2014

Intelligent Approaches For Modeling And Optimizing Hvac Systems

III Raymond Tesiero
North Carolina Agricultural and Technical State University

INTELLIGENT APPROACHES FOR MODELING AND OPTIMIZING HVAC SYSTEMS

Raymond Charles Tesiero III

North Carolina A&T State University

A dissertation submitted to the graduate faculty

in partial fulfillment of the requirements for the degree of

DOCTOR OF PHILOSOPHY

Department: Computational Science and Engineering

Major Professor: Dr. Nabil Nassif

Greensboro, North Carolina

2014

The Graduate School
North Carolina Agricultural and Technical State University
This is to certify that the Doctoral Dissertation of

Raymond Charles Tesiero III

has met the dissertation requirements of
North Carolina Agricultural and Technical State University

Greensboro, North Carolina
2014

Approved by:

Dr. Nabil Nassif Major Professor	Dr. Harmohindar Singh Committee Member
Dr. Kenneth Flurchick Committee Member	Dr. Ahmed Megri Committee Member
Dr. Marwan Bikdash Department Chair & Committee Member	Dr. Ram Mohan Graduate School Representative

Dr. Sanjiv Sarin
Dean, The Graduate School

Biographical Sketch

Raymond Charles Tesiero III was born on January 25, 1970 in Albany, New York. He has 20 years of experience, starting his engineering employment in the private sector during college at a general mechanical contracting company in 1989 and worked at a variety of companies as a co-op during college. He received his Associate of Applied Science degree in Civil Engineering Technology from Hudson Valley Community College (H.V.C.C.) in 1991 and his Bachelor of Science degree in Mechanical Engineering from Rochester Institute of Technology (R.I.T.) in 1995. He was then employed for an additional 16 years and has extensive experience in executive level roles in the private sector where he rose to the position of President of a signal communication and system integration company which was a contractor for the federal government with top secret clearance. He has worked for a variety of companies and has held the following titles: Mechanical Engineer, Project Engineering Manager, Plant Engineer, Plant Manager, Division Manager, Executive Vice President and General Manager. He is currently a PhD candidate in Computational Science and Engineering at North Carolina A&T State University (NC A&T) where he also received a Master's of Science degree in Civil Engineering in 2010. He is currently employed as a Research Coordinator and is responsible for government grant proposals, energy audits, building thermal modeling and analysis for the Center for Energy Research and Technology (C.E.R.T.) and provides input to academic curricula in the HVAC and energy areas. Ray also provides training and outreach programs in the pursuit of reducing energy and water consumption, promoting sustainable design practices, and reduction measures. He has eight publications to his credit, taught numerous workshops, presented at several international conferences, has been the co-principle investigator of four grants, and is a member of ASHRAE.

Dedication

I dedicate this dissertation to my wife, Michelle S. Tesiero, for her support and encouragement and our two daughters, Charlie and Samantha, who sacrificed family time to allow me to continue my graduate education, and for being there for me throughout the entire master and doctorate programs. I also dedicate this to my parents, Raymond Charles Tesiero Jr. and Mary C. Tesiero, who encourage me to excel in all that I do, instilled a great work ethic, taught the importance of hard work and higher education and always pushing my siblings and I to continue to pursue goals.

Acknowledgements

I would like to thank my research advisors at North Carolina Agricultural and Technical State University for guiding me through the masters' and doctoral dissertation programs. This includes my PhD advisor Dr. Nabil Nassif and my master's advisor Dr. Harmohindar Singh both from the Civil, Architectural and Environmental Engineering (CAEE) Department and my PhD committee members Dr. Marwan Bikdash and Dr. Kenneth Flurchick both from the Computational Science and Engineering (CSE) Department, and Dr. Ahmed Megri from CAEE, they have generously given their time and expertise to better my work. I thank them for their contribution and their good-natured support. I would like to especially thank my principal PhD research advisor Dr. Nabil Nassif for guiding me through the research and programming.

I would also like to thank Dr. Harmohindar Singh, director of The Center for Energy Research and Technology, C.E.R.T., who hired me during my master's degree and employed me full-time, enabling me to finance my education. Without my employment at NC A&T, my graduate advisors, my committee members, and my professors in CSE and CAEE, I would not be able to achieve the honor of obtaining a PhD in Computational Science and Engineering. I would also like to thank my wife, Michelle, children, Charlie and Samantha, and my parents, Mary and Ray, for their love and support to achieve my goals.

Table of Contents

List of Figures

List of Tables

List of Symbols

Symbols	Description	Typical Units
η_p	Pump efficiency	Unit-less
η_t	Total pump/motor efficiency	Unit-less
A	area	ft^2
a_i	Regression coefficients for head vs. flow	Unit-less
B	barometric pressure	psia or in. Hg
b_i	Regression coefficients for efficiency vs. flow	Unit-less
BF	Bypass factor	Unit-less
c	concentration	lb/ft^3, mol/ft^3
c	specific heat	Btu/lb·°F
c_p	specific heat at constant pressure	Btu/lb·°F
c_v	specific heat at constant volume	Btu/lb·°F
C	coefficient	—
C	fluid capacity rate	Btu/h·°F
C	thermal conductance	$Btu/h \cdot ft^2 \cdot °F$
C_L	loss coefficient	—
C_P	coefficient of performance	—
C_1	Capacity rate of stream 1	Btu/h ^oF
C_2	Capacity rate of stream 2	Btu/h ^oF
C_{min}	Minimum of the two capacity rates	Btu/h ^oF
C_{max}	Maximum of the two capacity rates	Btu/h ^oF
C	Ratio C_{min}/C_{max}	Unit-less

C_i	Regression coefficients for part-load performance	Unit-less
$c_{p,a}$	Specific heat of dry air	Btu/lb ^oF
$c_{p,sat}$	Effective specific heat of saturated air	Btu/lb ^oF
$c_{p,l}$	Specific heat of liquid	Btu/lb ^oF
$c_{p,v}$	Specific heat of water vapor	Btu/lb ^oF
d	Diameter of pump impeller	in
d	prefix meaning differential	—
d or D	diameter	ft
D_e or D_h	equivalent or hydraulic diameter	ft
D_v	mass diffusivity	ft^2/s
ε	Heat exchanger effectiveness	Unit-less
ε_m	Motor drive efficiency	Unit-less
e	base of natural logarithms	—
E	energy	Btu
E	electrical potential	V
f_D	friction factor, Darcy-Weisbach formulation	—
f_F	friction factor, Fanning formulation	—
F	force	lb_f
$f_{m,loss}$	Fraction of motor inefficiencies to airstream	Unit-less
f_{wet}	Fraction of surface area wet	Unit-less
g	gravitational acceleration	ft/s2
G	mass velocity	$lb/h \cdot ft^2$
h	heat transfer coefficient	$Btu/h \cdot ft^2 \cdot °F$

h	hydraulic head	ft
h	specific enthalpy	Btu/lb
h_a	enthalpy of dry air	Btu/lb
h_D	mass transfer coefficient	lb/h·ft^2·lb/ft^3
h_s	enthalpy of moist air at saturation	Btu/lb
H	total enthalpy	Btu
$h_{a,o}$	Leaving air enthalpy	Btu/lb
$h_{l,sat,ent}$	Saturated enthalpy of air at inlet liquid temp.	Btu/lb
$h_{lsat,lvg}$	Saturated enthalpy of air at exit liquid temp.	Btu/lb
$h_{sat,cond}$	Saturated air enthalpy at condensate temp	Btu/lb
$h_{a,ent}$	Entering air enthalpy	Btu/lb
$h_{a,lvg}$	Leaving air enthalpy	Btu/lb
J	mechanical equivalent of heat	ft·lb$_f$ /Btu
k	thermal conductivity	Btu/h·ft·°F
k (or γ)	ratio of specific heats, c_p/c_v	—
K	proportionality constant	—
KD	mass transfer coefficient	lb/h·ft^2
l or L	length	ft
m or M	mass	lb
M	molecular weight	lb/lb mol
m	Fluid mass flow rate	lb/h
m_a	Dry air mass flow rate	lb/h
$m_{a,rat}$	Dry air mass flow rate at rating	lb/h

m_l	Liquid mass flow rate	lb/h
$m_{l,rat}$	Liquid mass flow rate at rating	lb/h
m_w	Liquid mass flow rate	lb/h
n or N	number in general	—
N	rate of rotation	rpm
N	Number of transfer units, UA/C_{min}	Unit-less
NTU	Number of heat transfer units	Unit-less
p or P	pressure	psi
p_a	partial pressure of dry air	psi
p_s	partial pressure of water vapor in moist air	psi
p_w	vapor pressure of water in saturated moist air	psi
P	power	hp, watts
ΔP_{rat}	Rated pump head	psi
p_{ent}	Entering pressure	psi
p_{lvg}	Leaving pressure	psi
q	time rate of heat transfer	Btu/h
Q	total heat transfer	Btu
Q	volumetric flow rate	cfm
Q_{rat}	Rated volumetric fluid flow rate	cfm
q	Total heat transfer rate	Btu/h
q_{loss}	Heat transfer to air stream	Btu/h
q_{tot}	Total heat transfer rate	Btu/h
$q_{tot,rat}$	Total heat transfer rate at rating	Btu/h

q_{sen}	Sensible heat transfer rate	Btu/h
$q_{sen,rat}$	Sensible heat transfer rate at rating	Btu/h
r or R	thermal resistance	$ft^2 \cdot h \cdot °F/Btu$
R	gas constant	$ft \cdot lb_f / lb_m \cdot °R$
s	specific entropy	$Btu/lb \cdot °R$
S	total entropy	$Btu/°R$
t	temperature	°F
Δt_m or ΔT_m	mean temperature difference	°F
T	absolute temperature	°R
$T_{a,ent}$	Surface temperature at air entrance	F
t_{adp}	Apparatus dew point enthalpy	F
t_{dp}	Entering air dew point	F
$t_{l,ent}$	Entering water or liquid temperature	F
$t_{l,rat}$	Entering liquid temperature at rating	F
$t_{a,ent}$	Entering air dry bulb temperature	F
$t_{a,rat}$	Entering air dry bulb temperature at rating	F
$t_{l,lvg}$	Leaving water or liquid temperature	F
$t_{a,lvg}$	Leaving air dry bulb temperature	F
u	specific internal energy	Btu/lb
U	total internal energy	Btu
U	overall heat transfer coefficient	$Btu/h \cdot ft^2 \cdot °F$
UA	Overall heat transfer coefficient	$Btu/h\ ft^2\ ^oF$
UA_h	Overall enthalpy heat transfer coefficient	lb/h

UA_{int}	Liquid-side heat transfer coefficient	Btu/h ^{o}F
UA_{ext}	Air-side heat transfer coefficient	Btu/h ^{o}F
v	specific volume	ft^3/lb
V	total volume	ft^3
V	linear velocity	fps
w	mass rate of flow	lb/h
W	weight	lb_f
W	humidity ratio of moist air	lb(water)/lb(dry air)
W	work	ft·lb_f
W_t	Pump power	hp, Watts
W_s	Shaft power	hp, Watts
$W_{t,rat}$	Rated pump/motor power	hp, Watts
w_{adp}	Apparatus dew point humidity ratio	Unit-less
$w_{a,ent}$	Entering air humidity ratio	Unit-less
$w_{a,rat}$	Entering air humidity ratio at rating	Unit-less
$w_{a,lvg}$	Leaving air humidity ratio	Unit-less
W_s	humidity ratio of moist air at saturation	lb(water)/lb(dry air)
x	mole fraction	—
x	quality, mass fraction of vapor	—
$X_{1,ent}$	Inlet state of stream 1	F
$X_{2,ent}$	Inlet state of stream 2	F
$X_{1,lvg}$	Outlet state of stream 1	F
$X_{2,lvg}$	Outlet state of stream 2	F

α	linear coefficient of thermal expansion	per °F
α	thermal diffusivity	ft^2/h
β	volume coefficient of thermal expansion	per °F
γ *(or k)*	ratio of specific heats, c_p/c_v	—
γ	specific weight	lb_f/ft^3
Δ	difference between values	—
ε	emissivity, emittance (radiation)	—
θ	time	s, h
η	efficiency or effectiveness	—
μ	degree of saturation	—
μ	dynamic viscosity	lb/ft·h
ν	kinematic viscosity	ft^2/h
ρ	density	lb/ft^3
τ	time	s, h
ϕ	relative humidity	—

Abbreviations and Symbols

Term	Text	Drawings	Program
absolute	abs	ABS	ABS
air condition(-ing, -ed)	—	AIR COND	—
air-conditioning unit(s)	—	ACU	ACU
air-handling unit	—	AHU	AHU
ambient	amb	AMB	AMB
apparatus dew point	adp	ADP	ADP
approximate	approx.	APPROX	—
atmosphere	atm	ATM	—
average	avg	AVG	AVG
barometer(-tric)	baro	BARO	—
boiling point	bp	BP	BP
brake horsepower	bhp	BHP	BHP
British thermal unit	Btu	BTU	BTU
Celsius	°C	°C	°C
coefficient	coeff.	COEF	COEF
coefficient, valve flow	C_v	C_v	CV
coil	—	—	COIL
compressor	cprsr	CMPR	CMPR
condens(-er, -ing, -ation)	cond	COND	COND
conductance	—	—	C
contact factor	—	—	CF

cooling load	clg load	CLG LOAD	CLOAD
cubic feet	ft^3	CU FT CUFT,	CFT
cubic inch	in_3	CU IN CUIN,	CIN
cubic feet per minute	cfm	CFM	CFM
cfm, standard conditions	scfm	SCFM	SCFM
cubic ft per sec, standard	scfs	SCFS	SCFS
degree	deg. or °	DEG or °	DEG
density	dens	DENS	RHO
dew-point temperature	dpt	DPT	DPT
difference or delta	diff., Δ	DIFF	D, DELTA
dry	—		DRY
dry-bulb temperature	dbt	DBT	DB, DBT
effectiveness	—		EFT
effective temperature[2]	ET*	ET*	ET
efficiency	eff	EFF	EFF
efficiency, fin	—		FEFF
efficiency, surface	—		SEFF
entering	entr	ENT	ENT
entering water temperature	EWT	EWT	EWT
entering air temperature	EAT	EAT	EAT
enthalpy	—	—	H
entropy	—	—	S
equivalent direct radiation	edr	EDR	—

equivalent feet	eqiv ft	EQIV FT	EQFT
equivalent inches	eqiv in	EQIV IN	EQIN
evaporat(-e, -ing, -ed, -or)	evap	EVAP	EVAP
face velocity	fvel	FVEL	FV
factor, friction	—	—	FFACT, FF
Fahrenheit	°F	°F	F
fan	—	—	FAN
feet per minute	fpm	FPM	FPM
feet per second	fps	FPS	FPS
flow rate, air	—	—	QAR, QAIR
flow rate, fluid	—	—	QFL
flow rate, gas	—	—	QGA, QGAS
foot or feet	ft	FT	FT
foot-pound	ft·lb	FT LB	—
gage or gauge	ga	GA	GA, GAGE
gallons	gal	GAL	GAL
gallons per hour	gph	GPH	GPH
gallons per minute	gpm	GPM	GPM
grains	gr	GR	GR
gravitational constant	*G*	G	G
head	hd	HD	HD
heat	—	—	HT
heat gain	HG	HG	HG, HEATG

heat gain, latent	LHG	LHG	HGL
heat gain, sensible	SHG	SHG	HGS
heat loss	—	—	HL, HEATL
heat transfer	—	—	Q
heat transfer coefficient	*U*	U	U
horsepower	hp	HP	HP
hour(s)	h	HR	HR
humidity, relative	rh	RH	RH
humidity ratio	*W*	W	W
inch	in.	in.	IN
kilowatt hour	kWh	KWH	KWH
latent heat	LH	LH	LH, LHEAT
least mean temp. difference	LMTD	LMTD	LMTD
least temp. difference	LTD	LTD	LTD
leaving air temperature	lat	LAT	LAT
leaving water temperature	lwt	LWT	LWT
liquid	liq	LIQ	LIQ
logarithm (natural)	ln	LN	LN
logarithm to base 10	log	LOG	LOG
low-pressure steam	lps	LPS	LPS
low-temp. hot water	lthw	LTHW	LTHW
mass flow rate	mfr	MFR	MFR
maximum	max.	MAX	MAX

minimum	min.	MIN	MIN
minute	min	MIN	MIN
not applicable	na	N/A	—
number	no.	NO	N, NO
outside air	oa	OA	OA
percent	%	%	PCT
pounds	lb	LBS	LBS
pounds per square foot	psf	PSF	PSF
psf absolute	psfa	PSFA	PSFA
psf gage	psfg	PSFG	PSFG
pounds per square inch	psi	PSI	PSI
psi absolute	psia	PSIA	PSIA
psi gage	psig	PSIG	PSIG
pressure	—	PRESS	PRES, P
pressure, barometric	baro pr	BARO PR	BP
pressure, critical	—	—	CRIP
pressure, dynamic (velocity)	vp	VP	VP
pressure drop or difference	PD	PD	PD, DELTP
pressure, static	sp	SP	SP
pressure, vapor	vap pr	VAP PR	VAP
Rankine	°R	°R	R
recirculate	recirc.	RECIRC	RCIR, RECIR
refrigerant (12, 22, etc.)	R-12, R-22	R12, R22	R12, R22

relative humidity	rh	RH	RH
return air	ra	RA	RA
revolutions	rev	REV	REV
revolutions per minute	rpm	RPM	RPM
revolutions per second	rps	RPS	RPS
roughness	rgh	RGH	RGH, E
safety factor	sf	SF	SF
saturation	sat.	SAT	SAT
second	s	s	SEC
sensible heat	SH	SH	SH
sensible heat gain	SHG	SHG	SHG
sensible heat ratio	SHR	SHR	SHR
shaft horsepower	sft hp	SFT HP	SHP
solar	—	—	SOL
specific gravity	SG	SG	—
specific heat	sp ht	SP HT	C
sp ht at constant pressure	c_p	c_p	CP
sp ht at constant volume	c_v	c_v	CV
specific volume	sp vol	SP VOL	V, CVOL
square	sq.	SQ	SQ
standard	std	STD	STD
static pressure	SP	SP	SP
supply	sply	SPLY	SUP, SPLY

supply air	sa	SA	SA
surface	—	—	SUR, S
surface, dry	—	—	SURD
surface, wet	—	—	SURW
system	—	—	SYS
tee	—	—	TEE
temperature	temp.	TEMP	T, TEMP
temperature difference	TD, Δt	TD	TD, TDIF
temperature entering	TE	TE	TE, TENT
temperature leaving	TL	TL	TL, TLEA
thermal conductivity	k	K	K
thermal expansion coeff.	—	—	TXPC
thermal resistance	R	R	RES, R
thermostat	T STAT	T STAT	T STAT
time	—	T	T
ton	—	—	TON
tons of refrigeration	tons	TONS	TONS
total	—	—	TOT
total heat	tot ht	TOT HT	—
U-factor	—	—	U
unit	—	—	UNIT
valve	v	V	VLV
variable	var	VAR	VAR

variable air volume	VAV	VAV	VAV
velocity	vel.	VEL	VEL, V
ventilation, vent	vent	VENT	VENT
viscosity	visc	VISC	MU, VISC
volume	vol.	VOL	VOL
volumetric flow rate	—	—	VFR
water	—	—	WTR
watt	W	W	WAT, W
watt-hour	Wh	WH	WHR
wet bulb	wb	WB	WB
wet-bulb temperature	wbt	WBT	WBT
year	yr	YR	YR
zone	z	Z	Z, ZN

Dimensionless Numbers

Re	Reynolds number	$\rho VD/\mu$

Abbreviations and Definitions

AHU	- Air Handling Unit
ANN	- Artificial Neural Network
ASHRAE	- American Society of Heating Refrigeration and Air Conditioning Engineers
BAS	- Building Automation System
BEP	- Building Energy Performance
BDA	- Building Design Advisor
BTU	- British Thermal Unit
DCV	- Demand Controlled Ventilation
DDC	- Digital Direct Control
DOE	- Department of Energy
DX	- Direct Expansion
EIA	- Energy Information Administration
EMCS	- Energy Management Control System
EP	- Evolutionary Programming
FMBMPC	- fuzzy model-based multivariable predictive functional control
GA	- Genetic algorithm
HVAC	- Heating, Ventilation and Air Conditioning
IAQP	- Indoor Air Quality Procedure
IIR	- Infinite Impulse Response
MEP	- Mechanical, Electrical and Plumbing
MPC	- Model-based Predictive Controller
NVP	- Natural Ventilation Procedure

OA - Outside Air

OAT - Outside Air Temperature

OLSTM - On-line, self-tuning model

OLSTOP - On-line, self-tuning, optimization process

OP - Optimization Process

OSP - Occupied Set Point

OVSP - Optimal Variable Set-point

PPD - Predicted Percent Dissatisfied

SATR - Supply Air Temperature Reset

SATRC - Supply Air Temperature Reset Control

ST - Self-tuning

STD - Set Temperature Distribution

STM - Self-tuning Model

VAV - Variable Air Volume

VRC - Ventilation Reset Control

VRP - Ventilation Rate Procedure

WNN - Wavelet Artificial Neural Network

Subscripts

a,b,...	referring to different phases, states or physical conditions of a substance, or to different substances
a	air
a	ambient
b	barometric (pressure)
c	referring to critical state or critical value
c	convection
db	dry bulb
dp	dew point
e	base of natural logarithms
f	referring to saturated liquid
fg	referring to evaporation or condensation
F	friction
g	referring to saturated vapor
h	referring to change of phase in evaporation
H	water vapor
i	referring to saturated solid
i	internal
if	referring to change of phase in melting
ig	referring to change of phase in sublimation
k	kinetic
L	latent

m	mean value
M	molar basis
p	referring to constant pressure conditions or processes
p	potential
r	refrigerant
r	radiant or radiation
s	referring to moist air at saturation
s	sensible
s	referring to isentropic conditions or processes
s	static (pressure)
s	surface
t	total (pressure)
T	referring to isothermal conditions or processes
v	referring to constant volume conditions or processes
v	vapor
v	velocity (pressure)
w	water
wb	wet bulb
0	referring to initial or standard states or conditions
1,2,...	different points in a process, or different instants of time

Abstract

Advanced energy management control systems (EMCS), or building automation systems (BAS), offer an excellent means of reducing energy consumption in heating, ventilating, and air conditioning (HVAC) systems while maintaining and improving indoor environmental conditions. This can be achieved through the use of computational intelligence and optimization. This research will evaluate model-based optimization processes (OP) for HVAC systems utilizing MATLAB, genetic algorithms and self-learning or self-tuning models (STM), which minimizes the error between measured and predicted performance data. The OP can be integrated into the EMCS to perform several intelligent functions achieving optimal system performance. The development of several self-learning HVAC models and optimizing the process (minimizing energy use) will be tested using data collected from the HVAC system servicing the Academic building on the campus of NC A&T State University.

Intelligent approaches for modeling and optimizing HVAC systems are developed and validated in this research. The optimization process (OP) including the STMs with genetic algorithms (GA) enables the ideal operation of the building's HVAC systems when running in parallel with a building automation system (BAS). Using this proposed optimization process (OP), the optimal variable set points (OVSP), such as supply air temperature (T_s), supply duct static pressure (P_s), chilled water supply temperature (T_w), minimum outdoor ventilation, reheat (or zone supply air temperature, T_z), and chilled water differential pressure set-point (D_{pw}) are optimized with respect to energy use of the HVAC's cooling side including the chiller, pump, and fan. HVAC system component models were developed and validated against both simulated and monitored real data of an existing VAV system. The optimized set point variables minimize energy use and maintain thermal comfort incorporating ASHRAE's new ventilation standard

62.1-2013. The proposed optimization process is validated on an existing VAV system for three summer months (May, June, August).

This proposed research deals primarily with: on-line, self-tuning, optimization process (OLSTOP); HVAC design principles; and control strategies within a building automation system (BAS) controller. The HVAC controller will achieve the lowest energy consumption of the cooling side while maintaining occupant comfort by performing and prioritizing the appropriate actions. Recent technological advances in computing power, sensors, and databases will influence the cost savings and scalability of the system. Improved energy efficiencies of existing Variable Air Volume (VAV) HVAC systems can be achieved by optimizing the control sequence leading to advanced BAS programming. The program's algorithms analyze multiple variables (humidity, pressure, temperature, CO_2, etc.) simultaneously at key locations throughout the HVAC system (pumps, cooling coil, chiller, fan, etc.) to reach the function's objective, which is the lowest energy consumption while maintaining occupancy comfort.

CHAPTER 1

Introduction

The recent global trend shows as fuel costs rise, improving energy efficiency in buildings is a major concern for owners and building managers. The buildings sector account for more than 40% of the overall energy consumption in the US. In particular, within the buildings sector, heating and cooling applications account for more than half of all the energy consumed. With the significant demand for energy, especially in the building heating ventilation and air-conditioning (HVAC) systems, it is essential to develop new technologies that can improve energy efficiency (Narayanan, S. et al., 2014). Several reasons are behind the push towards a reduction in energy consumption:

- Energy costs
- Government grants
- Utility rebates
- Carbon footprint awareness (Greenhouse gas emissions)
- LEED certification
- Improving bottom line profits
- Net-zero energy objectives

Navigant Research forecasts that global advanced HVAC controls revenue will grow from $7.0 billion in 2014 to $12.7 billion in 2023. The Navigant Research report analyzes the global market for advanced HVAC controls, with a focus on the following components: sensors, field devices, floor-level controllers, and building-level controllers. Building owners, operators, and especially governments and regulatory agencies are increasingly focusing on optimizing

commercial building energy use through improved HVAC controls ("Advanced HVAC Controls," 2014).

From the 2011 Buildings Energy Data Book published by the U.S. D.O.E., U.S. building's primary energy consumption increased by 48% between 1980 and 2009. The Energy Information Administration (EIA) projects that this growth will stagnate due to the recession until 2016, when steady growth is predicted through 2035. Total primary energy consumption is expected to reach more than 45 quads by 2035, a 17% increase over 2009 levels. This growth in buildings sector energy consumption is fueled primarily by the growth in population, households, and commercial floor-space, which are expected to increase 27%, 31%, and 28%, respectively, between 2009 and 2035 (D&R International, L., 2012).

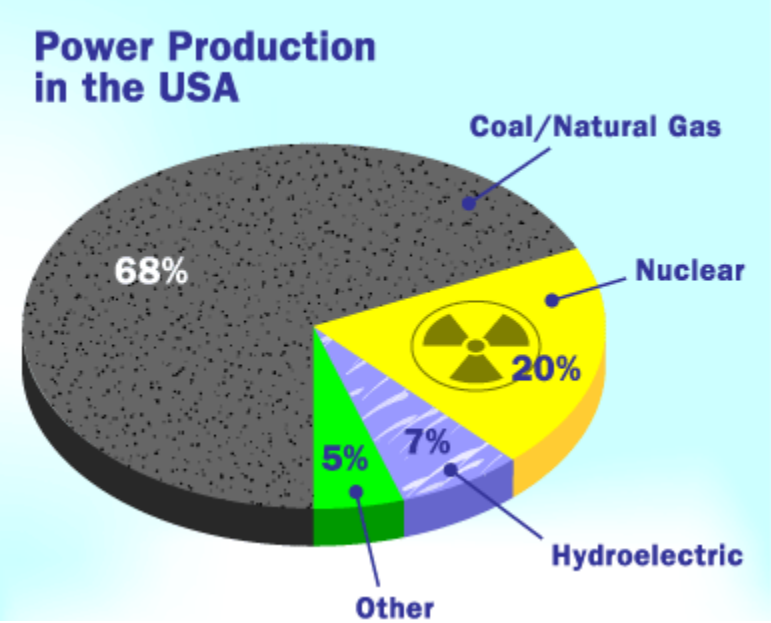

Figure 1. Power production in the USA.

Today electricity is generated mainly from non-renewable energy sources, and over consumption leads to faster depletion of the energy reserves on earth, see Figure 1. The majority of electricity in the United States is produced by power plants that burn coal, with 464 such plants producing 56 percent of all electricity. These power plants also are the nation's single

biggest source of mercury pollution. Each year, the plants spew a total of 48 tons of mercury into the atmosphere, roughly a third of all human-generated mercury emissions. When coal is burned in power plants, the trace amount of mercury that it contains passes along with the flue gas into the atmosphere. The mercury eventually falls back to earth in rain, snow, or as dry particles, either locally or sometimes hundreds of miles distant. Once the mercury is deposited on land or in water, bacteria often act to change the metal into an organic form, called methylmercury, which easily enters the food chain and "bioaccumulates." At the upper reaches of the food chain, some fish and other predators end up with mercury levels more than a million times higher than those in the surrounding environment. For the humans and wildlife that ultimately consume these species, these concentrations can be poisonous (Little, M., 2002).

Electricity is becoming more expensive and generation of electricity from conventional fuels is extremely damaging to the environment because great quantities of carbon dioxide and monoxide, sulphur dioxide and other hazardous materials are released into the atmosphere, see Figure 2.

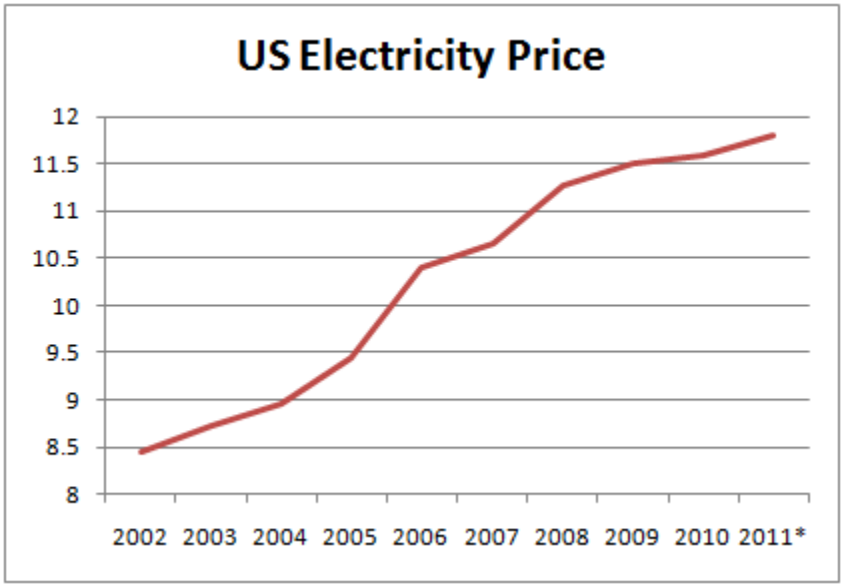

Figure 2. US electricity price.

Reducing the consumption of electricity will prolong the existence of the natural energy reserves and limit pollution of the atmosphere while at the same time save money, see Figure 3. There are several efforts in energy efficiency legislation that will create jobs, save consumers and taxpayers money, and reduce pollution by lowering energy consumption across the country like the Energy Savings and Industrial Competitiveness Act (S.1392), also known as Shaheen-Portman bill. Shaheen-Portman is a bipartisan effort that reflects an affordable approach to boost the use of energy efficiency technologies. It will help create private-sector jobs, save businesses and consumers money, reduce pollution and make our country more energy independent. A study by experts at the American Council for an Energy Efficient Economy found that 2013's version would have saved consumers $4 billion by 2020 and helped businesses add 80,000 jobs to the economy. It would also cut carbon-dioxide emissions by the equivalent of taking 5 million cars off the road ("Shaheen: Energy Efficiency Bill Will Create Jobs, Save Money, Reduce Pollution," 2013).

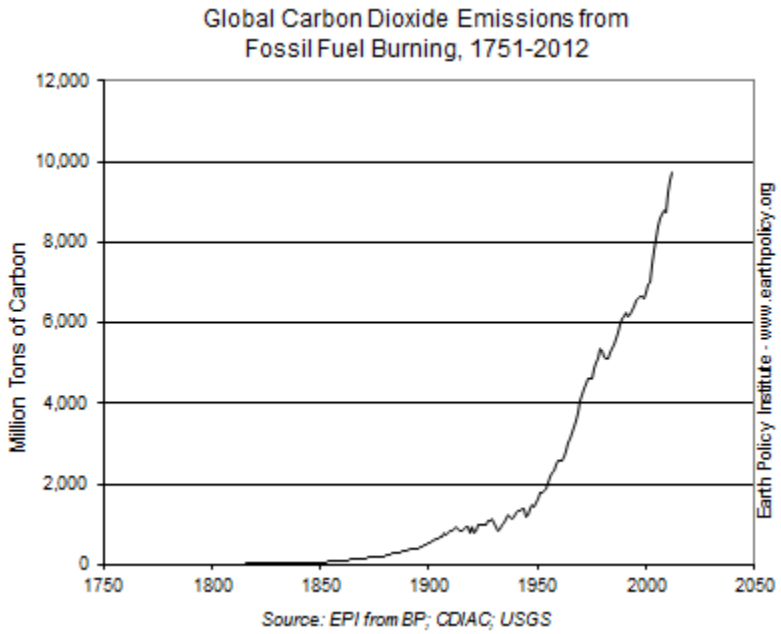

Figure 3. Global carbon dioxide emissions from fossil fuels.

A structured approach to energy management can help to identify and implement the best ways to reduce energy costs for a facility. Today buildings in the U.S. consume 72 percent of electricity produced, and use 55 percent of U.S. natural gas. Buildings account for about 48 percent of the energy consumed in the United States (costing $350+ billion per year), more than industry and transportation. Of this energy, heating and cooling systems use about 55 percent (HVAC, Ventilation, and Hot Water Heating), while lights and appliances use the other 35 percent. *(Architecture, D., 2012)* See Figures 4 and 5.

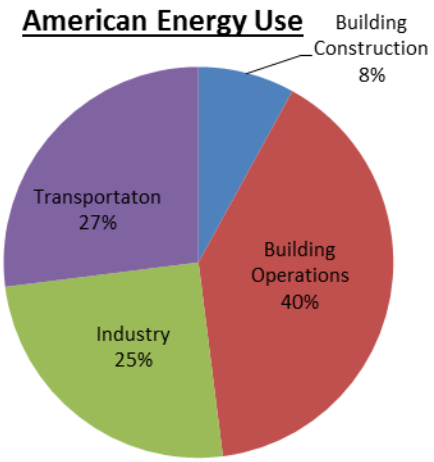

Figure 4. American energy use.

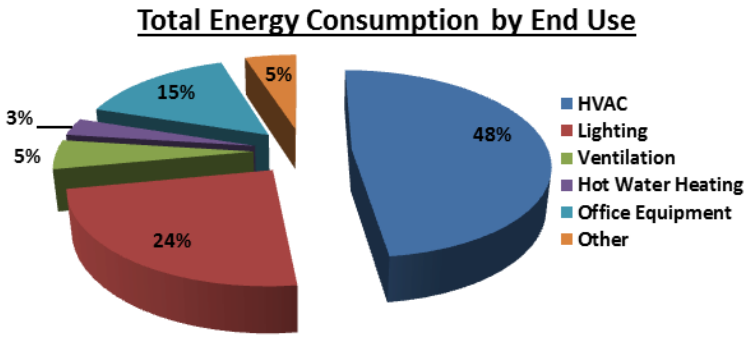

Figure 5. Total building energy consumption by end use.

Buildings are complex engineering systems determined by its structure, functions, and the required installations. As a building consists of a high number of components differing in characteristics and operation times, Building Energy Management Systems (BEMS) needs this environment to be divided into multiple zones, e.g. office rooms, common areas, halls etc., with a set of energy demand and control variables. Therefore, an adequate and reliable model is necessary for each zone in a building (Hurtado, L. A. et al., 2013).

Projected world marketed energy consumption in the next 20 years is in the 600+ quadrillion BTU range (Mincer, S., 2011), see Figure 6. Power usage in buildings is often inefficient with regard to the overall building operability. The development of building energy savings methods and models becomes apparently more necessary for a sustainable future. The development of a physical model representing the HVAC system, utilizing MATLAB software and incorporating HVAC design principles and major system components, are improved methodologies to estimate and accurately control a building's HVAC systems with minimum energy consumption while maintaining occupant comfort. Creating an OP with self-learning models has advantages over other techniques due to, simplicity in analysis and adaptability to changes in a building's energy use.

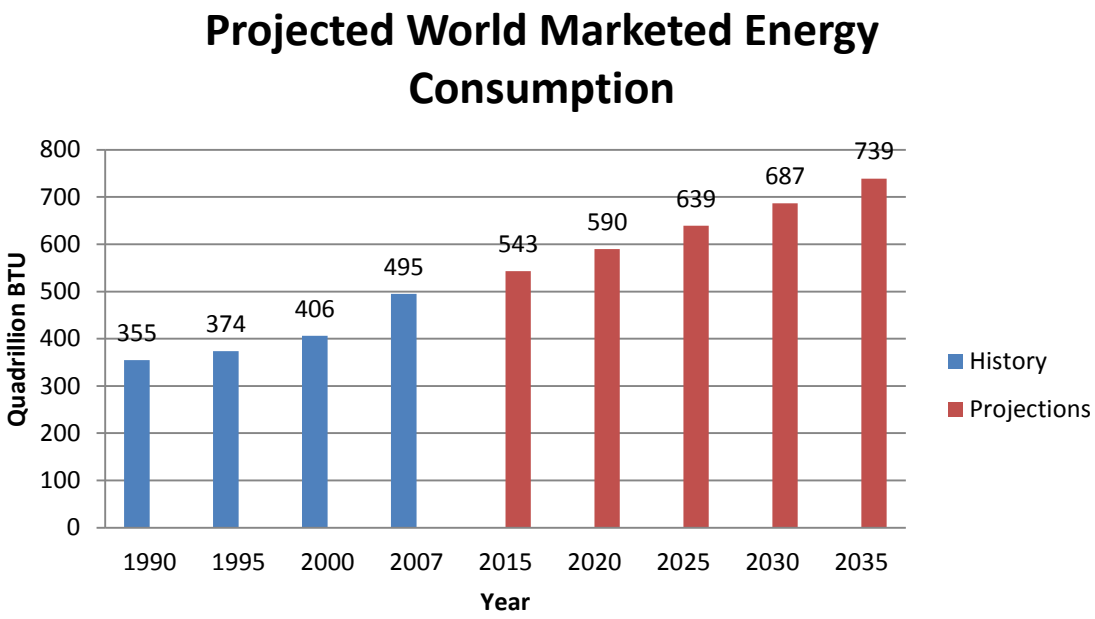

Figure 6. Projected world marketed energy consumption.

The capacity of the HVAC system is typically designed for the maximum or extreme conditions for the building. The HVAC system mainly operates in partial load from the design variables such as solar loads, occupancy levels, ambient temperatures, building and office equipment, lighting loads, etc. These variables are constantly changing throughout the course of the day. Deviation from the HVAC system design can result in drastic swings or imbalance since design capacity is greater than the actual load in most operating scenarios. Without proper HVAC programming control sequences, the system can become unstable and the building will overheat or overcool spaces, wasting energy. The self-learning model training process simply involves modification of input variables until the calculated output is in close agreement with the actual output. There are several different forms of self-learning models to improve the accuracy of component modeling. Previous research utilizing optimization processes claim to achieve 10 - 20% savings in building HVAC energy consumption which can equate to 35+ billion dollars and over 100 quadrillion BTU's.

The air supply temperature (T_s), duct static pressure (P_s), chilled water supply temperature (T_w), and chilled water differential pressure set-point (D_{pw}) set points for this system are determined as a function of the outdoor air temperatures, zone sensible and latent loads, and system design parameters. Decreasing the supply air temperature may result in a lower supply duct static pressure and fan energy. Applying some reheat in the low-load zone (ventilation critical zone) significantly reduces the system's outdoor air ventilation. The zone air temperature set-points of the investigated HVAC system are kept constant in the comfort zone during occupied periods. The optimization of the cooling side of the HVAC system set points during occupied periods proves to reduce system energy use. Two techniques are implemented in this research problem; genetic algorithms (GA) are utilized, one to optimize the variable set points and another GA to minimize the error in system component validation for the chiller and cooling coil, and a new interpolation method to minimize the error in the models for the fan and pump. The OP provides an opportunity to maintain the thermal comfort and minimize the energy use according to the time of day (Nassif, N. et al., 2005).

1.1 Research Goals and Objectives

The objective of the research is to develop the methodology and validate on-line, self-tuning models (OLSTM) against actual data from an existing building; and utilize these models with a new optimization process that optimize key variable set points to minimize the energy use of a specific HVAC system configuration. The goals of the work are:

- To develop functional models for typical HVAC systems; to give the overview of various HVAC system components; to analyze the impacts of optimal variable set points on the energy performance.

- To identify the criteria for on-line, self-tuning models and optimal variable set point system selection; to identify the feasible simulation and optimization tools for the research approach; to give an overview of tools and methods used for the research approach; to identify criteria for suitable selection of optimization algorithms for solving optimal variable settings; to identify optimization variables for the specific HVAC system components; to define the optimization objective function and constraints.
- To develop component models capable to estimate the HVAC system's performance annually for commercial applications; to calibrate and validate the models.
- To train and test the models utilizing simulated data and automatically modify the component models to match with current real-time system operation and validate the modified component models.
- To develop an optimization process for variable set-points from a multifunctional modeling approach for a typical building HVAC system; to develop HVAC system models for different components that are transferrable; to evaluate the optimal variables of the HVAC system in the simulated building; to select the optimal variable set-points for the system configuration in an actual building that utilizes a building automation system and has real time data.
- To summarize the research, draw conclusions, and provide directions for the future research.

1.2 The Scientific Contribution

The scientific contribution is the development of systematic, simulation-based, self-tuning models (STM) for the effective and efficient validation of various HVAC system components, to automatically select the optimal variable set-points to minimize energy use

incorporating control strategies and current ASHRAE standards in an on-line self-tuning optimization process (OLSTOP). This approach could be implemented in existing building automation systems (BAS) with real-time data. Additionally, the models would minimize the limitations of HVAC theory based knowledge and BAS operator‘s expertise for specific systems under certain climate conditions.

In this research, new equation-based modeling and simulation approaches are compared with ASHRAE’s HVAC 2 Toolkit, EnergyPlus, and eQuest models and calculations. The new STMs utilized are improved techniques for more accurate validation of the HVAC system components and are all programmed into MATLAB for analysis. A building is simulated in eQuest to determine the load required for the optimization process (OP) evaluations or testing. Actual data from a building automation system (BAS) is used during the optimization process that establishes the optimal variable set-points through MATLAB programming incorporating genetic algorithms to minimize HVAC energy use without sacrificing thermal comfort. The methods are presented with respect to HVAC system component modeling in the MATLAB environment. This optimization process using STMs can be applied to automatically select optimal variable set-points in real time by coupling MATLAB’s output and a building’s automation system’s current HVAC operational performance data.

The developed methods are implemented for optimization of a real HVAC system installed in the New Academic Classroom building on the campus of NC A&T State University in North Carolina, USA. The optimization process implementation presents new set-point variables (T_s, T_w, P_s, D_{pw}) that minimized energy use for the system configuration. The validated ST component models are used to enhance the system optimization model; then confirmation is performed at the system optimization level. The validated system optimization model is used for

performance analysis of the real HVAC system configurations in North Carolina. In the study, only the cooling side of each HVAC system configuration is analyzed. The evaluation resulted that the performance of HVAC cooling system with the new optimized set-point variables configuration is much more energy efficient than the original set-points. See Table 1 for the optimal set-point variable comparisons. The overall optimization of the HVAC system with real time building load demands resulted with the cooling side power consumption reduction between 13% and 73% depending on the outside conditions and time of day. The average savings was 22% comparing the optimal set-point variables for the three month analysis to standard practice (SP or SATR) and fixed or override mode (FOM).

Table 1

OLSTOP Results Table

OLSTOP RESULTS TABLE: Ts (F) Ps (in wc) Tw (F) Dpw (psi)														
Scheme	Optimal Variables (OV)				Standard Practice (SP) - SATR				Fixed or Override Mode (FOM)				Outside Conditions	
Variable	Ts	Ps	Tw	Dpw	Ts	Ps	Tw	Dpw	Ts	Ps	Tw	Dpw	WBT (F)	DBT (F)
Max	63.14	2.26	54.84	19.92	65.00	2.5	45	20	55	2.5	45	20	82.00	93.00
Min	55.00	1.00	45.67	10.00	55.00	2.5	45	20	55	2.5	45	20	49.00	51.00
Average	57.82	1.35	50.02	12.55	55.56	2.5	45	20	55	2.5	45	20	67.04	75.43
Scheme	Optimal Power (kW)				SP (SATR) Power (kW)				FOM Power (kW)				Savings	
Power	Total	Chiller	Pump	Fan	Total	Chiller	Pump	Fan	Total	Chiller	Pump	Fan	OV to SP	OV to FOM
Max	112.65	96.75	3.59	23.16	131.17	106.81	5.08	32.14	131.17	106.81	5.08	19.42	73.94%	64.37%
Min	5.24	0.00	0.00	4.56	11.93	0.00	0.00	10.05	14.71	5.21	0.05	8.53	13.02%	13.02%
Average	63.76	50.68	1.42	11.67	79.62	61.50	2.49	15.63	79.32	61.96	2.50	14.86	22.54%	22.21%

The dissertation also contributes at the component level in which the Fan, Pump, Chiller, Cooling Coil, Zone, VAV System, and Ventilation models are developed for optimal performance analysis of typical commercial system operation using genetic algorithms. These new models have the capability to handle real-time control strategies with respect to free cooling economizers and ASHRAE's 62.1-2013 ventilation standard operational modes and sensor functionalities. The models are validated and compared to the published data and measurements from ASHRAE's HVAC 2 Toolkit, EnergyPlus, and eQuest, which are recognized HVAC

simulation building modeling programs and software, and the real building data from the BAS of the New Academic Building on the campus of NC A&T State University.

The existing optimal set-point variable studies do not address the following points that are in this research:

1. the incorporation of reheat, penalties, and constraints with the cooling system
2. the interaction between the optimal variable set-points including both the air and water side of the cooling system
3. controlling and varying the optimal variable set points while maintaining thermal comfort during the day as a function of daily energy use by utilizing genetic algorithms and accurately tune parameter coefficients with STMs, which leads to further energy savings.
4. the ventilation requirements based on the newest version of ASHRAE 62.1-2013
5. the interaction between the outside airflow rates and other optimal variables

This paper presents a system approach that takes into account the interaction involving reheat, penalties, and constraints, including supply air temperature (T_s), supply duct static pressure (P_s), chilled water supply temperature (T_w), chilled water differential pressure set-point (D_{pw}), and the new minimum outdoor ventilation requirements (ASHRAE 62.1-2013) using an OP while engaging OLSTMs and genetic algorithms. The following methodology is employed:

1. collecting data from the investigated existing HVAC system
2. modeling and validation of self-tuning (self-learning) HVAC components, including ASHRAE-62.1-2013 standard multi-zone ventilation calculation procedure
3. development of optimization algorithms
4. development of proposed optimization process
5. testing the developed optimization process on multi-zone HVAC systems

Self-learning (or self-tuning) models (Fan, Pump, Chiller, and Cooling Coil) of HVAC components with the capability for online tuning of coefficient parameters that fit the system performance curves, are proposed in this research and ensure more reliability and accuracy. The structure of the program consists of several component models that represent the system, a set of tuning parameters integrated into the models to improve accuracy and a means to intelligently update the parameters online with the measured data of the system. The model parameters are periodically adjusted online by an intelligent optimization method, the genetic algorithm, to reduce the error between measured and predicted data.

Finally, the developed models present the dynamic, real-time concept of predicting optimal set-point variables in HVAC systems; and considerably ease the complex task of minimizing energy use in HVAC system configurations. The energy savings are presented by comparing the actual existing operation of the HVAC system which is calculated using the monitored and validated models, to the STM's optimization of the building automation system's controller set point variables. Additionally, the approach is a step forward toward the development of software systems able to synthesize, in real-time, new and optimal variable set-points in varying system configurations and integrate easily into a BAS.

1.3 Dissertation Outline

The dissertation is composed of 6 chapters. A brief summary of all chapters is presented here:

1. Chapter 1 gives an overview of the basic idea of the research in terms of motivation based on the statistical data related to energy consumption of HVAC systems in the building sector. Additionally, the research approach is also briefly discussed along with the basic goals, objective and scientific contribution.

2. Chapter 2 provides the literature review of HVAC system optimization through numerous research studies, including several different computational techniques.
3. Chapter 3 is related to the methodology of the HVAC system components (equipment). It defines the various types of HVAC systems components and describes the Building Automation System (BAS). It is focused on: the various aspects of the research methodology, describing in detail the formulas utilized in the programming in MATLAB for the components and subroutines, the steps required to analyze the data, and performing the self-tuning and optimization process. Chapter 3 presents the dissertation contribution at the component level in which 27 models are programmed into MATLAB capable of implementing control strategies and the new ASHRAE standards utilizing genetic algorithms to validate tuning parameters of component models and optimize system set-point variables to minimize energy.
4. Chapter 4 concerns model training and testing, where the initial results are validated against the component models including their respective tuning parameters with the GA and the optimization process utilizing its genetic algorithm is discussed. The methods of HVAC system modeling and simulation are discussed through examples of model training, testing and validation. This is the proof of concept chapter for the proposed methodology for automated optimal selection of system set-point variables. The optimization process is discussed and the genetic algorithms are presented. The approach is implemented on the system design and configuration level of a real HVAC cooling system operating in North Carolina. The optimization process which minimizes energy use is implemented and validated for performance. Chapter 4 presents the dissertation contributions at the data entry level in which an input file called UserInput.xlsx is created

with several worksheets that are read during simulation, model testing, training, and validation. Another file is created during output called UserOutput.xlsx where the results are automatically saved after running the program. There is also a discussion of a user-interface that has been designed and will be further developed in post-doctoral work.

5. Chapter 5 presents the optimal variable set point results from the optimization process in graphical form.
6. Chapter 6 presents the summary of key conclusions and directions for the future research activities for further enhancement.
7. Following Chapter 6 is the reference and the appendix section.

CHAPTER 2

Literature Review

The problems surrounding building energy performance arise from the infinite architectural and mechanical building designs and multiple energy analysis methods and tools available. Energy efficiency is achieved through properly functioning equipment and control systems, whereas problems associated with building controls and operation are the primary causes of inefficient energy usage. There is an obvious relationship between energy consumption and control-related problems. The most significant problems associated with energy inefficiency are found to be:

- Software
- Hardware
- Equipment Maintenance
- Energy Management Strategies
- Human Factors

When a BAS is not present, a more "hands-on" approach is necessary. Training and commitment to control strategies will save money; as long as the building's energy use systems are running properly it can be controlled efficiently. Failure to utilize available features restricts equipment use, especially with controls. Most buildings are using only a small portion of their control capabilities. There are a number of common human factors that contribute to this problem, see Table 2. Human factors, including controller programming issues, occur at a significantly higher rate than any other subcategory of problem. There are several objectives of a controller: reduce energy costs, improve building occupant comfort, fault detection and diagnostic capability (Martin, R. A. et al., 2002).

Table 2

Human Factors that Waste Energy in Buildings

Common Factors	
Fear of change	Lack of energy conservation awareness from top-down approach
Lack of training	Need to please co-workers' individual comfort levels
Lack of planning	Simplicity of "overriding" system parameters
Insufficient staffing	Lack of fundamental HVAC theory
Fear of internal politics	Lack of programming knowledge
Failure to tune the system	Failure to maintain the system

2.1 HVAC System Modeling and Simulation

Today, modeling and simulation are recognized techniques for solving energy cost issues in several engineering fields. A wide range of tools are available in the design, analysis, and optimization of system performance. Design, test, operation, and management of HVAC systems rely increasingly on modeling and simulation techniques. Such techniques together with model-based analysis of HVAC systems provide an important tool enabling engineers to carry out detailed tests of the systems by matching their performance on a computer through simulation (Ali, M. et al., 2013). Several studies have been addressed to optimize HVAC systems, Treado, S. J. (2010), Kelly, G. E. et al. (2012), Bravo, R. H. et al. (2011), Lu, L. et al. (2005), Platt, G. et al. (2010), Xu, G. (2012), Counsell, J. et al. (2013), and Wemhoff, F. et al. (2010) are just a few.

Modeling of HVAC systems is rapidly gaining more interest for system energy performance evaluation. Energy performance, system, and control analysis optimization are gaining momentum in research applications with the rising costs of building utilities. Available tools are not fully suited for modeling and simulation of real-time analysis of building automation system (BAS) data, nor have the compatibility to adjust optimal variables set-points.

Numerous modeling and simulation methods have been extensively analyzed in different research activities for HVAC system operation. HVAC modeling related to controls and system

components are currently being researched. However, they lack a user-friendly interface for entering and reviewing data input and output. In 1986, Berkeley Lab researchers began to conceptualize an interface program that would address this very issue and more. The end result of Berkeley's efforts is the Building Design Advisor (BDA), a program that allows for the integrated use of multiple analysis and visualization tools. BDA by itself is not a simulation too. Instead, it provides the interface that makes it easier for designers to use sophisticated modeling tools. Another important development in HVAC modeling is the planned merger of two energy simulation tools: Building Loads Analysis and System Thermodynamics and DOE-2 into a new program known as EnergyPlus (Cook, H., 1998).

2.2 HVAC Design Optimization

Real-time optimization techniques to reduce energy implemented in HVAC system controls while developing and tuning component models is what this research paper is exploring. An on-line, self-tuning, optimization process (OLSTOP) simulation tool is useful for a detailed investigation of existing HVAC systems and applying efficient energy management strategies and controls. HVAC systems are by nature, discrete, non-linear and highly constrained. By linking such a program to an appropriate optimization algorithm (in our research - genetic algorithms, GA) the saving potentials for the overall building energy consumption can be identified. In a study by Fong, Hanby and Chow, a simulation - evolutionary programming (EP) coupling approach which incorporated the component-based simulation and EP optimization was linked for such purpose. From the optimization results, the component-based HVAC model and the EP technique worked well together in providing the optimum combination of the chilled water and supply air temperatures for effective energy management throughout a year (Fong, K. F. et al., 2006). A study by Vakiloroaya, V. et al. (2013) developed a gradient projection-based

optimization-simulation algorithm to find the optimizing set-points of the supply chilled water temperature, refrigerant flow rate and supply air temperature; by applying this approach, an air-cooled central cooling plant HVAC system can achieve significant improvements in energy-efficiency and performance, especially in part-load conditions (Vakiloroaya, V. et al., 2013).

Finding optimal set-points of local-loop controllers has been researched by Ke, Y.-P. et al. (1997). They examined the relation connecting the supply air temperature (T_s) reset controls (SATRC) and the ventilation requirement applying zone reheat to optimize supply air temperature. Their simulation results illustrated that the use of the optimized SATRC saves more energy than a conventional one. Englander, S. L. et al. (1992) minimized the supply duct static pressure (P_s) set-point without sacrificing occupant thermal comfort and continued to maintain adequate ventilation. Braun, J. E. et al. (1989) controlled the chilled water supply temperature (T_w) set-point by optimizing chilled water systems (Nassif, N. et al., 2005). Another study by Preglej, A. et al. (2014) took the approach of a fuzzy model-based multivariable predictive functional control (FMBMPC) of a heating ventilating and air conditioning (HVAC) system. The control law is derived in the state-space domain and is given in an analytical form without an optimization algorithm. The results show that the FMBMPC approach performs well due to the HVACs' nonlinear dynamics. In case of interactions influence rejection by the HVAC system, the FMBMPC algorithm outperforms the classical proportional-integral (PI) approach. The results also show that the proposed approach exhibits better reference-model tracking across a wider operating range (Preglej, A. et al., 2014).

Megri and Yu investigated the possibility of improving the heating energy demand calculation accuracy by the integration of a zonal model into a multi-room thermal model. Comparisons between the predictions of the thermal multi-room model and the integrated zonal

model were performed to demonstrate the importance of considering the room temperature distribution in energy predictions. The objective of their study was to develop a new energy model that takes into account the distribution of the temperature within the room. This model predicts energy based on the new concept of set temperature distribution (STD) (Megri, A. C. et al., 2014a). They also developed a comprehensive heat transfer attic model and integrated it into the building thermal model for the transient-state situation by including thermal capacitances of both indoor air and building envelope. The objective is not only to accurately take into account the characteristics of attics into building simulation programs, but also to study the effects of the attic temperature and ventilation rate on the energy demands and thermal comfort of the building. This model is based on energy conservation equations and uses the analogy between electrical circuits and mechanical systems. The ultimate objective is to improve the prediction of multi-room thermal models by taking into account the heat and mass transfer phenomena within the attic (Megri, A. C. et al., 2014b).

Genetic algorithms (GA) are also explored in simulation-based HVAC system optimization. GAs will be more widely used when there are publicly available and easy-to-use interfaces with energy-simulation codes. It has been necessary to develop a custom interface, to convert the GA's specified value for a given variable to an appropriate input value in the simulation code. An interface is also required to obtain output from the simulation package and form the objective function (Caldas, L. G. et al., 2003).

Kusiak, A. et al. (2010) used a data-driven approach for minimizing air conditioning energy. They implemented eight data-mining algorithms applied to model the nonlinear relationship among energy consumption, control settings (supply air temperature (T_s) and supply air static pressure (P_s)), and a set of uncontrollable parameters. A particle swarm optimization

algorithm was selected to model a chiller, pump, fan, and a reheat device; which were integrated into an energy model optimizing T_s and P_s of an AHU (Kusiak, A. et al., 2010).

A paper by Huh and Brandemuehl describes research into the optimal operation of building heating, ventilation, and air-conditioning (HVAC) systems focusing on both temperature and humidity control. Their analysis is based on a combination of a realistic simulation of a direct expansion (DX) air-conditioning system and a direct-search numerical optimization technique. Building loads were modeled using an extended bin method that allows consideration of the interactions between loads and indoor conditions. Results indicate that minimum energy use typically occurs at low airflow rates, with indoor humidity levels below the upper comfort limit (Huh, J.-H. et al., 2008).

A data-driven approach utilizing predictive models with controllable and uncontrollable I/O variables through a dynamic neural network was investigated by Kusiak and Xu. The minimization of energy was accomplished with a multi-objective particle swarm optimization algorithm model and solved with three variants (Kusiak, A. et al., 2012). Research from Djuric, Novakovic, Holst, and Mitrovic optimizes the insulation thickness of the building envelope, the supply-water temperature, and the heat exchange area of the radiators which influence the energy, investment cost, and the thermal comfort. A combination of the building energy simulation software *EnergyPlus* and the generic optimization program *GenOpt* was used. The thermal comfort was represented by Predicted Percentage of Dissatisfied (PPD) (Djuric, N. et al., 2007).

Regardless of what type of mechanical, electrical, and plumbing (MEP) system exists in a facility, it can be controlled intelligently, effortlessly and more efficiently with a BAS using typical energy management strategies as shown in Table 3. These strategies can be implemented

without a BAS, using thermostats and/or time control time-of-day schedulers, and a bit of common sense. Typically a building's single largest expense is energy costs. Utilizing a BAS, to monitor and manage your building's lighting, HVAC and other systems automatically, and building specific scheduling programs will gain control of energy costs.

Table 3

Typical Energy Management Strategies

Typical Energy Management Strategies	
Time of day scheduling	Chilled/hot water reset
Avoid conservative scheduling	Separate schedules for area or zone usage
Night setback	Zone temperature sensors
Optimal start/stop	Chiller/tower optimization
Implement an energy awareness program	Develop energy competition (NEED)
Economizers	VAV fan pressure optimization
Occupied standby mode	Systems integration
Demand limiting	Demand Control Ventilation (DCV)
Supply air reset	Variable flow pump pressure optimization

Over the last two decades or so, efforts have been undertaken to develop supervisory and optimal control strategies for building HVAC systems thanks to the growing scale of BAS integration and the convenience of collecting large amounts of online operating data by the application of BASs. These energy or cost-efficient control settings are optimized in order to minimize the overall system energy input, or operating cost, without violating the operating constraints of each component and without sacrificing indoor environmental air quality. One of the main achievable goals of the effective use of BASs is to improve the building's energy efficiency, lowering costs, and providing better performance (Wang, S. et al., 2008a).

Energy savings and thermal comfort are important to both facility managers and building occupants. As a result, new innovations in the field are constantly under investigation, including self-tuning or self-learning models. Commercial building HVAC systems consume large quantities of electricity. Therefore it is important for facility managers to take advantage of

lower energy rates. The evolution of design, operation, and maintenance of buildings has changed significantly in the past 20 years since the advancement of controls, simulation and programming software and data driven tools like self-learning models.

2.3 Control Functions

Control functions are the basic functions of BASs. Energy savings can be achieved using several key control strategies while operating a VAV HVAC system. The six key control strategies are:

1. Optimal Start/Stop
2. Fan - Pressure Optimization (P_s)
3. Pump - Pressure Optimization (D_{pw})
4. Supply-Air-Temperature Reset (T_s)
5. Chilled Water Supply Temperature (T_w)
6. Ventilation Optimization (ASHRAE 62.1-2013)

The optimal start strategy utilizes a BAS to calculate the length of time required to bring each zone to its occupied set-point temperature from its current drift temperature. The system will not start until the minimum energy use is achieved while reaching occupied set-point (OSP) temperature just in time for occupancy. The optimal stop strategy is shutting off the system prior to the end of the work day, allowing the temperature to drift from OSP, assuming the building occupants may not mind a few degree changes prior to leaving the building. During optimal stop only cooling and heating are shut-off, the outdoor air supply fan would continue to ventilate the building during occupied hours.

Fan-Pressure Optimization utilizes communicating controllers in a VAV system to optimize the static-pressure control function to minimize duct pressure and save energy. Several benefits are achieved with this strategy:

- Reduced supply fan energy use
- Lower sound levels
- Reduced risk of fan surge
- Flexibility of sensor location (Trane, 2006)

Supply-Air Temperature Reset (SATR) consists of raising the supply-air temperature thus saving compressor and reheat energy. An air-side economizer is beneficial to this strategy because when the outdoor air is cooler than the supply air temperature set-point, the compressors are shut off and the outdoor air dampers modulate to meet the desired supply-air temperature. SATR will reduce energy consumption considering compressor, reheat, fan and humidity levels.

Ventilation Optimization involves resetting intake airflow per occupancy levels. This strategy can be implemented utilizing CO_2 sensors, occupancy sensors, and time-of-day schedules; this is more commonly known as Demand Controlled Ventilation or DCV. Several benefits are achieved with this strategy:

- Assures proper ventilation without requiring a CO_2 sensor in every zone.
- Enables documentation of actual ventilation system performance.
- Uses system-level ventilation reset equations (ASHRAE 62.1-2013).

These strategies implemented for VAV systems will reduce energy consumption in buildings (Murphy, J., 2006).

These control strategies and others are thoroughly described in Murphy's article, Using Time-of-Day Scheduling to Save Energy, published in ASHRAE Journal, May 2009. Murphy

mentions that fresh outdoor air louvers can be shut during unoccupied periods to further save energy. If a manual system is installed or the operations department is hesitant to completely turn-off systems at night, then the systems can at the very minimum be adjusted a few degrees (+/-10^{o}F depending on cooling or heating mode) so the HVAC systems don't work as hard during unoccupied periods (evenings and weekends).

Too many K-12 schools, colleges, and universities have extremely conservative schedules; which means the systems are started too early (6:00am) and stopped too late (6:00pm). Colleges and universities have a bad habit of keeping systems on 24/7 in some buildings on campus. If K-12 students start getting to the classrooms by 7:25am and the majority leave around 2:30pm, then a schedule should mirror the occupancy patterns. Why are we conditioning these spaces in the same manner when the building has 500 fewer occupants? Typically K-12 teachers get to their classrooms between 15 and 30 minutes prior to the children, and leave closer to 5:00pm. The majority of school administration and custodial staff are on similar schedules. The building's HVAC systems could be turned on at 6:30am if the teachers begin their day at 7:00am and turned off at 4:30pm if the teachers tend to leave at 5:00pm. Large spaces in schools like the cafeteria, gymnasium, media center, library, stage and computer labs are perfect opportunities to modify specific mechanical and electrical systems. Several school audits consistently show energy waste in lighting and HVAC systems in hallways, stairwells, restrooms, and other large spaces. The habits do not change whether the audit is performed during the summer months, during the school day, or in the afternoons when the students have left the building. There is a strange habit of leaving cafeteria and gymnasium lights on when they are unoccupied. Several schools leave hallway lights on around the clock. These practices can be costly from an energy perspective, since the entire school may be operating to maintain

occupied temperature set-points, although only a few spaces are occupied (Murphy, J., 2006), such as during the summer months when only the administrative and custodial staff is working. K-12 schools go from hundreds of occupants to under ten during school breaks. Colleges and universities have similar reduced occupancy patterns between semester breaks and holidays.

In a paper by Kusiak, A. et al. (2014), a study to control HVAC systems with a data-driven approach modeled with a NN algorithm is presented. The objective is to minimize energy consumption while maintaining the indoor temperature within a specified range. The Poisson and uniform distributions are applied to simulate the behavior of the occupants impacting the internal heat balance. A nonlinear interior-point algorithm is used to solve the model. The solutions are the set points of the supply air static pressure and the supply air temperature (Kusiak, A. et al., 2014).

Another energy saving strategy is to set the override feature for a 2-hour period of time. If a space or zone needs conditioned air during an unoccupied mode and the override is employed, ensure it is not on indefinitely; therefore, automatically returning the zone to the unoccupied mode after the 2 hour defined time limit. This feature goes hand-in-hand with less conservative time-of-day operating schedules.

Create separate time-of-day operating schedules for areas of the school with significantly different usage patterns. This author has seen a Media Center's schedule that specifies no classes on Mondays and no classes until 8:50 am Tuesday-Friday, with nothing after 2:40 pm. This specific media center is occupied roughly 28 hours per week when school is in session or 17% of the week it needs MEP equipment running. Gymnasiums, cafeterias, and all specials (music, art, etc.) have separate schedules that can save energy. If administration, teachers and custodians

communicate with the operations departments per school in a district, millions of dollars in utility costs can be conserved (Tesiero, R. C. et al., 2014).

Nassif, et al (2013) studied ice thermal storage technology to reduce energy costs by shifting the cooling cost from on-peak to off-peak periods. The paper discusses the application of ice thermal storage and its impact on energy consumption, demand, and total energy cost. Energy simulation software along with a chiller model is used to simulate the energy consumption and demand for an existing building. The study presents a case study to demonstrate through real monthly utility bills the cost saving achieved by the ice storage applications. The results show that although the energy consumption may increase by using ice thermal storage, the energy cost drops significantly, mainly depending on the local utility rate structure (Nassif, N. et al., 2013).

Control functions of BASs can be divided into two categories, local control functions and supervisory control (or energy management) functions. Local control functions are the basic control and automation that allow the building services systems to operate properly and provide adequate services. In the control of HVAC systems, supervisory and optimal control aims at seeking the minimum energy input or operating cost to provide the satisfied indoor comfort and healthy environment, taking into account the dynamic indoor and outdoor conditions as well as the characteristics of HVAC systems (Wang, S. et al., 2008b).

When the whole building is considered, the energy performance is divided into two categories, complicating the analysis and optimization process. Figures 7 - 9 shows the major components of a building's energy consumption. The present study focuses on the HVAC related components since they are usually the most complicated part of building energy analysis (Hui, C. M., 1996).

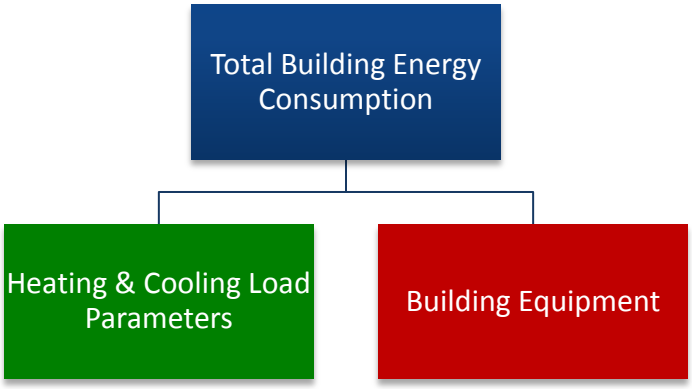

Figure 7. Major components of building energy consumption.

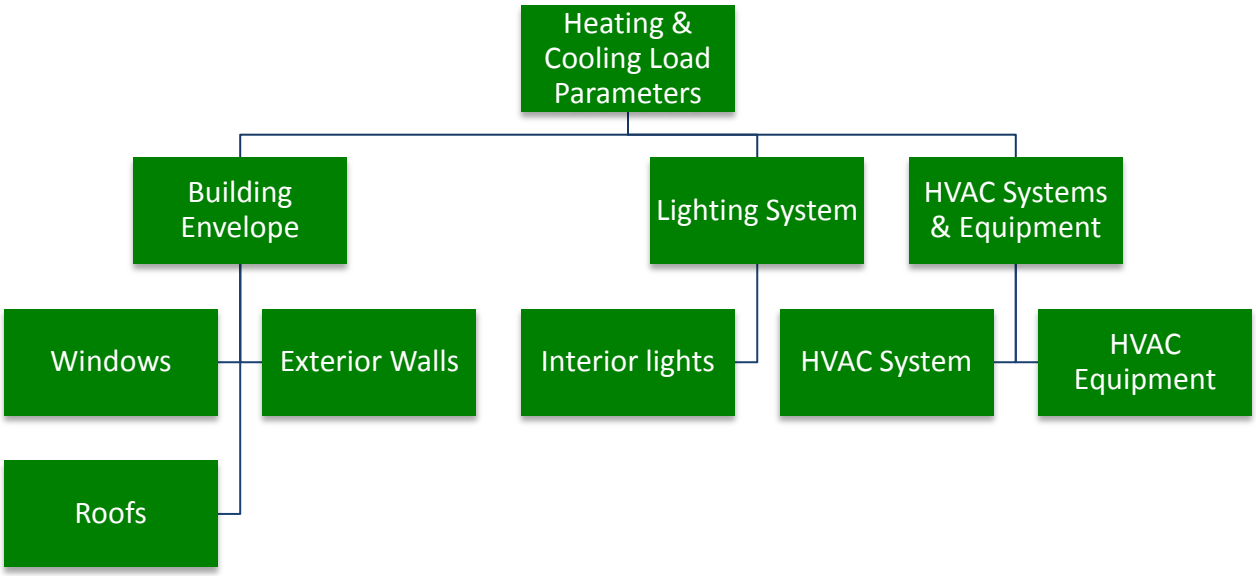

Figure 8. Major components of HVAC load parameters.

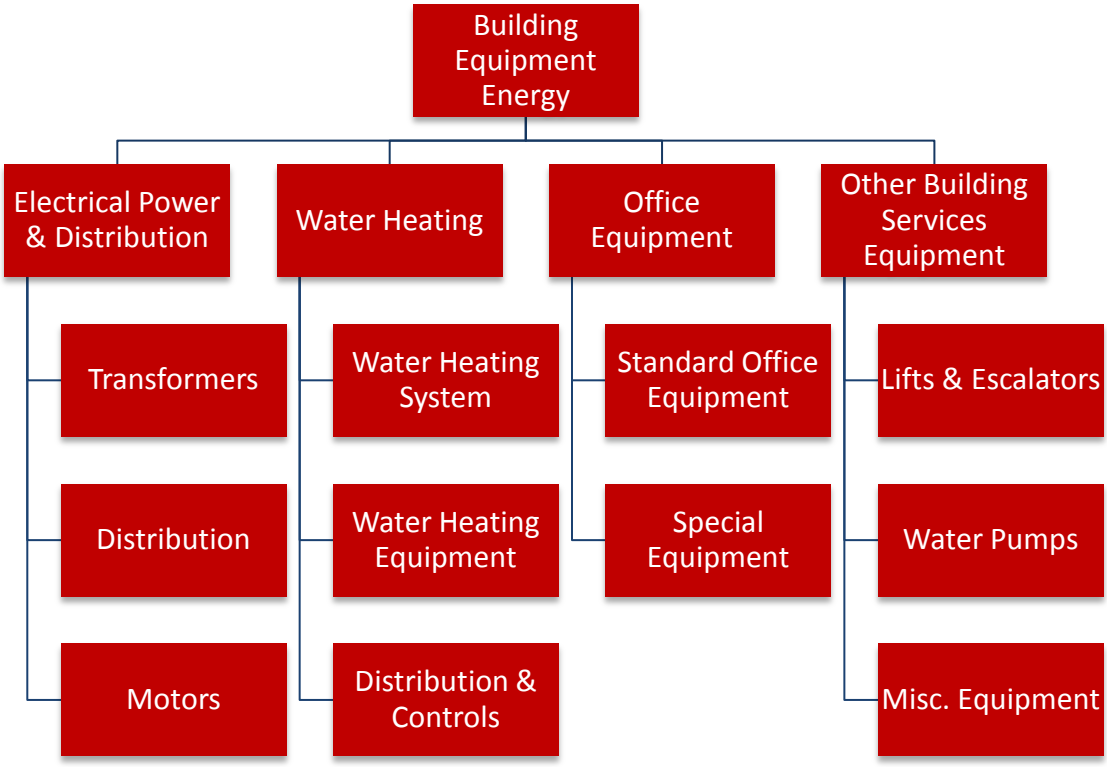

Figure 9. Major components of building equipment.

Energy savings and thermal comfort are important to both facility managers and building occupants. As a result, new innovations in the field are constantly under investigation, including "self-tuning" programming. Building performance can be improved with attention to the relationship between design variables and energy performance (Martin, R. A. et al., 2002). Building performance (see Figure 10) can be divided into three categories:

1. Thermal performance or thermal loads
2. Energy performance or energy-consuming equipment
3. Environmental performance or indoor environmental factors including thermal comfort, lighting, air movement, etc.

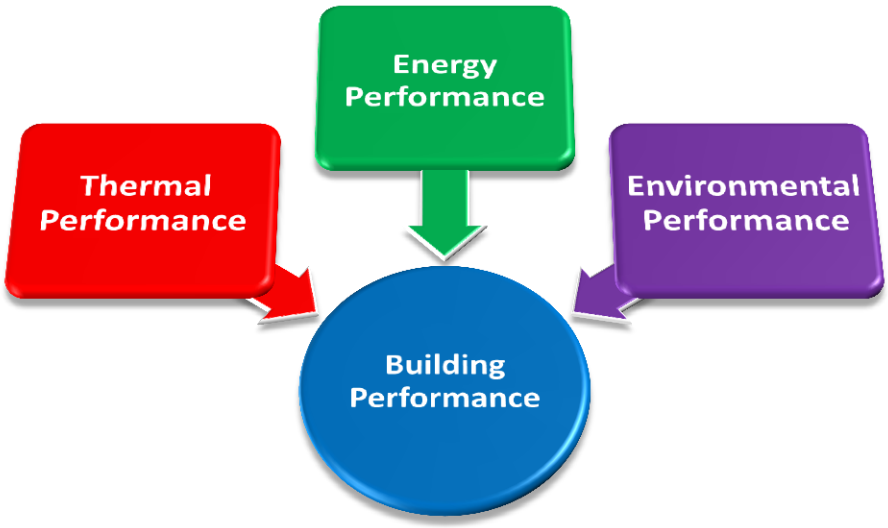

Figure 10. Energy, thermal, and environmental performances of buildings.

Korolija, I. et al. (2011), examine the relationship between building heating and cooling load and subsequent energy consumption with different HVAC systems. The results presented in their paper indicated that it is not possible to form a reliable judgment about building energy performance based only on building heating and cooling loads. Castilla, M. et al. (2011) presents a comparison among several predictive control approaches, that allow a high thermal comfort level optimizing the use of an HVAC system by means of different cost functions. Real results obtained in a solar energy research center were included with the selected strategy of a Model-based Predictive Control (MPC) controller.

Anderson, M. et al. (2007) discusses the construction and modeling of an experimental system for testing advanced HVAC controllers. A simple HVAC system, intended for controlling the temperature and flow rate of the discharge air, was built using standard components. While only a portion of an overall HVAC system, it is representative of a typical hot water to air heating system. In his article, a single integrated environment was created that is

used for data acquisition, controller design, simulation, and closed loop controller implementation and testing.

Nassif, N. (2010) investigated strategies to operate economizer dampers to minimize both the supply and return fan energy use in HVAC systems. Another paper by Nassif, N. and S. Moujaes (2008) proposes a new operating strategy for the outdoor, discharge, and recirculation air dampers of the economizer in VAV system, called split-signal damper control strategy. The strategy controls the outdoor air by only one damper while keeping the remaining two dampers fully open. The discharge or recirculation air damper is modulated to control the amount of outdoor air introduced into the system. The simulation results show annual energy savings in the supply and return fans of an existing system, compared to the traditional strategy of three-coupled modulating dampers.

2.4 Current Self-Learning Research Efforts

The self-learning or self-tuning models (STM) terminology will be used extensively in this report, like artificial neural networks (ANN), they operate without detailed information about the system. They learn the relationships between input and output variables by studying the historical or previous time-step's data. The main advantages of STMs and ANNs are their abilities to map nonlinear functions, to learn and generalize by experience, as well as to handle multivariable problems. Active solutions can provide alternative methods where analyses and optimization become useful for the purpose of energy reductions. Optimal controllers are hailed as the theoretical upper bound (best possible) for achieving their specified objective, minimizing some given cost function by the use of dynamic programming.

Yang's article states that building energy prediction using adaptive ANN models can be achieved with real-time, on-line, incoming data that will have unexpected pattern changes.

Building and facility managers can combine automated energy data collection with a reliable ANN scheme to identify minimum energy consumption strategies and maintenance issues. Utilizing the dynamic, adaptive ANN model that updates real-time data will make short-term energy predictions (Yang, J. et al., 2005).

The self-learning model's capability can approximate the nonlinear relationship between the input and output variables of a complex HVAC system. The objective of this research is to develop an accurate model that predicts the HVAC electrical consumption in order to conserve building energy. Congradac, V. et al. (2009) describe the use of genetic algorithms (GAs) for operating standard HVAC systems in order to optimize performance, primarily with regard to power saving. Genetic algorithms were introduced as an instrument for solving optimization problems. A simulation was conducted in order to demonstrate how much power can be saved by using the suggested method of CO_2 concentration control in a standard HVAC system. This simulation was verified using MATLAB Simulink and EnergyPlus software. Application of values that one obtains by using the genetic algorithm in MATLAB and in EnergyPlus gave expected results in energy and cost savings.

Bichiou, Y. et al. (2011) conducted a comprehensive energy simulation environment which was developed and presented to optimally select both building envelope features and heating and air conditioning system design and operation settings. The simulation environment was able to determine the building design features that minimize the life cycle costs. Three optimization algorithms were considered in the simulation environment including Genetic Algorithm, the Particle Swarm Algorithm and the Sequential Search algorithm. Platt, G. et al. (2010) focused on real-time HVAC zone model fitting and prediction techniques based on physical principles, as well as the use of genetic algorithms for optimization. The proposed

approach was validated by comparing real-time HVAC zone model fitting and prediction against the corresponding experimental measurements. In addition, comparison with prediction results using an algorithm based on feedback-delayed Kalman filters demonstrated the superiority of the proposed approach in terms of prediction accuracy (Platt, G. et al., 2010).

A study by Nassif, N., S. Moujaes, et al. (2008) tuned model parameters online by using a genetic algorithm which minimizes the error between measured and estimated performance data. The validation results show that the component models augmented with an online parameter tuner significantly improved the accuracy of predicted outputs. The use of such models offers several advantages such as designing better real-time control, optimization of overall system performance, and online fault detection. Nassif's article using a two-objective genetic algorithm (2OGA) allowed optimization of the operation of the HVAC systems in buildings. The savings were achieved without jeopardizing thermal comfort and required minimum zone airflow rates (Nassif, N. et al., 2005).

Wang, S. et al. (2000) presented a supervisory control strategy using a system approach for VAV air-conditioning systems in which simplified physical models were utilized to predict the overall system performance, and a GA was used to solve the optimization problem of multiple control variables. The simulation results showed that this online supervisory control strategy can improve the overall system energy and environment performance since it took into consideration the system level characteristics and interactions among the system variables.

2.5 Self-Tuning/Learning Supervisory Control Strategies

Self-learning programs operate without detailed information about the system. STMs learn the relationships between input and output variables by studying the historical data. The main advantages of these models are their abilities to map nonlinear functions, to learn and

generalize by experience, as well as to handle multivariable problems. These desirable properties make the self-learning models feasible for control applications.

Studies using self-tuning-based supervisory control strategies demonstrate that they can play a role in the supervisory control of building HVAC systems. Energy or cost savings are possible when such controllers are used. However, most of these studies were performed from the view point of academic research. Significant control errors might result when the system operates outside the range of training data, and/or the measurement faults, and/or component degradations occur. Moreover, the training of the models always requires extensive computational cost and memory demand, which makes it almost impossible and unacceptable to apply adaptive control in practice to improve the prediction accuracies of these models. The online practical application of such methods needs to be cautious (Wang, S. et al., 2008a).

The objective of a study by Jahedi, G. et al. (2012) was to develop and simulate a wavelet-based artificial neural network (WNN) for self-tuning of a proportional-derivative (PD) controller for a decoupled bi-linear HVAC system with variable air volume and variable water flow responsible for controlling temperature and relative humidity (RH) of a thermal zone, where thermal comfort and energy consumption of the system are evaluated. To achieve the objective, a WNN was used in series with an infinite impulse response (IIR) filter for faster and more accurate identification of system dynamics, as needed for on-line use and off-line batch mode training. The simulation results show that the WNN-IIR controller performance was superior, as compared with classical PD controller (Jahedi, G. et al., 2012).

House, J. M. et al. (1991) and House, J. M. et al. (1995) proposed a system-based optimal control and operation method for optimizing multi-zone building HVAC schemes, recognizing energy use without sacrificing the thermal comfort. Another HVAC system online control

strategy was planned by Zaheer-Uddin, M. et al. (1993) and Zheng, G. R. et al. (1996) in which set-points variables are optimized simultaneously in order to improve the system responses and lower energy. Wang, S. et al. (2000) presented a control methodology operating a system approach centered on calculating the responses of the overall system environment and energy performance to variations in the control settings utilizing a genetic algorithm. The optimal control strategy based on steady-state models of HVAC systems has been researched by Zheng, G. R. et al. (1996). These models are interconnected to simulate the responses of the VAV system. The studies based on system approaches show that an optimal control strategy can improve the system responses and reduce energy use compared to traditional control strategies (Zaheer-Uddin, M. et al., 1993), (MacArthur, J. W. et al., 1993), (Nassif, N. et al., 2005).

2.6 Literature Review Summary

It can be concluded from the literature review that several modeling, optimization, validation and simulation tools and techniques based on various approaches are currently researched and implemented for energy performance analyses of HVAC systems. Existing tools and methods have their own projections and limitations. Self-tuning or self-learning modeling for variable set point optimization is an emerging modeling and simulation tactic. Limited studies have utilized the methodology for HVAC system simulation and variable set point optimization. However, instantaneous self-tuning variable set point optimization of HVAC system configurations has not yet been achieved due to computational power and processor speed. Therefore, it becomes essential to apply the equation-based, self-tuning modeling approach for optimization because it offers significant benefits in terms of system energy performance and can be applied to any building automation system. As computer technology advances, the iteration process to obtain and predict the optimal set-point variables for

reasonable time steps (1 minute to 5 minutes) within an HVAC system configuration will greatly increase the practicality (computer cost including interface) of this theory.

Control strategies and optimization techniques focusing on component modeling are currently researched. Optimization algorithms, utilizing genetic algorithms and artificial neural networks are the most popular. With new emerging technologies in computer advancement, HVAC building automation systems, and building energy simulation tools it becomes important to merge these instruments through smart programming practices to optimize energy savings.

The principal concentration of this research is to develop an efficient methodology for predictive optimal selection of HVAC system's set point variables in both the air and water side while maintaining occupant comfort and incorporating ASHRAE's new ventilation standard 62.1-2013. The exploration to further enhance proven FORTRAN based methods (Psychrometric routines) in ASHRAE's HVAC 2 Toolkit, Algorithms and Subroutines for Secondary HVAC System Energy Calculations, by Michael J. Brandemuehl by modeling system components utilizing the improved self-tuning techniques in MATLAB and programming, exploiting the built-in genetic algorithm syntax, is the essence of this research. This work focuses on the coupling between real-time building system's performance, modeling and simulation, and optimization tools for predictive selection of HVAC system set-point variables, which possess the term "self-tuning modeling" (STM) or "self-learning modeling."

A supervisory controller must be designed to be applicable to a broad spectrum of disturbance patterns, operating conditions, modes, building envelops, and HVAC systems. At the same time it should be structured hierarchically, and use advanced intelligent agent-controller methodology and task coordination. Optimizing processes using on-line (OL) STMs with genetic algorithms require extensive computational cost and memory demand. With the recent

technological advances in computing processing power, sensors, and databases, direct digital control (DDC) automation of these algorithms should become practically feasible (Martin, R. A. et al., 2002).

CHAPTER 3

Methodology

During the simulation and optimization calculations, the mathematical representation of the HVAC system includes all of the individual component models that influence energy use. Component models were developed and validated against measured, monitored, or calculated variables from other proven models. Improved energy efficiencies of existing VAV HVAC systems can be achieved by optimizing the control sequence through the development of OLSTOPs leading to advanced BAS programming. The program's algorithms analyzes multiple variables (humidity, pressure, temperature, CO_2, etc.) simultaneously at key locations throughout the HVAC system (pumps, cooling coil, chiller, fan, etc.) and the program runs simultaneous processes to reach the function's objective which is the lowest energy consumption while maintaining occupancy comfort. The process can be integrated into the EMCS to perform intelligent functions and achieve optimal whole-system performance. The HVAC optimization problems are dynamic, changing over the course of the optimization. The OLSTOP has been developed and utilized with the proper enhancement and the ability to continuously track the movement of the optimum (lowest energy consumption) over time.

Component models are required for the optimization process. For practical purposes simple, accurate, and reliable models will be developed to better match the real behavior of the systems over the entire operating range. We will explore MATLAB's software options to develop functional models that are data-driven and self-tuning for HVAC applications, focusing on energy optimization and control sequencing. The proposed models and the optimization process will be tested and evaluated using data collected from a typical existing HVAC system in the New Academic Building on the campus of NC A&T State University.

3.1 Materials and Methods - System Configuration

The component models, including STMs with the genetic algorithms developed in this research are intended for applications in optimizing control and thus minimizing energy consumption of HVAC systems. When the models are used for constructing an optimal control sequence, the STMs are specified with variable set point parameters specific to the HVAC system. When the OLSTOP is running the model parameters are tuned to improve the model accuracy utilizing the previous time step's conditions (15 minutes). This is done by employing genetic algorithms that optimize the set point variables minimizing component performance errors and total energy. In the prediction mode, the models forecast the optimal performance (minimal energy consumption) during the next time step period (15 minutes). For optimal controller set points, the predicted performance is based on the assumption that the actual thermal and ventilation loads and outdoor air conditions from the previous time step will remain constant. The HVAC system set points such as supply air temperature (T_s), duct static pressures (P_s), chilled water temperature (T_w), and chilled water differential pressure set-point (D_{pw}), including optimal outdoor airflow rate are determined by the optimizer (genetic algorithm-based) and kept constant for the next time step. During a short optimization calculation period (depending on the number of generations and population settings in the GA), the process uses data from the previous time step(s) readings. The operation sequence for the prediction and on-line, self-tuning models' optimal control strategy can be summarized as follows:

- At every predefined time period (daily and adjustable by user), the model parameters will be tuned from the previous data (tuning mode), these updated parameters are then used in the model to forecast the system performance at the next period (prediction mode).

- There are five main controlled variables: supply air temperature T_s, duct static pressure P_s, chilled water temperature T_w, chilled water differential pressure set-point D_{pw}, and zone air temperature T_z (thermal comfort). It also includes the outdoor airflow rate based on ASHRAE Standard 62.1-2013.
- These variables are simulated by the following models: central plant, chiller, cooling coil, fan, HVAC simulation, pump, VAV system, ventilation, and zone model.
- These following programs and subroutines are imposed on the chilled water loop and VAV boxes: System Calculation, constraint, hydronic, and total pressure.

The component models will be developed and validated against the monitored data. The following required variables will be measured:

- Outdoor, mixed, and return air temperatures
- Supply air and water temperatures
- Zone airflow rates
- Supply duct static pressure
- Fan speed
- Fan power
- Cooling coil valve positions
- Fan and outdoor airflow rates
- Inlet and outlet cooling coil relative humidity

Figure 11 shows a flow diagram of the HVAC simulation system with the on-line, self-tuning, optimization process (OLSTOP). Included in this diagram are the proposed STMs and how they interact within the overall system. The EMCS collects the measured data (real data or training data) from components or subsystems. The STMs are continuously trained using the real

data to better match the real behavior of the systems. At each time interval (15 minutes), the OP provides optimal whole system performance by determining optimal set points and operation sequences.

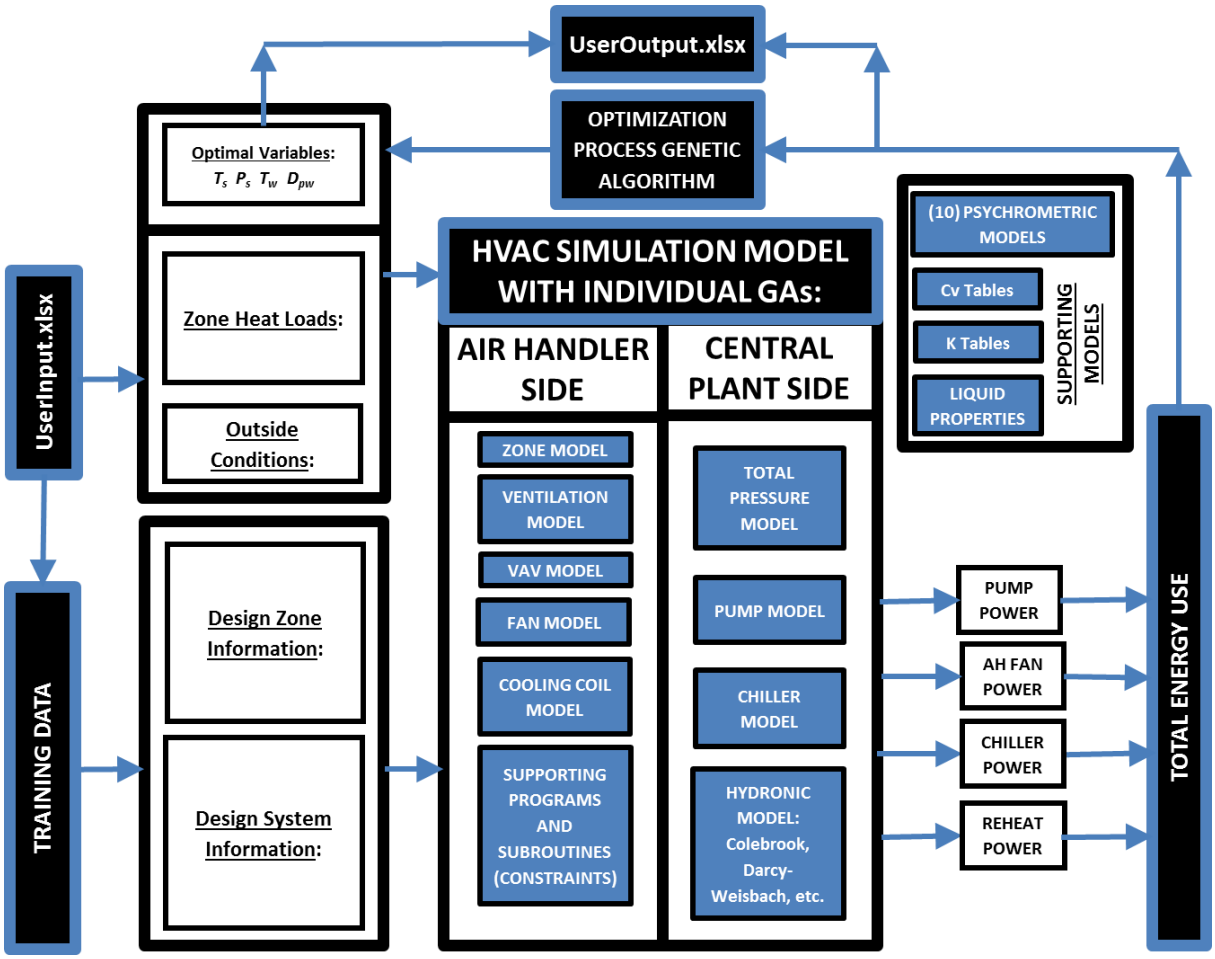

Figure 11. HVAC simulation system OLSTOP.

Psychrometric routines and C_v and *k* tables are included as supporting routines/programs developed in MATLAB. The loss coefficient for valves appears as C_v, a dimensional coefficient expressing the flow through a valve at a specified pressure drop. The C_v values for a variety of valves including check, ball, butterfly, strainer, etc. are found in supporting models. The k-values (geometry- and size-dependent loss coefficient) for steel pipe fittings including elbows

(45^o and 90^o) and tees (straight and branch) are also included. Valves and fittings cause pressure losses greater than those caused by the pipe alone.

In this research, there are many variables measured including the optimal set-point variables: supply air temperature (T_s), duct static pressure (P_s), chilled water supply temperature (T_w), chilled water differential pressure set-point (D_{pw}), and outdoor air flow rate. The objective function is the total energy consumption over the optimization period, determined by the OP incorporating self-learning component models. The HVAC component models and the OP will be developed and theoretically utilized in the energy management control system (EMCS) to perform the advanced and intelligent functions. The energy consuming equipment templates for the dissertation contribution are the fan, pump, cooling coil, and chiller models. Those models can be used for various applications but the inputs and the outputs have to be clearly defined. For the optimization, the model outputs are estimates of the energy consumptions (the objective function) such as fan, pump, and chiller power.

We are attempting to comply with both ASHRAE Standard 62.1-2013 and Standard 90.1. The minimum requirements of ventilation in Standard 62.1-2013, and the energy-limiting requirements of Standard 90.1 using VAV systems are incorporated. In the dynamic reset (DR) section of Standard 62.1-2013, changing conditions in zones allow optimal control sequencing to reset air intake or ventilation requirements based on airflow values (CO_2 monitoring) is incorporated into the logic of the program. Other operational logic is reviewed and programmed, including:

- Demand controlled ventilation (DCV) – resets zone outdoor airflow (V_{oz}) as zone population or effective outside air (OA) per person varies (zone-level control).

- Ventilation reset control (VRC) – resets outdoor air intake flow (V_{ot}) in multiple-zone systems as system ventilation efficiency (E_v) varies (system-level control).
- Ventilation optimization - combines DCV and VRC for multiple-zone VAV systems.

3.1.1 The VAV air handling system. The Variable Air Volume (VAV) device controls the temperature inside a space by modulating, thus regulating the amount of air supplied to a room, space, zone, etc. Typically, a zone is made up of several rooms or areas, and each zone will have its own VAV box, and several zones are connected to an air handling unit. Each zone will be comprised of multiple rooms or spaces. A VAV system, which is the system in the Academic Building at NC A&T State University campus, is analyzed, modeled and simulated. The air handling system, which provides air to the VAV system, is also studied and analyzed. When modeling the different components of the VAV system in eQuest, which is a building energy simulation tool, theoretical models are explored to depict the distinctive properties of the system. The VAV system components explored in this research are programmed in MATLAB utilizing the built-in genetic algorithm tool. The unique models are developed to simulate the VAV system response and calculate the specific performance of the system. All of the models used in this research are derived using English IP (Inch Pound) units. Table 4 shows the typical IP unit abbreviations used in this report.

Table 4

IP Unit Abbreviations

Abbreviation	Definition
BTU	British Thermal Units
CFM	Cubic Feet per Minute
^{o}F	Degrees Fahrenheit
ft	Feet
in	Inches
lb	Pounds
sqft	Square Feet

The primary HVAC system in most buildings is the air handling unit (AHU). This unit, which can be located outside on the ground or roofs, inside on mezzanines, attics, cellars, crawl spaces, or mechanical rooms, is the main system that delivers conditioned air to the entire building. The key responsibility of the air handling unit is to distribute fresh, conditioned air to the building's zones, and exhaust contaminated, carbon dioxide (CO_2) air. The size and configuration of the air handling unit, depends on the heating and cooling loads of the particular zone it controls within a building.

VAV boxes are installed in the building's supply air ducts. Each air handling unit is comprised of outside, relief and mixed air dampers, heating and cooling coils, supply and return air fans, and electronic control hardware that operates the air handling system.

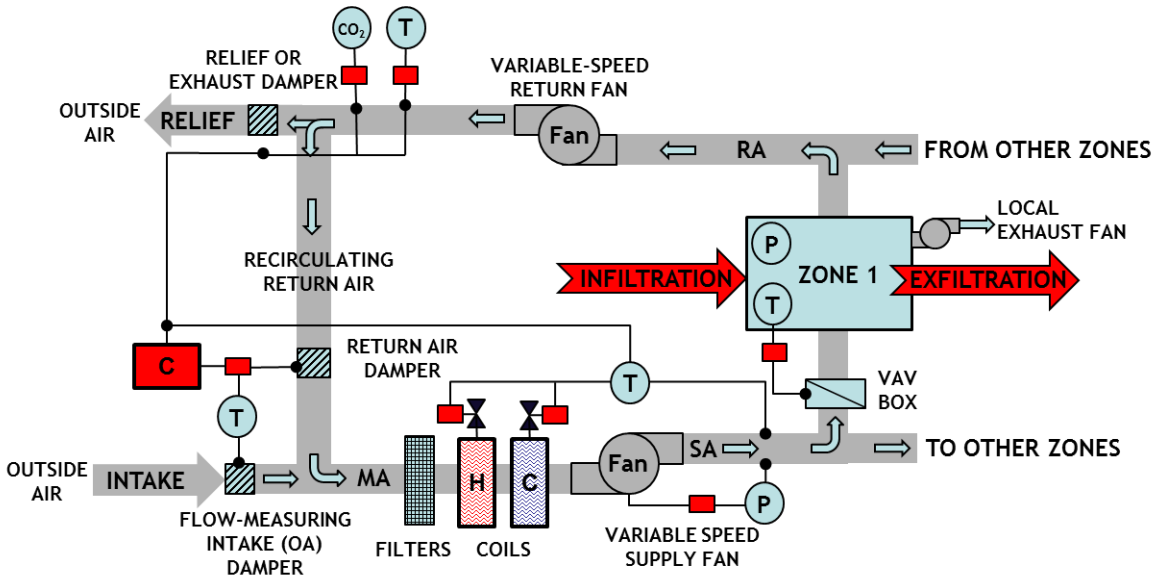

Figure 12. VAV air handling system.

3.1.2 VAV system with return fan with direct control. Figure 12 illustrates a typical VAV system with a local reheat VAV box:

1. A flow sensor monitors intake airflow to maintain the proper volume of outdoor air for ventilation through the fresh air intake damper. The mixed air pressure changes modulating the linked intake and recirculating dampers.
2. A pressure sensor monitors supply-duct static pressure adjusting supply-fan speed accordingly.
3. The room thermostat detects the dry-bulb temperature and controls the supply airflow.
4. Local exhaust fans (in rest rooms, for example) remove some of the air from the occupied spaces. The remaining air either ex-filtrates; or, it returns to the air handler, with infiltrated air.
5. A temperature sensor monitors the return air temperature.
6. The return air either passes through the recirculating damper into the mixed air or exits the building through the relief damper (Trane, 2002).

3.1.3 The VAV system. The indoor air temperature control of a single zone space in air conditioning systems is a practical problem of considerable interest. This problem is also of economic significance, since an improved control strategy can reduce cooling/heating costs without sacrificing the thermal comfort of the occupants (Yamakawa, Y. et al., 2009). In a typical building the cooling mode is usually run throughout the year, independent of the outdoor air temperature. Solar radiation, human occupancy, computers and various office equipment, and lighting and other utility operation generate heat requiring the VAV system to supply cold air to maintain occupant comfort. Following ASHRAE's standards for energy (90.1-2013), thermal environmental conditions for occupancy (55-2013), and ventilation for acceptable indoor air quality (62.1-2013) the operation of the VAV control system is described by the following steps:

1. The temperature in the room is monitored by the VAV controller.
2. If the room is warm or cold, the VAV controller opens or shuts the supply air damper to control the amount of cold air into the room (dual damper setting).
3. If the room is occupied, the VAV supply air damper cannot be fully shut. The VAV controller has to maintain a minimum amount of fresh air as stated in ASHRAE's ventilation standard 62.1-2013.

3.1.4 The conditioned space, area, or room. When the room is occupied ASHRAE's standard 62.1-2013 specifies the minimum ventilation rates and other measures intended to provide indoor air quality that is acceptable to human occupants and that minimizes adverse health effects. The standard has evolved to include three procedures for ventilation design, the Indoor Air Quality Procedure (IAQP), the Ventilation Rate Procedure (VRP), and the Natural Ventilation Procedure (NVP). The VAV controller modulates the damper in the zone supply duct to the room in accordance with room temperature fluctuations to maintain room temperature set-point and ventilation requirements. The mixing of the return air and outdoor air and the exchange of energy between the air volumes follows the laws of thermodynamics; mainly the first law referred to as the law of conservation of energy. The law of conservation of energy states that the total energy of an isolated system cannot change and it is said to be conserved over time. Heat into a space or energy input into the system minus the work output or energy extracted from the system will equal the change in energy or the energy stored in the system, which is the First law of thermodynamics (Conservation of Energy). From ASHRAE's 2013 Fundamentals Handbook the equation describing the first law of thermodynamics is (ASHRAE, 2013):

$$\sum m_{in}\left(u + pv + \frac{V^2}{2} + gz\right)_{in} - \sum m_{out}\left(u + pv + \frac{V^2}{2} + gz\right)_{out} + Q - W$$
$$= \left[m_f\left(u + \frac{V^2}{2} + gz\right)_f - m_i\left(u + \frac{V^2}{2} + gz\right)_i\right]_{system} \quad (3.1)$$

where:

m = mass

g = local acceleration of gravity

z = elevation above horizontal reference plane

p = pressure

v = specific volume

u = internal energy per unit mass

i = initial state

f = final state

V = velocity of a fluid stream crossing the system boundary

Q = heat mechanism that transfers energy from higher temperature to lower temperature

W = work or energy delivered or absorbed by a mechanism

Simplifying the equation yields:

$$Q_{in} - Q_{out} = \frac{d(Q)}{dt} \quad (3.2)$$

where:

Q_{in} = energy entering the room space

Q_{out} = energy leaving the space

$d(Q)/dt$ = rate of change of the stored energy

The energy (Q) of a gas is defined by the following equation:

$$Q = m \times C_p \times (\Delta t) \quad (3.3)$$

where:

m = mass of the gas, m of the gas is also defined as $(V_g \times \rho_g)$

C_p = specific heat constant

Δt = room temperature differential. It is also equal to $d(T_g)/dt$

V_g = volume of the gas

ρ_g = density of the gas

T_g = temperature of the gas

Combining equations yields:

$$(Q_i + Q_e + Q_s) - Q_{out} = (V_r \rho_a) \times C_p \times \frac{d(T_r)}{dt} \tag{3.4}$$

where:

ρ_a = density constant of air

V_r = volume of the room

T_r = temperature of the room

Q_i = energy generated by interior loads, (people, lights, and computers)

Q_e = energy generated by exterior loads, (thermal radiation and outdoor temperatures)

Q_s = energy of the supply air

Simplifying the equations yields:

$$Q_{out} = M \times C_p \times (T_r - T_{alr}) \tag{3.5}$$

$$T_r = T_{alr} \tag{3.6}$$

$$Q_{out} = 0 \tag{3.7}$$

$$Q_s = M \times C_p \times (T_s - T_r) \tag{3.8}$$

$$Q_s = k \times V_{SAF} \times (T_s - T_r) \tag{3.9}$$

where:

V_{SAF} = volume of the air flow supplied into the room

k = a constant1.08 (cfm Btu)/(Hour °F)

T_s = the temperature of supplied air into the room

T_{alr} = the temperature of air leaving the room (or return air temperature)

C_p = 0.241 Btu/(lb °F)

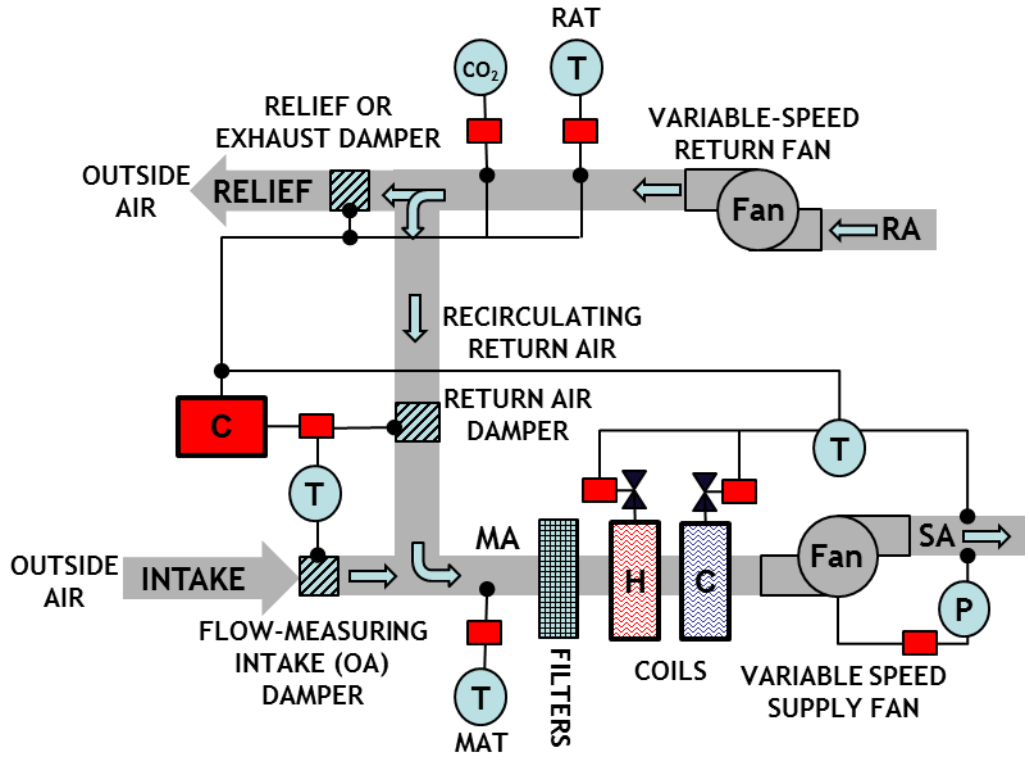

Figure 13. Typical air handling unit (AHU) system showing dampers.

3.1.5 The VAV damper. Automatic dampers are used in air conditioning and ventilation to control airflow. They may be used to modulate control to maintain a controlled variable, such as mixed air temperature or supply air duct static pressure; or for two-position control to initiate operation, such as opening minimum outside air dampers when a fan is started, see Figure 13. Multi-blade dampers are typically available in two arrangements: parallel-blade and opposed-blade, although combinations of the two are manufactured. They are used to control flow

through large openings typical of those in air handlers. Both types are adequate for two-position control (ASHRAE, 2013).

3.1.6 The various sensors. A sensor responds to a change in the controlled variable (flow, temperature, pressure, etc.). The response, which is a change in some physical or electrical property of the primary sensing element, is available for translation or amplification by mechanical or electrical signal. This signal is sent to the controller (ASHRAE, 2013). Temperature-sensing equipment commonly detects variations in a relative dimension (produced by changes in thermal expansion), the state of a liquid or vapor, or certain electrical properties. There are a variety of sensors to measure the temperature in a space, ductwork, surfaces or water. Temperature-sensing technologies commonly installed in HVAC systems are as follows:

- A bimetal element.
- A rod-and-tube element
- A sealed bellows element
- A remote bulb element
- A thermistor
- A resistance temperature device (RTD)

Sensors that measure relative humidity, dew point, or absolute humidity of ambient or moving air are called humidity sensors or hygrometers. There are a number of pressure sensing and fluid flow measuring devices and ventilation or contamination protection equipment available. Lighting and power measuring devices are also available to monitor and save energy.

3.1.7 VAV system simulation and observations. The zone, space, or room model has three main load components:

1. Interior loads

2. Exterior loads
3. Negative loads

The interior loads are created by people, computer equipment, or electrical equipment. The exterior loads are produced by the outdoor climate conditions and negative loads are from the HVAC system controls to maintain set-point temperatures. The VAV system controls the damper position which regulates the amount of conditioned air supplied to the room and the temperature of the room. By generating a negative load from the supply air the VAV system matches all internal and external loads to maintain the room's temperature set-point. The damper position modulates with the differing load patterns of a room throughout the day, this correlation between damper position and load disturbances can be monitored and used to perform energy analysis on a building.

In some cases a VAV damper can be "starved" which means the temperature in the room is above the temperature set-point, the loads are greater than the system's capacity and the damper is fully open at its maximum position (100% open) but there isn't enough air pressure to eliminate the disturbance loads. This occurs more frequently in hot climates and in over-sized and under pressurized VAV systems, see constraint model section 3.3.2.7 for further information on damper starvation.

3.1.8 HVAC system. An air handling unit (AHU) is a device used to circulate conditioned air as part of a heating, ventilating, and air-conditioning (HVAC) system. An air handler usually contains:

- blower or fans (supply and/or return)
- heating and/or cooling elements
- filter racks or chambers

- dampers (outside air, return air, exhaust air)
- temperature sensors (return air, mixed air, supply air)

Air handlers typically connect to a supply air and return air ductwork ventilation system that distributes the conditioned air through the building and returns it to the AHU.

In a chilled-water (CHW) system, the air conditioner cools water to between 40 and 45 degrees Fahrenheit. The chilled water is then piped throughout the building and connected to multiple air handler's cooling coils. The length of the chilled-water piping is not a concern as long as the CHW system is well insulated.

In a building's HVAC system, a chiller is a piece of equipment that removes heat from a liquid through the vapor-compression or absorption refrigeration cycle, see Figures 14 - 15. The vapor compression cycle involves the circulation of refrigerant; during phase changing the refrigerant absorbs heat through evaporation and gives up heat during condensation. The heat that is gained or lost during the phase change is called latent heat of vaporization. Both the vapor absorption and compression refrigeration system have the similar processes of compression, condensation, expansion and evaporation. In the vapor absorption system the refrigerant condenses in the condenser, releasing heat to the atmosphere; and it evaporates in the evaporator, producing a cooling effect. The refrigerant can then be circulated through a heat exchanger to cool the air. From the compressor the refrigerant is a high temperature, high pressure, super-heated gas and is sent to the condenser. The condenser changes the refrigerant to a warm temperature liquid, and sends it to a receiver or the Thermal Expansion Valve (TXV). The TXV measures the appropriate quantity of refrigerant and converts the high pressure warm liquid into a low pressure saturated gas. This saturated gas enters the evaporator where it is converted to a

cool dry gas (no liquid present) and then re-enters the compressor to be heated and pressurized again.

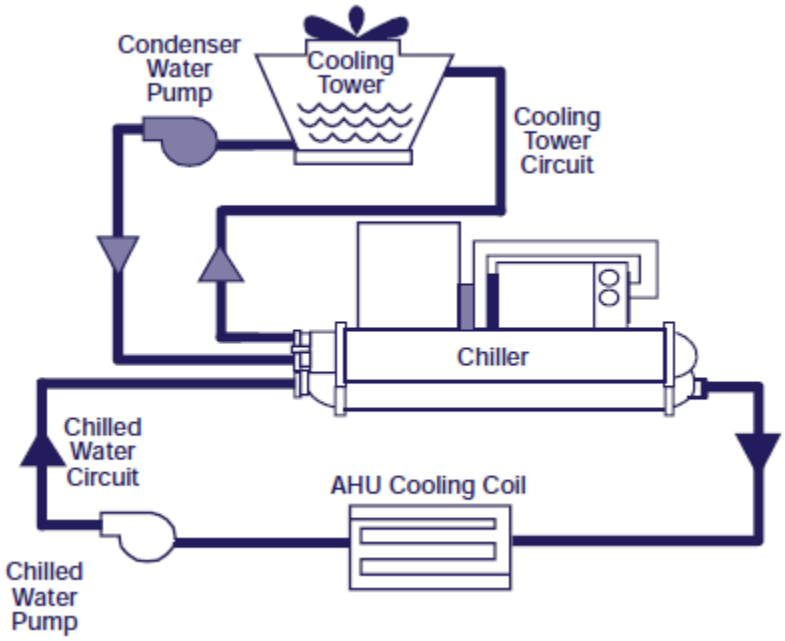

Figure 14. Central plant – chiller piping system.

In the vapor compression system, the compressor pulls the refrigerant from the evaporator and compresses it under high pressure, and the energy input is from an electric motor. In the vapor absorption cycle, the process of suction and compression are carried out by the absorber and the generator, which replace the compressor in the vapor compression cycle, and the energy input is given in the form of the heat. Even though there is a large range in sizes and variety of air conditioning systems used in buildings, most systems utilize the vapor compression cycle to produce the desired cooling and dehumidification. Compared with water-cooled air conditioning systems which cannot work in each climatic condition, air-cooled systems have become more famous due to their ability to work in various weather conditions (Vakiloroaya, V. et al., 2014).

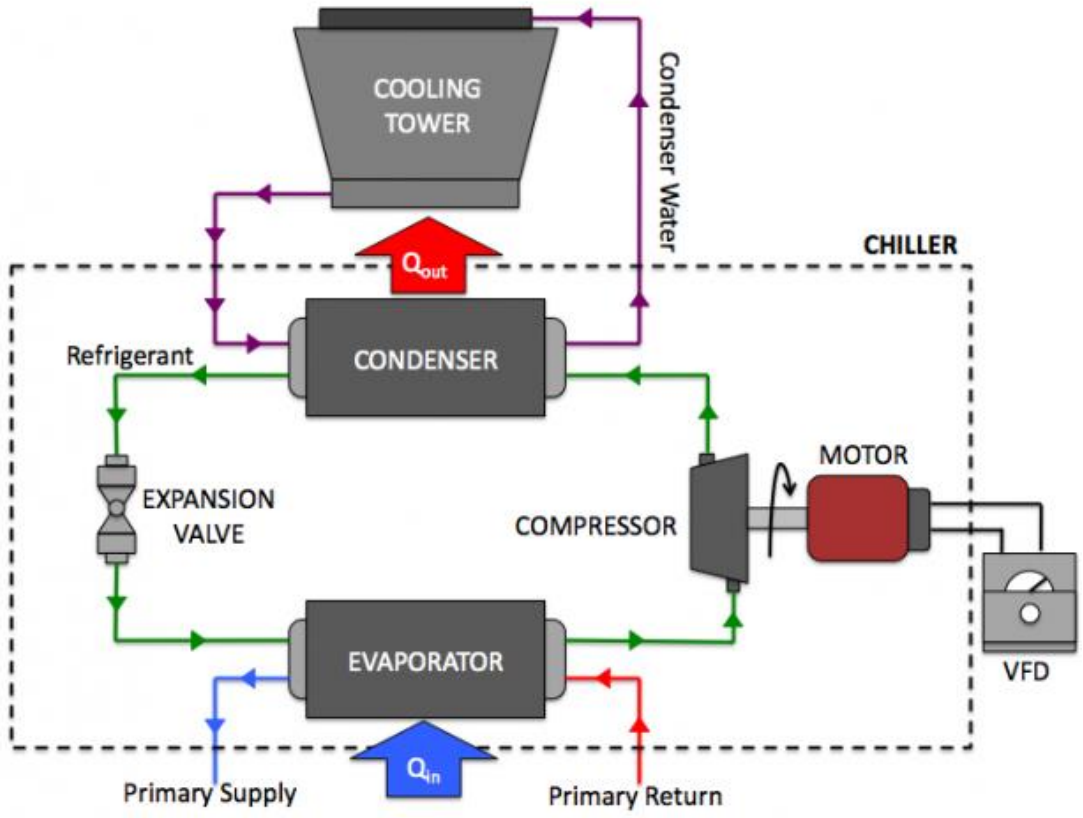

Figure 15. Typical chiller.

In some large HVAC systems, a cooling tower is installed to dissipate heat from the compressor coils. A large fan blows air through a stream of water causing some of the water to evaporate, thus cooling the water and sending it through a heat exchanger to cool the hot condenser coils. In a cooling tower, water has to be added regularly due to the evaporation. The relative humidity and the barometric pressure of the outside air affect the amount of cooling that an air conditioning system receives from a cooling tower.

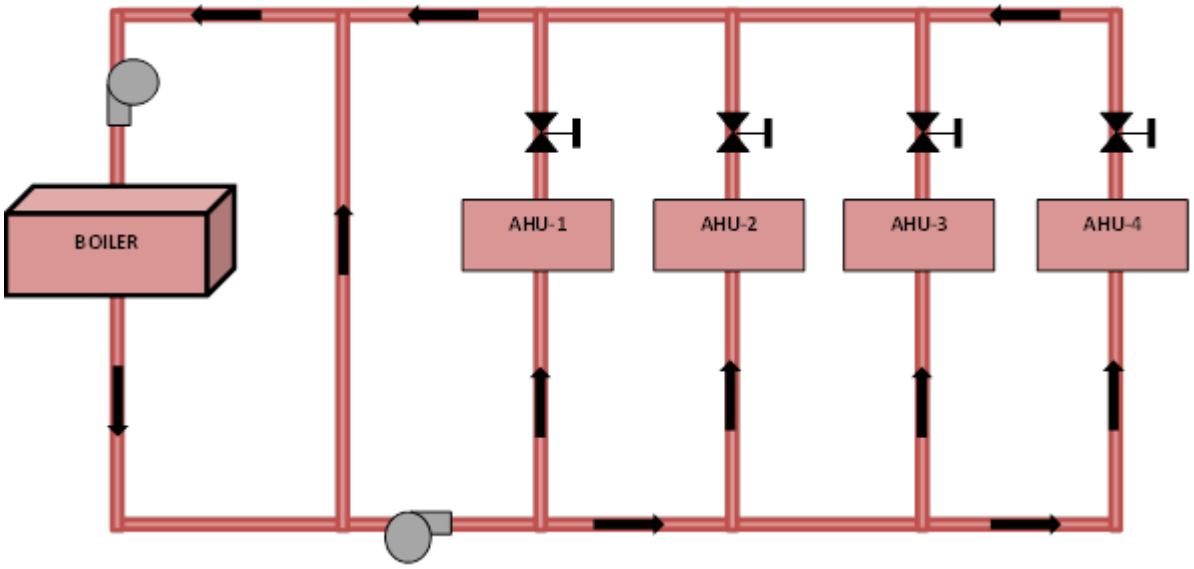

Figure 16. Typical boiler piping system to heating coils in AHUs.

A boiler is a closed vessel in which water or another fluid is heated, typically generating steam, see Figure 16. The heated or vaporized fluid exits the boiler for use in various processes or heating applications. We did not optimize the heating side in this research.

3.2 The Building Automation System (BAS)

North Carolina A&T State University has the building automation system (BAS) BACnet product for building automation control, see Figure 17. BACnet is the term used to refer to ANSI/ASHRAE Standard 135-2008, and is a data communication protocol for building automation and control networks. The BAS monitors and controls buildings with graphical software from any computer terminal that has internet connectivity and allows access to real-time data and energy management features. As-built drawings, floor plans and specific graphics of the HVAC equipment were customized for the Academic Building at NC A&T.

Commercial building automation systems (BASs) continue to evolve from point solutions built from proprietary products toward open and integrated systems based on modern digital information technologies. Integrated by new building management systems (BMSs), the

automation of HVAC, lighting, fire & life safety, and security & access controls is increasingly forming the foundational infrastructure for advanced energy management products and services. The adoption of new embedded computing, communications, sensing, and software technologies is fundamentally changing the underlying products and services within the commercial BAS market, presenting risks and rewards for various industry stakeholders ("Commercial Building Automation Systems," 2013).

Figure 17. NC A&T BAS website.

The building we choose for our research is the Academic Classroom Building; see Figure 18, because it had the HVAC system components we required for analysis. The Academic Classroom Building consists of three floors, six variable air volume (VAV) air handling units (AHU) with variable frequency drive (VFD), a hot water system, cooling tower, and chiller.

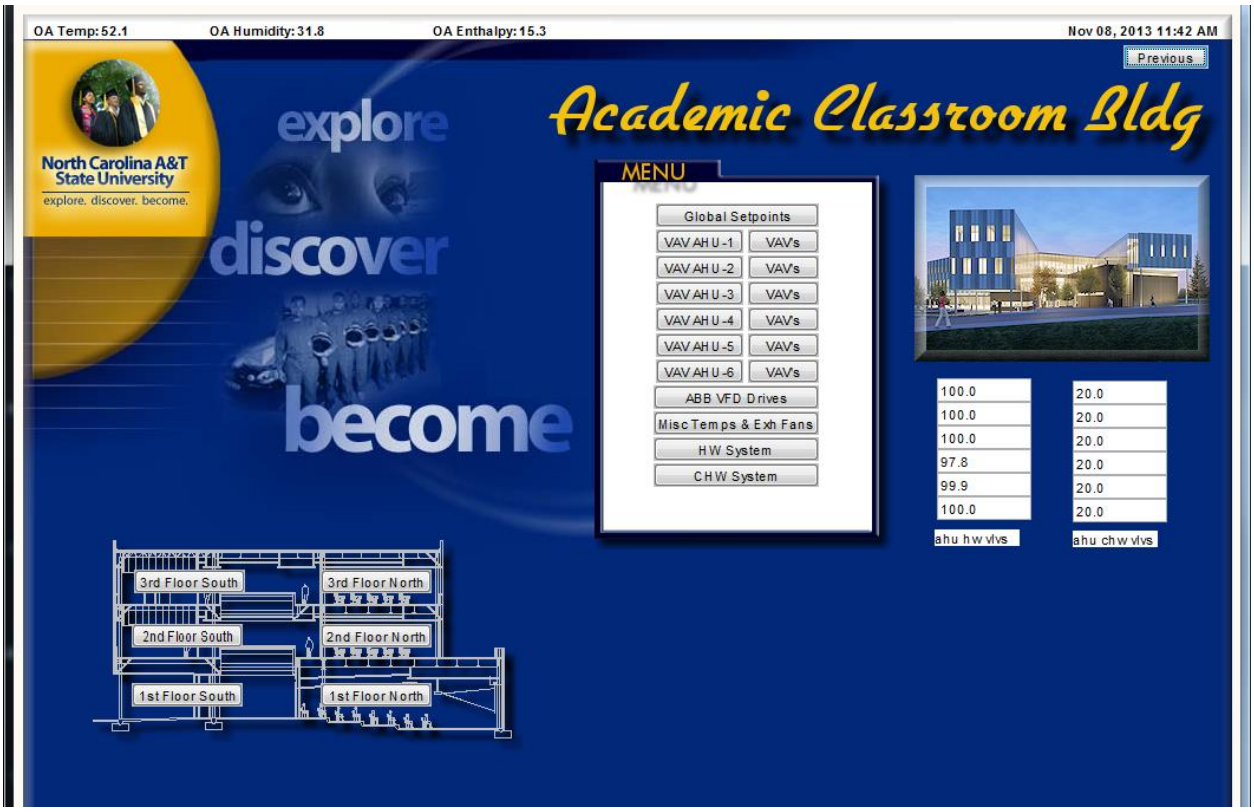

Figure 18. Academic classroom building menu.

The HVAC system configuration for each AHU includes a supply and return fans, relief, return, bypass, and outside air (OA) dampers, heat exchanger coils for preheat and cooling, see Figure 19. In each screen shot OA conditions including outside air temperature (OAT), outside air humidity (OAH), and Date/Time are shown across the top of the frame, and all settings and conditions of each component are also shown in the 3D image of the system.

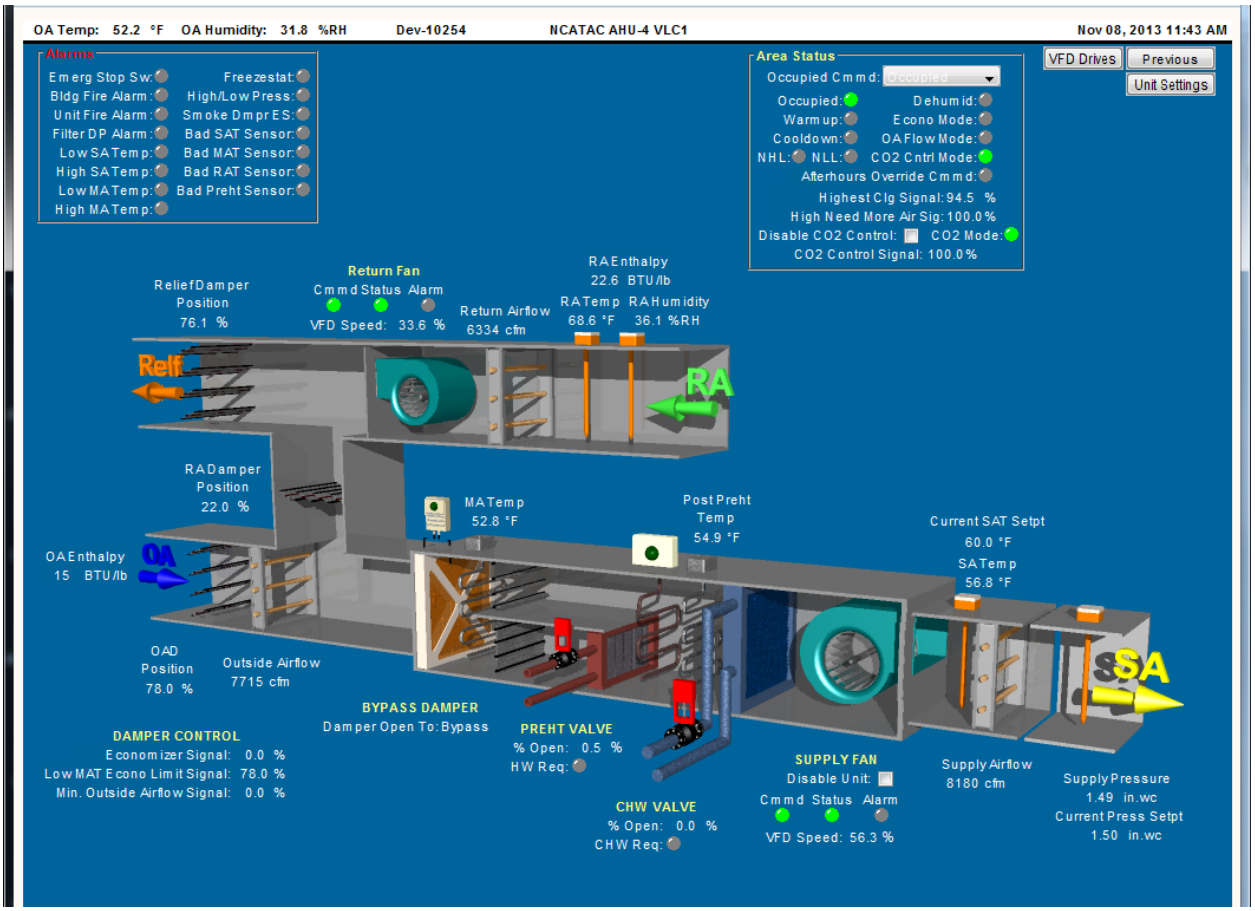

Figure 19. Academic classroom building's air handling unit 4.

The ABB VFD Drive Points, see Figure 20, shows each individual VFD and its corresponding RPM, Output Frequency, AC Output Voltage, Output Current, and Power Output.

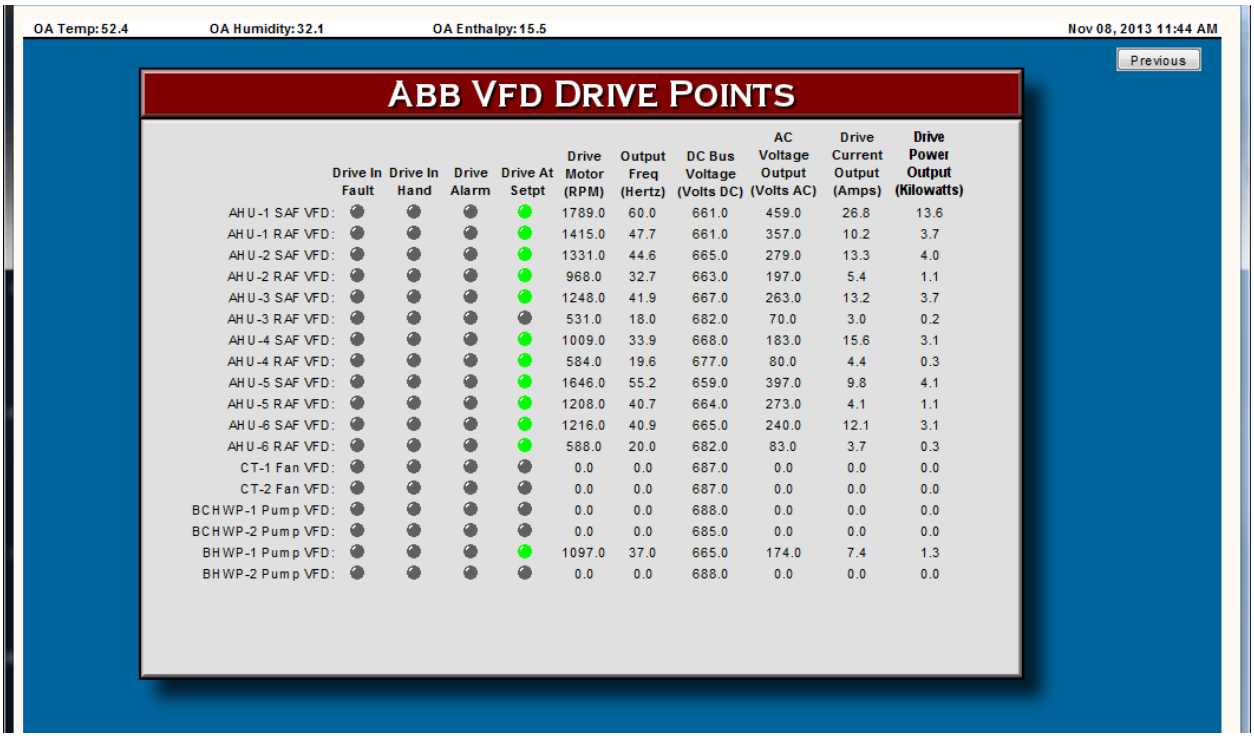

	Drive In Fault	Drive In Hand	Drive Alarm	Drive At Setpt	Drive Motor (RPM)	Output Freq (Hertz)	DC Bus Voltage (Volts DC)	AC Voltage Output (Volts AC)	Drive Current Output (Amps)	Drive Power Output (Kilowatts)
AHU-1 SAF VFD:					1789.0	60.0	661.0	459.0	26.8	13.6
AHU-1 RAF VFD:					1415.0	47.7	661.0	357.0	10.2	3.7
AHU-2 SAF VFD:					1331.0	44.6	665.0	279.0	13.3	4.0
AHU-2 RAF VFD:					968.0	32.7	663.0	197.0	5.4	1.1
AHU-3 SAF VFD:					1248.0	41.9	667.0	263.0	13.2	3.7
AHU-3 RAF VFD:					531.0	18.0	682.0	70.0	3.0	0.2
AHU-4 SAF VFD:					1009.0	33.9	668.0	183.0	15.6	3.1
AHU-4 RAF VFD:					584.0	19.6	677.0	80.0	4.4	0.3
AHU-5 SAF VFD:					1646.0	55.2	659.0	397.0	9.8	4.1
AHU-5 RAF VFD:					1208.0	40.7	664.0	273.0	4.1	1.1
AHU-6 SAF VFD:					1216.0	40.9	665.0	240.0	12.1	3.1
AHU-6 RAF VFD:					588.0	20.0	682.0	83.0	3.7	0.3
CT-1 Fan VFD:					0.0	0.0	687.0	0.0	0.0	0.0
CT-2 Fan VFD:					0.0	0.0	687.0	0.0	0.0	0.0
BCHWP-1 Pump VFD:					0.0	0.0	688.0	0.0	0.0	0.0
BCHWP-2 Pump VFD:					0.0	0.0	685.0	0.0	0.0	0.0
BHWP-1 Pump VFD:					1097.0	37.0	665.0	174.0	7.4	1.3
BHWP-2 Pump VFD:					0.0	0.0	688.0	0.0	0.0	0.0

Figure 20. Variable frequency drive (VFD) points.

The VAV Box Summary screen, see Figure 21, identifies each AHU's multiple VAV box settings including: temperature set-point, space temperature, supply air temperature, heating set-point, cooling set-point, current airflow rate, area status (occupied or unoccupied) and sensor's location and other various details.

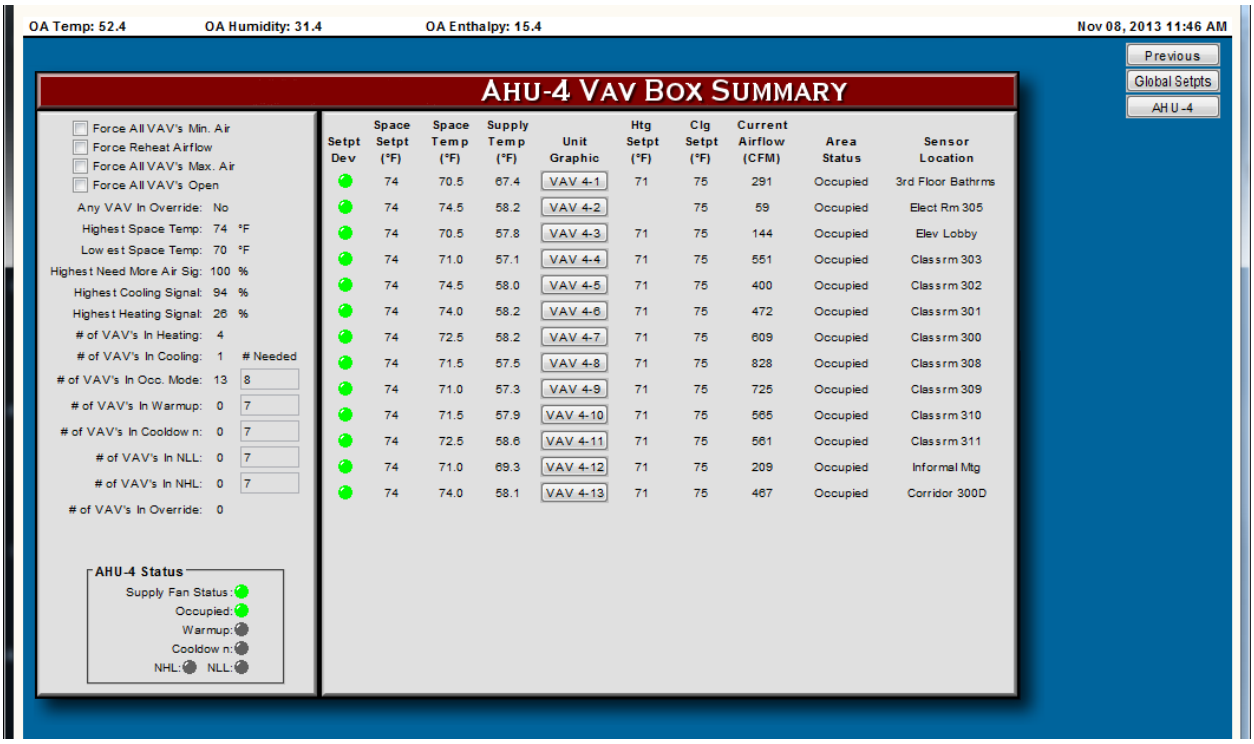

Figure 21. AHU-4 variable-air-volume (VAV) box summary.

Each AHU has a Summary Status and Set-points screen, see Figure 22, which includes information about the specific AHU's status, fans, runtime, sensor readings, alarms, set-points and controls.

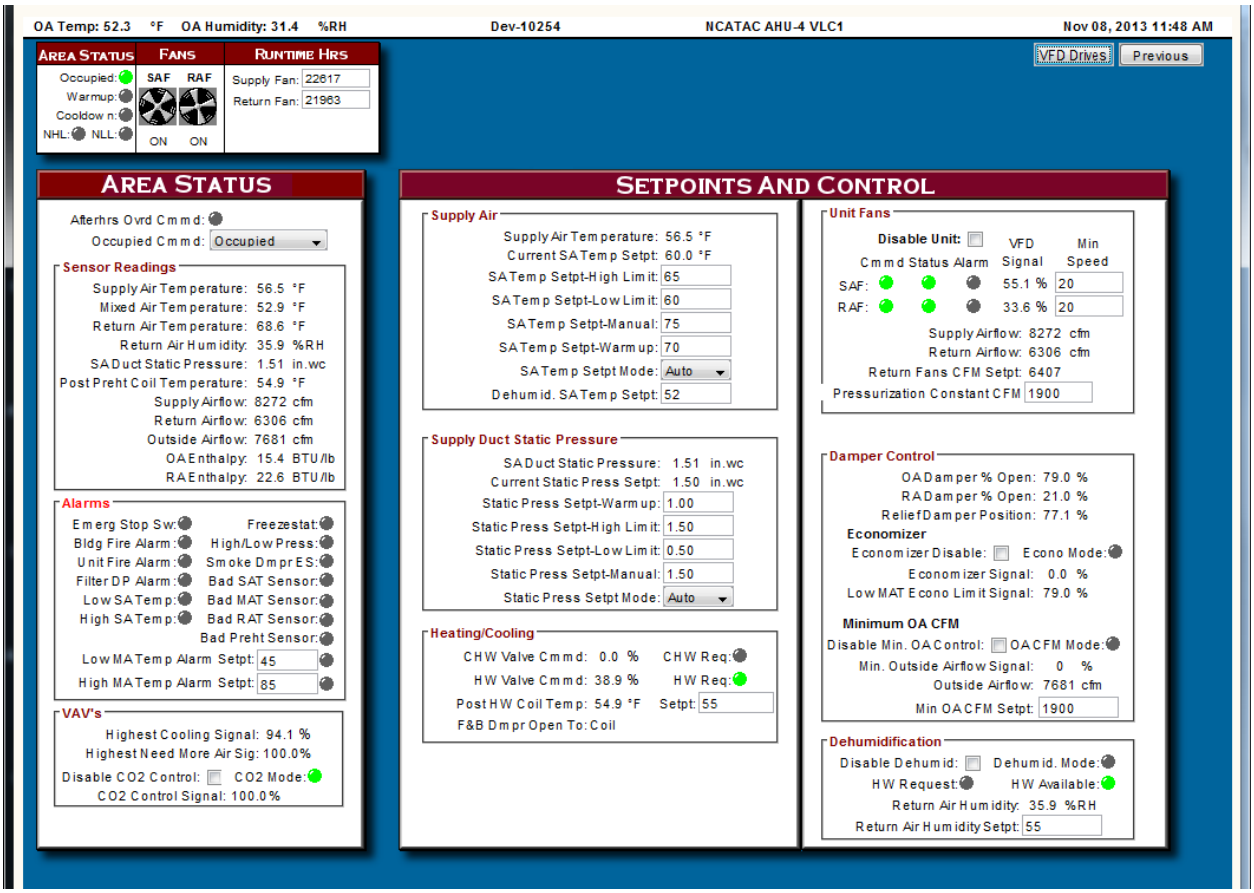

Figure 22. AHU-4 summary status and set-points.

The BAS system also includes layout drawings of the AHU's zones, see Figures 23 and 24. In the layout drawings each VAV box is identified with a green dot and the overall building floor plans are identified.

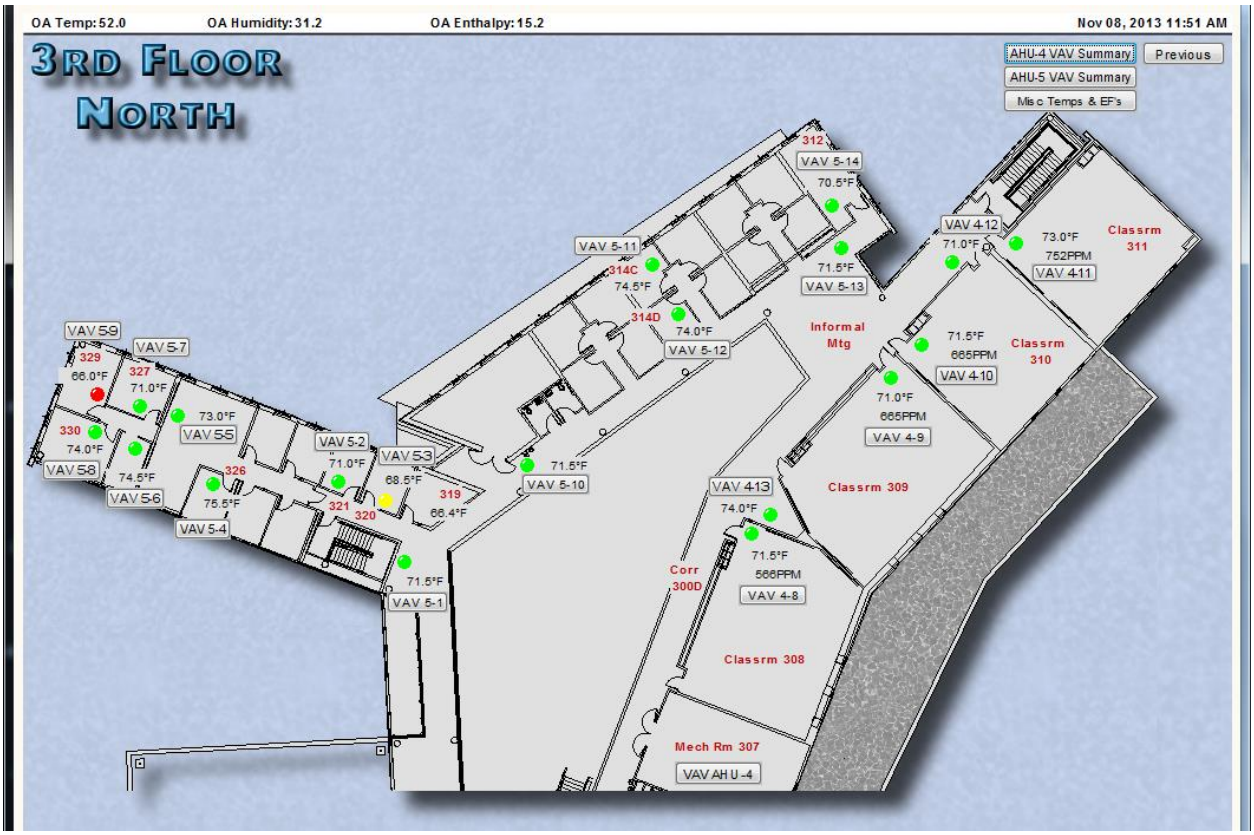

Figure 23. Academic classroom building AHU-4 3rd floor north zone.

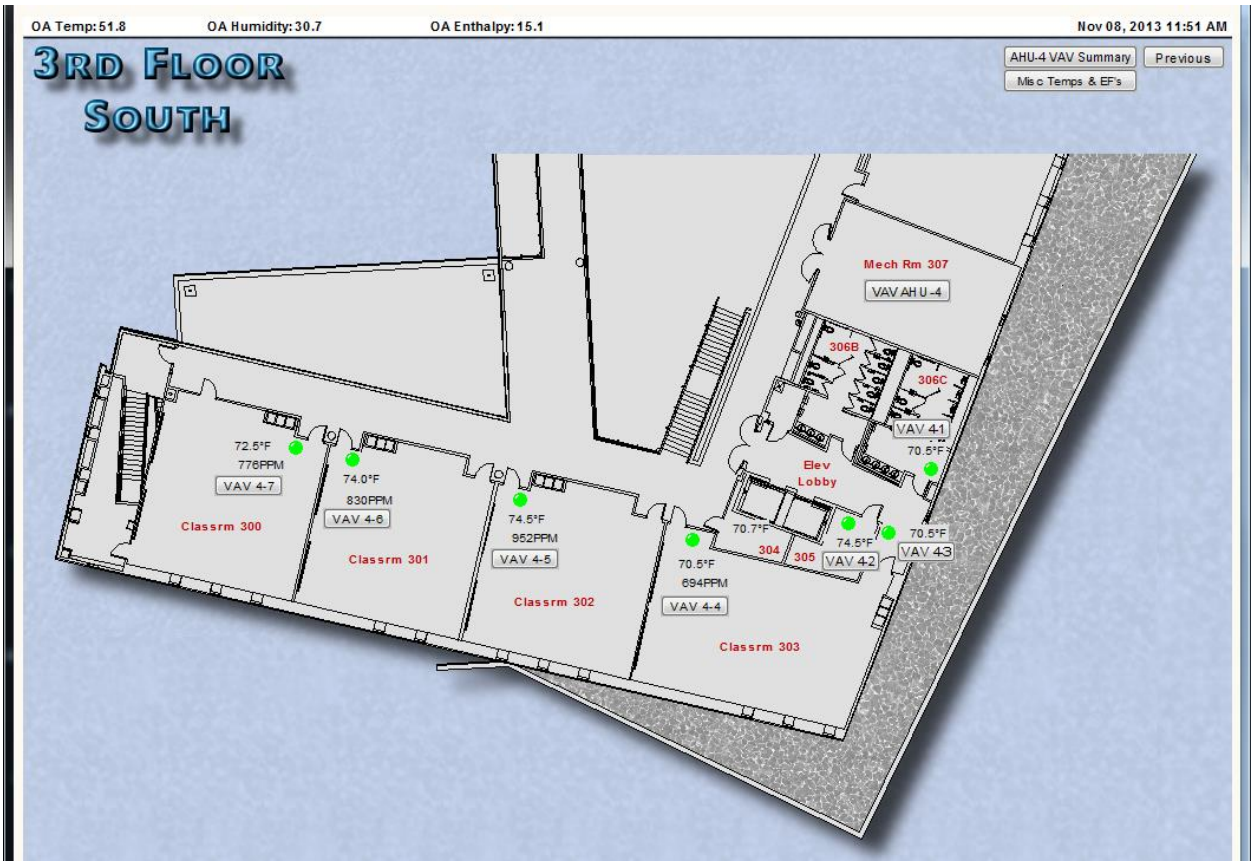

Figure 24. Academic classroom building AHU-4 3rd floor south zone.

The data was trended using the BAS in the Academic Classroom Building on the campus of North Carolina A&T State University. We collected data for our training model every minute for an entire year and are currently monitoring real data. We did not use the whole data for modeling and randomly selected a period of 13 days from September 25, 2013 to October 7, 2013 (17,269 arrays) which included date, time, Building outside air temperature (OAT), OAT at unit, relative humidity at unit (RH), supply air temperature (SAT) and set point, supply air pressure (SAP) and set point, supply air flow (SAF) and fan speed, chilled water valve open position (%), GHRH, chilled water temperature (CHWT), mixed air temperature (MAT), outside air damper position open (%), outside air flow (OAF), outside air enthalpy (OAE), return fan speed, return air flow (RAF), supply air fan power (kW), and return air fan power (kW), the

same data was collected from October 8, 2013 to October 15, 2013 (9,982 arrays) for validation, see Table 5 for a small section of the data and Figures

Table 5

Collected Data from BAS to Microsoft Excel

	Date (D/M/Y)	Time (minute)	Outide Air Temp (OAT) °F	OAT at Unit °F	Relative Humidity (RH) at Unit (%)	Supply Air Temperature (SAT) Set Point (SP)	Supply Air Temperature °F	Supply Air Pressure (in wc)	Supply Air Pressure SP (in wc)	Supply Air Flow (cfm)	Supply Air Speed (%)	Chilled Water Valve Position Open (%)
1	7-Oct-13	9:00:00 PM	67.5	66.2	62.9	60	60.5	1.5	1.5	10164.1	57.4	18
2	7-Oct-13	8:59:00 PM	67.5	66.2	63	60	60.1	1.5	1.5	9438.3	57.3	16.8
3	7-Oct-13	8:58:00 PM	67.5	66.2	63.3	60	59.7	1.5	1.5	9065.5	57.4	16.1
4	7-Oct-13	8:57:00 PM	67.5	66.2	63.3	60	59.2	1.5	1.5	8623.6	57.1	15.7
5	7-Oct-13	8:56:00 PM	67.5	66.2	63.3	60	58.9	1.5	1.5	8249.3	57.2	15.6
6	7-Oct-13	8:55:00 PM	67.6	66.2	63.3	60	59	1.5	1.5	9370	57.3	17
7	7-Oct-13	8:54:00 PM	67.6	66.2	63.3	60	59.5	1.5	1.5	11408.3	57.4	18.5
8	7-Oct-13	8:53:00 PM	67.6	66.2	63.3	60	60.2	1.5	1.5	8256	57.4	20.3
9	7-Oct-13	8:52:00 PM	67.6	66.2	63.3	60	60.5	1.5	1.5	12191.7	57.4	20.6
10	7-Oct-13	8:51:00 PM	67.7	66.2	63.3	60	60.6	1.5	1.5	8853.3	57.4	20.3
11	7-Oct-13	8:50:00 PM	67.7	66.2	63.3	60	60.5	1.5	1.5	11743.6	57.4	19.5
12	7-Oct-13	8:49:00 PM	67.7	66.2	64.2	60	60.3	1.5	1.5	10008.2	57.4	18.7
13	7-Oct-13	8:48:00 PM	67.8	66.2	65.3	60	59.9	1.5	1.5	9229	57.3	17.7
14	7-Oct-13	8:47:00 PM	67.8	66.2	64.1	60	59.4	1.5	1.5	10910.4	57.1	17.2
15	7-Oct-13	8:46:00 PM	67.7	66.3	64.1	60	58.9	1.5	1.5	11366	57.2	16.8
16	7-Oct-13	8:45:00 PM	67.9	66.2	64.7	60	58.7	1.5	1.5	8576.3	57.2	17.2
17	7-Oct-13	8:44:00 PM	67.9	66.2	64.9	60	58.8	1.5	1.5	10028.1	57.2	18.6
18	7-Oct-13	8:43:00 PM	67.9	66.3	65.3	60	59.4	1.5	1.5	8128.4	57.2	20.7
19	7-Oct-13	8:42:00 PM	67.9	66.3	65.8	60	60	1.5	1.5	8058.8	57.3	22.3
20	7-Oct-13	8:41:00 PM	67.9	66.4	65.7	60	60.5	1.5	1.5	8920.1	57.3	23.1

	Date (D/M/Y)	Time (minute)	GH Relative Humidity (%)	Chilled Water Temperature °F	Mixed Air Temperature °F	Outside Air Damper Position Open (%)	Outside Air Flow (cfm)	Outside Air Enthalpy (Btu/lb)	Return Fan Speed (%)	Return Air Flow (cfm)	Supply Fan Power (kW)	Return Fan Power (kW)
1	7-Oct-13	9:00:00 PM	91.8	52.8	65	100	8054.3	25.3	27.6	10027.5	3.2	0.3
2	7-Oct-13	8:59:00 PM	91.9	52	65	100	8108.7	25.3	33.5	6256.9	3.2	0.3
3	7-Oct-13	8:58:00 PM	92	50.9	64.9	100	7813.3	25.3	28.9	8783.7	3.2	0.4
4	7-Oct-13	8:57:00 PM	92	50.4	65	100	8091.2	25.3	30.2	8506.4	3.1	0.3
5	7-Oct-13	8:56:00 PM	92.1	51.2	64.9	100	8153.6	25.3	24.4	5982.9	3.2	0.3
6	7-Oct-13	8:55:00 PM	92.2	52.5	64.9	100	8014.9	25.3	23.1	8914.4	3.2	0.3
7	7-Oct-13	8:54:00 PM	92.2	53.6	64.9	100	8144.3	25.3	21.3	10140.1	3.1	0.3
8	7-Oct-13	8:53:00 PM	92.2	54	64.9	100	8019.8	25.3	20	10624.4	3.1	0.3
9	7-Oct-13	8:52:00 PM	92.3	54.1	64.9	100	8202.7	25.3	22.5	5723.4	3.2	0.3
10	7-Oct-13	8:51:00 PM	92.3	53.7	64.8	100	8430.3	25.3	20	7373.1	3.2	0.3
11	7-Oct-13	8:50:00 PM	92.3	53.2	64.9	100	8091.4	25.4	20	5654.8	3.3	0.3
12	7-Oct-13	8:49:00 PM	92.3	52.5	64.9	100	8157	25.6	21.4	5893.3	3.1	0.3
13	7-Oct-13	8:48:00 PM	92.3	51.5	64.9	100	8079.8	25.6	26.2	5673.6	3.2	0.3
14	7-Oct-13	8:47:00 PM	92.4	50.4	64.9	100	8123.8	25.4	31.4	8871.8	3.1	0.3
15	7-Oct-13	8:46:00 PM	92.5	50.5	64.9	100	8080.9	25.5	33.5	6416.6	3.1	0.3
16	7-Oct-13	8:45:00 PM	92.5	52	65	100	8046	25.6	29.7	7755.1	3.2	0.3
17	7-Oct-13	8:44:00 PM	92.5	53.2	65	100	8216.9	25.6	26.4	9450.1	3.1	0.3
18	7-Oct-13	8:43:00 PM	92.6	54	65	100	8074	25.7	29.1	9213.9	3.2	0.3
19	7-Oct-13	8:42:00 PM	92.6	54.4	65	100	8148.3	25.7	31.6	7379.9	3.2	0.3
20	7-Oct-13	8:41:00 PM	92.7	54.2	65	100	8173.5	25.8	29.5	6056.8	3.1	0.3

Notice in table, which is a small section of the real building data that the system is in fixed or over-ride mode (FOM) as shown by the supply air temperature (SAT) set point (SP) is fixed at a constant 60°F and the supply air pressure set point is fixed at 1.5 in w.c. See Figures 25 and 26 for graphs representing the chilled water temperature and SAT over time and the supply and return fan power over time respectively. Also note the outside air damper position is fully open at 100% and the outside air temperature is between 67°F - 68°F.

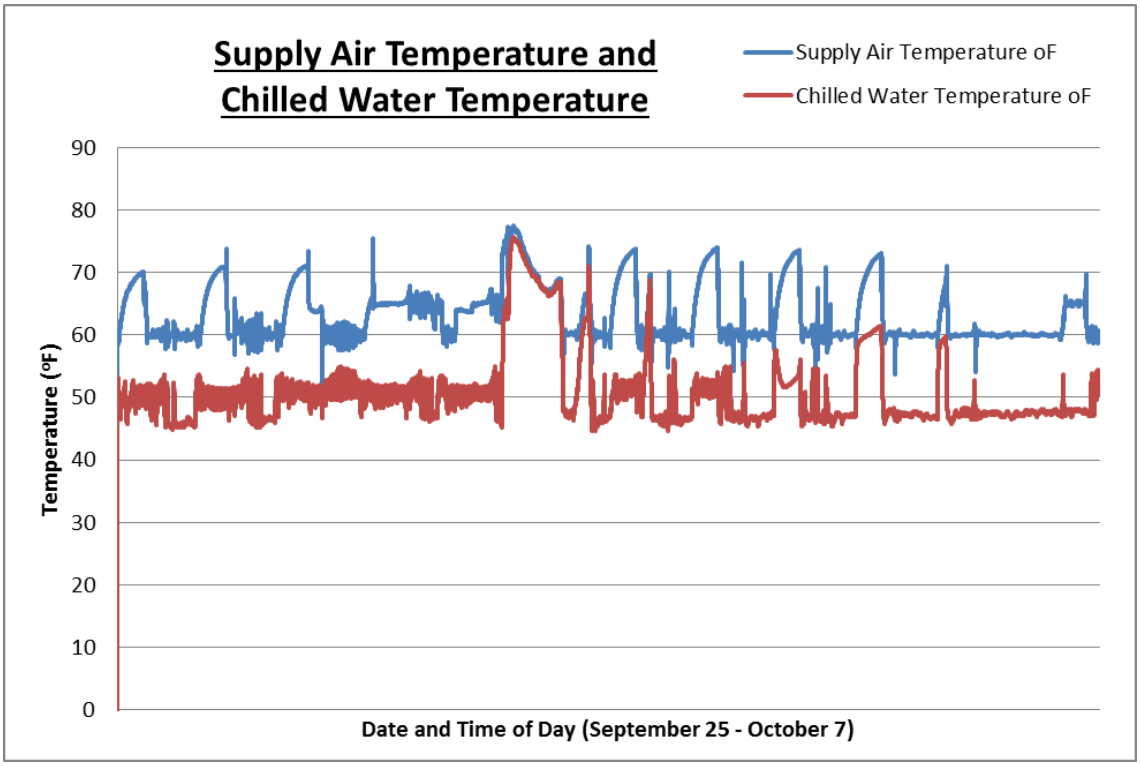

Figure 25. Real BAS data SAT and CHWT over time.

As shown in Figures 24 & 25 which are graphs of the real data from the BAS of the New Academic Classroom Building at NC A&T State University, the chiller had a problem and shut off causing the T_s and T_w to increase for a long period of time, which in turn caused both the return and supply fans to try to make-up the zone or thermal comfort temperature and the fan power spiked.

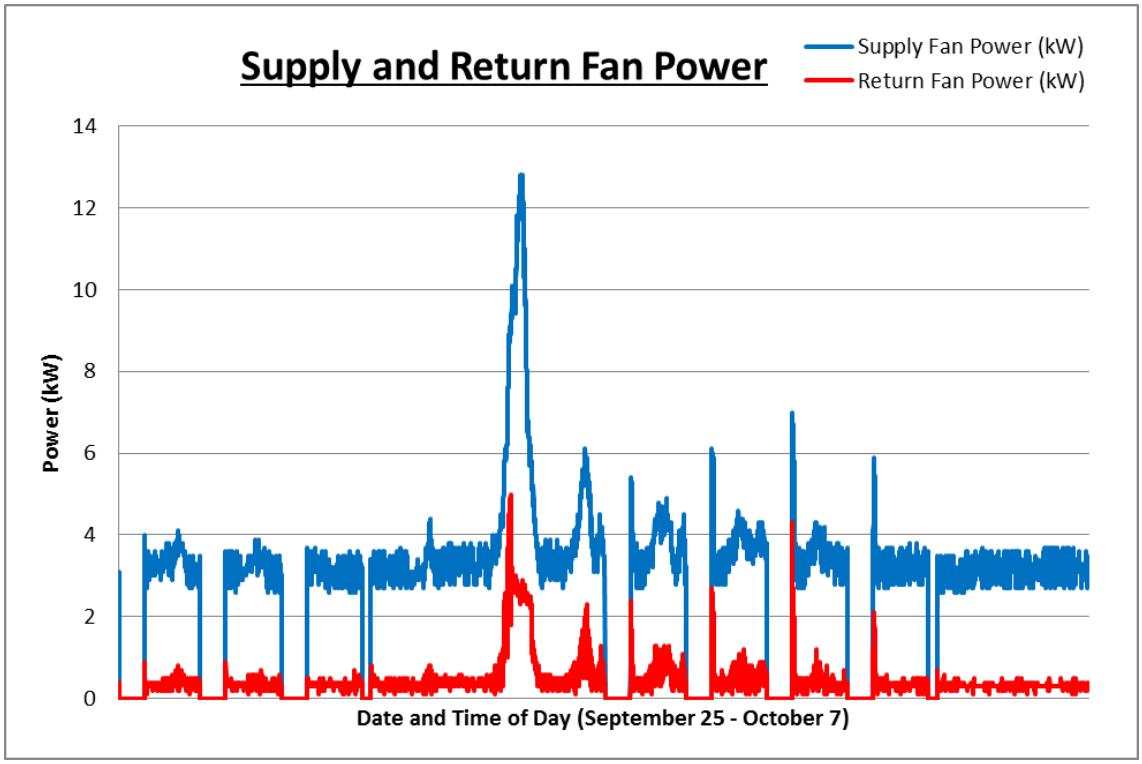

Figure 26. Real BAS data SA and RA fan power over time.

3.2.1 Tool for simulation and analysis. In this research we utilized MATLAB to simulate the dynamic behavior and modeled the individual components of the HVAC system using a choice of mathematical integration and GA methods. Utilizing a genetic algorithm we then used the command line for running a batch of simulations. We were able to see the simulation results while the simulation runs. We then changed parameters to see what happens for further exploration. The simulation results were entered into a user interface in the MATLAB workspace for post processing and visualization, which we then copied to a spreadsheet for further analysis. Model analysis tools include linearization, iterative exploration, optimization numerical integration, built-in graphics for visualizing data and custom plots and building applications with custom graphical interfaces. This research collected real data from the building automation system, then we simulated the building using eQuest to test the optimization process

and then we ran the MATLAB simulation with the real data to collect the results for optimization and energy savings.

3.2.2 Interaction with MATLAB environment. The BAS for the Academic Classroom Building on the campus of North Carolina A&T State University was investigated and analyzed; using MATLAB software the system was modeled. Using the training data from the BAS, optimal variables, loads, outside air conditions, design zone conditions, and design system information were then developed and entered as input to the HVAC Simulation Model. Each component model was then developed to generate individual power output readings that could then be summed for the total power function of the HVAC system.

The Optimal Variables include: supply air temperature (T_s), duct static pressure (P_s), chilled water temperature (T_w), and the chilled water differential pressure set-point (D_{pw}). The Loads include three: total, sensible, and latent loads in kBTU per zone. The Outside Air Conditions include, *DBT*, *WBT*, *RH*, and W_o. The Design Zone Information includes: temperature, airflow rate per person (R_p) and per unit area (R_a), area, and number of people. The System Design Information includes: efficiency, fluid capacity rate (*C)*, and standard differential pressure (P_{sd}), chiller size (tons), pipe roughness (e), number of tees, elbows, valves, pipe diameter, etc..

The HVAC Simulation Model was developed to optimize the input variables utilizing the genetic algorithm to minimize total system energy while computing or running the VAV System Model inside the program, which had the output variables: Fan Power, Reheat, and Power Penalty. The VAV System Model, Optimal Variables and Design System Information were linked to the Central Plant Model as input, and the Chiller Power, Pump Power, and Fan Power

were the output. The genetic algorithm utilizes an iterative process that calculates the optimal variables to minimize the HVAC system's energy.

The VAV System Model includes: Variable Definitions, Zone Model, Ventilation Model, Pressure and Fan Model, Constraint Model, and Cooling Coil Model. The Variable Definition is a set of variables identified by name: Supply Air Temperature (T_s), Duct Static Pressure (P_s), chilled water temperature (T_w), and the chilled water differential pressure set-point (D_{pw}). The Zone Model calculates Q_z, Q_{sys}, Reheat_z, and Reheat, with input variables T_s, Load, and Design Zone.

3.2.3 Component models. The model development is necessary for the study of the energy consumption of HVAC systems. Models are also required to simulate the different supervisory and local loop control strategies to improve the energy consumption efficiency. HVAC systems have complex structures consisting of heat and mass transfer equipment such as chiller, boiler, heating/cooling coils, and supply air ducts. HVAC systems also consist of several sensors and controllers for regulating the controllable variables such as zone temperature, supply air temperature, supply air fan speed, duct static pressure, and chilled water temperature at their set-points. To predict the energy consumption by the HVAC systems accurately, one needs to model the individual components either from the measured data or based on the knowledge of the underlying physical phenomenon (Afram, A. et al., 2014). Developing the process for the optimization of the supervisory control strategy in an existing HVAC system requires the use of component models (Nassif, N. et al., 2005). The process required in optimizing the supervisory control strategy includes (see Figure 26 for OP flow chart):

- the models (components, psychrometrics, control functions, etc.)
- the optimization programs (energy and component accuracy)

- data acquisition (BAS and system data entry for program)
- indoor load prediction (BAS and simulation)
- software tools (MATLAB, BAS, MS Excel)

The VAV model consists of the fan, the damper, the cooling coils, the chiller, etc. At each optimization period the optimization program (OP) will send the trial controller set points to the VAV system model (component models), where the energy use and thermal comfort (objective function) will be simulated and then returned to the OP, see Table 6.

Table 6

Component Models

Component Models	Objective Function	Independent Variables	Dependent Variables
VAV Model	Energy use and thermal comfort	Outdoor air temperature, indoor sensible loads	Controller set points
Fan Model	Fan power	System airflow rate, static pressure	Controller set points
Pump Model	Pump power	System fluid flow rate, pressure drop	Controller set points
Ventilation Model	Outdoor air flow rate	Outdoor damper position, static pressure	Controller set points
Cooling Coil Model	Cooling load	Fan airflow rate, entering liquid temperature, entering air DBT, humidity ratio, leaving air DBT	Controller set points
Chiller Model	Compressor power	Cooling Coil Load, chilled water supply temperature	Controller set points

The HVAC chiller and cooling coil component models include a genetic algorithm and the fan and pump models utilize an iterative process to inhibit the “self-learning” capability that was developed and utilized in the STM to perform the advanced and intelligent functions. The models can be used for various applications but the inputs and the outputs have to be clearly defined. For the optimization, the model outputs are estimates of the energy consumptions (the objective function) such as fan, pump, and chiller power. The models will be validated and tested for both cases. Additional System Calculations are also required for the optimization.

The zone model is to establish zone airflow rates, local energy use, and return air conditions based on thermal loads. The calculations are constructed on the steady state heat balance equation for each zone. The sensible load is a function of airflow rate and the difference between the space and supply air temperatures; and the humidity is determined using the latent load. The loads are determined from the same model but with an inverse form using measured data of the previous period (15 minutes) and then the loads are assumed to be constant during the current optimization period (15 minutes).

The electric reheat is initiated only when the airflow rate reaches its minimum level (20% of design airflow rate) and when space temperature is lower than the heating set-point. The system airflow rate is applied as the input for cooling in the fan model and is equal to the sum of zone airflow rates calculated by the zone model. An iteration process is applied to estimate the return air conditions; the initial cooling coil leaving air humidity ratio is assumed, and the new value is calculated and reused. This iterative process continues calculating through the loop several times until the values of cooling coil leaving air humidity ratio stabilize within a specified tolerance.

The minimum air flow rate based on the ASHRAE standard 62.1-2013 is included in the optimization calculations. The outdoor air is determined by the multi-zone procedure of ASHRAE 62.1-2013 standard based on the actual zone airflow rates. The advantage of including the minimum outdoor standard procedure in the whole optimization process is to minimize the energy use while respecting the ventilation requirements by ASHRAE's current standard.

3.3 Model Development

First generation of building performance simulation (BPS) tools is based on simplified methods found in handbooks (calculations based on analytical formulations that embody many

simplifying assumptions). Second generation tools are based on methods that assume simplified (still analytical) modeling of dynamics in buildings. Third generation tools use numerical methods and provide partial integration of different performance aspects of buildings, e.g. thermal energy, visual, and acoustical. The current fourth generation tools tend to be fully integrated with respect to different building performance aspects, with new developments concerned with intelligent knowledge-based user interfaces, application quality control and user training. The current tools can capture reality much better than earlier tools, but are more complex to use (Trčka, M. et al., 2010). The majority of models in building and system performance simulation are:

- Continuous in state
- Discrete in time, as time is specified to proceed in discrete steps.
- Deterministic.
- Time varying, since the rules of interaction are different at different times.
- Both steady state and dynamic.
- Forward, as they are used to predict the response of output variables based on a known structure and known parameters when subjected to input and forcing variables.
- Backward (data-driven) models tend to be much simpler but are relevant only for cases when system-specific and accurate models of specific building components are required (Trčka, M. et al., 2010).

As a need for global energy conservation technology has been recognized, the design and implementation of optimizing set-points within HVAC system models has proven to be a logical pathway to saving energy and therefore money for building owners. Programming methodology follows mathematical theorems and can be provable. A program can be proved correct as it is

developed and its results are used to tackle a single problem area (in our case building energy). The logic for model development is: algorithm development, language, structure, correctness validation, code generation, documentation, and training or testing. See the optimization flow chart in Figure 27 for a brief summary of the models developed and the key calculations within each sub-routine.

3.3.1 Psychometric programs. For our research the psychrometric routines were all written in MATLAB to assist our research and obtain our optimal variables to reduce energy through MATLAB's built-in genetic algorithm tool. The psychrometric details and standard formulas are found in Appendix A. The psychrometirc section consists of routines that calculate these individual basic psychrometric moist air properties:

- humidity ratio (*W*)
- relative humidity (*RH*)
- enthalpy
- wet bulb temperature (*WBT or* t_{wb})
- dewpoint temperature (*DPT or* t_d)
- dry and moist air densities
- saturated water vapor pressure
- saturated water vapor temperature
- saturated moist air enthalpy
- saturated moist air temperature
- atmospheric pressure
- dry bulb temperature

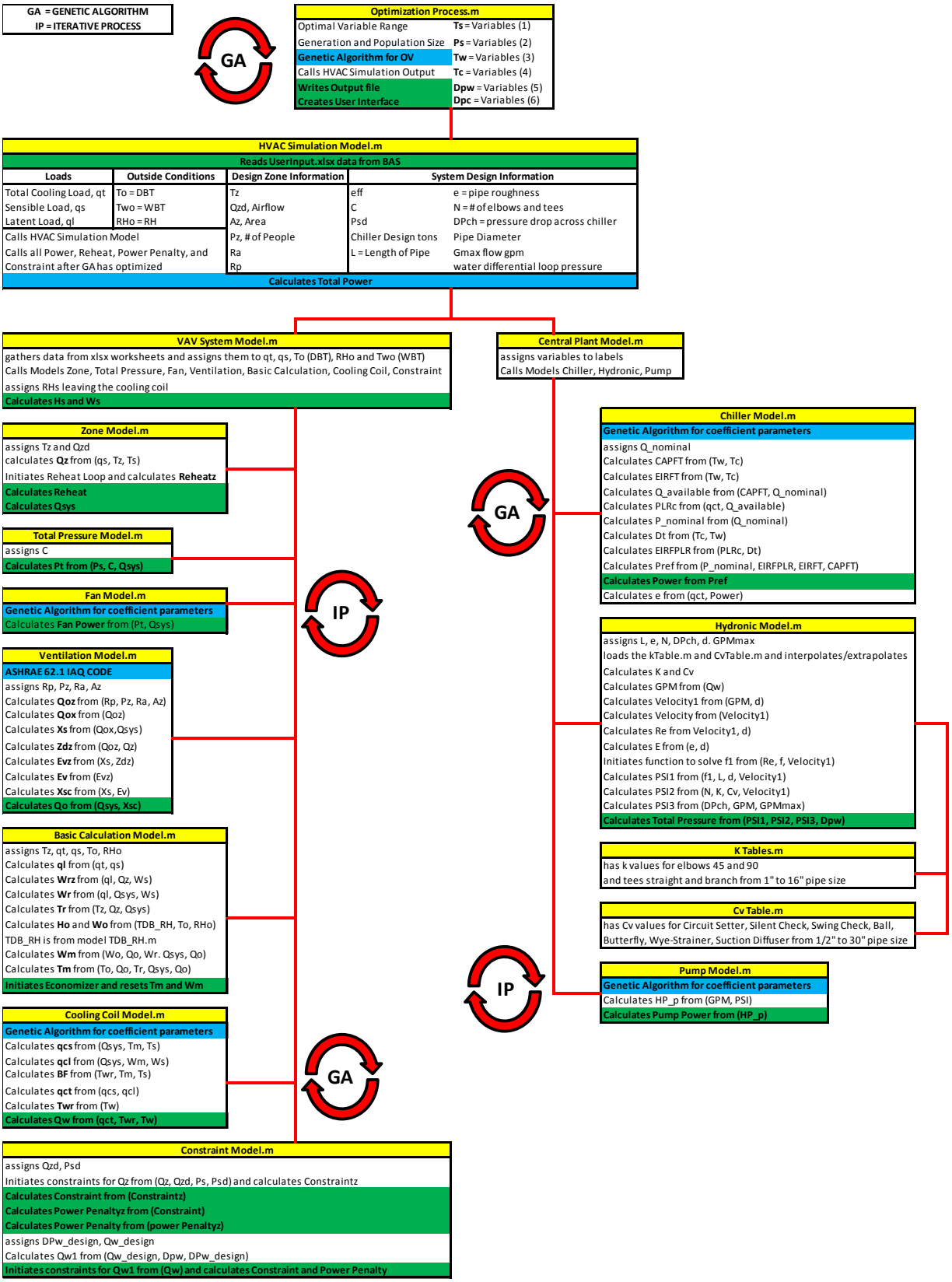

Figure 27. Optimization process flow chart.

3.3.2 VAV system model. A variable air volume model with reheat system maintains a constant supply air temperature by regulating the air flow which controls zone temperature. VAV terminal units or boxes, located in the ductwork system at each zone, modulate air flow contingent on its cooling load, while maintaining zone temperature set point. Reheat coils are included in the building system in this research to provide the required heating. The reheat coil will be triggered to meet the zone load if the VAV box has reduced the air flow to its minimum position and the cooling load has continued to decrease.

The VAV System model: calls the ordered values, sets them equal to the variables T_s, P_s, T_w, and D_{pw} during the iterative process of finding the optimal variable set points, and runs through its functions. The model calls for the total and sensible zonal loads from the input data and sets them equal to q_t and q_s respectively. The outdoor dry-bulb temperature, relative humidity, wet-bulb temperature, and relative humidity leaving the cooling coil from the input data are also set to variables T_o, RH_o, T_{wo}, and RH_s respectively. The following programs/sub-routine models are called:

- zone
- total pressure
- fan
- ventilation
- System Calculation
- cooling coil
- constraints

See the description and functionality of the models in their sections below.

3.3.2.1 Zone model. The balance laws are essential when modeling HVAC systems. The law of conservation of mass maintains that for any system closed to all transfers of matter and energy, the mass of the system remains constant over time or the quantity of mass is "conserved" over time. The law indicates that mass can neither be created nor destroyed, although it may be rearranged in space, or the entities associated with it may be changed in form. This means that mass stored in a fixed volume is only altered due to mass inputs and mass outputs. This is illustrated in Figure 28 and is often referred to as mass balance. The law of conservation of energy, illustrated in Figure 29, states that the total energy of an isolated system cannot change and it is said to be conserved over time. Energy can be neither created nor destroyed, but can change form.

Figure 28. Conservation of mass.

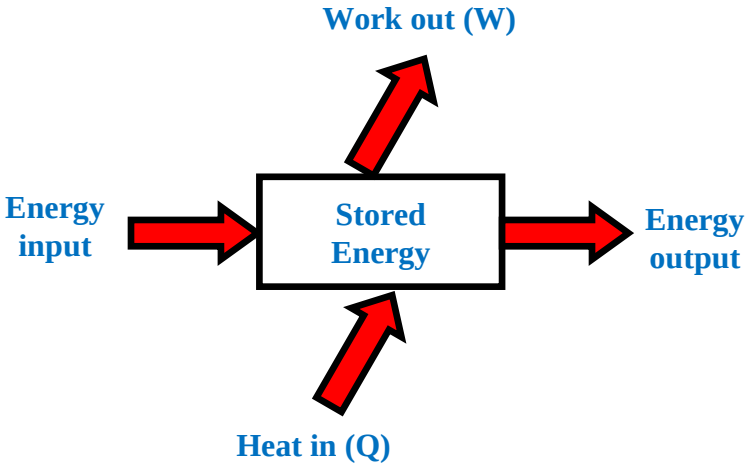

Figure 29. Conservation of energy.

No system without an external energy supply can deliver an unlimited amount of energy to its surroundings. It can however change form, as an example kinetic energy can become

thermal energy due to friction. The Zone model utilizes these laws, shown in Figure 30. Heat into a space or energy input into the system minus the work output or energy extracted from the system will equal the change in energy or the energy stored in the system, which is the First law of thermodynamics (Conservation of Energy).

AHU SIDE - HVAC Component Model Theory & Equations:

Zone Model: First Law of Thermodynamics (Conservation of Energy)

Heat balance equation: $H - W = \Delta E$ (3.10)

Heat H: Energy input to the system.

Work W: Energy extracted from the system.

Internal heat E: Energy stored in the system (can only measure/calculate its change).

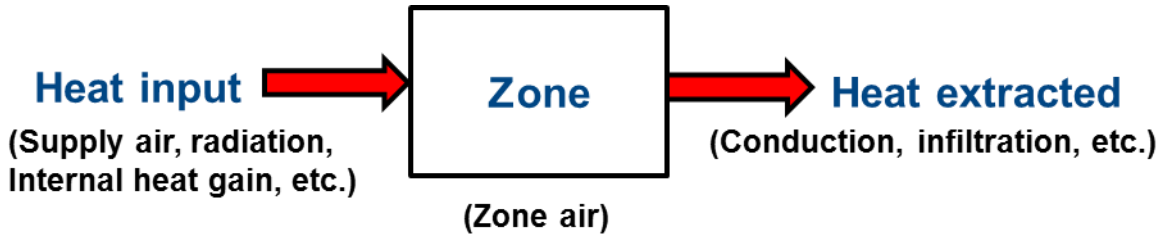

Figure 30. Zone diagram.

The second law of thermodynamics states that heat can flow from a mass with higher temperature to a mass with lower temperature, but never from low to high. Heat loss in buildings is due to heat transfer by conduction, convection and radiation. Heat conduction is the flow of heat through walls, windows, doors, etc. influenced by temperature differences. When radiation waves hits an object some of the radiation is absorbed by the object therefore, radiation contributes to the total energy or heat transference. The rest of the radiation waves or energy is reflected or travels through the object. Zone temperature and airflow data is assigned to

variables T_z and Q_{zd} from the design zone information input. The zone model calculates the zone requirements from the UserInput.xlsx building model data. Each zone's load is calculated:

$$Q_{zone} = \frac{q_{z,senible} or\ q_s}{\left(1.1(T_z - T_s)\right)} \tag{3.11}$$

System air flow rate is calculated:

$$Q_{sys} = \sum_{i=0}^{no.of\ zones} Q_{zone,i} \tag{3.12}$$

The reheat loop is initiated; if the zone's load is less than 20 percent of the design load then it requires the reheat coil to turn on in zone (i), following this equation:

$$Reheat_{zone}(i) = \frac{q_s(i) - 1.1Q_{zone}(i)(T_z(i) - T_s) \times 0.2}{3410} \tag{3.13}$$

The function calculates the sum of all of the zone's reheat to get the total reheat power usage for the system at that specific time.

3.3.2.2 Total pressure model. Fan energy use in variable-air-volume (VAV) systems can be reduced by resetting the supply duct pressure. The standard way to reset duct pressure is by controlling the most open terminal damper to a nearly open position. The standard way to control VAV fan systems is to regulate the static pressure in the main supply duct. This strategy ensures that zone terminals have enough pressure to operate properly, but it is inefficient because the pressure setpoint will be higher than necessary all of the time. Considerable energy savings can be achieved if the supply duct pressure is reduced at part load (Federspiel, C. C., 2005). The Total Pressure Model calculates the total pressure for the air handling system, see Figure 31. The data is read from the UserInput.xlsx spreadsheet's worksheet labeled System Design Information. Utilizing the system load to pressure drop relationship from the fan laws we can calculate the total pressure drop across the air handler.

$$\frac{dp_1}{dp_2} = \left(\frac{Q_1}{Q_2}\right)^2 \tag{3.14}$$

$$P_t = P_s + CQ_{sys}^2 \tag{3.15}$$

C is the flow coefficient considering the pressure drop between the Ps sensor and the fan outlet.

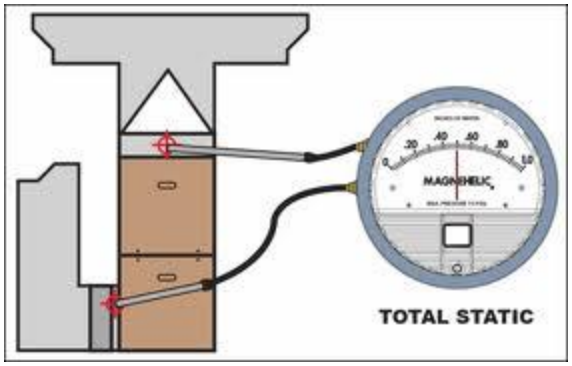

Figure 31. Total static pressure.

3.3.2.3 Fan and pump models. This is a new model that includes an iterative process that applies to both pumps and fans (see Figures 32 and 33). This model will allow the user to select any two variables as model inputs (*MI*) or model outputs (*MO*) among four variables of flow (air or water) *Q*, total pressure *P*, speed *N*, and power *W*. This is compared to the well known simple and detailed models from HVAC 2 Toolkit, that uses the perfect fan or pump laws through the application of dimensionless flow (ϕ) and pressure (ψ) coefficients. The only fundamental difference is in the calculation of fluid properties. The pump model uses a constant density and specific heat of the fluid and the fan model uses psychrometric routines to calculate fluid density and temperature rise. These models use a fourth-order equation to predict fan and pump efficiency from the dimensionless flow parameter.

Fan Flow

$$\Phi = c_1 \times \frac{Q}{N \times D^3} \tag{3.16}$$

Fan Pressure

$$\Psi = c_2 \times \frac{\Delta P}{\rho \times N^2 \times D^2} \tag{3.17}$$

where,

Q = airflow (cfm)

N = fan speed

D = fan diameter

ρ = average air density

ΔP = fan static pressure

c_1 *and* c_2 = constants that make the coefficients dimensionless

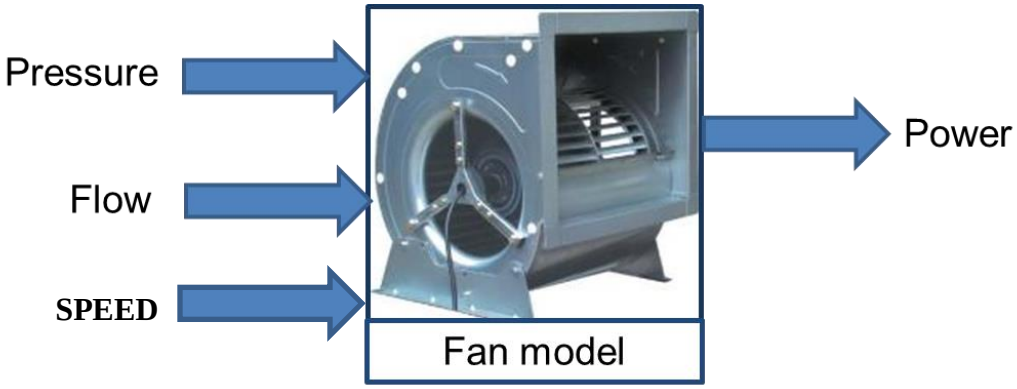

Figure 32. OLSTM fan model parameters predicted with iterative process.

Dimensionless Pump Flow Coefficient

$$\phi = \frac{\dot{m}}{\rho N d^3} \tag{3.18}$$

Dimensionless Pump Head Pressure Coefficient

$$\psi = \frac{\Delta P}{\rho N^2 d^2} \tag{3.19}$$

where,

m = mass flow rate

ρ = density of liquid

N = rotation speed

d = diameter of pump impeller

P = head pressure

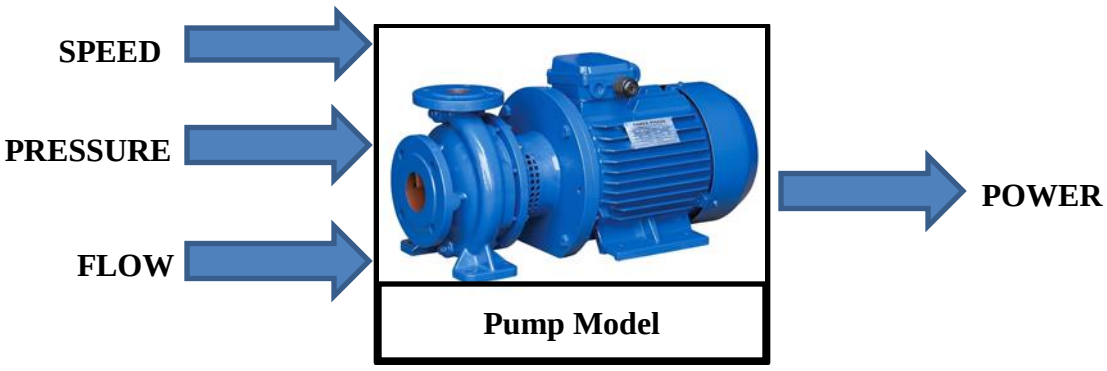

Figure 33. OLSTM pump model parameters predicted with iterative process.

Accurate estimation of fan and pump performance is a key element in reducing energy consumption associated with fan and pump operations. In existing systems, optimization, intelligent control, and fault detection and diagnostic need an accurate model to estimate fan/pump flow rate and power or static/head pressure and power. Another application is the use of the modern airflow station technique (Joo, I.-S., 2007). The fan and pump model can determine the airflow or fluid flow by using the measured fan differential pressure (pump head pressure) and fan or pump speed. The success of this technique is related to the model accuracy and the amount of data to be collected on site for calibration. In simulation software application, the designer has to use airflow and fan pressure (fluid flow and head pressure) as inputs to the fan/pump model in order to calculate fan/pump power.

There are several models proposed in literature (Brandemuehl, M., 1993; Clark, D. R., 1985; Nassif, N., 2010; Nassif, N., S. Moujaes, et al., 2008; Stein, J. et al., 2004). Those models do not provide flexibility in selecting the input and output variables and have their limitations in many applications. The simple fan model (SFM) in DOE-2 (DOE, 1980) and HVAC 2 Toolkit (Brandemuehl, M., 1993) uses a third order regression model in order to estimate the power W_s as a function of airflow or fluid flow rate Q. The detailed fan model (DFM) in HVAC 2 toolkit (Brandemuehl, M., 1993), based on Clark's model (Clark, D. R., 1985), characterizes the

fan/pump performance in terms of pressure rise across the fan/pump and shaft power. The detailed model does not permit the direct calculation of fan/pump power from airflow (fluid flow) and pressure. It requires both airflow (fluid flow) and fan/pump speed as inputs to correlate the efficiency to the dimensionless flow term.

These new fan and pump models can be used in several applications, and also be incorporated into any commercial building models. The fan/pump model uses numerical methods based on an interpolation technique from data generated by basic fan/pump laws. It can be calibrated with two or more data points for better accuracy. Using the variables of airflow or fluid flow rate, total fan or pump pressure, speed, and power, the models are flexible in using any two of those variables as inputs or outputs. The models proposed in this research will overcome the existing model limitations by selecting any input or output variables and any set of data for calibrations. To test the model, two different manufacturers' data of roof top unit packages with capacity ranging from 2 tons to 20 tons (7 kW to 70.2 kW) are first used. Then the model is tested and evaluated on an actual variable air volume (VAV) system using the real annual measured data from the BAS of the New Academic Classroom Building at NC A&T State University.

$$\frac{W_s}{W_{rat}} = C_0 + C_1 \frac{Q}{Q_{rat}} + C_2 \left(\frac{Q}{Q_{rat}}\right)^2 + C_3 \left(\frac{Q}{Q_{rat}}\right)^3 \tag{3.20}$$

See equation 3.20 for the SFM, the W_{rat} and Q_{rat} are the rated power and airflow rate. This model requires at least four different operating points to find the polynomial coefficients (C_0, C_1, C_2, and C_3). Simulation software generally uses default values, or left options, as user inputs. The model is based on the assumption of a single system curve and constant pressure rise across the fan (Stein, J. et al., 2004). However, in real applications such as VAV systems, the

system curve varies with the relative changes in the damper positions of VAV boxes, and the pressure rise is not constant due to various load and static pressure reset control algorithm.

The other model in the HVAC toolkit is a detailed fan model (DFM) (Brandemuehl, M., 1993; Clark, D. R., 1985). In this model, the fan performance is characterized in terms of pressure rise across the fan (ΔP) and shaft power (W). It uses the dimensionless coefficients of flow (Φ), pressure head (ψ), and shaft power (η_f), as follows:

$$\phi = \frac{Q}{Nd^3} \tag{3.21}$$

$$\psi = \frac{\Delta P}{\rho N^2 d^2} \tag{3.22}$$

$$\eta_f = \frac{Q\Delta P}{W} \tag{3.23}$$

where d is the fan diameter, ρ is the air density, and N is the fan speed. The performance of a fan is represented by a fourth order polynomial regression of the manufacturer's data using these dimensionless coefficients.

$$\psi = a_0 + a_1\phi + a_2\phi^2 + a_3\phi^3 + a_4\phi^4 \tag{3.24}$$

$$\eta_f = b_0 + b_1\phi + b_2\phi^2 + b_3\phi^3 + b_4\phi^4 \tag{3.25}$$

where,

a_i = regression coefficients of head vs. flow

b_i = regression coefficients of efficiency vs. flow

The coefficients, a_i and b_i are determined from the manufacturer's data.

The main problem of this model is that the model assumes fixed peak efficiency for fans of all sizes (Stein, J. et al., 2004). In addition, the model does not allow direct calculation of fan efficiency from airflow and pressure. It is required to use airflow and fan pressure as inputs to calculate fan speed and efficiency.

The proposed model is based on numerical analysis and an interpolation technique for the data obtained by the principle fan laws. This model will allow the user to select any two variables as model inputs (*MI*) or model outputs (*MO*) among all four variables of air flow *Q*, total pressure *P*, speed *N*, and power *W*. The model needs at least two different operating points for calibrations, obtained from manufacturer's data (*MD*) or measurements. The procedure to find the model output (*MO*) is described below.

Given: *MD =[Q, P, N, W] = [Flow, Pressure, Speed, Power]*

Inputs: *MI = [MI_1,MI_2] = [P,N], [Q,P], [Q,N], [P,Q], or etc.*

Outputs: *MO =[MO_1,MO_2] = [Q,W],[N,W],[P,W],[W,N],or etc.*

To find the outputs, the internal variables (*IV*) are first generated from fan laws and using one variable of the input (MI_1): *IV = fan laws (MD, MI_1).* Second, the model outputs *MO* are then found from any interpolation/extrapolation techniques such as linear or polynomial interpolation: *MO=interpolation/extrapolation (IV, MI_2).* Three examples showing the implementation of these procedures are found in chapter 4 which is the model testing and validation section.

3.3.2.4 Ventilation model. The purpose of this function is to specify the minimum ventilation rates and other measures intended to provide indoor air quality that is acceptable to human occupants and that minimizes adverse health effects taking into account the new ASHRAE 62.1-2013 ventilation for acceptable indoor air quality code. Step one of the program reads the data from the UserInput.xlsx spreadsheet and the Design Zone Information worksheet, and assigns values for each zone to people outdoor air rate or R_p (cfm/person), zone population or the number of people (P_z), area outdoor air rate or R_a (cfm/ft^2), and zone floor area or A_z (ft^2).

Ventilation air is the amount of outdoor air required to maintain Indoor Air Quality (IAQ) for the occupants and makeup for air leaving the space due to equipment exhaust, ex-filtration and pressurization. The standard load calculations are utilized:

$$q_s = 1.08 \times Q \times (T_o - T_c) \tag{3.26}$$

$$q_l = 0.68 \times Q \times \Delta W_g \tag{3.27}$$

$$q_l = 4840 \times Q \times \Delta W_{lb} \tag{3.28}$$

$$q_T = 4.5 \times Q \times (h_o - h_c) \tag{3.29}$$

$$q_T = q_s + q_l \tag{3.30}$$

where:

q_s = Sensible heat gain (Btu/hr)

q_l = Latent heat gain (Btu/hr)

q_T = Total heat gain (Btu/hr)

Q = Ventilation airflow rate in cubic feet per minute (cfm)

T_o = Outside dry bulb temperature, °F

T_c = Dry bulb temperature of air leaving the cooling coil, °F

ΔW_g = Humidity Ratio Difference (Gr H_2O/lb of dry air) = (W_o – W_c)

ΔW_{lb} = Humidity Ratio Difference (lb H_2O /lb of dry air) and = (W_o – W_c)

W_o = Outside humidity ratio, lb H_2O per lb (dry air)

W_c = Humidity ratio of air leaving the cooling coil, lb H_2O per lb (dry air)

h_o = Outside/Inside air enthalpy, Btu per lb (dry air)

h_c = Enthalpy of air leaving the cooling coil Btu per lb (dry air) for determining infiltration

Step two in the program calculates the breathing zone outdoor airflow following the ASHRAE 62.1-2013 ventilation for acceptable indoor air quality code. The following equations are utilized to follow the new standard:

$$V_{bz} = R_p \times P_z + R_a \times A_z \tag{3.31}$$

$$V_{oz} = \frac{V_{bz}}{E_z} \tag{3.32}$$

$$Z_{dz} = \frac{V_{oz}}{V_{dz}} \tag{3.33}$$

$$V_{ou} = \sum R_p + P_z + \sum R_a \times A_z = R_p \times P_b + \sum R_a \times A_z \tag{3.34}$$

$$X_s = \frac{V_{ou}}{V_{ps}} \tag{3.35}$$

$$E_{vz} = 1 + X_s - Z_{dz} \tag{3.36}$$

$$E_v = min(E_{vz}) \tag{3.37}$$

$$V_{ot} = \frac{V_{ou}}{E_v} \tag{3.38}$$

$$X_{sc} = \frac{V_{ot}}{V_{ps}} \tag{3.39}$$

$$V_{ot} = V_{ps} \times X_{sc} \tag{3.40}$$

where:

A_z = zone floor area, m^2 (ft^2)

C_o = CO_2 concentration in outdoor air (ppm)

C_r = CO_2 concentration in return air (ppm)

C_s = CO_2 concentration in supply air (ppm)

C_z = CO_2 concentration in breathing zone (ppm)

E_v = system efficiency

E_{vz} = zone efficiency

E_z = zone air distribution effectiveness

N_z = CO_2 generation rate, L/person (cfm/person)

P_b = building population, persons

P_z = zone population, persons

R_a = area outdoor air rate, L/s per m^2 (cfm/ft^2)

R_p = people outdoor air rate, L/s per person (cfm/person)

V_{bz} = breathing zone outdoor airflow, L/s (cfm)

V_{dz} = discharge air supplied to the zone, L/s (cfm)

V_{ot} = outdoor air intake flow, L/s (cfm)

V_{ou} = uncorrected outdoor air intake flow, L/s (cfm)

V_{oz} = zone outdoor airflow, L/s (cfm)

V_{ps} = system supply air flow, L/s (cfm)

X_s = uncorrected outdoor fraction in supply air

X_{sc} = corrected outdoor fraction in supply air

Z_{dz} = outdoor air fraction in discharge air supplied to each zone, L/s (cfm)

3.3.2.5 System calculation model. This routine assigns data to the variables for the zone temperature (T_z), the total heat load (q_t), the sensible heat load (q_s), the outside dry bulb temperature (T_o), and the Outside relative humidity (RH_o). These values are read from the data stored in our UserInput.xlsx spreadsheet, which has all of the data from our building model. Various worksheets in the UserInput.xlsx spreadsheet labeled Loads, Outside Conditions, Design Zone Information, and System Design Information have specific building data values stored at each time step. Common air-conditioning processes involve transferring heat via air transport or

leakage. Next the model calculates the latent heat load, zone humidity ratio, return temperature, mixed air temperature, and economizer control functionality utilizing these equations:

Latent Load $$q_l = q_t - q_s \tag{3.41}$$

Zone Humidity Ration $$W_{rz} = \frac{q_l}{4840 \times Q_{sys}} + W_s \tag{3.42}$$

Humidity ratio $$W_r = \frac{\sum q_l}{4840 \times Q_{sys}} + W_s \tag{3.43}$$

Return Air Temperature $$T_r = \frac{\sum (T_z \times Q_z)}{Q_{sys}} \tag{3.44}$$

Mixed Air Humidity Ratio $$W_m = \frac{\left(W_o \times Q_o + W_r \times \left(Q_{sys} - Q_o\right)\right)}{Q_{sys}} \tag{3.45}$$

Mixed Air Temperature $$T_m = \frac{\left(T_o \times Q_o + T_r \times \left(Q_{sys} - Q_o\right)\right)}{Q_{sys}} \tag{3.46}$$

Also, the economizer section is identified: if the outside temperature is less than the return temperature and the outside temperature is greater than 55^{o}F then the mixed air temperature equals the outside air temperature and the mixed air humidity ratio equals the outside air humidity ratio. See Figure 34, the outside (fresh air) dampers and exhaust (relief) dampers are opened and the return air damper is closed allowing the “free” cooling to take place, thus saving energy for the system.

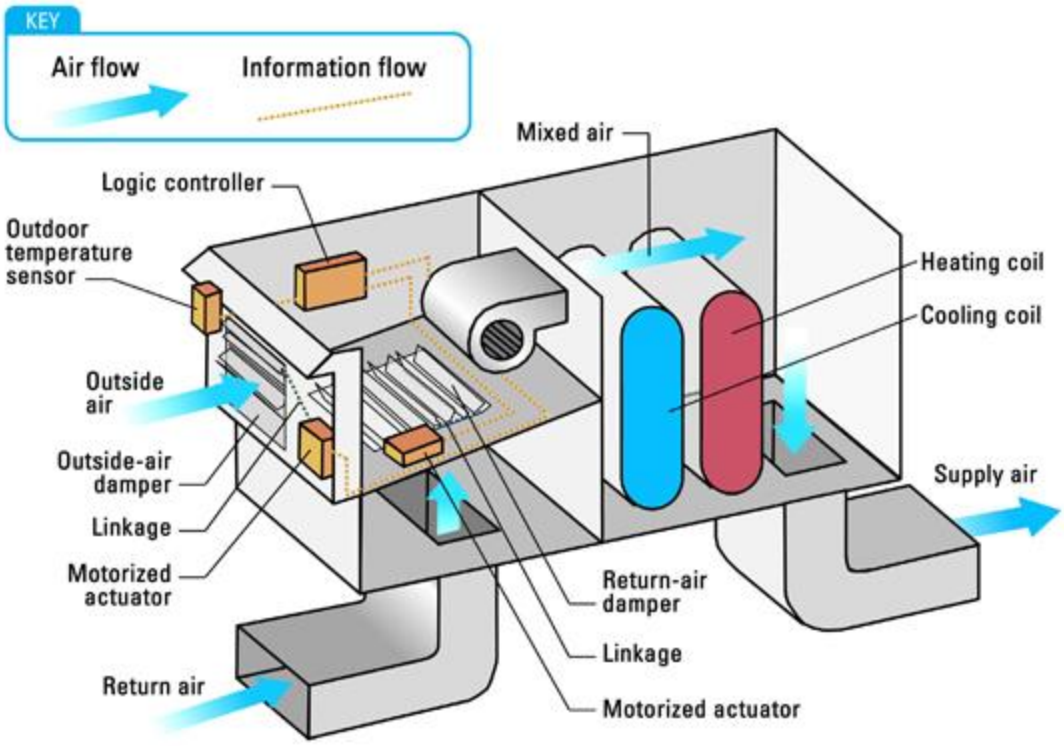

Figure 34. Economizer mode air handling unit (AHU) system.

3.3.2.6 Cooling coil model. The models for a cooling and dehumidifying coil determine whether the finned surface is completely or partially dry or wet, and using the following equations it calculates:

- the outlet liquid temperature
- air dry bulb temperature
- humidity ratio
- the total and sensible cooling capacity
- the heat transfer coefficients and mass transfer associated with condensation on the finned air-side surface in accordance with ASHRAE standards and methods.

Enthalpy effectiveness $$\varepsilon = \frac{C_a\left(h_{a,ent} - h_{a,lvg}\right)}{C_{min}\left(h_{a,ent} - h_{l,ent,sat}\right)} \quad (3.47)$$

$$C_a = \dot{m}_a \tag{3.48}$$

$$C_w = \left(\dot{m}\frac{c_p}{c_{p,sat}}\right)_l \tag{3.49}$$

$$\Delta h_{sat} = c_{p,sat}\Delta t_{sat} \tag{3.50}$$

$$UA_h = \frac{UA}{c_p} \tag{3.51}$$

$$\frac{1}{UA_{h,tot}} = \frac{c_{p,sat}}{UA_{int}} + \frac{c_{p,a}}{UA_{ext}} \tag{3.52}$$

$$UA_{ext} = -\left(\dot{m}c_p\right)_a \ln(BF) = -\left(\dot{m}c_p\right)_a \ln(1-\varepsilon) \tag{3.53}$$

where:

$h_{a,o}$ = Leaving air enthalpy, Btu/lb

$h_{l,sat,ent}$ = Saturated enthalpy of air at inlet liquid temp., Btu/lb

$h_{lsat,lvg}$ = Saturated enthalpy of air at exit liquid temp., Btu/lb

$h_{a,ent}$ = Entering air enthalpy, Btu/lb

$h_{a,lvg}$ = Leaving air enthalpy, Btu/lb

m = Fluid mass flow rate, lb/h

m_a = Dry air mass flow rate, lb/h

$c_{p,a}$ = Specific heat of dry air, Btu/lb ^{o}F

$c_{p,sat}$ = Effective specific heat of saturated air, Btu/lb ^{o}F

$c_{p,l}$ = Specific heat of liquid, Btu/lb ^{o}F

q_a = heat transfer rate of air, Btu/h

q_w = heat transfer rate of water, Btu/h

$t_{l,ent}$ = Entering water or liquid temperature, F

$t_{a,ent}$ = Entering air dry bulb temperature, F

$t_{l,lvg}$ = Leaving water or liquid temperature, F

$t_{a,lvg}$ = Leaving air dry bulb temperature, F

UA_h = Overall enthalpy heat transfer coefficient, lb/h

UA_{int} = Liquid-side heat transfer coefficient, Btu/h ^oF

UA_{ext} = Air-side heat transfer coefficient, Btu/h ^oF

For further details and calculations on heat and mass transfer properties see Appendix B.

Chilled water flow rate is calculated as a function of valve opening by the hydronic model. A simple **s**elf-**t**uning steady state **c**ooling **c**oil **m**odel (STCCM) was developed for the New Academic Building at North Carolina A&T State University. The existing ASHRAE HVAC 2 Toolkit cooling coil models consider the internal and external heat transfer coefficients (UA_{int} & UA_{ext}) constant and are calculated by design conditions and water and air flow rates; this will not produce accurate results as the UA_{int} & UA_{ext} change over time. To improve the accuracy we varied the UA_{int} & UA_{ext} based on the water and air flow rate. The parameters of this relationship are determined based on the actual BAS coiling coil data and found with a genetic algorithm to tune the model. In this model, the internal and external heat transfer coefficients (UA_{int} & UA_{ext}) are determined from the performance of the coil at a single rating point, and are assumed to vary as functions of the liquid and airflow rates $(Q_{gpm}\ and\ Q_{sys})$:

$$UA_{int} = UA_{int,rate}\left(\frac{Q_{gpm}}{Q_{gpm,rate}}\right)^{a_1} \tag{3.54}$$

$$UA_{ext} = UA_{ext,rate}\left(\frac{Q_{sys}}{Q_{sys,des}}\right)^{a_2} \tag{3.55}$$

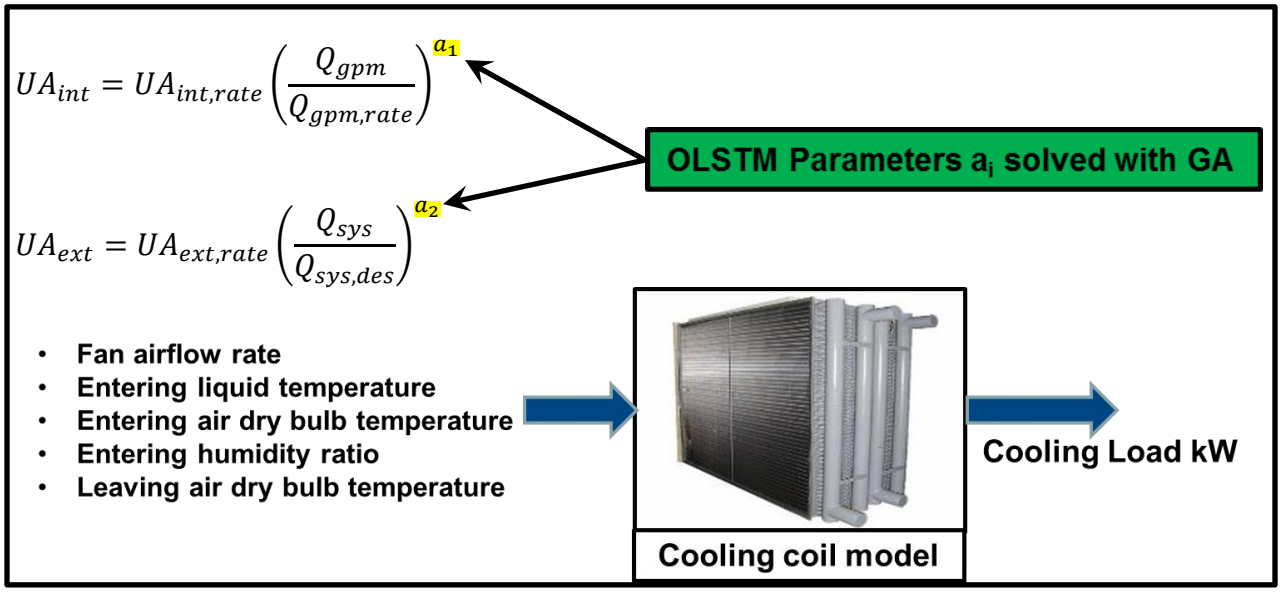

Figure 35. Cooling coil model diagram.

In this research the genetic algorithm (see section 3.4 for GA) determines the tuning parameters a_1 and a_2 considering the relation between the heat transfer coefficients and the liquid and airflow rates. The tuning parameter corrects the error in determining liquid flow rate as a function of valve opening using the valve model; see Figure 35 for the cooling coil model diagram. The cooling coil model is calculated using equations for latent load, zone humidity ratio, humidity ratio, return temperature, mixed air humidity ratio, mixed air temperature (3.47 - 3.55) and the following equations:

Bypass Factor

$$BF = \frac{h_{lvg} - h_{adp}}{h_{ent} - h_{adp}} = \frac{w_{lvg} - w_{adp}}{w_{ent} - w_{adp}} \tag{3.56}$$

$$\frac{h_{ent} - h_{lvg}}{w_{ent} - w_{lvg}} = \frac{h_{ent} - h_{adp}}{w_{ent} - w_{adp}} \tag{3.57}$$

3.3.2.7 Constraint model. The process for modeling and optimizing HVAC systems must involve several constraints. In a VAV system there is a correlation between the damper position and the magnitude of the cooling load. As the loads increase in the zone, more cold air is required and the damper position is increased; and when the loads decrease, the VAV control

throttles back the damper position to maintain the temperature set-point of the zone. The chiller model constraint is found in the chiller model section 3.3.3.1.

The term "starved" refers to a situation where the VAV controller senses a load in the zone and commands the damper to open and supply more cold supply air, but since there is not enough cold air pressure to eliminate the cooling loads, the VAV damper stays at 100% until the zone loads decrease. The VAV damper is said to be "starved" because it is at maximum opened position without it being able to satisfy the zone loads. When the VAV damper is at its maximum position then the temperature is above the temperature set-point of the zone. The system cannot satisfy the cooling loads, therefore it is under sized. If the supply air temperature is increased (to save energy), then the VAV system is not able to generate enough negative loads to satisfy the zone's cooling loads (Ben-Aissa, N., 1997).

If the static pressure set-point is too low, some of the VAV boxes will not be able to get enough air to provide comfort, and the fan will use little energy, starving VAV boxes. The actual flow is less than the desired flow, even though damper is 100% open, and the zone temperature will rise. A high static pressure set-point also reduces the controllability of the system (Rajkumar, C. V. et al., 2013).

The Constraint Model uses the "starved" VAV box scenarios explained above, and we decided to allow one VAV box to be starved within the system which adds a power penalty to the output allowing the program to continue but, it "kills" the solution during the optimization process. In other words, the optimization process will continue to find the optimal variables to reduce the energy in the system but will include constraints that prohibit the use of that particular optimal variable sequence because it will increase the energy to a value that is not acceptable for a viable solution to the optimization process.

Adequate supply airflow rate should be provided to every zone at the supply duct static pressure (P_s) setpoint which is an optimal variable. The total pressure model calculates the total fan static pressure drop for the system. The VAV system model is required to determine the optimal variables including the zone load conditions and outdoor air conditions while maintaining occupant comfort. The VAV system model calls the subroutines of the zone, total pressure, fan, ventilation, System Calculation, cooling coil and constraints models. These models require detailed information on the system which is entered in the UserInput.xlsx Excel file in the Loads, Outside Conditions, Design Zone Information, and System Design Information worksheets. A simplified simulation method is used to meet the requirements described above without using intensive calculations.

The design zone airflow rates $\left(Q_{zd_{design}}\right)$, are the maximum airflow rates introduced into zones at the design supply duct static setpoints when the VAV dampers are wide open. However, these "maximum limit" airflow rates $\left(Q_{z_{max}}\right)$, are functions of the supply duct static setpoint (P_s), using the following standard equations $\Delta P = CQ^2$ and $Q = \sqrt{\frac{C}{\Delta P}}$ we can establish the following equation:

$$\left(Q_{z_{max}}\right) = Q_{zd_{design}} \sqrt{\frac{P_s - \Delta P_{duct}}{P_{s,design} - \Delta P_{duct,design}}} \tag{3.58}$$

The term ΔP_{duct} represents the pressure drop between the static pressure sensor location and the zone VAV box inlet. Since the airflow rate velocity is not significantly changed between sensor location and the VAV box inlet, the dynamic pressure part is not included in the equation above. To ensure that every individual zone at the trial duct static pressure setpoint (P_s) receives adequate supply air, the "zone airflow rate constraint" must be respected so that the zone

airflow(Q_z), obtained by optimization is equal to or lower than the maximum limit of zone airflow rate calculated by $\left(Q_{z_{max}}\right)$. This equation can be simplified within the normal fan operation range as follows:

$$\left(Q_{z_{max}}\right)_{simplified} = Q_{zd_{design}}\sqrt{\frac{P_s}{P_{s,design}}} \tag{3.59}$$

Given that $\Delta P_{duct,design} > \Delta P_{duct}$ and consequently , $\left(Q_{z_{max}}\right)_{simplified} = Q_{z_{max}}$this simplification further ensures, for a given supply duct static pressure setpoint, that no zone box is starved for supply air. Therefore, the "zone airflow rate constraint" could be expressed as $Q_z \leq \left(Q_{z_{max}}\right)_{simplified}$. For the optimization process, the fan airflow rate and fan static pressure are required, as the inputs of the fan model, to calculate the fan power. The fan airflow rate (Q_{sys}) is determined as the sum of zone airflow rates. However, the fan static pressure ($P_{s,fan}$) can be determined using a formula represented by the operation curve expressed in terms of known design points (static pressure and airflow rate of fan) and supply duct static pressure setpoint.

$$P_{s,fan} = \left(\frac{Q_{sys}}{Q_{sys,design}}\right)^2 \left(P_{s,fan,design} - P_s\right) + P_s \tag{3.60}$$

The constraints result from restrictions on the operation of the HVAC system. They cover the lower and upper limits of variables, such as supply air temperature, zone air temperatures, etc. The constraints also cover the design capacity of components. The fan and zone airflow rates, for instance, are restricted within the maximum and minimum limits:

- The fan airflow rate must be less than the design value and higher than 40% of the design value.

- The zone airflow rates must be higher than the minimum limits for the modified HVAC system and derived from the operation manual for the existing HVAC system (30% of design value).
- The zone airflow rates must be lower than the "maximum limits" corresponding to the optimal duct static pressure set-point.

3.3.3 Central plant model. The central plant model calls the sub-routines in the Chiller Model, Total Pressure Model, Pump Model and Hydronic Models with the corresponding optimal variables (T_w and D_{pw}) performing the iterative process of finding the optimal variable set points, and runs through its functions. These models that make up the central plant are described in the next sections. The central plant may include equipment to provide heat only, cooling only, both heat and cooling, or any of these three options in conjunction with electric power generation. Central cooling and/or heating plants generate cooling and/or heating in one location for distribution to multiple locations in one building. Central cooling and heating systems are used in almost all buildings, but particularly in very large buildings and complexes or where there is a high density of energy use. They are especially suited to applications where maximizing equipment service life and using energy and operational workforce efficiently are important. Central systems are characterized by large chilling and/or heating equipment located in one facility or multiple smaller installations interconnected to operate as one. Equipment configuration and ancillary equipment vary significantly, depending on the facility's use (ASHRAE, 2012).

Equipment can be located adjacent to the facility, or in remote stand-alone plants. Primary equipment (i.e., chillers and boilers) is available in different sizes, capacities, and configurations to serve a variety of building applications. Operating a few pieces of primary

equipment (often with back-up equipment) gives central plants different benefits from decentralized systems.

3.3.3.1 Chiller model. Chillers cool secondary coolant like water or brine for air conditioning or refrigeration. In our research the application is water chilling for air conditioning. The basic components of a vapor-compression, liquid-chilling system include a compressor, liquid cooler (evaporator), condenser, compressor drive, liquid-refrigerant expansion or flow control device, and control center; it may also include a receiver, economizer, expansion turbine, and/or subcooler (ASHRAE, 2013).

Liquid refrigerant evaporating at a lower temperature chills the liquid entering the cooler. The refrigerant vaporizes and is drawn into the compressor, which increases the pressure and temperature of the gas so that it may be condensed at the higher temperature in the condenser. The condenser cooling medium is warmed in the process. The condensed liquid refrigerant then flows back to the evaporator through an expansion device. In the expansion device, some of the liquid refrigerant changes to vapor (flashes) as pressure drops; flashing cools the liquid to the saturated temperature at evaporator pressure (ASHRAE, 2012).

The flow rate necessary to deliver the full output of the heat source at a specific temperature drop can be found using equation below:

$$Q_{gpm} = \frac{q}{(8.01 \times \rho \times C \times \Delta T)} \tag{3.61}$$

where:

Q_{gpm} = Water volume flow rate (GPM)

q = Heat load (BTU/hr)

ΔT = Intended temperature drop (°F)

ρ = Fluid's density at the average system temperature (lb/ft^3)

C = the fluid's specific heat at the average system temperature (Btu/lb/°F)

8.01 = a constant

In small to medium size hydronic systems, the product of ($8.01 \times \rho \times c$) can be taken as 500 for water, 479 for 30% glycol, and 450 for 50% glycol. The total heat removed by air condition chilled-water installation can thus be expressed as (Bhatia, A., 2012):

$$q = 500 \times Q_{gpm} \times \Delta T \tag{3.62}$$

where

q = total heat removed (Btu/h)

Q_{gpm} = water flow rate (GPM)

ΔT = temperature difference (^{o}F)

The chiller model is based on EnergyPlus' chiller model, however we improved the accuracy of the formulas which simulates the thermal performance of an electric liquid chiller and the power consumption of its compressor using leaving condenser water temperature. This model requires the use of three chiller performance curves provided in the reference datasets of EnergyPlus, this research revised this model to incorporate our own specific chiller's application by developing our own performance curves utilizing a genetic algorithm to minimize the error to solve for the coefficients (a_i, b_i, c_i, d_i, e_i, *and* f_i) of the bicubic curves (*CAPFT*, *EIRFT*, *EIRFPLR*). See Figure 36 for the chiller model diagram.

See section 3.4 for the genetic algorithm and chapter 4 for model training and testing section. The model, developed by (Hydeman, M., N. Webb, et al., 2002) is an empirical model similar to EnergyPlus' chiller model (USDOE, 2012). The model in this research uses performance information at reference conditions along with three curve fits for cooling capacity and efficiency to determine chiller operation at off-reference conditions, similar to EnergyPlus,

however the curve fitting parameters are determined utilizing a genetic algorithm. The model provides improved accuracy over other chiller models.

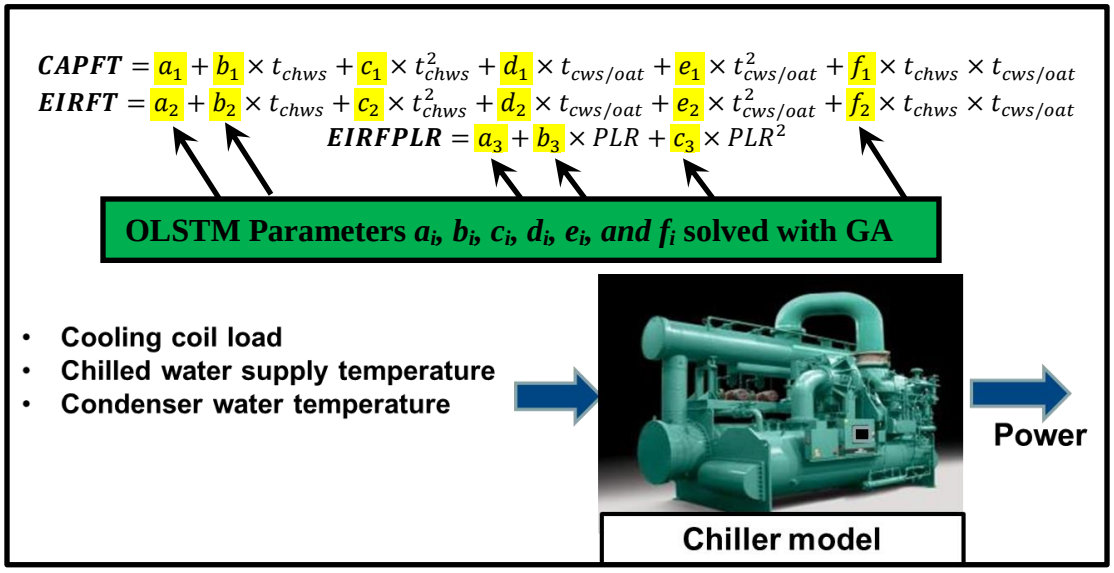

Figure 36. Chiller model diagram.

The Energy Input to Cooling Output function of Part Load Ratio (PLR) curve for this reformulated EIR chiller model includes the condenser leaving water temperature as an independent variable in addition to part-load ratio. The three performance curves are: (USDOE, 2012)

1. Cooling Capacity Function of Temperature Curve (*CAPFT*)
2. Energy Input to Cooling Output Ratio Function of Temperature Curve (*EIRFT*)
3. Energy Input to Cooling Output Ratio Function of Part Load Ratio Curve (*EIRFPLR*)

$$CAPFT = a_1 + b_1 \times t_{chws} + c_1 \times t_{chws}^2 + d_1 \times t_{\frac{cws}{oat}} + e_1 \times t_{cws/oat}^2 + f_1 \times t_{chws} \times t_{cws/oat} \quad (3.63)$$

$$EIRFT = a_2 + b_2 \times t_{chws} + c_2 \times t_{chws}^2 + d_2 \times t_{\frac{cws}{oat}} + e_2 \times t_{cws/oat}^2 + f_2 \times t_{chws} \times t_{cws/oat} \quad (3.64)$$

$$P = P_{ref} \times CAPFT\left(t_{chws}, t_{\frac{cws}{oat}}\right) \times EIRFT\left(t_{chws}, t_{\frac{cws}{oat}}\right) \quad (3.65)$$

$$\times EIRFPLR\left(QT, t_{chws}, t_{cws/oat}\right)$$

$$EIRFPLR = a_3 + b_3 \times PLR + c_3 \times PLR^2 \quad (3.66)$$

$$PLR = \frac{QT}{Q_{ref} \times CAPFT\left(t_{chws}, t_{cws/oat}\right)} \quad (3.67)$$

where:

CAPFT = a curve that represents the available capacity as a function of evaporator and condenser temperatures

EIRFT = a curve that represents the full-load efficiency as a function of evaporator and condenser temperatures

EIRFPLR = a curve that represents the efficiency as a function of the percentage unloading a given chiller performance model is defined by the regression coefficients (a_i, b_i, c_i, d_i, e_i, *and* f_i), the reference capacity (Q_{ref}), and the reference power (P_{ref}).

t_{chws} = the chilled water supply temperature (^{o}F),

$t_{cws/oat}$ = the condenser water supply temperature (^{o}F) for water-cooled equipment or the outdoor air dry-bulb temperature (^{o}F) for air-cooled equipment,

QT = the capacity (ton),

Q_{ref} = the capacity (ton) at the reference evaporator and condenser temperatures where the curves come to unity,

PLR = a function representing the part-load operating ratio of the chiller.

P = the power (kW) and

P_{ref} = the power (kW) at the reference evaporator and condenser temperatures where the curves come to unity.

The chiller model requires the optimal variable T_w which is the chilled water supply temperature (^{o}F) and the condensing chilled water temperature T_c which is approximately equal

to the wet-bulb temperature + 8 ^{o}F (for Water-Cooled chiller) however for this program the condenser water supply temperature (^{o}F) for water-cooled equipment was set at 85^{o}F for simplicity. The design chiller capacity (rating capacity) in tons ($Q_{nominal}$) is read from the worksheet System Design Information in the Excel file UserInput.xlsx. The chilled capacity available under the current conditions in tons ($Q_{available}$) is calculated by:

$$Q_{available} = CAPFT \times Q_{nominal} \tag{3.68}$$

PLR_c is a function representing the part-load operating ratio of the chiller calculated by:

$$PLR_c = \frac{q_{ct}}{(Q_{available} \times 12{,}000)} \tag{3.69}$$

q_{ct} is calculated in the cooling coil model. The Chiller power (kW) $P_{nominal}$ is calculated by:

$$P_{nominal} = Q_{nominal} \times 0.6 \tag{3.70}$$

The change in temperature entering and leaving the chiller (Δt) is found by:

$$\Delta t = T_c - T_w \tag{3.71}$$

If $\Delta t < 0$ (or negative) then Δt is equal to zero. The power (kW) P_{ref} at the reference evaporator and condenser temperatures where the curves come to unity is calculated by:

$$P_{ref} = P_{nominal} \times EIRFPLR \times EIRFT \times CAPFT \tag{3.72}$$

$$Power = P_{ref} \tag{3.73}$$

If $q_{ct} \leq 0$ (if cooling load is negative or zero) then power is equal to zero. If $Q_{available} < 0$ (if chilled capacity is negative) then power is equal to zero or $Q_{available} = 0$. If Power < 0 (if Power is negative) then Power is equal to zero, Power = 0. Standard efficiency e (or COP) is calculated by:

$$e = \frac{q_{ct}}{\left(\frac{12{,}000}{Power \times 3.51}\right)} \tag{3.74}$$

3.3.3.2 Hydronic model. The Reynolds Number (Re) is central to evaluating any form of flow when there are significant velocities involved. The Reynolds Number reveals the importance of the viscous effect related to the inertia effect. The Reynolds number is proportional to inertial force divided by viscous force. The flow is laminar if Re < 4000 or turbulent when Re > 4000. Reynolds Number can be expressed as:

$$R_e = \frac{DV\rho}{\mu} = \frac{d_h V}{720\nu} \tag{3.75}$$

where:

D = characteristic length (For a pipe or duct the characteristic length is the pipe or duct diameter, in inches)

V = velocity (ft/s)

ρ = density (lb/ft^3)

μ = dynamic (absolute) viscosity (Ns/m^2) or (lb$_m$/ft s)

ν = kinematic viscosity, ft^2/s

The hydraulic diameter is not the same as the geometrical diameter in non- circular ducts or pipes and can be calculated from the generic equation:

$$d_h = \frac{4A}{P} \tag{3.76}$$

where:

d_h = hydraulic diameter (in)

A = area section of the pipe (in^2)

P = wetted perimeter of the pipe (in)

The Friction Coefficient (λ) for fully developed laminar flow, where the roughness of the duct or pipe can be discarded, will depend only on the Reynolds Number, R$_e$ and can be expressed as:

$$\lambda = \frac{64}{R_e} \tag{3.77}$$

The Darcy-Weisbach equation is effective for fully developed, steady, incompressible flow. The friction factor or coefficient is contingent on the flow (if it is laminar, transient or turbulent from the Reynolds Number) and the roughness of the tube or duct. The friction coefficient can be determined by the Colebrook Equation or by using the Moody Diagram. The Darcy-Weisbach equation can be expressed as head loss:

$$\Delta h = \lambda \frac{L}{d_h}\left(\frac{v^2}{(2g)}\right) = \left(\frac{\Delta p}{\rho}\right)\left(\frac{g_c}{g}\right) = f\left(\frac{L}{D}\right)\left(\frac{V^2}{2g}\right) \quad (3.78)$$

where:

Δh = head loss (ft)

v = velocity (ft/s)

λ = friction coefficient

L = length of duct or pipe (ft)

g = acceleration of gravity (32.2 ft/s^2)

d_h = The hydraulic diameter is used for calculating the dimensionless Reynolds Number (Re) to determine if the flow is turbulent or laminar.

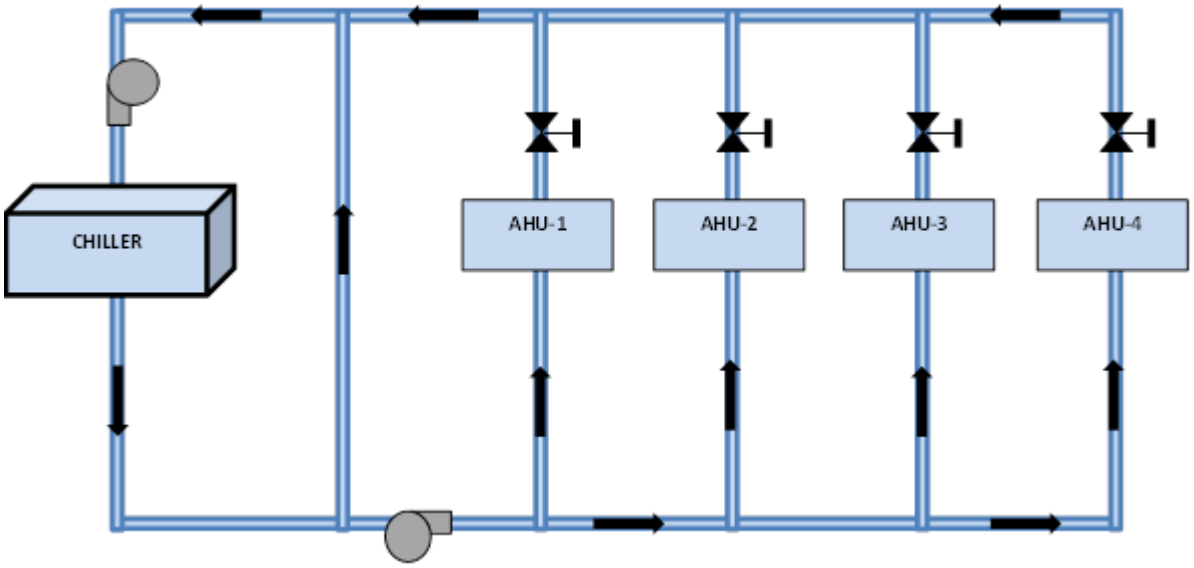

Figure 37. Typical head loss piping diagram for chiller to cooling coils in AHUs.

The Hydronic Model calculates the total pressure drop in the chiller's piping (see Figure 37) including information from the UserInput.xlsx spreadsheet and the imbedded worksheet labeled Design System where all the piping information is stored. The Darcy-Weisbach equation with friction factors from the Moody chart or Colebrook equation is fundamental to calculating pressure drop in chilled-water piping. Pressure drop caused by fluid friction in fully developed flows of all "well behaved" (Newtonian) fluids is described by the Darcy-Weisbach equation (ASHRAE, 2013):

$$\Delta p = f\left(\frac{L}{D}\right)\left(\frac{\rho}{g_c}\right)\left(\frac{V^2}{2}\right) \tag{3.79}$$

or

$$\Delta p_f = \left(\frac{12fL}{d_h}\right)(\rho)\left(\frac{V}{1097}\right)^2 \tag{3.80}$$

where:

Δp = pressure drop, lb_f/ft^2

Δp_f = friction losses in terms of total pressure, in. of water

f = friction factor, dimensionless

L = length of pipe, ft

D = internal diameter of pipe, ft

ρ = fluid density at mean temperature, lb_m/ft^3

V = average velocity, fps

g_c = units conversion factor, 32.2 ft lb_m/lb_f s^2

The density ρ of a fluid is its mass per unit volume. The densities of air and water at standard indoor conditions of 68°F and 14.696 psi (sea level atmospheric pressure) are ρ_{water} = 62.4 lb_m/ft^3, and ρ_{air} = 0.0753 lb_m/ft^3. In this form, the fluid's density does not appear explicitly (although it is in the Reynolds number, which influences *f*). The friction factor *f* is a function of pipe roughness ε, inside diameter *D*, and parameter Re. The friction factor is frequently

presented on a Moody chart giving *f* as a function of Re with *ε/D* as a parameter. A useful fit of smooth and rough pipe data for the usual turbulent flow regime is the Colebrook equation (ASHRAE, 2013):

$$\frac{1}{\sqrt{f}} = 1.74 - 2\log\left(\frac{2\varepsilon}{D} + \frac{18.7}{Re\sqrt{f}}\right) \tag{3.81}$$

or

$$\frac{1}{\sqrt{f}} = -2\log\left(\frac{12\varepsilon}{3.7D_h} + \frac{2.51}{Re\sqrt{f}}\right) \tag{3.82}$$

since *f* appears on both sides in this research it is obtained iteratively.

Valves and fittings cause pressure losses greater than those caused by the pipe alone. One formulation expresses losses as

$$\Delta p = K\left(\frac{\rho}{g_c}\right)\left(\frac{V^2}{2}\right) \; or \; \Delta h = K\left(\frac{V^2}{2g}\right) \tag{3.83}$$

Where *K* = geometry- and size-dependent loss coefficient known as *K* Factors. The loss coefficient for valves appears in another form as C_v, a dimensional coefficient expressing the flow through a valve at a specified pressure drop (ASHRAE, 2013).

$$Q_{gpm} = C_v\sqrt{\Delta p} \tag{3.84}$$

where:

Q_{gpm} = volumetric flow, gpm

C_v = valve coefficient, gpm at Δp = 1 psi

Δp = pressure drop, psi

The Hydronic Model uses the above formulas and reads data specific to the HVAC system in the UserInput.xlsx spreadsheet that defines the systems chilled water piping. Pipe roughness, length, diameter, number of elbows, tees and valves, pressure drop across the chiller (D_{pw}) and *K* factor and C_v tables are loaded into this routine. The Reynolds number, Relative roughness, Colebrook equation, Darcy-Weisbach equation (*DWE*), pressure loss for connections

($PL_{connections}$), and the pump affinity laws (PAL) are all calculated and the total pressure is finally obtained.

$$P_{total} = DWE + PL_{connections} + PAL + D_{pw} \quad (3.85)$$

3.3.3.3 Pump model. For a detailed explanation of the pump model see the fan and pump models section 3.3.2.3. This is a new model that includes an iterative process that applies to both pumps and fans. This model will allow the user to select any two variables as model inputs (MI) or model outputs (MO) among four variables of flow (water) Q, total pressure P, speed N, and power W. This is compared to well know simple and detailed models from HVAC 2 Toolkit, that uses the perfect pump laws through the application of dimensionless flow (ϕ) and pressure (ψ) coefficients. The only fundamental difference is in the calculation of fluid properties. The model was programmed in MATLAB to include an iterative process to tune the flow and head coefficient parameters. Energy consumption (kWh) is equal to power (kW) input multiplied by operating hours. The kW input will depend on the motor efficiency and pump power requirement (1 kW = 0.746 HP). The pump model relies on:

- pressure balancing
- flow performance
- water flow loop pressure drop characteristics
- power and pressure rise vs. volumetric flow
- dimensionless performance curve
- pressure rise or head and efficiency to fluid flow rate
- pressure rise across the device
- shaft power requirements at a given fluid flow rate
- pump affinity laws for changes in speed, density, and diameter

- nominal operating speed
- entering fluid density
- wheel diameter

3.4 Genetic Algorithm for Tuning Model Parameters.

A genetic algorithm (GA) is a familiar method exercised to find accurate solutions to optimization problems. These algorithms use iterative techniques instinctive to biology such as inheritance, mutation, selection and crossover. GAs are implemented using a computer's advanced computational capacity in which a population of theoretical representations (chromosomes) of solutions to an optimization problem that iteratively advances toward improved results. The evolution starts from a population of randomly generated solutions or individuals (in our research the optimal variable range) and occurs in periods which are called generations. In each generation, the fitness of every individual in the population is evaluated; multiple individuals are randomly selected from the current population based on their fitness, and altered to obtain a new population. This last population is then used in the next iteration of the algorithm. The algorithm terminates when either a maximum number of generations has been calculated, or an adequate fitness level has been attained for the population.

The EMCS collects the measured data "real data" from components or subsystems. At the same time the models integrated into the EMCS compute outputs from which a set of "estimated data" is obtained. The parameters of the models are tuned by a genetic algorithm (GA) at each sample time such that the error between the real and estimated data is minimized. It is expected that the OLSTM with updated parameters will better match the real behavior of the subsystems and overall system. Since the OLSTM is always tuned using online real data, the optimal values lead to the best performance of the HVAC system. At each time interval (15 minutes), the

genetic algorithm is used for tuning the model parameters by reducing the error between measured and estimated sample data S (real and estimated data) taken from previous periods. The component models are then used for determining optimal set points for the next operating interval J (next 15 min).

The OLSTOP including the component models for the chiller and cooling coil all use genetic algorithms (GA), and the fan and pump component models use a new iterative process. Given a set of measured data (MD) and estimated data (ED) for a sample S, the model parameters can be tuned with respect to the reference value δ_{ref} by the genetic algorithm optimization method as follows:

$$\delta_i \rightarrow \delta_i + a_i \cdot \delta_{ref,i} \tag{3.86}$$

where the term a_i is the tuning parameter included in the model. The reference value δ_{ref} could be the design value or any other value with a significant impact on the process. The tuning parameters of model a_i are determined by the genetic algorithm (GA) to minimize the error (least squares error) between the estimated and real data. The GA objective function f (least squares error), which should be minimized, is written as:

$$f = \sqrt{\frac{\sum_{k=1}^{n=size(S)} (MD_k - ED_k)^2 \cdot \lambda^k}{n}} \tag{3.87}$$

where n is the size of the data S. The term λ ($0 < \lambda < 1$) is a forgetting factor to give higher weight to more recent data (k = 1) than older data (k = n = size (S)).

Figure 38 shows the flowchart of genetic algorithm (GA) for parameter tuning. The GA starts with a random generation of the initial population (initial solution). The problem variables (model parameters a_i) are encoded to form a chromosome (a string of variables) that represents an individual (one solution) in the population. The performance or objective function *f* of each

individual of the first generation is estimated. The second generation is generated using operations on individuals such as selection, crossover, and mutation, in which individuals with higher performance (fitness) have a greater chance to survive.

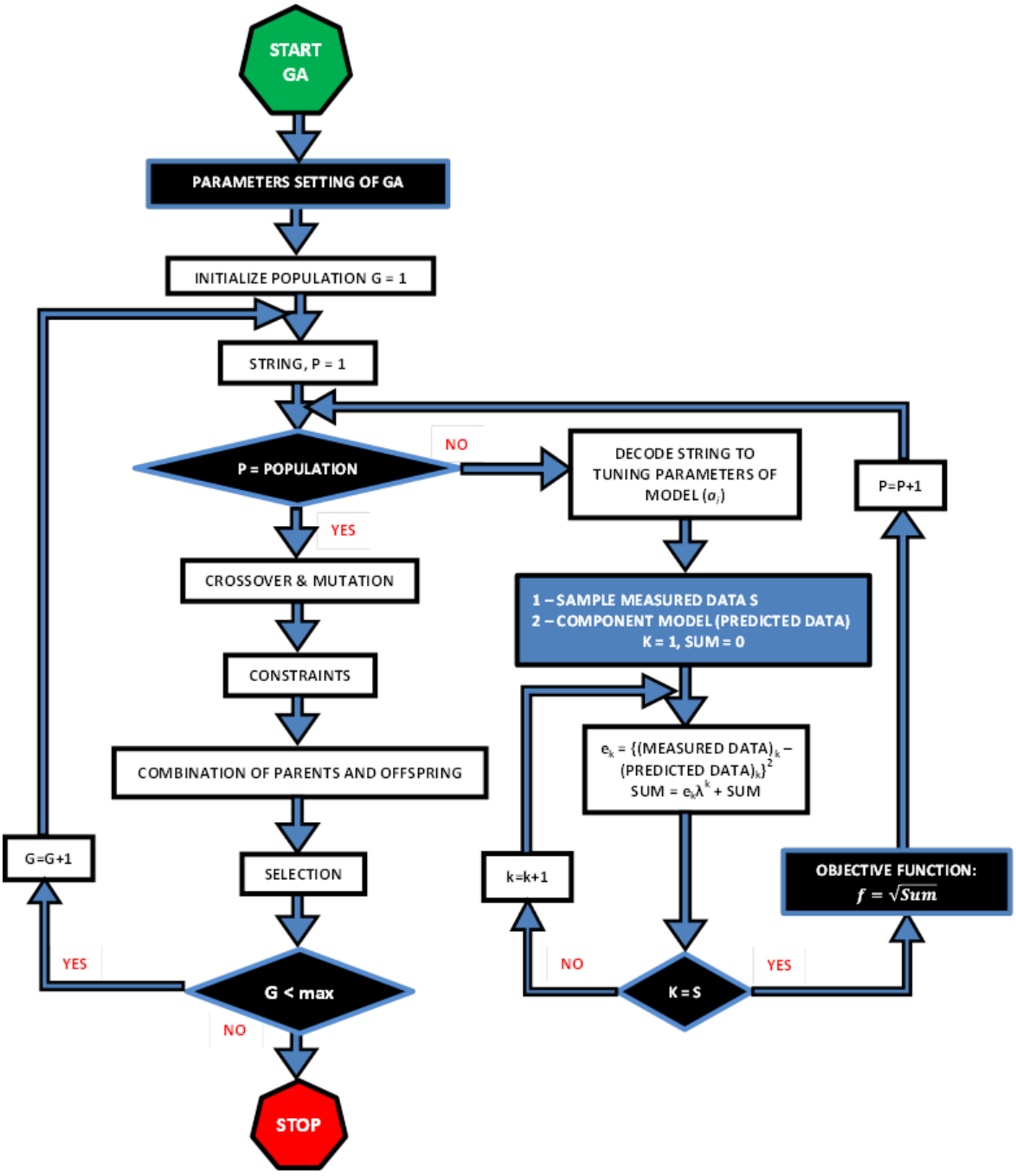

Figure 38. Genetic algorithm objective function = minimum error.

The performance of each new individual is again evaluated. The process is repeated until the maximum number of generations (G_{max}) is reached. After two offsprings are created using the crossover and mutation operators, they are compared with both of their parents to select two best solutions among the four parent–offspring solutions. To control the rate of tuning, the genetic algorithm search is restricted to the range of [I, +I], for instance [0.1, 0.1]. Since the design value is used as the reference value, the tuning parameters should be always in the range of [1, +1] (Nassif, N., S. Moujaes, et al., 2008).

3.5 Optimization Process

The optimization process including the genetic algorithm with minimum energy use as its objective function is the main program and objective of this research. The dynamic OLSTOP was evaluated using data from an existing VAV system, see schematic of the system in Figure 39.

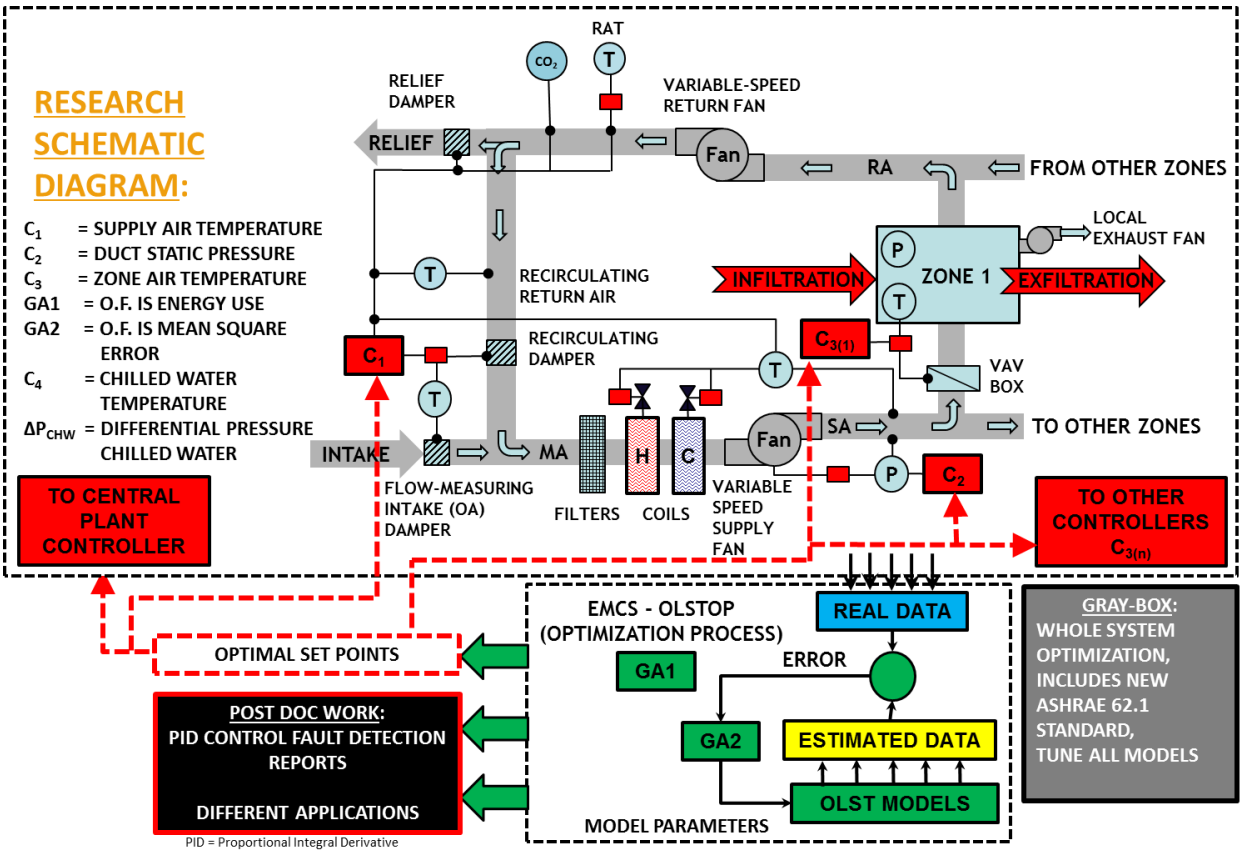

Figure 39. Research schematic diagram.

The optimization process adjusts the system for optimal energy performance over a period of 15 min (optimization period). During this short optimization period, the loads and outdoor air conditions are assumed to be constant and recorded from the measured data collected during the previous time step. The genetic algorithm is used to find the energy use by each component and then the total energy use in response to the controller set points and operating modes. The inputs are the controller variable set points (problem variables) and the output is the energy use (objective function).

3.5.1 Optimization process model. The Optimization Process Model incorporates the genetic algorithm tool in MATLAB. This process optimizes the variables at each time step from the UserInput.xlsx spreadsheet for supply temperature (T_s), duct static pressure (P_s), chilled

water temperature (T_w) and the pressure drop of the chilled water (D_{pw}). Optimizing these variables reduces the energy consumption or power for each specific time and generates an output file called UserOutput.xlsx. This output file gives the optimum variables at the specified time generated by the genetic algorithm and calculates the total power, chiller power, pump power, fan power, reheat, power penalty, and constraints. This output is then used to generate graphical images to further prove the energy savings.

The OP program controls the generations and population settings for the genetic algorithm and initiates the HVAC Simulation Model. The user output file is generated by xlswrite syntax and the user interface is also created in the optimization model.

At each optimization period (15 minutes), the genetic algorithm sends the controller's optimal set point variables to the VAV system model, where the energy use and thermal comfort (objective functions) are simulated and returned back to the OP model. The HVAC Simulation model determines the energy use and thermal comfort resulting from the time step change in outdoor and indoor load conditions (independent variables) and the controller set points (dependent variables). The multiple computations involved with both the OLSTM and the optimization process require ten minutes on a desktop computer with an Intel Core 2 Duo processor. In the OLSTOP there are approximately 100 variables and depending on how many generations are specified in the genetic algorithms for the STM and the OP, and how many data points for the iterative process in the fan and pump STM, there can be over 1,000 computations. This computation time allows the optimization process to be implemented online. The time could be decreased using a newer computer with a faster processor and smaller generations and population size with the genetic algorithms.

In simulation and optimization computations, the OLSTM of the HVAC system includes the individual component models that impact the objective functions (lowest error and minimal energy use). To simulate the responses of the HVAC system to the deviations in outdoor and indoor load conditions, which gradually fluctuate, compared to the optimization period (15 minutes), the steady state model can be managed. The developed models and a summary of calculations include:

- System Calculation Model – Zone mixed air humidity ratios, return and mixed air temperatures, and economizer section
- Chiller Model – chiller power based on EnergyPlus but improved accuracy with GA
- Constraint Model – constraint and power penalty calculations
- Cooling Coil Model – cooling coil with GA
- Fan Model – fan power with GA
- HVAC Simulation Model – calls all subroutines and data files and calculates total power
- Hydronic Model – flow parameters, piping, fittings, pressure drop
- Optimization Process Model – genetic algorithm (GA) to find optimal variables
- Pump Model – pump power with GA
- Total Pressure Model – static pressure from system design information
- VAV System Model – pulls all air-side subroutines and programs together with optimal variables
- Central Plant Model – pulls all water-side subroutines and programs together with optimal variables
- Ventilation Model – ASHRAE 62.1-2013 Ventilation Fresh Air Requirement Calculations

- Zone Model – calculates zone requirements and reheat loop
- Psychrometric Routines and Calculations – all required conversions and variables for all subroutines

3.5.1.1 HVAC simulation model. The HVAC Simulation Model calls all the sub-programs (Total Power, Chiller Power, Pump Power, Fan Power, Reheat, Power Penalty, and Constraint). It also reads all of the system data from the UserInput.xlsx spreadsheet. The final calculation for the overall HVAC system energy use or power consumption is calculated in this routine.

$$P_{total} = P_{chiller} + P_{pump} + P_{CTfan} + P_{fan} + P_{reheat} + P_{penalty} \quad (3.88)$$

3.5.1.2 Genetic algorithm for optimization process. In this research, a genetic algorithm search method based on the mechanics of Darwin's natural selection theory was developed to solve the optimization problem. Since energy use and thermal comfort are the objective functions, a genetic algorithm is investigated, see Figure 40.

Using the VAV model, the energy use and thermal comfort are determined. As a result of the constraint functions, a penalty must be imposed on the objective functions. The constraint violation is calculated using the penalty function approach. For a description of how a genetic algorithm work please review the GA section 3.4 of this chapter.

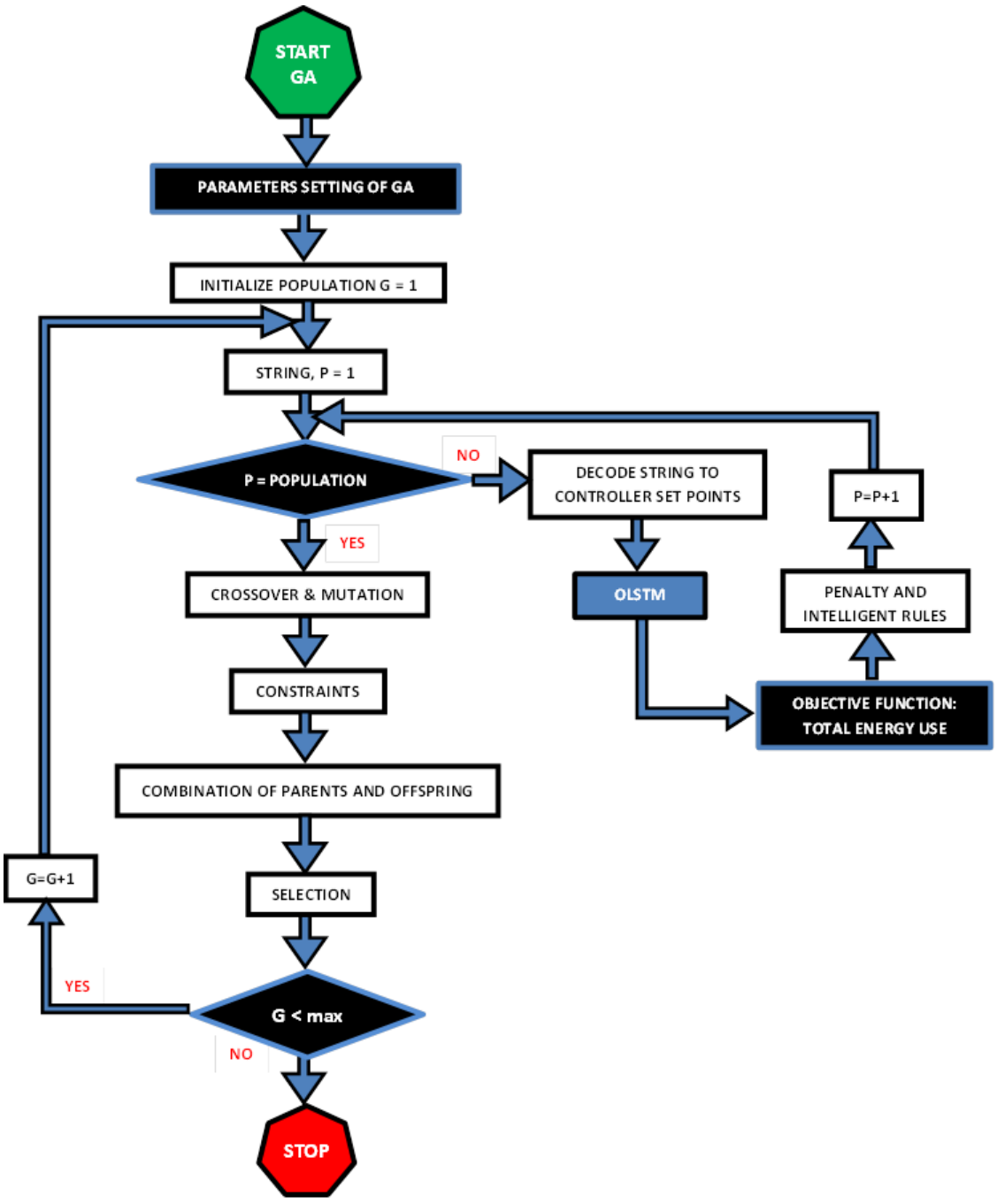

Figure 40. Genetic algorithm objective function = minimum total energy use.

3.5.2 User input. For the OLSTOP testing procedure we simulated the New Academic Classroom Building in eQuest and utilized the building simulation to generate the loads required for the OP to calculate the optimal set point variables. We exported, sorted, and stored the eQuest data including the loads in a file called UserInput.xlsx which is a spreadsheet and it has all of the building model simulated data that the program reads. The information stored in this file is massive and includes every time step's information for all cooling loads, outdoor conditions, system, and zone information.

Table 7

Loads Worksheet from User Input Spreadsheet

May 28, 11am	**Total**	**Sensible**	**Latent**
Zone	**Kbtu**	**Kbtu**	**Kbtu**
1	38630.1	32051.7	6578.38
2	40091.1	33512.8	6578.38
3	37250.7	30672.3	6578.38
4	38168.7	31590.3	6578.38
5	60083.3	46021.5	14061.8
6	41992.2	35413.8	6578.38
7	43258.9	36680.5	6578.38
8	40785.6	34207.2	6578.38
9	40992.2	34413.9	6578.38
10	63348.5	49286.7	14061.8
11	41992.2	35413.8	6578.38
12	43258.9	36680.5	6578.38
13	40785.6	34207.2	6578.38
14	40992.2	34413.9	6578.38
15	63348.5	49286.7	14061.8

Several worksheets are stored in the spreadsheet labeled: Loads, Outside Conditions, Design Zone Information, and System Design Information. The worksheet labeled Loads has the simulated building model's total load (BTU), sensible load (BTU), and latent load (BTU) per zone stored hourly for the entire year. Obviously, in a real implemented scenario running the

OLSTOP in a BAS the loads would be calculated based on the previous time step's data (15 minutes). See Table 7 showing the cooling loads from 15 zones of the building during one time step on May 28 at 11 am.

The next worksheet labeled Outside Condition has the outside dry bulb, wet bulb temperatures and relative humidity for the building's location recorded hourly for the entire year. See Table 8 showing the outdoor conditions during one time step on May 28 at 11 am.

Table 8

Outside Conditions Worksheet from User Input Spreadsheet

Dry Temp	WetBulb	RH
°F	°F	%
55	53	70

The worksheet labeled Design Zone Information has each zone's temperature, airflow rate, area, number of occupants, Ra (cfm/sf), and Rp (cfm/person). See Table 9 showing the design zone information during one time step on May 28 at 11 am.

The worksheet labeled System Design Information has the chiller efficiency, C, P_{sd}, Chiller design tonnage, and the flow parameters including length of pipe, pipe roughness (e), number of elbows and tees, pressure drop across the chiller (D_{Pch}), pipe diameter, flow gpm, and water differential loop pressure.

3.5.3 User output. The UserOutput.xlsx spreadsheet has the four optimal variables (T_s, P_s, T_w, D_{pw}) and the Energy used at that specific time interval including Total Power, Chiller Power, Pump Power, Fan Power, Reheat, Power Penalty, and number of Constraints. The output file is automatically generated at the end of the optimization process and saved in the optimization process file folder.

Table 9

Design Zone Information Worksheet from User Input Spreadsheet

Zones	Tz °F	Airflow cfm	Area Az sq ft	Population Pz number	OAR/Az Ra cfm/sf	OAR/Pz Rp cfm/per	OAR BZ Vbz CFM
1	75	4277	2973	21	0.06	5	285.31
2	75	4067	2973	20	0.06	5	280.06
3	75	4067	2973	20	0.06	5	280.06
4	75	4270	2973	21	0.06	5	285.13
5	75	3323	4775	116	0.06	7.5	1158.79
6	75	5346	2973	27	0.06	5	312.03
7	75	4800	2973	24	0.06	5	298.38
8	75	3363	2973	17	0.06	5	262.46
9	75	5146	2973	26	0.06	5	307.03
10	75	4258	4775	149	0.06	7.5	1404.23
11	75	5346	2973	27	0.06	5	312.03
12	75	4800	2973	24	0.06	5	298.38
13	75	3363	2973	17	0.06	5	262.46
14	75	5146	2973	26	0.06	5	307.03
15	75	4258	4775	149	0.06	7.5	1404.23
		65830					7457.57

3.5.3.1 User interface. The user interface section will be further developed during post-doc work. The initial testing mimics the UserOutput.xlsx information. However, further development will allow a user friendly interactive interface that will allow different HVAC system configurations and specifications to be entered as well as large data files for annual loads, outside conditions, etc. from BAS and then the optimal variables will be generated. See the diagram in Figure 41 that shows the User Interface, with the results of one time step, which automatically “pops-up” on the computer screen after the optimization program has run in MATLAB.

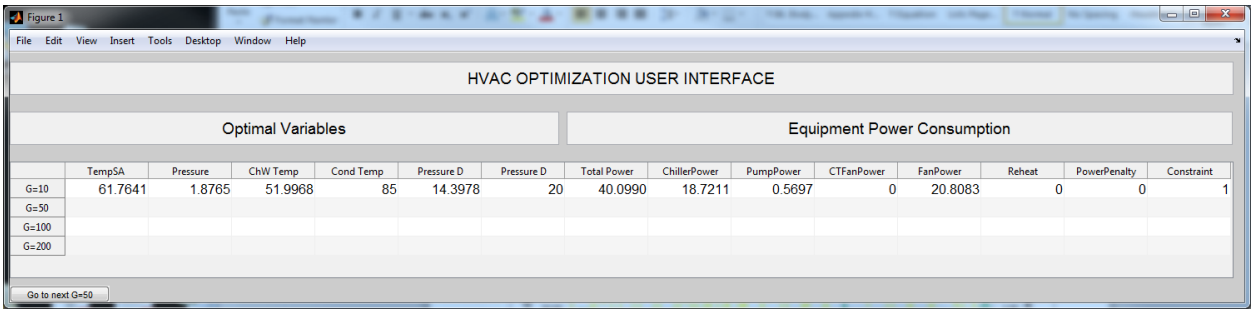

Figure 41. User interface from optimization process.

CHAPTER 4

Model Training and Testing

4.1 Model Training and Testing

A great majority of modern buildings are equipped with Energy Management and Control Systems (EMCS) which monitor and collect operating data from different components of heating ventilating and air conditioning (HVAC) systems. Models derived and tuned by using the collected data can be incorporated into the EMCS for online prediction of the system performance. HVAC component models with self-tuning parameters were developed and validated in this research. The model parameters were tuned online using genetic algorithms, which minimizes the error between the measured and estimated performance data as its objective function. The research also includes tools that analyze the thermal loads and incorporate ASHRAE's new ventilation load requirements and the optimization process that optimized the set point variables employing a genetic algorithm to minimize energy use as its objective function.

Empirical validation was employed in which the calculated results from the OLSTM's programs, subroutines, and algorithms were compared to monitored data from a real building. Analytical verification was also exercised in which the outputs from the OLSTM's programs, subroutines, and algorithms were compared to the results from known analytical solutions and the generally accepted numerical methods for similar building conditions in eQuest and EnergyStar simulation programs. Data from an existing VAV system was collected over the year. The data was randomly divided into two types of samples: 80% for training and 20% for validation. Data was then utilized for model testing and accuracy. The OLSTM's performance was measured by the coefficient of variation *CV*, which is defined as the ratio of the standard

deviation to the mean, $CV = \frac{\sqrt{\frac{\sum_{i=1}^{n}(Real\ data - Simulated\ data)^2}{n}} = standard\ deviation}{mean}$. The developed component models included:

- Fan Model (iterative process, IP)
- Pump Model (IP)
- Chiller Model (genetic algorithm, GA)
- Cooling Coil Model (GA)

The results of the model training, validation, and testing was graphed and analyzed. The testing results show how well the models capture the system performance and were used for the calculations required for the optimization process.

4.1.1 Fan and pump model training and testing. The proposed model is based on numerical analysis and an interpolation technique for the data obtained by the principle fan laws. This model will allow the user to select any two variables as model inputs (*MI*) or model outputs (*MO*) among all four variables of air flow *Q*, total pressure *P*, speed *N*, and power *W*. The model needs at least two different operating points for calibrations, obtained from manufacturer's data (*MD*) or measurements. The procedure to find the model output (*MO*) is described below.

Given: *MD =[Q, P, N, W] = [Flow, Pressure, Speed, Power]*

Inputs: *MI = [MI_1,MI_2] = [P,N], [Q,P], [Q,N], [P,Q], or etc.*

Outputs: *MO =[MO_1,MO_2] = [Q,W],[N,W],[P,W],[W,N],or etc.*

To find the outputs, the internal variables (*IV*) are first generated from fan laws and using one variable of the input (MI_1): *IV = fan laws (MD, MI_1).* Second, the model outputs *MO* are then found from any interpolation/extrapolation techniques such as linear or polynomial interpolation: *MO=interpolation/extrapolation (IV, MI_2).* Three examples below show the implementation of these procedures.

In example 1, it is assumed that there are two operating points (A_1 and A_2) obtained from the manufacturer's data or by performing on-site measurements. Those points are used for the model calibration and depicted in Figure 42 that also shows typical fan characteristic performance curves. The operating points (A_1 and A_2) contain the measured variables of flow rates (Q_{A1} and Q_{A2}), total static pressures (P_{A1} and P_{A2}), fan speed (N_{A1} and N_{A2}) and fan power (W_{A1} and W_{A2}). Thus, the objective is to find the airflow rate Q_{B0} and fan power W_{B0} (point B_0) from the total fan pressure P_{B0} and speed N_{B0}. Available data for calibrations A_1 and A_2:

$$MD = [Q_{A1,} P_{A1,} N_{A1,} W_{A1}, Q_{A2}, P_{A2}, N_{A2}, W_{A2}]$$

Inputs: total fan pressure P_{B0} and speed N_{B0}, $MI = [P_{B0}, N_{B0}]$.

Outputs: the airflow rate Q_{B0} and fan power W_{B0}, $MO = [Q_{B0}, W_{B0}]$

IV = internal variables generated from fan laws (B_1 and B_2) using the input fan static pressure (P_{B0}) where ($P_{B0} = P_{B1} = P_{B2}$) see Figure 42:

$$Q_{B1} = Q_{A1}\left(\frac{P_{B0}}{P_{A1}}\right)^{0.5}, Q_{B2} = Q_{A2}\left(\frac{P_{B0}}{P_{A2}}\right)^{0.5} \quad (4.0)$$

$$W_{B1} = W_{A1}\left(\frac{P_{B0}}{P_{A1}}\right)^{1.5}, W_{B2} = W_{A2}\left(\frac{P_{B0}}{P_{A2}}\right)^{1.5} \quad (4.1)$$

$$N_{B1} = N_{A1}\left(\frac{P_{B0}}{P_{A1}}\right)^{0.5}, N_{B2} = N_{A2}\left(\frac{P_{B0}}{P_{A2}}\right)^{0.5} \quad (4.2)$$

To find the variables of the point B_0, an interpolation technique such as linear or polynomial interpolation is used. Both the linear and polynomial interpolation techniques were tested and the results were about the same. Thus, to simplify our discussions, only the linear technique is discussed. Thus, the model outputs (B_0) are:

$$Q_{B0} = \frac{N_{B2} - N_{B0}}{N_{B2} - N_{B1}} \times Q_{B1} + \frac{N_{B0} - N_{B1}}{N_{B2} - N_{B1}} \times Q_{B2} \quad (4.3)$$

$$W_{B0} = \frac{N_{B2} - N_{B0}}{N_{B2} - N_{B1}} \times W_{B1} + \frac{N_{B0} - N_{B1}}{N_{B2} - N_{B1}} \times W_{B2} \tag{4.4}$$

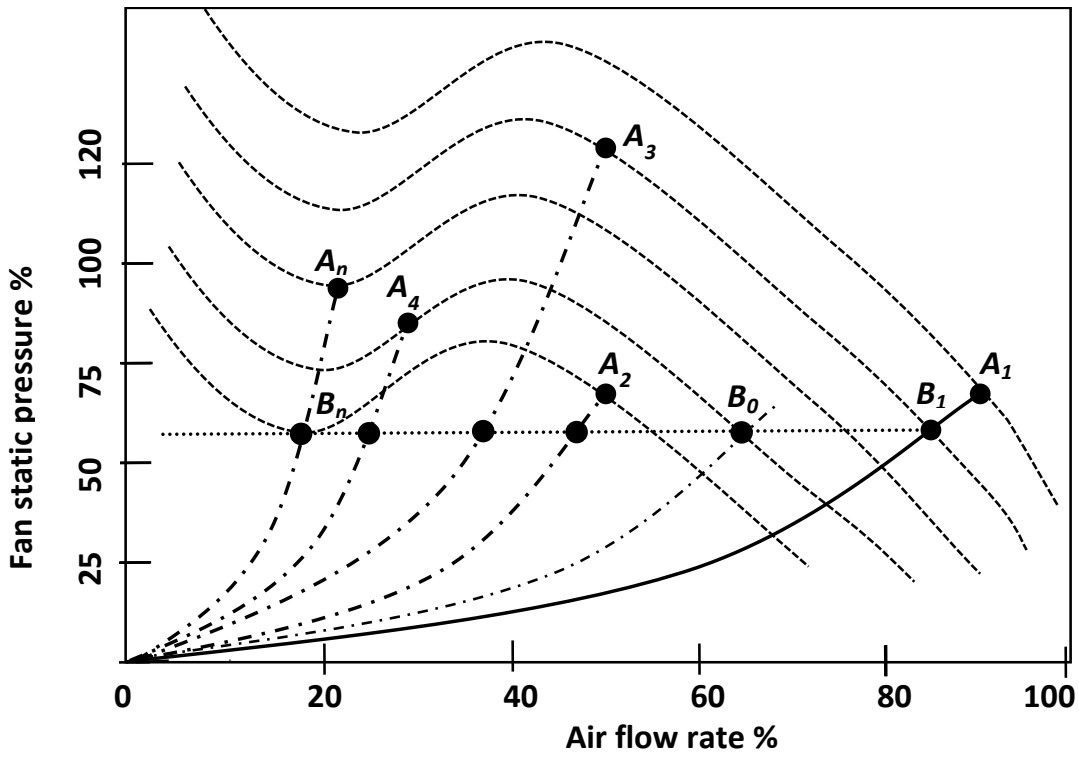

Figure 42. Fan and System Performance Curves.

In example 2, a set n of operating data is available for the model calibration:

$MD = [A_1, A_2, \ldots, A_n]$, measured data $A_1, A_2, \ldots, A_n$:

where:

$$A_n = [Q_{An}, P_{An}, N_{An}, W_{An}]^T$$

$$MI = [P_{B0}, N_{B0}]$$

$$MO = [Q_{B0}, W_{B0}]$$

The procedure to find the outputs (airflow rate Q_{B0} and fan power W_{B0}) is described below.

The data are first generated from fan laws based on input fan static pressure P_{B0}:

$$Q_{Bi} = Q_{B0}\left(\frac{P_{B0}}{P_{Bi}}\right)^{0.5}, W_{Bi} = W_{B0}\left(\frac{P_{B0}}{P_{Bi}}\right)^{1.5}, N_{Bi} = N_{B0}\left(\frac{P_{B0}}{P_{Bi}}\right)^{0.5} \tag{4.5}$$

for $i=1,\ldots..n$

Then, using linear interpolation, the model outputs are:

$$Q_{B0} = \frac{N_{Bi+1} - N_{B0}}{N_{Bi+1} - N_{Bi}} \times Q_{Bi} + \frac{N_{B0} - N_{Bi}}{N_{Bi+1} - N_{Bi}} \times Q_{Bi+1} \tag{4.6}$$

where $Q_{Bi} < Q_{B0} < Q_{Bi+1}$

$$W_{B0} = \frac{N_{Bi+1} - N_{B0}}{N_{Bi+1} - N_{Bi}} \times W_{Bi} + \frac{N_{B0} - N_{Bi}}{N_{Bi+1} - N_{Bi}} \times W_{Bi+1} \tag{4.7}$$

where $W_{Bj} < W_{B0} < W_{Bj+1}$

The proposed model is first evaluated using a set of fan performance data obtained from two different manufacturers A and B for roof top unit packages with capacity ranging from 2 tons to 20 tons (7 kW to 70.2 kW). Second, the model is validated against data collected from an existing system. The simple fan model (*SFM*) and detailed fan model (*DFM*) described in Chapter 3 are also considered along with the proposed fan model (*FM*). The coefficient of variance (*CV*) is used as a statistical index for the model accuracy. In the evaluation process, different sizes of data required for the model calibration are considered with three cases of variable combinations (Table 10):

Table 10

Fan Model Case Numbers

Case Number	Pressure (*P*)	Speed (*N*)	Airflow (*Q*)	Power (*W*)
I	Input	Input	Output	Output
II	Input	Output	Input	Output
III	Output	Input	Input	Output

To evaluate the model using the manufacturers' data, first three data points (n = 3) with low, medium, and high airflow rates for model calibration are selected from the available set of manufacturers' data (120 operating points). Then the model is validated against the remaining data (120 – 3 = 117). Figure 43 and Figure 44 show a comparison of the power and pressure obtained from manufacturer's data of a 15 ton (52.7 kW) package unit and simulated by FM,

SFM, and DFM. The straight line is a one-to-one line, indicating agreement between the actual and simulated data.

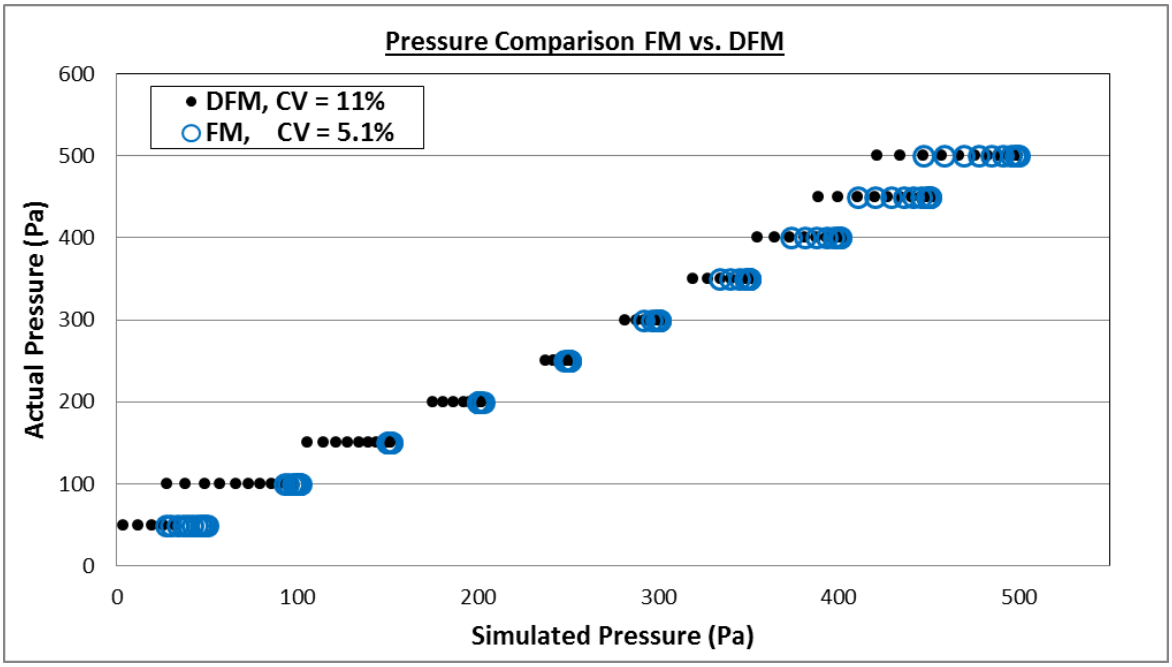

Figure 43. A pressure comparison of a 15 ton unit: FM and DFM.

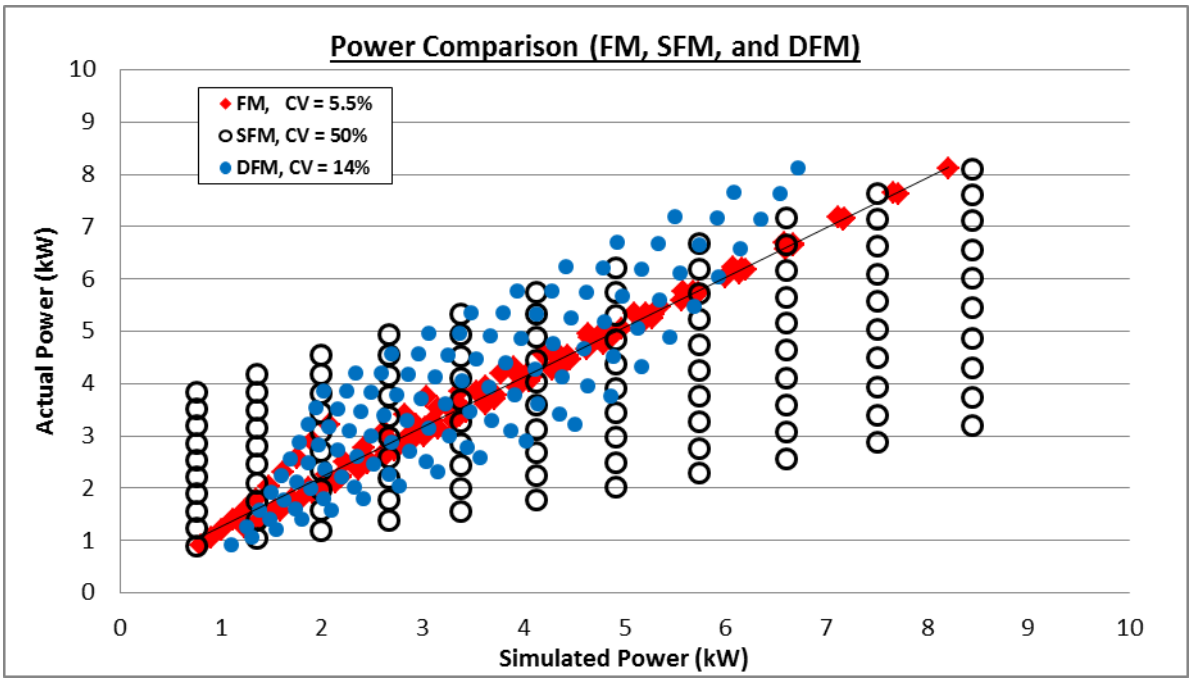

Figure 44. A power comparison of a 15 ton unit: MD, FM, SFM, and DFM.

As discussed before, the simple model is based on finding only the power as a function of airflow rate and the model does not respond to the variations of pressure at any given flow. As the manufacturer's data includes a set of power and pressure combinations at a given flow, the simple model produces always the same power and does not respond to the pressure variations. The SFM fails to follow the variation of the fan pressure at a given airflow rate, and the model errors are very large (the coefficient of variance *CV* is around 50%). The detailed model DFM can improve the results, and the simulated power somewhat follows the pressure patterns. Similarly, the proposed fan model FM can further improve the results and the *CV* drops to 5.5% when only three data points ($n = 3$) are used for calibration. However, the simple model needs four different operating points ($n = 4$), and the detailed model uses five points ($n = 5$) to find the polynomial coefficients. The accuracy of the proposed model depends on the size n of data used for calibration, for instance, by using four data points n = 4 instead of three n = 3, the *CV* will drop to 1.52%. Figure 45 shows the variations of *CV* due to the size n for a 15 ton package unit (for airflow rate of Case-I and Manufacturer A).

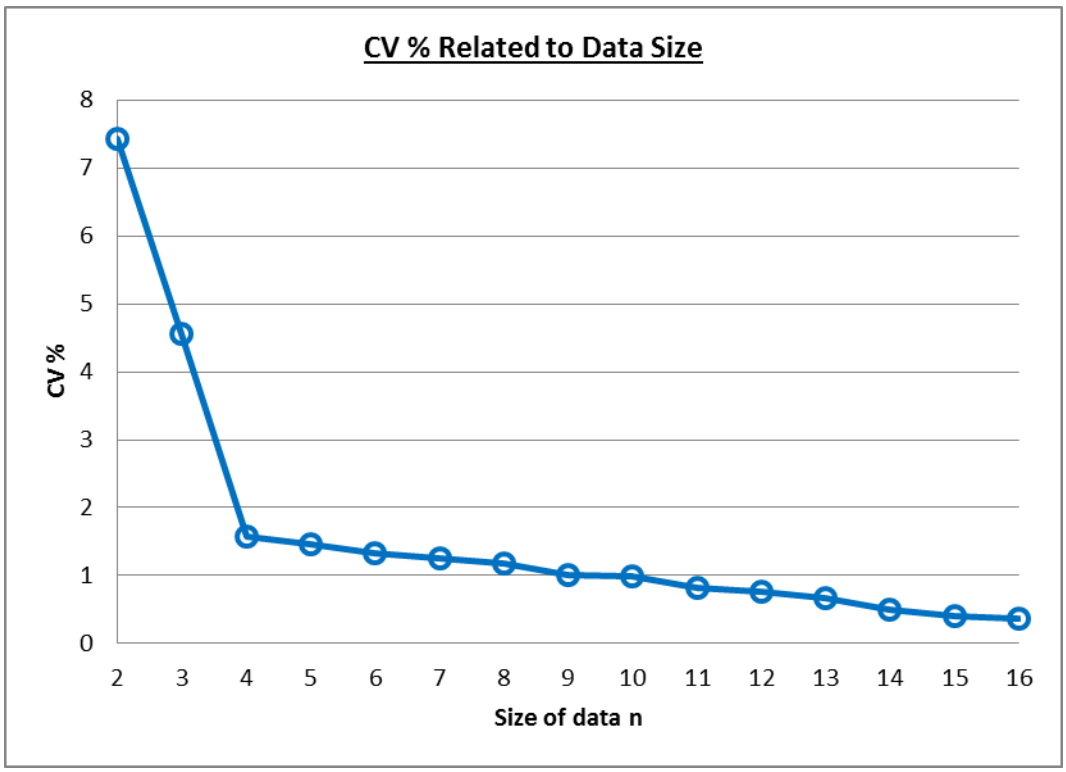

Figure 45. The CV for the 15 ton unit for airflow rate of case I & mfr. A.

The accuracy increases significantly with a larger set of data *n* used for model calibration, as a small interval will be used for interpolation.

Table 11 and Table 12 show the *CV*s resulted by comparing the airflow rates obtained from two different manufacturers and simulated by the proposed model for various sizes of rooftop package units. The tables show the *CV* for case-I and only for the airflow rate outputs, whereas the results of other cases are summarized in Table 13.

The average *CV* and the standard deviation STDs of the *CV*s are determined from the *CV*s' values obtained from various sizes of the package units (2 tons to 20 tons). It also includes the results from the detailed fan model calibrated by five operating points $n = 5$. In case-I, the detailed fan model DFM simulates the airflow rate using the iteration technique. Initial value of air flow rate is assigned and then the calculation is repeated until convergence.

Table 11

Case I Airflow Rate CVs from Manufacturer (A) simulated by the proposed model

Airflow Rates Coefficient of Variance Manufacturer A					
Unit Size	**Data Size**	**Size n = 2**	**Size n = 3**	**Size n = 5**	**Size n = 10**
2 tons (7 kW)		7.02	4.22	1.46	0.95
3 tons (10.5 kW)		8.34	5.67	1.12	0.98
4 tons (14 kW)		7.01	5.11	1.90	1.01
5 tons (17.6 kW)		6.55	4.99	1.22	0.97
6 tons (21.1 kW)		6.77	4.89	1.38	1.14
7.5 tons (26.3 kW)		8.21	5.35	1.77	1.11
8.5 tons (29.8 kW)		7.89	4.87	1.16	1.15
10 tons (35.1 kW)		6.88	4.76	1.67	1.33
12.5 tons (43.9 kW)		7.55	5.37	1.01	0.94
15 tons (52.7 kW)		7.42	5.55	1.51	1.19
17 tons (59.7 kW)		7.36	5.01	1.88	1.44
18 tons (63.2 kW)		6.87	4.66	1.57	1.03
20 tons (70.2 kW)		6.99	4.44	1.31	1.23
Average		7.30	4.99	1.46	1.11
Standard Deviation		0.54	0.41	0.28	0.15

Table 12

Case I Airflow Rate CVs from Manufacturer (B) simulated by the proposed model

Airflow Rates Coefficient of Variance Manufacturer B					
Unit Size	**Data Size**	**Size n = 2**	**Size n = 3**	**Size n = 5**	**Size n = 10**
2 tons (7 kW)		7.32	4.12	1.53	1.08
3 tons (10.5 kW)		9.78	4.89	1.11	1.11
4 tons (14 kW)		8.81	5.75	1.53	1.04
5 tons (17.6 kW)		7.89	5.11	1.88	1.03
6 tons (21.1 kW)		7.24	5.01	1.56	1.27
7.5 tons (26.3 kW)		6.89	5.43	1.88	1.26
8.5 tons (29.8 kW)		6.49	4.22	1.77	1.33
10 tons (35.1 kW)		7.81	5.76	1.04	1.49
12.5 tons (43.9 kW)		8.35	5.33	1.54	0.96
15 tons (52.7 kW)		8.32	5.66	1.54	1.12
17 tons (59.7 kW)		6.89	5.23	1.12	1.54
18 tons (63.2 kW)		7.17	4.75	1.07	1.36
20 tons (70.2 kW)		6.56	4.56	1.55	1.44
Average		7.99	5.06	1.47	1.23
Standard Deviation		0.92	0.52	0.28	0.18

The proposed model FM provides accurate results for the same size of data n = 5. For the data of manufacturer A, the average *CV* resulted by calculating the airflow rate (case-I) by the proposed model FM is 1.46%, compared to the CV of 12.5% in the detailed model. The average *CV* when the power is simulated by FM is 3.49%, compared to 9% for the detailed model.

Table 13

CVs comparing the simulated results and manufacturer's data for a period of three months

		Proposed Model				**DFM**	**SFM**
Cases	**Outputs**	**Size n = 2**	**Size n = 3**	**Size n = 5**	**Size n = 10**	**Size n = 5**	**Size n = 4**
Case I	Airflow	9.12	5.42	3.12	1.71	11.2	-
	Power	8.56	6.11	3.32	1.78	12.3	-
Case II	Speed	10.31	6.81	3.87	1.89	10.86	-
	Power	9.44	7.21	3.93	1.22	10.54	16.54
Case III	Pressure	8.45	4.89	3.05	1.46	9.59	-
	Power	9.02	6.12	3.75	1.37	10.54	17.21

The proposed model is evaluated on the existing VAV system at the New Academic Classroom Building at NC A&T State University. The simulated results are compared with measured data collected from the existing VAV system under normal operations and covering the entire year. The data were collected at 1 min intervals. Different operating data were selected for the model calibration. Figures 46 - 47 show the speed and power comparisons. The self-tuning model fan model provides very accurate results in terms of *CV* = 0.683 % for fan speed and *CV* = 6.64% for fan power. These results indicated that the self-tuning fan model can accurately simulate the airflow rate, pressure, speed, or power, and the accuracy increases significantly by increasing the data size *n* for the model calibration.

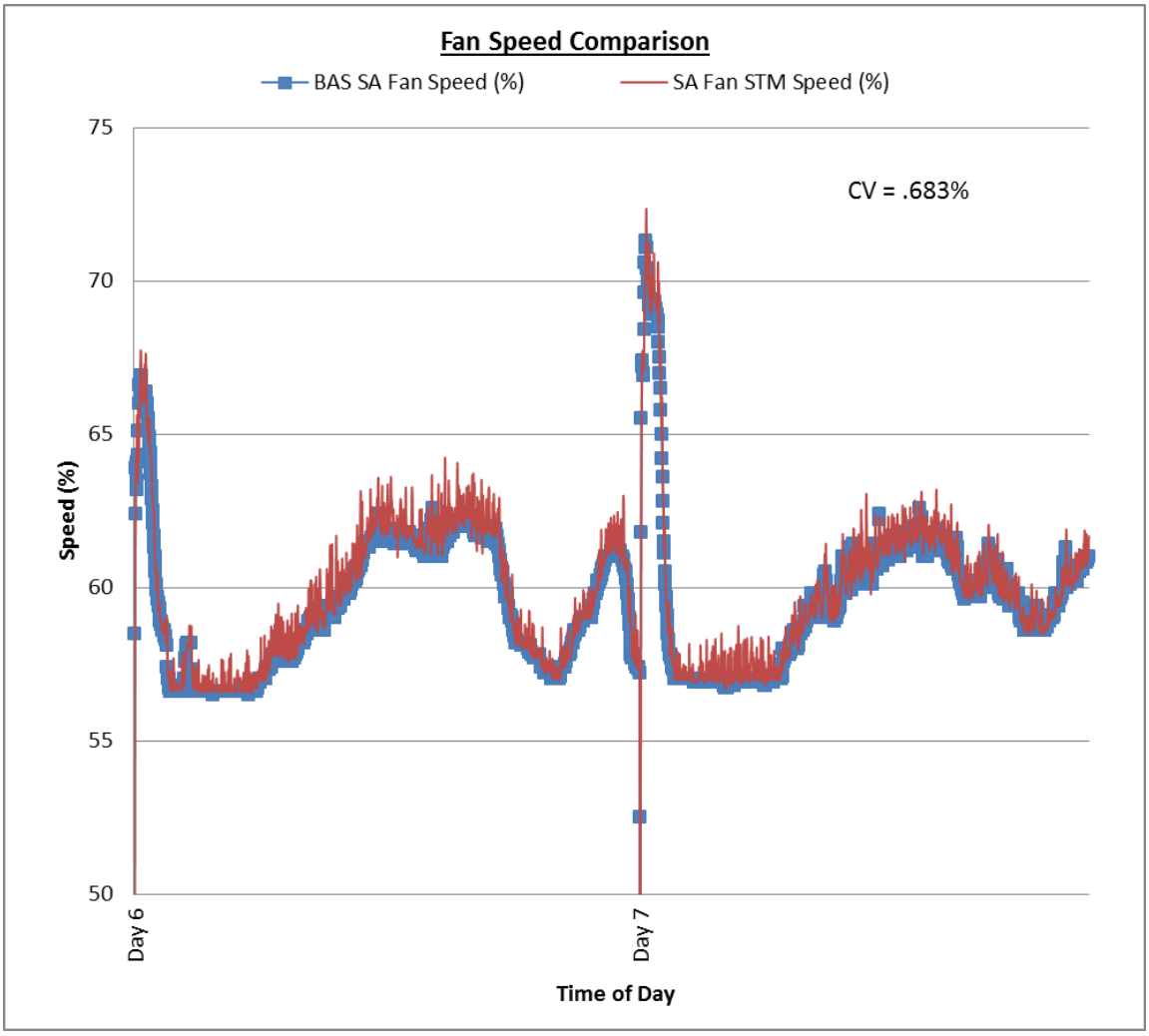

Figure 46. STM fan speed comparison.

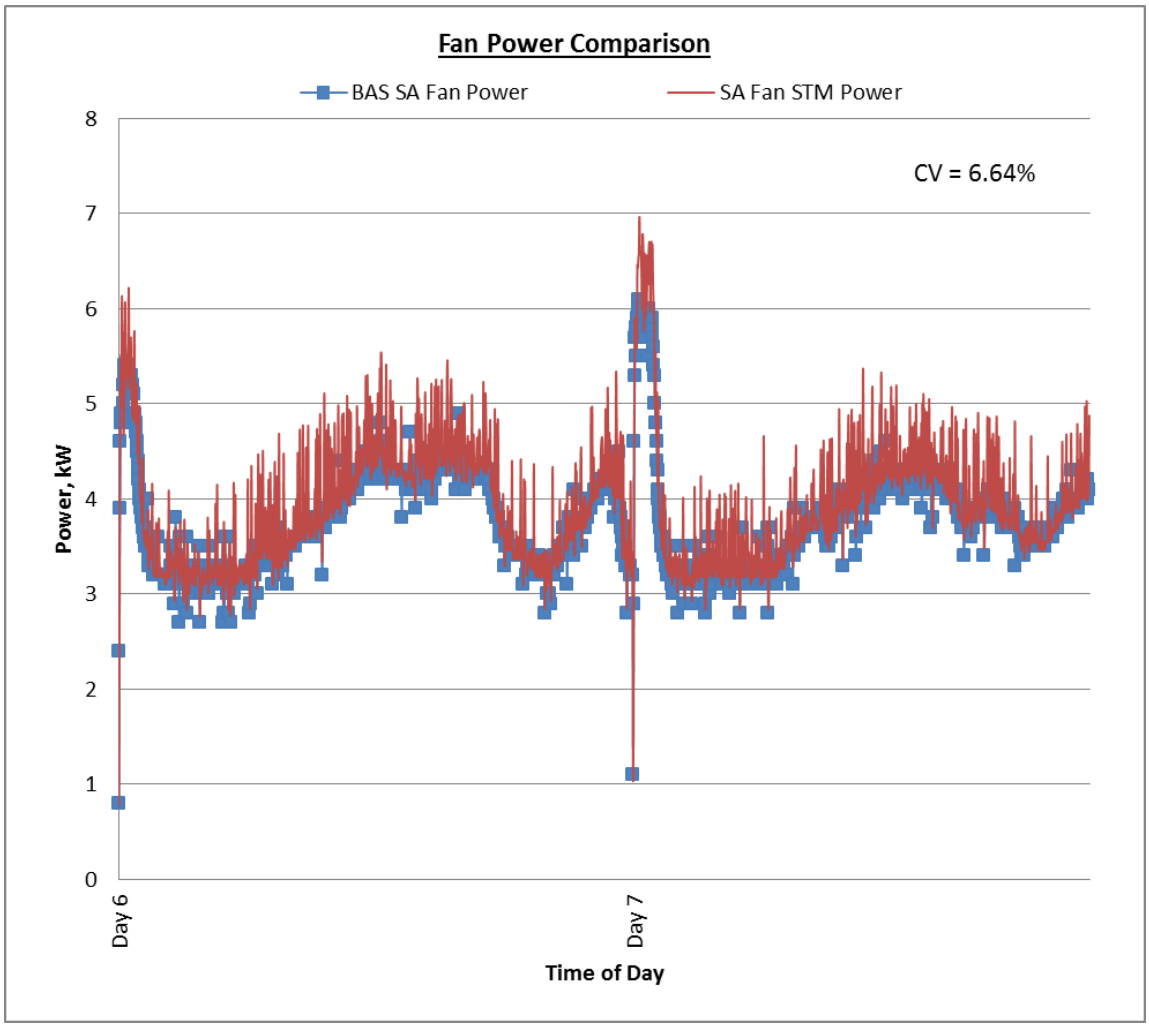

Figure 47. STM fan power comparison.

The fan model proposed in this research uses a numerical analysis based on the interpolation technique for the data generated by basic fan laws. The model was tested for accuracy using data obtained from two different manufacturers and an actual VAV system. The results indicated that the model can accurately simulate the airflow rate, pressure, speed, or power, and the accuracy in terms of the coefficient of variance *CV*. The model is able to use any two variables among all four variables of airflow rate, total fan pressure, speed, and power as inputs or outputs. Any size of data can be used for the model calibration, obtained either from manufacturers or field measured data. However, the accuracy increases significantly through

increasing the data size *n* for the model calibration. The fan model can be used for several applications such as optimization, fault detection, modern airflow station technique, and any commercial building models.

4.1.2 Chiller model training and testing. Chiller plants are challenging to accurately model due to the multifaceted interaction of the system components and controls. Precise computer modeling is demanding to establish the applicable design temperatures or flows, and control setpoints and algorithms to optimize chiller performance. Issues such as the optimal variable speed drives and flow rate are highly dependent on the performance of individual pieces of equipment, the configuration of the piping, and the control system design. These design and operational issues can only be answered correctly through simulation. The exactness of the simulations depends greatly on the calibration of the component models (Hydeman, M. & K. L. Gillespie, 2002).

The chiller model simulation program developed is similar to the DOE-2 model (DOE, 1980) but was improved to include a GA to select the optimal regression coefficients (a_i, b_i, c_i, d_i, e_i, *and* f_i) in a step function programmed in MATLAB, consisting of the following three curves:

- CAPFT - a curve that represents the available capacity as a function of evaporator and condenser temperatures or the Cooling **Cap**acity **F**unction of **T**emperature Curve
- EIRFT - a curve that represents the full-load efficiency as a function of evaporator and condenser temperatures or the **E**nergy **I**nput to Cooling Output **R**atio **F**unction of **T**emperature Curve
- EIRFPLR - a curve that represents the efficiency as a function of the percentage unloading unloading a given chiller performance model is defined by the regression

coefficients (a_i, b_i, c_i, d_i, e_i, *and* f_i), the reference capacity (Q_{ref}), and the reference power (P_{ref}) or the **E**nergy **I**nput to Cooling Output **R**atio **F**unction of **P**art **L**oad **R**atio Curve For further methodology and equations please review the chiller section 3.3.3.1 in chapter 3 of this research paper. The DOE-2 model assumes the regression coefficients to be constant. The BAS data sets of a real building's chiller were tested on the new model. The tuning parameters of the model (optimal regression coefficients, a_i,, b_i, c_i, d_i, e_i, *and* f_i) are determined by the genetic algorithm (GA) to minimize the error (least squares error) between the estimated and real data. The GA objective function f (least squares error), is minimized.

The chilled water supply temperature (t_{chws},^{o}F), the condenser water supply temperature ($t_{cws/oat}$, ^{o}F) for water-cooled equipment or the outdoor air dry-bulb temperature (^{o}F) for air-cooled equipment, the capacity (Q, ton), the capacity at the reference evaporator and condenser temperatures where the curves come to unity (Q_{ref}, ton), a function representing the part-load operating ratio of the chiller (PLR), the power (P, kW), the power (P_{ref}, kW) at the reference evaporator and condenser temperatures where the curves come to unity, and the chilled capacity available under the current conditions in tons ($Q_{available}$), are utilized and calculated in this chiller model (Hydeman, M. & K. L. Gillespie, 2002). The change in temperature entering and leaving the chiller is (Δt). If $\Delta t < 0$ (or negative) then Δt is equal to zero, and q_{ct} is calculated in the cooling coil model, if $q_{ct} \leq 0$ (if cooling load is negative or zero) then the power is equal to zero. If $Q_{available} < 0$ (if chilled capacity is negative) then power is equal to zero, ($Q_{available} = 0$). If Power < 0 (if Power is negative) then Power is equal to zero, (Power = 0). Standard efficiency e (or COP) is also calculated, see chapter 3 for equations.

The chiller model requires the optimal variable T_w which is the chilled water supply temperature (^{o}F) and the condensing chilled water temperature T_c which is approximately equal

to the wet-bulb temperature + 8 ^{o}F (for Water-Cooled chiller) however for this program the condenser water supply temperature (^{o}F) for water-cooled equipment was set at 85^{o}F for simplicity. The design chiller capacity (rating capacity) in tons ($Q_{nominal}$) is read from the worksheet System Design Information in the Excel file UserInput.xlsx. After calculating the CAPFT, EIRFT, PLR, and EIRFPLR, we can calculate the final curve coefficients. Reference power is calculated to minimize the predicted power error. The format of root mean square error is utilized in the GA:

$$Error = \sqrt{\frac{\sum_{i=1}^{n}\left(\frac{P_{ref} \times (CAPFT_i \times EIRFT_i \times EIRFPLR_i) - P_i}{P_i}\right)^2}{n}} \tag{4.8}$$

In a real BAS OLSTOP the reference power is from the previous time step (15 minutes) (P_{ref}), and utilizing the equation above we seek the minimum of this error function. For each curve in the subset and with reference capacity and power calculated as described above, we calculate a total error on the predicted power across the data set. The curve with the lowest prediction error is selected for the final model. Figure 48 shows the accuracy of the new self-tuning model for the chiller compared to the real data from a BAS with a CV = 3.804%.

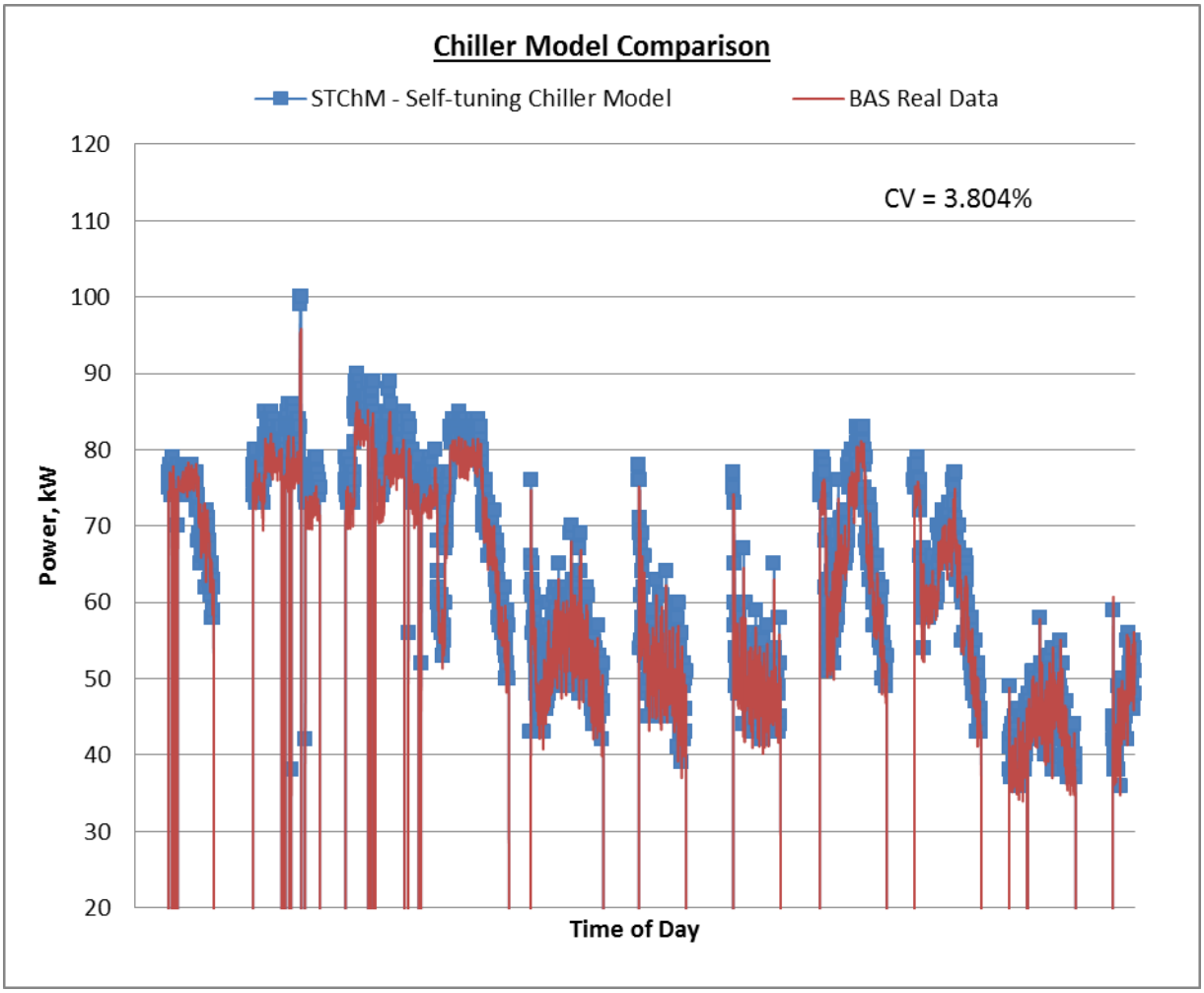

Figure 48. STM chiller comparison.

4.1.3 Cooling coil model training and testing. Reducing the water flow rate (gpm) in a cooling coil will increase the differential temperature (ΔT) on the coils; the coils would then have to heat up the water faster because there is less water to absorb the same amount of heat from the air, resulting in the need for larger coils. In an existing cooling coil, lowering both the entering water temperature and the water flow rate, the return water temperature will increase, raising ΔT; this strategy provides energy savings without negatively impacting the chilled water loop operation.

In a cooling coil, avoiding the "low ΔT syndrome" is paramount; this occurs when the system is required to supply more water than is available at a specific supply water temperature, or when the maximum water flow rate is achieved and the coil cannot supply the heat necessary to push the ΔT to the anticipated level. Lowering the supply chilled water temperature efficiently increases the ΔT and eliminates the "low ΔT syndrome." Lowering the supply chilled water temperature is a system optimization strategy that assists with reducing the supply air temperature to the building. Colder air temperature results in the opportunity to reduce fan energy. At lower temperatures, cooling coils can create more cooling with less water.

In an existing system, lowering the leaving chilled water temperature will result in a lower cooling coil entering water temperature, which will reduce the water flow rate, therefore reducing pump energy. The cooling coil leaving water temperature (return water temperature) will typically increase by the same amount as the chiller leaving water temperature is decreased (Trane, 2000). Theses optimization strategies are included in the OLSTOP incorporating the chiller and cooling coil STMs.

The existing models for a cooling and dehumidifying coil determine whether the finned surface is completely or partially dry or wet, and it calculates the outlet liquid temperature, air dry bulb temperature, humidity ratio, the total and sensible cooling capacity, and the heat transfer coefficients and mass transfer associated with condensation on the finned air-side surface in accordance with ASHRAE standards and methods. The self-tuning cooling coil model is calculated using equations for latent load, zone humidity ratio, humidity ratio, return temperature, mixed air humidity ratio, mixed air temperature, enthalpy effectiveness, overall enthalpy heat transfer coefficient, (UA_h, lb/h), liquid-side heat transfer coefficient, (UA_{int}, Btu/h ^{o}F), air-side heat transfer coefficient, (UA_{ext}, Btu/h ^{o}F), and bypass factor. For further details and

calculations on heat and mass transfer properties see the cooling coil method in chapter 3, section 3.3.2.6 and Appendix B.

Chilled water flow rate is calculated as a function of valve opening by the hydronic model. A simple **s**elf-**t**uning steady state **c**ooling **c**oil **m**odel (STCCM) was developed for the New Academic Building at North Carolina A&T State University. The existing ASHRAE HVAC 2 Toolkit cooling coil models consider the internal and external heat transfer coefficients (UA_{int} & UA_{ext}) constant and are calculated by design conditions and water and air flow rates; this will not produce accurate results as the UA_{int} & UA_{ext} change over time. To improve the accuracy we proposed to vary the UA_{int} & UA_{ext} based on the liquid and air flow rate. $UA_{int} = UA_{int,rate}\left(\frac{\dot{V}_l}{\dot{V}_{l,rate}}\right)^{a_1}$, $UA_{ext} = UA_{ext,rate}\left(\frac{\dot{V}_t}{\dot{V}_{t,des}}\right)^{a_2}$.The parameters of this relationship will be determined based on the actual BAS coiling coil data and found with a genetic algorithm to tune the model. In this model, the internal and external heat transfer coefficients (UA_{int} & UA_{ext}) are determined from the performance of the coil at a single rating point, and are assumed to vary as functions of the liquid and airflow rates $(\dot{V}_l \; and \; \dot{V}_t)$. The genetic algorithm (GA) determines the tuning parameters a_1 and a_2 considering the relation between the heat transfer coefficients and the liquid and airflow rates. The tuning parameter corrects the error between the simulated and measured supply air temperatures. Figure 49 clearly shows the cooling coil model comparison with the BAS real data and the CCSIM from ASHRAE HVAC 2 Toolkit and the new self-tuning model. The calculated *CV* = 0.713% for the new STCCM predicts a more accurate curve fit and determines the next time step's (15 minutes) internal and external heat transfer coefficients (UA_{int} & UA_{ext}) to use in the OLSTOP to reduce overall system energy comparing to the CCSIM with a *CV* = 2.256%.

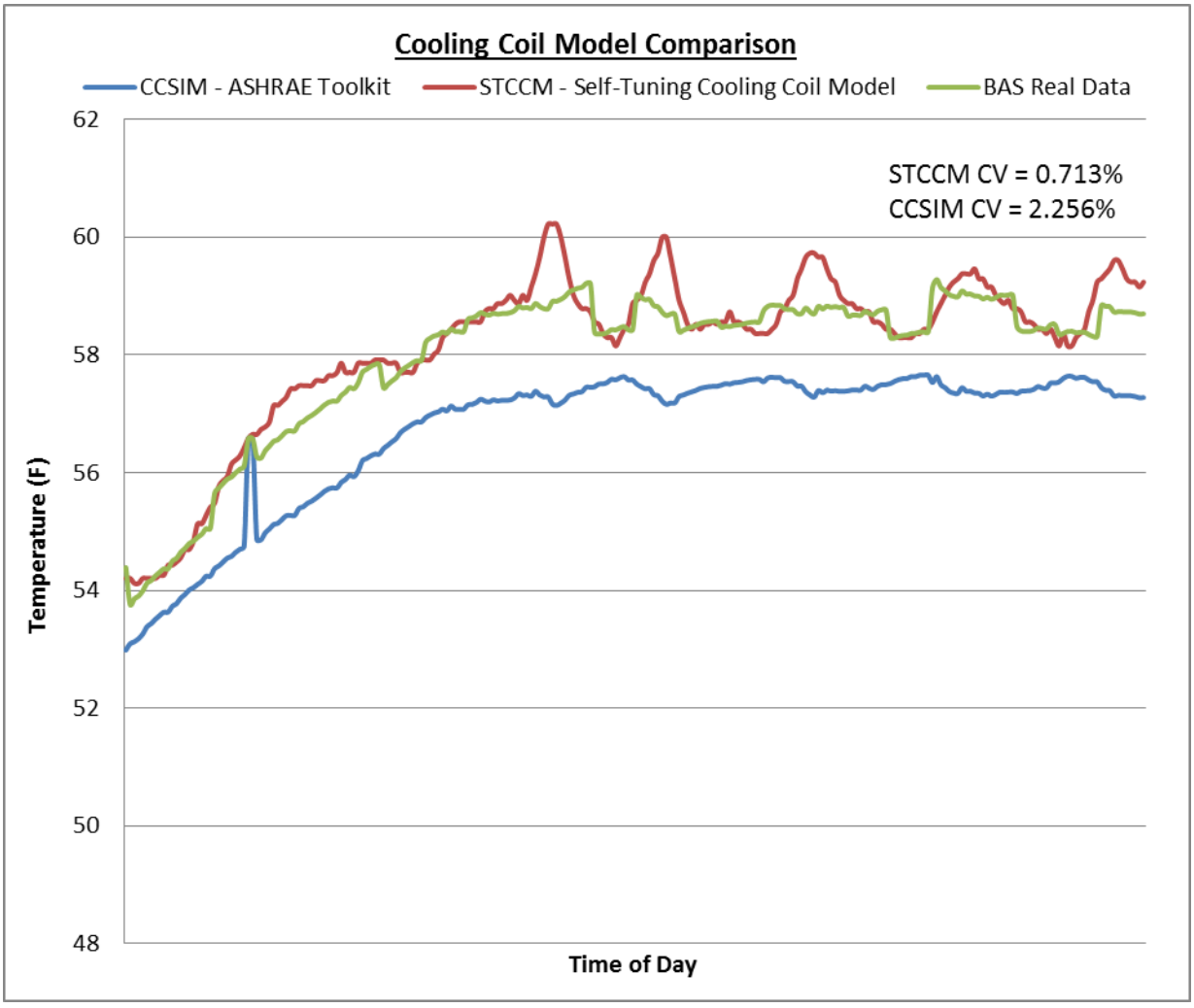

Figure 49. STM cooling coil comparison.

4.2 Component Models General Statement

The developed component models are validated against recorded data of an existing HVAC system. Utilizing the "real data" from the components or subsystems of the existing HVAC system the models compute outputs which we call the "estimated data." The minimum error objective function of the genetic algorithm that accurately portrays the component models tunes the model's parameters at each time step. When online self-tuning models are deployed, the components are tuned using real-time data that accurately matches the behavior of the system. As the component models are finely tuned, the optimal set-point variables are then

producing minimal energy usage with maximum precision. In the existing HVAC system, the data was recorded from the building automation system every minute and included:

- outside air and zone temperature
- air conditioner: fresh air intake temperature and relative humidity
- air handling unit: supply air temperature, pressure, and relative humidity, fan speed, power, chilled water and mixed air temperature, valve and outdoor air damper opening position, outdoor air fan power and enthalpy, return air fan speed and fan power
- supply duct static and mixing air box pressures, etc.

The zone total, sensible, latent, and ventilation loads that are the inputs for the models are calculated from the available recorded data at previous time periods, all model formulations are described in Chapter 3. The data from the previous time step is the input factors to tune the model parameters for the OLSTOP optimal control strategy application. The time step will need to be longer then the time required to run the optimization process with the genetic algorithms (which is dictated by how many generations and the population size that is set in the program). For example, if it takes 10 minutes to run the optimization process then the time steps need to be every ten minutes. The building automation system will take the previous time step's real data, run the online self-tuning models' calculations and adjust the set point variables to minimize the energy use of the HVAC system. It is assumed that the outdoor and indoor conditions remain constant during the optimization computation which allows the OLSTOP to operate. The resulting errors are negligible or the difference between the process time and the load condition changes within the time step. As computer technology advances the time step and optimization computation time can be improved. The component models are validated comparing the

measured data for three summer months (May, June, and August 2014). The statistical indicator utilized is the coefficient of variance (CV) between the predicted values and measured data.

CHAPTER 5

Results

The models were validated against real data recorded from existing HVAC systems in Chapter 4. We simulated the New Academic Classroom Building (NACB) in eQuest to obtain the zone loads every hour for an entire year. The OLSTOP is validated in this chapter with the simulated data from eQuest. The real data for the NACB obtained from the BAS showed that the system was in either standard practice mode (supply air temperature fluctuates with outdoor temperature) or fixed or override mode (T_s is set at a constant 55^{o}F) at different times throughout the year, both which waste energy when compared to the OLSTOP. For a wide range of the OLSTOP graphs depicting the results for May, June and August addressing the data by 3-month, per month, and per day timelines for each component and comparing the savings to standard practice (SP) and fixed or over-ride mode (FOM), see Appendix E. This research proves that by implementing an OLSTOP energy savings can be achieved, see Table 14.

Table 14

Optimization Process Comparison Results Table

OLSTOP RESULTS TABLE: Ts (F) Ps (in wc) Tw (F) Dpw (psi)														
Scheme	Optimal Variables (OV)				Standard Practice (SP) - SATR				Fixed or Override Mode (FOM)				Outside Conditions	
Variable	Ts	Ps	Tw	Dpw	Ts	Ps	Tw	Dpw	Ts	Ps	Tw	Dpw	WBT (F)	DBT (F)
Max	63.14	2.26	54.84	19.92	65.00	2.5	45	20	55	2.5	45	20	82.00	93.00
Min	55.00	1.00	45.67	10.00	55.00	2.5	45	20	55	2.5	45	20	49.00	51.00
Average	57.82	1.35	50.02	12.55	55.56	2.5	45	20	55	2.5	45	20	67.04	75.43
Scheme	Optimal Power (kW)				SP (SATR) Power (kW)				FOM Power (kW)				Savings	
Power	Total	Chiller	Pump	Fan	Total	Chiller	Pump	Fan	Total	Chiller	Pump	Fan	OV to SP	OV to FOM
Max	112.65	96.75	3.59	23.16	131.17	106.81	5.08	32.14	131.17	106.81	5.08	19.42	73.94%	64.37%
Min	5.24	0.00	0.00	4.56	11.93	0.00	0.00	10.05	14.71	5.21	0.05	8.53	13.02%	13.02%
Average	63.76	50.68	1.42	11.67	79.62	61.50	2.49	15.63	79.32	61.96	2.50	14.86	22.54%	22.21%

Comparing the results of the OLSTOP with the existing system yields considerable savings (between 13% and 73%) for the three months analyzed (May, June and August), see Table 14. The validation results confirm that the component models strengthened with an online

self-tuning model (OLSTM) which includes the genetic algorithm and a new iteration process, significantly improved the accuracy of system and the OP improved energy use. The application of online self-tuning models and optimization process presents several advantages such as designing superior real-time control and optimization of overall system performance. See Table 14 for the optimal set-point variable comparisons. The average savings comparing the optimal set-point variables to the standard practice (SP or SATR) and fixed or override mode (FOM) for the three month analysis was 22%.

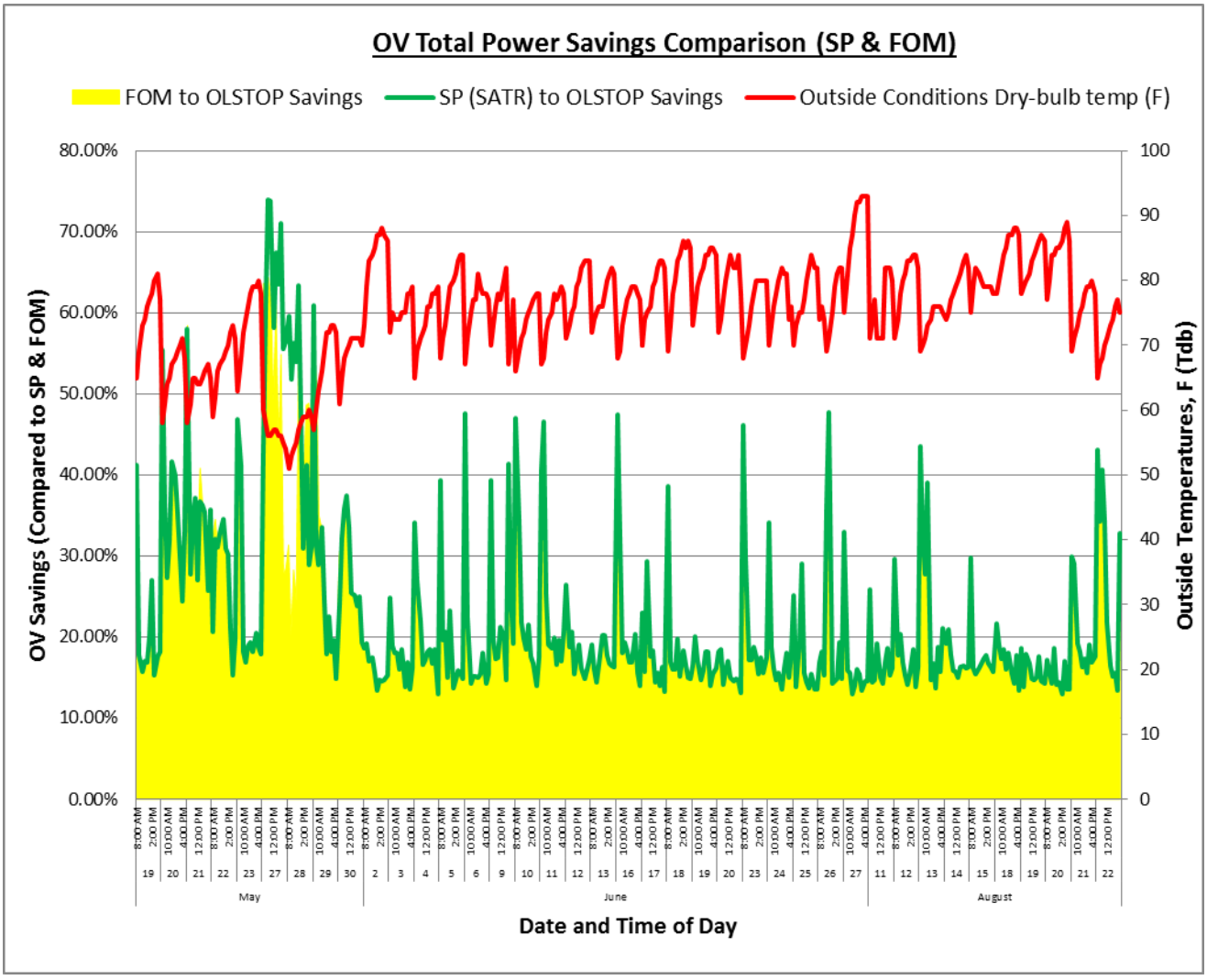

Figure 50. OLSTOP total power savings comparison to SP & FOM.

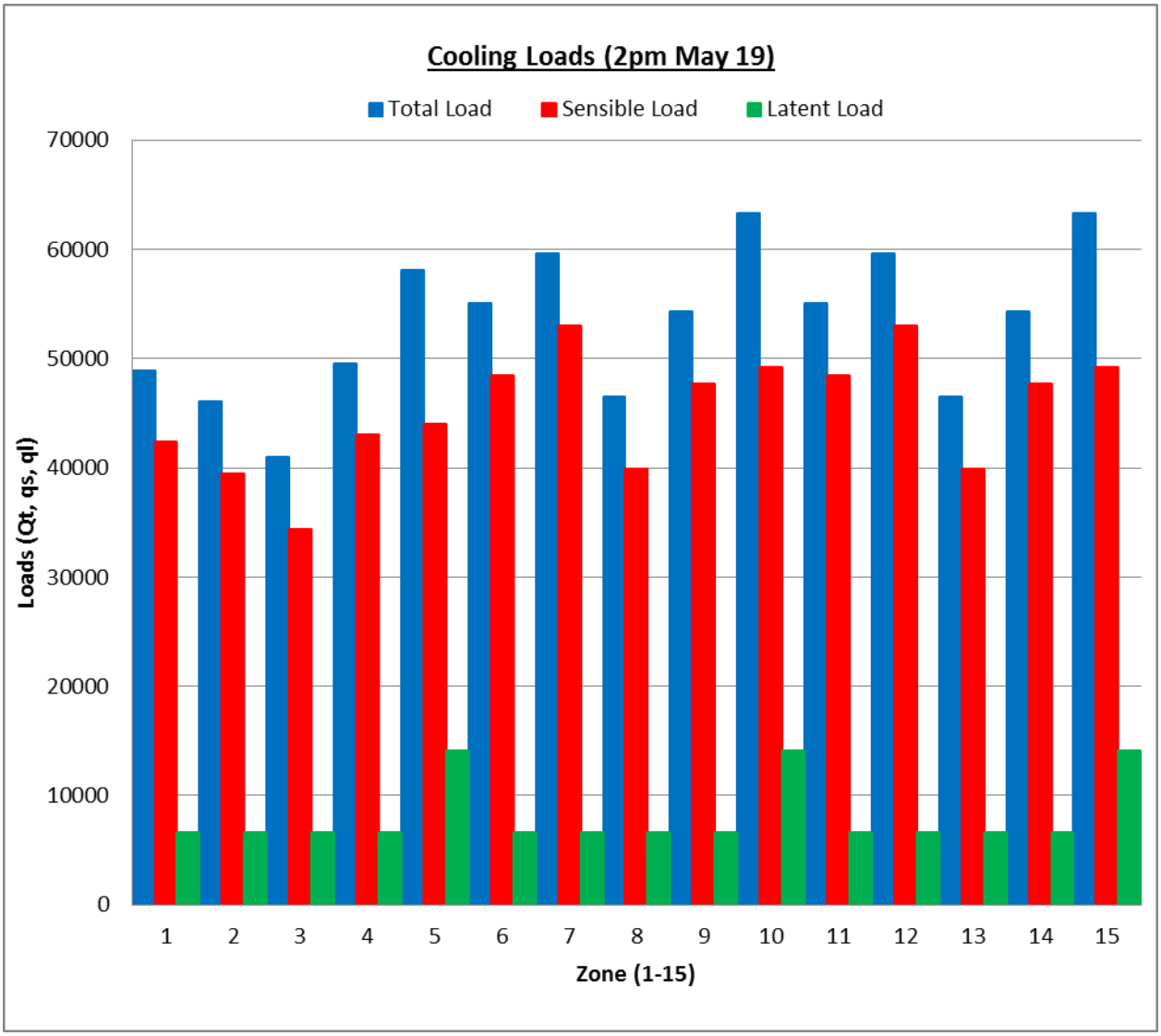

Figure 51. Cooling loads (2 pm May 19) obtained from eQuest.

In Figure 51, the zone loads are shown for 2 pm on May 19, the building was simulated for an entire year in eQuest and simplified to 15 zones with one system handling all 15 zones. The system parameters were sized according to the real building (New Academic Classroom Building at NC A&T State University). The simulated data was then compared to the real data for system validation. The simulated data was then utilized in the OLSTOP for savings comparison.

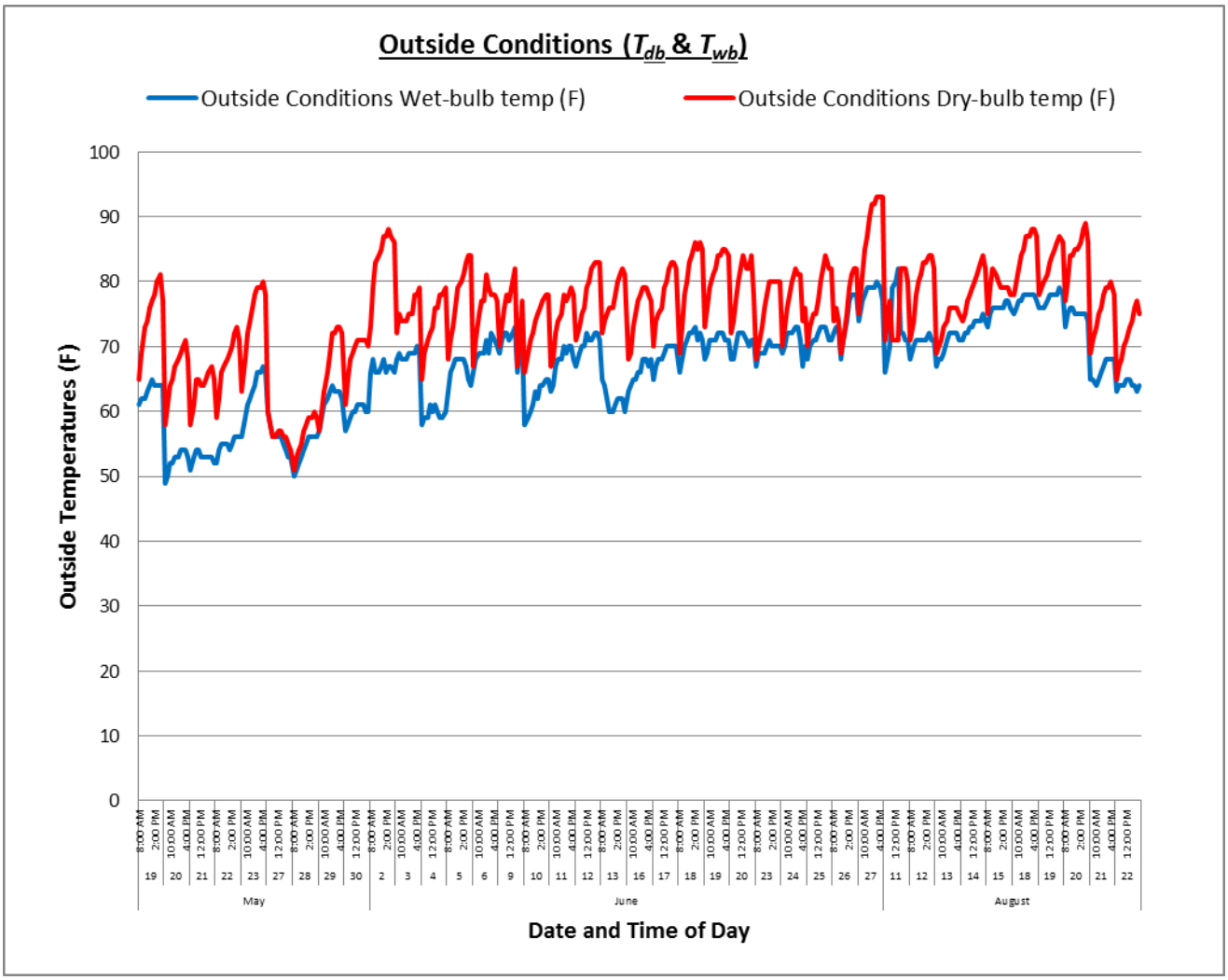

Figure 52. Outside temperatures (T_{db} & T_{wb}).

The outdoor temperatures were utilized in the OLSTOP and are shown in Figure 52. May had some cooler days where the economizer routine took advantage of the "free cooling" and June and August fluctuated averaging in the high 70°F's to low 80°F's. Temperatures spiked in the afternoons typically between 2 – 4 pm.

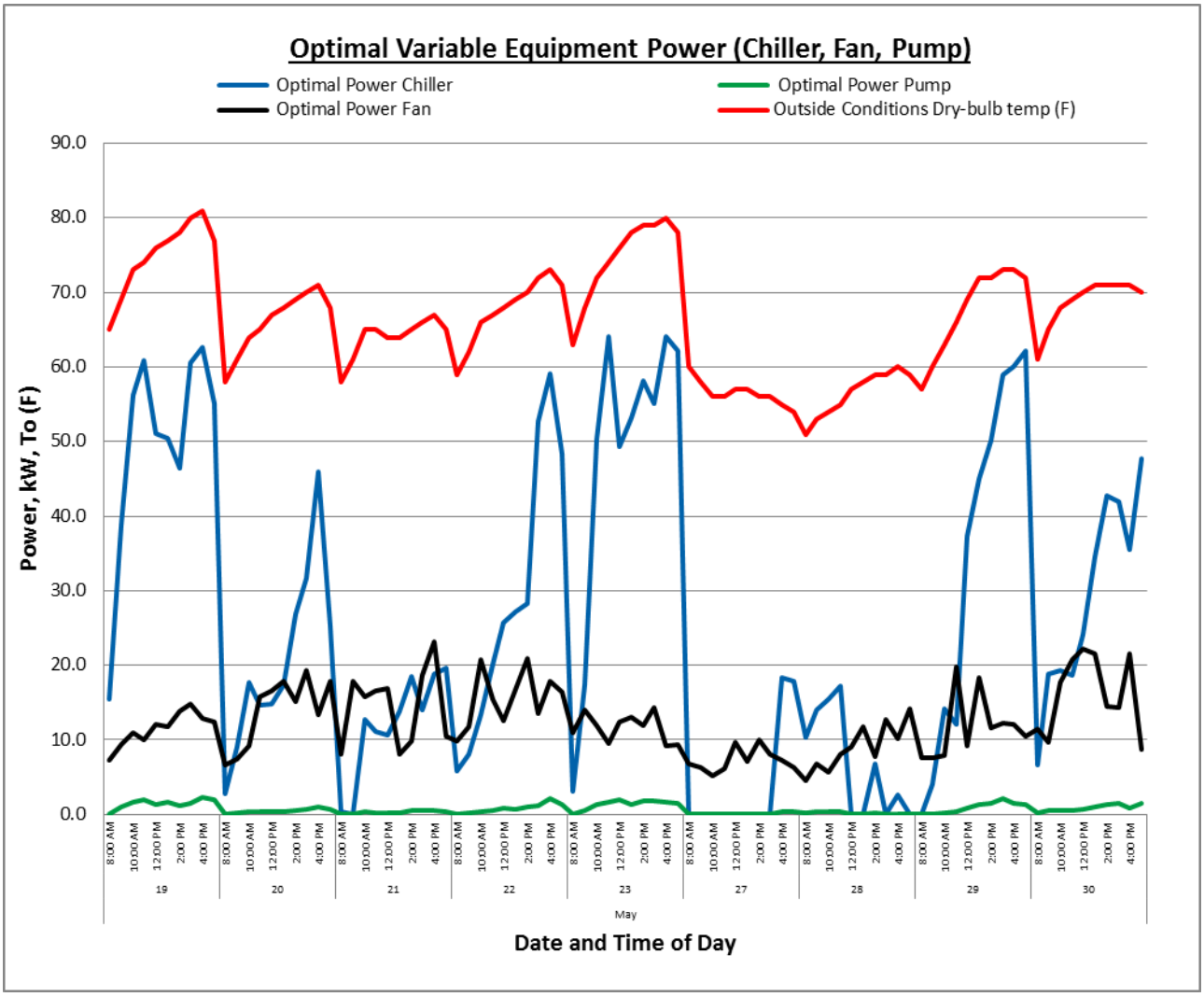

Figure 53. Optimal variable equipment power (chiller, fan, pump) – May.

In Figure 53, the optimal variable equipment's power profiles are shown for several days in May. The outside dry bulb temperature rises as expected, peaking between 2:00 - 4:00pm and the pump and chiller power have the similar contours as expected with the fan power increasing as the outdoor temperature rises. The power peaks shown in the graph relate to the zone loads that vary throughout the day depending on class size and occupancy levels during the semester.

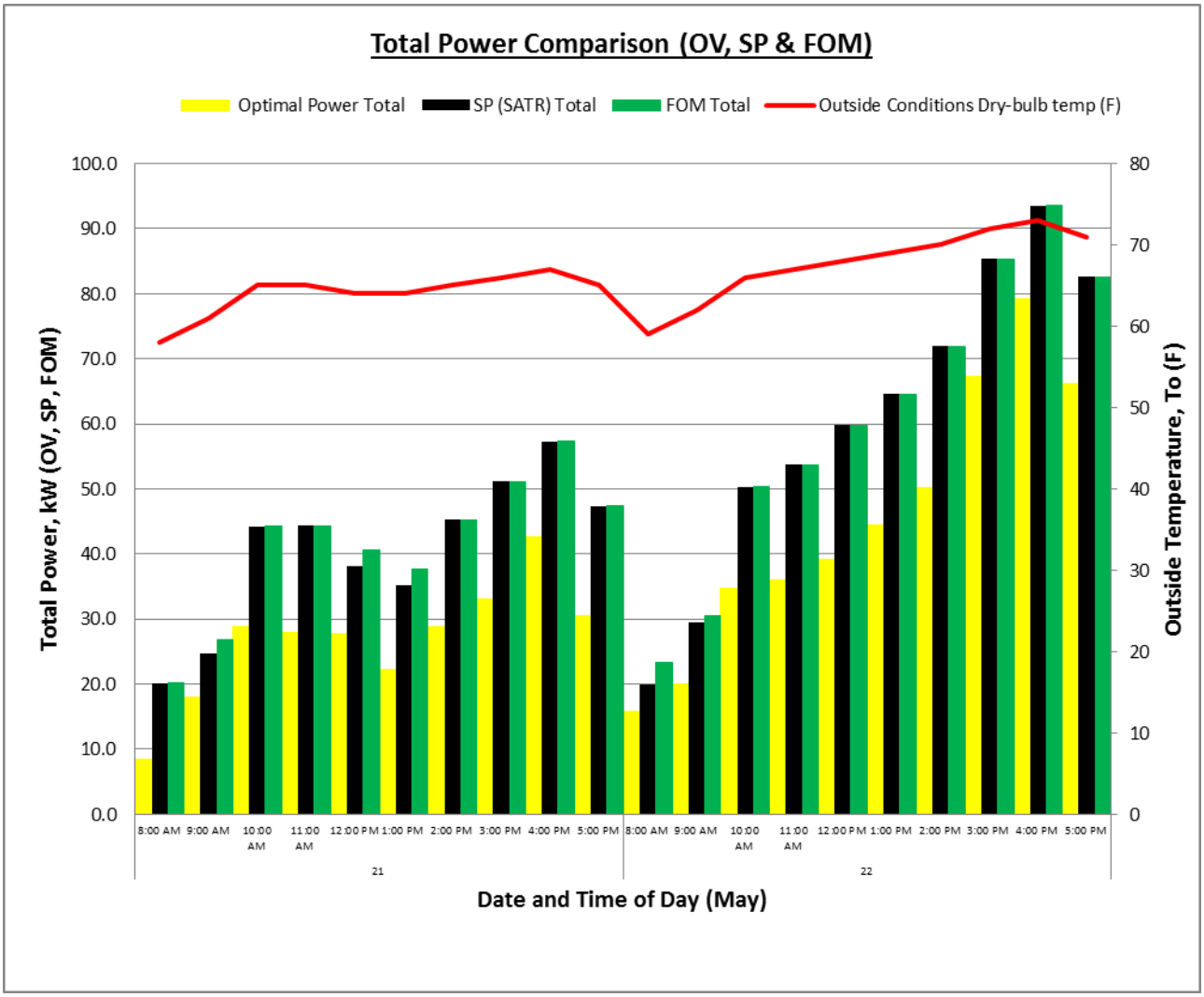

Figure 54. Total HVAC power comparison (OV, SP & FOM) - May 21 & 22.

In Figure 54, the total HVAC power comparison is shown for two days in May. The standard practice (SP) which is the supply air temperature reset (SATR) mode is compared to the fixed or over-ride mode (FOM) and the optimal power which is found by the OLSTOP. The FOM has the variables fixed in the BAS, typically by a HVAC technician, this is the most inefficient mode as the system is not able to save energy by modulating a set point variable, and is typically only controlled by thermostats in each zone. In the SP or SATR mode only the supply air temperature

(T_s) is controlled by outside dry bulb temperature (T_o or T_{db}) to save energy, with the other variable set-points fixed. The SATR control function to set T_s is found by the following logic:

If $T_o \leq 55\ ^oF$ then $T_s = 65\ ^oF$

If $T_o \geq 65\ ^oF$ then $T_s = 55\ ^oF$

If $55\ ^oF < T_o < 65\ ^oF$ then $T_s = (-1 \times T_o) + 120$ (equation of line, shown in Figure 55)

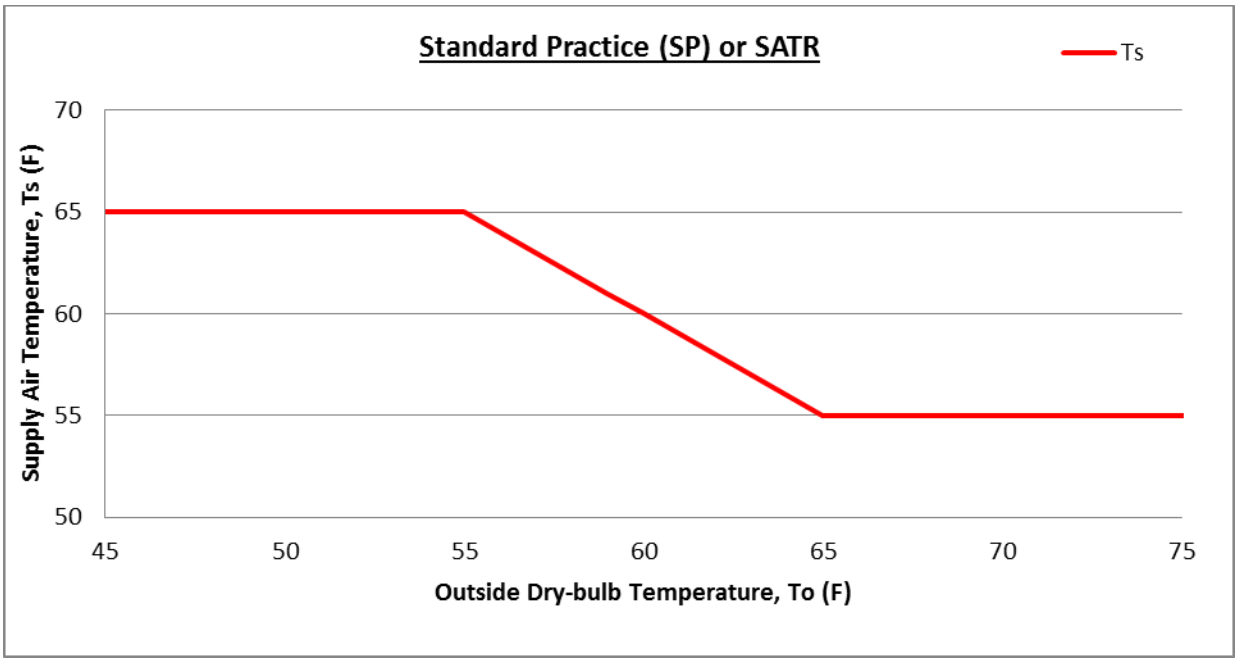

Figure 55. Standard practice (SP) or SATR T_s vs. T_o.

See Table 15 to show the comparison with the set-point variables by mode.

Table 15

Set-point Variable Comparison by Mode

Mode	T_s (F)	P_s (in wc)	T_w (F)	T_c (F)	D_{pw} (in wc)	D_{pc} (in wc)
FOM	55	2.5	45	85	20	20
SP	SATR	2.5	45	85	20	20
Optimal	Calculate OP	Calculate OP	Calculate OP	85	Calculate OP	20

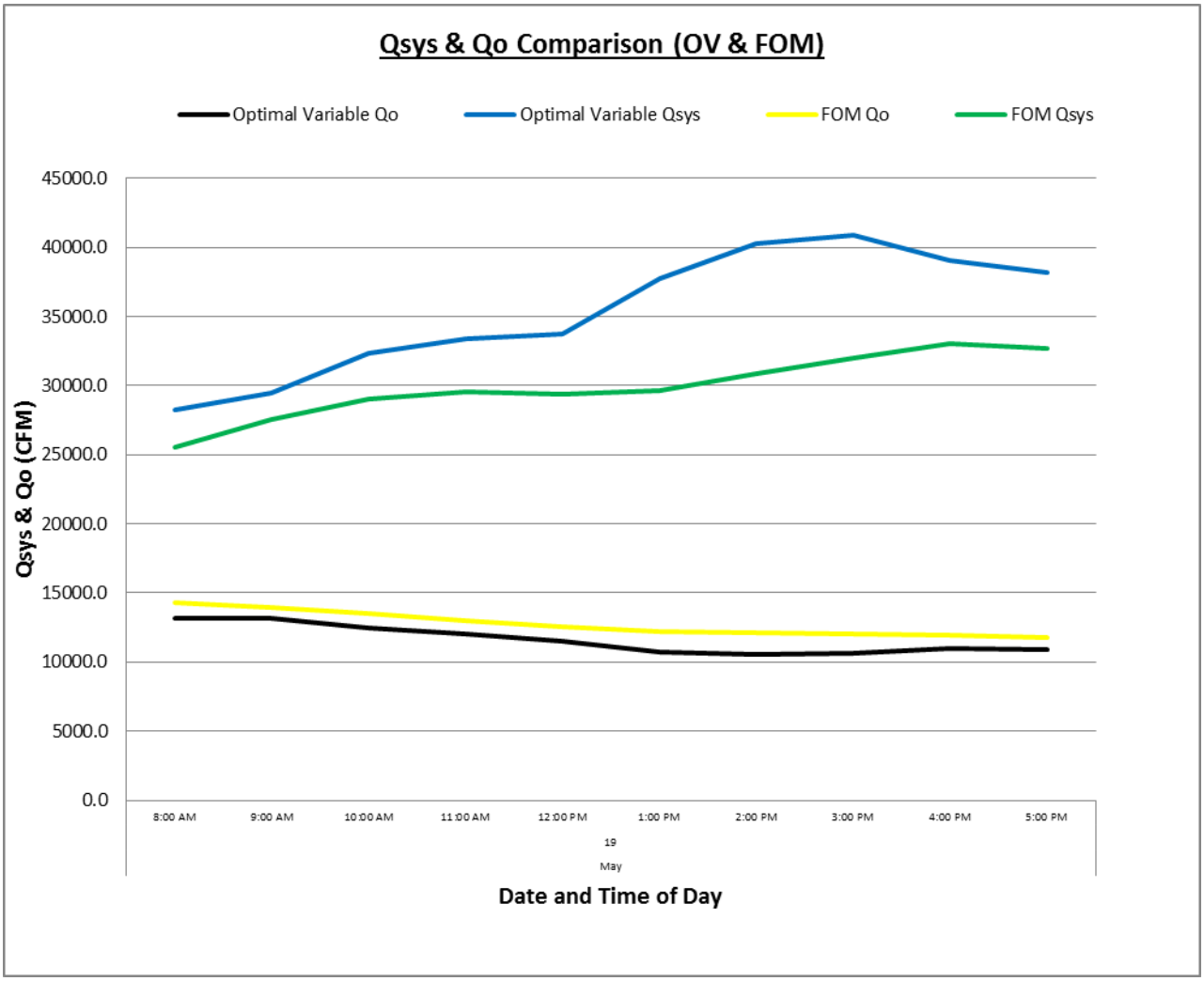

Figure 56. Q_{sys} & Q_o comparison (OV & FOM) - May 19.

In Figure 56, the total system supply airflow (Q_{sys}) and the total outdoor fresh air requirement (Q_o) which is found by calculating the breathing zone outdoor airflow following the ASHRAE 62.1-2013 ventilation for acceptable indoor air quality code comparing FOM and the OP, is shown for one day in May. This graph shows that when the supply air temperature T_s is set around 55°F in both the SP (SATR) and FOM, the optimal T_s is higher, say 60°F, so the fan power increases with the air flow to make up for the higher optimal T_s. Then the total system supply airflow (Q_{sys}) is higher and the ventilation efficiency improves, see chapter 3, section 3.3.2.4 equations.

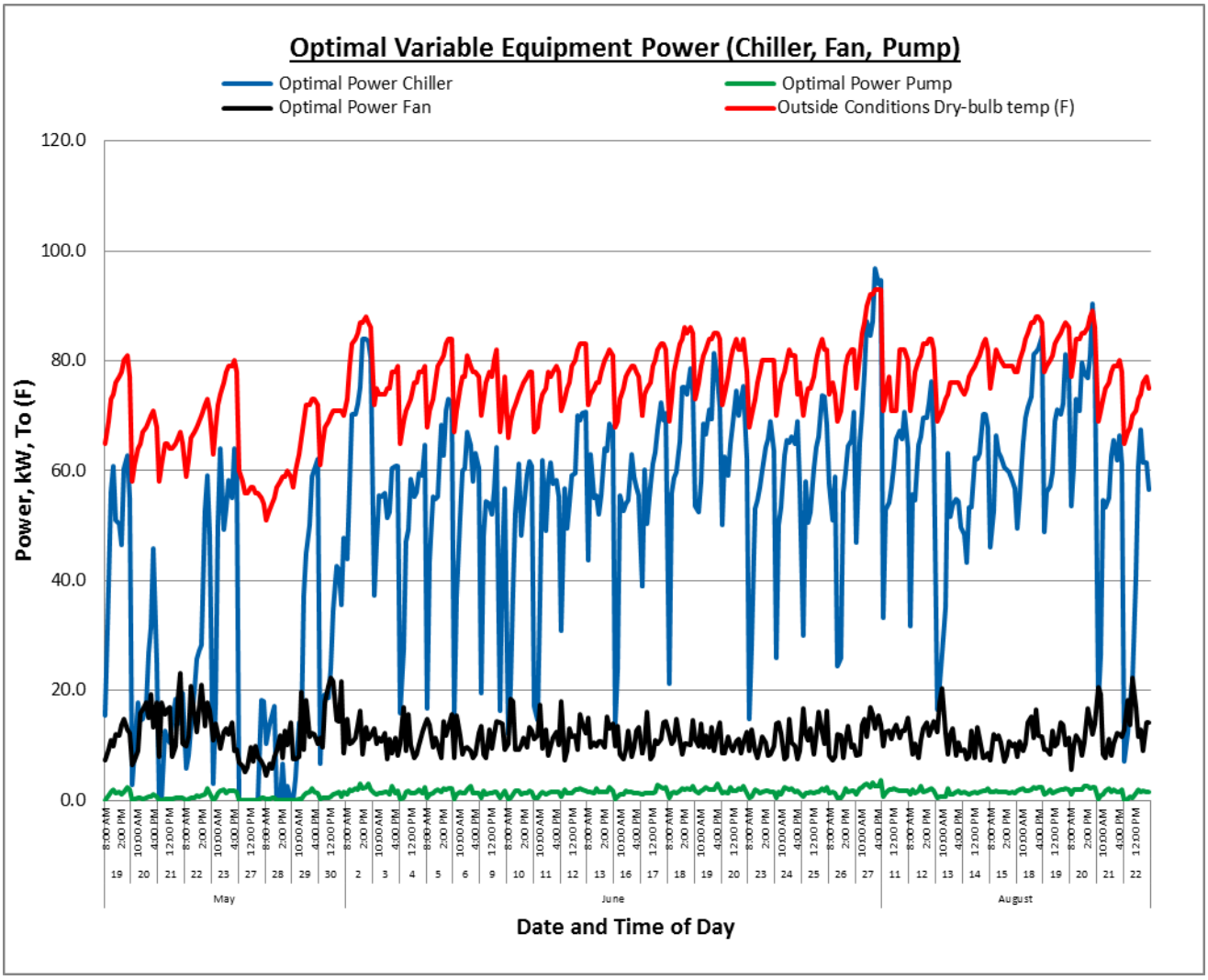

Figure 57. Optimal variable equipment power (chiller, fan and pump).

As shown in Figure 57, the optimal variable equipment power (chiller, pump, and fan) calculated by the OLSTOP are plotted for the three summer months (May, June and August). The chiller and pump power drop to minimum levels when the outdoor temperature is below 55^{o}F around May 27 to May 29 and they maximize with the peak outdoor temperature in the 90^{o}F's during June 27th.

The online self-tuning models constantly fluctuate, depending on zone load and outdoor conditions, to minimize energy use. Once the data is sorted by outside drybulb temperature the

graph clearly shows that overall HVAC system power increases in a linear trendline as outdoor temperature increases. This obvious relationship requires further analysis and more detailed interpretation of the results. The optimal supply temperature, T_s, to the fan and the optimal chilled water differential pressure, D_{pw}, both show a slight downward trendline as outdoor temperature increases. This relationship indicates that when the outdoor temperature is lower the "free" cooling or cool outdoor air can be utilized, thus reducing the chiller's energy use.

The optimal set point variables that control the energy use of the main components of the cooling side of the HVAC system work together to minimize energy use as outside temperature increases. The cooling side of an HVAC system has three main pieces of equipment which are the chiller, pump, and fan. There is a direct relationship in energy usage of the equipment with their corresponding set point variables and the individual zone load requirements and outdoor conditions. The optimization process is controlled by the building's thermal loads and outdoor conditions which directly influence the chiller and pump power that increase with respect to supply air temperature (T_s), chilled water temperature (T_w) and chilled water differential pressure set-point (D_{pw}) and the fluctuating fan power regarding T_s and duct static pressure (P_s).

When all OLSTMs and the OP are operating the objective function is to minimize the total energy use in the HVAC system at each time step. Figure 59 shows the OP's optimal variable (OV) total power comparison to the existing system when it was in fixed or override mode (FOM) and standard practice mode, SP (only T_s fluctuating).

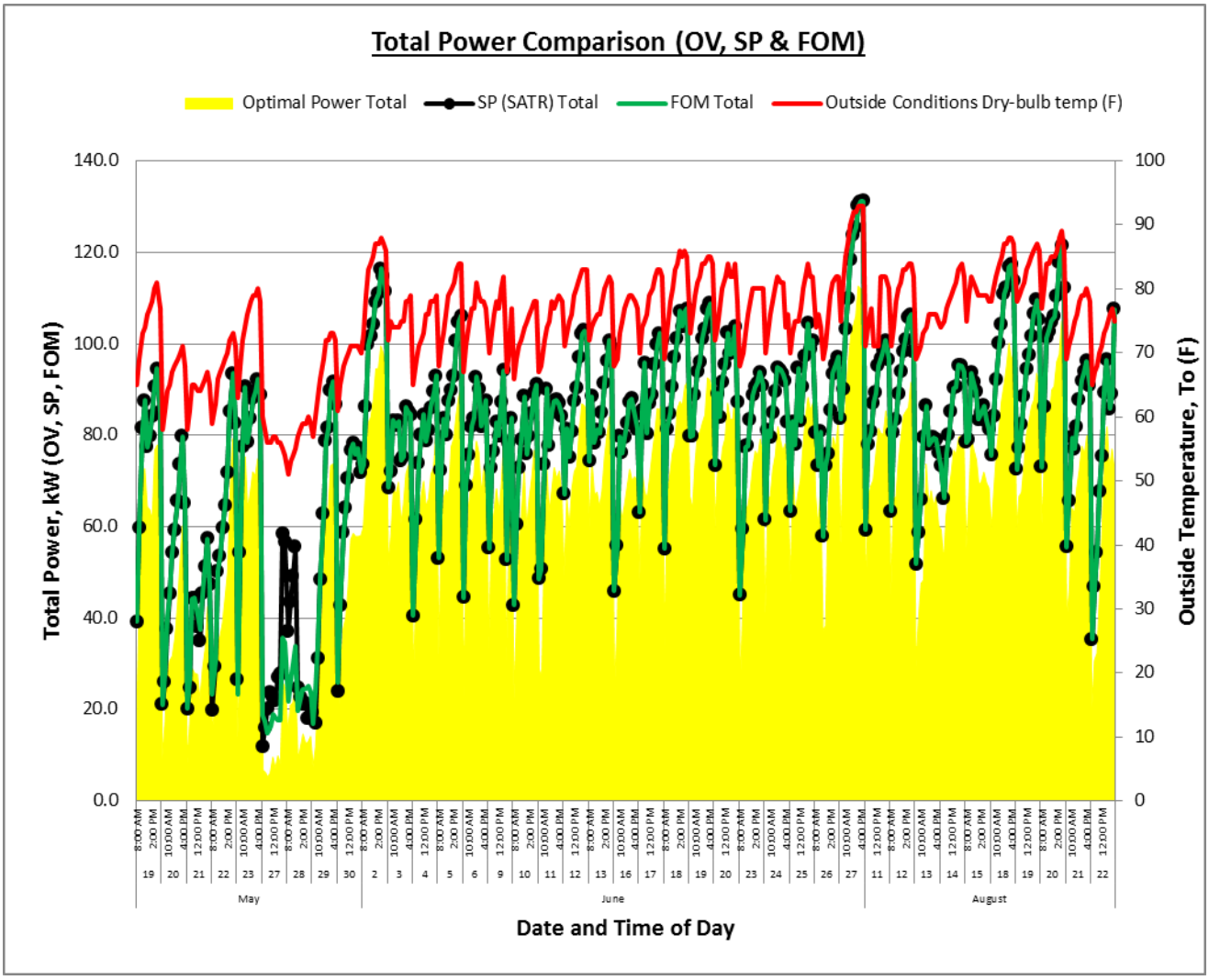

Figure 58. Total power comparison (OV, SP & FOM).

See Figure 58 for the total energy comparison after the OLSTM and OP completed. The optimal variables were selected at each time step and the component models were verified through the GA.

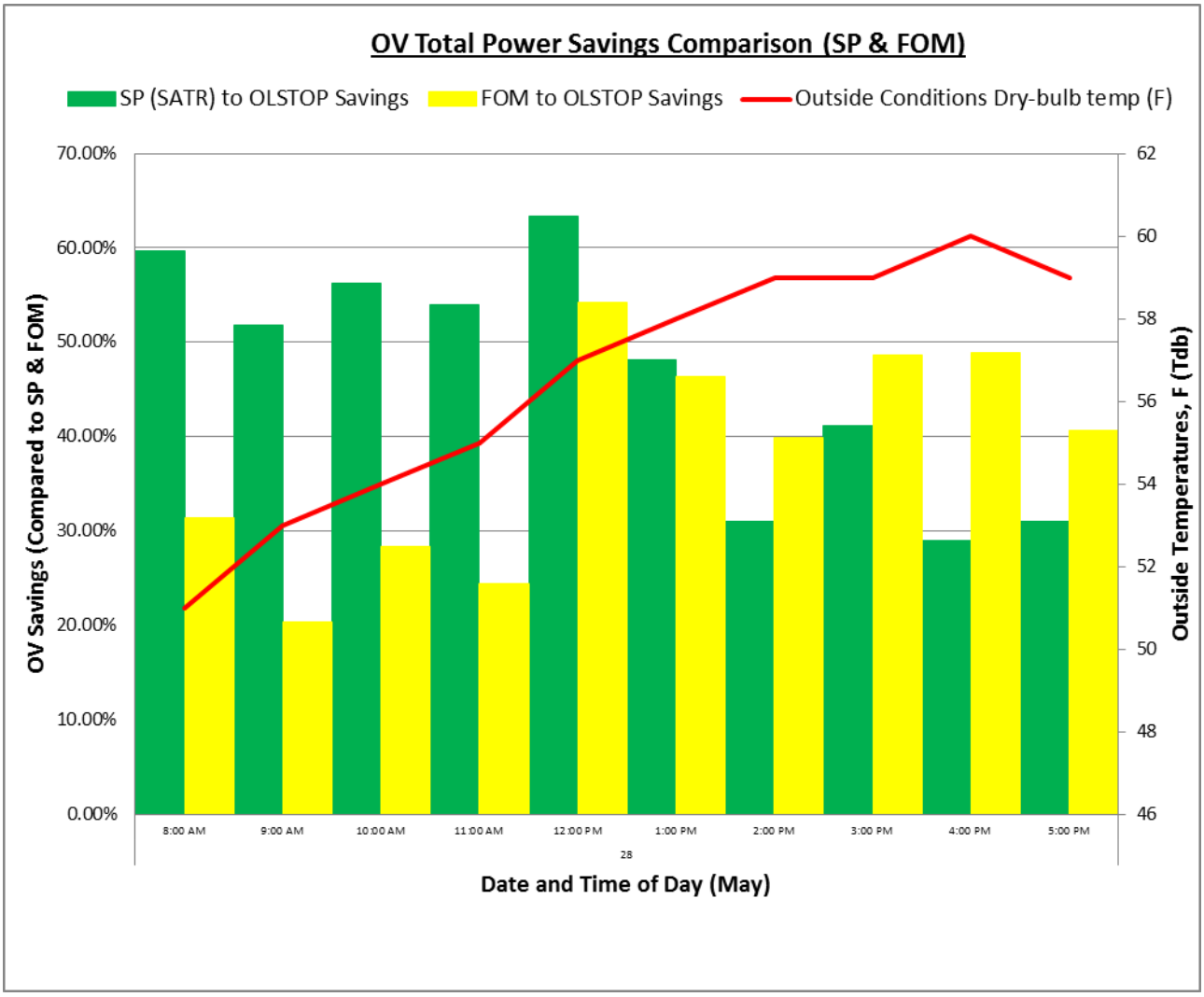

Figure 59. OV total power savings comparison (SP & FOM) - May 28.

By minimizing or optimizing duct static pressure the fan's energy use is reduced; this results in the fan generating enough static pressure to push the required quantity of air through the system to cool each zone adequately, instead of maintaining a set pressure. Friction pressure drop is lower at lower air flows thus by varying the fan speed a more energy efficient control is produced. The fan affinity law of fluid work (fan power) varying with the cube of air flow or speed applies in this application:

$$\frac{P_1}{P_2} = \left(\frac{n_1}{n_2}\right)^3 \tag{5.1}$$

where:

P = fan power (W)

n = fan speed (rpm) or flow (cfm)

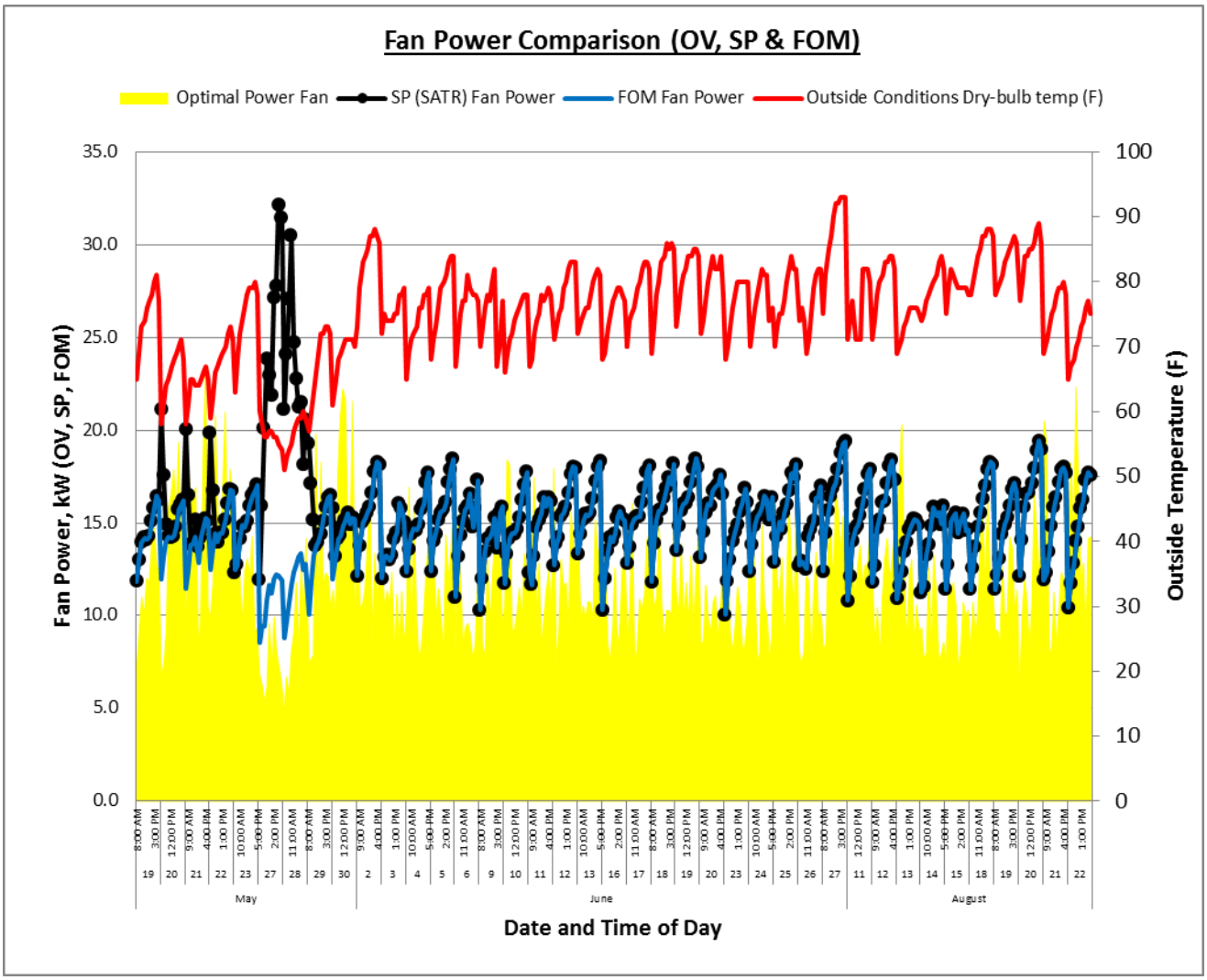

Figure 60. Fan power comparison (OV, SP & FOM).

Variable speed control is achieved by controlling fan speed with a variable-frequency drive. The basis of the fan power law is that the pressure rise through a centrifugal blower is proportional to the square of the speed, while at the same time, the pressure loss through a

system of fixed-flow resistances tends to be proportional to the square of the flow. As a result, the flow ends up being proportional to the blower speed. Since power is proportional to flow times pressure, power is proportional to the speed cubed (Dieckmann, J. et al., 2010). However, in the VAV system's case, typically the duct static pressure is maintained at a constant pressure, and therefore will not exactly follow the square of the flow.

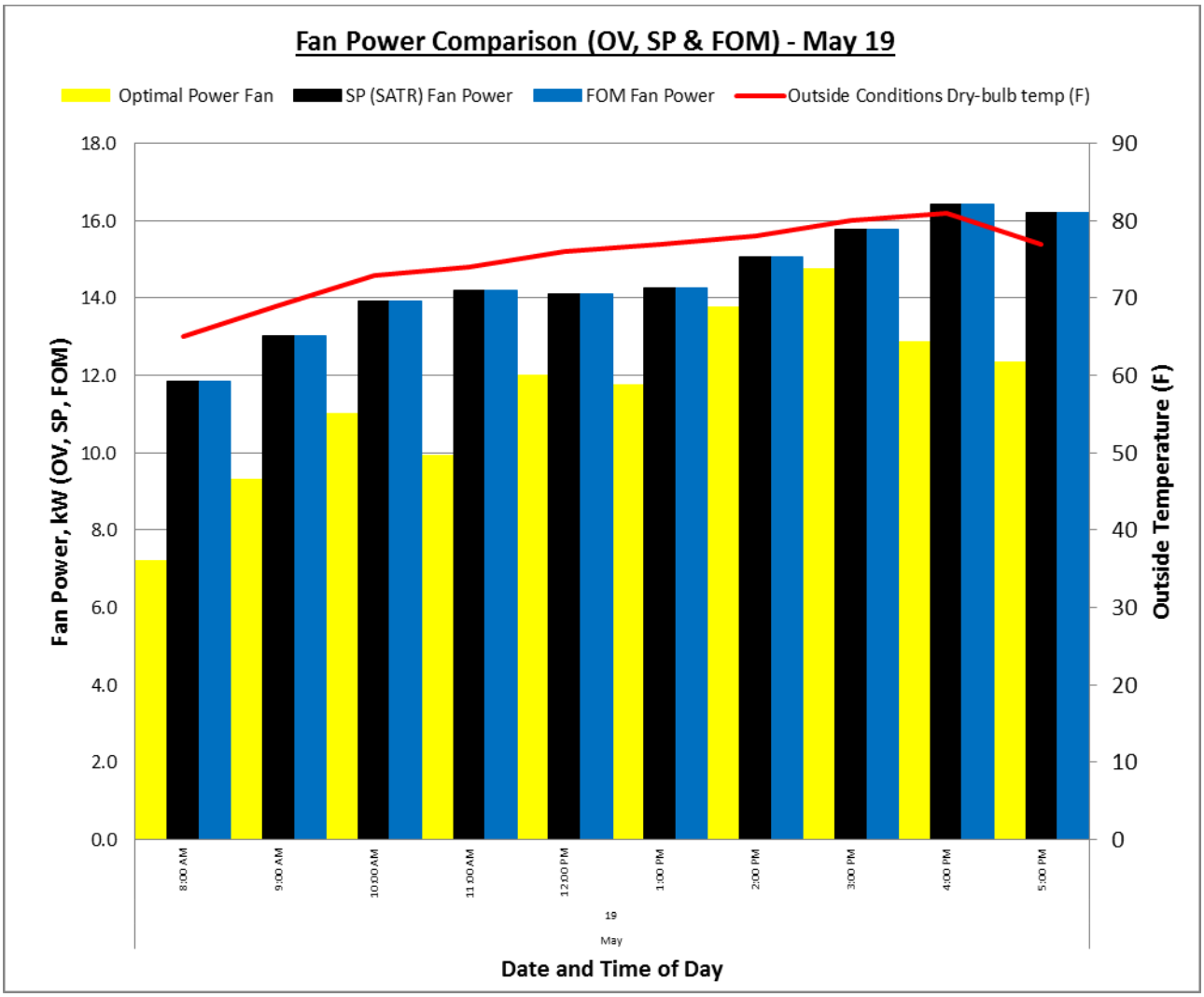

Figure 61. Fan power comparison (OV, SP & FOM) - May 19.

In Figures 60 and 61 the obvious fan power savings is when the outside temperature is under 57 ^{o}F the SATR or SP mode automatically resets the T_s to a higher temperature which

increases the fan power. In the OLSTOP the variable set-points work in conjunction with each other to minimize overall system energy use and the fan power is at its minimum energy use in this scenario.

Similar to fan energy use, pump energy savings from reducing chilled water flow rate is apparent. The flow rate is related to the chilled water pressure drop across the system. The pump affinity laws apply in this situation; the pressure varies with the square of the speed and the power varies with the cube of the speed:

Head or Pressure

$$\frac{dp_1}{dp_2} = \left(\frac{n_1}{n_2}\right)^2 \tag{5.2}$$

Power

$$\frac{P_1}{P_2} = \left(\frac{n_1}{n_2}\right)^3 \tag{5.3}$$

Reducing the flow rate reduces pumping costs and improves system effectiveness. The energy savings potential from reducing the flow rate is shown in Figures 62 & 63. In the OLSTOP, this is achieved by monitoring the pressure drop in relation to the other optimal variables of the chilled water and reducing flow respectively.

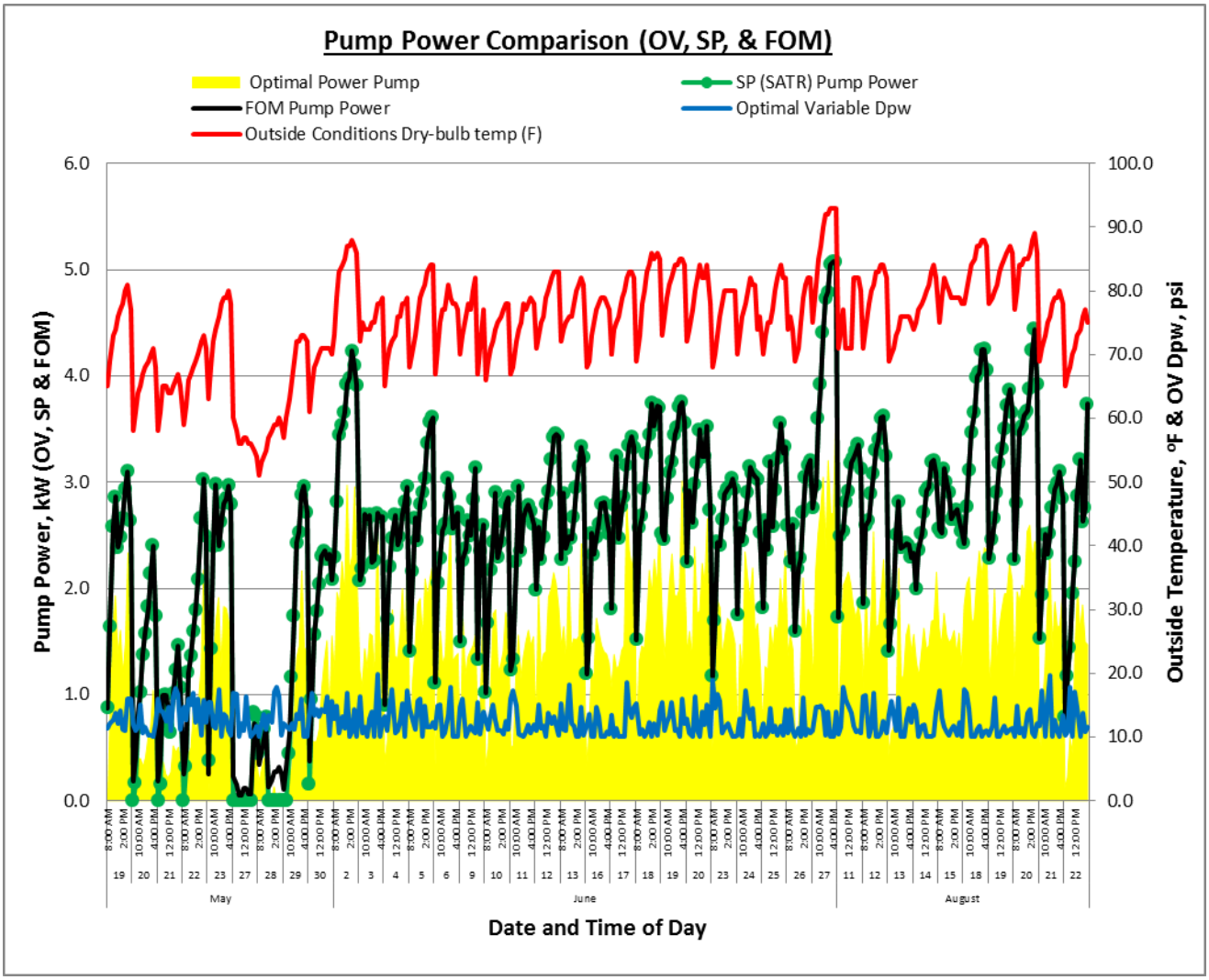

Figure 62. Pump power comparison (OV, SP & FOM).

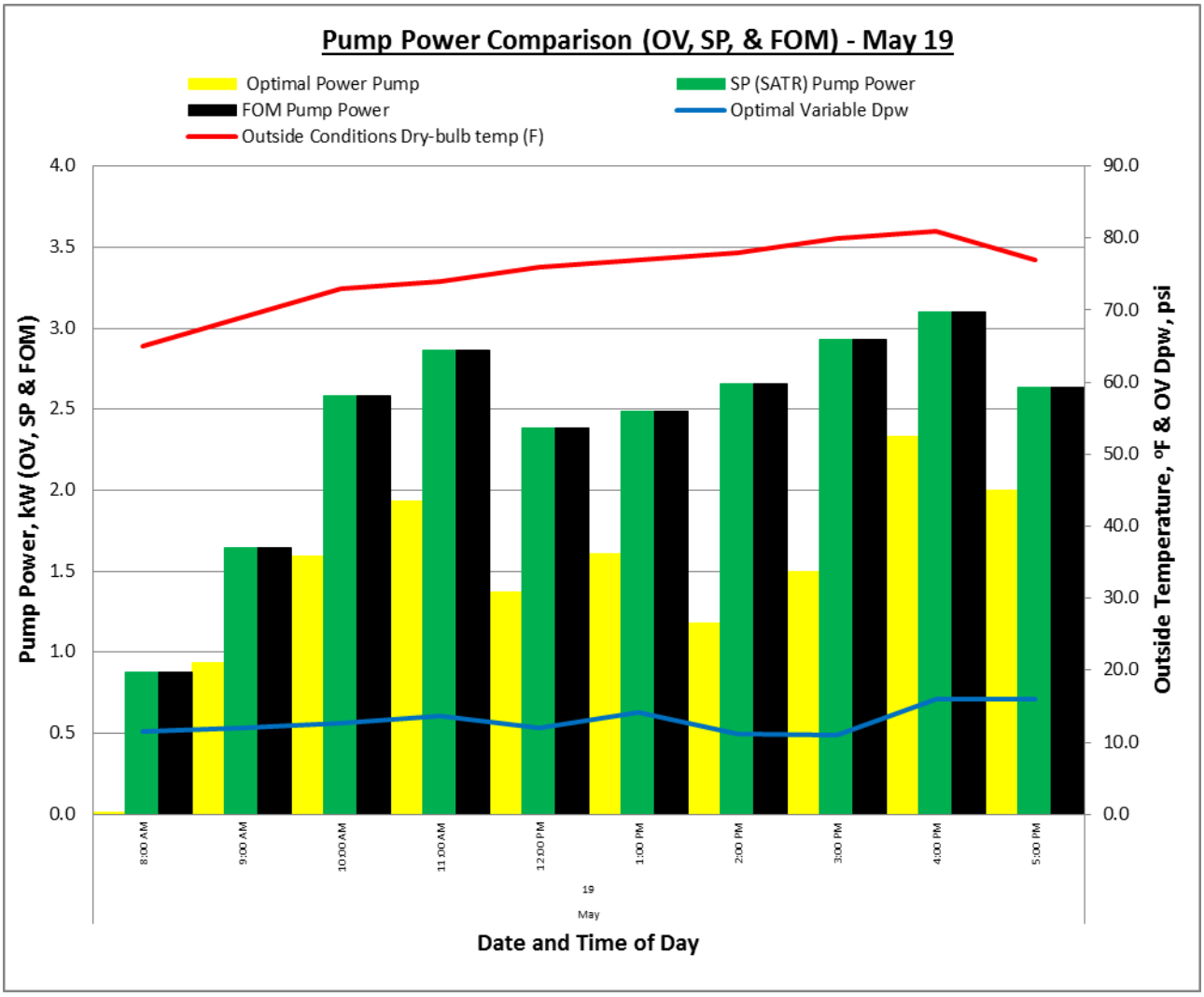

Figure 63. Pump power comparison (OV, SP & FOM) - May 19.

The system's efficiency improves with optimum supply air temperature (T_s), duct static pressure (P_s), pressure drop across the chilled water (D_{pw}) and chilled water temperature (T_w). These variables work together to minimize the fan, pump, and chiller's energy use. The effect on the total cooling electricity use is modeled by solving a system of equations that includes the chiller performance (see Chapter 3). The OLSTOP utilizes the real time loads and provides the capability to vary the energy use of the pumps, fans and chillers with variable frequency drives.

Variable flow control significantly reduces energy use over constant flow systems, as shown in Figures 64 & 65.

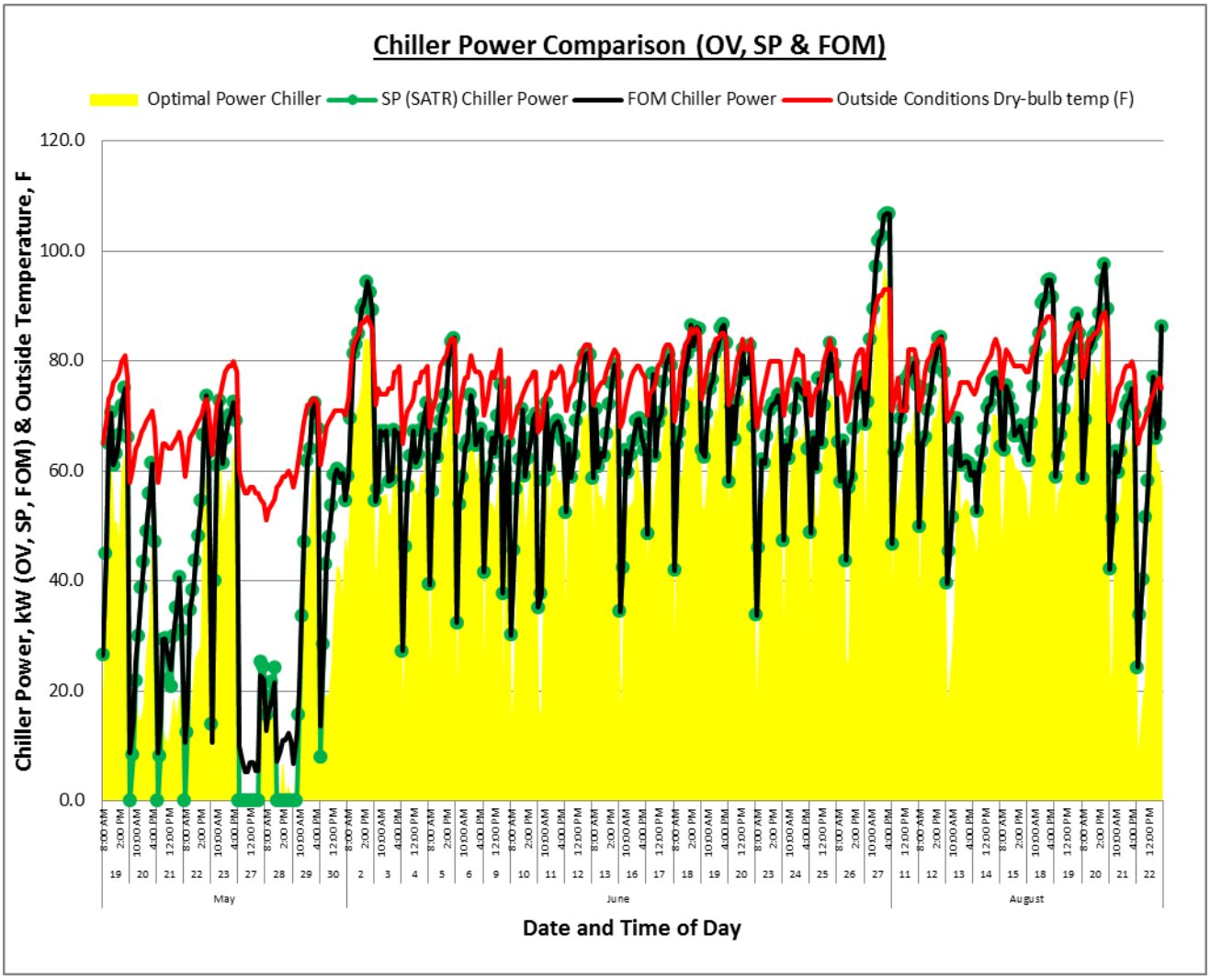

Figure 64. Chiller power comparison (OV, SP & FOM).

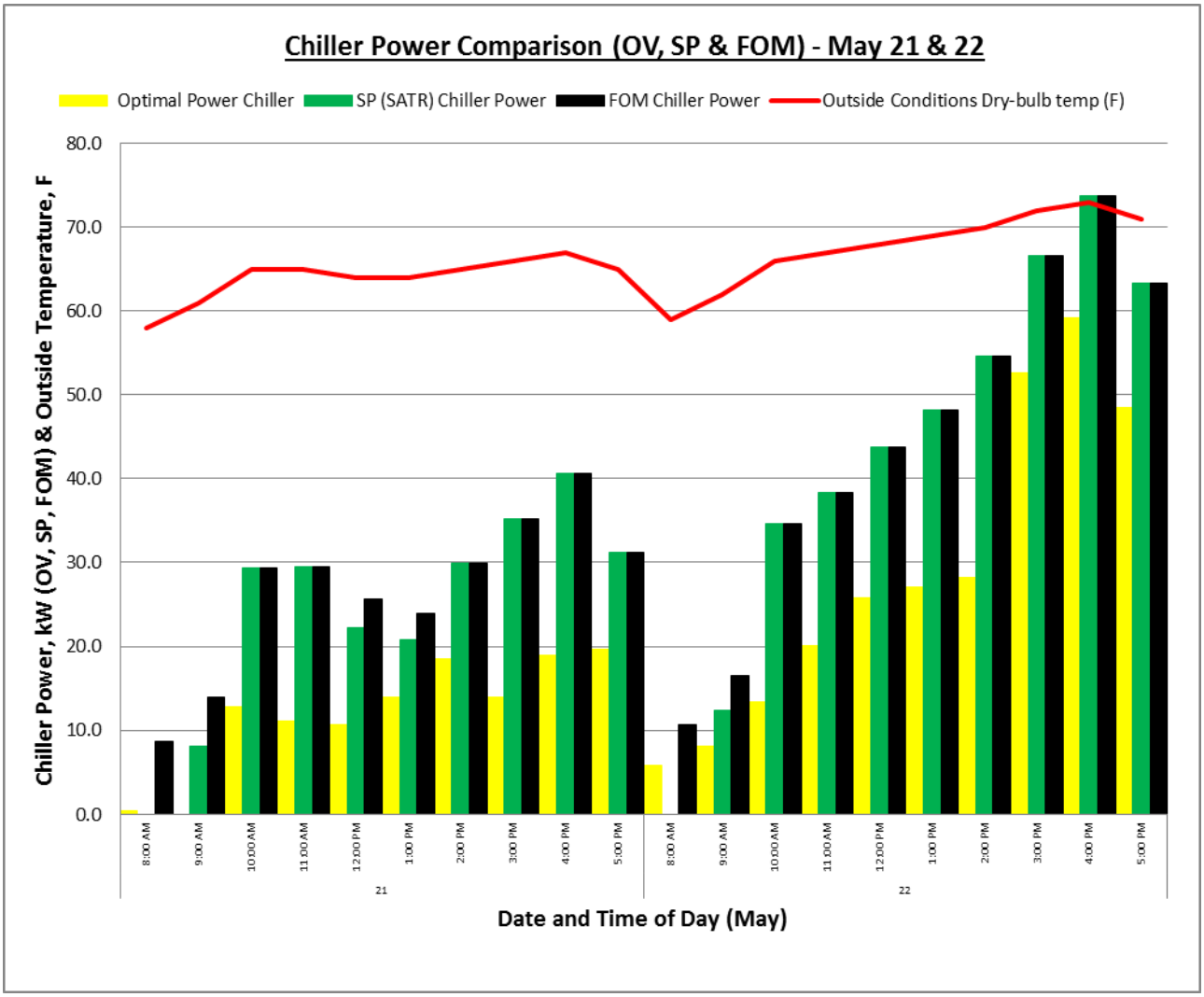

Figure 65. Chiller power comparison (OV, SP & FOM) - May 21 & 22.

To save energy in a chiller there is a significant opportunity to increase chilled water supply temperature (T_w). This is accomplished by modifying the chilled water supply temperature (T_w) while tracking the outside air dry bulb temperature. As shown in the graph in Figures 66 & 67, the chilled water supply temperature (T_w) will typically range between 45°F - 55°F based on outdoor conditions. The OLSTOP allows the chilled water supply temperature (T_w) set point to adjust relative to the outside and internal zone conditions reducing system energy use and improving the humidity control. The energy efficiency of the cooling side of an

existing HVAC system will improve for every degree that the chilled water supply temperature (T_w) is increased. As shown in Figure 66 the chilled water supply temperature averages about 49 ^{o}F. The chilled water temperature requirements change with respect to internal loads and outdoor conditions and the chiller is required to provide mechanical cooling to the building. The chiller power is obvious in the graph in Figure 67 by the large spike in electricity consumption when outside drybulb temperature peaks. During late fall, winter and through early spring, the building will operate entirely in free cooling or economizer mode significantly reducing the chiller's energy use.

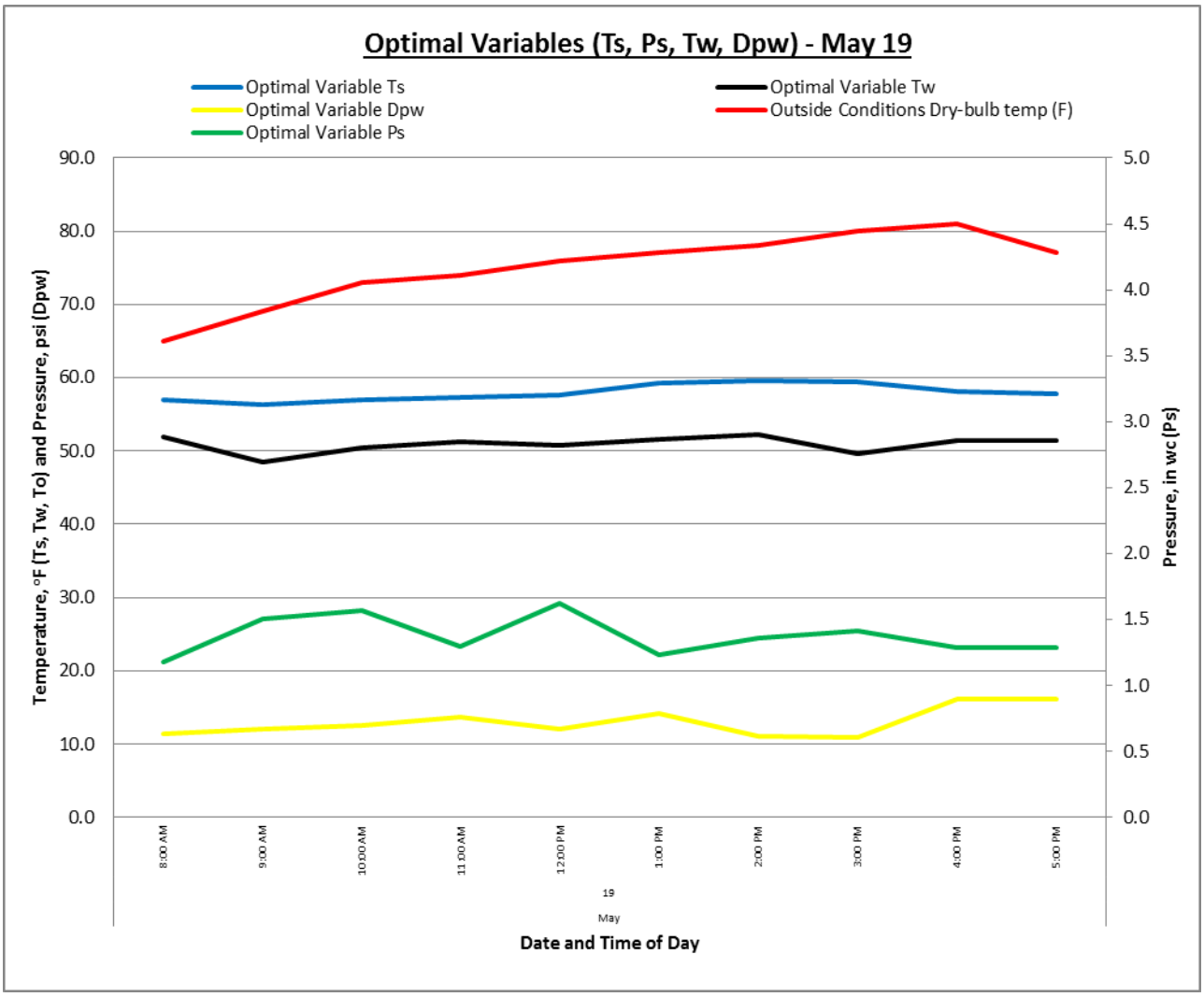

Figure 66. Optimal variables (T_s, P_s, T_w, D_{pw}) - May 19.

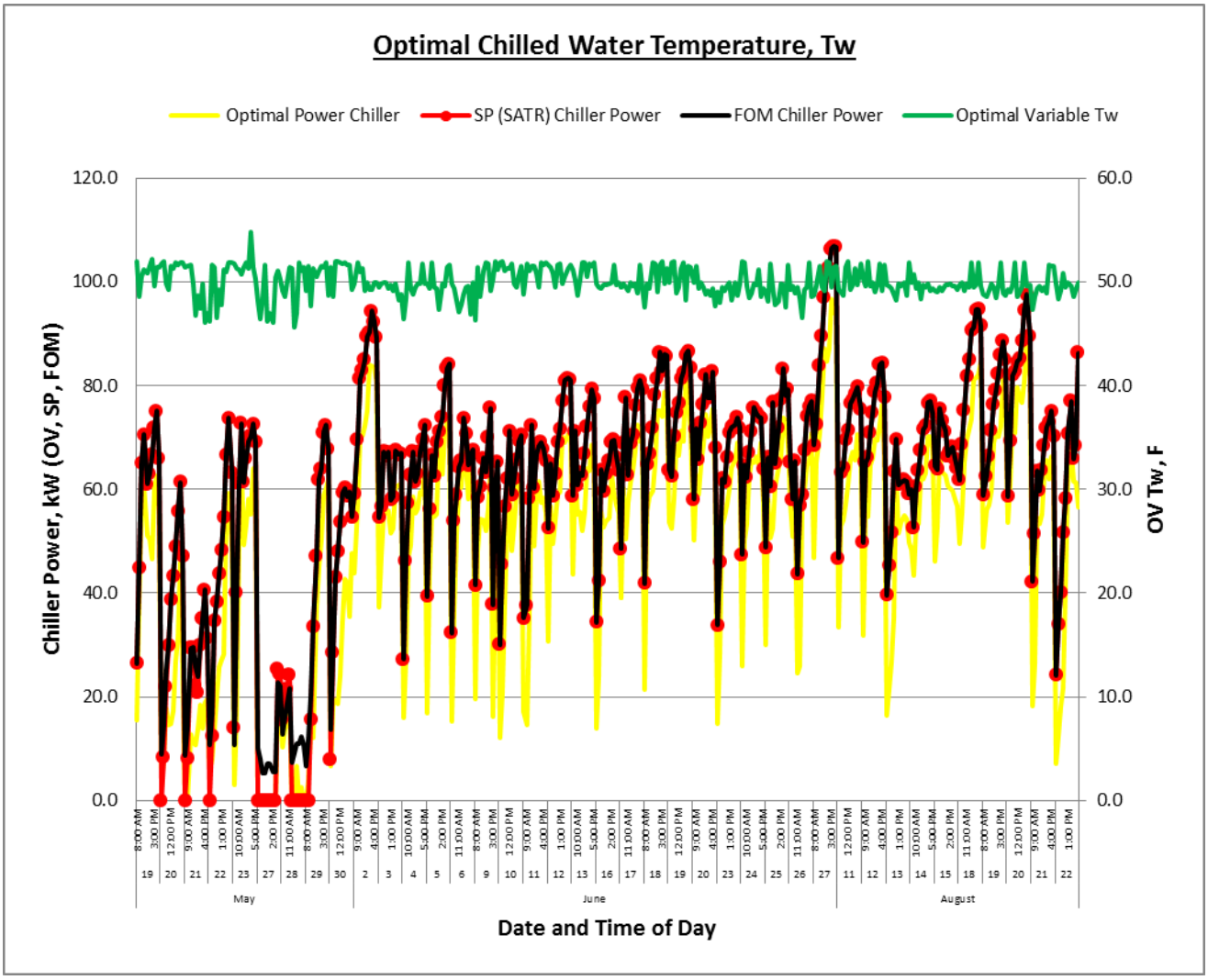

Figure 67. Optimal chilled water temperature, T_w.

Changing the chilled water differential pressure set-point (D_{pw}), obviously affects the flow rate (pump speed), influences pump's energy usage. Chilled water pump speed is controlled to maintain the pressure drop through the chilled water piping or the supply-to-return differential pressure. As discussed earlier, reducing the D_{pw} will decrease the pump energy, as shown in Figure 68. Pump energy can be close to the ideal pump curve by controlling both pump speed and valve position to optimally set the D_{pw}. Modulating valve position and minimizing the differential pressure (D_{pw}) allows pumps to operate closer to their maximum efficiency.

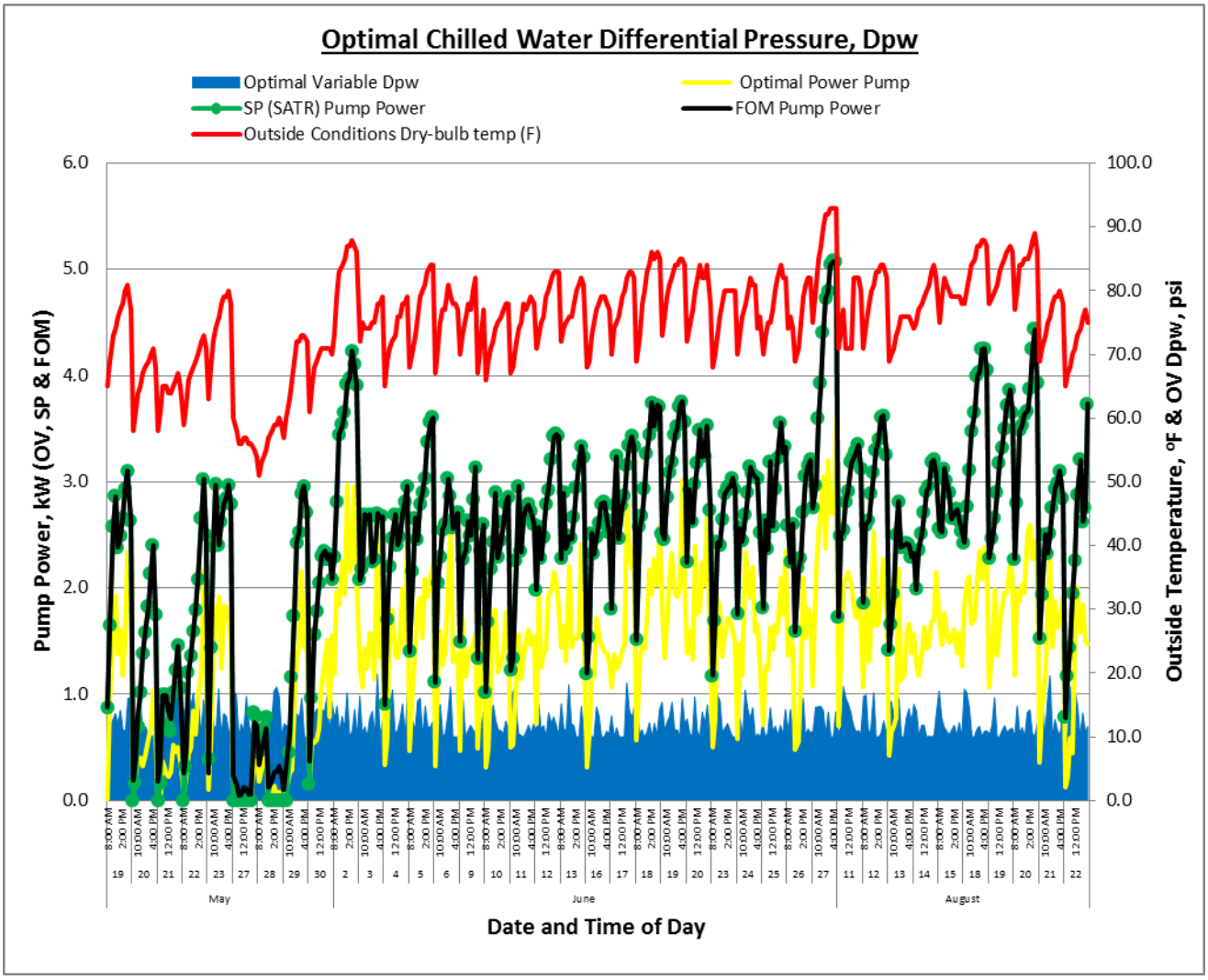

Figure 68. Chilled water differential pressure set-point, $D_{pw.}$

The standard practice (SP) or supply air temperature reset (SATR) mode proves that raising the supply-air temperature (T_s) will save energy when comparing to fixed or over-ride mode (FOM); however, controlling only T_s will increase fan energy and depending on the chilled water control strategy, this will decrease chiller power. Higher T_s may lead to poor humidity control; the OLSTOP will identify the optimal T_s in a systematic procedure, minimizing whole system energy use, not only the chiller or fan. "Free cooling," typically known as an airside economizer, is when the outdoor air is cooler than the T_s set-point, and the

outdoor and return air dampers modulate to deliver the desired supply-air temperature to the system. There are three types of economizer strategies:

1. single temperature control
2. dual temperature control (used in this research with the OLSTOP)
3. dual enthalpy control

For dual temperature control, when the outdoor temperature is cooler than the return air temperature, the economizer ("free cooling") will be active.

In a DX rooftop system, increasing the T_s set-point has a direct impact on HVAC system energy conservation because the compressors turn off sooner and the economizers are on and providing the cooling. This does not necessarily apply in the research as the NACB is a chilled water VAV system. Where zones require reheat due to minimum airflow and internal loads, raising the T_s will reduce the need for reheat advancing energy savings. Obviously, when T_s is warmer, zones that demand cooling will need additional air to satisfy the load, increasing supply fan energy, which seems counterintuitive. This research optimized multiple set point variables in unison to calculate the minimal energy use of the cooling system at each time step. The graph in Figures 69 & 70 shows when the outdoor temperature in May was in the 50^{o}Fs the chiller power was at or near zero, taking advantage of the "free cooling" concept. Optimizing supply-air-temperature (T_s) minimizes overall system energy use, but it requires knowledge of the impact on space humidity levels, chiller, reheat, and fan energy. In some situations the increase in fan energy may be larger than the chiller and reheat energy; these are the factors that an OLSTOP automatically resolves with the single objective function in the genetic algorithm, which is minimal system energy use.

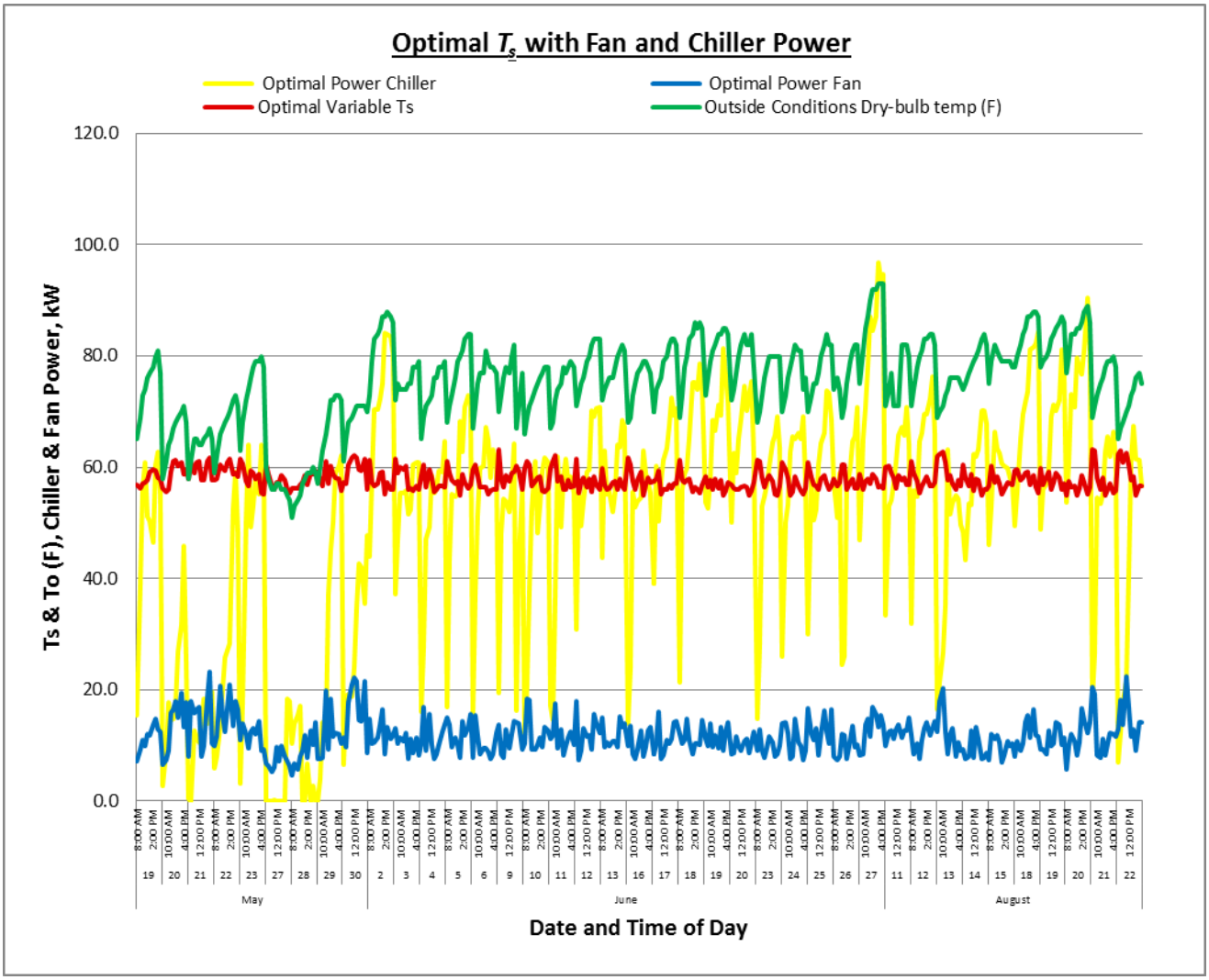

Figure 69. Optimal supply temperature, T_s with fan and chiller power.

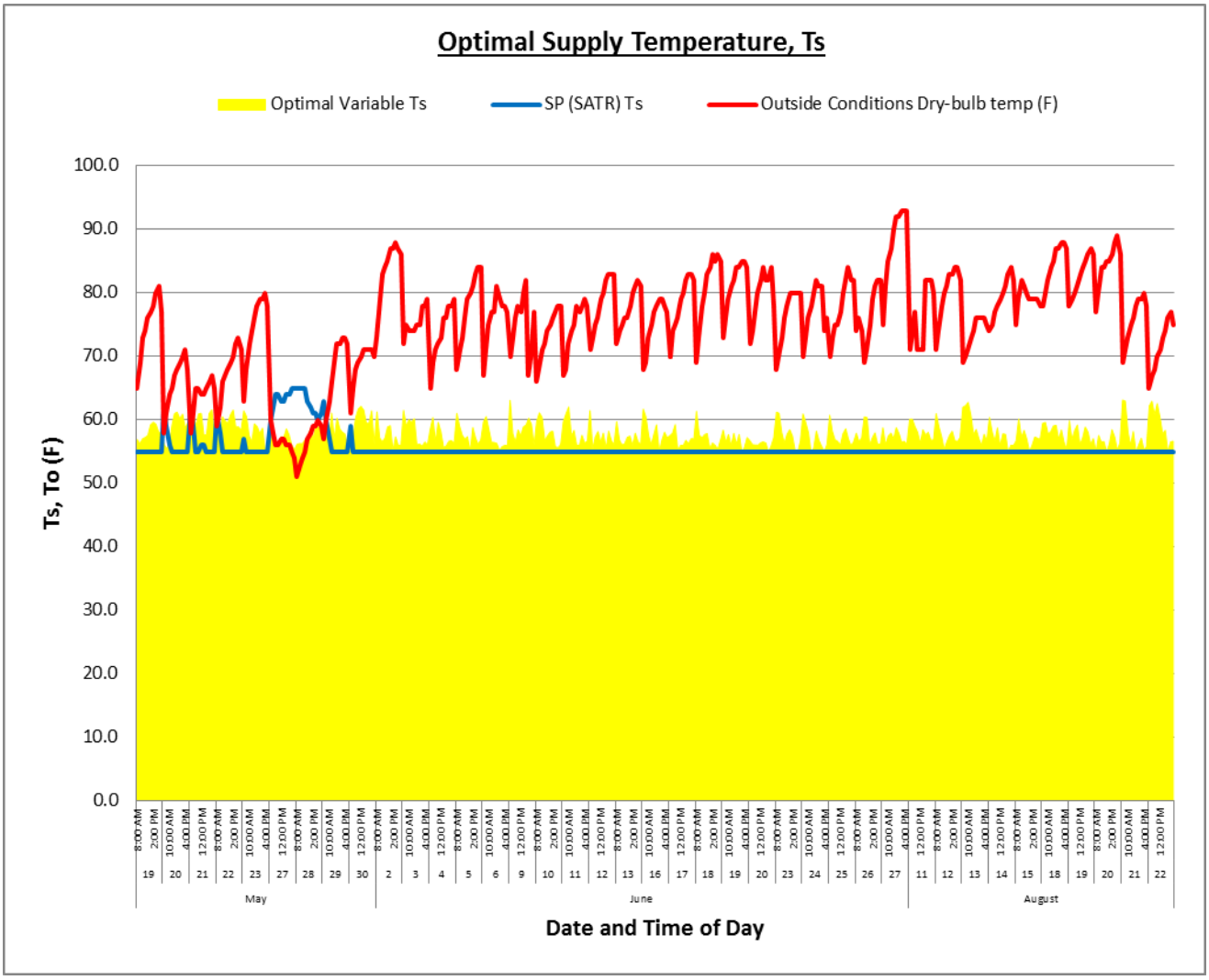

Figure 70. Optimal supply temperature, T_s.

Optimizing duct static pressure (P_s) saves fan energy. The VAV boxes inside the ductwork modulate to adjust airflow supplied to the zones depending on load conditions. With the fluctuating VAV boxes, the duct static pressure changes, this modifies the fan performance to maintain the static pressure set-point. The OLSTM and OP optimizes the static-pressure, minimizing duct static pressure (P_s) and saving fan energy. In Figure 71, the graph clearly shows the fan energy is directly related to the duct static pressure and has the same profile.

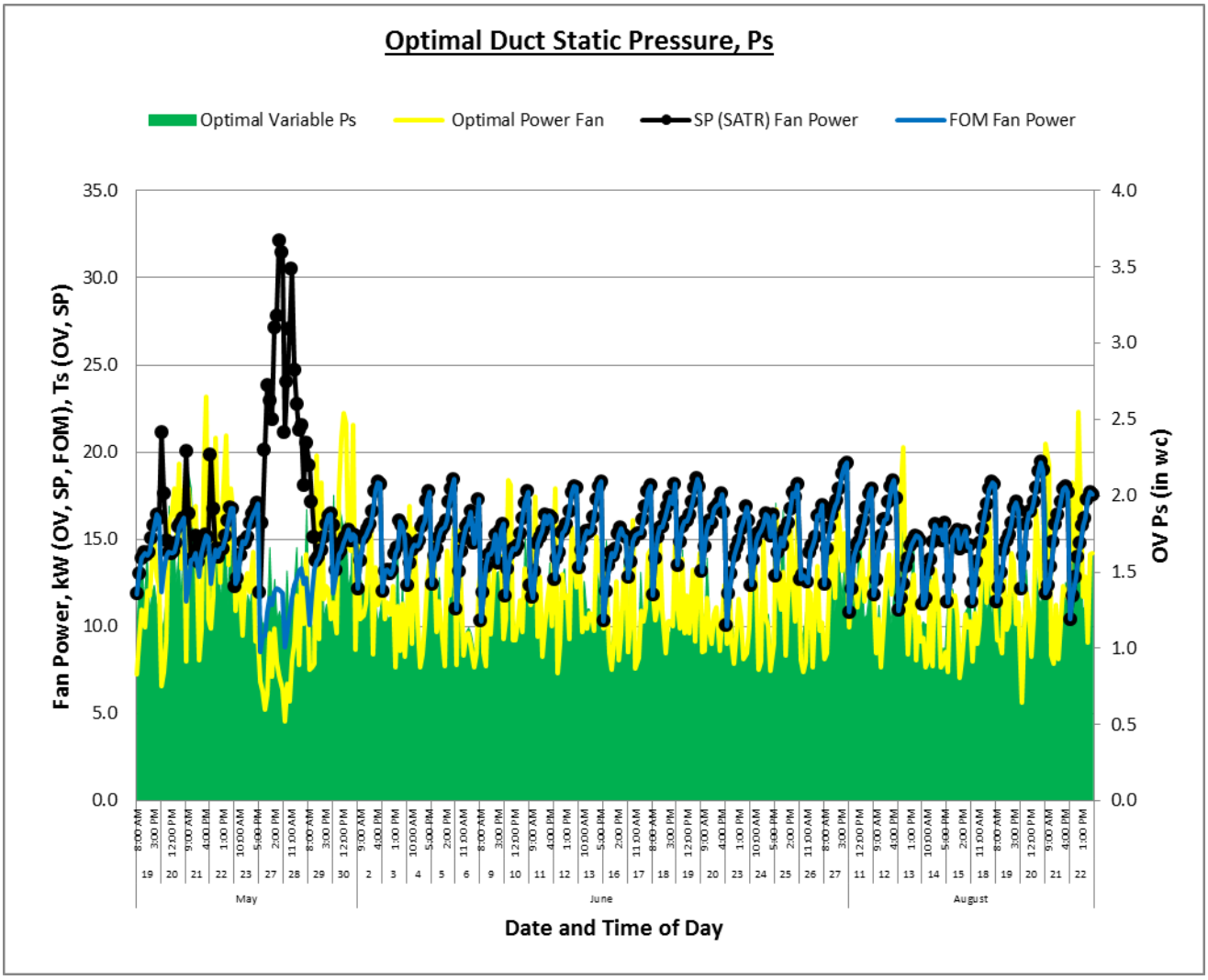

Figure 71. Optimal duct static pressure, P_s.

The optimal duct static pressure (P_s) set-point for the fan is based on providing just enough pressure to the one damper that is 100% open ("critical unit") in the system. This is called fan-pressure optimization and saves supply fan energy use. As described in Chapter 3, the Constraint Model uses the "starved" VAV box scenario, and we decided to allow one VAV box to be starved within the whole HVAC system and add a power penalty to the output allowing the program to continue but that particular solution will not survive in following generations in the GA during the optimization process. In other words, the optimization process will continue to find the optimal variables to reduce the energy in the system but will include constraints that

"kill" that particular optimal variable sequence because it will increase the energy to a value that is not acceptable for a viable solution to the optimization process.

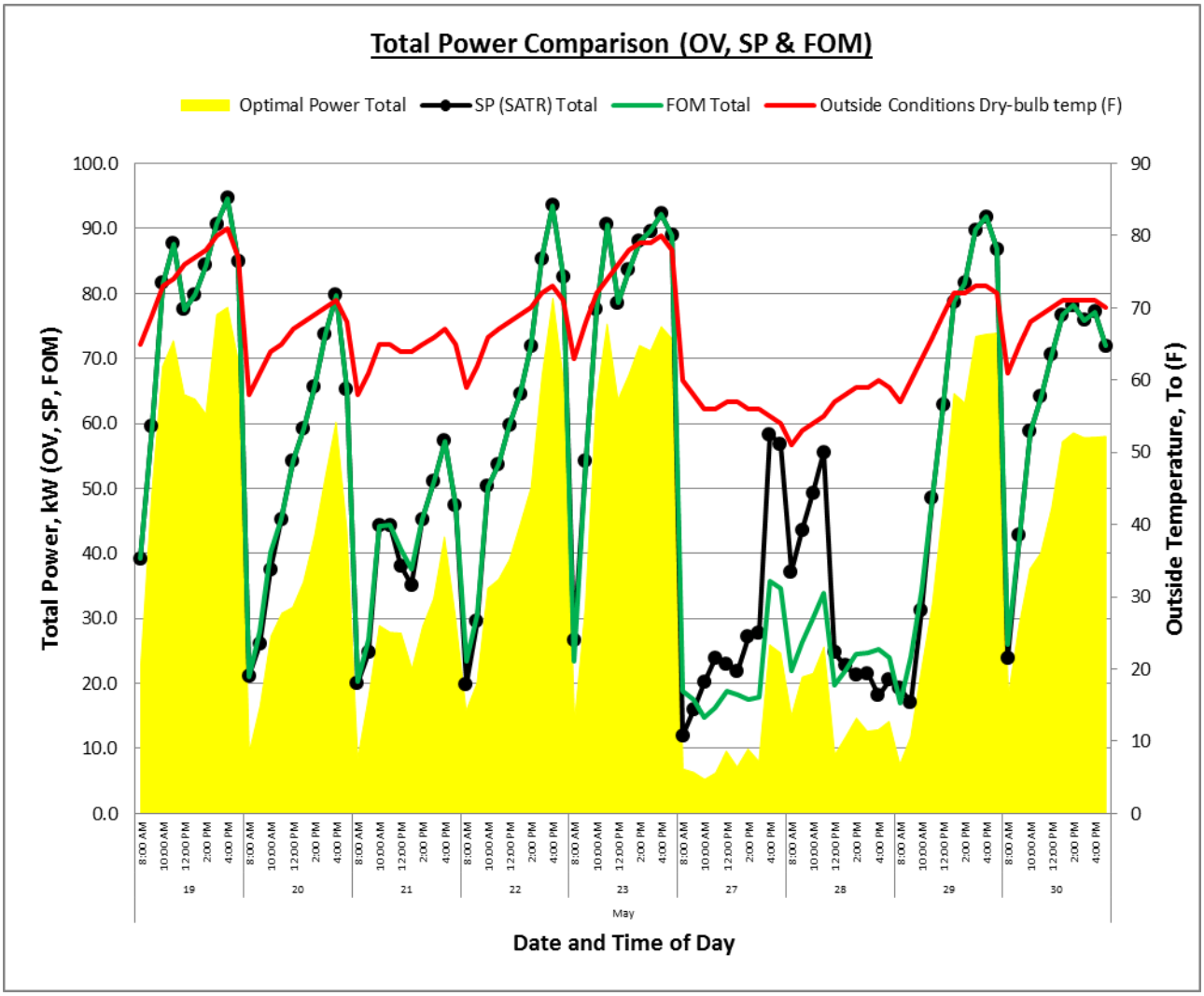

Figure 72. Total power comparison (OLSTOP, SP & FOM) – May.

CHAPTER 6

Conclusion and Future Work

Self-learning or self-tuning approaches are proposed for use in HVAC control and to advance the EMCS. Self-tuning HVAC component models were developed and validated against data collected from the existing HVAC system. The testing results show that the models exhibit good accuracy and fit the input-output data well. An infinite variety of optimal processes can be used for this purpose, but in the interest of conserving computer time genetic algorithms in MATLAB were utilized. The errors of the fan, pump, cooling coil, and chiller models in terms of the coefficient of variation (CV) were calculated. The models could be incorporated into the EMCS to perform several intelligent functions including energy management and optimal control. A whole system optimization process based on genetic algorithms was developed and tested. The testing results indicated that the optimization process can provide energy saving.

The proposed optimization process was applied to an existing HVAC system that is installed at the New Academic Building on the campus of North Carolina A&T State University. The set-points, such as the supply air temperature (T_s), the supply duct static pressure (P_s), chilled water differential pressure set-point (D_{pw}), and the chilled water supply temperature (T_w), are optimized for the existing HVAC system while maintaining or improving the zone air temperatures, T_z (thermal comfort). The existing HVAC providing conditioned air to internal zones, was investigated. In this case, the optimization process using genetic algorithms was performed for three summer months (May, June and August). The results show that by comparing actual and optimal energy use, the OLSTMs running in conjunction with the OP could save energy between 13% - 73% depending on the time of day and load conditions, while satisfying minimum zone airflow rates and zone thermal comfort. These results indicate that the

OP with the required constraints could improve the operating performance of the existing HVAC system. The results show that the program optimizes all controller set-points, including, zone reheat, T_s, T_w, D_{pw}, and P_s, performs better and provides more energy savings while maintaining zone temperature and thermal comfort. Other results indicate that the application of the on-line, self-tuning, optimization process (OLSTOP) could help control daily energy use and daily building thermal comfort while providing further energy use savings.

The models consist of tuning parameters which intelligently adapt to the actual behavior of the HVAC system. The model parameters were periodically adjusted online by a genetic algorithm optimization method to reduce the error between measured and predicted data.

Steady state models were developed and validated against measured data from an existing HVAC system. The coefficient of variance (*CV*) between the predicted and measured data was used as a measure of comparison. The validation results showed that the accuracy of proposed OLSTM is significantly better than that of pure physical models without the tuning parameters in the case of the fan model. For instance, the coefficient of variance (*CV*) of the cooling coil model decreased from 2.256% for the well documented CCSIM from ASHRAE's HVAC 2 Toolkit to 0.713% with the new self-tuning cooling coil model. The chiller model's *CV* = 3.804% and the Fan Model had a *CV* = 0.683% comparing speed and a *CV* = 6.64% comparing power. Thus, the use of such models offer several advantages such as designing better real-time control, optimization of overall system performance, and online fault detection.

6.1 Future Work

There are various enhancements that could be implemented to the research for post-doctoral work. By introducing supplementary advanced models, utilizing other methods and techniques by replacing the genetic algorithms, it is possible to achieve more accurate

simulations than the ones explored in this report. Launching models that optimize more set-point variables approximating condenser water temperature (T_c), the pressure drop of the condenser water piping (D_{pc}) and others can be investigated. Including additional components resembling the cooling tower and the entire heating side (boiler, heating coil, etc.) of the HVAC system can also be modeled. Including these new component models and optimizing additional set-point variables will enable further energy savings by simulating extra scenarios. This report indicates that the OLSTOP is able to maintain occupant comfort and meet the new ASHRAE 62.1-2013 fresh air requirements.

The OLSTOP has the ability to obtain optimal set-point variables implementing constraints, power penalties (to "kill" a solution), new ASHRAE standards, and control strategies. The OLSTOP compares set-point variables (T_s, P_s, T_w, and D_{pw}) by running the same programs and subroutines with the Standard Practice (SP) which is typical in existing buildings where only T_s is adjusted, and Fixed or Over-ride Mode (FOM) which has the fixed settings for the set-point variables $T_s = 55^oF$, $P_s = 2.5$ in w.c., $T_w = 45^oF$ and $D_{pc} = 20$ in w.c. Creating a program that does not provide these constraints, penalties, ASHRAE standards and control strategies on the FOM and SP mode and running it would gain a realistic "higher" energy savings per time step versus the OLSTOP. We assume that the HVAC operator in the existing building is running in a SATR (supply air temperature reset) mode where the T_s is adjusted with outside dry-bulb temperature (T_o); this mode sets T_s at 55^oF if $T_o > 65^oF$ and sets T_s at 65^oF if $T_o < 55^oF$ and calculates T_s on a linear basis if $55^oF < T_o < 65^oF$). However, that process would require more time and effort for code and data collection and calibration that is counter-productive to implementing new programming techniques and accuracy for the OLSTOP.

This research program was sequenced from 8 am to 5 pm, Monday through Friday (main time of occupancy) for three summer months (May, June, and August) but not on weekends or overnight where occupancy levels drop off significantly and would signal the program to bring in fresh air only when necessary. This would lead to a more economical usage of fresh air and prove to increase energy savings. The program should be evaluated and the resulting data compared at each time step for the entire year (24/7/365).

The OLSTOP is used for operation and control but could be further developed to influence architect's and engineer's decisions during the conceptual building design phase, which will have an essential outcome on the building energy performance (BEP). The consequences of these findings are often overlooked; therefore a more strategic approach to the interaction between the OLSTOP, which has a direct impact on BEP, and the conceptual building design should be investigated. The selection of efficient heating and cooling systems partnered to a specific building and component models that accurately portray the equipment's interactions and performance becomes increasingly vital to the building design process. This dissertation investigated the relationship between the primary and secondary HVAC systems and the real and simulated building design. The goal was to quantify the OLSTOP with its energy savings capability in an existing building. The relationship concerning the initial design decisions and the configuration, energy consumption and emissions of the HVAC system would reduce a building's carbon footprint and save money. In order to accomplish this, a program supporting the following should to be developed:

- an HVAC system design optimization program, providing a configuration suitable to satisfy the thermal conditioning demand of the provided building with the OLSTOP

implemented in the BAS (this will help avoid component oversizing, increase the system efficiency, and decrease the investment cost and carbon emission).

- qualify the fuel consumption and carbon emissions of the proposed system while optimally conditioning the designed building
- the cost assessment, including both the investment and the energy consumption annually

Several future exploits that could benefit from incorporating the OLSTOP are:

- building systems that currently operate independently from one another; HVAC and building lighting systems do not communicate with each other and could benefit with additional energy savings by becoming intelligent, cooperative systems.
- simplifying the building modeling and energy simulation phases with interactive interfaces and smooth transitions from model, simulation and BAS
- implementing a software upgrade to an existing BAS that would incorporate the OLSTOP

In this research standard components and HVAC theory are utilized due to the complexity of modeling a specific building's HVAC system and trying to reuse the system components in other buildings. Calculation subroutines include the new ASHRAE standards, control strategies, constraints and power penalties to develop the OLSTOP. All HVAC system components were not modeled and the program wasn't run against every conceivable situation and parameter (lighting level control, seasonally (Fall, Winter, Spring), optimal window shade usage, etc.). HVAC modelling and simulation is complicated from a user stand point and analyzing the results can be problematic due to HVAC system operator error, equipment maintenance, and other unknowns that directly effect that data output. The OLSTOP should be further developed to include:

- new programming in different languages like C++ or FORTRAN including faster and multiple processors in a message passing interface (MPI) environment to speed up the process
- a new user interface that allows the user to directly input system data and automatically run all time steps generating each individual output sequentially; and input to be read from a standard file format that is directly down loaded from a simulation tool like eQuest or EnergyPlus or a building automation system (BAS).
- proving that the GA parameters achieve optimal variables and finding the technology or processor speed to gain the ability to run the genetic algorithm at a higher generation and population to achieve true optimal set-point variables attaining higher energy savings
- Other optimizing techniques to compare to the GA, like non-linear curve fitting, non-linear least squares, etc.
- Additional HVAC system component models from both primary and secondary systems including the heating side that will determine more set-point variables.

REFERENCES

Advanced HVAC Controls. (2014, 2014 Aug 19). *PR Newswire*.

Afram, A., & Janabi-Sharifi, F. (2014). Review of modeling methods for HVAC systems. *Applied Thermal Engineering, 67*(1-2), 507-519. doi: 10.1016/j.applthermaleng.2014.03.055

Ali, M., Sahir, M., H., Qureshi, A., Akhtar, K., & Gondal, I. (2013). *Optimization of Heating, Ventilation, and Air-Conditioning (HVAC) System Configurations.* (PhD in Mechanical Engineering), University of Engineering & Technology Taxila, Pakistan. (08-UET/PhD-ME-45)

Anderson, M., Buehner, M., Young, P., Hittle, D., Anderson, C., Tu, J., & Hodgson, D. (2007). An experimental system for advanced heating, ventilating and air conditioning (HVAC) control. *Energy and Buildings, 39*(2), 136-147. doi: 10.1016/j.enbuild.2006.05.003

Architecture, D. (2012). Sustainability and the Impacts of Building, 2012, from http://doerr.org/services/sustainability.html

ASHRAE. (2012). *2012 HVAC Systems and Equipment*. Atlanta, GA: ASHRAE.

ASHRAE. (2013). *2013 ASHRAE Handbook Fundamentals Inch-Pound Edition*. Atlanta, GA: ASHRAE.

Ben-Aissa, N. (1997). HVAC Controls: Variable Air Volume Systems. *VisSim Tutorial Series*. Retrieved from

Bhatia, A. (2012). HVAC Refresher - Facilities Standard for the Building Services (Part 2). Retrieved from

Bichiou, Y., & Krarti, M. (2011). Optimization of envelope and HVAC systems selection for residential buildings. *Energy and Buildings, 43*(12), 3373-3382. doi: 10.1016/j.enbuild.2011.08.031

Brandemuehl, M. (1993). *HVAC 2 Toolkit: Algorithms and Subroutines for Secondary HVAC System Energy Calculations*: ASHRAE.

Braun, J. E., Klein, S. A., Mitchell, J. W., & Beckman, W. A. (1989). Methodologies for Optimal Control to Chilled Water Systems without Storage. *ASHRAE Transactions, 95*(1), 652-662.

Bravo, R. H., & Flocker, F. W. (2011). Designing HVAC Systems Using Particle Swarm Optimization. *ASHRAE Transactions, 117*, 565-578.

Caldas, L. G., & Norford, L. K. (2003). Genetic Algorithms for Optimization of Building Envelopes and the Design and Control of HVAC Systems. *Journal of Solar Energy Engineering, 125*(3), 343-351. doi: 10.1115/1.1591803

Castilla, M., Álvarez, J. D., Berenguel, M., Rodríguez, F., Guzmán, J. L., & Pérez, M. (2011). A comparison of thermal comfort predictive control strategies. *Energy and Buildings, 43*(10), 2737-2746. doi: 10.1016/j.enbuild.2011.06.030

Clark, D. R. (1985). *HVACSIM+ building systems and equipment simulation program: Reference Manual*. Washington, D.C.: U.S. Department of Commerce.

Commercial Building Automation Systems. (2013, 2013 Nov 26). *PR Newswire*. Retrieved from https://sheba.ncat.edu/validate?url=/docview/1461734878?accountid=12711

Congradac, V., & Kulic, F. (2009). HVAC system optimization with CO2 concentration control using genetic algorithms. *Energy and Buildings, 41*(5), 571-577. doi: 10.1016/j.enbuild.2008.12.004

Cook, H. (1998). Modeling energy-efficient HVAC. *Building Design & Construction, 39*(1), 64-66.

Counsell, J., Zaher, O., Brindley, J., & Murphy, G. (2013). Robust nonlinear HVAC systems control with evolutionary optimisation. *Engineering Computations, 30*(8), 1147-1169. doi: http://dx.doi.org/10.1108/EC-04-2012-0079

D&R International, L. (2012). 2011 Buildings Energy Data Book U. S. D. o. Energy (Ed.) Retrieved from http://buildingsdatabook.eere.energy.gov/.

Dieckmann, J., McKenney, K., & Brodrick, J. (2010). Variable Frequency Drives, Part 2: VFDs for Blowers. [Article]. *ASHRAE Journal, 52*(5), 58-62.

Djuric, N., Novakovic, V., Holst, J., & Mitrovic, Z. (2007). Optimization of energy consumption in buildings with hydronic heating systems considering thermal comfort by use of computer-based tools. *Energy and Buildings, 39*(4), 471-477. doi: http://dx.doi.org/10.1016/j.enbuild.2006.08.009

DOE. (1980). *DOE-2 Reference Manual, Part 1, Version 2.1*: Lawrence Berkeley Laboratory.

Englander, S. L., & Norford, L. K. (1992). Saving Fan Energy in VAV Systems, Part 2: Supply Fan Control for Static Pressure Minimization using DDC zone Feedback. *ASHRAE Transactions, 98*(1), 19-32.

Federspiel, C. C. (2005). Detecting Critical Supply Duct Pressure/DISCUSSION. *ASHRAE Transactions, 111*, 957-963.

Fong, K. F., Hanby, V. I., & Chow, T. T. (2006). HVAC system optimization for energy management by evolutionary programming. *Energy and Buildings, 38*(3), 220-231. doi: http://dx.doi.org/10.1016/j.enbuild.2005.05.008

House, J. M., & Smith, T. F. (1995). A System Approach to Optimal Control for HVAC and Building Systems. *ASHRAE Transactions, 101*(2), 647-660.

House, J. M., Smith, T. F., & Arora, J. S. (1991). Optimal Control of a Thermal System. *ASHRAE Transactions, 97*(2), 991-1001.

Huh, J.-H., & Brandemuehl, M. J. (2008). Optimization of air-conditioning system operating strategies for hot and humid climates. *Energy and Buildings, 40*(7), 1202-1213. doi: http://dx.doi.org/10.1016/j.enbuild.2007.10.018

Hui, C. M. (1996). *Energy Performance of Air-conditioned Buildings in Hong Kong.* (PhD), City University of Hong Kong, City University of Hong Kong.

Hurtado, L. A., Nguyen, P. H., Kling, W. L., & Zeiler, W. (2013, 2-5 Sept. 2013). *Building Energy Management Systems — Optimization of comfort and energy use.* Paper presented at the Power Engineering Conference (UPEC), 2013 48th International Universities'.

Hydeman, M., & Gillespie, K. L. (2002). Tools and techniques to calibrate electric chiller component models. *ASHRAE Transactions, 108*(1), 733-741.

Hydeman, M., Webb, N., Sreedharan, P., & Blanc, S. (2002). Development and testing of a reformulated regression-based electric chiller model. *ASHRAE Transactions, 108*(2), 1118-1127.

Jahedi, G., & Ardehali, M. M. (2012). Wavelet based artificial neural network applied for energy efficiency enhancement of decoupled HVAC system. *Energy Conversion and Management, 54*(1), 47-56. doi: 10.1016/j.enconman.2011.10.005

Joo, I.-S. (2007). Application of fan Airflow Stations In Air-handling Units. *Energy Engineering, 104*(2), 66.

Ke, Y.-P., & Mumma, S. A. (1997). Optimized supply-air temperature (SAT) in variable-air-volume (VAV) systems. *Energy, 22*(6), 601-614. doi: http://dx.doi.org/10.1016/S0360-5442(96)00154-5

Kelly, G. E., & Bushby, S. T. (2012). Are intelligent agents the key to optimizing building HVAC system performance? *HVAC & R Research, 18*(4), 750.

Korolija, I., Marjanovic-Halburd, L., Zhang, Y., & Hanby, V. I. (2011). Influence of building parameters and HVAC systems coupling on building energy performance. *Energy and Buildings, 43*(6), 1247-1253. doi: 10.1016/j.enbuild.2011.01.003

Kusiak, A., Li, M., & Tang, F. (2010). Modeling and optimization of HVAC energy consumption. *Applied Energy, 87*(10), 3092-3102. doi: http://dx.doi.org/10.1016/j.apenergy.2010.04.008

Kusiak, A., & Xu, G. (2012). Modeling and optimization of HVAC systems using a dynamic neural network. *Energy, 42*(1), 241-250. doi: http://dx.doi.org/10.1016/j.energy.2012.03.063

Kusiak, A., Xu, G., & Zhang, Z. (2014). Minimization of energy consumption in HVAC systems with data-driven models and an interior-point method. *Energy Conversion and Management, 85*(0), 146-153. doi: http://dx.doi.org/10.1016/j.enconman.2014.05.053

Little, M. (2002). Reducing mercury pollution from electric power plants. *Issues in Science and Technology, 18*(4), 27-30.

Lu, L., Cai, W., Xie, L., Li, S., & Soh, Y. C. (2005). HVAC system optimization—in-building section. *Energy and Buildings, 37*(1), 11-22. doi: http://dx.doi.org/10.1016/j.enbuild.2003.12.007

MacArthur, J. W., & Woessner, M. A. (1993). Receding Horizon Control: A Model-based Policy for HVAC Applications. *ASHRAE Transactions, 99*(1).

Martin, R. A., Federspiel, C. C. P. D., & Auslander, D. M. P. D. (2002). Supervisory control for energy savings and thermal comfort in commercial building HVAC systems.

Megri, A. C., & Yu, Y. (2014a). Energy Prediction of Electric Floor Radiation Systems Using a New Integrated Modeling Approach. *ASHRAE Transactions, 120*, 356-365.

Megri, A. C., & Yu, Y. (2014b). An Integrated Heat Transfer Attic and Multiroom Thermal Building Model. *ASHRAE Transactions, 120*, 236-247.

Mincer, S. (2011). Dealmaking International Electricity Woes 2012, from http://energy.aol.com/2011/08/03/international-electricity-woes/

Murphy, J. (2006). Energy-saving Control Strategies for Rooftop VAV Systems. *Trane Engineers Newsletter, 35*(4). Retrieved from

Narayanan, S., Yang, S., Kim, H., & Wang, E. N. (2014). Optimization of adsorption processes for climate control and thermal energy storage. *International Journal of Heat and Mass Transfer, 77*(0), 288-300. doi: http://dx.doi.org/10.1016/j.ijheatmasstransfer.2014.05.022

Nassif, N. (2010). Performance analysis of supply and return fans for HVAC systems under different operating strategies of economizer dampers. *Energy and Buildings, 42*(7), 1026-1037. doi: 10.1016/j.enbuild.2010.01.015

Nassif, N., & Moujaes, S. (2008). A new operating strategy for economizer dampers of VAV system. *Energy and Buildings, 40*(3), 289-299. doi: 10.1016/j.enbuild.2007.02.030

Nassif, N., Moujaes, S., & Zaheeruddin, M. (2008). Self-tuning dynamic models of HVAC system components. *Energy and Buildings, 40*(9), 1709-1720. doi: 10.1016/j.enbuild.2008.02.026

Nassif, N., Stanislaw, K., & Sabourin, R. (2005). Optimization of HVAC Control System Strategy Using Two-Objective Genetic Algorithm. *HVAC&R Research, 11*(3), 459-486.

Nassif, N., Tesiero, R. C., & Singh, H. (2013). Impact of Ice Thermal Storage on Cooling Energy Cost for Commercial HVAC Systems. *ASHRAE Transactions, 119*, S1-S7.

Platt, G., Li, J., Li, R., Poulton, G., James, G., & Wall, J. (2010). Adaptive HVAC zone modeling for sustainable buildings. *Energy and Buildings, 42*(4), 412-421. doi: http://dx.doi.org/10.1016/j.enbuild.2009.10.009

Preglej, A., Rehrl, J., Schwingshackl, D., Steiner, I., Horn, M., & Škrjanc, I. (2014). Energy-efficient fuzzy model-based multivariable predictive control of a HVAC system. *Energy and Buildings, 82*(0), 520-533. doi: http://dx.doi.org/10.1016/j.enbuild.2014.07.042

Rajkumar, C. V., & Dattabhimaraju, S. P. (2013). Optimization of AHU Control Strategy. *International Journal of Innovative Technology and Research, 1*(2), 124-129.

Shaheen: Energy Efficiency Bill Will Create Jobs, Save Money, Reduce Pollution. (2013, 2013 Aug 01). *Targeted News Service*. Retrieved from https://sheba.ncat.edu/validate?url=/docview/1416577697?accountid=12711

Stein, J., & Hydeman, M. M. (2004). Development and Testing of the Characteristic Curve Fan Model. *ASHRAE Transactions, 110*, 347-356.

Tesiero, R. C., Nassif, N., Graydon, C., & Singh, H. (2014). "Low-Cost" Strategies to Save Energy in K-12 Schools. *American Journal of Engineering and Applied Sciences, 7*(1), 45-57. doi: 10.3844/ajeassp.2014.45.57

Trane. (2000). Chilled Water System Design and Operation - Cost-Reducing Optimization Strategies. La Crosse: Trane.

Trane. (2002). Managing the Ins and Outs of Commercial Building Pressurization. *Trane Engineers Newsletter, 31*. Retrieved from

Trane. (2006). Energy-Saving Control Strategies for Rooftop VAV Systems. *Engineers Mewsletter, 35*(4). Retrieved from doi:October 2006

Trčka, M., & Hensen, J. L. M. (2010). Overview of HVAC system simulation. *Automation in Construction, 19*(2), 93-99. doi: http://dx.doi.org/10.1016/j.autcon.2009.11.019

Treado, S. J. (2010). An Agent-Based Methodology for Optimizing Building HVAC System Performance. *ASHRAE Transactions, 116*, 124-134.

USDOE. (2012). EnergyPlus Engineering Reference. In T. B. o. T. o. t. U. o. I. a. t. R. o. t. U. o. C. t. t. E. O. L. B. N. Laboratory (Series Ed.) U. D. o. Energy (Ed.) *The Reference to EnergyPlus Calculations*

Vakiloroaya, V., Ha, Q. P., & Samali, B. (2013). Energy-efficient HVAC systems: Simulation–empirical modelling and gradient optimization. *Automation in Construction, 31*(0), 176-185. doi: http://dx.doi.org/10.1016/j.autcon.2012.12.006

Vakiloroaya, V., Samali, B., Cuthbert, S., Pishghadam, K., & Eager, D. (2014). Thermo-economic optimization of condenser coil configuration for HVAC performance enhancement. *Energy and Buildings, 84*(0), 1-12. doi: http://dx.doi.org/10.1016/j.enbuild.2014.07.079

Wang, S., & Jin, X. (2000). Model-based optimal control of VAV air-conditioning system using genetic algorithm. *Building and Environment, 35*(6), 471-487. doi: 10.1016/s0360-1323(99)00032-3

Wang, S., & Ma, Z. (2008a). Supervisory and optimal control of building HVAC systems: a review. [Technical report]. *HVAC & R Research*.

Wang, S., & Ma, Z. (2008b). Supervisory and Optimal Control of Building HVAC Systems: A Review. *HVAC&R Research, 14*(1), 3-32.

Wemhoff, F., & V., M. (2010). Predictions of energy savings in HVAC systems by lumped models. *Energy and Buildings, 42*(10), 1807-1814. doi: http://dx.doi.org/10.1016/j.enbuild.2010.05.017

Xu, G. (2012). *HVAC system study: A data-driven approach.* (1514516 M.S.), The University of Iowa, Ann Arbor. ProQuest Dissertations & Theses Full Text database.

Yamakawa, Y., Yamazaki, T. P., Kamimura, K. P., & Kurosu, S. P. (2009). Stability of Temperature Control in VAV Systems. *ASHRAE Transactions, 115*, 613-621.

Yang, J., Rivard, H., & Zmeureanu, R. (2005). On-line building energy prediction using adaptive artificial neural networks. *Energy and Buildings, 37*(12), 1250-1259. doi: http://dx.doi.org/10.1016/j.enbuild.2005.02.005

Zaheer-Uddin, M., & Patel, R. (1993). The Design and Simulation of a Sub-optimal Controller for Space Heating. *ASHRAE Transactions, 98*(1).

Zheng, G. R., & Zaheer-Uddin, M. (1996). Optimization of thermal processes in a variable air volume HVAC system. *Energy, 21*(5), 407-420. doi: http://dx.doi.org/10.1016/0360-5442(96)00114-4

APPENDIX A

Psychrometric Properties

The following psychrometric properties were programmed and written in MATLAB in standard IP units:

A.1 Perfect Gas Relationship for Dry and Moist Air.

All equations, identification, and nomenclature are identical to the 2013 ASHRAE Handbook – Fundamentals. When moist air is considered a mixture of independent perfect gases (dry air and water vapor), each is assumed to obey the perfect gas equation of state as follows:

Dry air: $$p_{da}V = n_{da}RT \quad \text{(A.1)}$$

Water vapor: $$p_wV = n_wRT \quad \text{(A.2)}$$

where:

p_{da} = partial pressure of dry air

p_w = partial pressure of water vapor

V = total mixture volume

n_{da} = number of moles of dry air

n_w = number of moles of water vapor

R = universal gas constant, 1545.349 ft-lb_f/lb mol-^oR

T = absolute temperature, ^oR

The mixture also obeys the perfect gas equation:

$$pV = nRT \quad \text{(A.3)}$$

or

$$(p_{da} + p_w)V = (n_{da} + n_w)RT \quad \text{(A.4)}$$

where $p = p_{da} + p_w$ is the total mixture pressure and therefore the humidity ratio, W is

$$W = 0.621945\frac{p_w}{p - p_w} \quad \text{(A.5)}$$

A.2 Dew Point Temperature.

The dew point temperature t_d is a function of:

- saturation temperature
- air-water vapor partial pressure
- humidity ratio

$$p_{ws}(t_d) = p_w = \frac{(pW)}{(0.621945 + W)} \quad \text{(A.6)}$$

Where p_w is the water vapor partial pressure for the moist air and $p_{ws}(t_d)$ is the saturation vapor pressure at temperature t_d (ASHRAE, 2013). Alternatively, the dew-point temperature can be calculated directly by:

$$t_d = C_{14} + C_{15}\alpha + C_{16}\alpha^2 + C_{17}\alpha^3 + C_{18}(p_w)^{0.1984} \quad \text{(A.7)}$$

For dew point temperature between 0 ^{o}C and 93^{o}C or 32 ^{o}F and 200^{o}F

Below 0^{o}C,

$$t_d = 6.09 + 12.608\alpha + 0.4959\alpha^2 \quad \text{(A.8)}$$

where:

t_d = dew-point temperature, ^{o}C

α = $ln(p_w)$

p_w = water vapor partial pressure, kPa

C_{14} = 6.54

C_{15} = 14.526

C_{16} = 0.7389

C_{17} = 0.09486

C_{18} = 0.4569

or below 32^{o}F,

$$t_d = 90.12 + 26.142\alpha + 0.8927\alpha^2 \quad \text{(A.9)}$$

where:

t_d = dew-point temperature, ^{o}F

α = $ln(p_w)$

p_w = water vapor partial pressure, psia

C_{14} = 100.45

C_{15} = 33.193

C_{16} = 2.319

C_{17} = 0.17074

C_{18} = 1.2063

A.3 Dry Bulb Temperature.

The dry bulb temperature *t* is a function of:

- moist air enthalpy
- humidity ratio
- saturation enthalpy

$$h = c_{p,a}t + w\left(h_{fg} + c_{p,v}t\right) \quad \text{(A.10)}$$

A.4 Enthalpy and Humidity Ratio.

The moist air enthalpy *h* is a function of:

- dry bulb temperature
- humidity ratio

$$h = h_{da} + Wh_g \quad \text{(A.11)}$$

where h_{da} is the specific enthalpy for dry air in Btu/lb$_{da}$ (I-P) and h_g is the specific enthalpy for saturated water vapor in Btu/lb$_w$ (I-P) at the mixture's temperature. As an approximation,

$$h_{da} \approx 1.006t \; for \; SI \; or \; \approx 0.240t \; for \; I - P \quad \text{(A.12)}$$

$$h_g \approx 2501 + 1.86t \; for \; SI \; or \; \approx 1061 + 0.444t \; for \; I - P \quad \text{(A.13)}$$

where *t* is the dry-bulb temperature in ^{o}C or ^{o}F. The moist air specific enthalpy in Btu/lb$_{da}$ then becomes

$$h = 1.006t + W(2501 + 1.86t) \; for \; SI \; or \quad \text{(A.14)}$$

$$h = 0.240t + W(1061 + 0.444t) \; for \; I - P \quad \text{(A.15)}$$

The above formulas and nomenclature are from the 2013 ASHRAE Handbook – Fundamentals.

A.5 Saturation Enthalpy.

Specific enthalpy of moist air can be expressed as:

$$h = h_a + W h_w \quad \text{(A.16)}$$

where:

h = specific enthalpy of moist air (kJ/kg, Btu/lb)

h_a = specific enthalpy of dry air (kJ/kg, Btu/lb)

W = humidity ratio (kg/kg, lb/lb)

h_w = specific enthalpy of water vapor (kJ/kg, Btu/lb)

First calculate the saturation pressure at a given dry bulb temperature, and then the humidity ratio from the saturation pressure.

A.6 Relative Humidity.

The relative humidity ϕ is calculated as a function of the saturation pressure and the humidity ratio. The relative humidity is defined as the ratio of the mole fraction of water vapor in a given moist air sample to the mole fraction in an air sample saturated at the same temperature and pressure (ASHRAE, 2013). The water vapor partial pressure is calculated as a function of humidity ratio, see equation A.17. The relative humidity is calculated as a function of water vapor partial pressure and saturation pressure.

$$\phi = \frac{p_w}{p_{ws}} \tag{A.17}$$

A.7 Dry Air Density.

The density of dry air is calculated as a function of the atmospheric pressure, dry bulb temperature and the humidity ratio and from the ideal gas relationship.

$$\rho_d = \frac{p_{da}}{R_a(t + 273.15)} \tag{A.18}$$

$$p_{da} = p_a \frac{0.62198W}{0.62198 + W} \tag{A.19}$$

A.8 Moist Air Density.

The density of moist air ρ_m is calculated as a function of the humidity ratio and dry air density and is the ratio of total mass to total volume of a moist air mixture.

$$\rho_m = \rho_d(1 + w) \tag{A.20}$$

$$\rho = \frac{(M_{da} + M_w)}{V} = \left(\frac{1}{v}\right)(1 + W) \tag{A.21}$$

where v is the moist air specific volume, ft^3/lb_{da} or m^3/kg_{da} and M_{da} is mass of dry air and M_w is mass of water vapor.

A.9 Saturation Pressure.

The saturation pressure is calculated as a function of temperature using a correlation. The water vapor saturation pressure is required to determine a number of moist air properties, principally the saturation humidity ratio (ASHRAE, 2013). Convert user temperature to Kelvin, if below freezing then calculate saturation pressure over ice.

$$p_{ws} = exp\left(\frac{C_1}{T} + C_2 + C_3T + C_4T^2 + C_5T^3 + C_6T^4 + C_7\ln(T)\right) \tag{A.22}$$

If above freezing then calculate saturation pressure over liquid water. Convert pressure in pascals to user pressure.

$$p_{ws} = exp\left(\frac{C_8}{T} + C_9 + C_{10}T + C_{11}T^2 + C_{12}T^3 + C_{13}\ln(T)\right) \quad (A.23)$$

Where variables are identified in Table 16:

Table 16

Saturation Pressure Programming and Formula Nomenclature

C_1 = -5674.5359	C_2 = 6.3925247	C_3 = -0.9677843E-2	C_4 = 0.62215701E-6
C_5 = 0.20747825E-8	C_6 = -0.9484024E-12	C_7 = 4.1635019	C_8 = -5800.2206
C_9 = 1.3914993	C_{10} = -0.04860239	C_{11} = 0.41764768E-4	C_{12} = -0.14452093E-7
C_{13} = 6.5459673			

A.10 Saturation Temperature of Water Vapor.

The maximum saturation pressure of the water vapor in moist air changes with the temperature of the air vapor mixture by the following equation:

$$p_{ws} = \frac{e^{\left(77.3450+0.0057T-\frac{7235}{T}\right)}}{T^{8.2}} \quad (A.24)$$

where:

p_{ws} = water vapor saturation pressure (Pa)

e = the constant 2.71828.....

T = dry bulb temperature of the moist air (K)

The density of water vapor can be expressed as:

$$\rho_w = \frac{0.0022p_w}{T} \quad (A.25)$$

where:

p_w = partial pressure water vapor (Pa, N/m^2)

ρ_w = density water vapor (kg/m^3)

T = absolute dry bulb temperature (K)

A.11 Saturated Air Dry Bulb Temperature.

The air dry bulb temperature is calculated as a function of saturated air enthalpy using an iterative method. Estimate saturated air temperature and initialize iteration. First estimate saturation enthalpy for estimated temperature; then compare estimated enthalpy with known enthalpy and calculate new estimate of temperature.

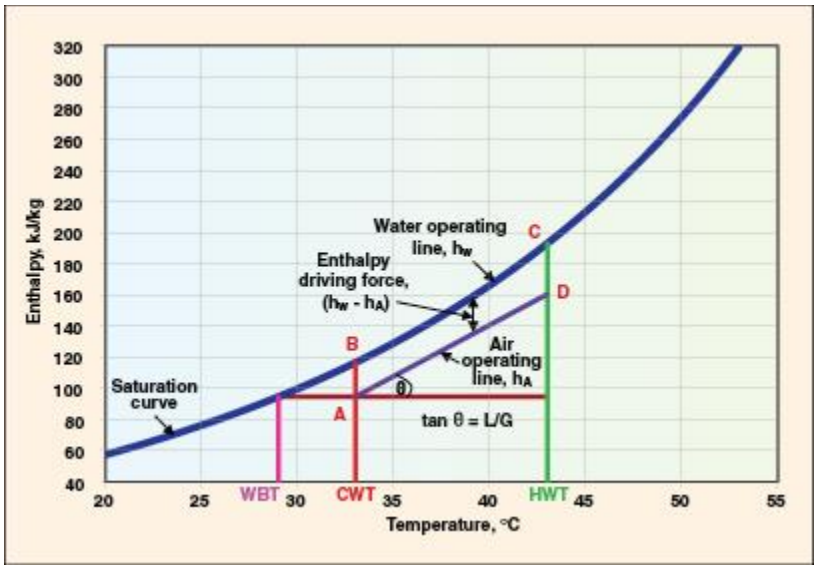

Figure 73. Enthalpy versus temperature for water and air.

A.12 Wet and Dry Bulb Temperature.

The wet bulb temperature is calculated as a function of dry bulb temperature and the humidity ratio using an iterative method, using equations below.

$$W = \frac{\left[h_{fg} - \left(c_{p,w} - c_{p,v}\right)t^*\right]W_s^* - c_{p,a}(t - t^*)}{h_{fg} + c_{p,v}t - c_{p,w}t^*} \tag{A.26}$$

or

$$W = \frac{(2501 - 2.326t^*)W_s^* - 1.006(t - t^*)}{2501 + 1.86t - 4.186t^*} \; for\ SI \tag{A.27}$$

and

$$W = \frac{(1093 - 0.556t^*)W_s^* - 0.240(t - t^*)}{1093 + 0.444t - t^*} \; for\ I - P \tag{A.28}$$

where t and t^* are in ^oC or ^oF. Below freezing, the corresponding equations are

$$W = \frac{(2830 - 0.24t^*)W_s^* - 1.006(t - t^*)}{2803 + 1.86t - 2.1t^*} \; for\ SI \tag{A.29}$$

and

$$W = \frac{(1220 - 0.04t^*)W_s^* - 0.240(t - t^*)}{1220 + 0.444t - 0.48t^*} \; for\ I - P \tag{A.30}$$

Thermodynamic wet-bulb temperature t^*

$$h + (W_s^* - W)h_w^* = h_s^* \tag{A.31}$$

A psychrometer consists of two thermometers; one thermometer's bulb is covered by a wick that has been thoroughly wetted with water. When the wet bulb is placed in an airstream, water evaporates from the wick, eventually reaching an equilibrium temperature called the wet-bulb temperature. This process is not one of adiabatic saturation, which defines the thermodynamic wet-bulb temperature, but one of simultaneous heat and mass transfer from the wet bulb (ASHRAE, 2013).

A.13 Psychrometrics from Dry Bulb Temperature and Enthalpy.

First, calculate the saturation pressure at a given temperature; then calculate the humidity ratio as a function of dry bulb temperature and enthalpy using the equation below.

$$W = \frac{\left(h - c_{p,a}t\right)}{\left(h_{fg} + c_{p,v}t\right)} \tag{A.32}$$

Next calculate:

- the relative humidity as a function of water vapor partial pressure and saturation pressure.
- wet bulb temperature as a function of dry bulb temperature and humidity ratio.
- dewpoint temperature as a function of water vapor partial pressure.
- dry air and moist air densities.

A.14 Psychrometrics from Dry Bulb Temperature and Relative Humidity.

First, calculate the saturation pressure at a given dry bulb temperature; then calculate the water vapor partial pressure as a function of the saturation pressure and relative humidity, using the equation below.

$$p_w = \phi p_{ws} \tag{A.33}$$

Next calculate:

- the humidity ratio as a function of the water vapor partial pressure.
- the enthalpy as a function of dry bulb temperature and humidity ratio.
- the wet bulb temperature as a function of dry bulb temperature and humidity ratio.
- the dewpoint temperature as a function of the water vapor partial pressure.
- dry and moist air densities .

A.15 Psychrometrics from Dry Bulb Temperature and Humidity Ratio.

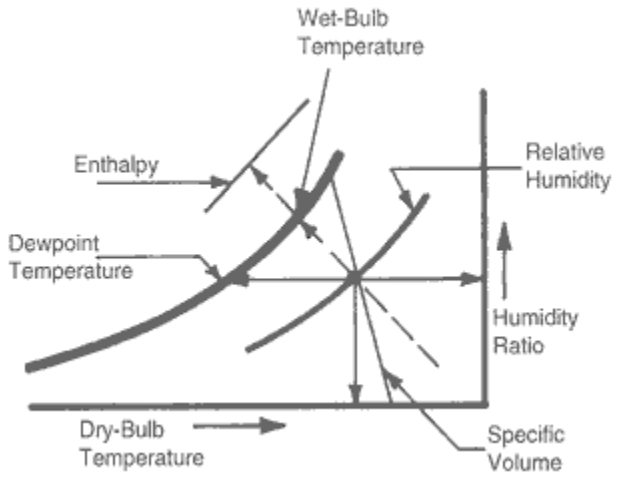

Figure 74. Properties of moist air on psychrometric chart.

Calculate:

- the saturation pressure at a given temperature.

- the relative humidity as a function of the partial pressure of water vapor and the saturation pressure of water vapor.
- the wet bulb temperature as a function of dry bulb temperature and humidity ratio.
- the enthalpy as a function of dry bulb temperature and humidity ratio.
- the dewpoint temperature as a function of the partial pressure of water vapor.
- dry and moist air densities .

APPENDIX B

Heat and Mass Transfer Components

The following properties were programmed in MATLAB based on the heat and mass transfer component routines similar to the HVAC 2 Toolkit by (Brandemuehl, M., 1993):

B.1 NTU-Effectiveness Analysis.

This section is similar to the HVAC 2 Toolkit: Algorithms and Subroutines for Secondary HVAC System Energy Calculations by Michael J. Brandemuehl. The subroutine calculates the outlet states of six different heat exchanger configurations heat exchanger using the effectiveness-NTU method of analysis:

1. Counterflow
2. Parallel flow
3. Cross flow, both streams unmixed
4. Cross flow, both streams mixed
5. Cross flow, stream 1 unmixed
6. Cross flow, stream 2 unmixed

The heat exchanger effectiveness ε is defined as the ratio of the actual heat transfer rate to the maximum heat transfer rate for the given entering fluid conditions and flow rates, and can be determined using these relationships:

$$q = C_1\left(X_{1,ent} - X_{1,lvg}\right) = C_2\left(X_{2,lvg} - X_{2,ent}\right) \tag{B.1}$$

$$q_{max} = C_{min}(X_{max} - X_{min}) \tag{B.2}$$

$$q = \varepsilon q_{max} \tag{B.3}$$

While the state variable, *X*, is typically a temperature, it could be another state variable that drives a heat or mass transfer process. The capacity rate, *C*, relates the transfer to the state

variable. For a given flow configuration, the effectiveness of a heat exchanger can be expressed as a function of two dimensionless variables: the number of transfer units, *N* or *NTU*, and the fluid capacity rate ratio, *C*.

$$N = NTU = \frac{UA}{C_{min}} \tag{B.4}$$

$$C = \frac{C_{min}}{C_{max}} \tag{B.5}$$

Where C_{min} is the minimum capacity rate and C_{max} is the maximum capacity rate of the two streams and *UA* is the overall heat transfer coefficient for the heat exchanger.

For calculation of enthalpy, the capacity rate has units of mass flow rate and the *UA* is modified to reflect enthalpy exchange. While the definition of *q*, *X*, C_i, and *UA* may vary with application, the effectiveness is related to *C* and *N* by the same equations, given below.

If *C* is equal to zero then the effectiveness is independent of configuration and the following holds.

$$\varepsilon = 1 - e^{-N} \tag{B.6}$$

Counterflow:

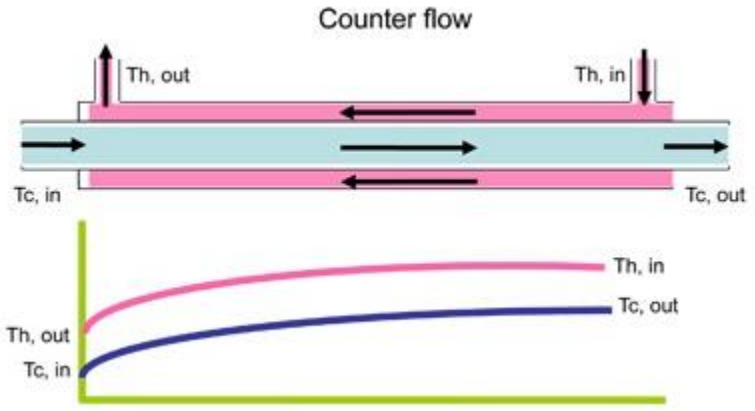

Figure 75. Counter flow.

$$\varepsilon = \frac{1 - e^{-N(1-C)}}{1 - Ce^{-N(1-C)}} \tag{B.7}$$

$$\varepsilon = \frac{N}{N+1} \qquad if\ C = 1 \tag{B.8}$$

Parallel flow:

$$\varepsilon = \frac{1 - e^{-N(1+C)}}{1+C} \tag{B.9}$$

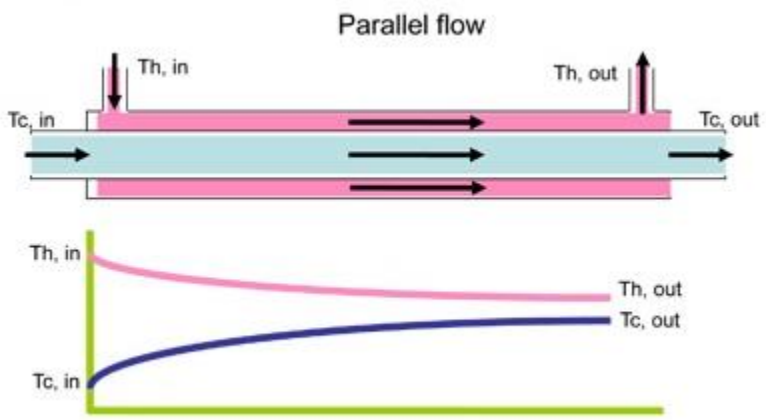

Figure 76. Parallel flow.

Cross flow, both streams unmixed:

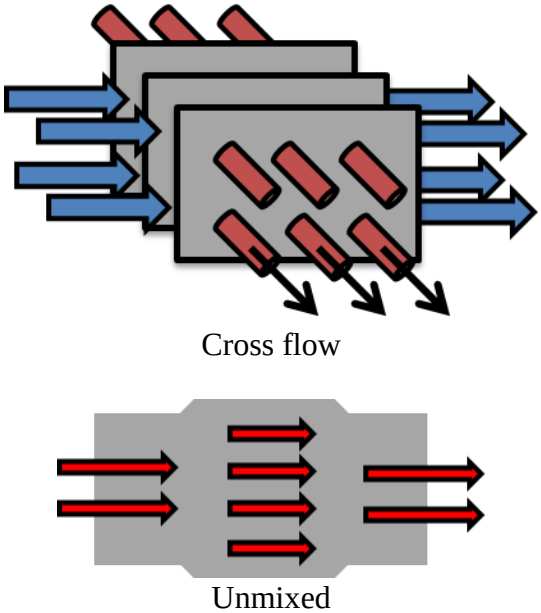

Figure 77. Cross flow unmixed.

$$\varepsilon = 1 - exp\left[\frac{e^{-NC_r} - 1}{Cn}\right] \tag{B.10}$$

$$n = N^{-0.22} \tag{B.11}$$

Cross flow, both streams mixed:

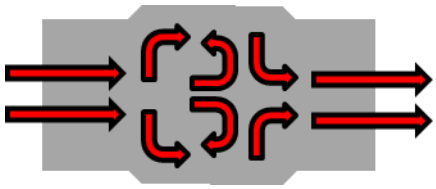

Figure 78. Mixed flow.

$$\varepsilon = \left[\frac{1}{1 - e^{-N}} + \frac{C}{1 - e^{-NC}} - \frac{1}{N}\right]^{-1} \tag{B.12}$$

Cross flow, minimum capacity rate stream unmixed:

$$\varepsilon = \frac{\left[1 - e^{-C\left(1 - e^{-N}\right)}\right]}{C} \tag{B.13}$$

Cross flow, maximum capacity rate stream unmixed:

$$\varepsilon = 1 - e^{-\frac{1 - e^{-NC}}{C}} \tag{B.14}$$

Outlet fluid conditions are calculated from the definition of the effectiveness.

$$X_{1,lvg} = X_{1,ent} - \varepsilon \frac{C_{min}}{C_1}\left(X_{1,ent} - X_{2,ent}\right) \tag{B.15}$$

$$X_{2,lvg} = X_{2,ent} + \varepsilon \frac{C_{min}}{C_2}\left(X_{2,ent} - X_{2,ent}\right) \tag{B.16}$$

Calculate:

- heat exchanger parameters for use in effectiveness relationships
- effectiveness for selected configuration
- leaving fluid conditions

B.2 Heat Exchanger UA from Rating Information.

This subroutine is based on the HVAC 2 Toolkit by (Brandemuehl, M., 1993) and ASHRAE Handbook Fundamentals, it calculates the overall heat transfer coefficient, *UA*, for a heat exchanger given design or rating information. Rating information required includes fluid capacity rates, inlet state variables, and heat transfer rate. Check for *Q* out of range (effectiveness > 1); then estimate the initial value of *UA*. Next calculate the heat transfer rate for estimated *UA* and given fluid conditions and heat exchanger configuration. Finally, calculate the new estimate for *UA* using the iteration routine. .

Heat exchanger theory leads to the basic heat exchanger design equation:

$$Q = (UA)LMTD \tag{B.17}$$

where:

Q = the rate of heat transfer between the two fluids in the heat exchanger in Btu/hr,

U = the overall heat transfer coefficient in Btu/hr-ft^2-^{o}F,

A = the heat transfer surface area in ft^2,

LMTD = the log mean temperature difference in ^{o}F, calculated from the inlet and outlet temperatures of both fluids.

There are two fluids involved with changing temperatures as they pass through the heat exchanger so the log mean temperature difference (*LMTD*) was derived. That log mean temperature is defined in terms of the temperature differences; T_{Pin} and T_{Pout} are the inlet and outlet temperatures of the primary fluid and T_{Sin} and T_{Sout} are the inlet and outlet temperatures of the secondary fluid .

$$LMTD = \frac{(\Delta T_2 - \Delta T_1)}{\ln\left(\frac{\Delta T_2}{\Delta T_1}\right)} \tag{B.18}$$

where:

LMTD = Logarithmic Mean Temperature Difference (^{o}F, ^{o}C)

For parallel flow:

$\Delta T_1 = T_{Pin} - T_{Sin}$ = inlet primary and secondary fluid temperature difference (^{o}F, ^{o}C)

$\Delta T_2 = T_{Pout} - T_{Sout}$ = outlet primary and secondary fluid temperature difference (^{o}F, ^{o}C)

For counter flow:

$\Delta T_1 = T_{Pin} - T_{Sout}$ = inlet primary and outlet secondary fluid temperature difference (^{o}F, ^{o}C)

$\Delta T_2 = T_{Pout} - T_{Sin}$ = outlet primary and inlet secondary fluid temperature difference (^{o}F, ^{o}C)

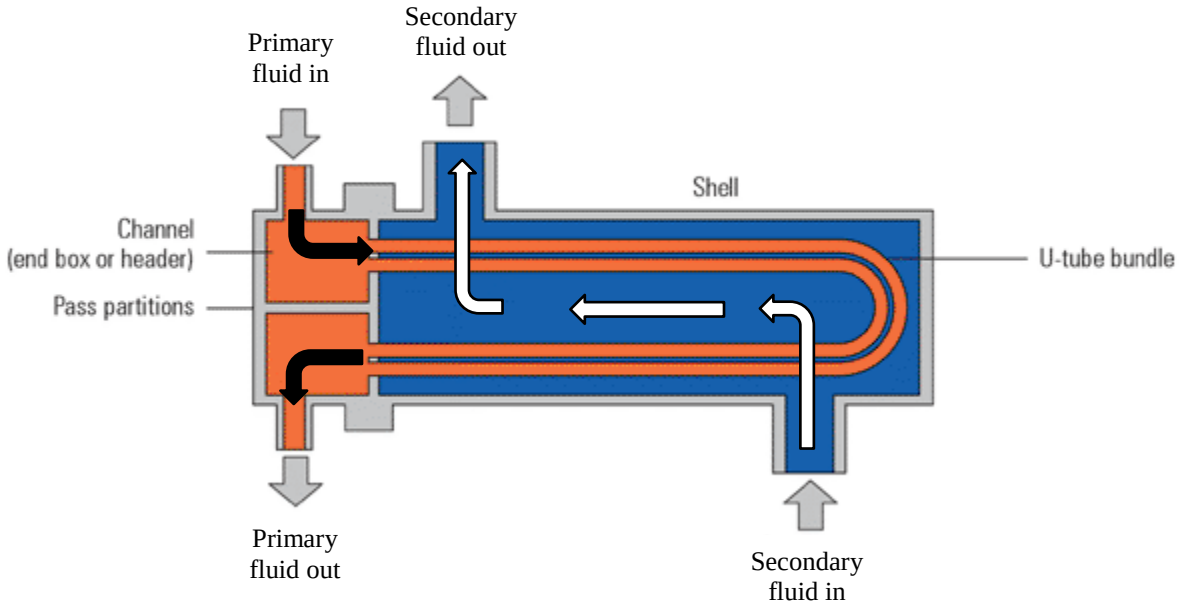

Figure 79. Schematic diagram of a shell and tube heat exchanger.

The heat transfer rate, *Q*, can be calculated from the known flow rate of the primary or the secondary fluids, its heat capacity, and the required temperature change, using the equation below:

$$Q = m_P C_{pP}(T_{Pin} - T_{Pout}) = m_S C_{pS}(T_{Sout} - T_{Sin}) \quad \text{(B.19)}$$

where:

m_P = mass flow rate of primary fluid, slugs/hr,

C_{pP} = heat capacity of the primary fluid, Btu/slug-^{o}F

m_S = mass flow rate of secondary fluid, slugs/hr,

C_{pS} = heat capacity of the secondary fluid, Btu/slug-^{o}F

The overall heat transfer coefficient, *U*, depends on the conductivity and convection coefficients on both sides of the material separating the two fluids. The heat transfer coefficient is often determined empirically by measuring all parameters in the basic heat exchanger equation (Brandemuehl, M., 1993).

Valve model equations, 2-way valve pressure drop:

$$P_i - P_o = K\dot{m}^2 \tag{B.20}$$

where

K = valve flow resistance coefficient, (1/kg m)

P_i = entering fluid pressure, (Pa)

P_o = leaving fluid pressure, (Pa)

m = mass flow rate, (kg/s)

W_f = weighing factor for valve characteristic, (1/kg m)

C = valve position (0 = closed, 1 = open)

λ = leakage parameter

3-way valve pressure drop through each port:

$$P_{i,1} - P_o = K_1\dot{m}_1^2 \tag{B.21}$$

$$P_{i,2} - P_o = K_2\dot{m}_2^2 \tag{B.22}$$

$$K = \frac{W_f K_o}{[(1-\lambda)C + \lambda]^2} + \left(1 - W_f\right)K_o\lambda^{(2C-2)} \tag{B.23}$$

$$K_o = \frac{1.736 \times 10^{12}}{(\rho C)^2} \tag{B.24}$$

The overall heat transfer coefficients are calculated in terms of R_i, R_m, R_o, and R_f.

Thermal resistance, R_m due to conduction through the coil tube and fouling is:

$$R_m = \frac{A_o}{A_i}\left[\frac{(r_o - r_i)}{k_t} + F_t\right] \tag{B.25}$$

The air-side and water-side surface resistances are:

$$R_o = \frac{1}{h_o} \tag{B.26}$$

$$R_i = \frac{A_o}{A_i}\frac{1}{h_i} \tag{B.27}$$

The resistance due to fin inefficiencies is:

$$R_f = \frac{(1 - \eta_o)}{\eta_o}\frac{1}{h_o} \tag{B.28}$$

where the surface effectiveness is defined in terms of the fin efficiency.

$$\eta_o = 1 - \frac{A_s}{A_o}\left(1 - \eta_f\right) \tag{B.29}$$

where:

A_o = external surface area/face area, unitless

A_i = internal surface area/face area, unitless

A_s = secondary surface area/face area, unitless

k_t = tube thermal conductivity, W/m C

F_t = fouling factor for tubes, C m^2/W

h_o = air-side film coefficient, W/m^2 C

h_i = water film coefficient, W/m^2 C

η_o = surface effectiveness, unitless

η_f = fin efficiency, unitless

Drycoil:

$$UA = \frac{A_o}{R_m + R_o + R_f + R_i} \tag{B.30}$$

Wetcoil:

$$UA_{int} = \frac{A_o}{R_m + R_i} \tag{B.31}$$

$$UA_{ext} = \frac{A_o}{R_f + R_o} \tag{B.32}$$

B.3 Heat Transfer for Air-Liquid Coil with Dry Fin Surface.

This program is similar to the HVAC 2 Toolkit and it calculates the leaving liquid, air conditions and the rate of heat transfer between the liquid and air fluid streams for a sensible (no mass transfer or moisture removal) heat exchanger. The performance of a coil with a dry fin surface is modeled using the effectiveness-NTU method. For sensible heat exchange, the capacity rates for the air and water streams are defined as follows:

$$q = C_a\left(t_{a,ent} - t_{a,lvg}\right) = C_l\left(t_{l,lvg} - t_{l,ent}\right) \tag{B.33}$$

$$C_a = \left(\dot{m}c_p\right)_a \tag{B.34}$$

$$C_l = \left(\dot{m}c_p\right)_l \tag{B.35}$$

where:

C_a = capacity rate of dry air stream, W/C

C_l = capacity rate of liquid stream, W/C

m = fluid mass flow rate, kg/s

$c_{p,a}$ = specific heat of dry air, J/kg C

$c_{p,l}$ = specific heat of liquid, J/kg C

$t_{l,ent}$ = entering water or liquid temperature, C

$t_{a,ent}$ = entering air dry bulb temperature, C

$t_{l,lvg}$ = leaving water or liquid temperature, C

$t_{a,lvg}$ = leaving air dry bulb temperature, C

q = total heat transfer rate, W

Calculate:

- fluid capacity rates for air and liquid
- the outlet air and liquid temperature conditions by modeling coil as a counterflow heat exchanger
- heat transfer rate

B.4 Cooling Coil with Completely Wet Surface.

The algorithm calculates the outlet water temperature, air dry bulb temperature and humidity ratio, and the total and sensible cooling capacity for a coil with a completely wet fin surface. The coil is considered to be operating under "all wet" surface conditions if the surface temperature at the air inlet is lower than the inlet air dewpoint temperature. A counterflow effectiveness model for enthalpy exchange is used which closely approximates the performance of multi-row counter-crossflow heat exchanger. Heat transfer in the wet coil is calculated based on enthalpy rather than temperature to include latent effects. The corresponding enthalpies of the coil and water are related to that of the air through "fictitious enthalpies," defined as the enthalpy of saturated air at the temperature of the coil or water. Enthalpy-based heat transfer calculations for a wet surface use the fundamental relationship between heat transfer, enthalpy, and capacity (Brandemuehl, M., 1993).

$$q_a = C_a\left(h_{a,ent} - h_{a,lvg}\right) \tag{B.36}$$

$$q_w = C_l\left(h_{l,sat,lvg} - h_{l,sat,ent}\right) = \left(\dot{m}c_p\right)_l\left(t_{l,lvg} - t_{l,ent}\right) \tag{B.37}$$

The enthalpy subscript *l,sat* refers to the enthalpy of saturated air evaluated at the liquid (chilled water) temperature and represents the "fictitious enthalpy." The capacity rates depend on the relationship between the heat transfer and the enthalpies (Brandemuehl, M., 1993). For enthalpy capacity rates and overall enthalpy transfer coefficient see equations 3.66 - 3.70.

Local heat transfer, q (W):

$$q = UA_{h,tot}\left(h_a - h_{w,sat}\right) \quad \text{(B.38)}$$

For a cooling coil with a completely wet surface, calculate:

- enthalpy of entering air and fictitious enthalpy of entering water
- $c_{p,sat}$ using entering air dewpoint and entering water temperature.
- the outlet air and water conditions by modeling coil as a counterflow enthalpy exchanger
- entering fin surface conditions from air and water conditions and the ratio of resistances
- water outlet temperature from "fictitious" water outlet enthalpy
- outlet air temperature and humidity from enthalpies

B.5 Cooling Coil with Partially Wet Surface.

This program calculates the outlet water temperature, air dry bulb temperature, humidity ratio, and the total and sensible cooling capacity for a coil with partly wet and partly dry fin surface. The coil is considered to be operating under "part wet" surface conditions if the surface temperature at the inlet is higher than the inlet air dewpoint temperature, but the surface temperature at the air outlet is lower than the entering dew point temperature. Heat transfer in a coil with part of the fin surface dry and part of it wet is calculated by treating the two sections of the coil as separate heat exchangers with a common boundary. The dry portion of the coil is analyzed by equations 3.93 – 3.95. The wet portion of the coil is analyzed by equations 3.66 - 3.70 and 3.96 - 3.98 (Brandemuehl, M., 1993).

The objective of the algorithm is to determine exactly what fraction of the total external surface area is wet. The area is determined through the knowledge that moisture in the air will begin condensing on the coil surface when the surface temperature is equal to the entering air

dewpoint temperature. The fraction wet surface area is iteratively adjusted to achieve this surface temperature at the dry/wet boundary (Brandemuehl, M., 1993).

B.6 Outlet Conditions for Wet Coil.

This subroutine calculates the leaving air temperature, the leaving air humidity ratio, and the sensible cooling capacity for a wet or partially wet coil given the total capacity, entering air conditions, and air-side overall heat transfer coefficient (Brandemuehl, M., 1993). The following can be calculated:

Effectiveness:

$$\varepsilon = 1 - e^{-NTU} \tag{B.39}$$

Saturated enthalpy at the condensate temperature for the calculated effectiveness:

$$h_{sat,cond} = h_{a,ent} - \frac{h_{a,ent} - h_{a,lvg}}{\varepsilon} \tag{B.40}$$

Given condensate temperature, t_c, the leaving dry bulb temperature is:

$$t_{a,lvg} = t_{a,ent} - \varepsilon\left(t_{a,ent} - t_c\right) \tag{B.41}$$

The sensible cooling capacity:

$$q_{sen} = \left(\dot{m}c_p\right)_a\left(t_{a,ent} - t_{a,lvg}\right) \tag{B.42}$$

The steps are as follows, calculate:

- the effectiveness of heat exchange between the air and the condensate.
- coil surface enthalpy using the effectiveness relationships
- condensate temperature from saturated enthalpy by psychrometric
- leaving air conditions and sensible capacity using condensate temperature

APPENDIX C

Fans and Pumps

The following properties and formulas are for basic reference only for fans and pumps:

C.1 Outlet Power.

The actual horsepower a fan requires because no fan is 100% efficient. BHP can be expressed as:

$$BHP = \frac{Q \times P_t}{(6356 \times Fan_{eff})} \tag{C.1}$$

Assuming 100% efficiency, AHP is the power required to move a given volume against a given pressure. AHP can be expressed as

$$AHP = \frac{Q \times P_t \times SG}{6356} \tag{C.2}$$

where:

BHP = Brake Horsepower

AHP = Air Horsepower

P_t = Total pressure, in-WG

Q = Air flow rate in CFM

SG = Specific Gravity (air = 1.0)

Fan_{eff} = Fan efficiency usually in 65–85% range

C.2 Fan Motor Horsepower.

The energy consumption of the pumps depends on two factors:

$$BHP_{pump} = \frac{Q_{gpm} \times h_d \times SG}{(3960 \times Efficiency)} \tag{C.3}$$

$$BHP_{pump} = \frac{Q_{gpm} \times PSI \times SG}{(1713 \times Efficiency)} \tag{C.4}$$

where:

BHP = brake horse power

Q_{gpm} = water flow, gallons per minute (GPM)

h_d = Total Dynamic Head, ft

SG = Specific Gravity, for water it is 1

Efficiency = Pump efficiency from its pump curves for the water flow and TDH

$$Motor\ hp = \frac{BHP}{Motor_{eff}} \tag{C.5}$$

where:

BHP = Break Horsepower

$Motor_{eff}$ = Motor drive efficiency usually 80-95%

C.3 Velocity in Duct.

Velocity in duct can be expressed as:

$$V = \frac{Q}{A} = \frac{144 \times Q}{a \times b} \tag{C.6}$$

where:

V = air velocity in ft per minute (FPM)

Q = air flow through duct in cubic ft per minute (CFM)

A = cross-section of duct in sq-ft

C.4 Rectangular Ducts.

a = Width of duct side (inches)

b = Height of other duct side (inches)

C.5 Equivalent Round Duct Size for a Rectangular Duct.

Equivalent round duct size for a rectangular duct can be expressed as

$$D_{eq} = 1.30 \times \frac{(a \times b)^{0.625}}{(a + b)^{0.25}} \tag{C.7}$$

where:

D_{eq} = equivalent diameter

a = one dimension of rectangular duct (inches)

b = adjacent side of rectangular duct (inches)

C.6 Equations for Flat Oval Ductwork.

$$P = 2\pi\left(\frac{1}{2}\left[\left(\frac{a}{2}\right)^2 + \left(\frac{b}{2}\right)^2\right]\right)^{\frac{1}{2}} \quad \text{(C.8)}$$

$$D_{eq} = \frac{(1.55 \times A^{0.625})}{P^{0.25}} \quad \text{(C.9)}$$

$$A = \frac{\pi ab}{4} \quad \text{(C.10)}$$

where:

a = Major Axis Dimension (Inches)

b = Minor Axis Dimension (Inches)

A = Cross-Sectional Area (Sq-ft)

P = Perimeter or Surface Area (Sq-ft per linear feet)

D_{eq} = Equivalent Round Duct Diameter

C.7 Duct Air Pressure Equations.

$$TP = SP + VP \quad \text{(C.11)}$$

where:

TP = Total Pressure

SP = Static Pressure, friction losses

VP = Velocity Pressure, dynamic losses

C.8 Velocity Pressure.

$$VP = \left(\frac{V}{4005}\right)^2 \quad \text{(C.12)}$$

where:

VP = Velocity pressure

V = Air velocity in FPM

The Affinity Laws of centrifugal pumps or fans indicates the influence on volume capacity, head (pressure) and/or power consumption of a pump or fan due to:

- change in speed of wheel - revolutions per minute (rpm)
- geometrically similarity - change in impeller diameter

There are two sets of affinity laws:

- affinity laws for a specific centrifugal pump - to approximate head, capacity and power curves for different motor speeds and /or different diameter of impellers
- affinity laws for a family of geometrically similar centrifugal pumps - to approximate head, capacity and power curves for different motor speeds and /or different diameter of impellers

In our case the **wheel diameter is constant** - change in pump wheel velocity can simplify the affinity laws to:

Volume Capacity

$$\frac{q_1}{q_2} = \left(\frac{n_1}{n_2}\right) \tag{C.13}$$

Head or Pressure

$$\frac{dp_1}{dp_2} = \left(\frac{n_1}{n_2}\right)^2 \tag{C.14}$$

Power

$$\frac{P_1}{P_2} = \left(\frac{n_1}{n_2}\right)^3 \tag{C.15}$$

C.9 Pump Motor Horsepower.

$$Motor\ HP = \frac{BHP}{Motor\ Efficiency} \tag{C.16}$$

where:

BHP = Break Horsepower

Motor Efficiency = Motor drive efficiency usually 80-95%

C.10 Pump Affinity Laws.

The Affinity Laws of centrifugal pumps or fans indicates the influence on volume capacity, head (pressure) and/or power consumption of a pump or fan due to:

- change in speed of wheel - revolutions per minute (rpm)
- geometrically similarity - change in impeller diameter

Be aware that there are two sets of affinity laws

- affinity laws for a specific centrifugal pump - to approximate head, capacity and power curves for different motor speeds and /or different diameter of impellers
- affinity laws for a family of geometrically similar centrifugal pumps - to approximate head, capacity and power curves for different motor speeds and /or different diameter of impellers

C.11 Pump Affinity Laws for a Specific Centrifugal Pump.

Volume Capacity

The volume capacity of a centrifugal pump can be expressed like:

$$\frac{q_1}{q_2} = \left(\frac{n_1}{n_2}\right)\left(\frac{d_1}{d_2}\right) \quad \text{(C.17)}$$

where:

q = volume flow capacity (m^3/s, gpm, cfm, ..)

n = wheel velocity - revolution per minute - (rpm)

d = wheel diameter

Head or Pressure

The head or pressure of a centrifugal pump can be expressed like:

$$\frac{dp_1}{dp_2} = \left(\frac{n_1}{n_2}\right)^2 \left(\frac{d_1}{d_2}\right)^2 \quad \text{(C.18)}$$

where:

d_p = head or pressure (m, ft, Pa, psi, ..)

Power

The power consumption of a centrifugal pump can be expressed as:

$$\frac{P_1}{P_2} = \left(\frac{n_1}{n_2}\right)^3 \left(\frac{d_1}{d_2}\right)^3 \quad \text{(C.19)}$$

where:

P = power (W, bhp, ..)

If the **wheel diameter is constant** - change in pump wheel velocity can simplify the affinity laws to:

Volume Capacity $$\frac{q_1}{q_2} = \left(\frac{n_1}{n_2}\right) \quad \text{(C.20)}$$

Head or Pressure $$\frac{dp_1}{dp_2} = \left(\frac{n_1}{n_2}\right)^2 \quad \text{(C.21)}$$

Power $$\frac{P_1}{P_2} = \left(\frac{n_1}{n_2}\right)^3 \quad \text{(C.22)}$$

C.12 Changing the Impeller Diameter.

If wheel velocity is constant a change in impeller diameter can simplify the affinity laws to:

Volume Capacity

$$\frac{q_1}{q_2} = \left(\frac{d_1}{d_2}\right) \quad \text{(C.23)}$$

Head or Pressure

$$\frac{dp_1}{dp_2} = \left(\frac{d_1}{d_2}\right)^2 \quad \text{(C.24)}$$

Power

$$\frac{P_1}{P_2} = \left(\frac{d_1}{d_2}\right)^3 \tag{C.25}$$

C.13 Specific Gravity.

Specific gravity is direct ratio of any liquid's weight to the weight of water at 62°F. Water at 62°F weighs 8.33 lbs per gallon and is designated as 1.0 specific gravity. By definition, the specific gravity of a fluid is:

$$SG = \frac{PF}{PW} \tag{C.26}$$

where:

PF = fluid density

PW = water density at standard conditions.

C.14 Head and Pressure.

$$PSI = \frac{Head(ft) \times SpecificGravity}{2.31} \tag{C.27}$$

C.15 Velocity Head.

$$h_v = \frac{v^2}{2g} \tag{C.28}$$

where:

h_v = Velocity head (ft)

v = Velocity (ft/s)

g = Acceleration due to gravity (32.17 ft/s^2)

C.16 Bernoulli's Equation.

$$h + \frac{p}{y} + \frac{v^2}{2g} = E = Constant \tag{C.29}$$

where:

h = elevation in ft

p = pressure lb/sq-in

y = fluid specific weight

v = velocity in ft/s

g = acceleration due to gravity (32.17 ft/s^2)

E = specific energy or energy per unit mass

Note: A centrifugal pump develops head not pressure. All pressure figures should be converted to feet of head taking into considerations the specific gravity.

C.17 Pump Net Positive Suction Head (NPSH).

To determine the NPSH available, the following formula may be used

$$NPSHA = HA \pm HS - HF - HVP \quad \text{(C.30)}$$

where:

NPSHA = Net Positive Suction Available at Pump expressed in feet of fluid

NPSHR = Net Positive Suction Required at Pump (Feet)

HA = Absolute pressure on the surface of the liquid where the pump takes suction, expressed in feet. This could be atmospheric pressure or vessel pressure (pressurized tank). It is a positive factor (34 Feet for Water at Atmospheric Pressure)

HS = Static elevation of the liquid above or below the centerline of the impeller, expressed in feet. Static suction head is positive factor while static suction lift is a negative factor.

HF = Friction and velocity head loss in the piping, also expressed in feet. It is a negative factor.

HVP = Absolute vapor pressure of the fluid at the pumping temperature, expressed in feet of liquid. It is a negative pressure.

The Net Positive Suction Head (N.P.S.H.) is the pressure head at the suction flange of the pump less the vapor pressure converted to fluid column height of the fluid.

C.18 Pump Specific Speed.

Equation below gives the value for the pump specific speed;

$$N_s = \frac{N_r \times Q_{gpm}}{(h)^{3/4}} \tag{C.31}$$

where:

N_s = Specific speed

Q_{gpm} = Flow in US gallons per minute (GPM)

N_r = Pump speed, RPM

h = Head, ft

C.19 Pump Loads and Motors.

Three different equations are used under different scenarios:

1. Heat gain of power driven equipment and motor when both are located inside the space to be conditioned:

$$q = 2545 \times \frac{P}{Eff} \times F_u \times F_l \tag{C.32}$$

where

q = Sensible heat gain (Btu/hr)

P = Horsepower rating from electrical power plans or manufacturer's data (HP)

Eff = Equipment motor efficiency, as decimal fraction

F_u = Motor use factor (normally = 1.0)

F_l = Motor load factor (normally = 1.0)

Note: F_u = 1.0, if operation is 24 hours

2. Heat gain of when driven equipment is located inside the space to be conditioned space

and the motor is outside the space or air stream

$$q = 2545 \times P \times F_u \times F_l \tag{C.33}$$

3. Heat gain of when driven equipment is located outside the space to be conditioned space and the motor is inside the space or air stream

$$q = 2545 \times P \times \left[\frac{(1.0 - Eff)}{Eff}\right] \times F_u \times F_l \tag{C.34}$$

C.20 Simple System Pump.

The algorithm is similar to HVAC 2 Toolkit and used in the comparison cases and calculates pump power and leaving fluid temperature for a given flow rate and entering fluid conditions.

$$PLR = \frac{\dot{m}/\rho}{Q_{rat}} \tag{C.35}$$

$$FFLP = C_0 + C_1 PLR + C_2 PLR^2 + C_3 PLR^3 \tag{C.36}$$

$$\dot{W}_l = FFLP \cdot \dot{W}_{t,rat} \tag{C.37}$$

$$\eta_t = \frac{Q_{rat}\Delta P_{rat}}{\dot{W}_{t,rat}} \tag{C.38}$$

$$\eta_p = \frac{\eta_t}{\eta_m} \tag{C.39}$$

$$f_{m,loss}(1 - \eta_m)\dot{W}_t + \left(1 - \eta_p\right)\eta_m \dot{W}_t = \dot{m} c_p \Delta T \tag{C.40}$$

The first term on the left account for the effect of motor inefficiency on the fluid temperature rise and the second term accounts for the effect of pump inefficiency. The factor $f_{m,loss}$ is the fraction of motor losses that are transferred to the fluid stream. Calculate:

1. Total system and pump efficiencies
2. Flow part load ratio based on rated flow
3. Fraction of full load power from the empirical relation
4. Pump shaft power and motor power at part load conditions
5. Leaving fluid conditions

C.21 Liquid Properties.

This routine has the properties of water (type 1), brine (type 2) and wet air, which include the specific heat and density, etc. In many refrigeration applications, heat is transferred to a secondary coolant, which can be any liquid cooled by the refrigerant and used to transfer heat without changing state. These liquids are also known as heat transfer fluids, brines, or secondary refrigerants. Water solutions of calcium chloride and sodium chloride have historically been the most common refrigeration brines.

C.22 C_v Table.

This routine has the C_v values for a variety of valves including check, ball, butterfly, strainer, etc. The loss coefficient for valves appears as C_v, a dimensional coefficient expressing the flow through a valve at a specified pressure drop.

$$Q = C_v\sqrt{\Delta p} \tag{C.41}$$

where:

Q = volumetric flow, gpm

C_v = valve coefficient, gpm at Δp = 1 psi

Δp = pressure drop, psi

C.23 K Table.

This routine has the k-values for steel pipe fittings including elbows (45^o and 90^o) and tees (straight and branch). Valves and fittings cause pressure losses greater than those caused by the pipe alone. One formulation expresses losses as

$$\Delta p = K\left(\frac{\rho}{g_c}\right)\left(\frac{V^2}{2}\right) \;\; or \;\; \Delta h = K\left(\frac{V^2}{2g}\right) \tag{C.42}$$

where:

K = geometry- and size-dependent loss coefficient

APPENDIX D

Zone and Ventilation

The following properties are for reference only for zone and ventilation calculations:

D.1 Roofs, External Walls and Conduction through Glass.

The conduction through glass is:

$$Q_s = U \times A \times (CLTD) \tag{D.1}$$

where:

Q_s = Sensible heat flow (Btu/Hr)

U = Thermal Transmittance for roof or wall or glass. (Unit- Btu/Hr Sq-ft °F)

A = area of roof, wall or glass calculated from building plans (sq-ft)

$CLTD$ = Cooling Load Temperature Difference (in °F) for roof, wall or glass. For winter months CLTD is (T_i - T_o). For summer cooling load, this temperature differential is affected by thermal mass, daily temperature range, orientation, tilt, month, day, hour, latitude, solar absorbance, wall facing direction and other variables and therefore adjusted CLTD values are used.

D.2 Partitions, Ceilings and Floors.

The equation used for sensible loads from the partitions, ceilings and floors:

$$Q_s = U \times A \times (T_a - T_r) \tag{D.2}$$

where:

Q_s = Sensible heat gain (Btu/Hr)

U = Thermal Transmittance for roof or wall or glass. (Unit- Btu/Hr Sq-ft °F)

A = area of partition, ceiling or floor calculated from building plans (sq-ft)

T_a = Temperature of adjacent space in °F (Note: If adjacent space is not conditioned and temperature is not available, use outdoor air temperature less 5 °F)

T_r = Inside room design temperature of conditioned space in °F (assumed constant usually 75°F)

D.3 People.

The heat load from people is both sensible load and the latent load. Sensible heat is transferred through conduction, convection and radiation while latent heat from persons is transferred through water vapor released in breathing and/or perspiration.

$$Q_{sensible} = N \times (HS) \times (CLF) \tag{D.3}$$

$$Q_{latent} = N \times (HL) \tag{D.4}$$

where:

$Q_{sensible}$ = Total Sensible heat gain (Btu/hr)

Q_{latent} = Total latent heat gain (Btu/hr)

N = number of people in space.

HS, HL = Sensible and Latent heat gain from occupancy (Btu/hr per person depending on nature of activity)

CLF = Cooling Load Factor, by hour of occupancy. Note: CLF = 1.0, if operation is 24 hours or of cooling is off at night or during weekends.

The sensible heat influence on the air temperature and latent heat influence the moisture content of indoor space.

D.4 Conductive Heat Transfer.

The equation used to express heat transfer by conduction is known as Fourier's Law and is expressed as:

$$Q = k \times A \times \frac{\Delta T}{t} \tag{D.5}$$

where:

Q = Heat transferred per unit time (Btu/hr)

A = Heat transfer area (ft^2)

k = Thermal conductivity of the material (Btu/ ($hr^oF\ ft^2/ft$))

ΔT = Temperature difference across the material (°F)

t = material thickness (ft)

D.5 R-values/U-values.

$$R = \frac{1}{C} = \frac{1}{K} \times t \tag{D.6}$$

$$U = \frac{1}{\sum R} \tag{D.7}$$

where:

R = R-Value (Hr Sq-ft °F/Btu)

U = U-Value (Btu/Hr Sq-ft °F) The lower the U-factor, the greater the material's resistance to heat flow and the better is the insulating value. U-value is the inverse of R-value (hr sq-ft °F /Btu).

C = Conductance (Btu/hr Sq-ft °F)

K = Conductivity (Btu in/ hr Sq-ft °F)

$\sum R$ = Sum of the thermal resistances for each component used in the construction of the wall or roof section.

t = thickness (ft)

D.6 Heat Loss through Infiltration and Ventilation.

$$Q_s = V \times \rho_{air} \times C_p \times (T_i - T_o) \tag{D.8}$$

where:

Q_s = Sensible heat loss

V = volumetric air flow rate

ρ_{air} = density of the air

C_p = specific heat capacity of air at constant pressure

T_i = indoor air temperature

T_o = outdoor air temperature

The energy quantity associated with net loss of moisture from the space is latent heat loss which is given by:

$$Q_l = V \times \rho_{air} \times hfg \times (W_i - W_o) \quad \text{(D.9)}$$

where:

Q_l = Latent heat loss

V = volumetric air flow rate

ρ_{air} = density of the air

W_i = humidity ratio of indoor air

W_o = humidity ratio of outdoor air

hfg = latent heat of evaporation at indoor air temperature

D.7 Air Change Rate Equations.

$$ACH = CFM \times \frac{60\frac{min}{hr}}{room\ volume} \quad \text{(D.10)}$$

$$CFM = ACF \times \frac{room\ volume}{60\frac{min}{hr}} \quad \text{(D.11)}$$

where:

ACH = Air Change Rate per Hour

CFM = Air Flow Rate (Cubic Feet per Minute)

room volume = Space Volume (Cubic Feet)

D.8 Ventilation Formula.

The equation below is used in calculating ventilation (or infiltration) due to the stack effect.

$$Q = C \times A \times \frac{[h \times (t_i - t_o)]}{t_i} \quad \text{(D.12)}$$

where:

Q = Air Flow Rate (CFM)

C = constant of proportionality = 313 (This assumes a value of 65 percent of the maximum theoretical flow, due to limited effectiveness of actual openings. With less favorable conditions, due to indirect paths from openings to the stack, etc., the effectiveness drops to 50 percent, and C = 240.)

A = area of cross-section through stack or outlets in sq ft. (Note: Inlet area must be at least equal to this amount)

t_i = (higher) temperature inside (°F), within the height h

t_o = (lower) temperature outside (°F)

h = height difference between inlets and outlets (ft)

D.9 Outdoor Air.

The equation for calculating outdoor quantities using carbon dioxide measurements is:

$$Outdoor\ air\ (\%) = \frac{(C_r - C_s) \times 100}{(C_r - C_o)} \quad \text{(D.13)}$$

where:

C_s = ppm of carbon dioxide in the mixed air (if measured at an air handler) or in supply air (if measured in a room)

C_r = ppm of carbon dioxide in the return air

C_o = ppm of carbon dioxide in the outdoor air

D.10 Dilution Ventilation.

Dilution ventilation is to control the vapors from organic liquids. To determine the correct volume flow rate for dilution (Q_d), it is necessary to estimate the evaporation rate of the contaminant (q_d) according to the following equation:

$$q_d = \frac{387(lbs)}{MW \times T \times \rho} \tag{D.14}$$

where:

q_d = Evaporation rate in CFM

387 = Volume in cubic feet formed by the evaporation of one lb-mole of a substance, e.g. a solvent

MW = Molecular weight of the emitted material

lbs = Pounds of evaporated material

T = Time of evaporation in minutes

ρ = density correction factor

The appropriate dilution volume flow rate for toxics is:

$$Q_d = \frac{q_d \times K_m \times 106}{C_a} \tag{D.15}$$

where:

Q_d = Volume flow rate of air, in CFM

q_d = Evaporation rate in CFM

K_m = Mixing factor to account for poor or random mixing (note K_m = 2 to 5; K_m = 2 is optimum)

C_a = Accessible airborne concentration of the material

APPENDIX E

OLSTOP Graphs

This section has the results of the OLSTOP in graph format.

E.1 Optimal Variables (T_s, P_s, T_w, D_{pw}) Graphs.

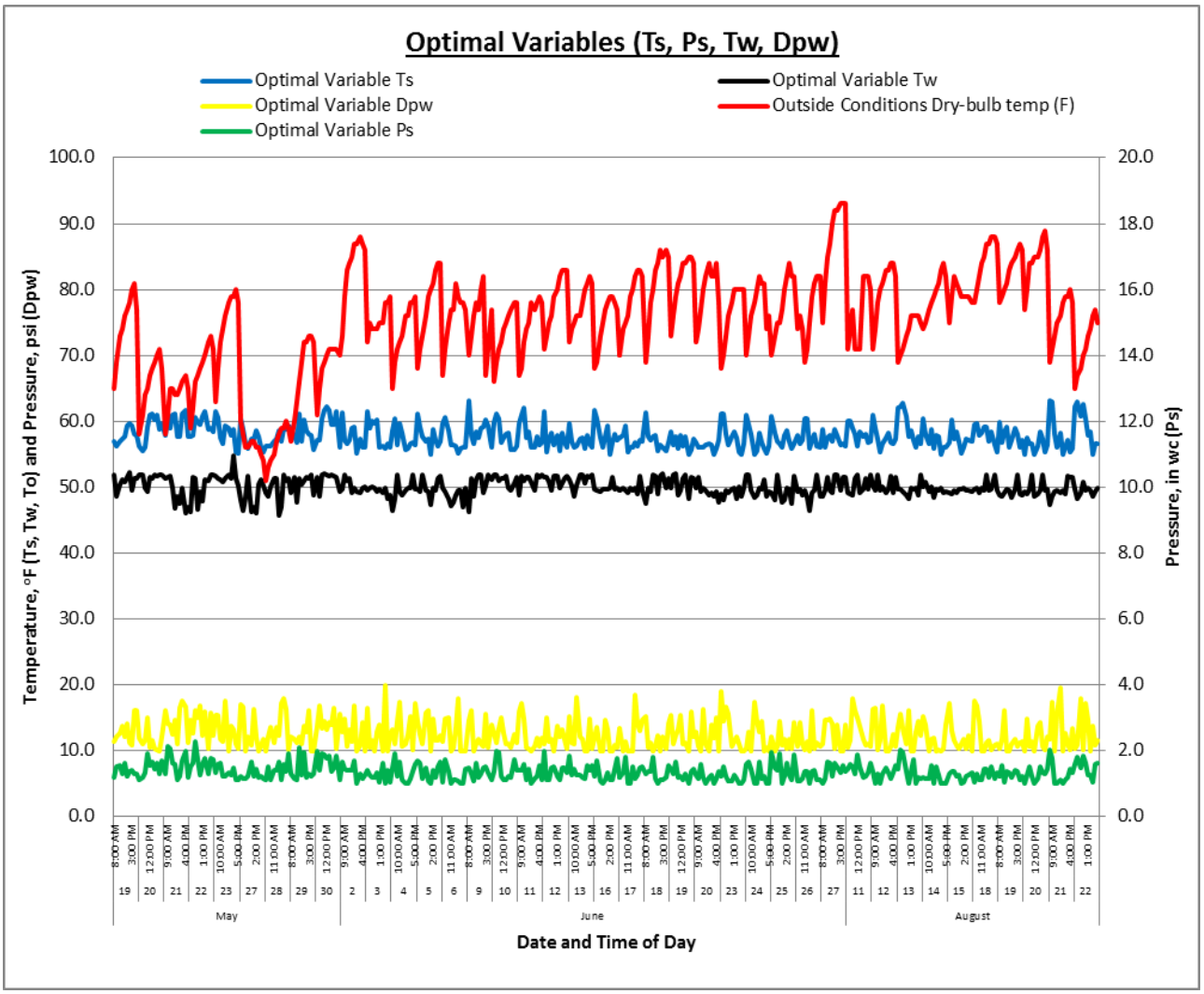

Figure 80. Optimal variables (May, June, August).

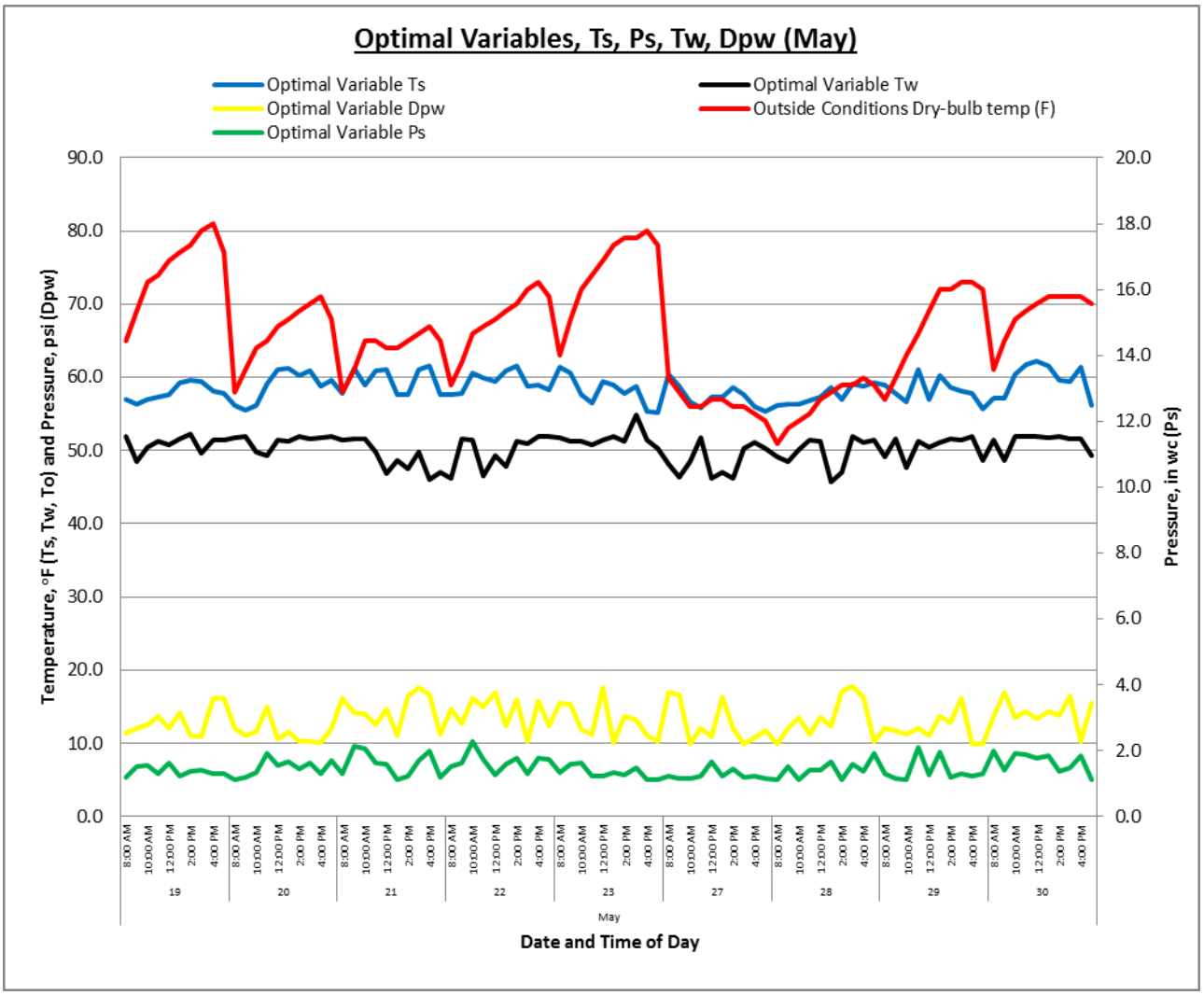

Figure 81. Optimal variables (May).

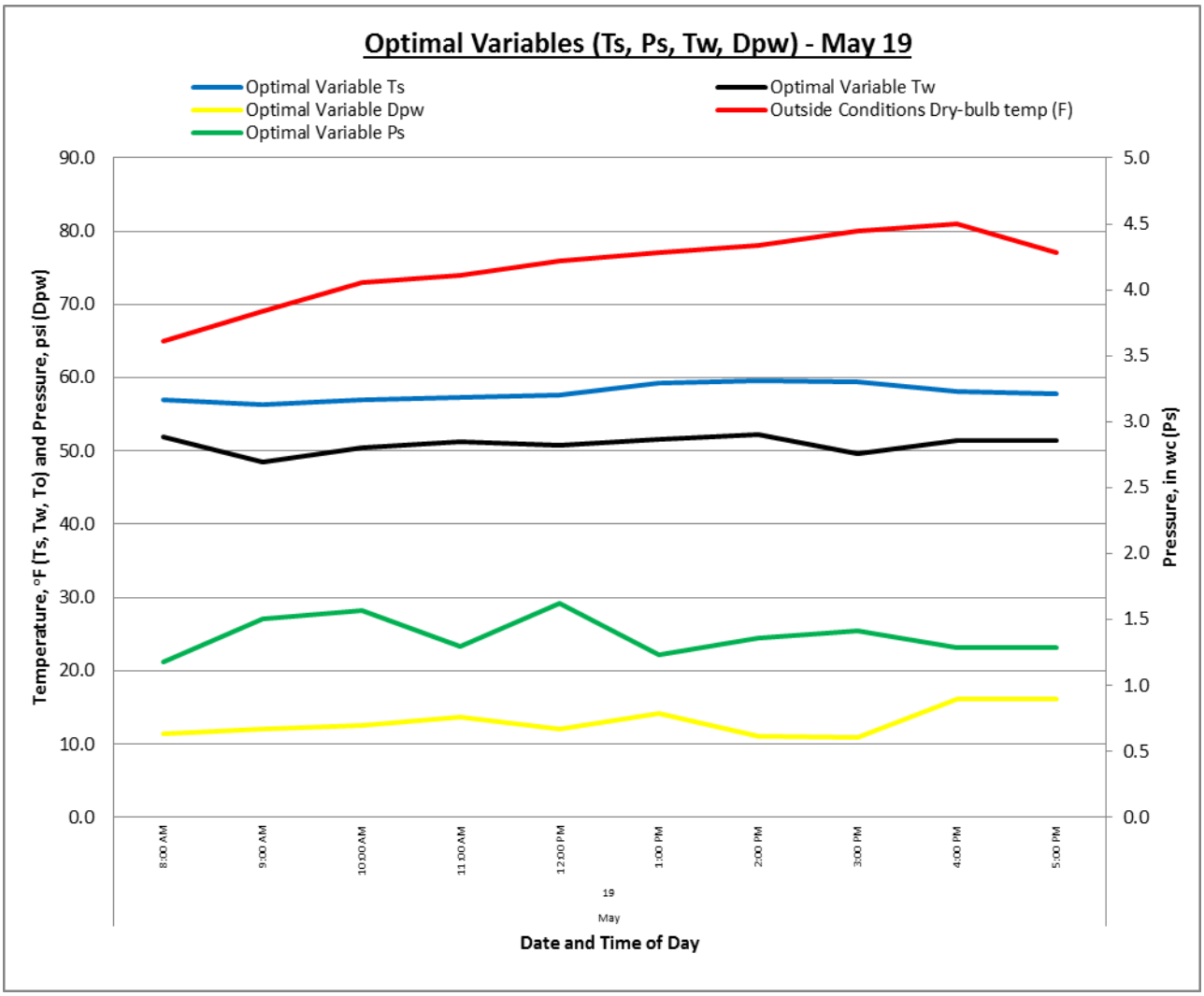

Figure 82. Optimal variables (May 19).

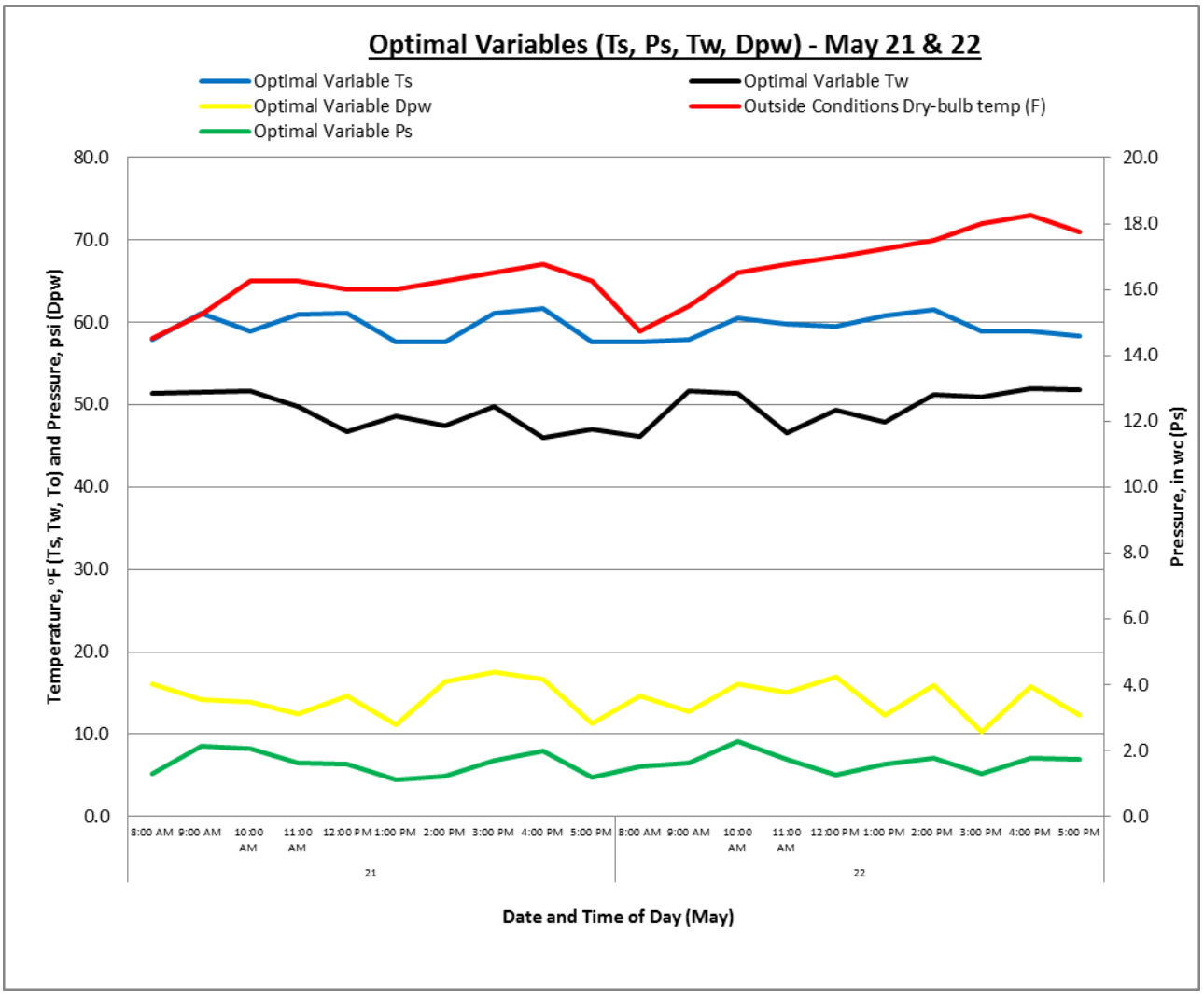

Figure 83. Optimal variables (May 21 & 22).

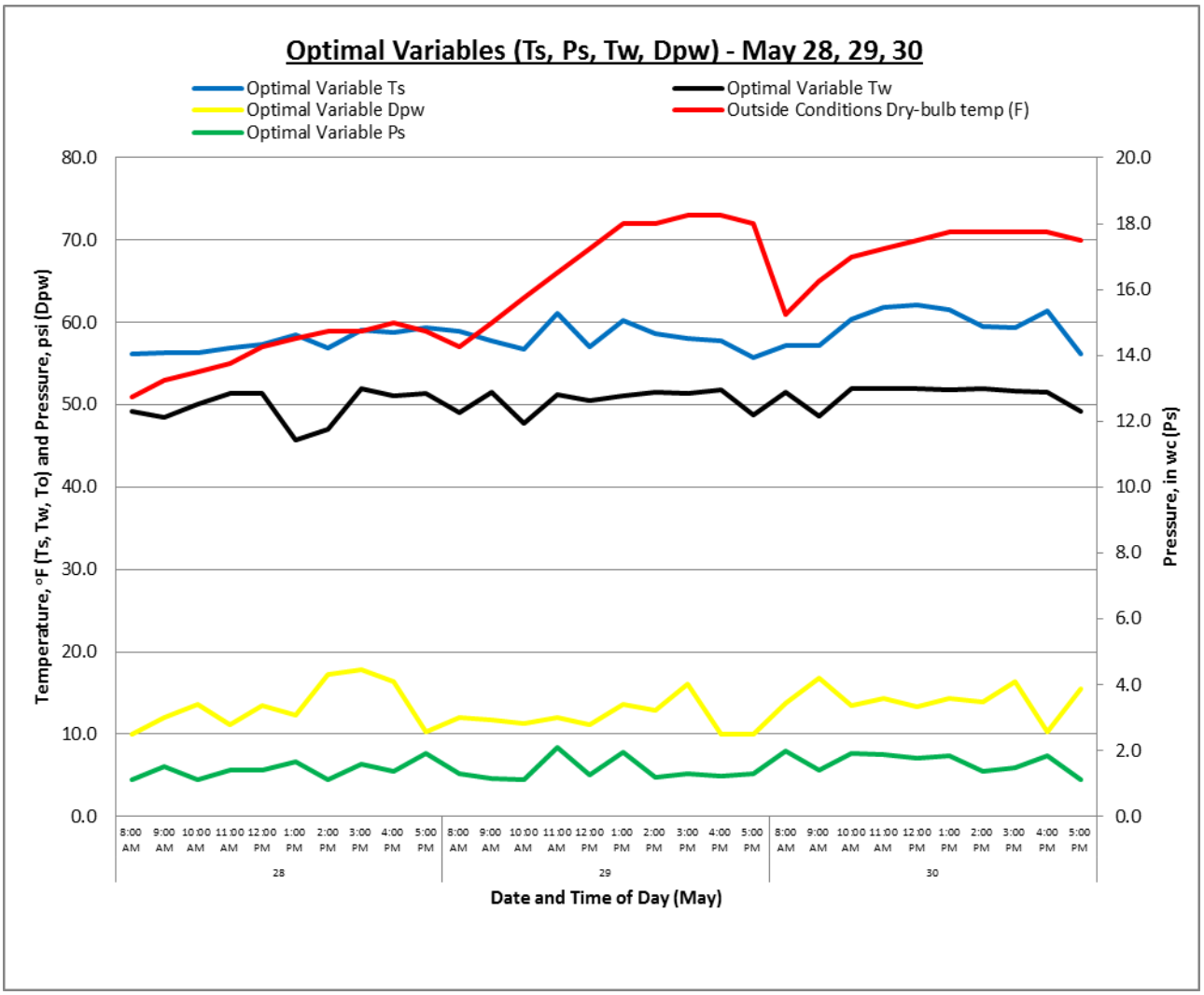

Figure 84. Optimal variables (May 28, 29, 30).

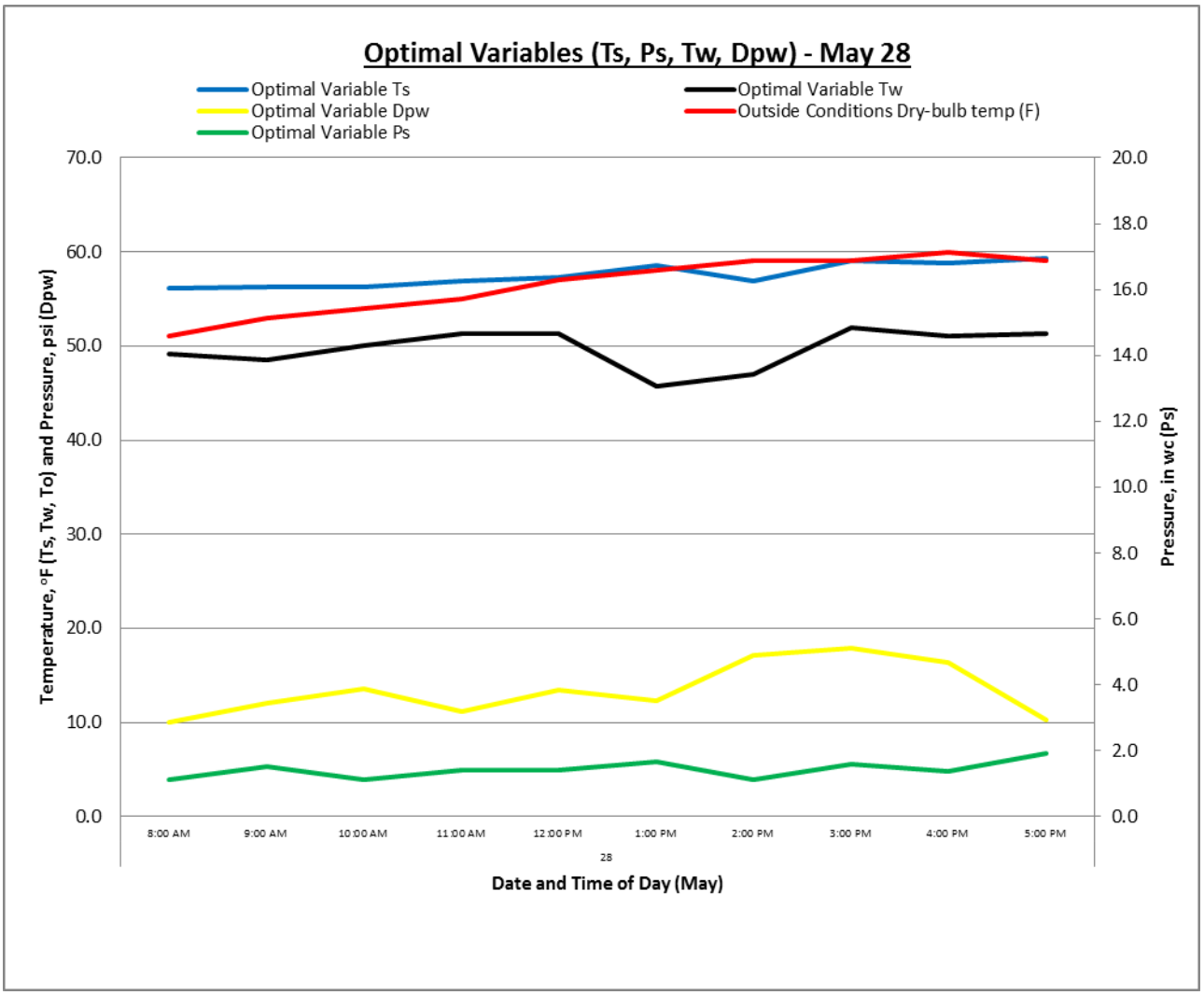

Figure 85. Optimal variables (May 28).

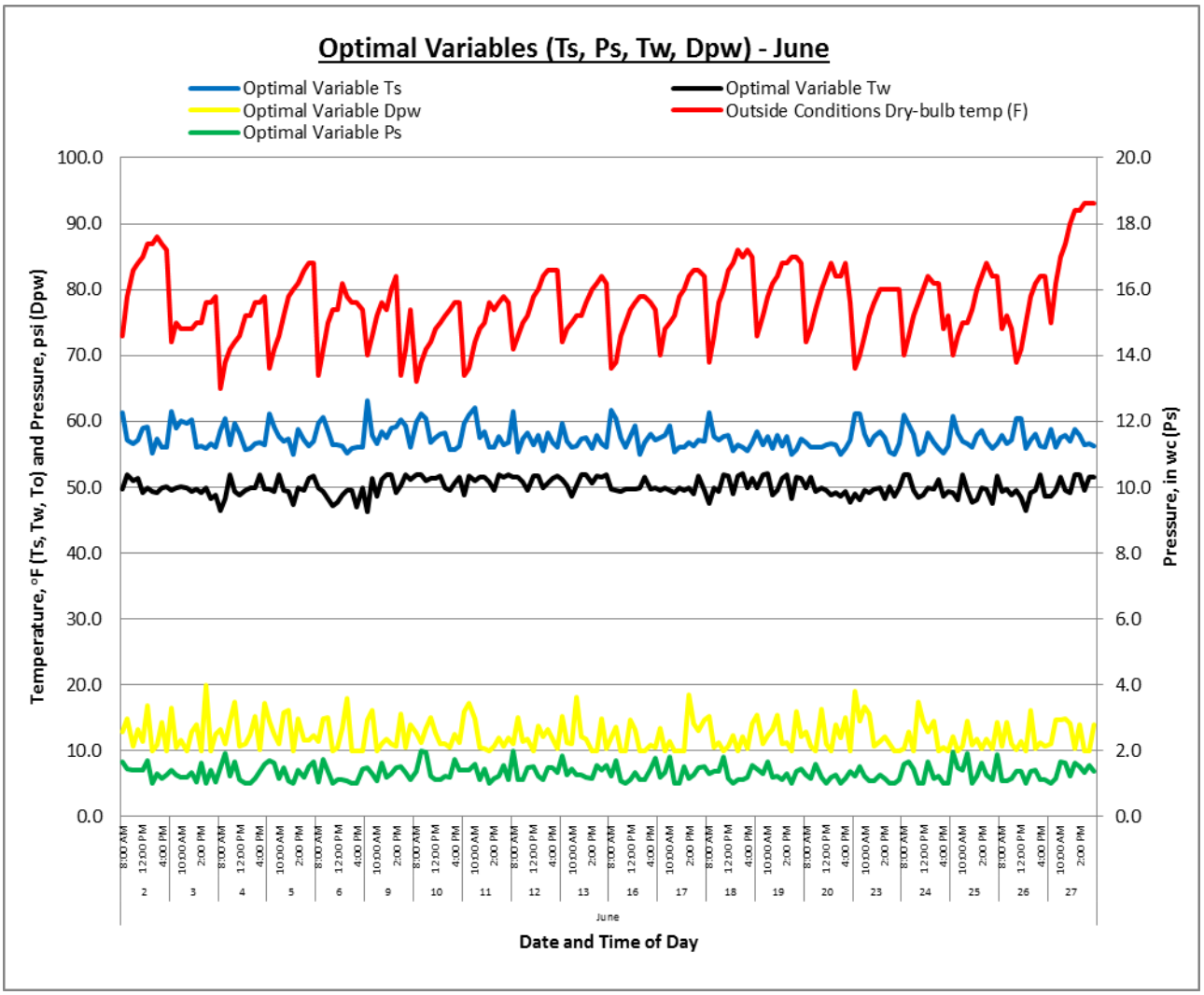

Figure 86. Optimal variables (June).

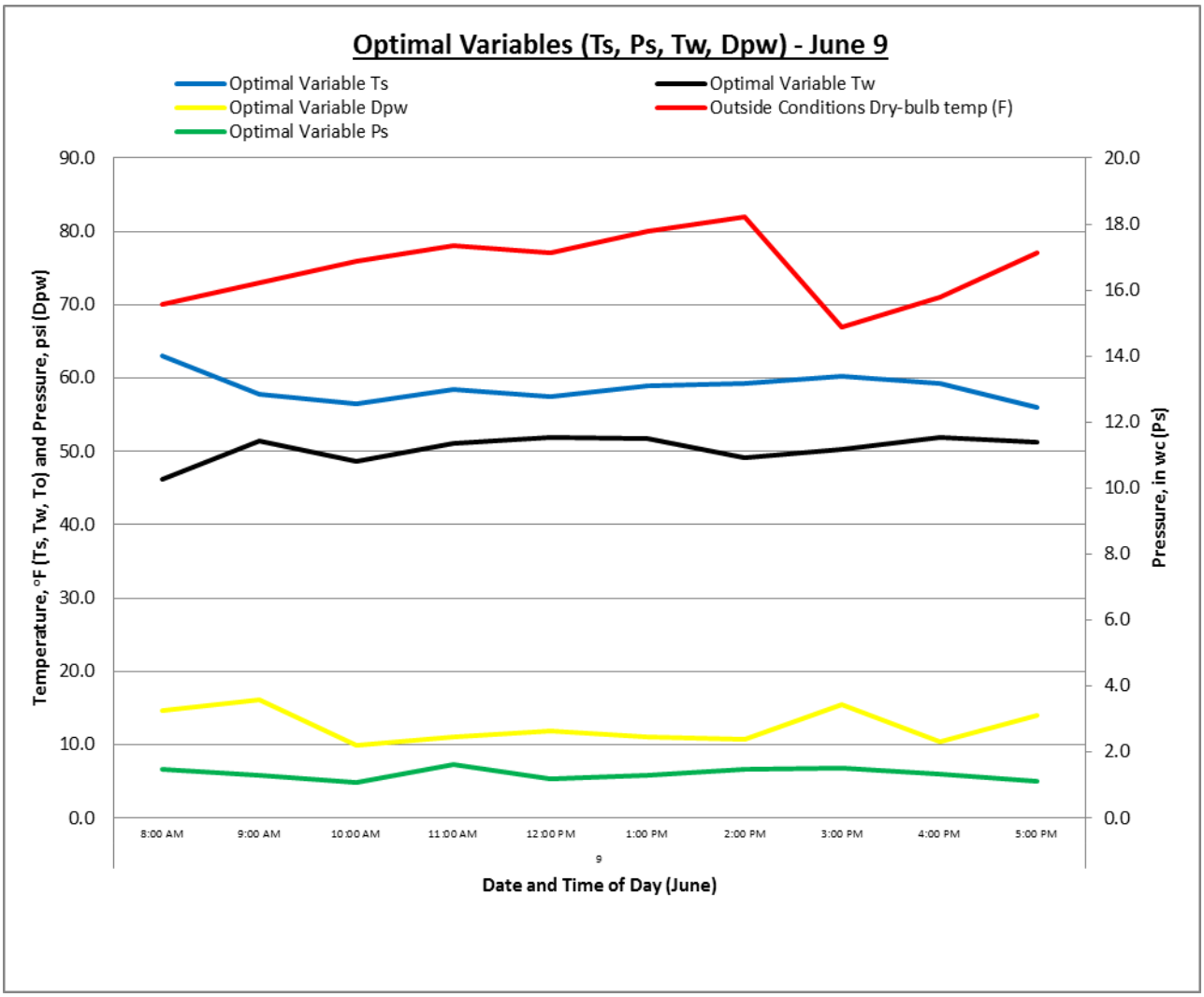

Figure 87. Optimal variables (June 9).

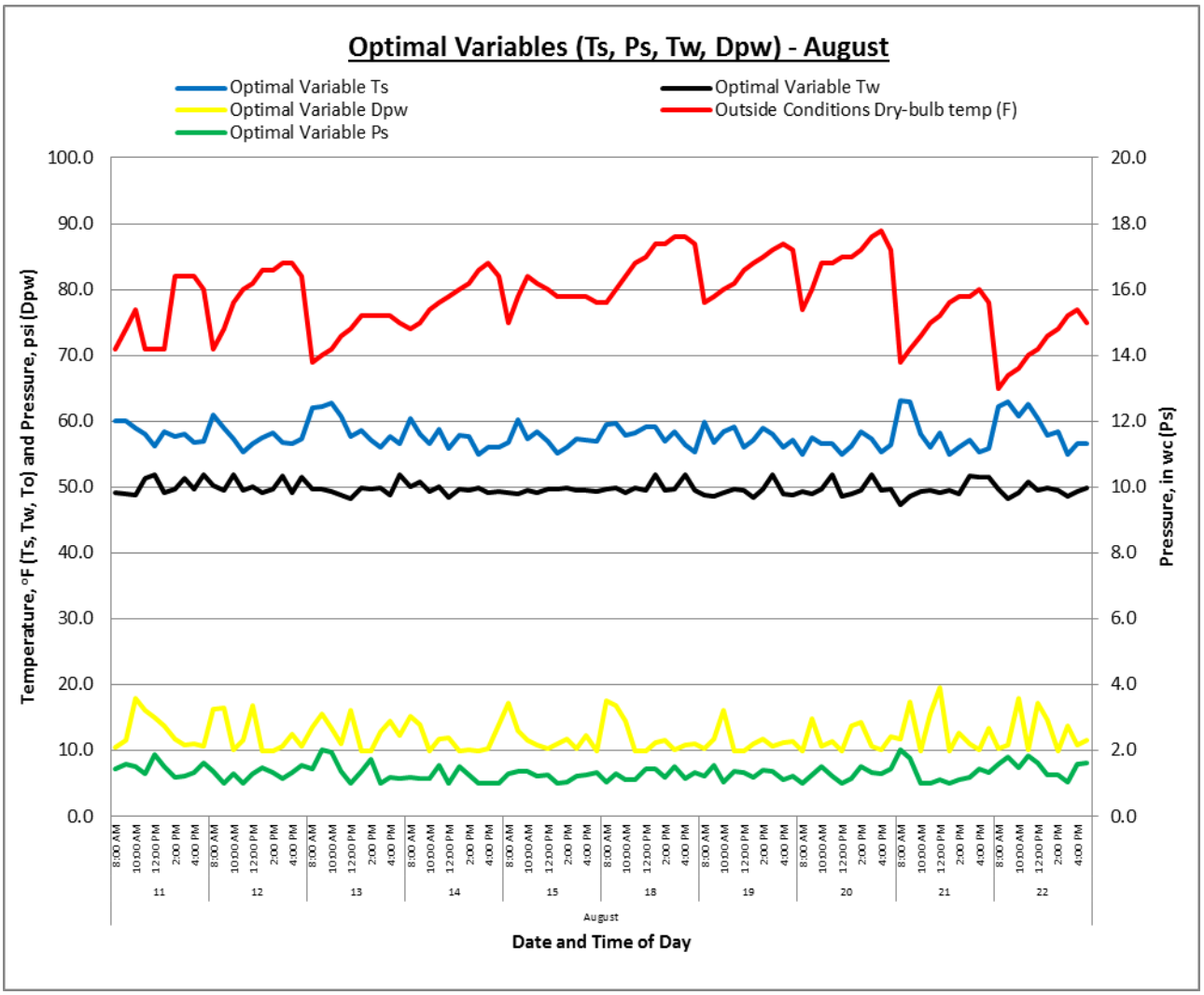

Figure 88. Optimal variables (August).

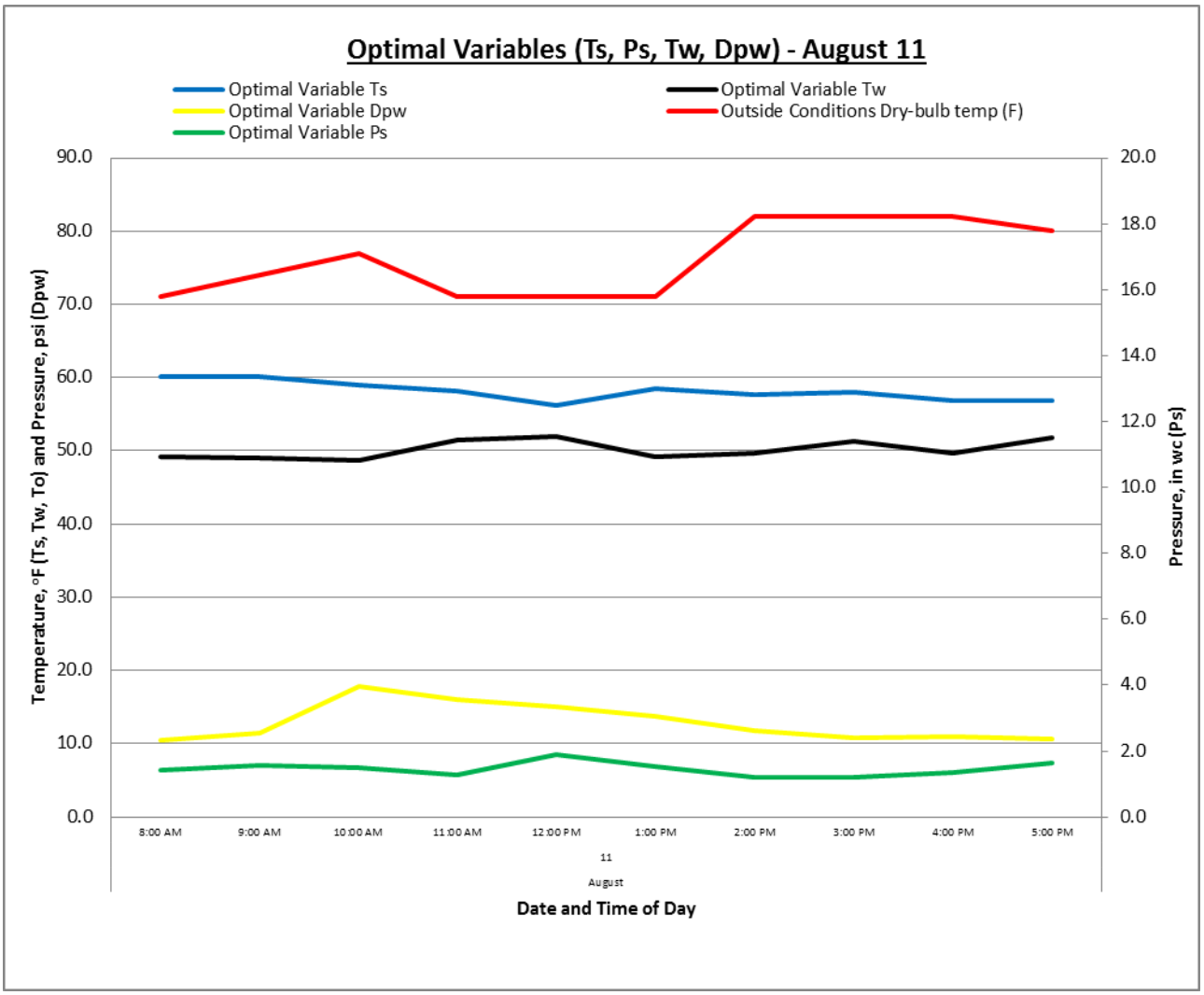

Figure 89. Optimal variables (August 11).

E.2 Pump Power Comparison (OV, SP & FOM) Graphs.

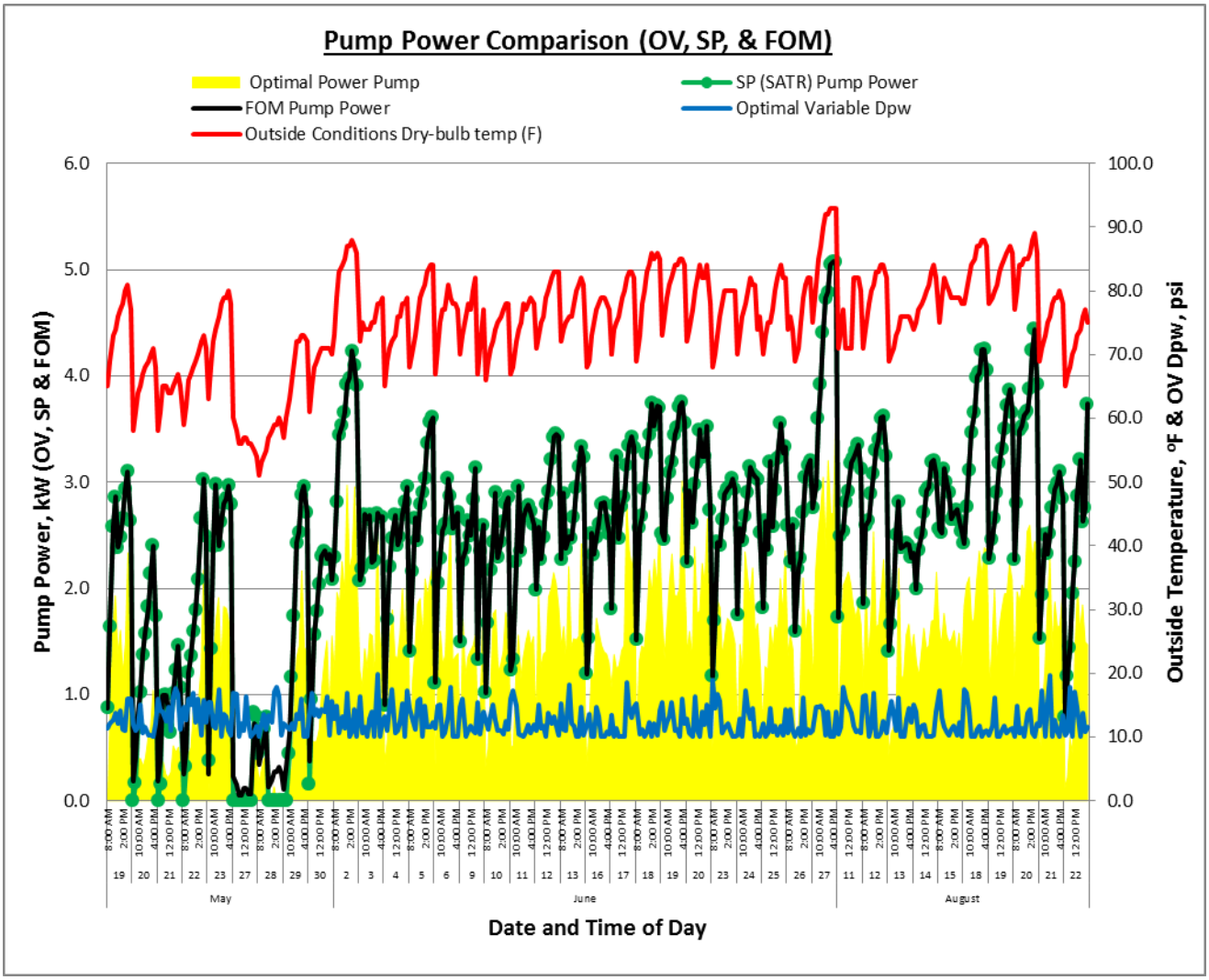

Figure 90. Pump power comparison (May, June, August).

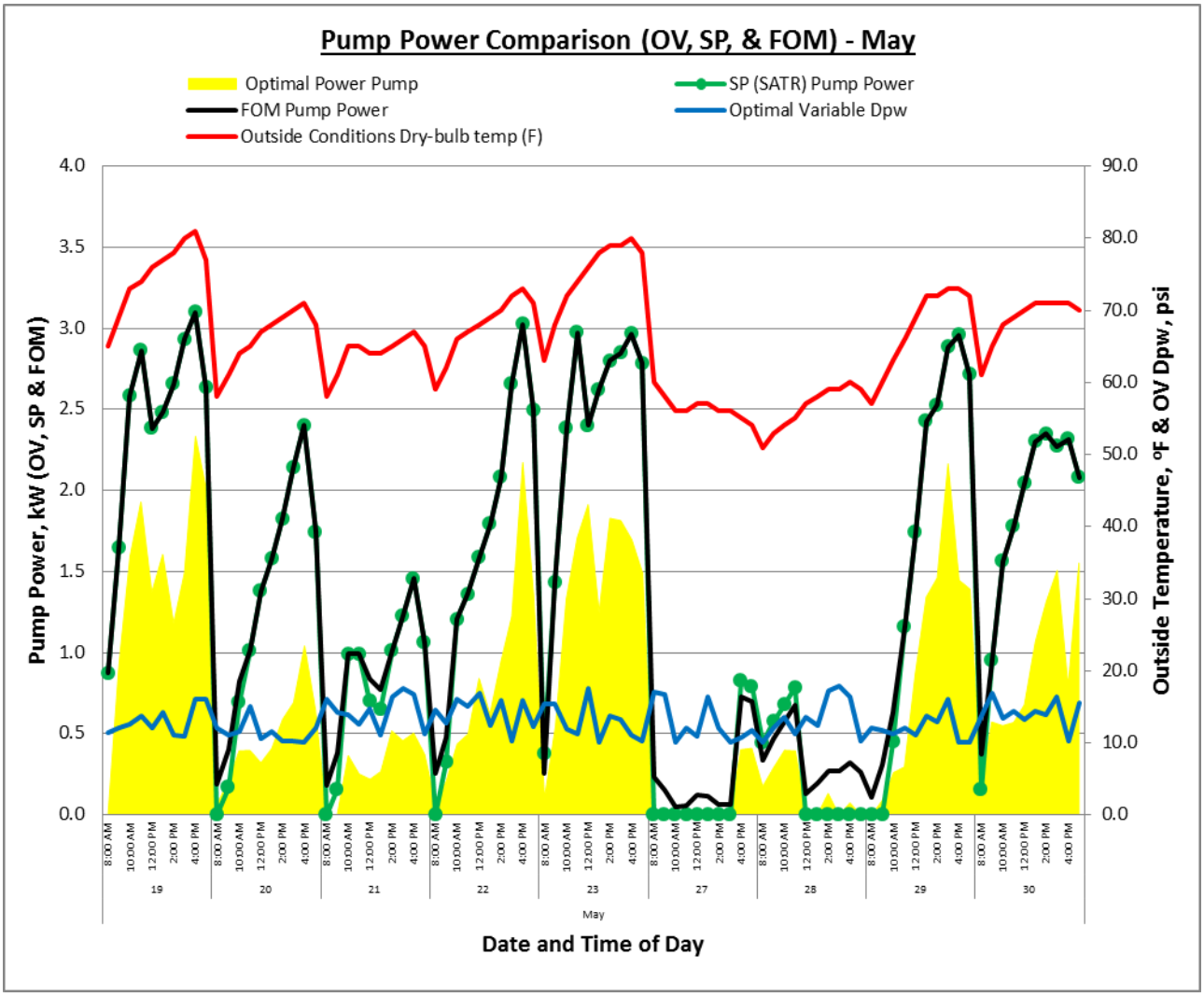

Figure 91. Pump power comparison (May).

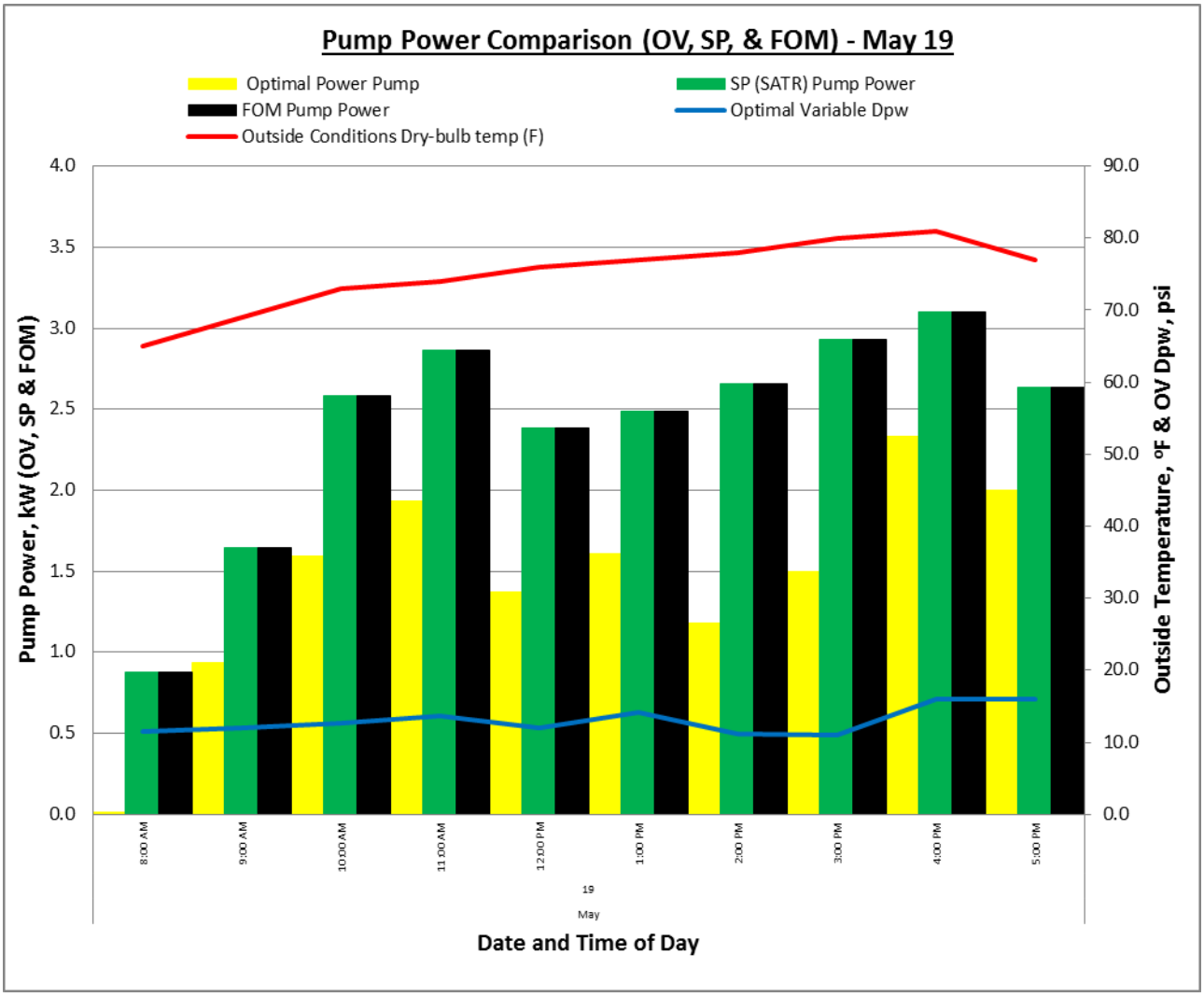

Figure 92. Pump power comparison (May 19).

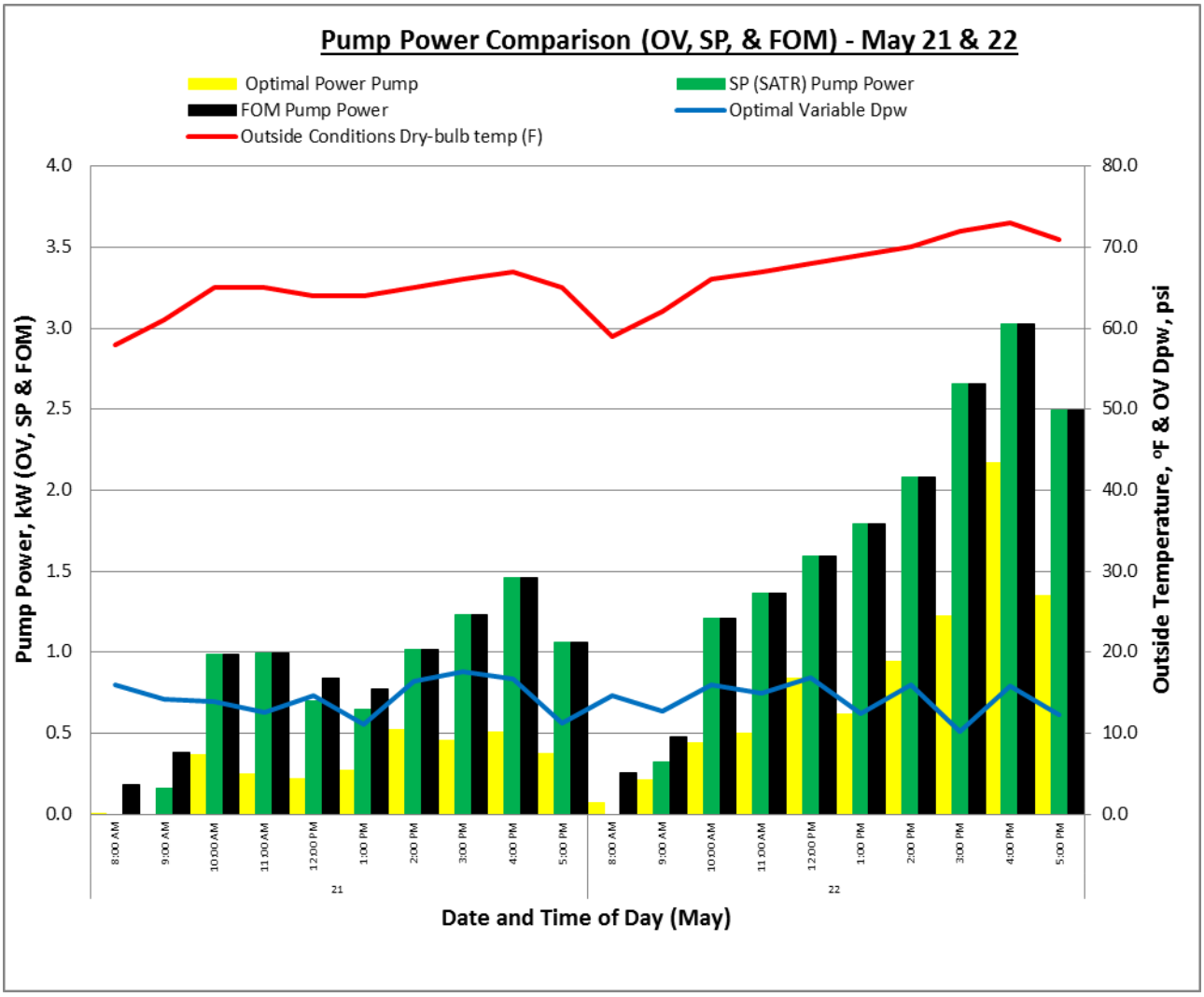

Figure 93. Pump power comparison (May 21 & 22).

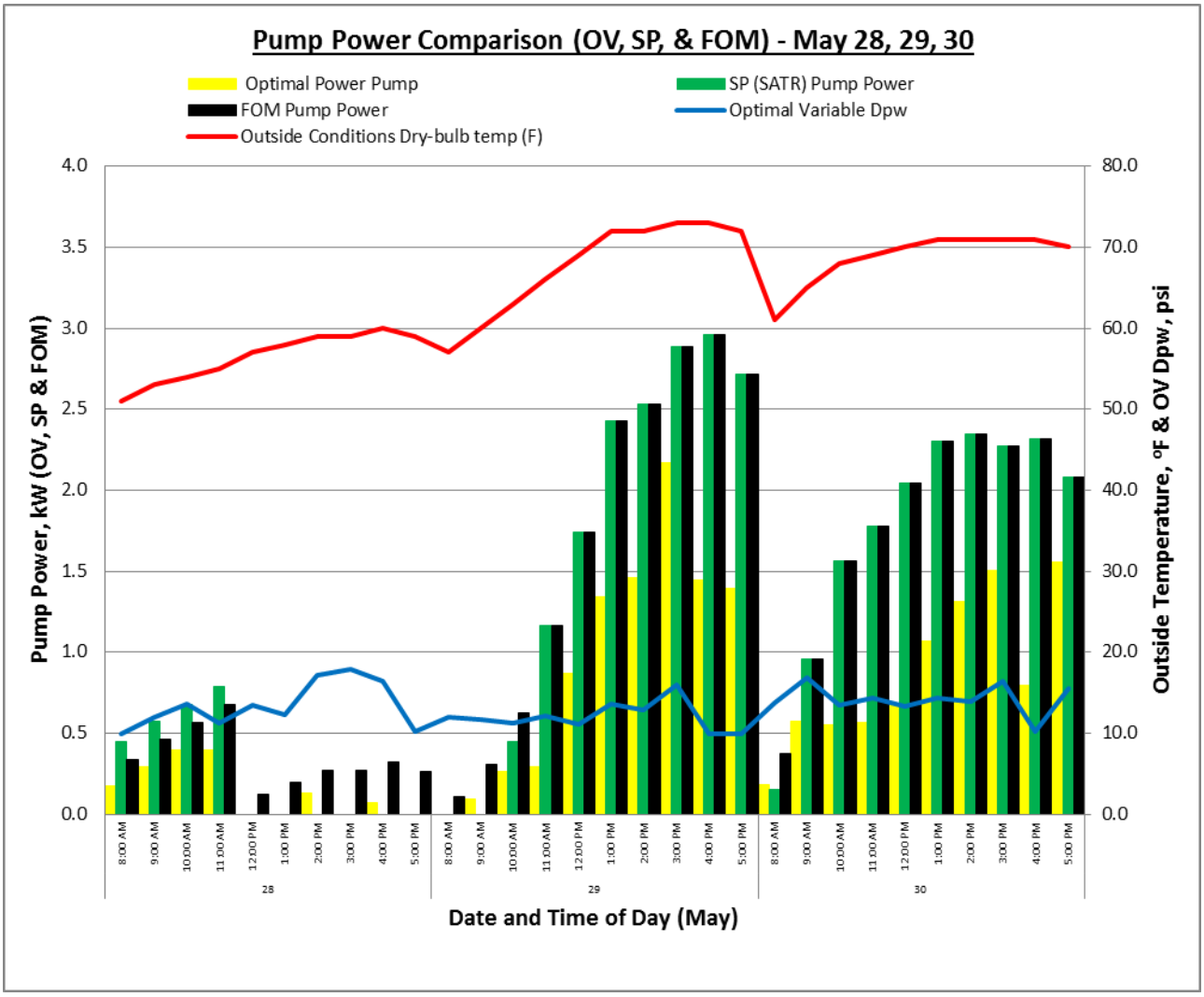

Figure 94. Pump power comparison (May 28, 29, 30).

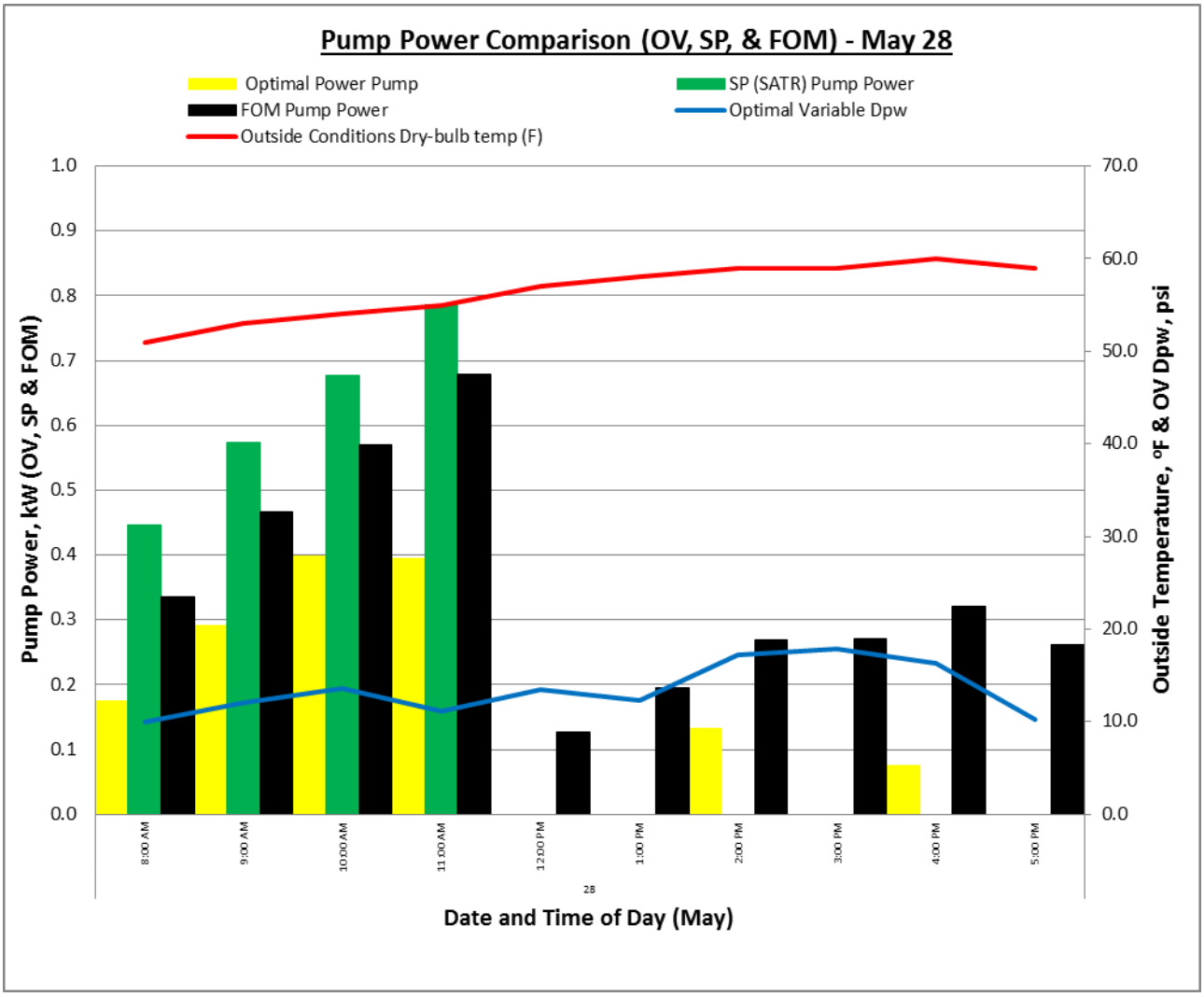

Figure 95. Pump power comparison (May 28).

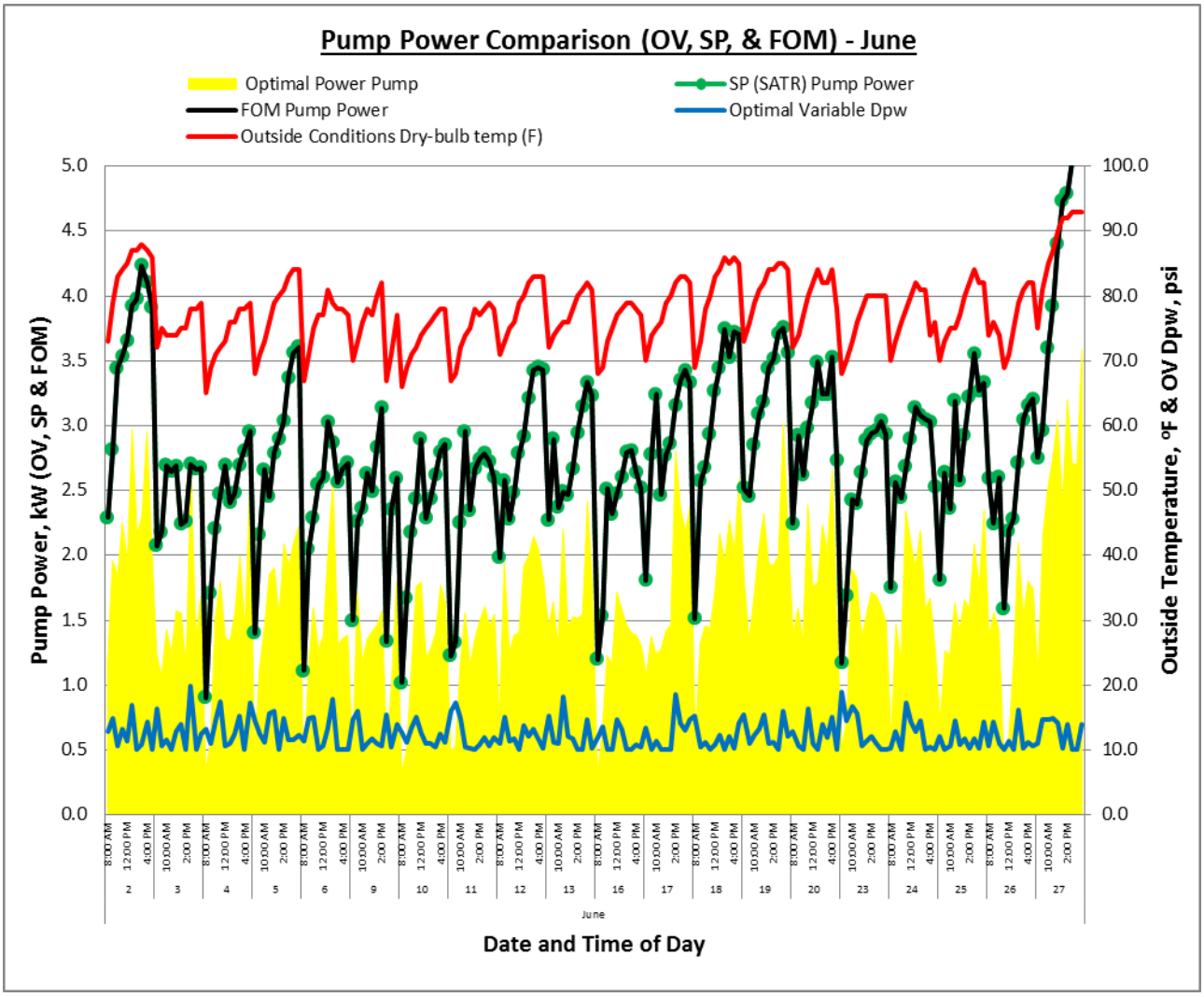

Figure 96. Pump power comparison (June).

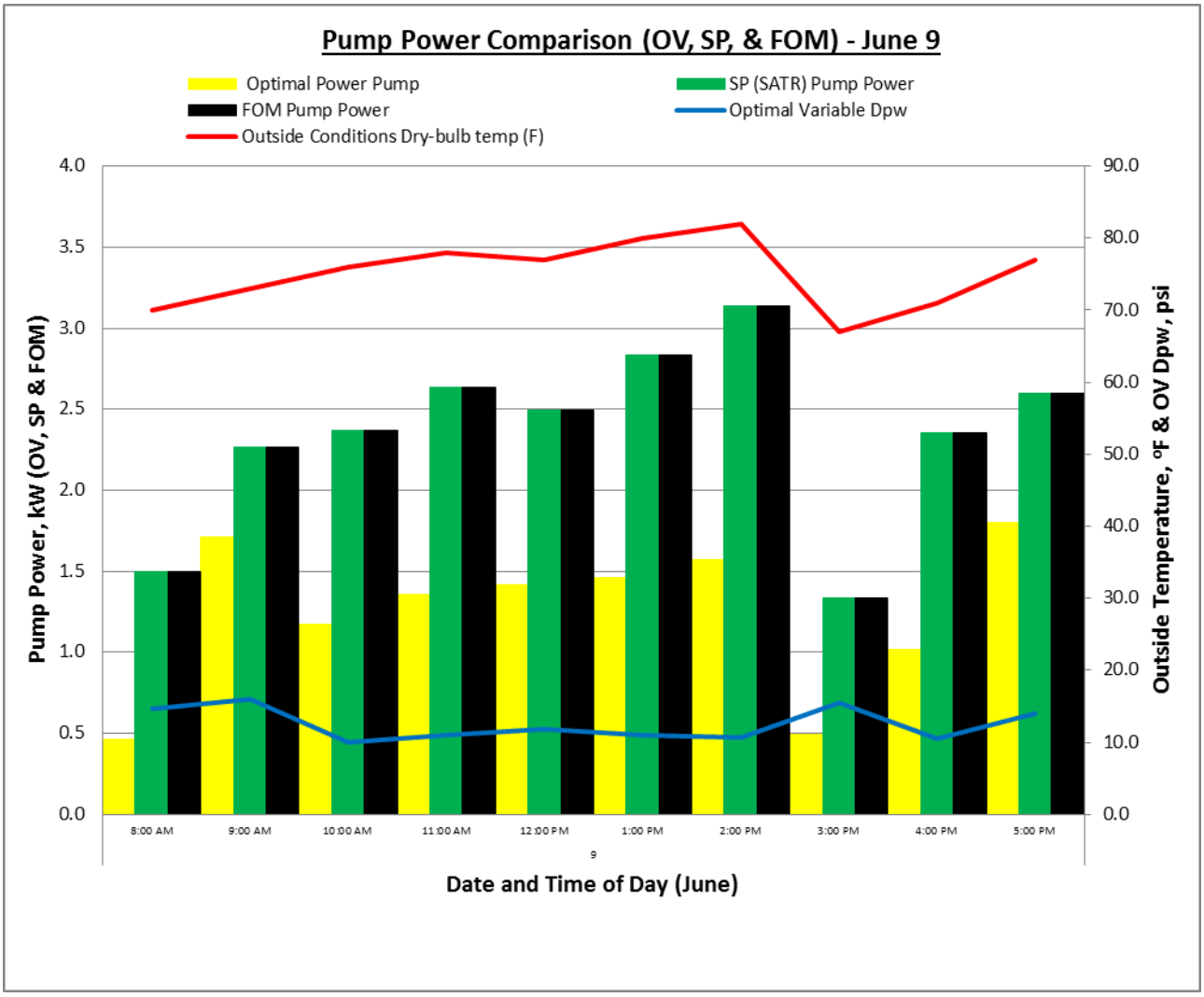

Figure 97. Pump power comparison (June 9).

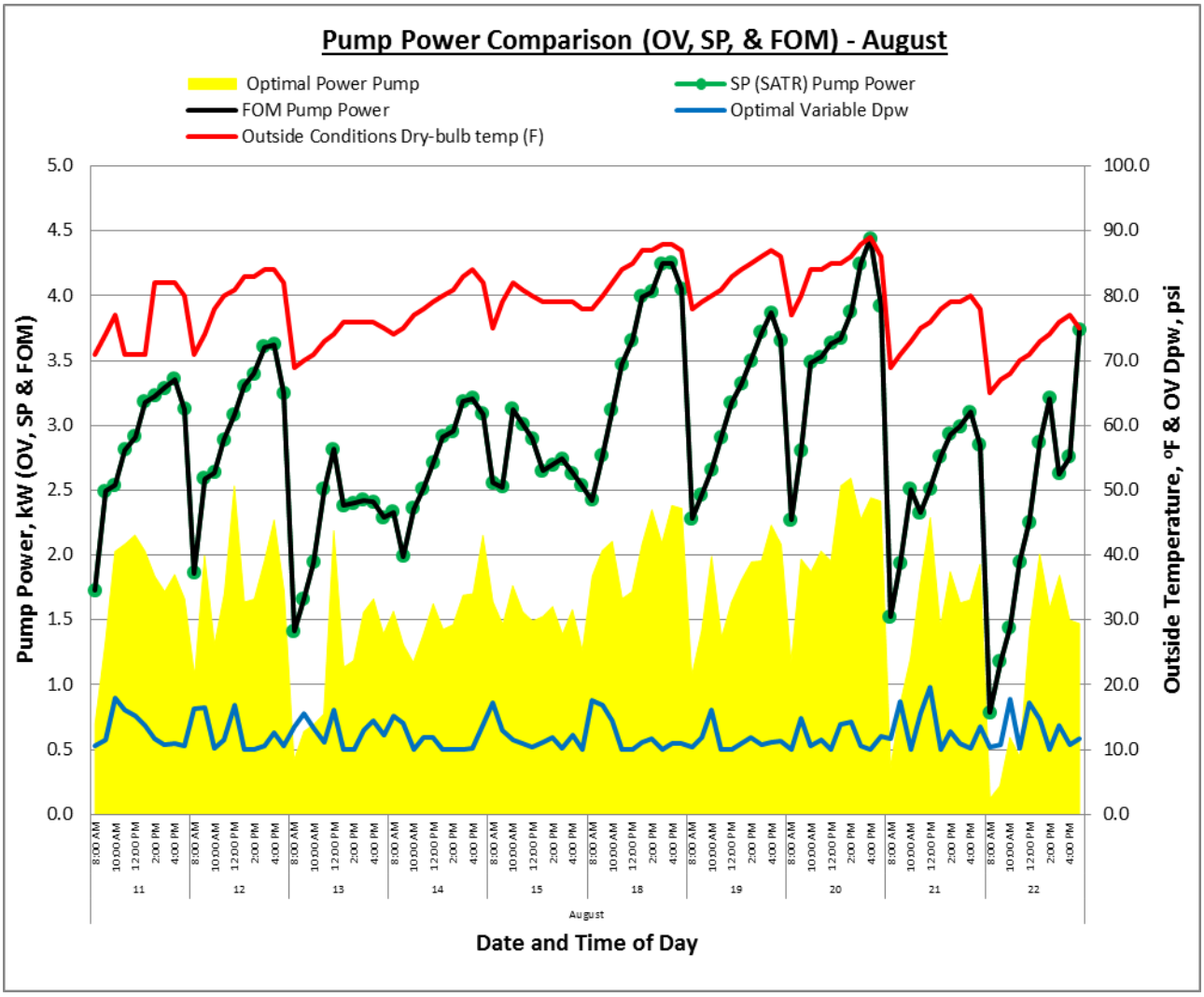

Figure 98. Pump power comparison (August).

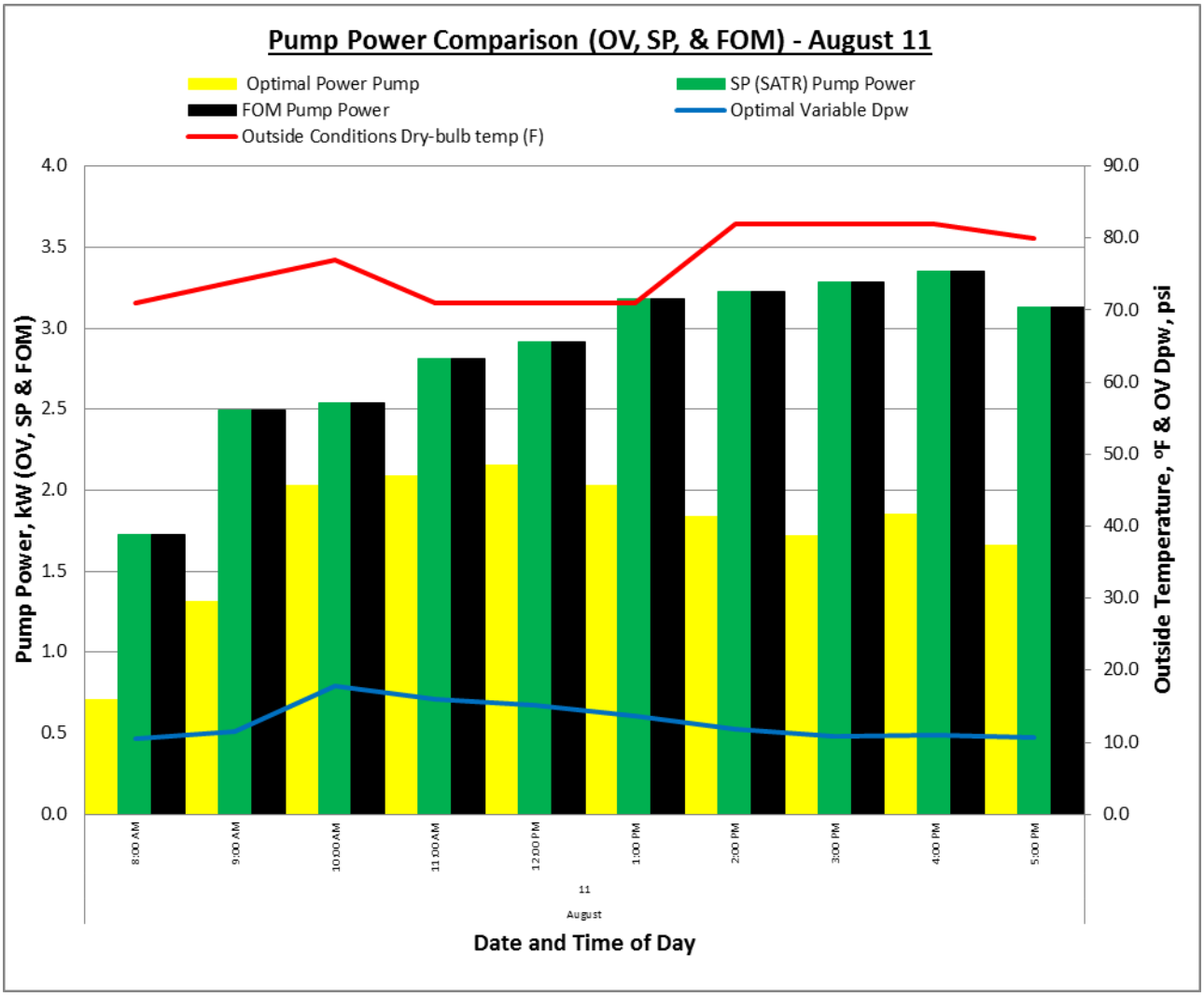

Figure 99. Pump power comparison (August 11).

E.3 Chiller Power Comparison (OV, SP & FOM) Graphs.

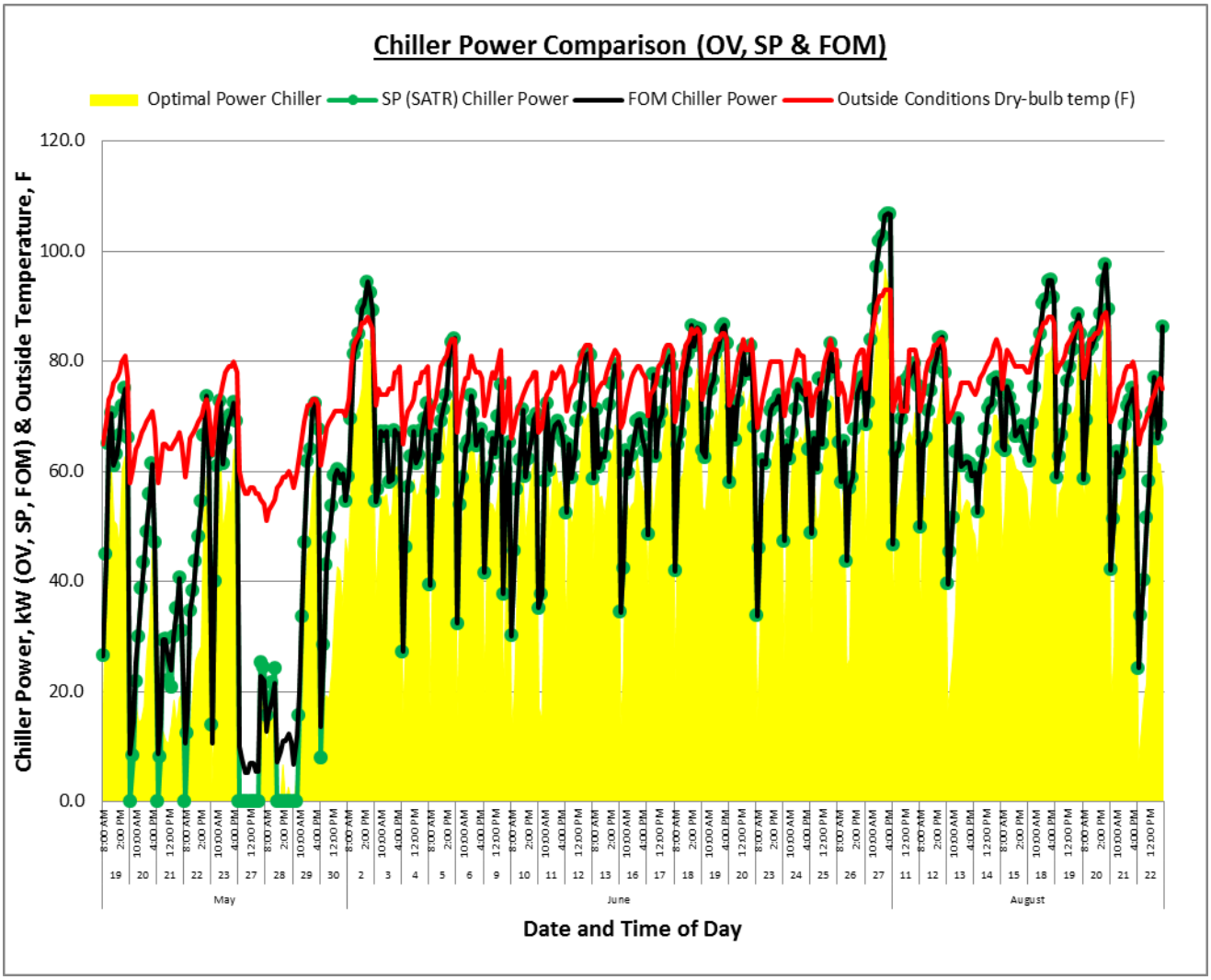

Figure 100. Chiller power comparison (May, June, August).

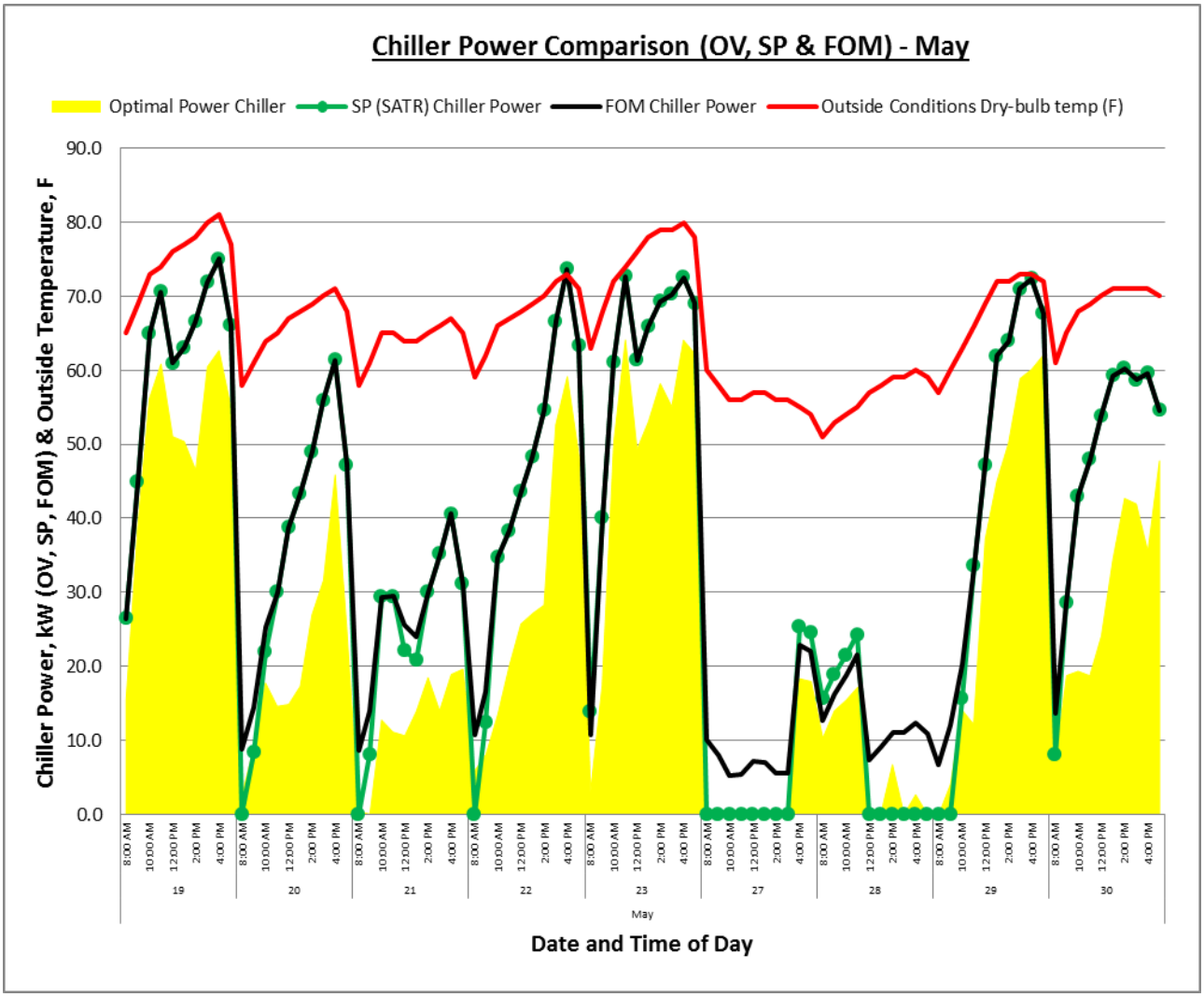

Figure 101. Chiller power comparison (May).

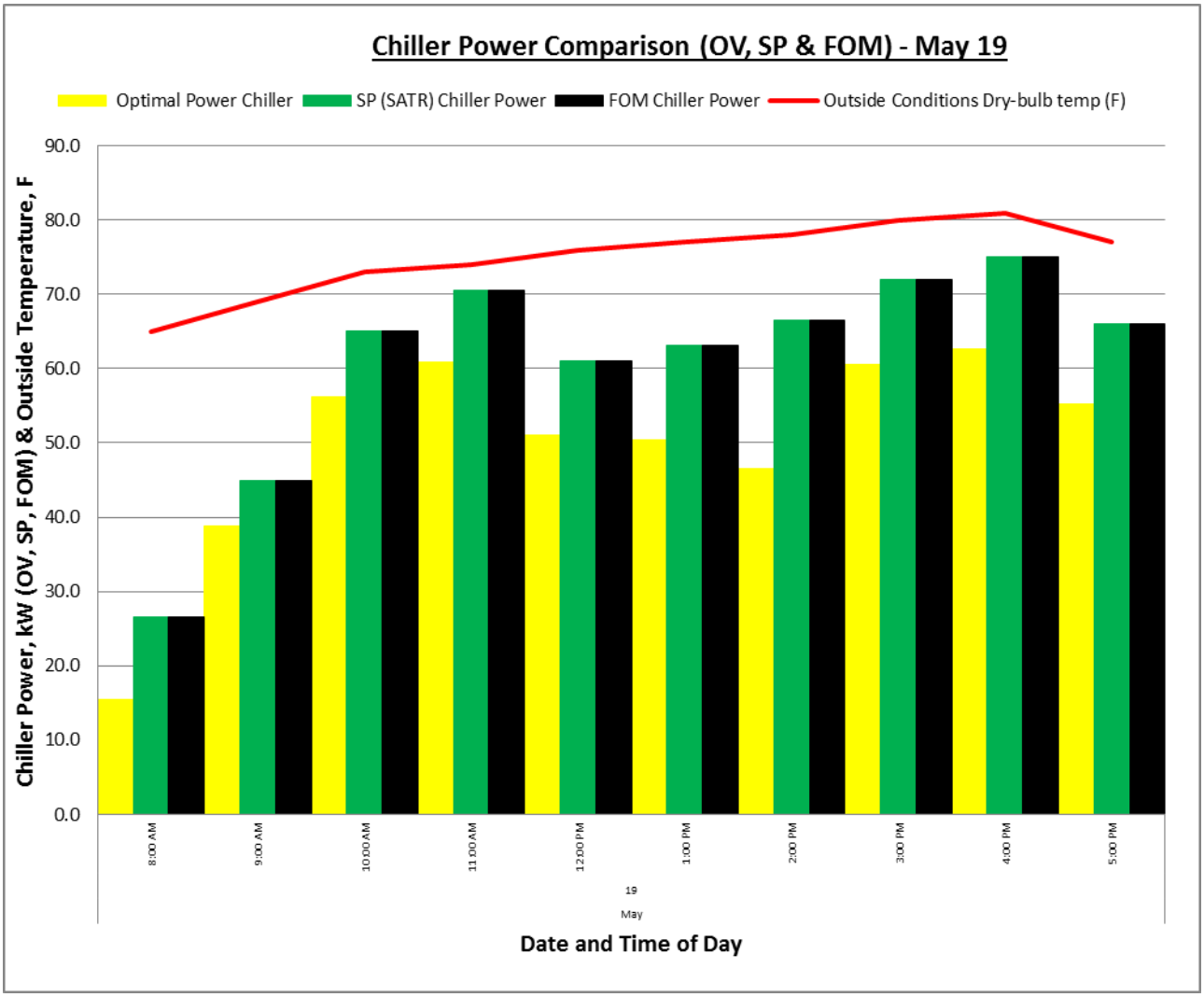

Figure 102. Chiller power comparison (May 19).

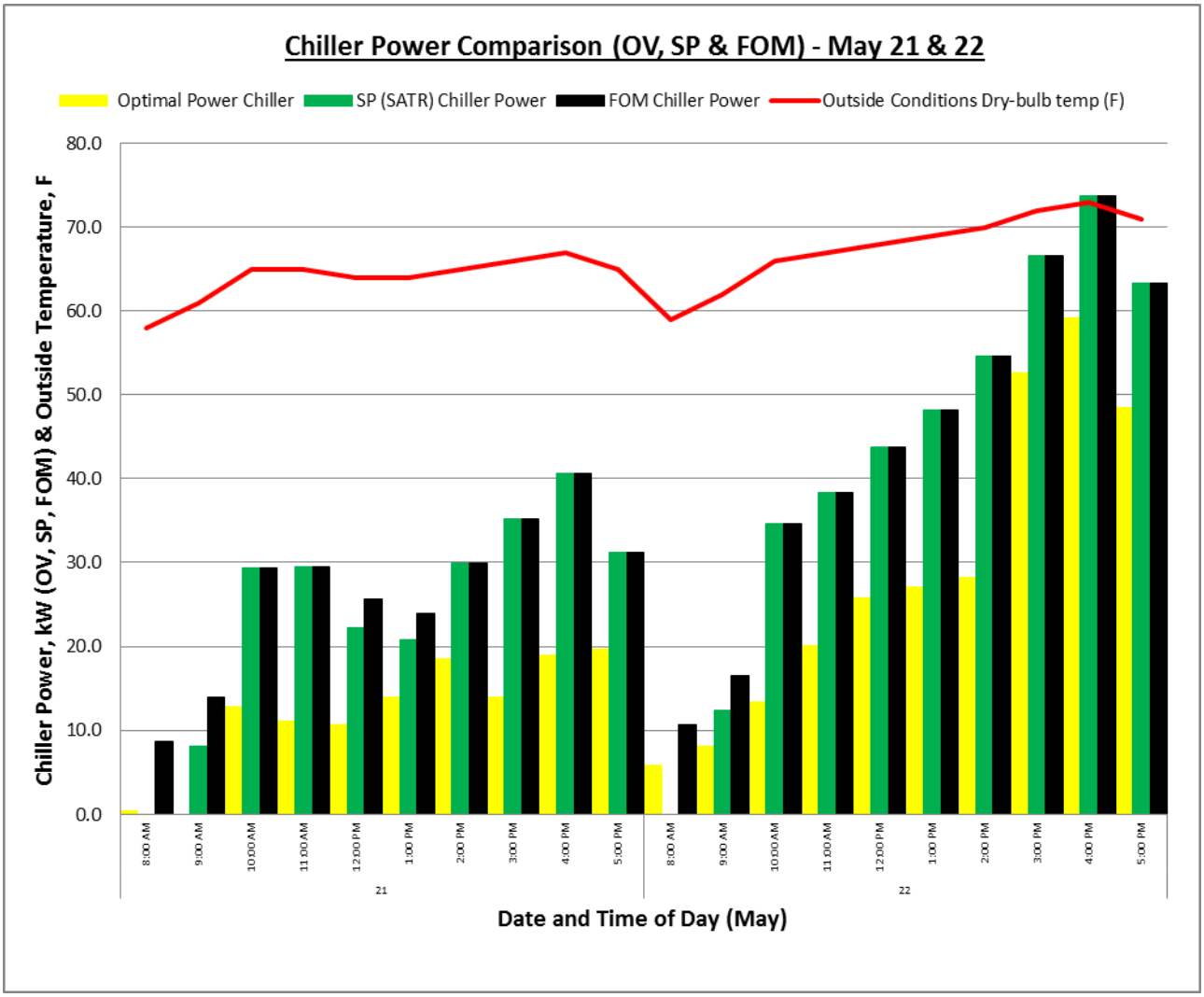

Figure 103. Chiller power comparison (May 21 & 22).

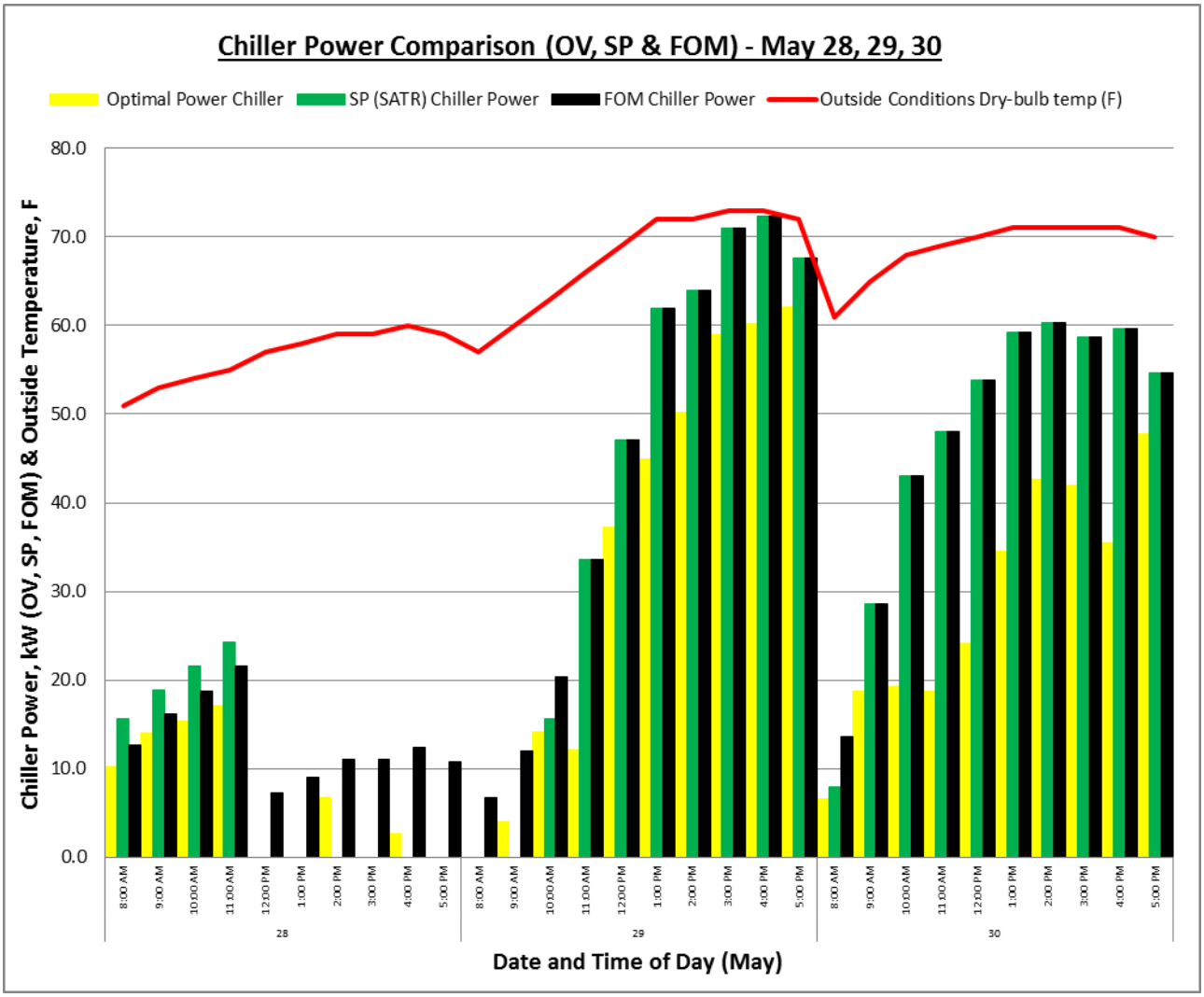

Figure 104. Chiller power comparison (May 28, 29, 30).

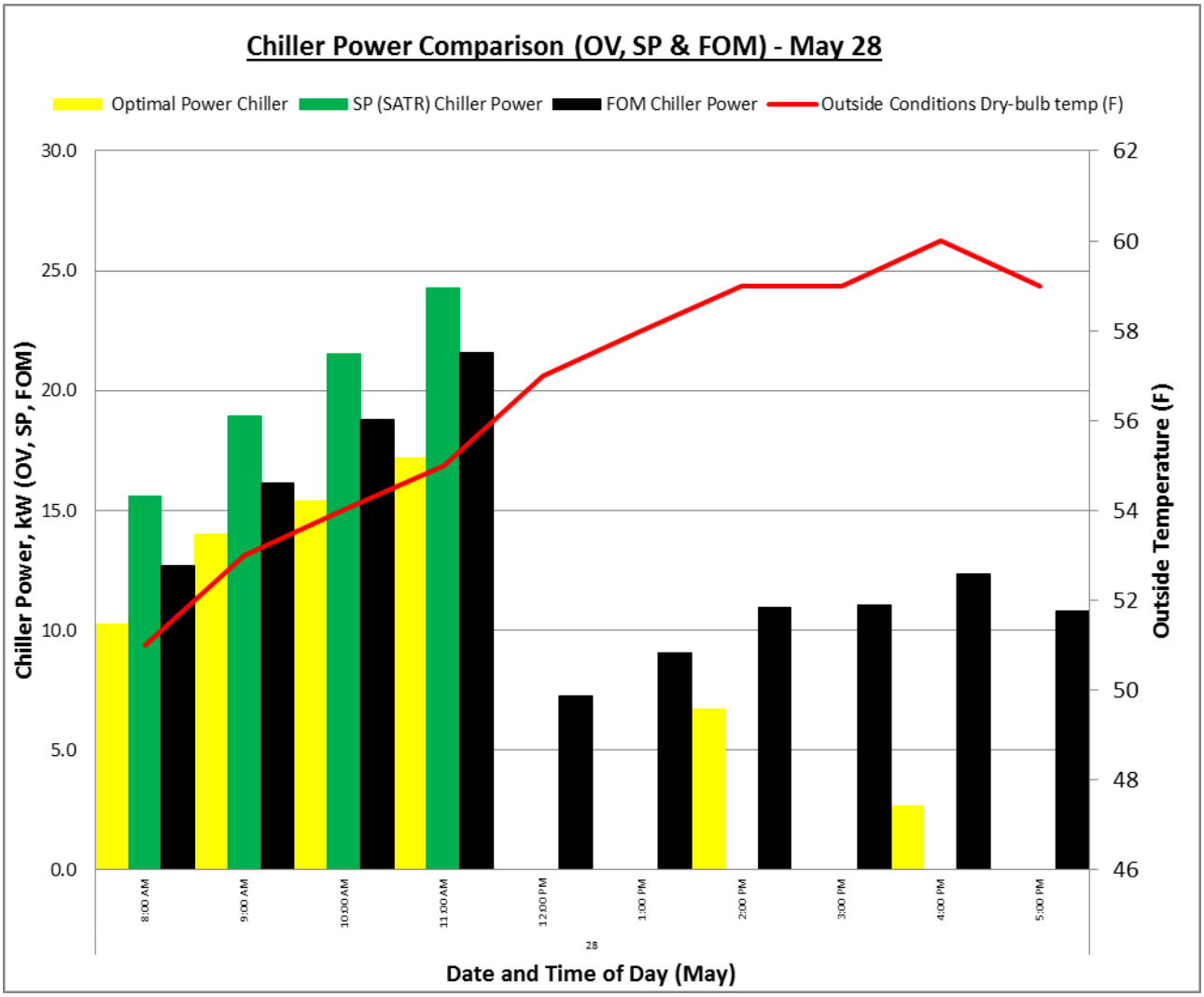

Figure 105. Chiller power comparison (May 28).

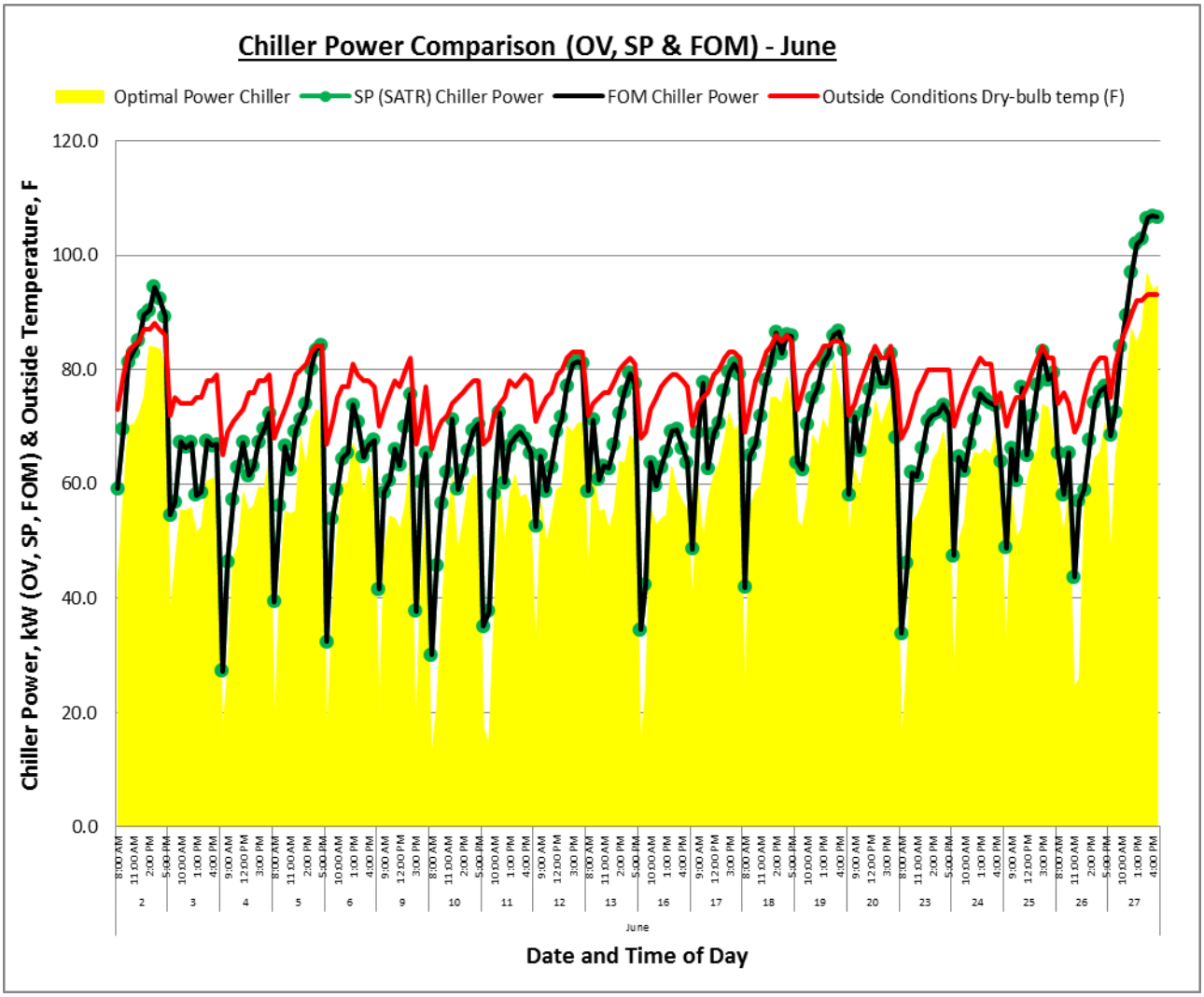

Figure 106. Chiller power comparison (June).

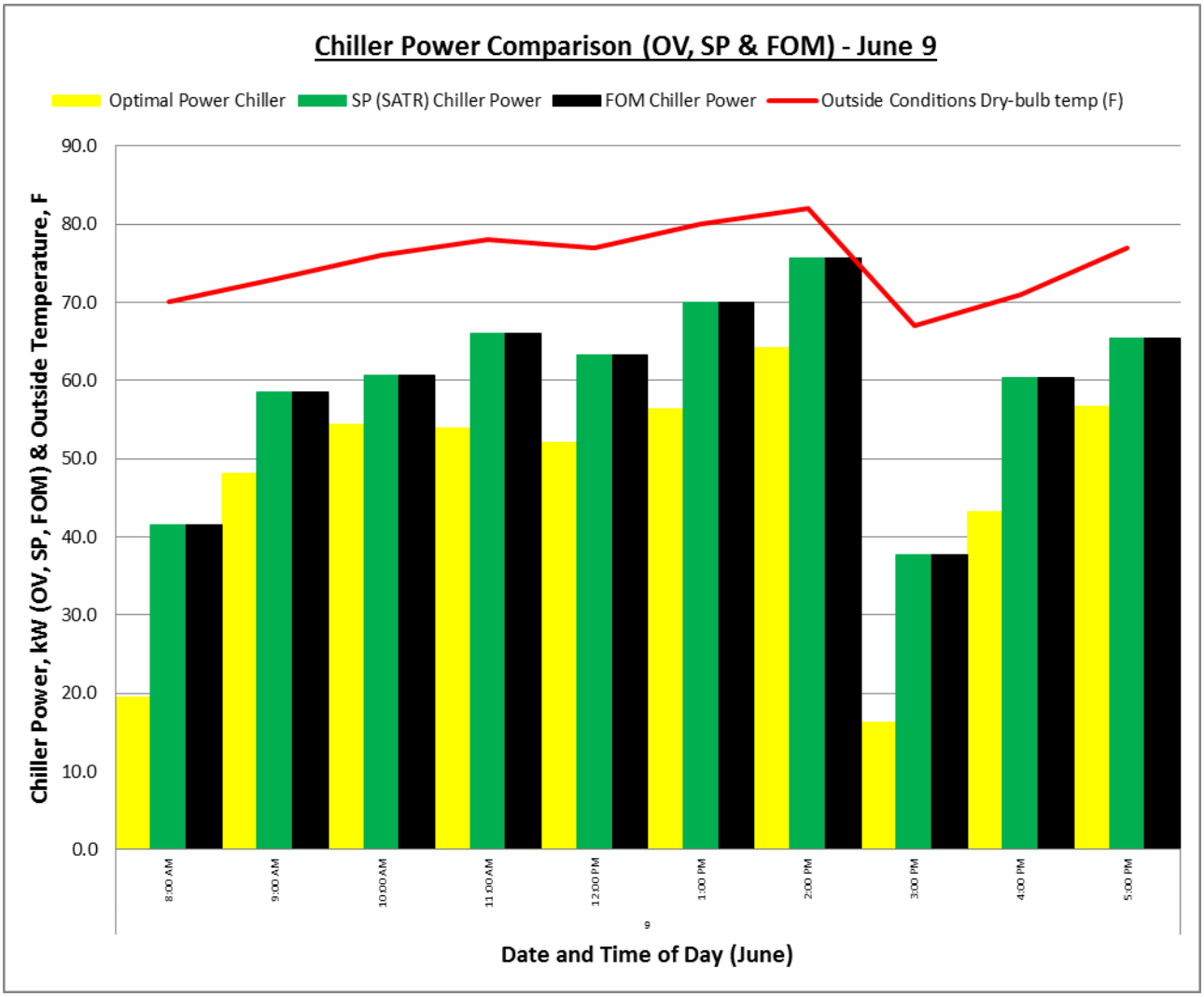

Figure 107. Chiller power comparison (June 9).

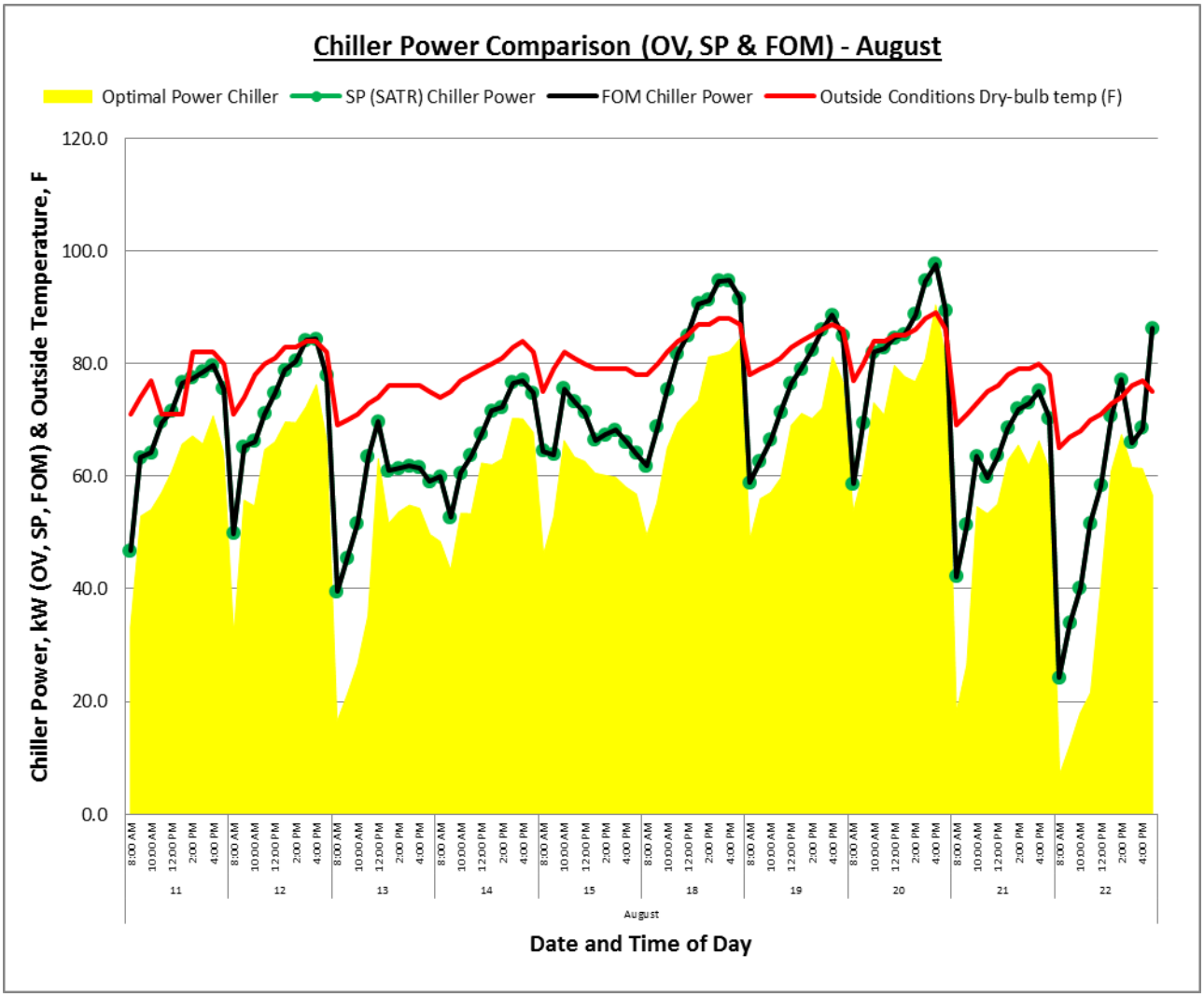

Figure 108. Chiller power comparison (August).

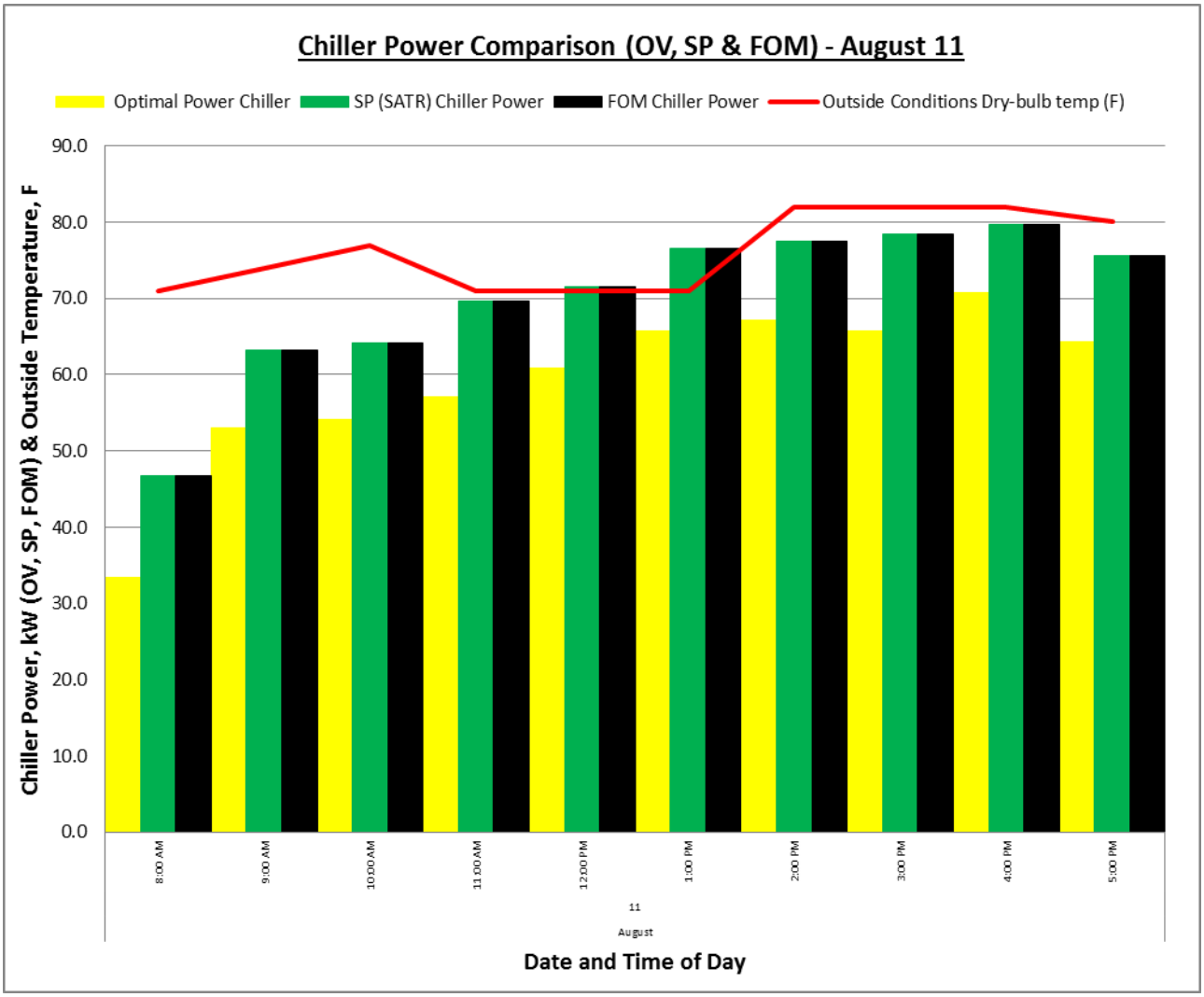

Figure 109. Chiller power comparison (August 11).

E.4 Optimal Chilled Water Temperature, T_w Graphs.

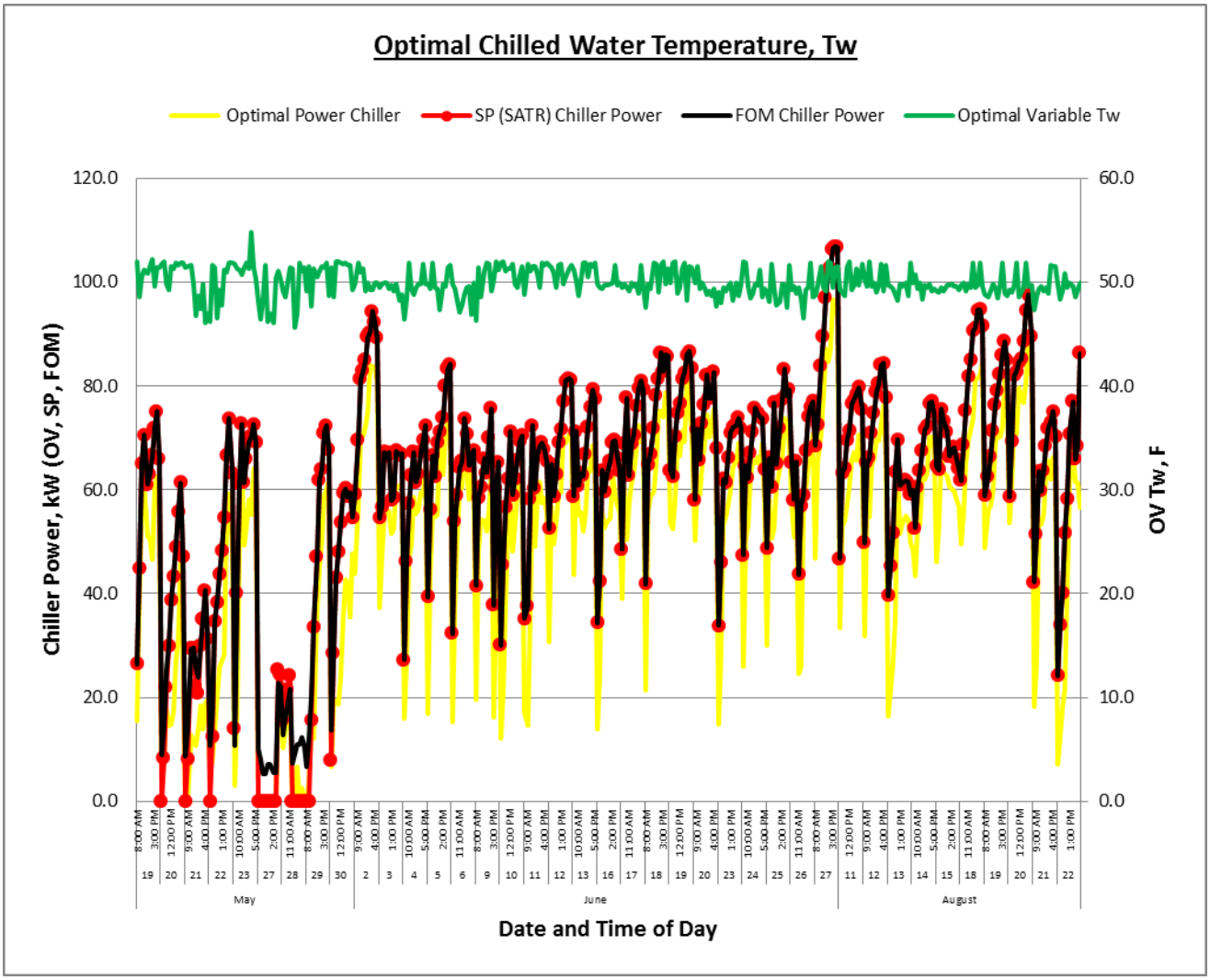

Figure 110. Optimal chilled water temperature T_w (May, June, August).

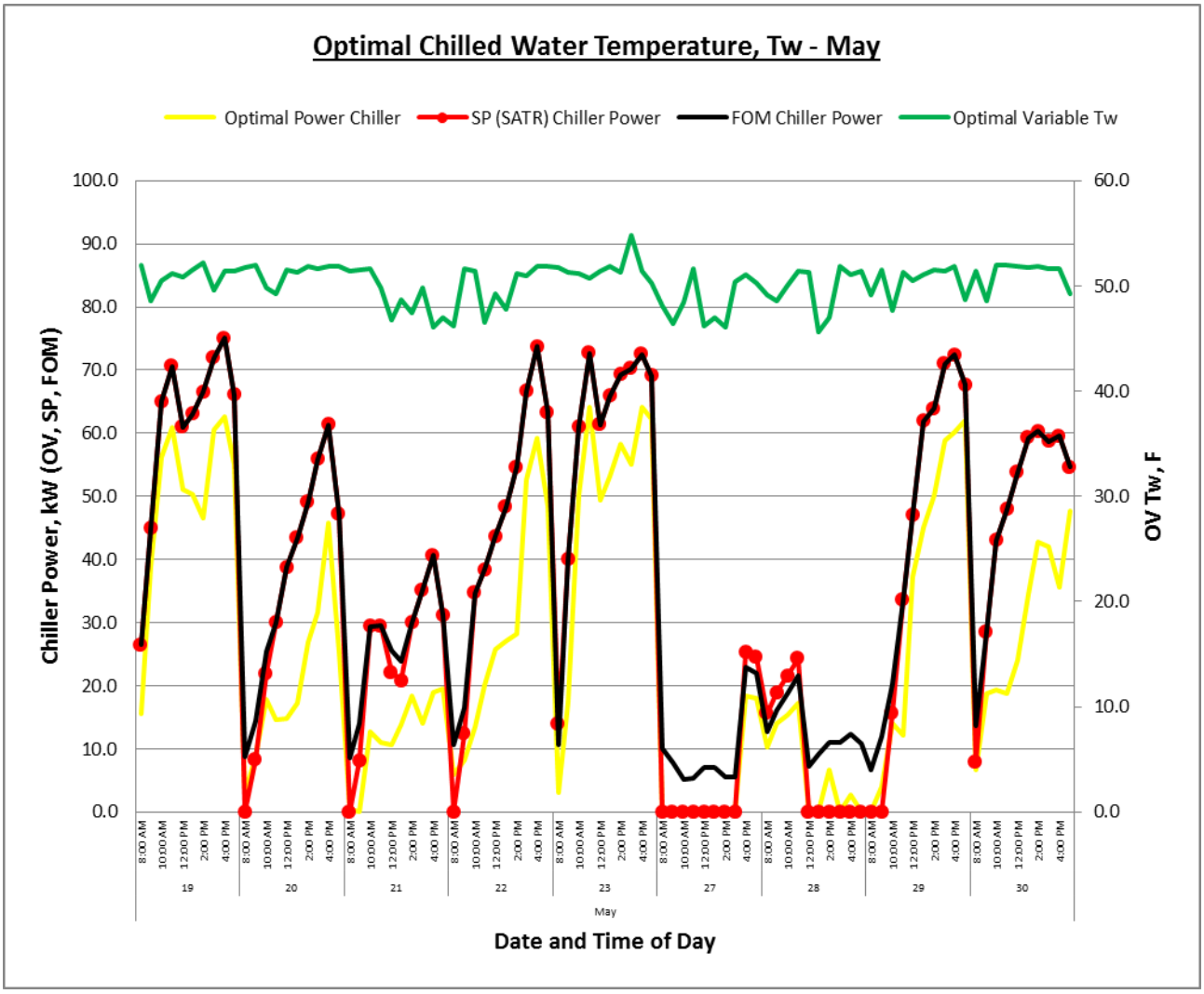

Figure 111. Optimal chilled water temperature T_w (May).

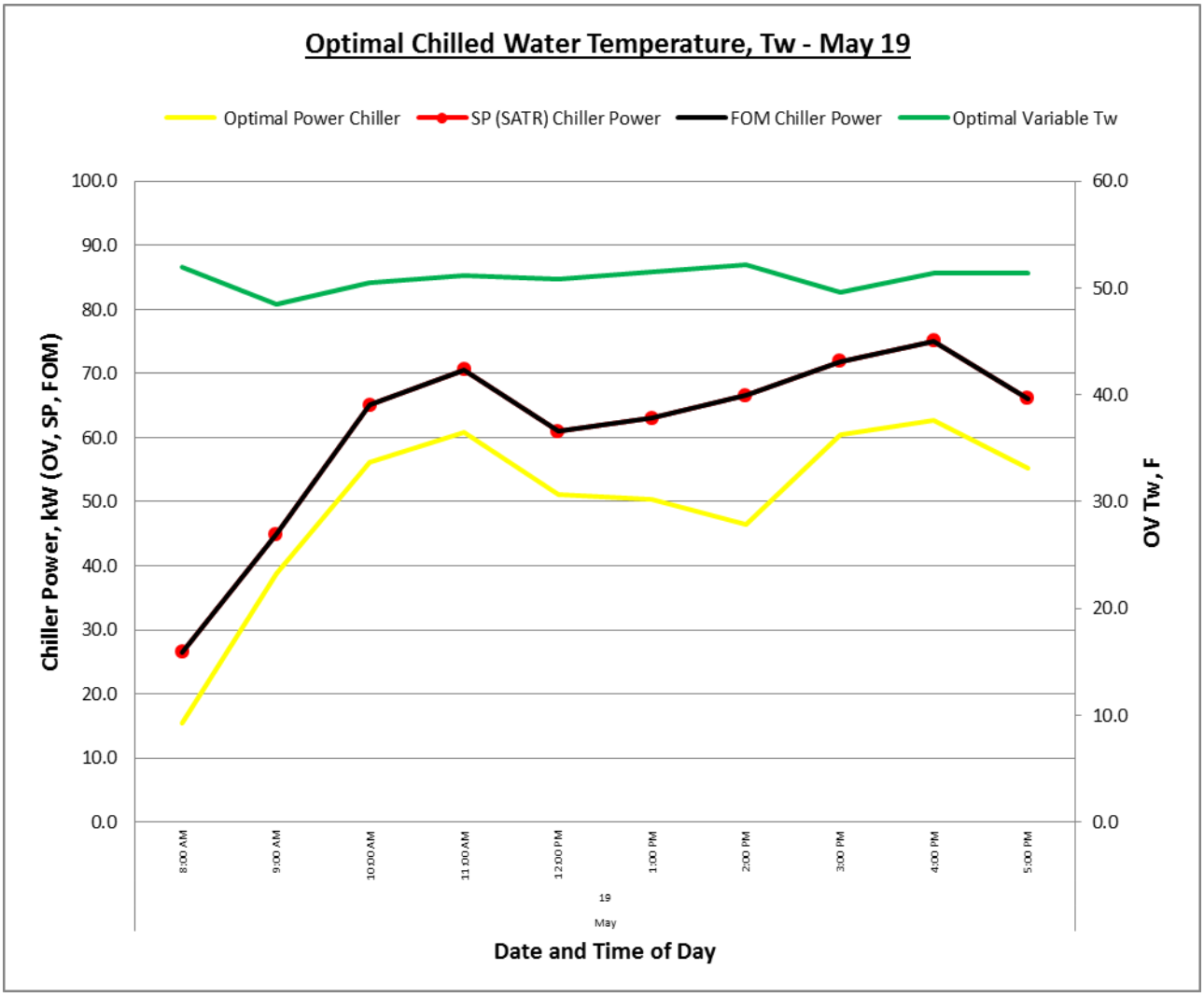

Figure 112. Optimal chilled water temperature T_w (May 19).

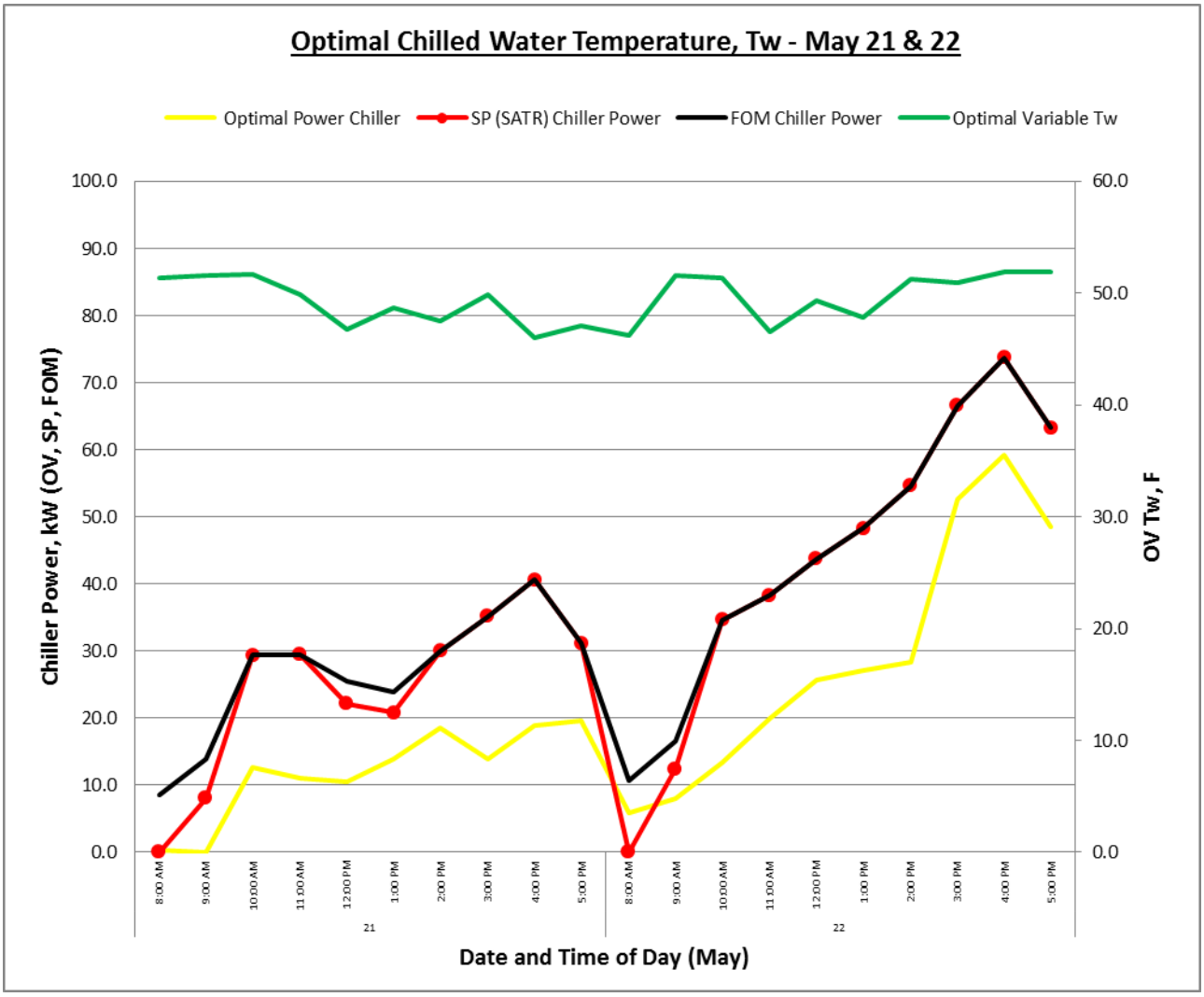

Figure 113. Optimal chilled water temperature T_w (May 21 & 22).

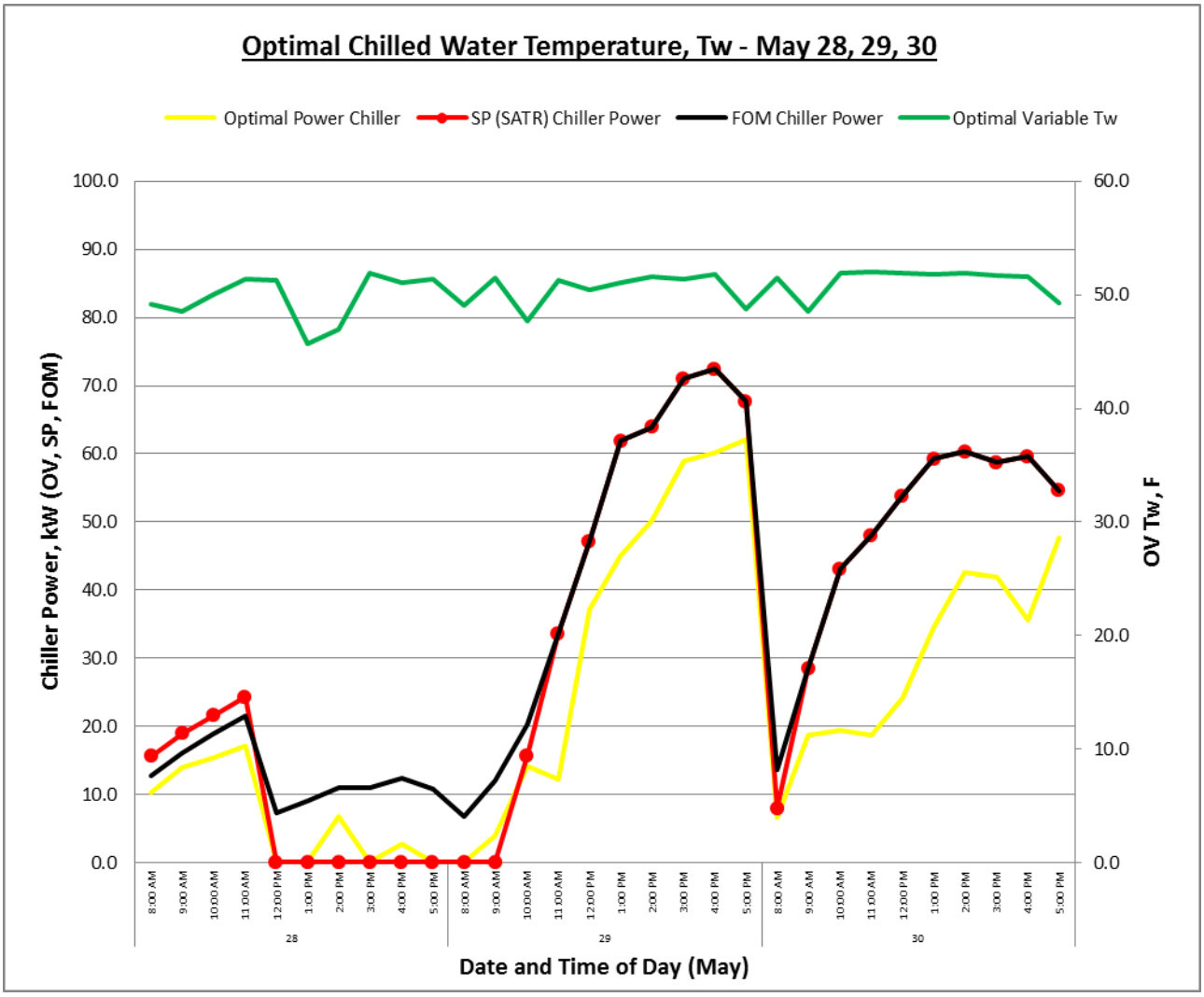

Figure 114. Optimal chilled water temperature T_w (May 28, 29, 30).

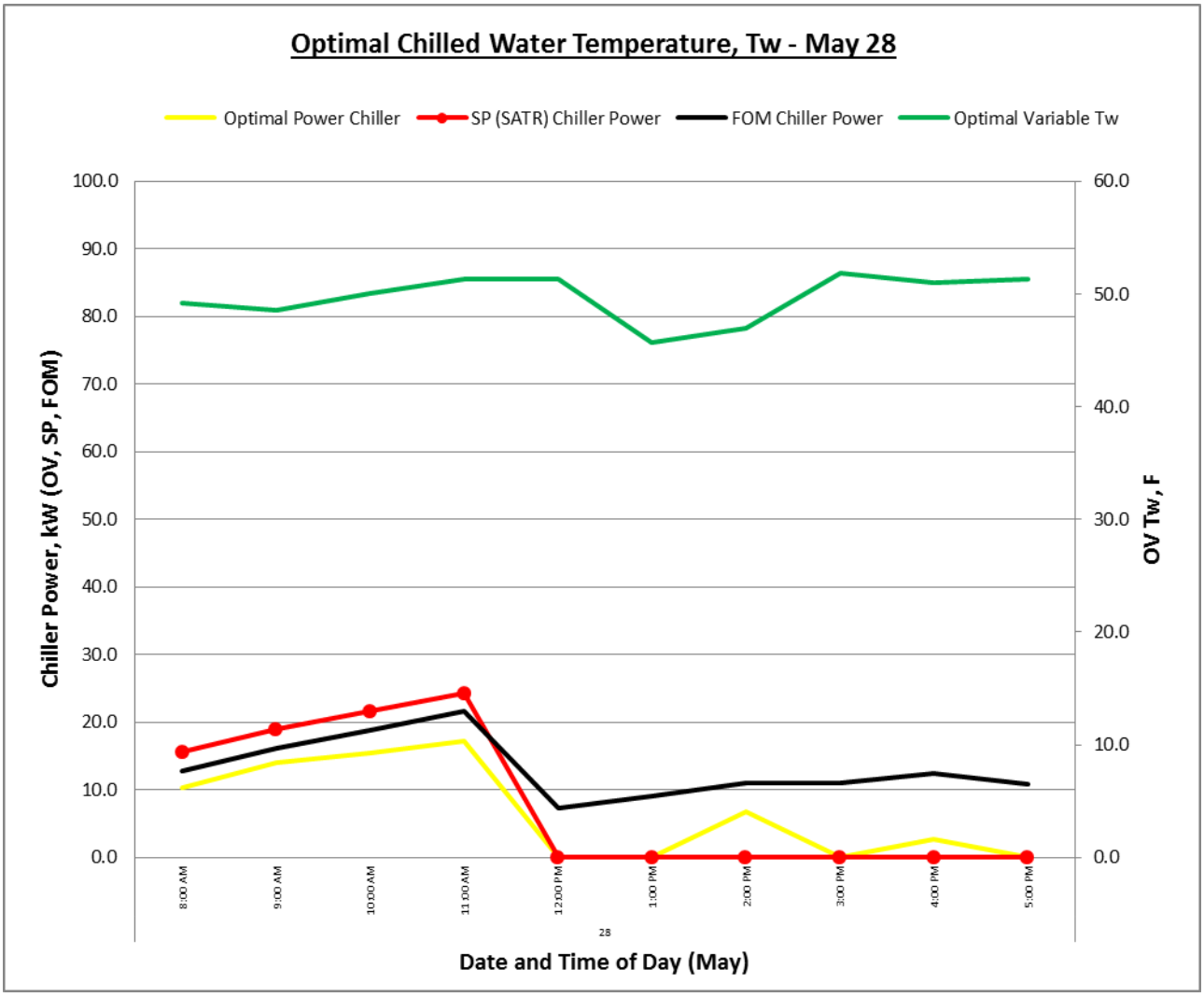

Figure 115. Optimal chilled water temperature T_w (May 28).

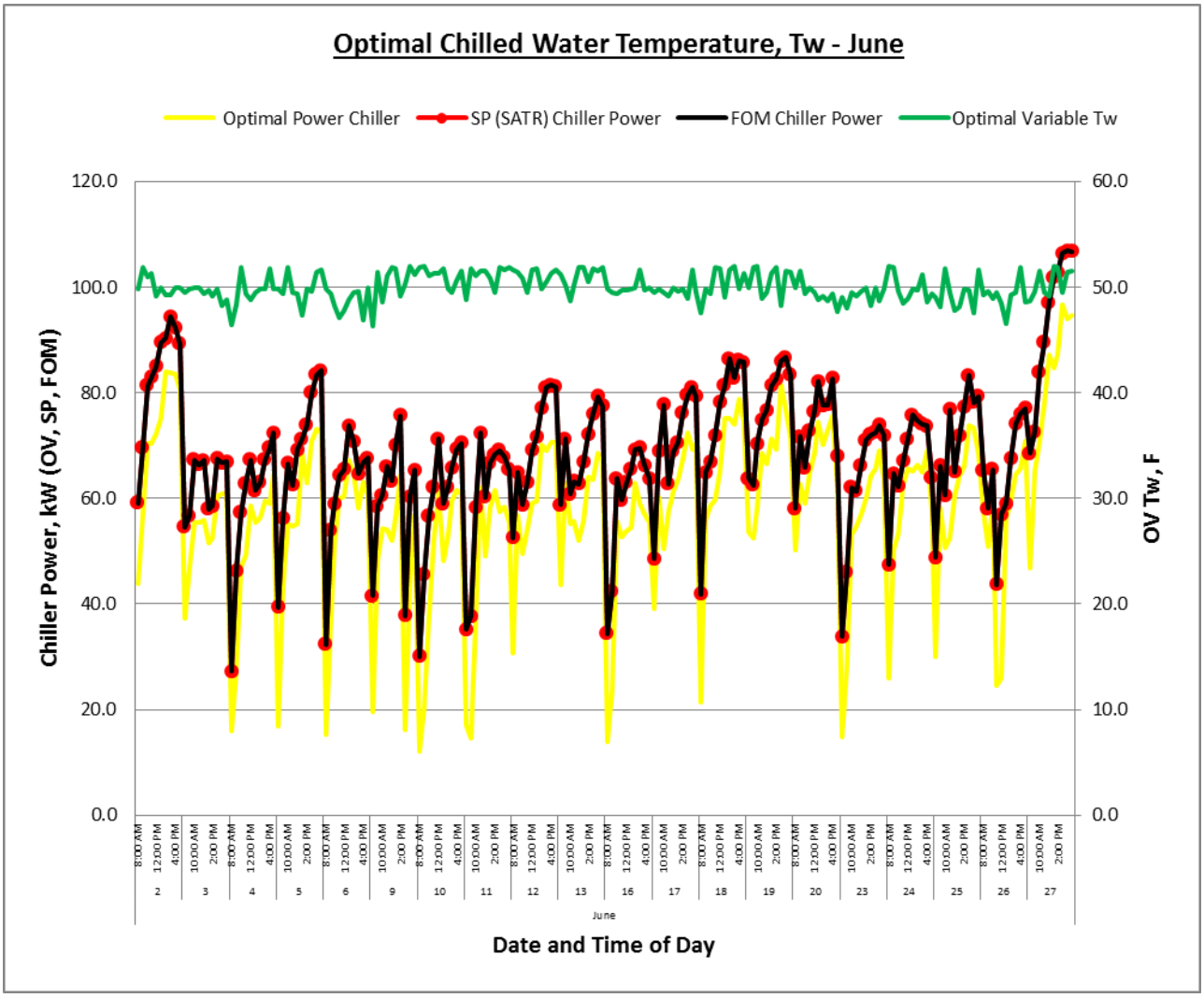

Figure 116. Optimal chilled water temperature T_w (June).

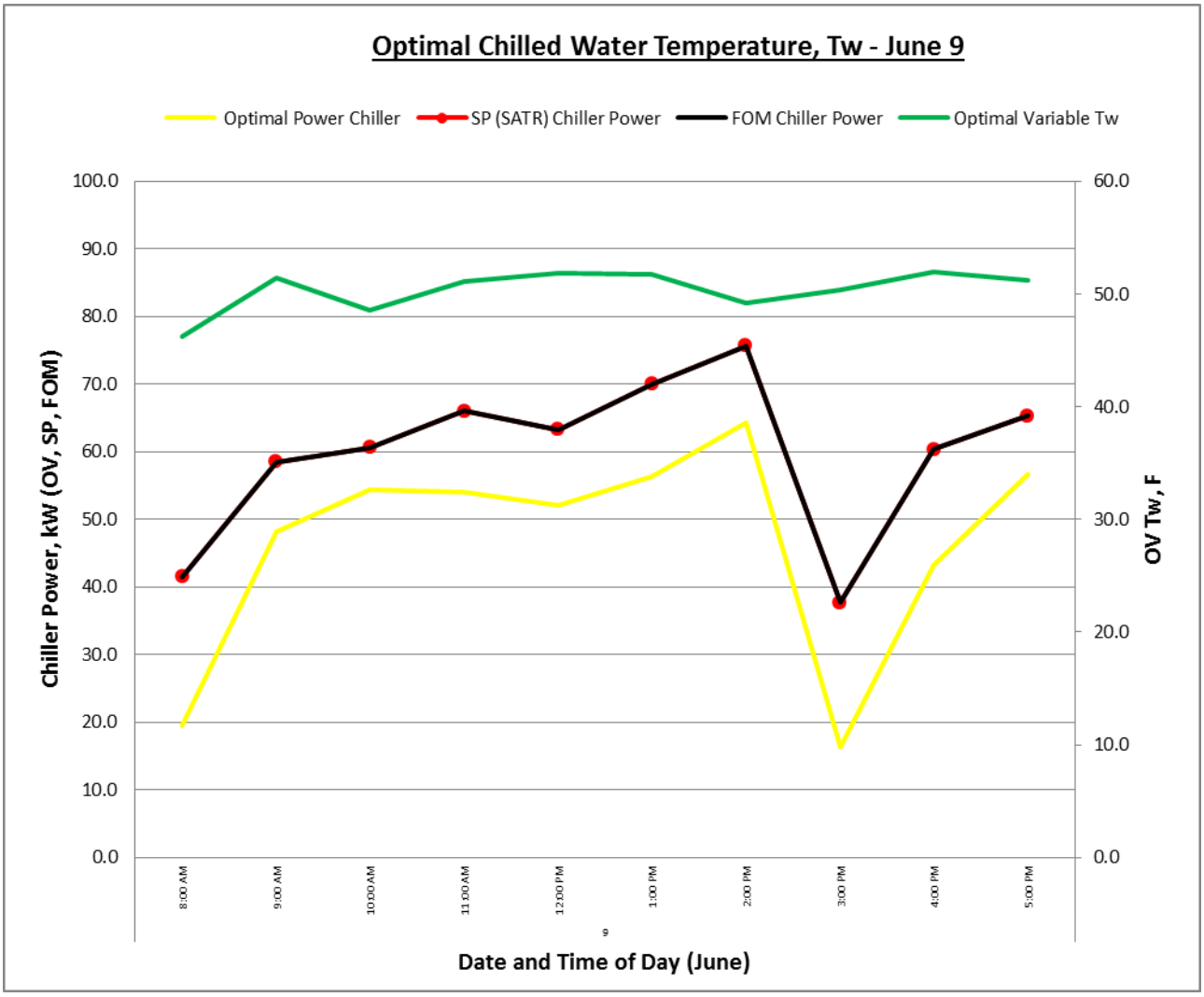

Figure 117. Optimal chilled water temperature T_w (June 9).

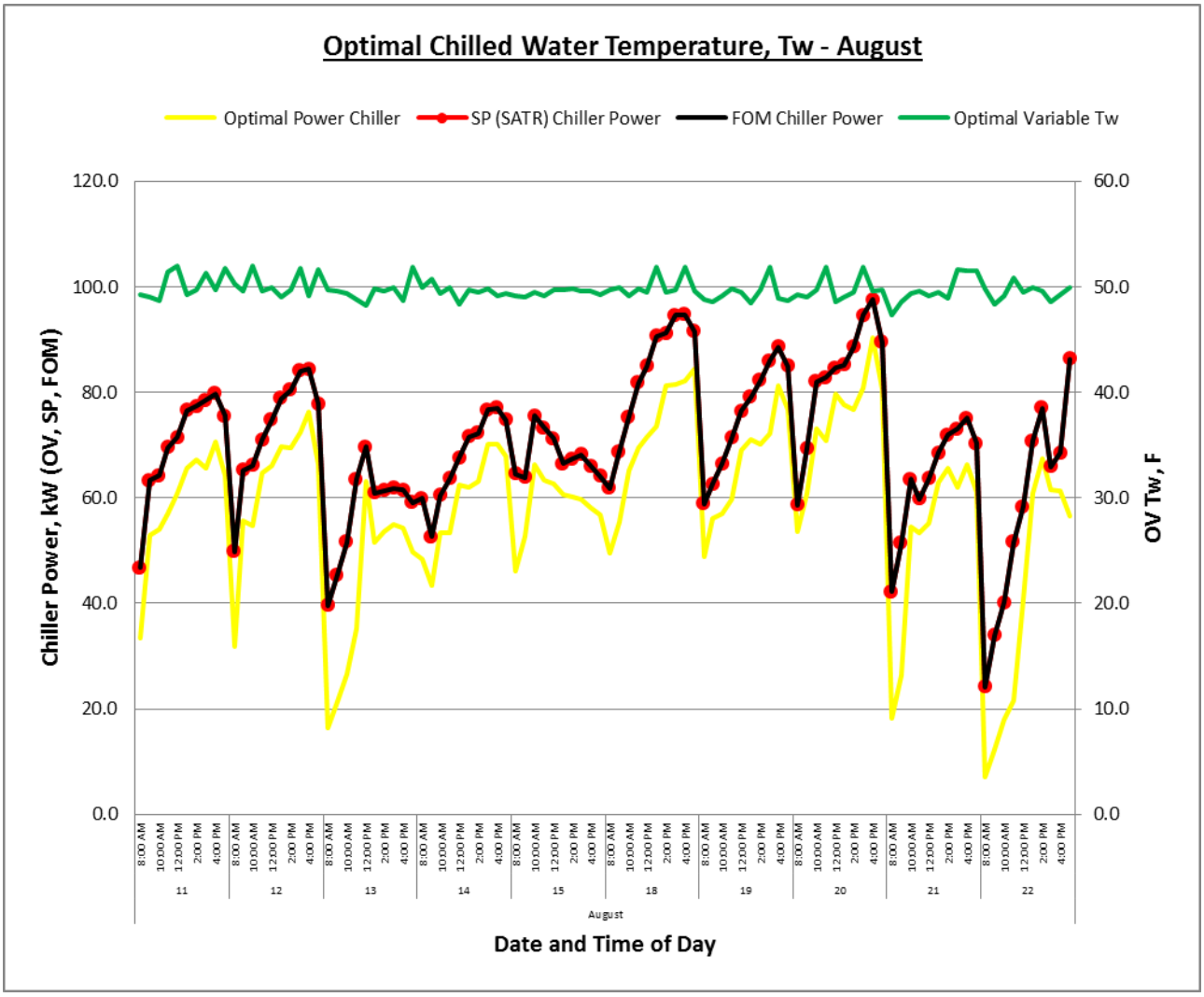

Figure 118. Optimal chilled water temperature T_w (August).

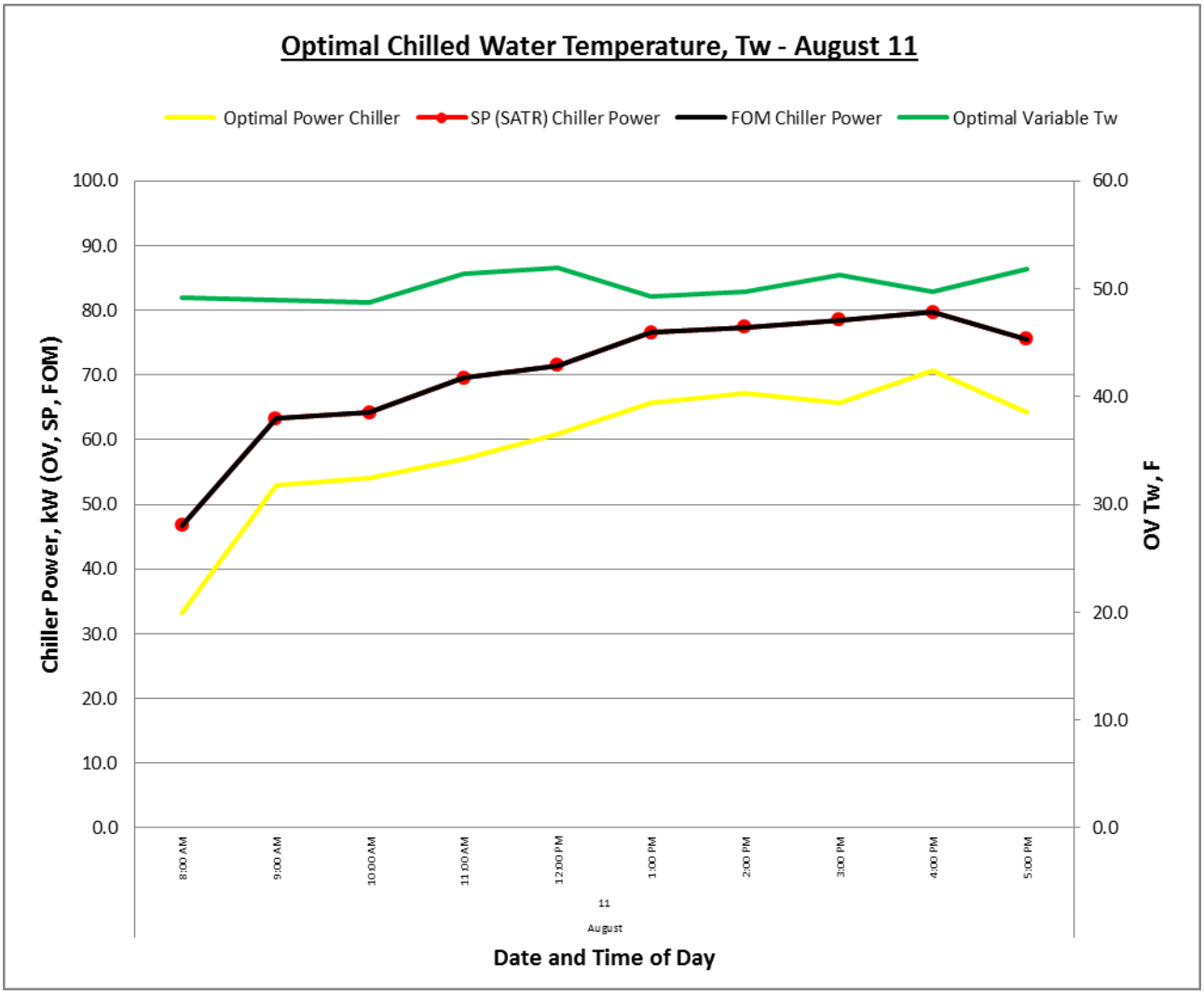

Figure 119. Optimal chilled water temperature T_w (August 11).

E.5 Optimal T_s with Fan and Chiller Power Graphs.

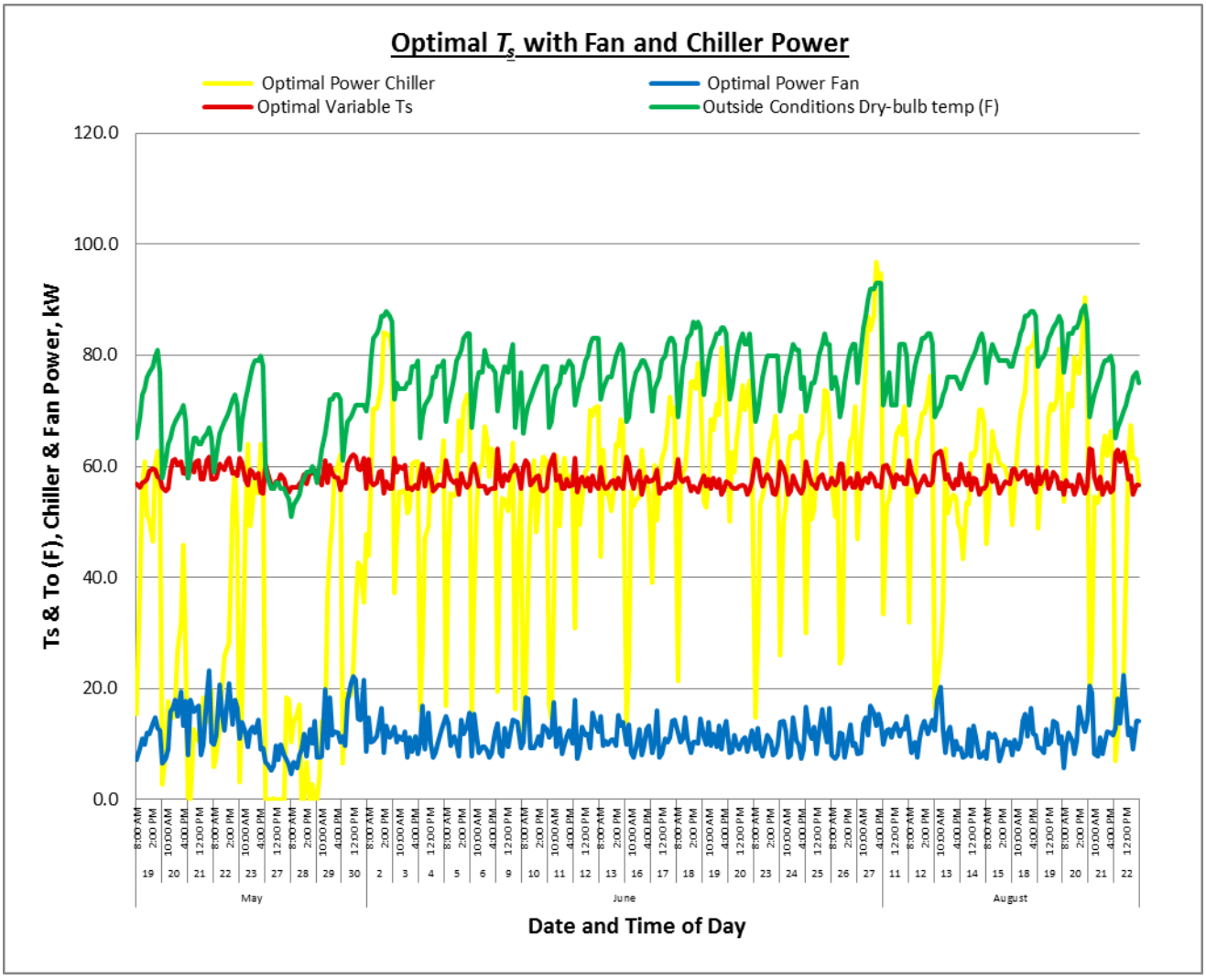

Figure 120. Optimal T_s with fan and chiller power (May, June, August).

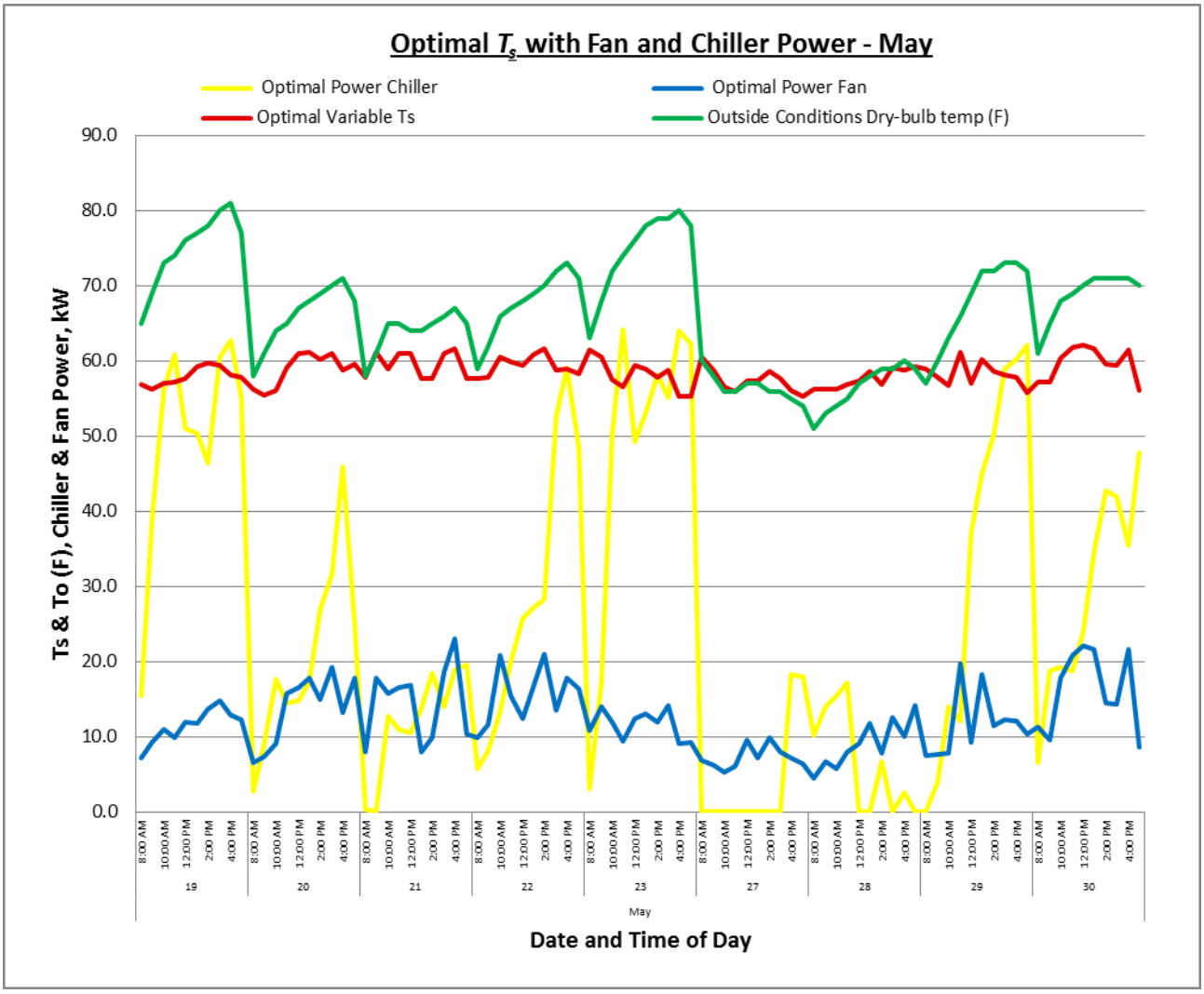

Figure 121. Optimal T_s with fan and chiller power (May).

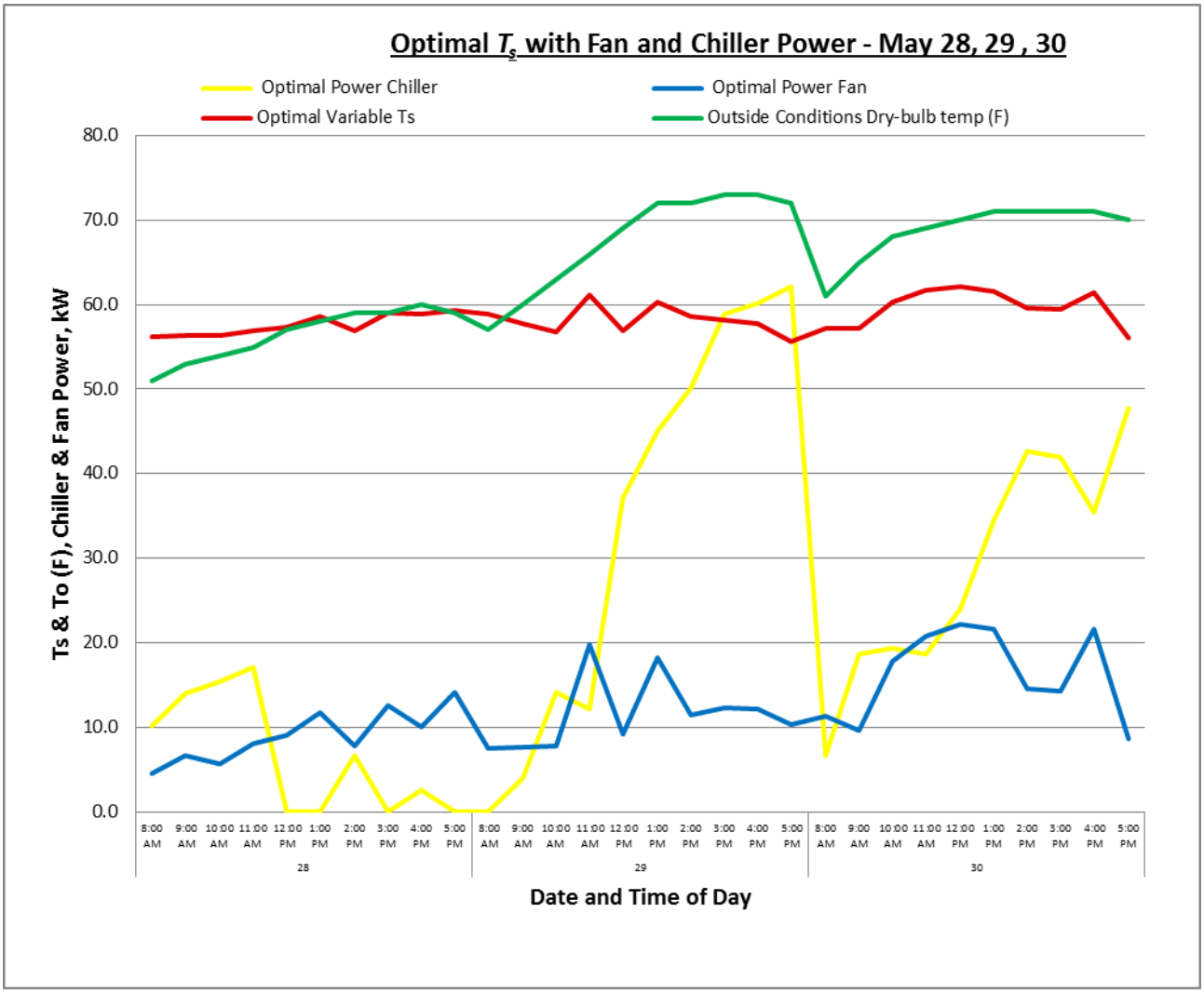

Figure 122. Optimal T_s with fan and chiller power (May 28, 29, 30).

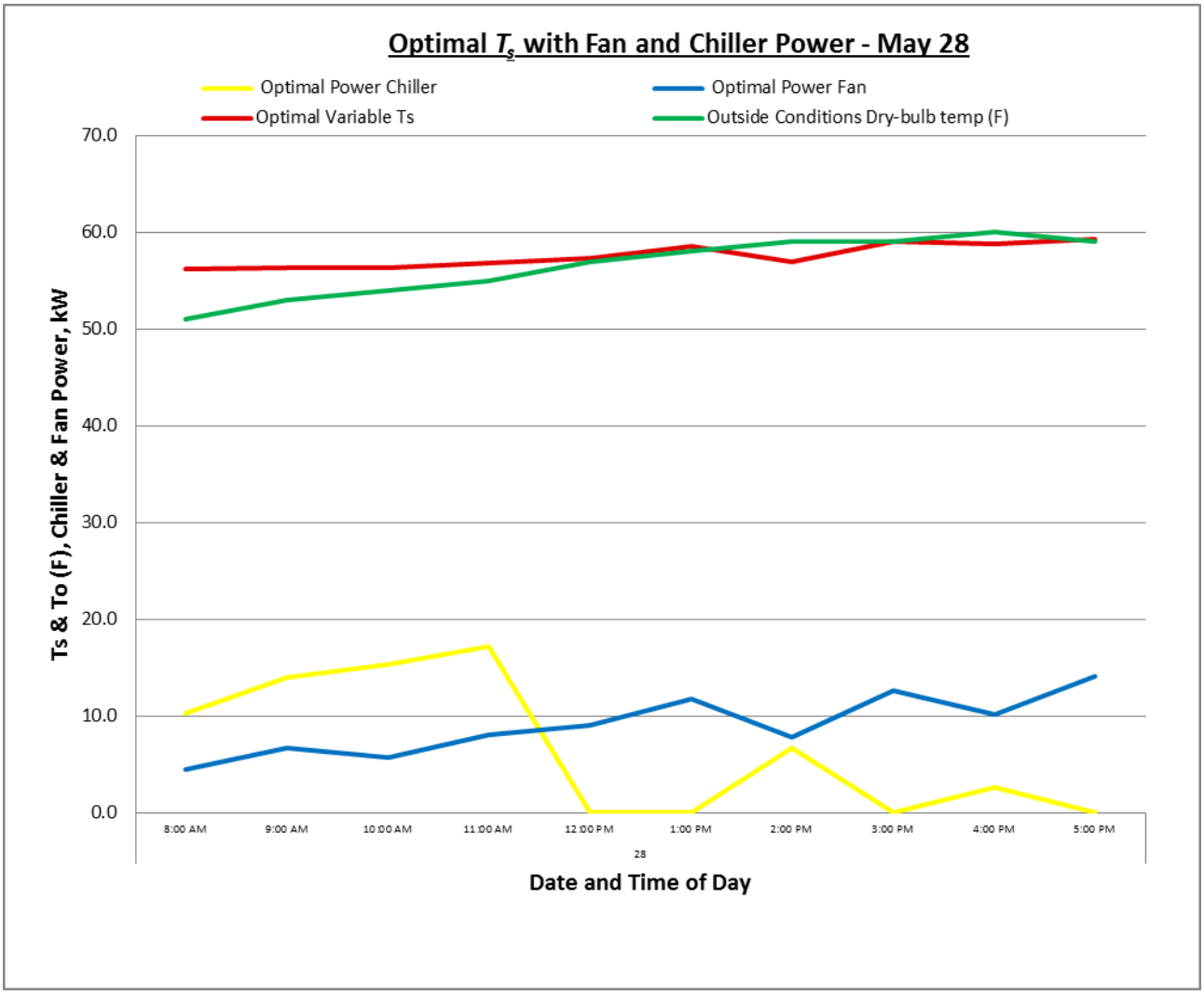

Figure 123. Optimal T_s with fan and chiller power (May 28).

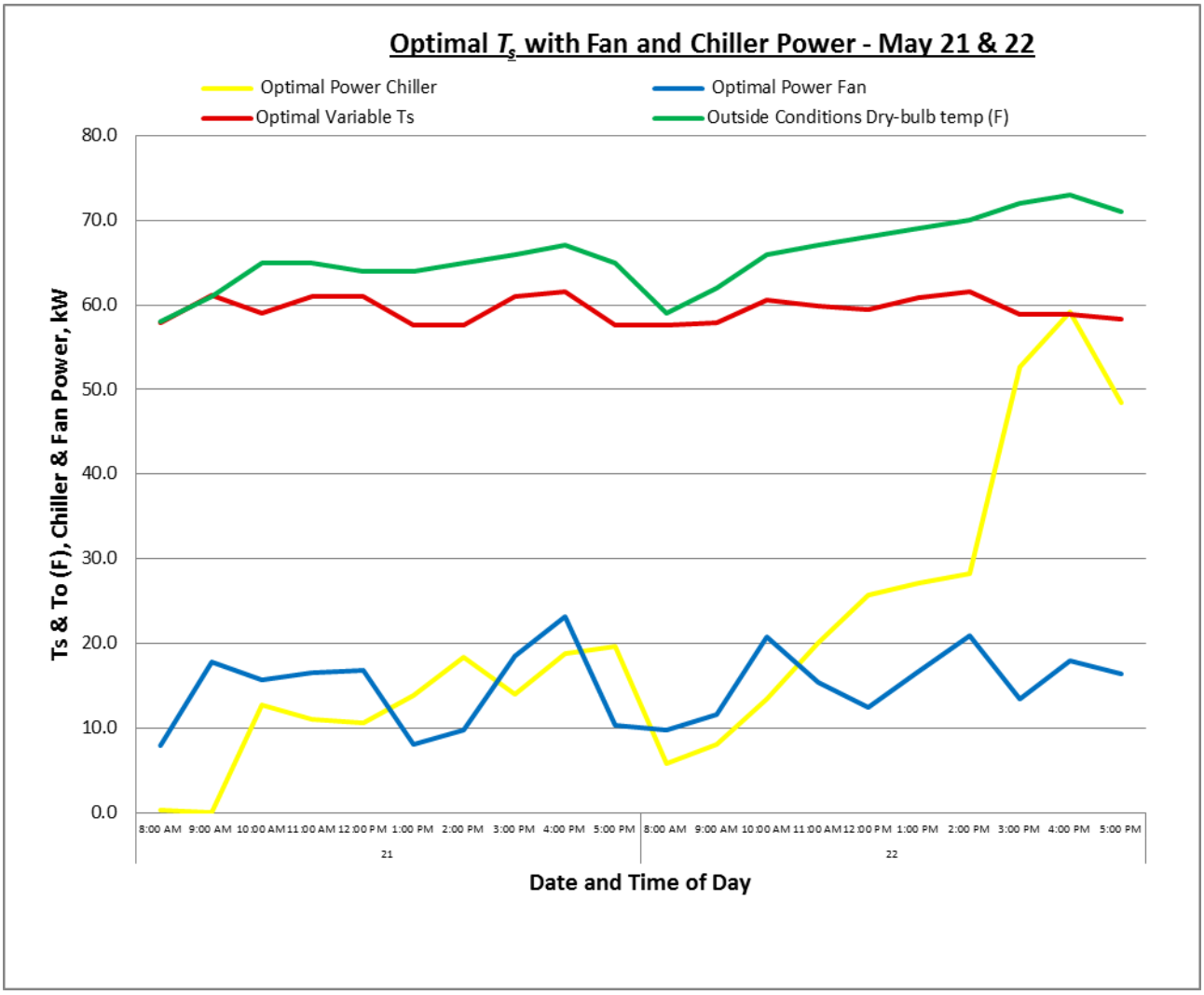

Figure 124. Optimal T_s with fan and chiller power (May 21 & 22).

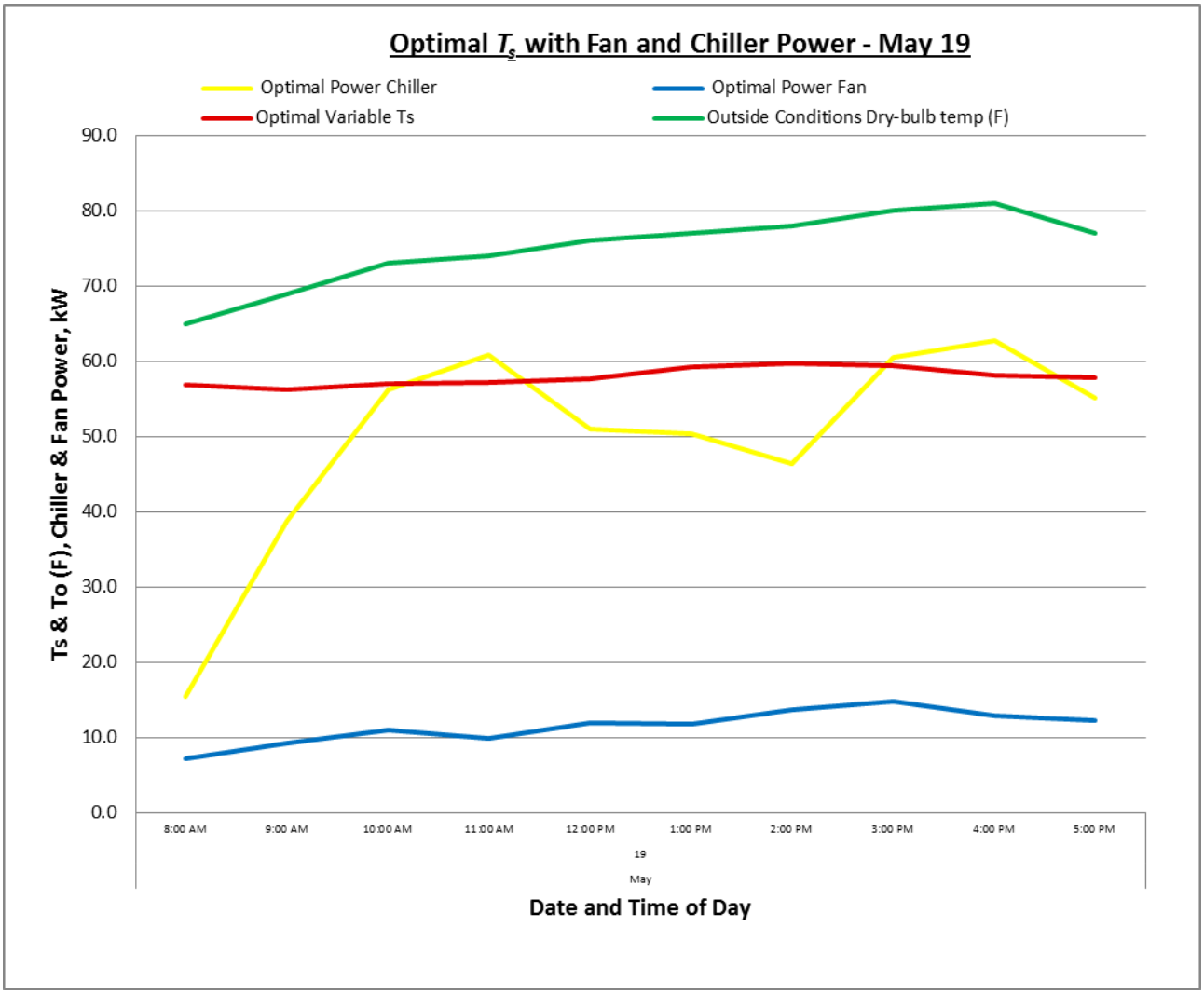

Figure 125. Optimal T_s with fan and chiller power (May 19).

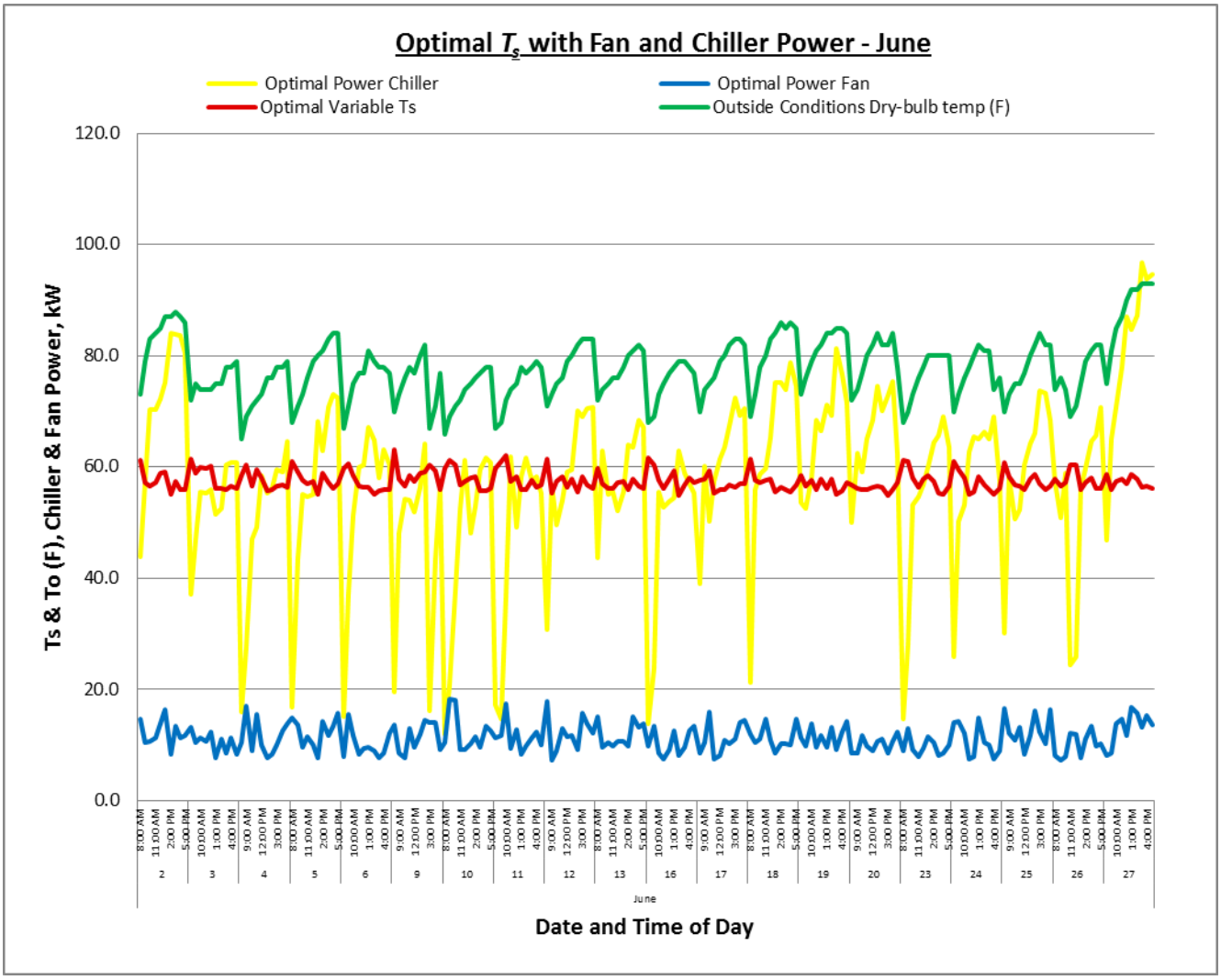

Figure 126. Optimal T_s with fan and chiller power (June).

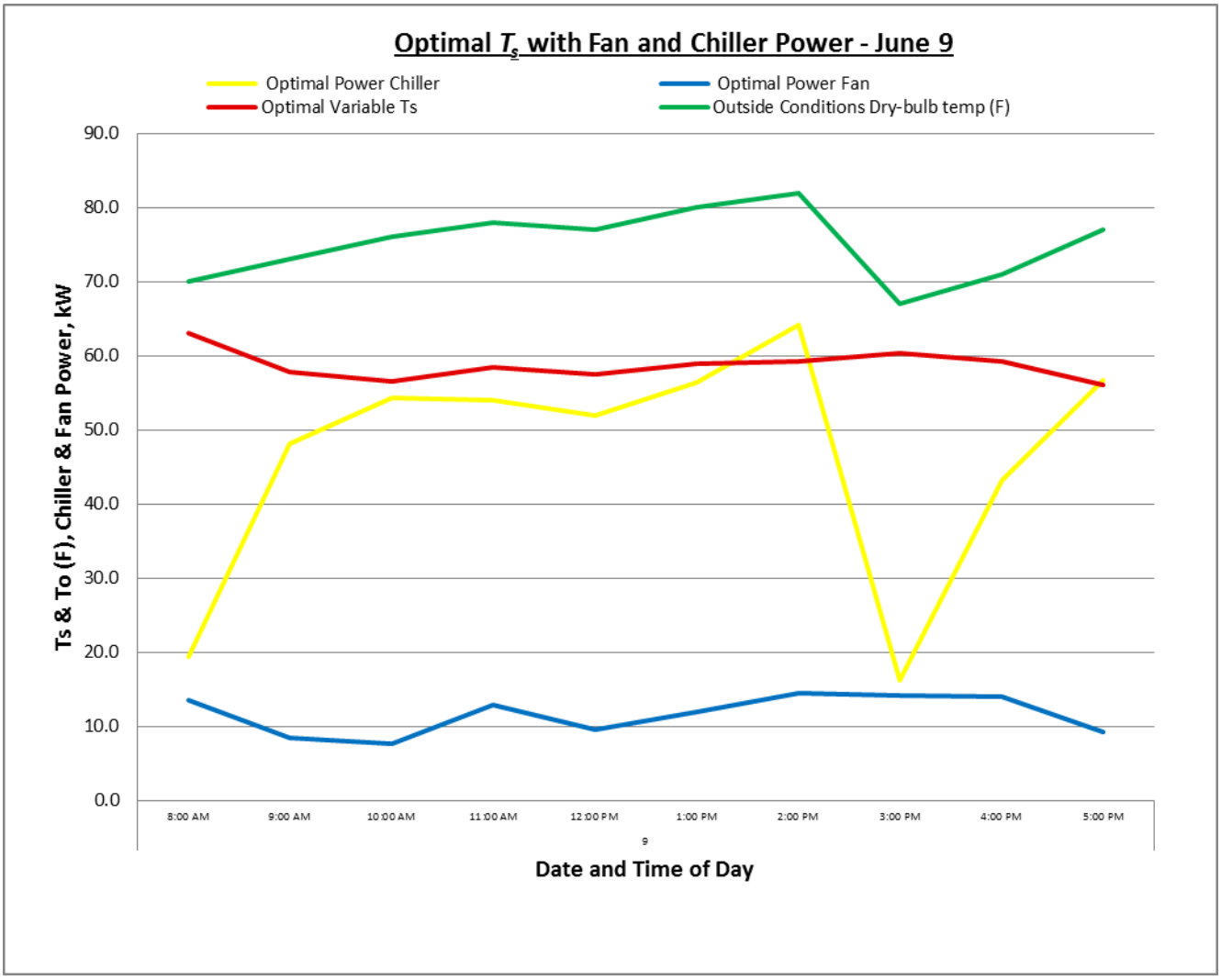

Figure 127. Optimal T_s with fan and chiller power (June 9).

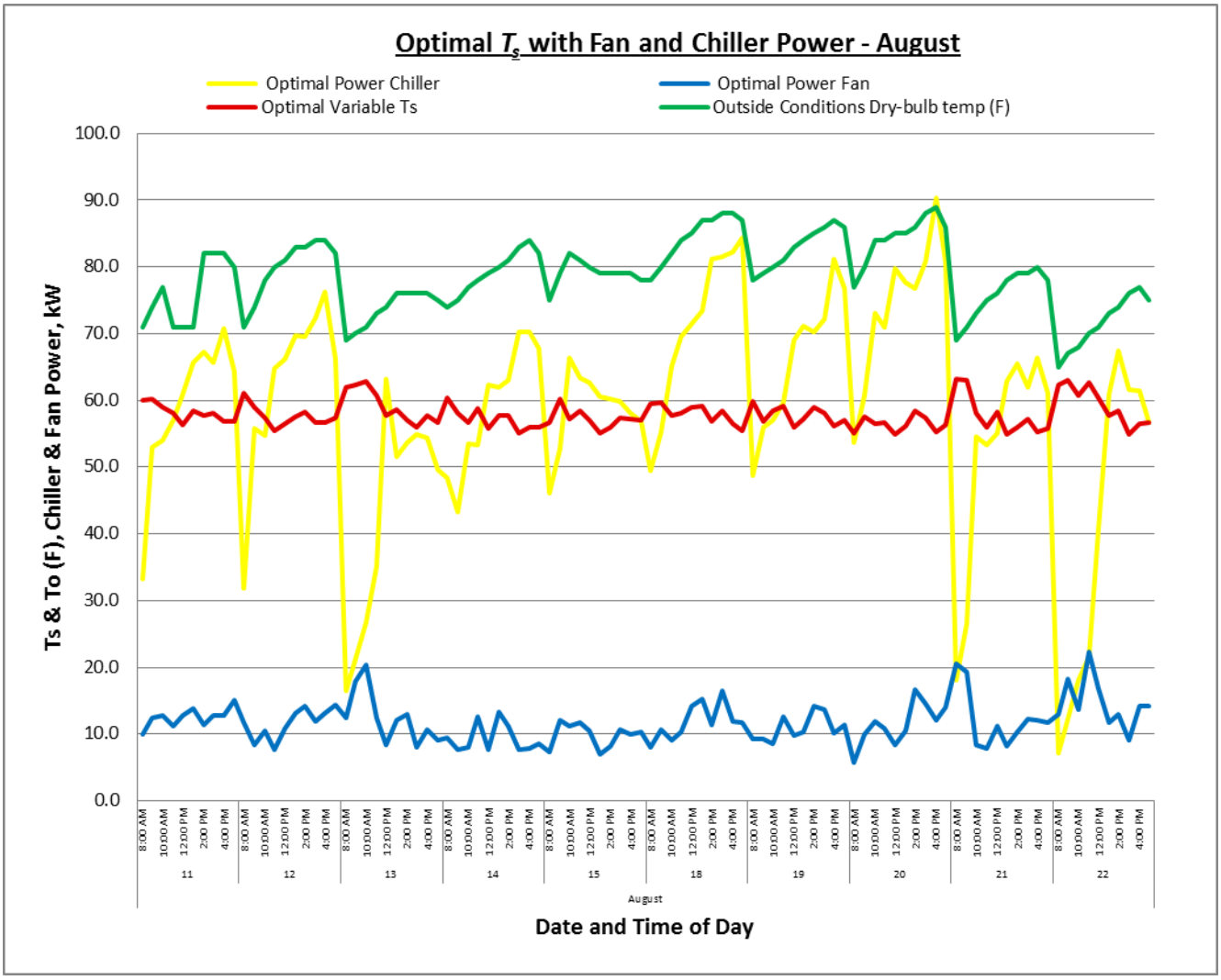

Figure 128. Optimal T_s with fan and chiller power (August).

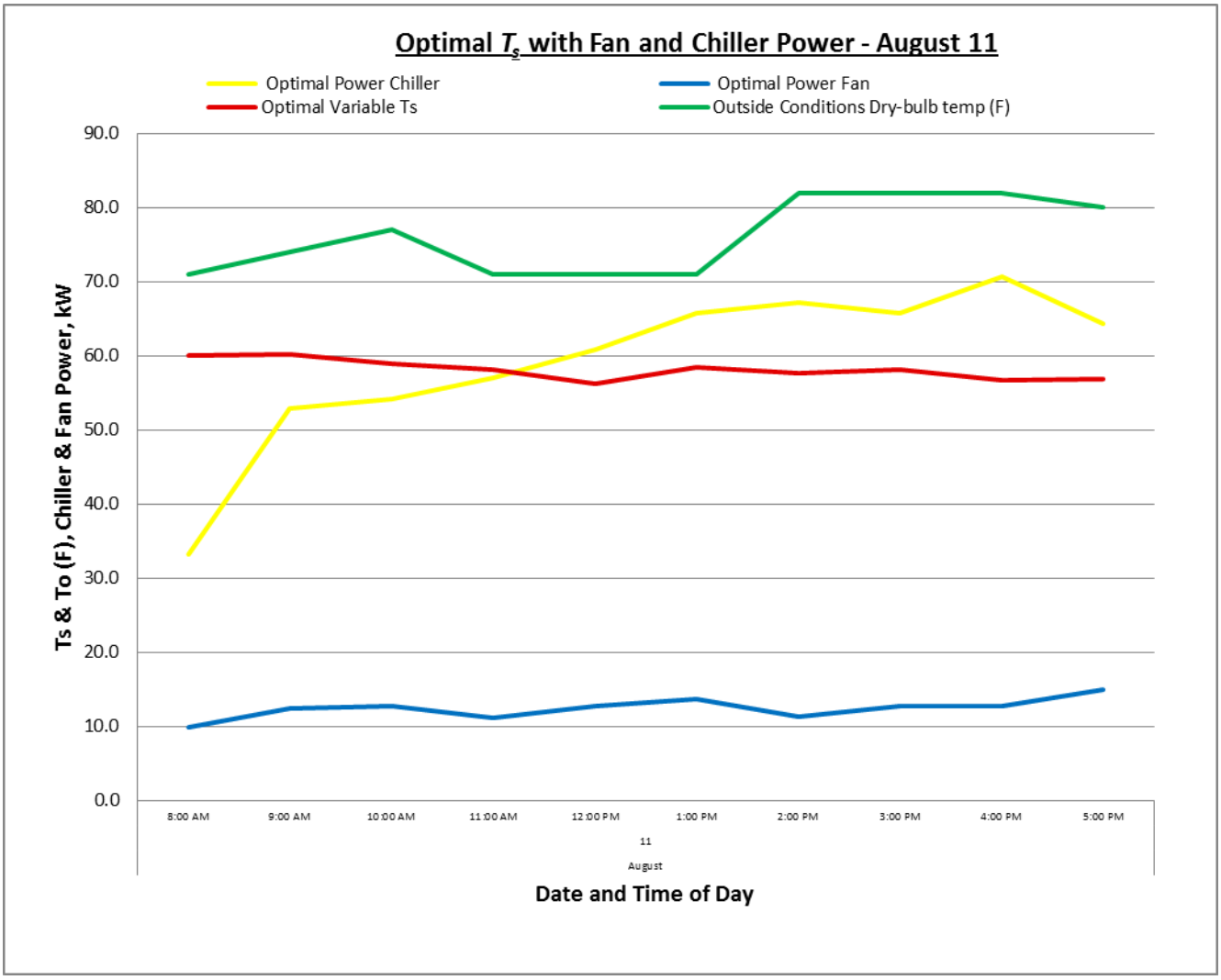

Figure 129. Optimal T_s with fan and chiller power (August 11).

E.6 Fan Power Comparison (OV, SP & FOM) Graphs.

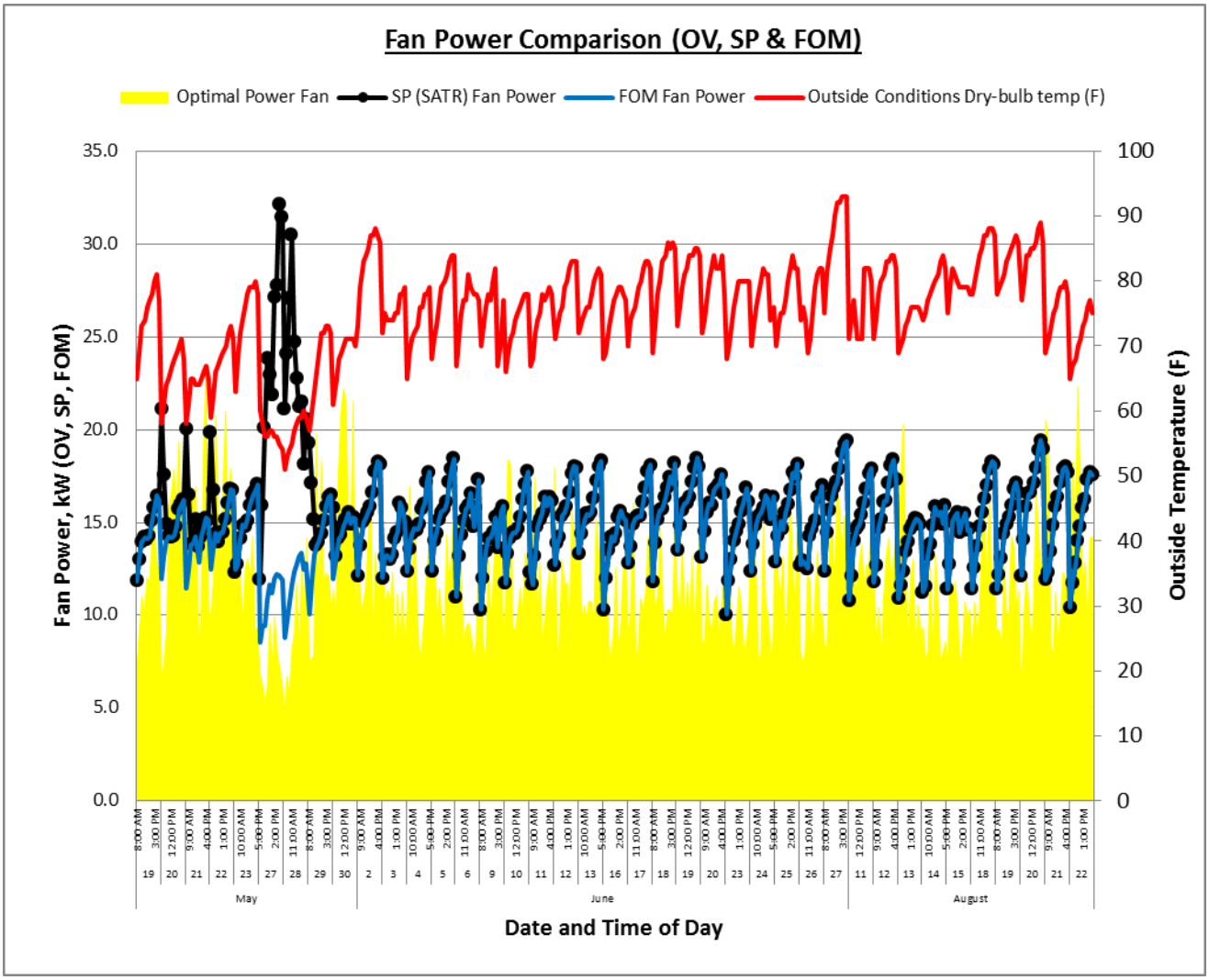

Figure 130. Fan power comparison (May, June, August).

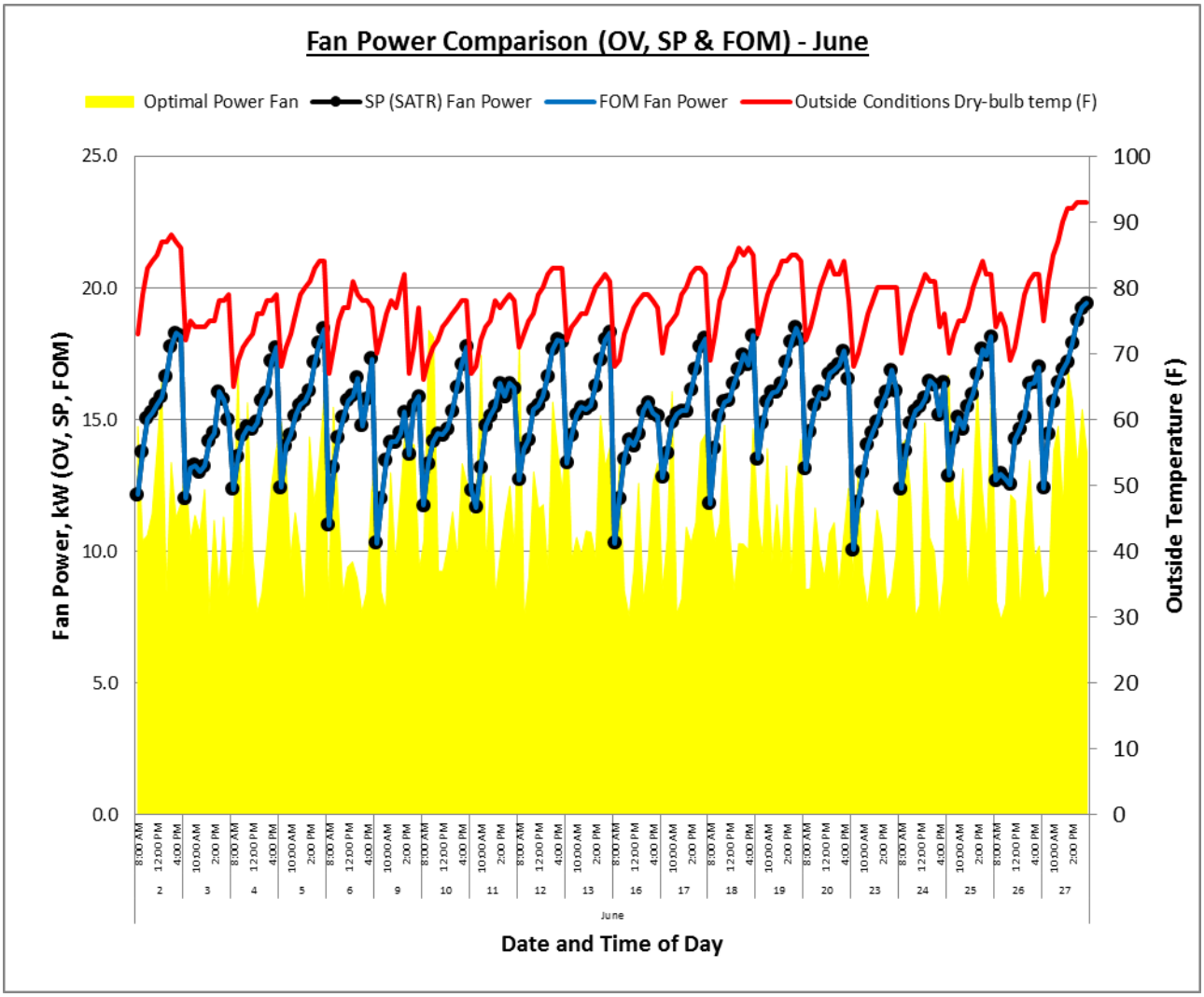

Figure 131. Fan power comparison (June).

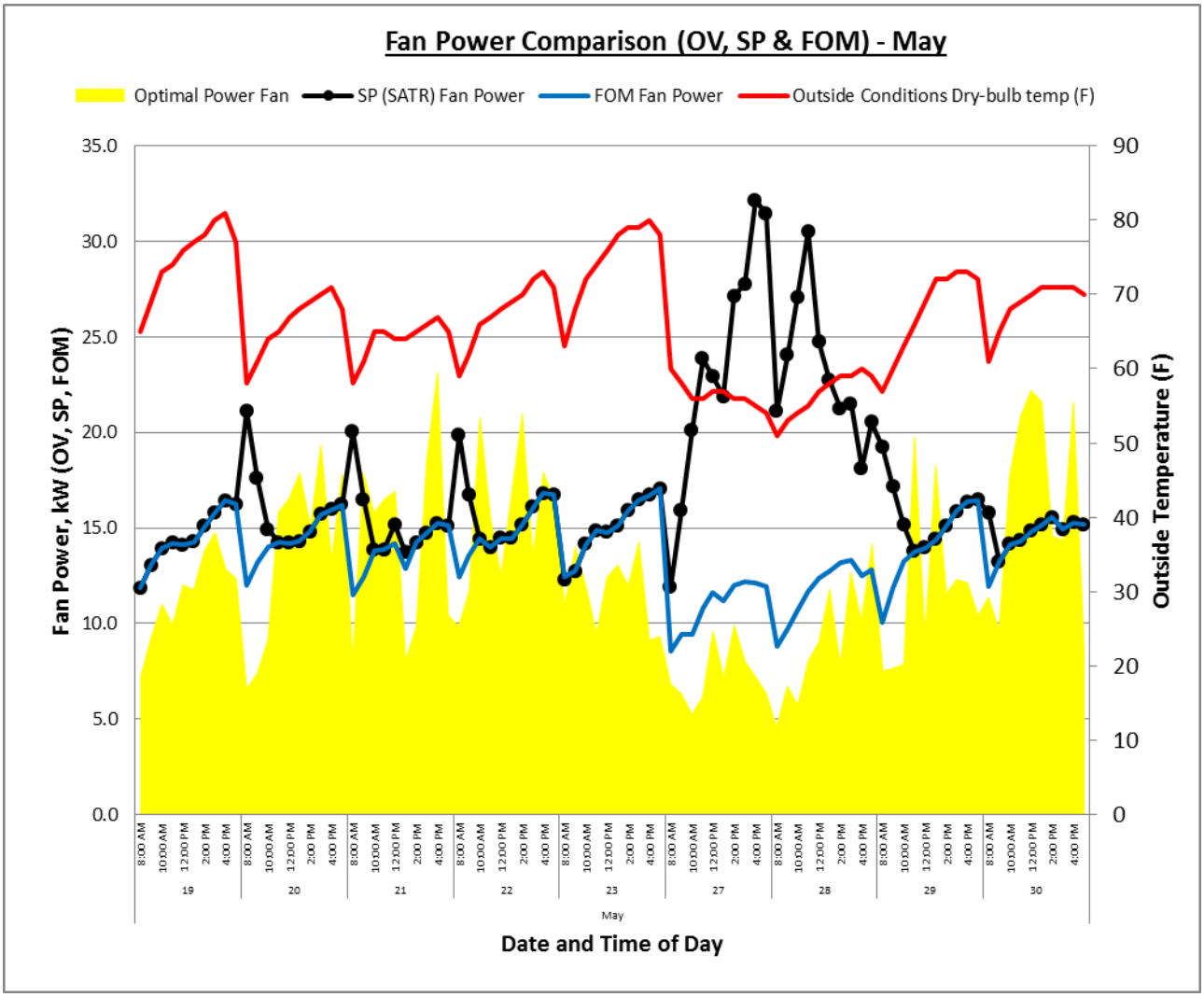

Figure 132. Fan power comparison (May).

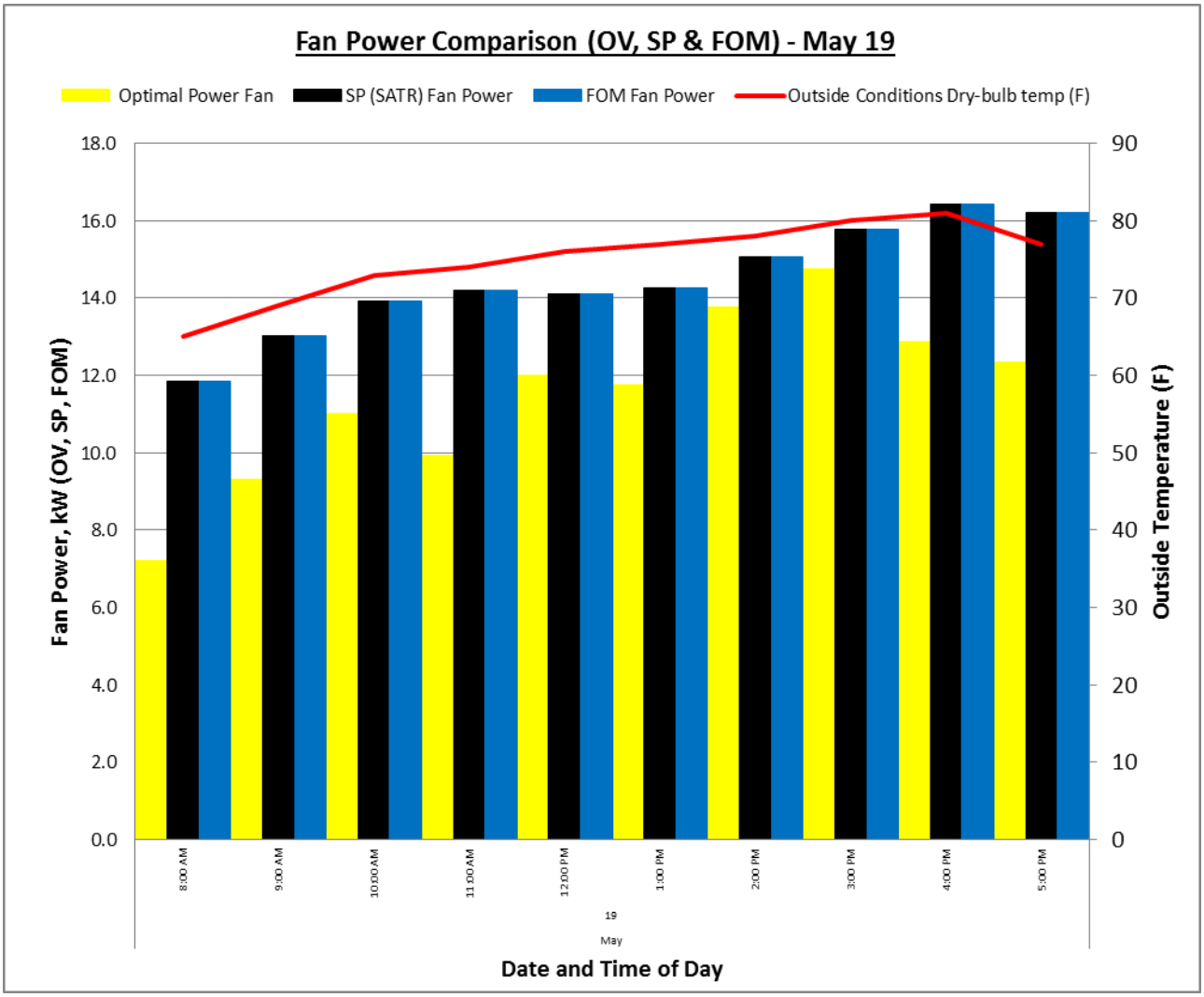

Figure 133. Fan power comparison (May 19).

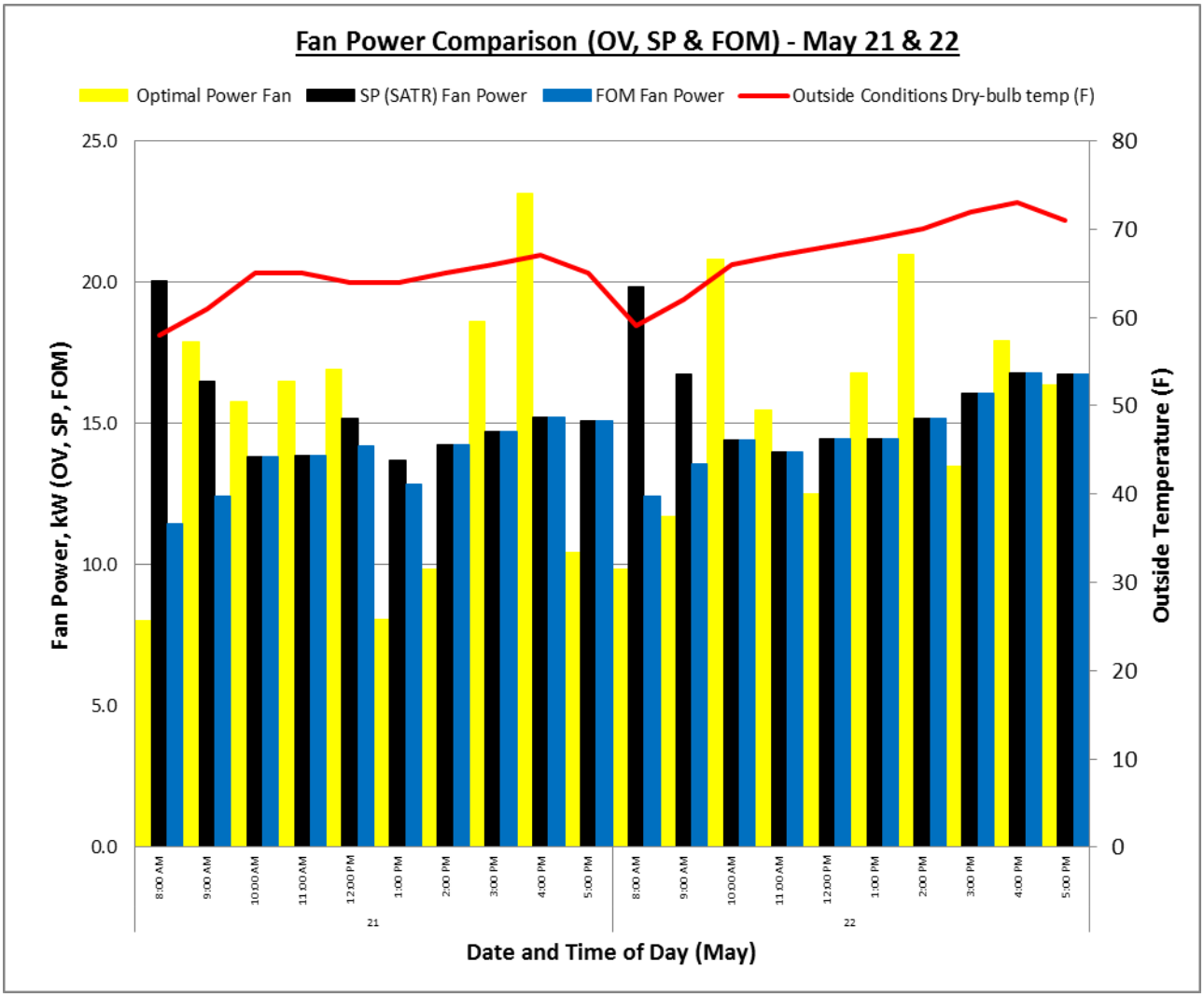

Figure 134. Fan power comparison (May 21 & 22).

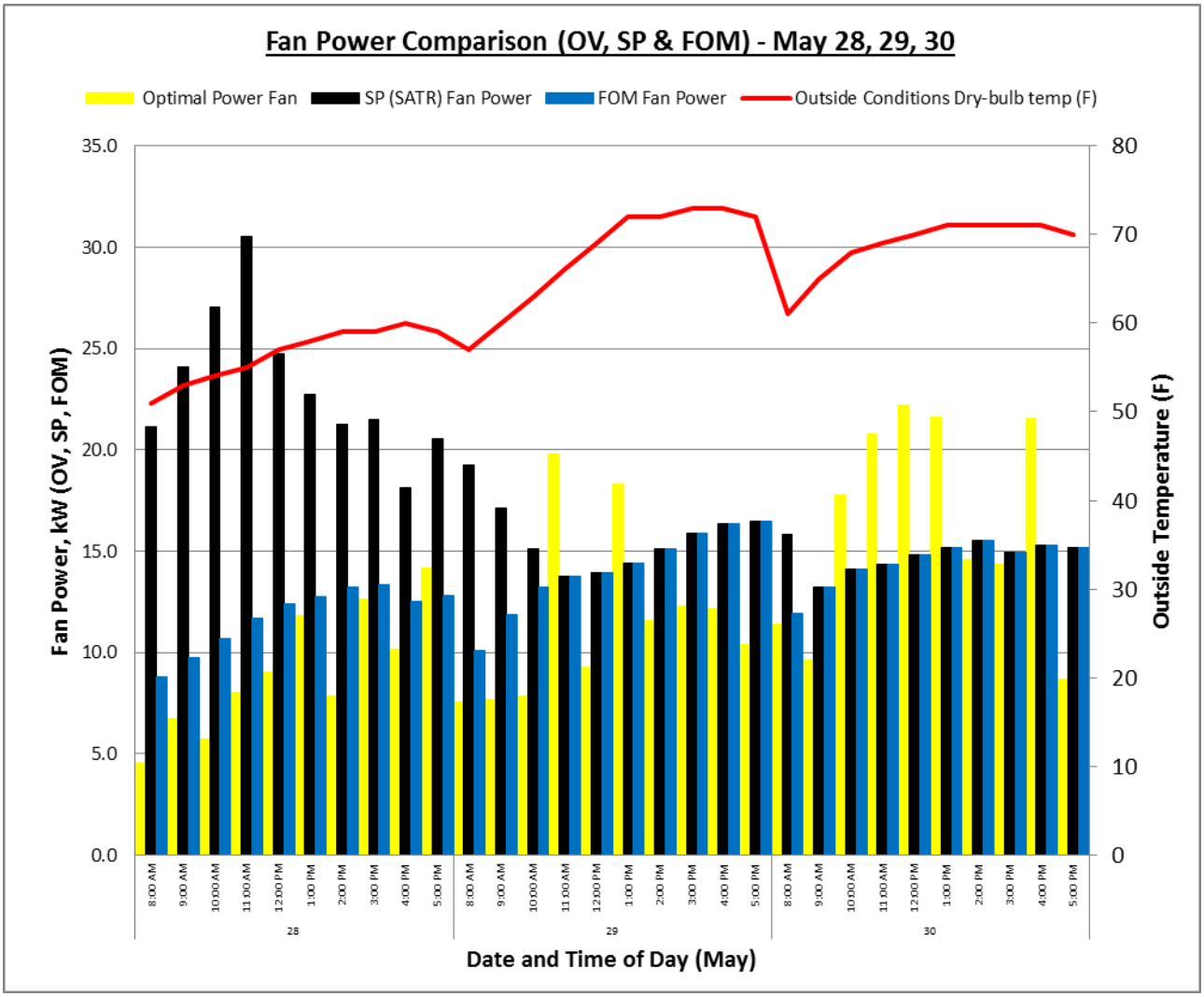

Figure 135. Fan power comparison (May 28, 29, 30).

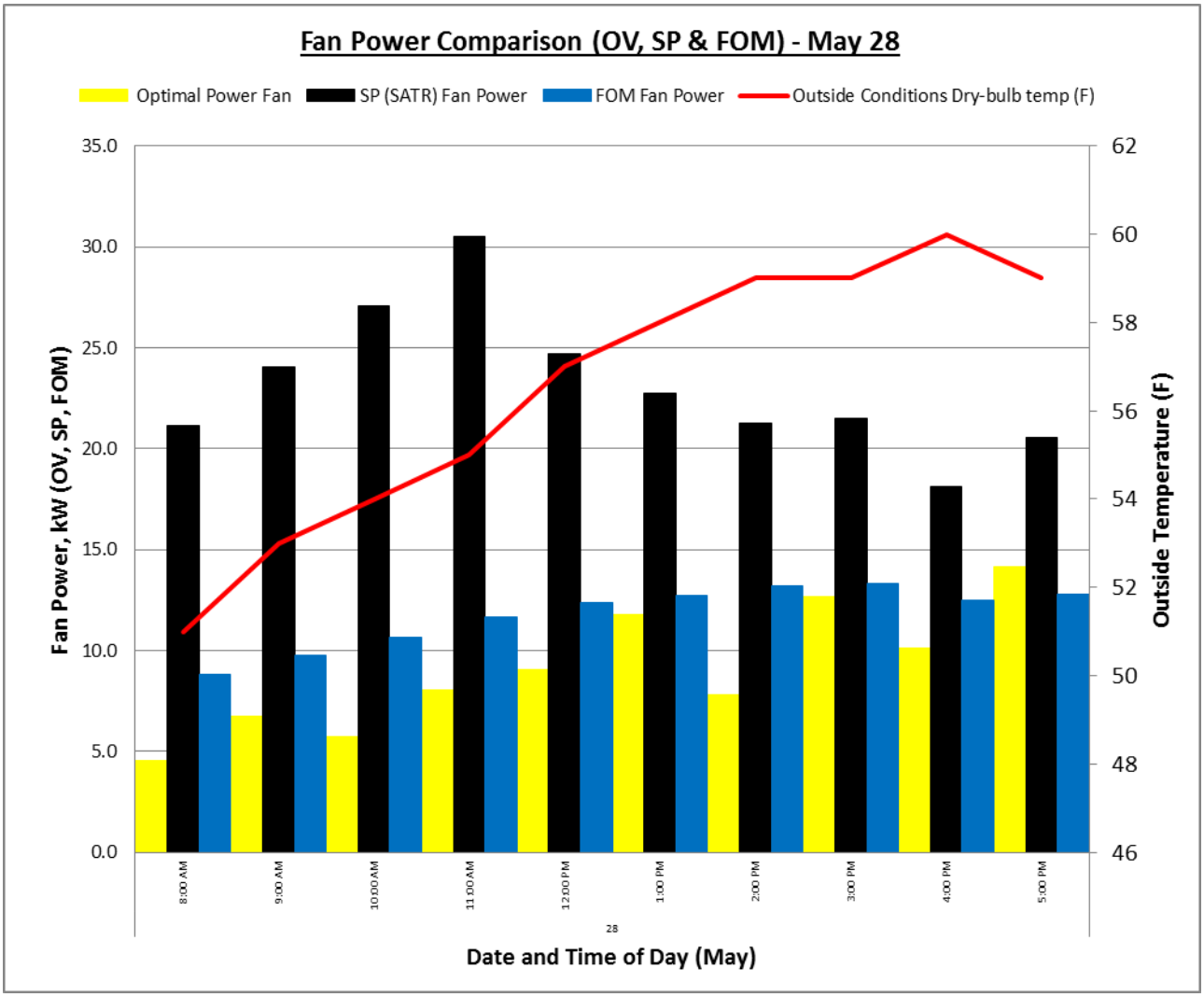

Figure 136. Fan power comparison (May 28).

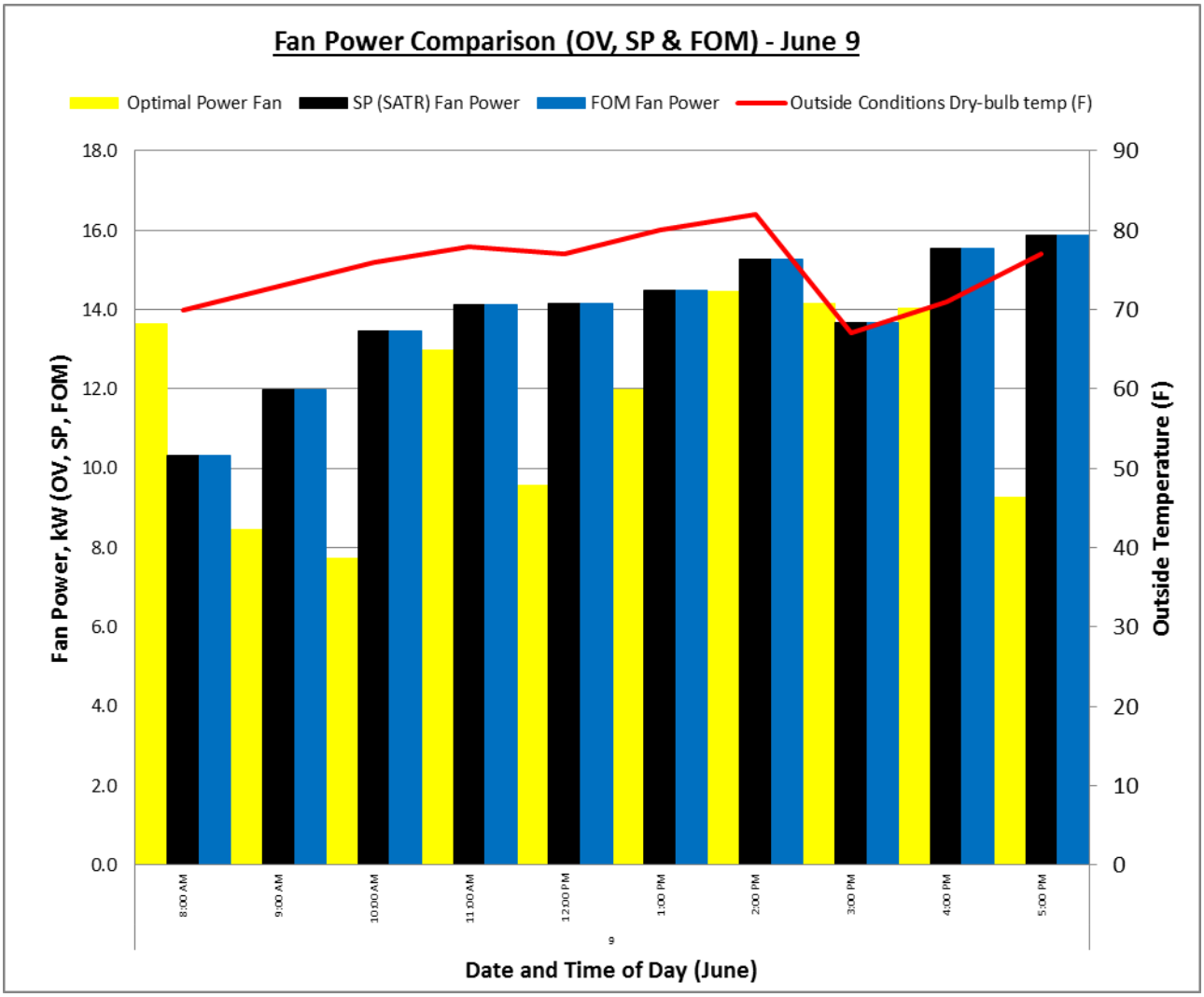

Figure 137. Fan power comparison (June 9).

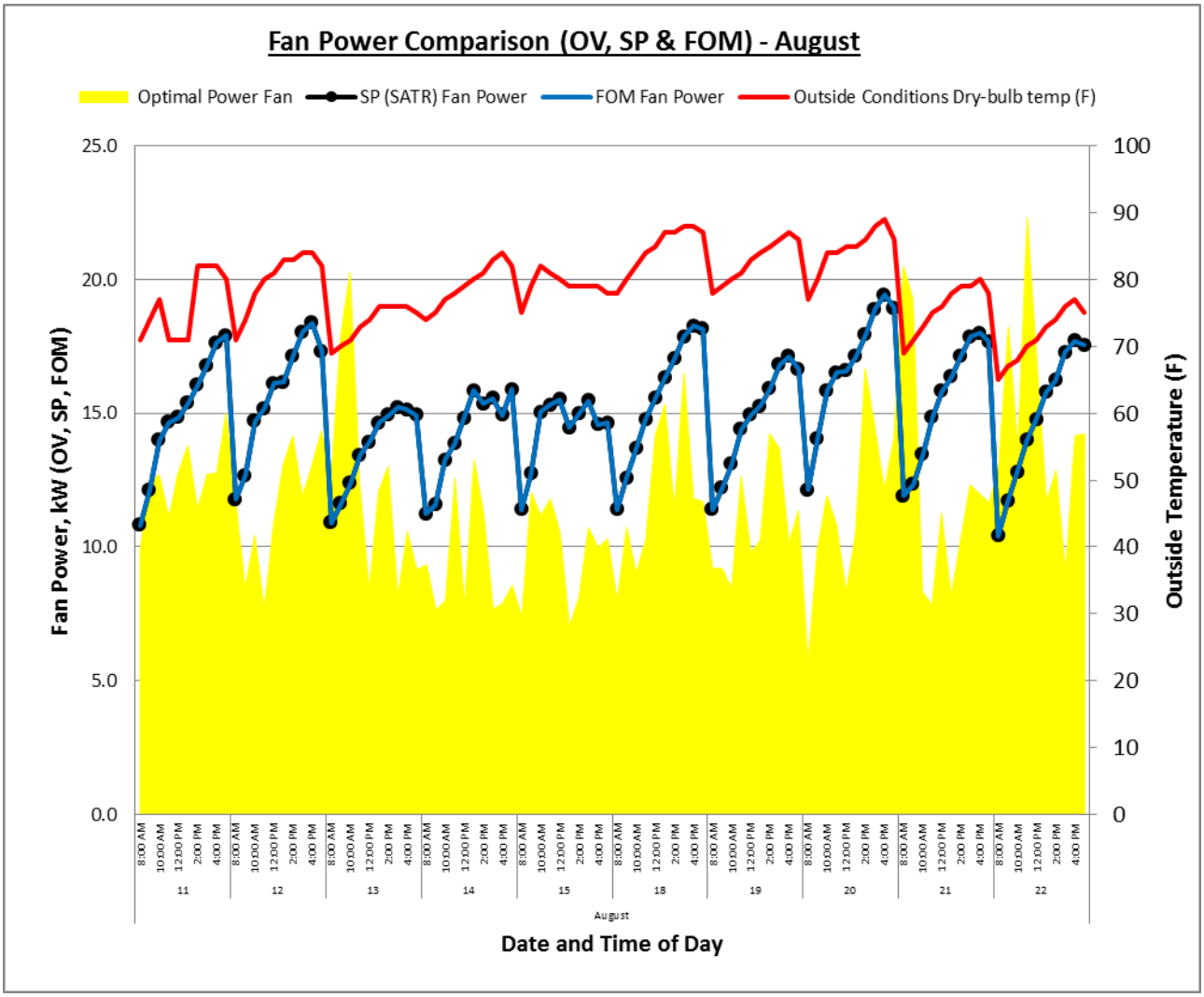

Figure 138. Fan power comparison (August).

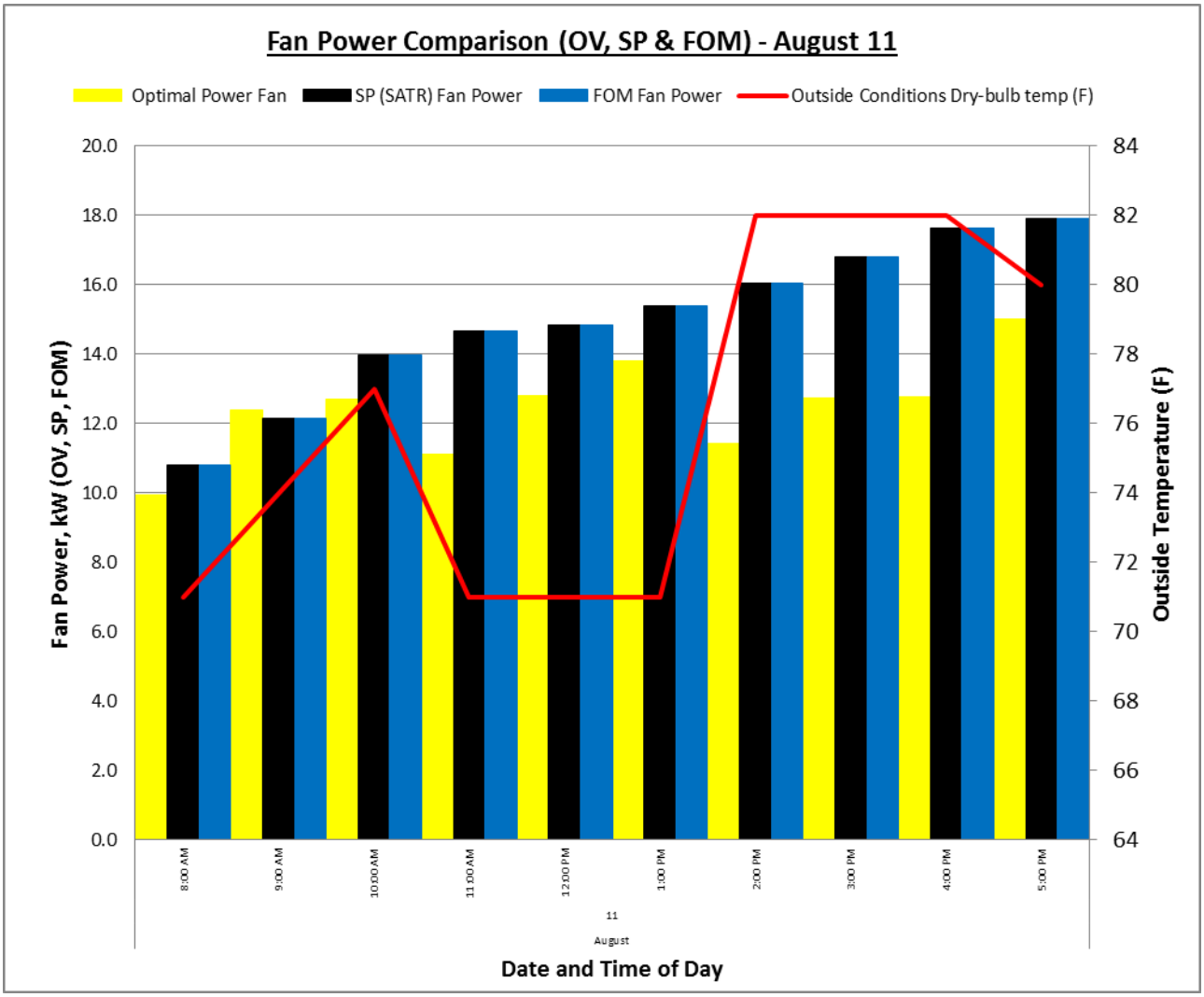

Figure 139. Fan power comparison (August 11).

E.7 Optimal Chilled Water Differential Pressure, D_{pw} Graphs.

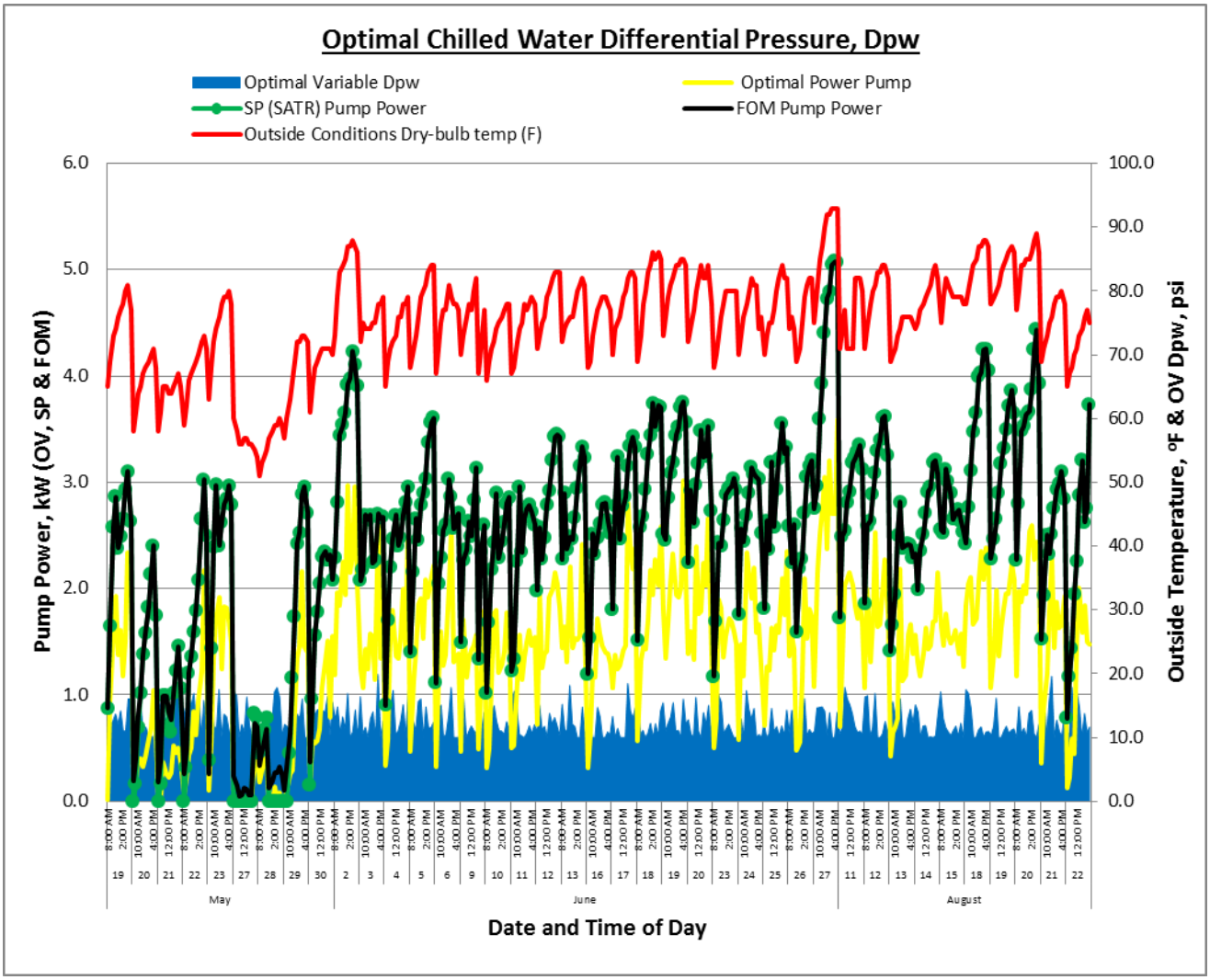

Figure 140. Optimal chilled water differential pressure D_{pw} (May, June, August).

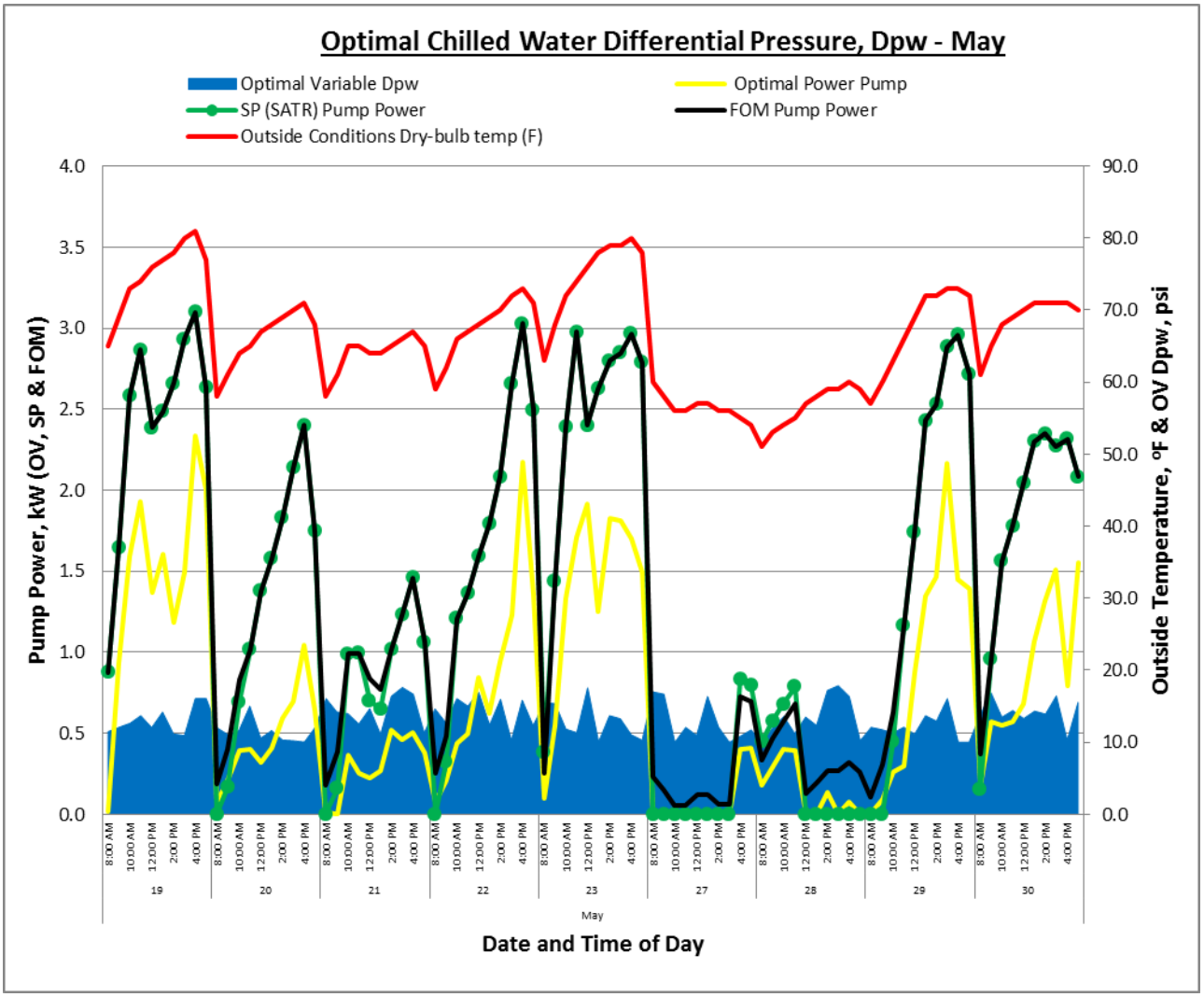

Figure 141. Optimal chilled water differential pressure D_{pw} (May).

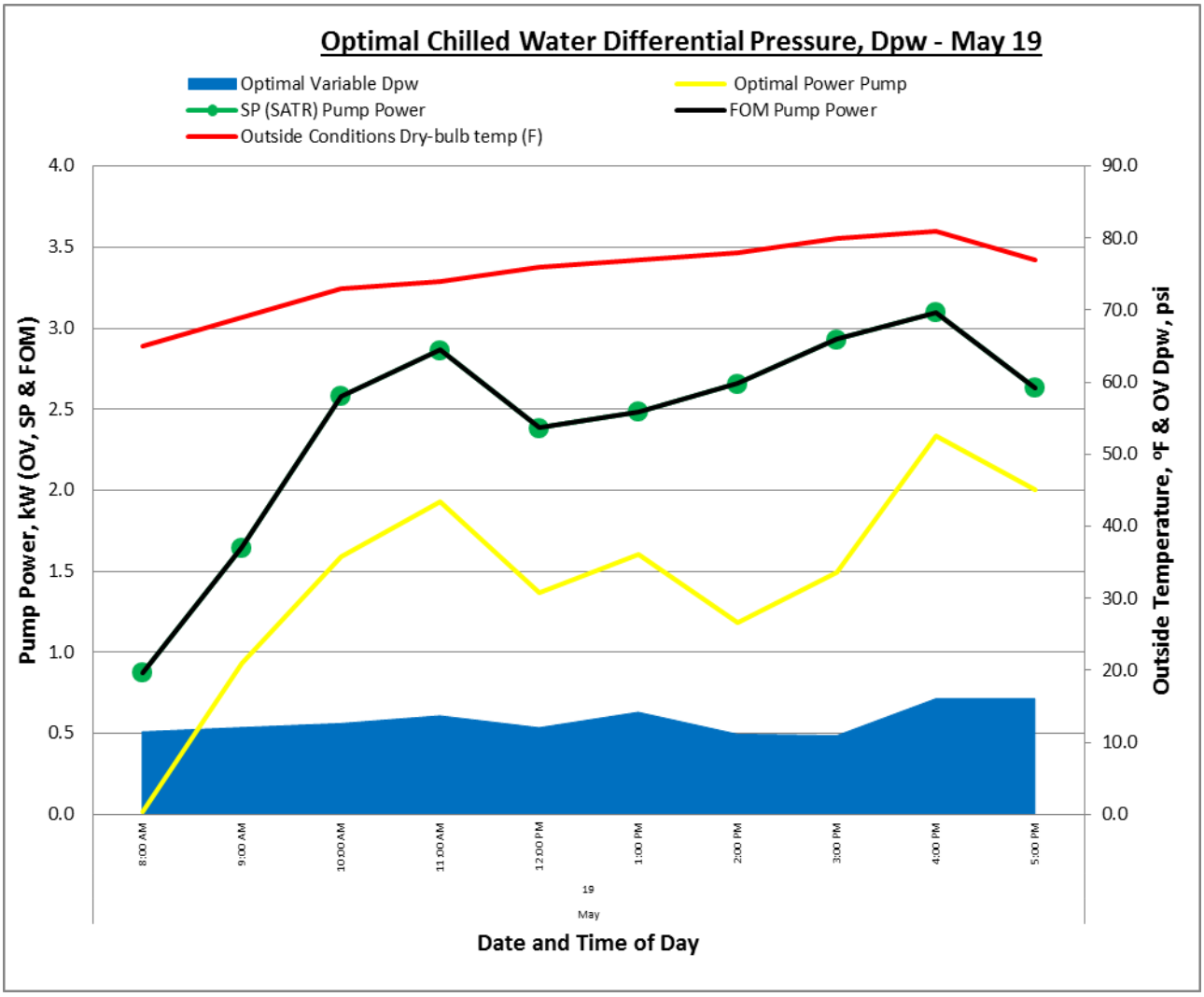

Figure 142. Optimal chilled water differential pressure D_{pw} (May 19).

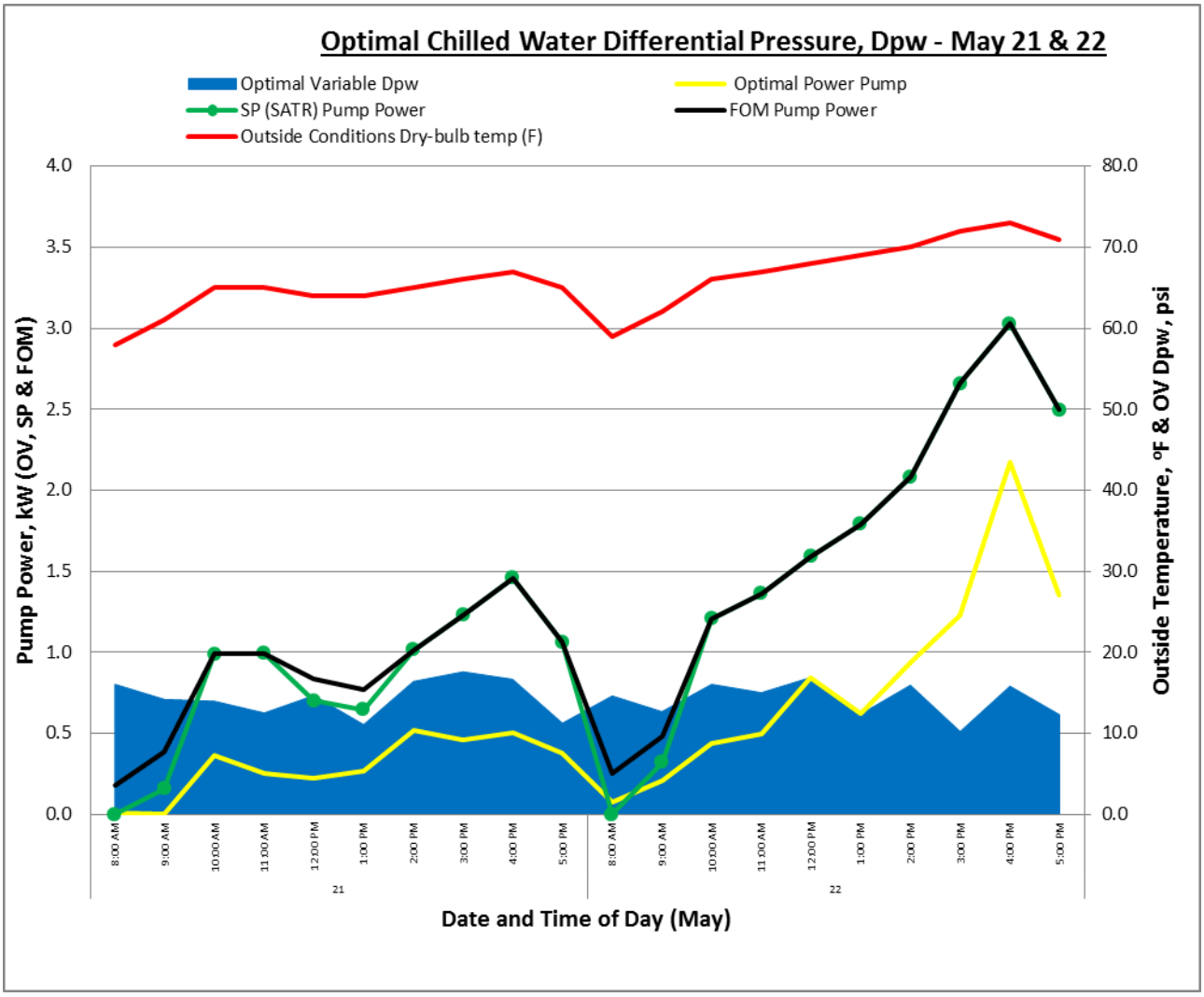

Figure 143. Optimal chilled water differential pressure D_{pw} (May 21 & 22).

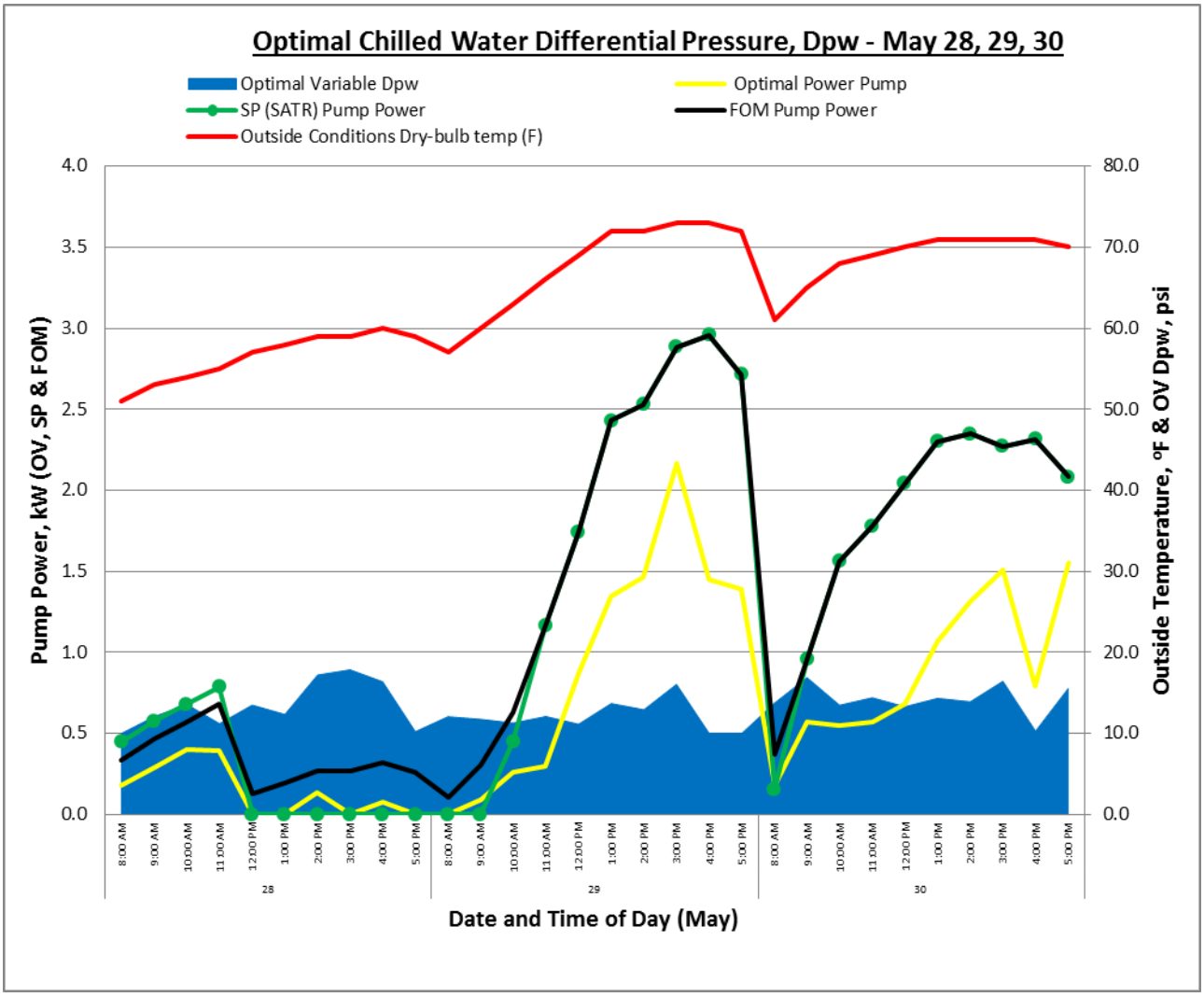

Figure 144. Optimal chilled water differential pressure D_{pw} (May 28, 29, 30).

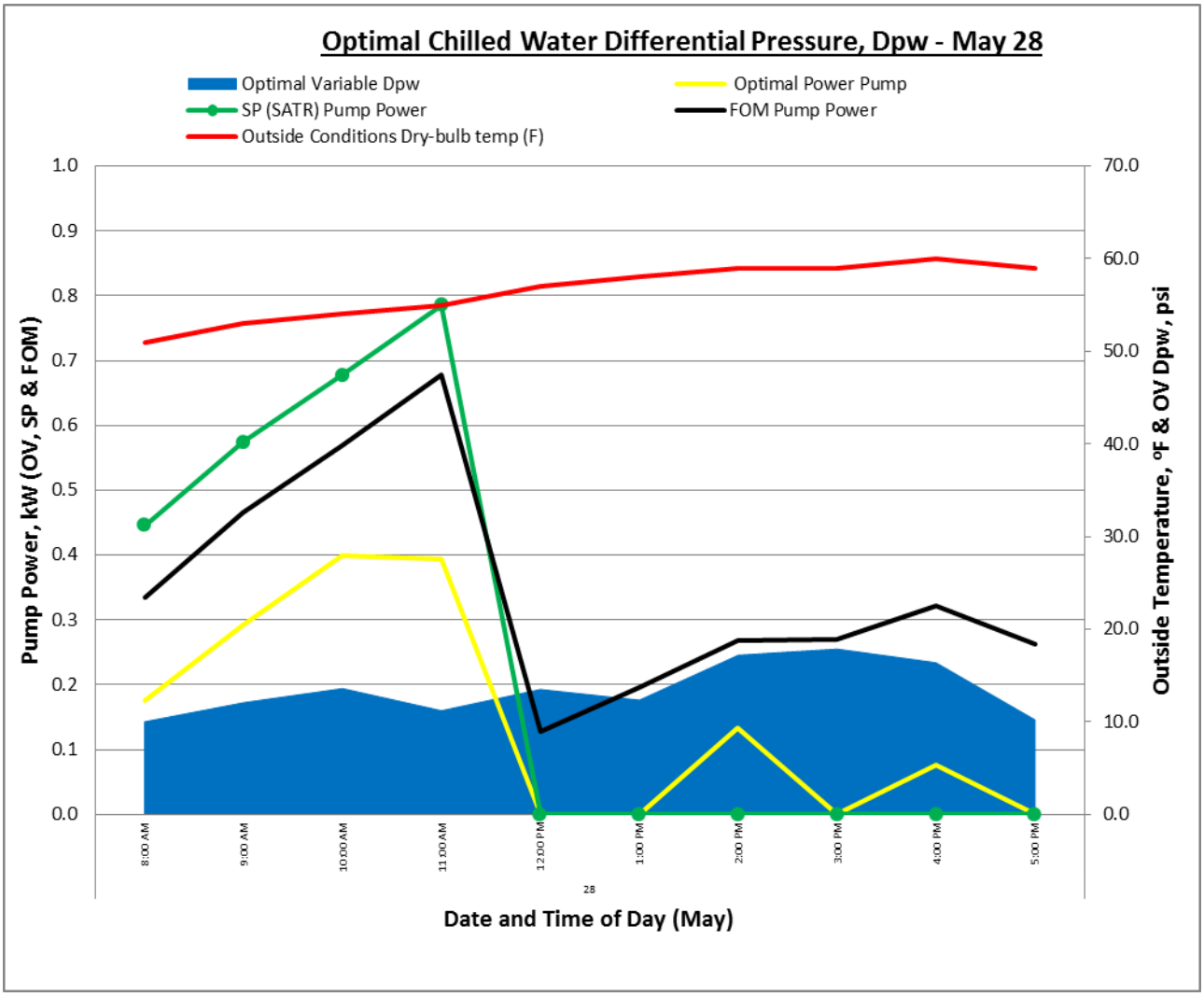

Figure 145. Optimal chilled water differential pressure D_{pw} (May 28).

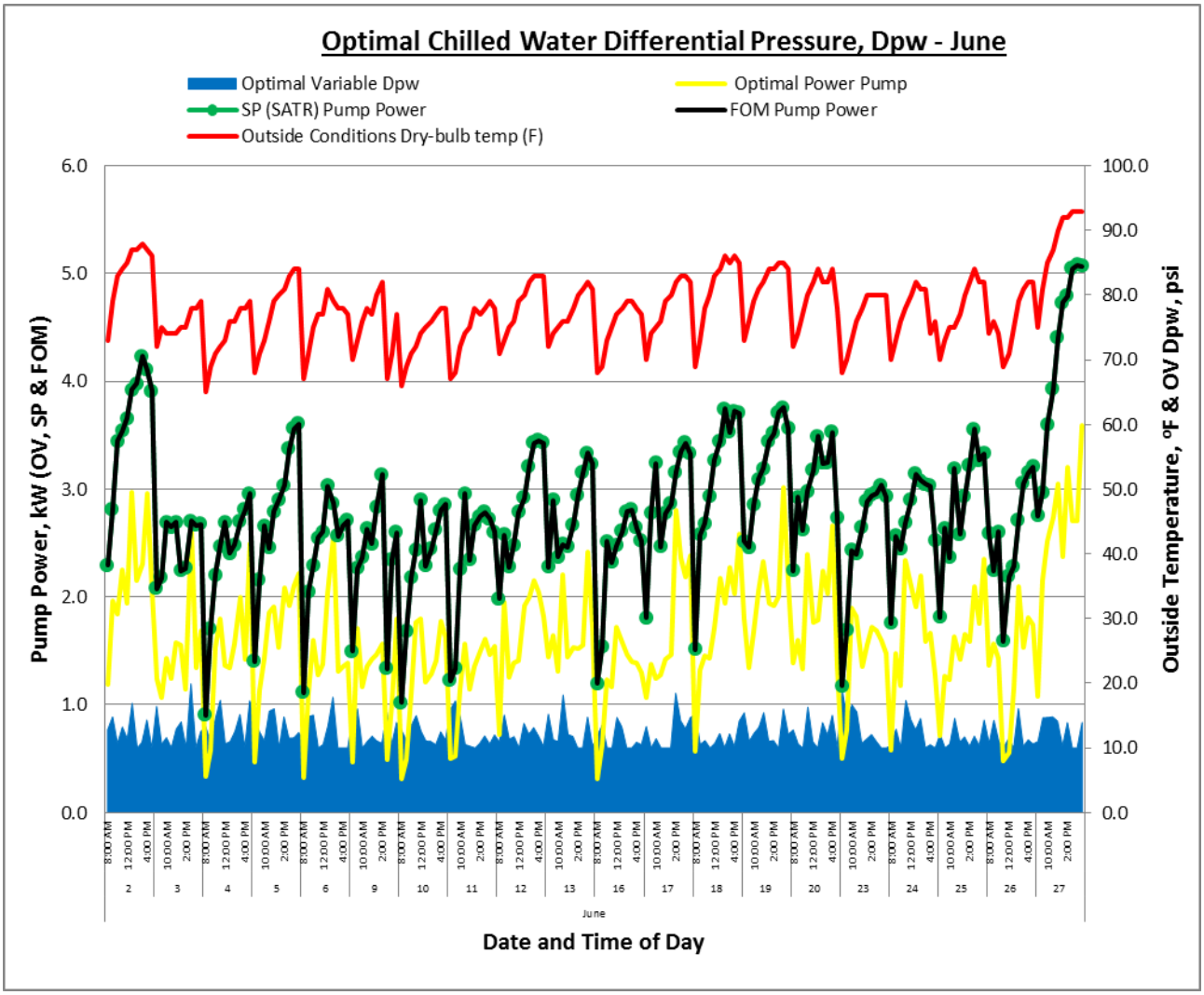

Figure 146. Optimal chilled water differential pressure D_{pw} (June).

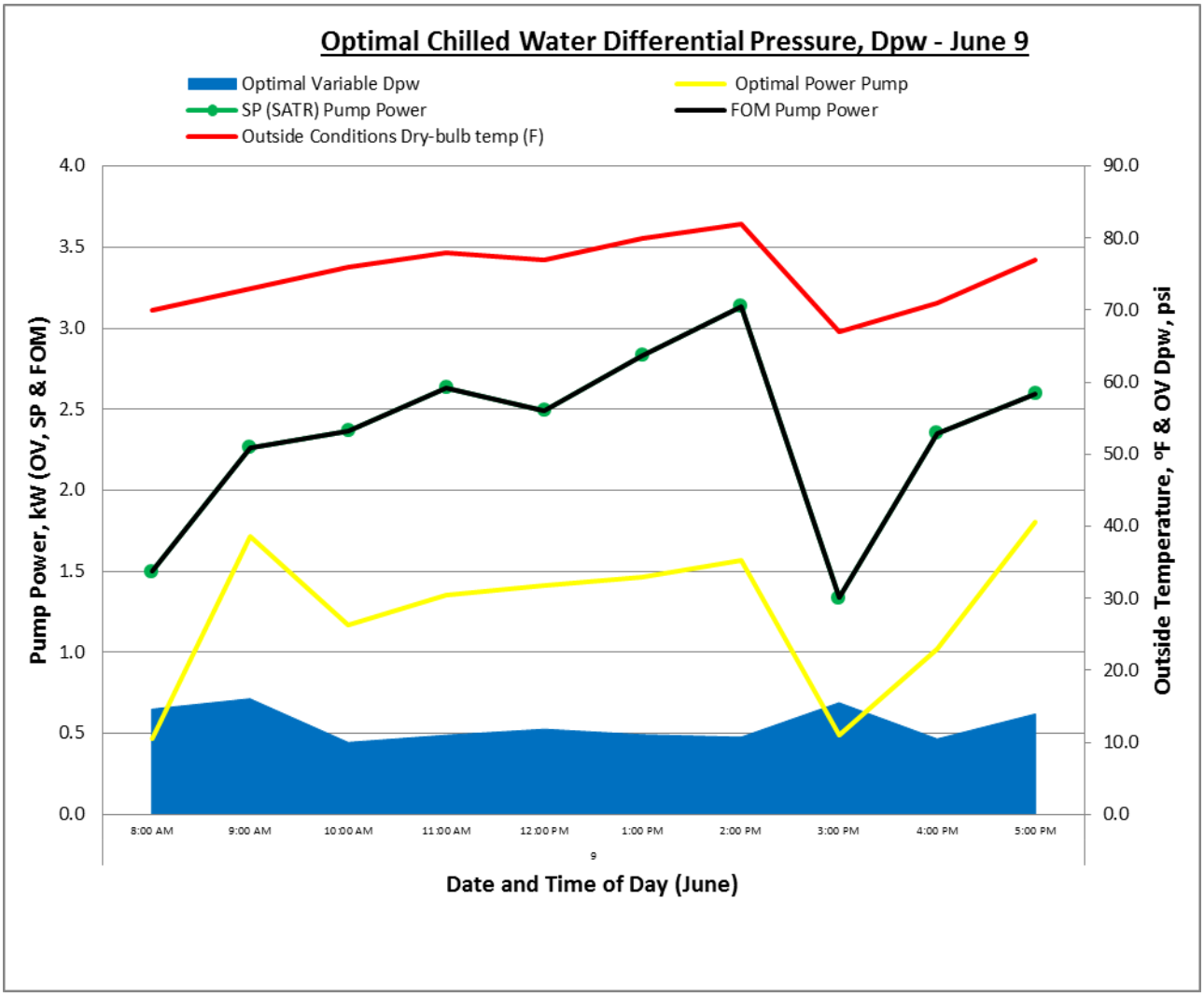

Figure 147. Optimal chilled water differential pressure D_{pw} (June 9).

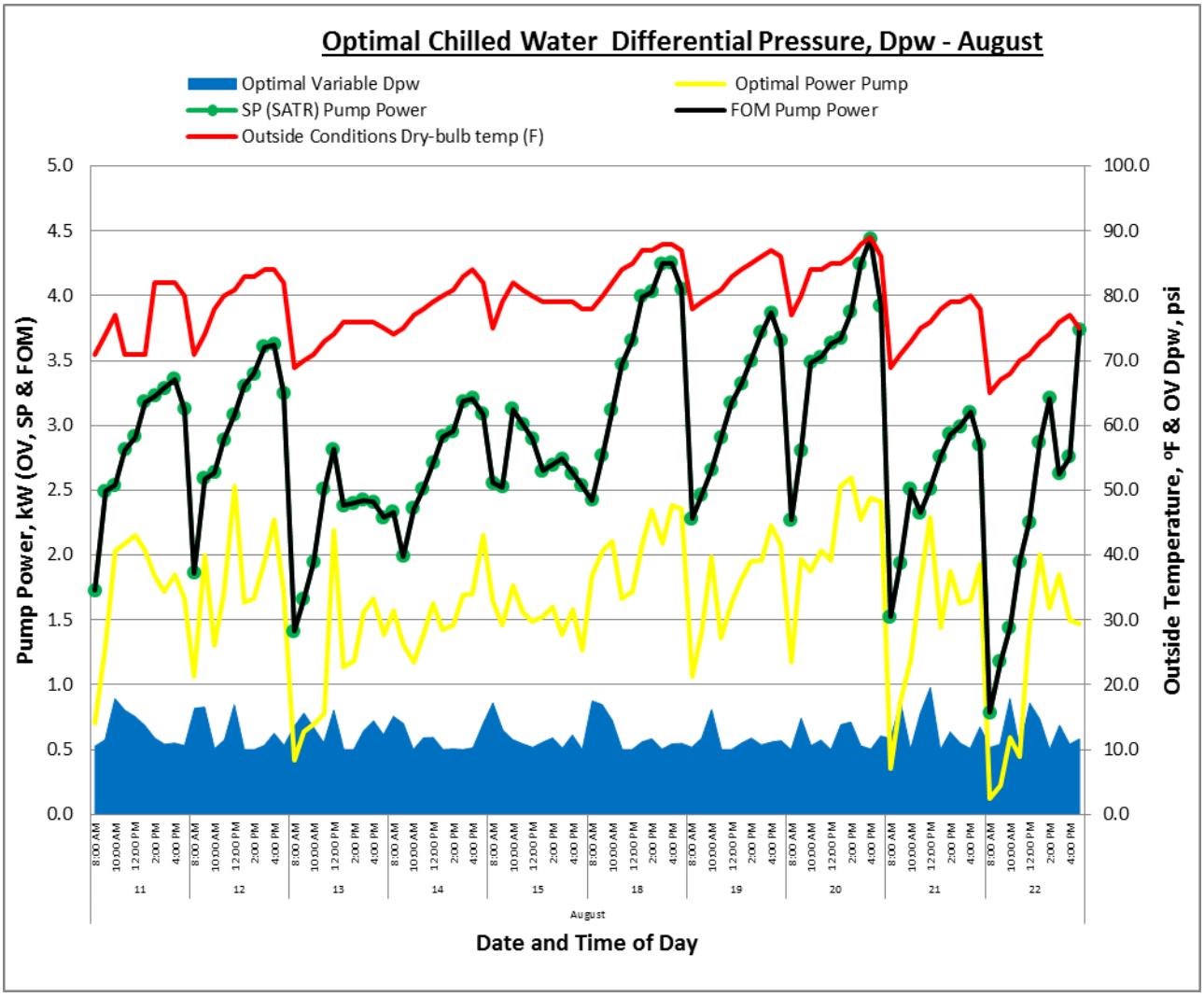

Figure 148. Optimal chilled water differential pressure D_{pw} (August).

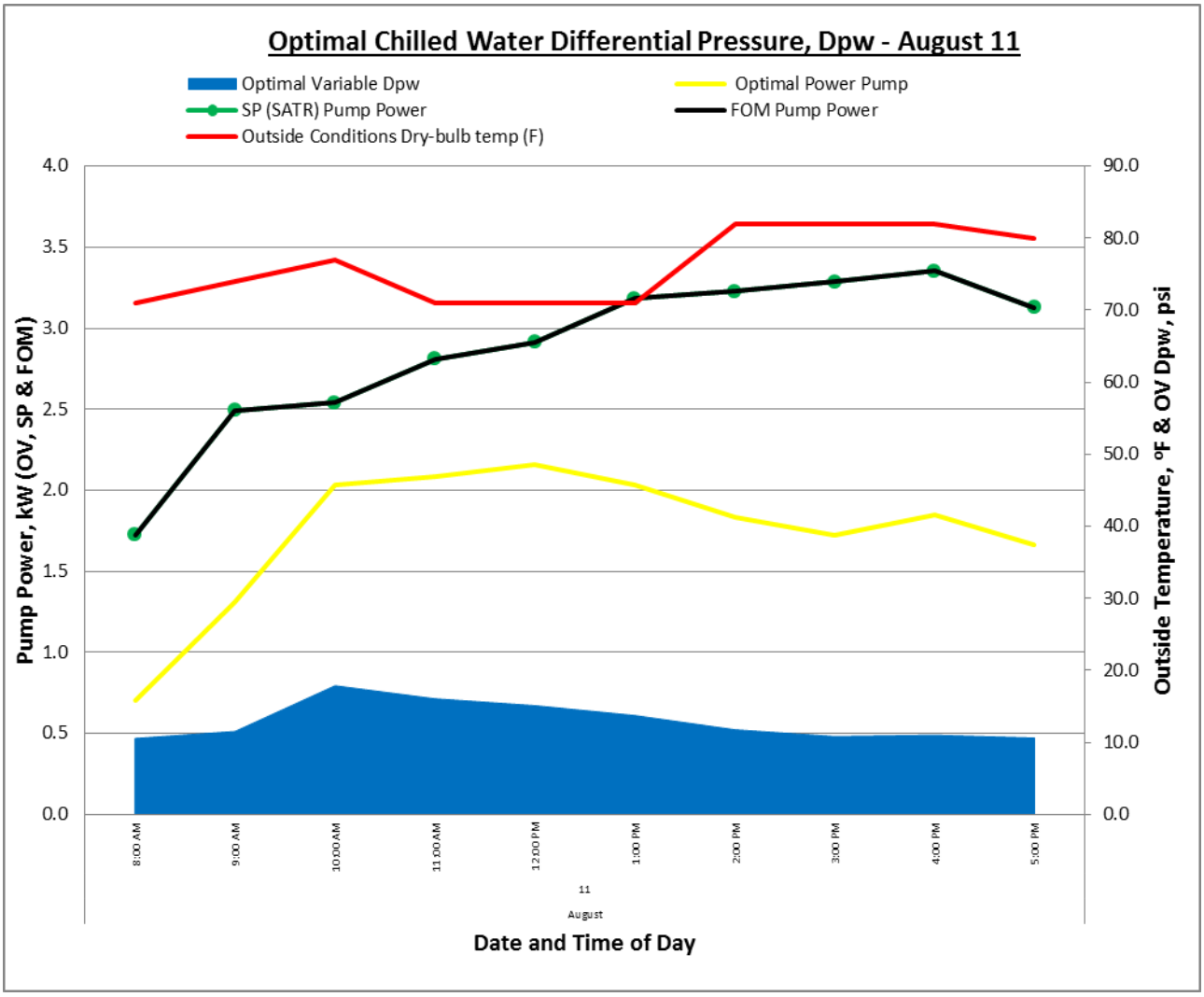

Figure 149. Optimal chilled water differential pressure D_{pw} (August 11).

E.8 Optimal Supply Temperature, T_s Graphs.

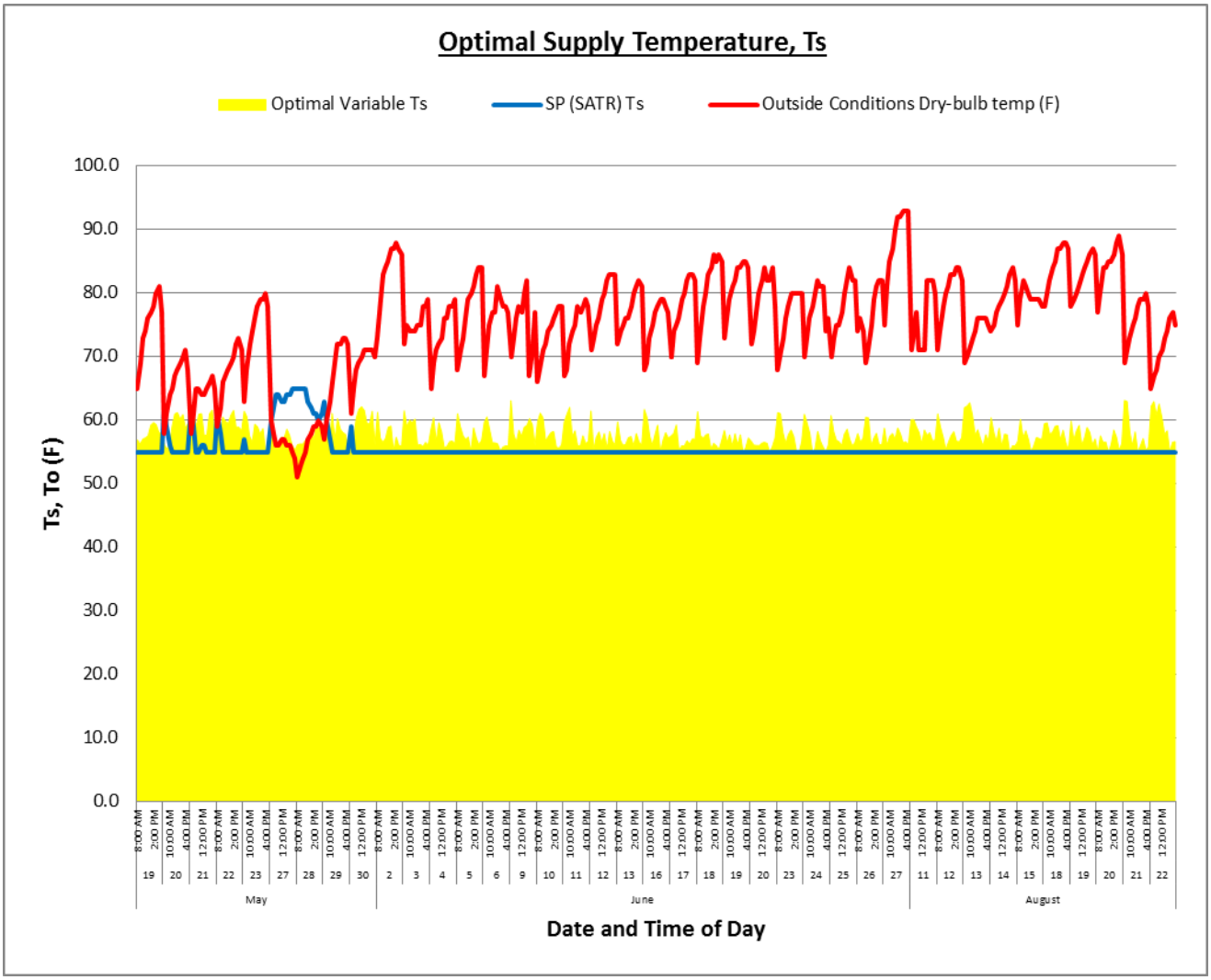

Figure 150. Optimal supply temperature T_s (May, June, August).

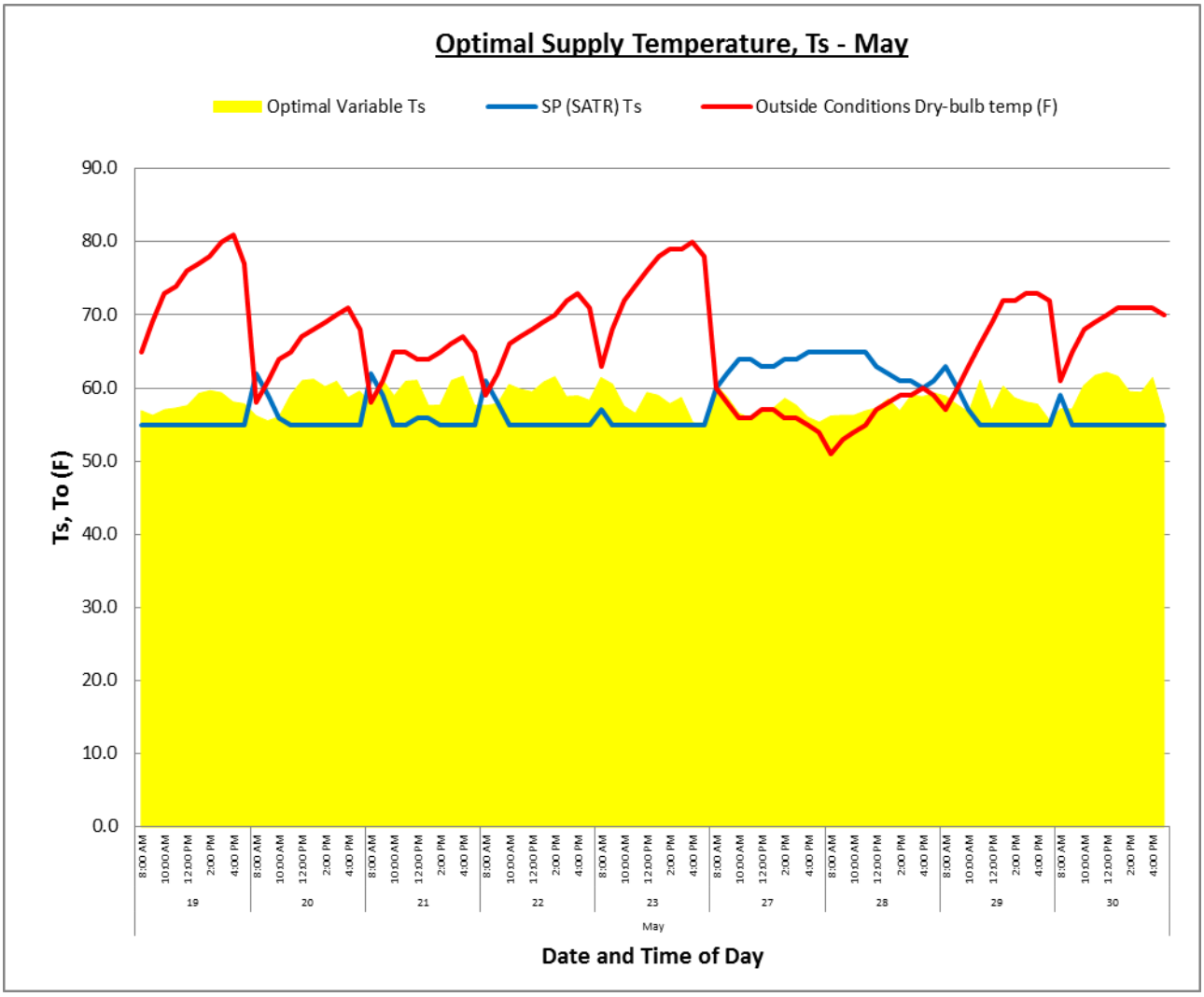

Figure 151. Optimal supply temperature T_s (May).

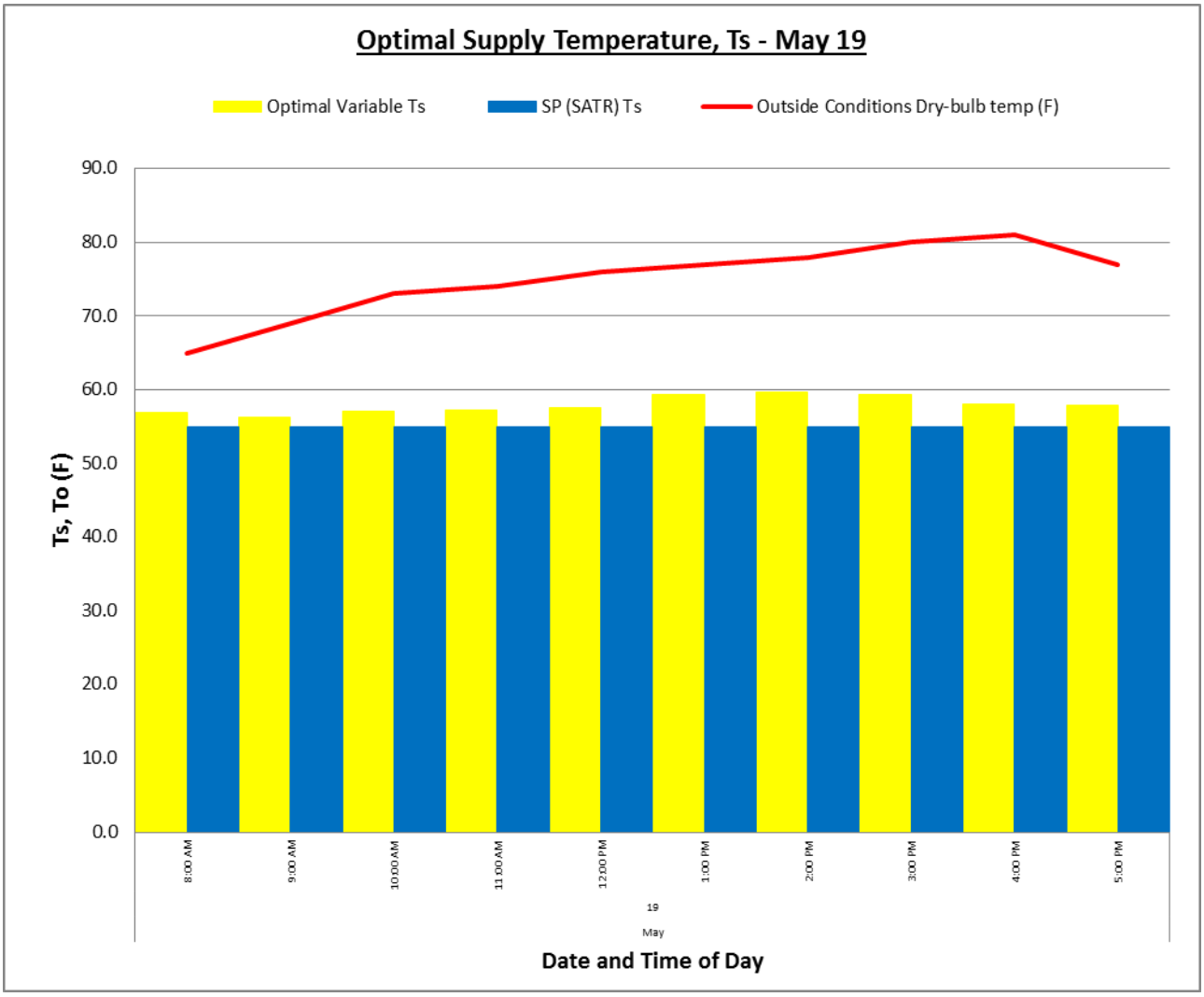

Figure 152. Optimal supply temperature T_s (May 19).

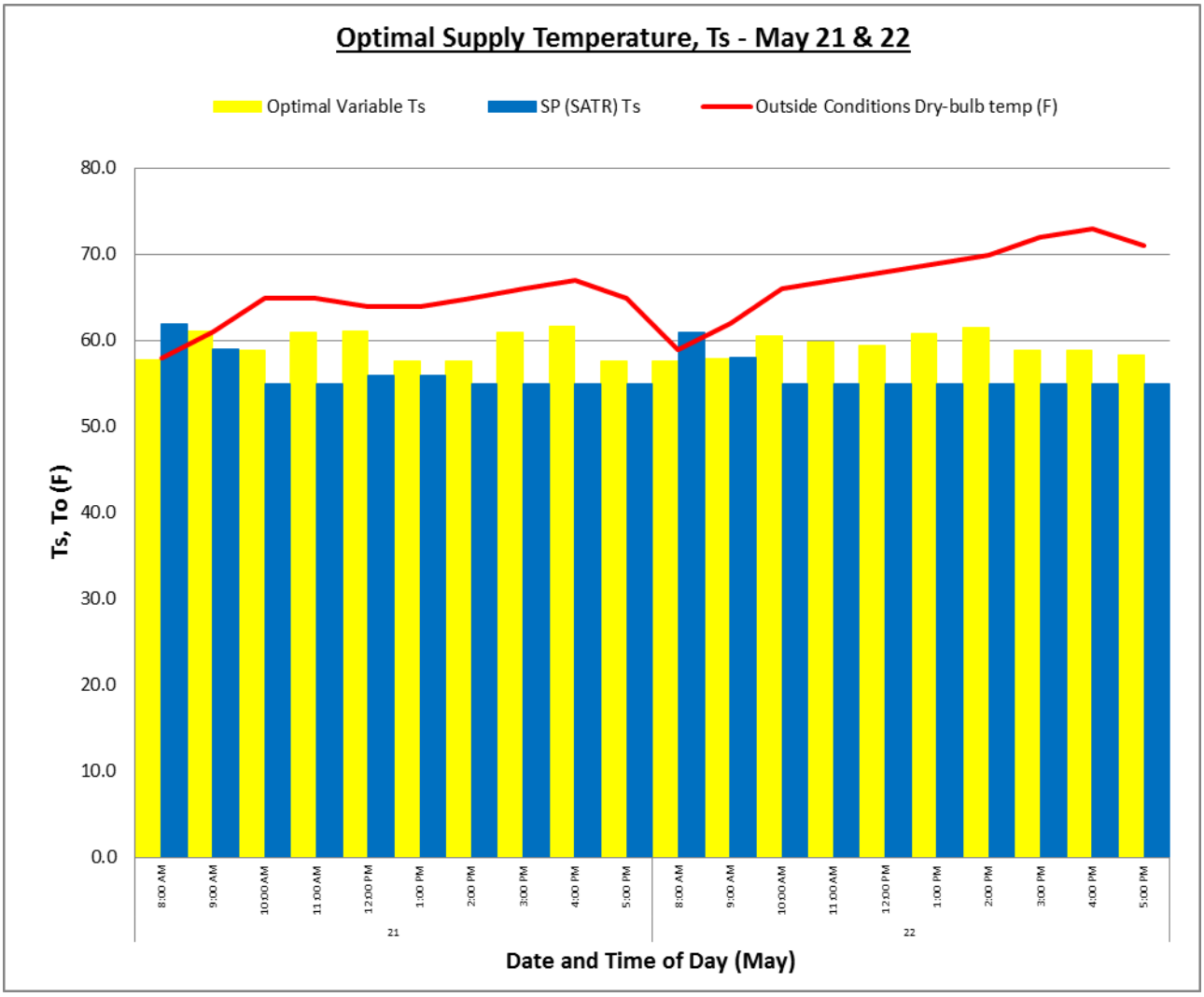

Figure 153. Optimal supply temperature T_s (May 21 & 22).

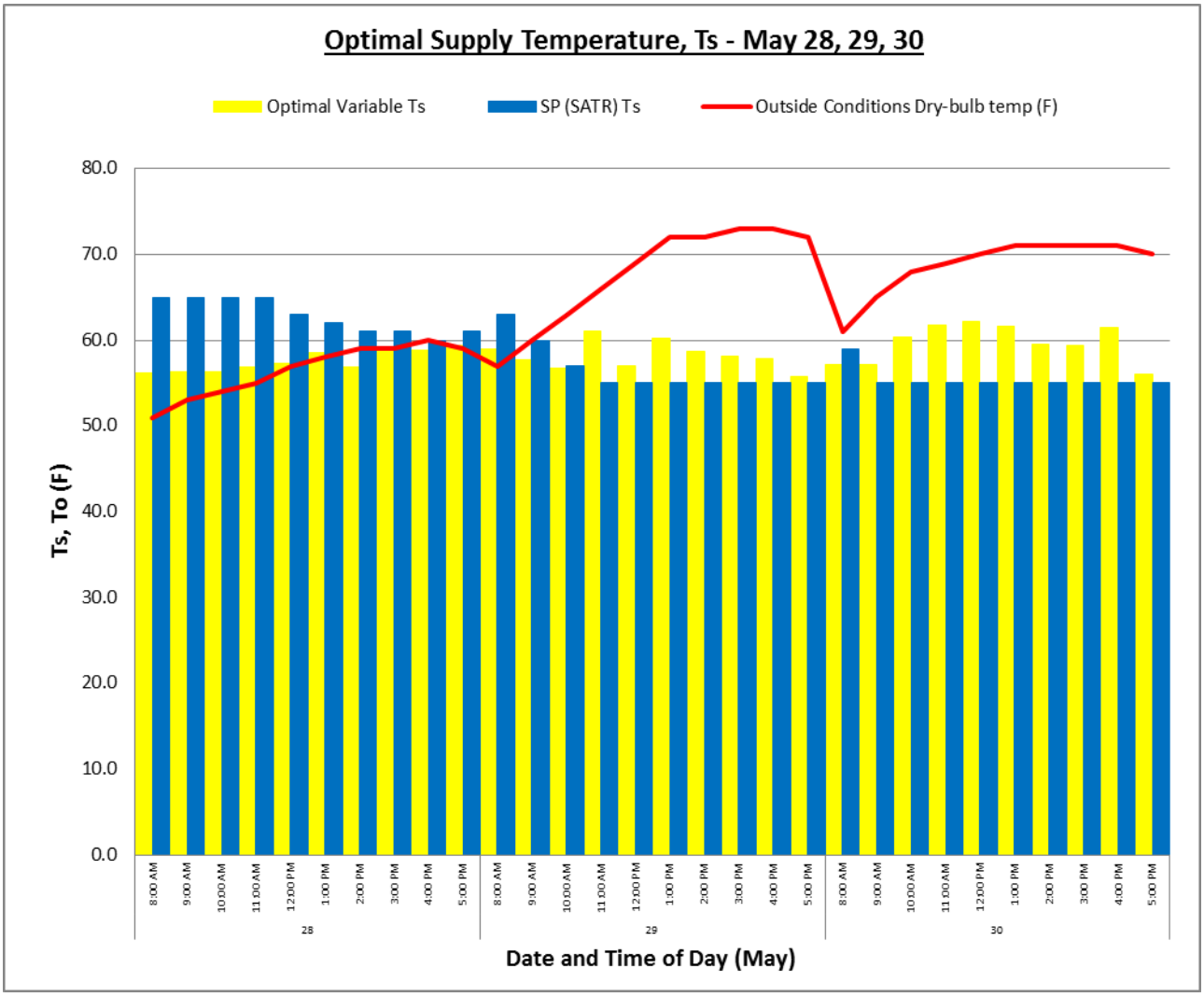

Figure 154. Optimal supply temperature T_s (May 28, 29, 30).

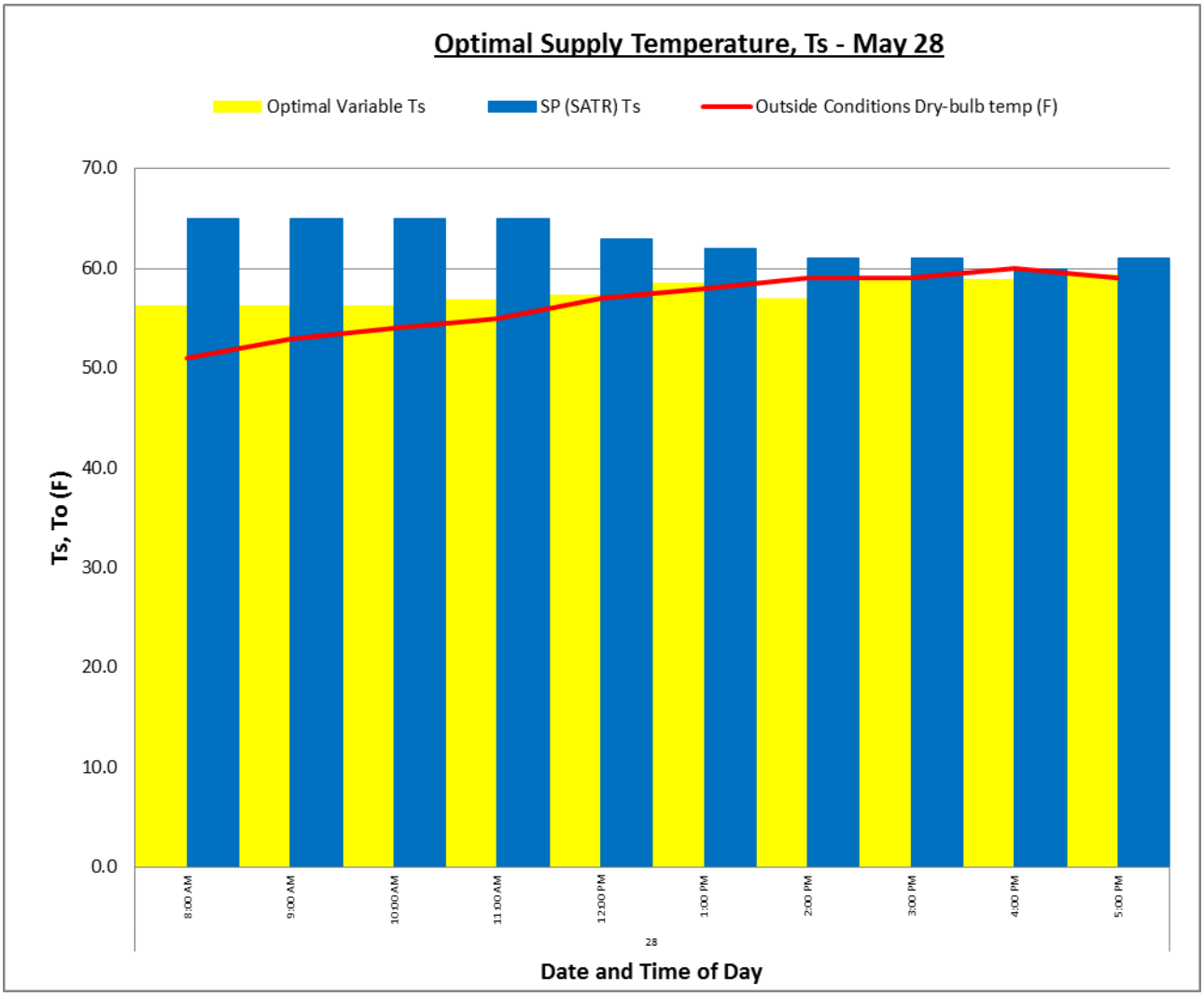

Figure 155. Optimal supply temperature T_s (May 28).

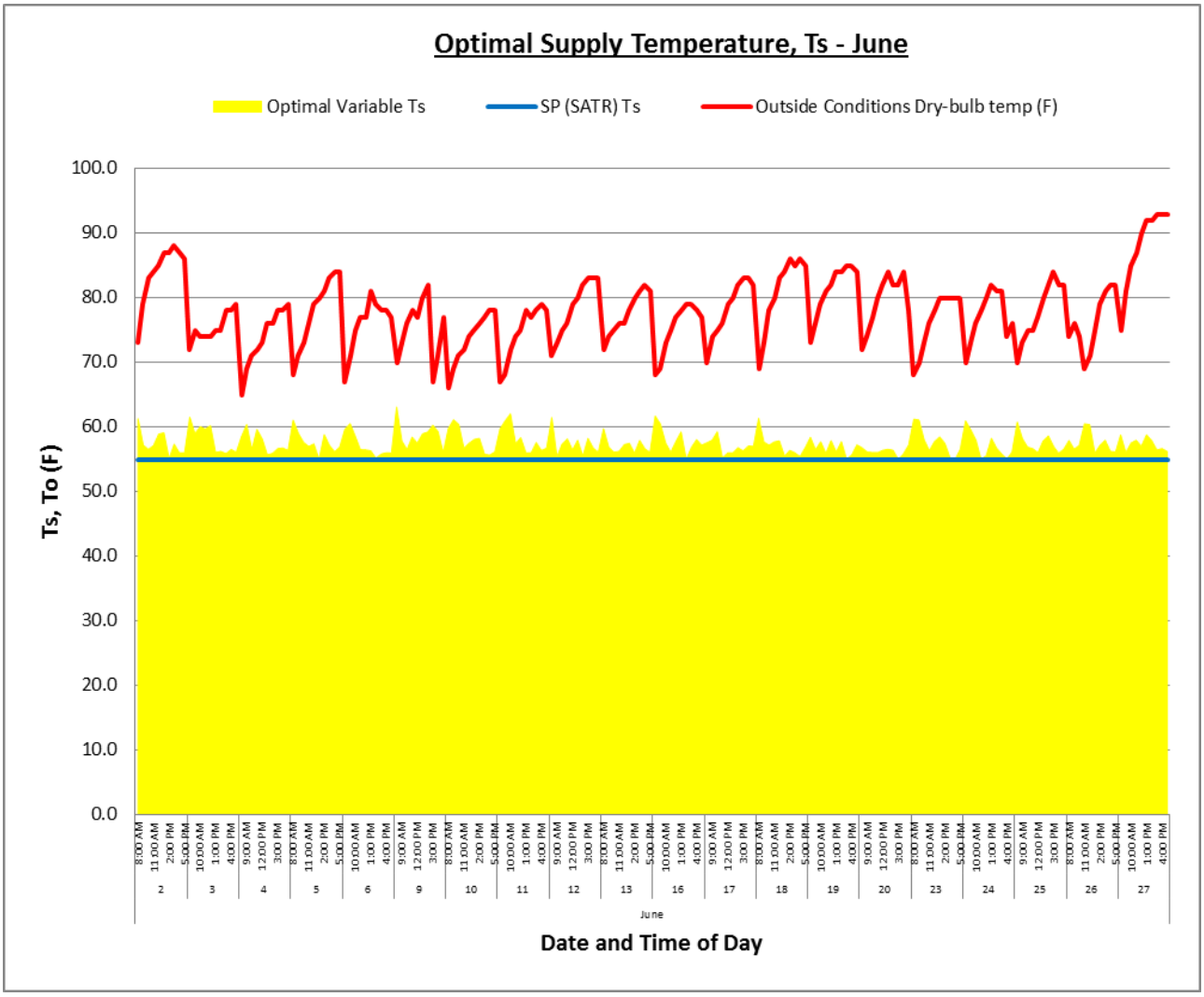

Figure 156. Optimal supply temperature T_s (June).

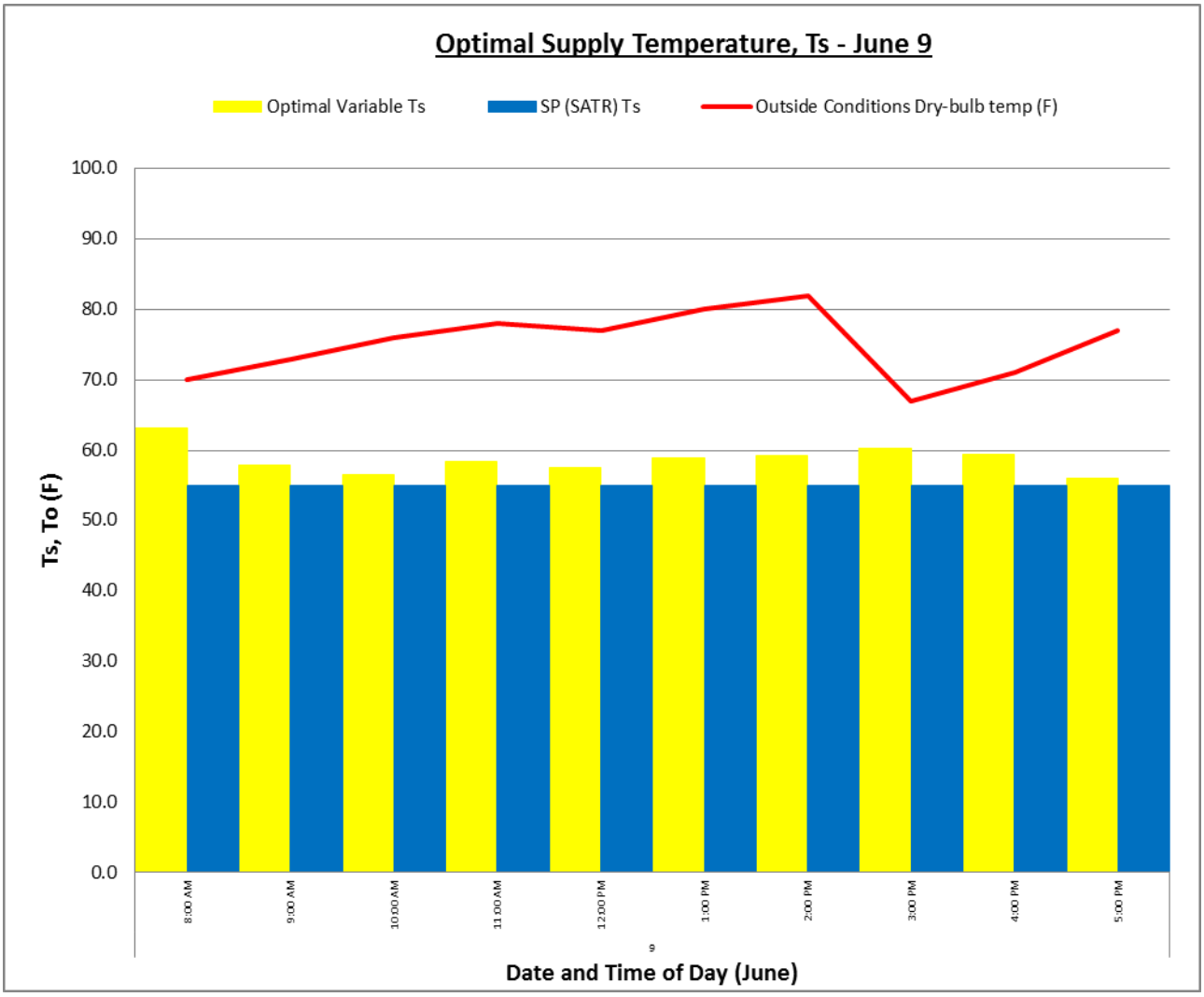

Figure 157. Optimal supply temperature T_s (June 9).

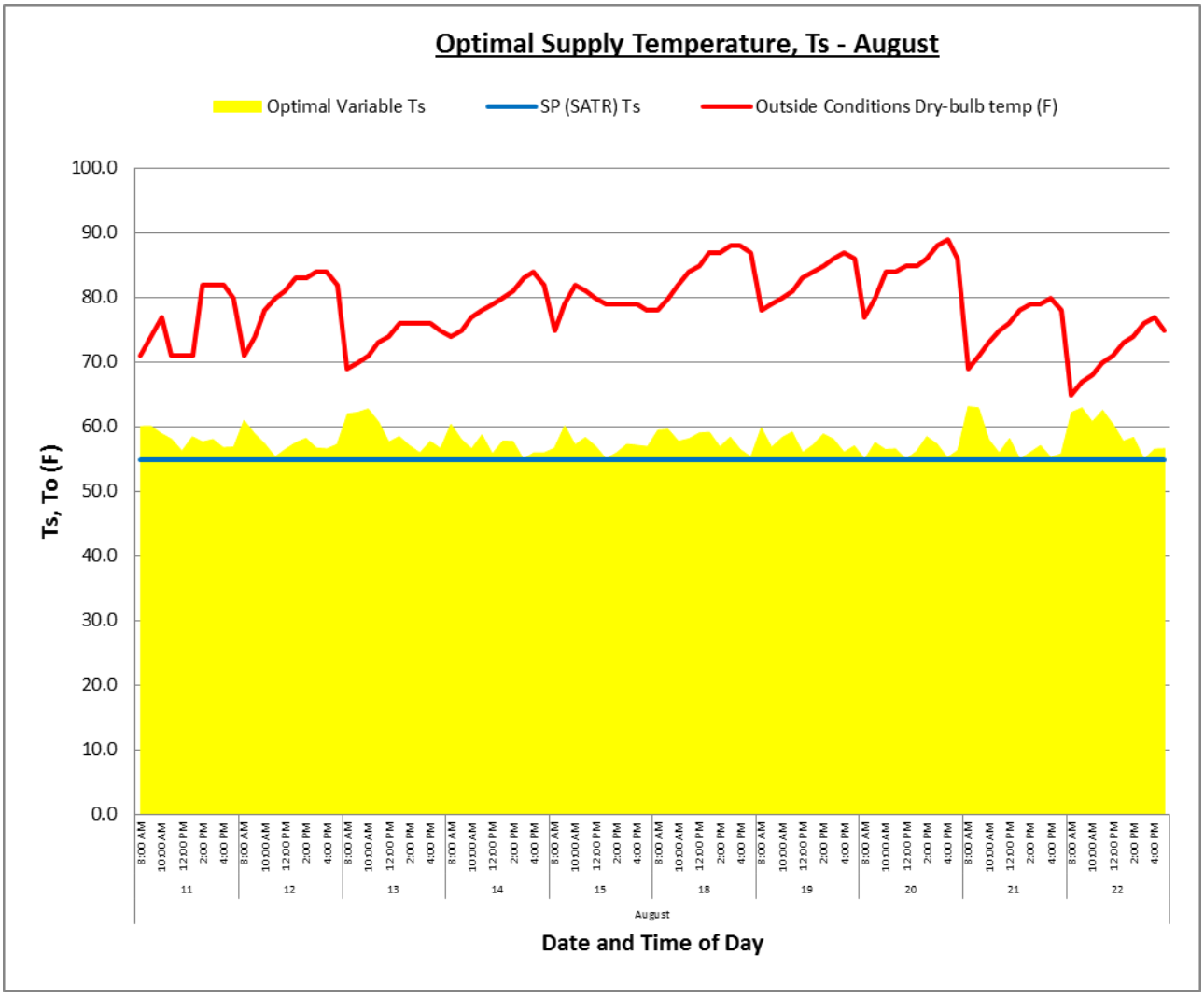

Figure 158. Optimal supply temperature T_s (August).

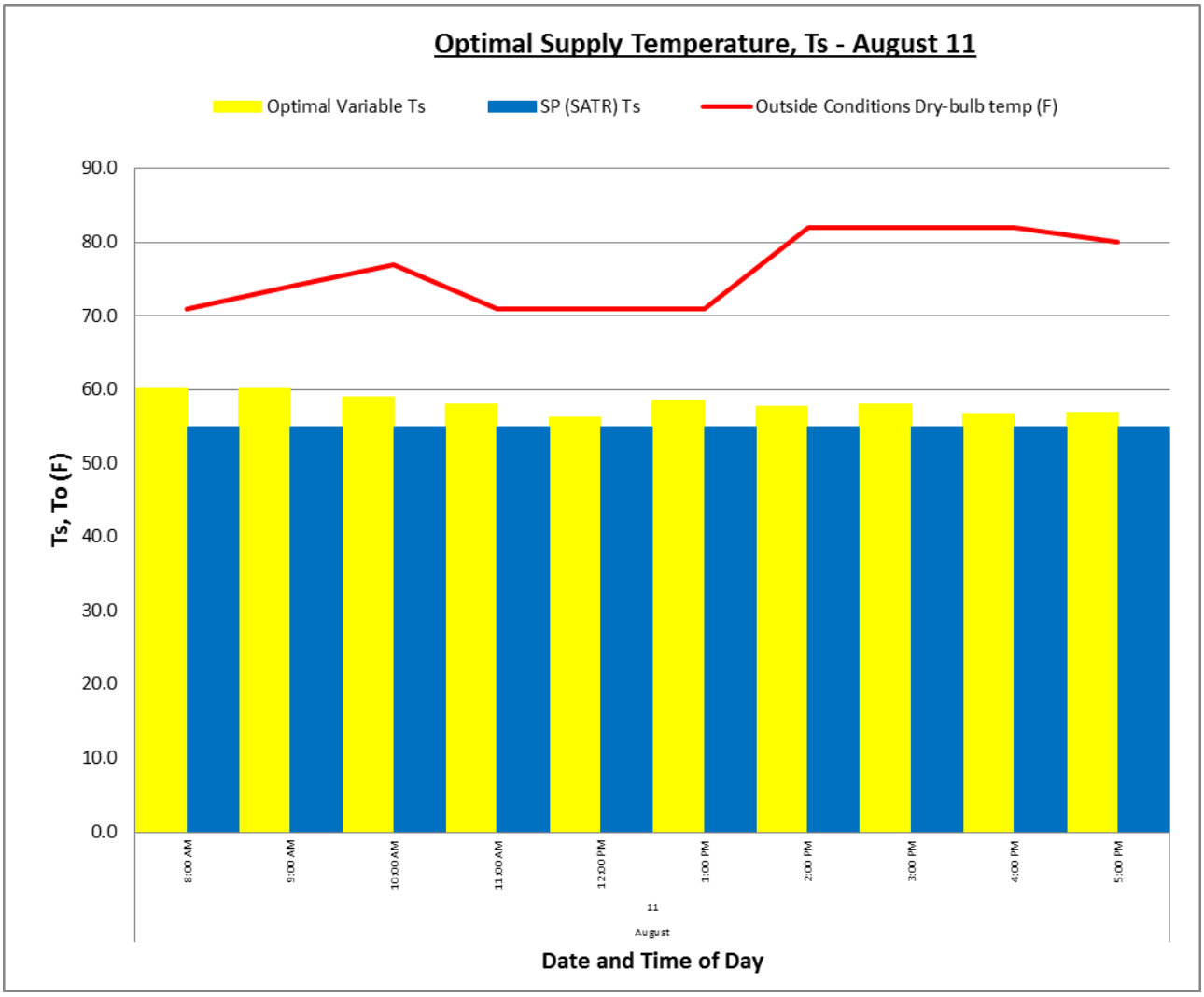

Figure 159. Optimal supply temperature T_s (August 11).

E.9 Optimal Duct Static Pressure, P_s Graphs.

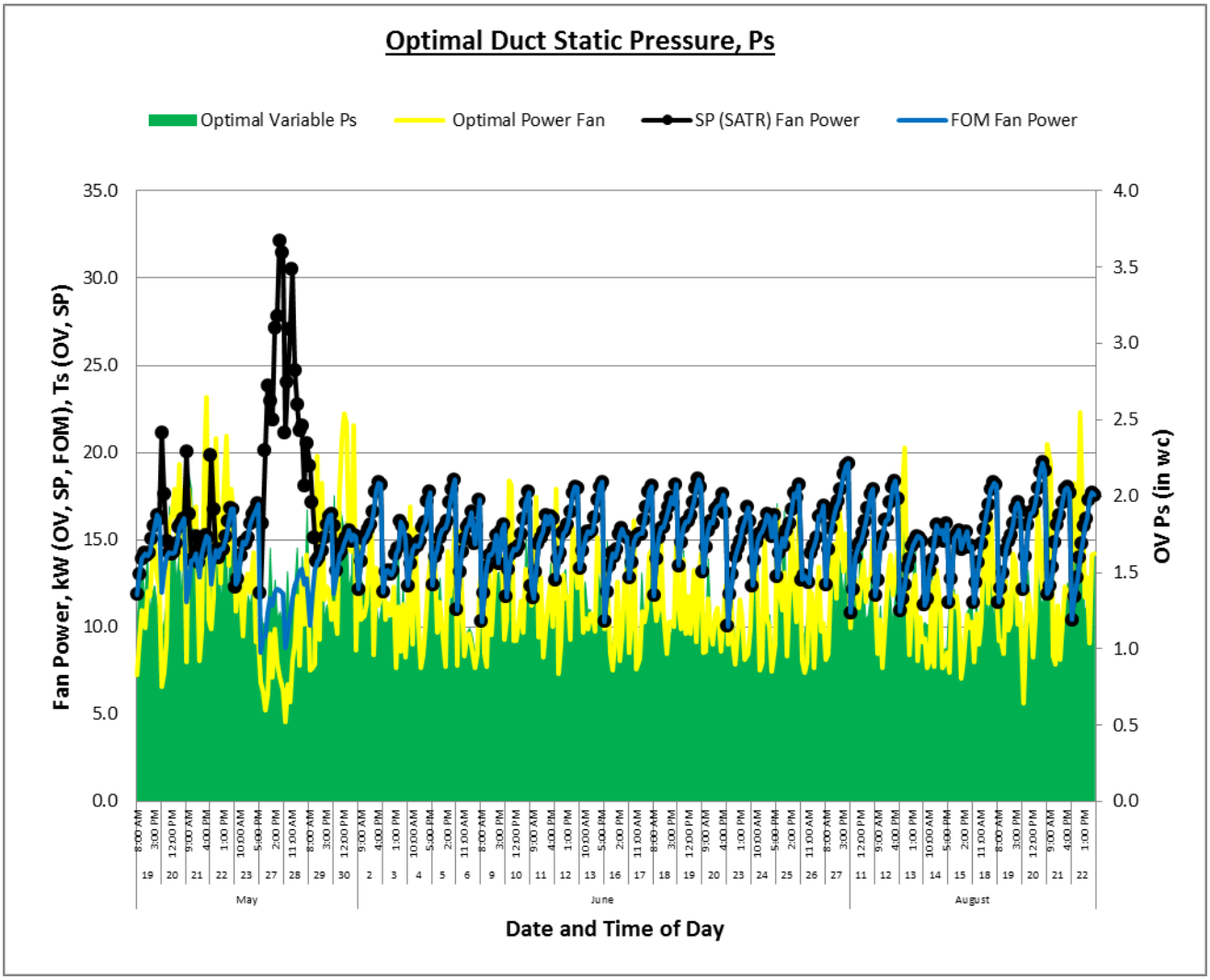

Figure 160. Optimal duct static pressure P_s (May, June, August).

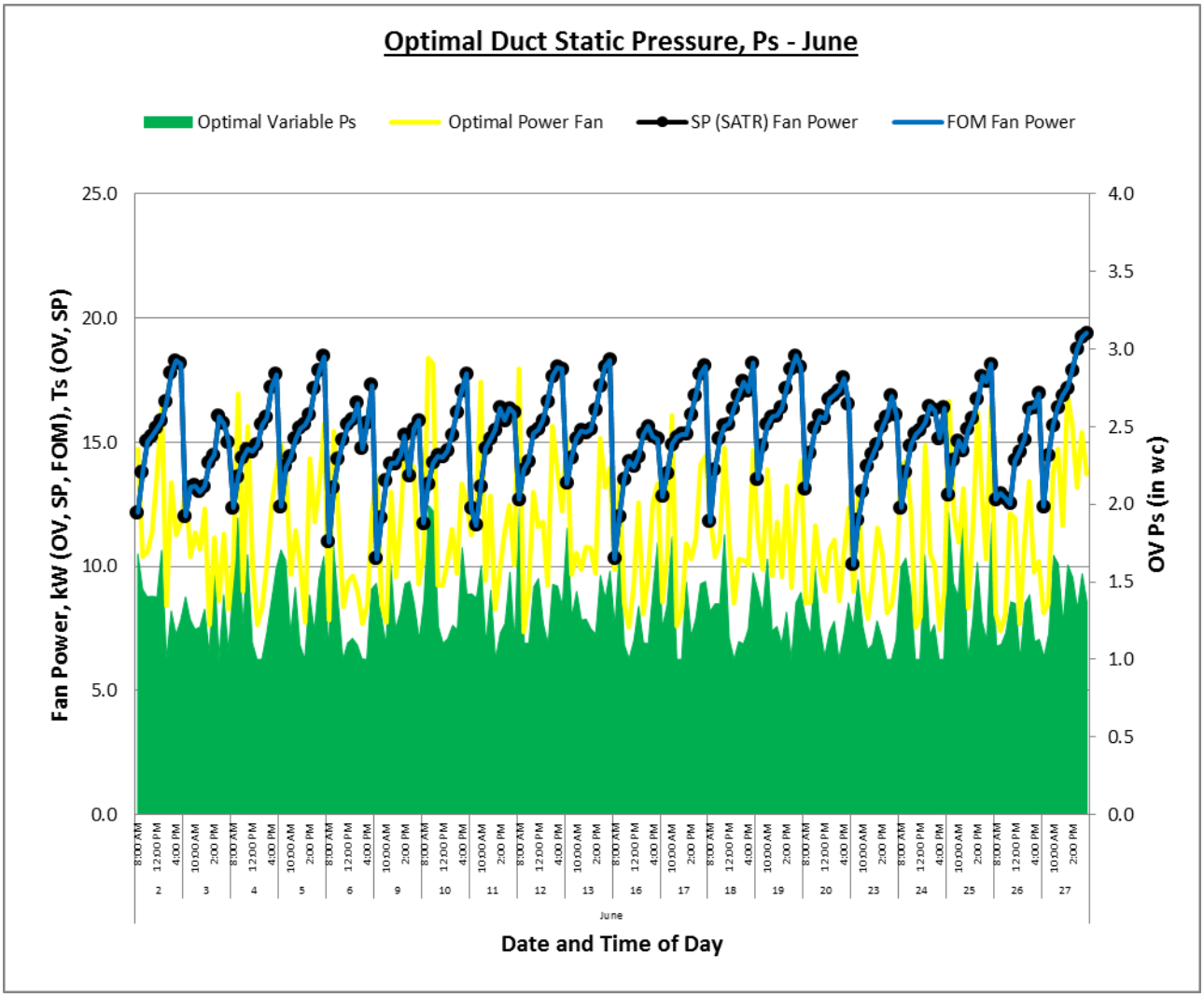

Figure 161. Optimal duct static pressure P_s (June).

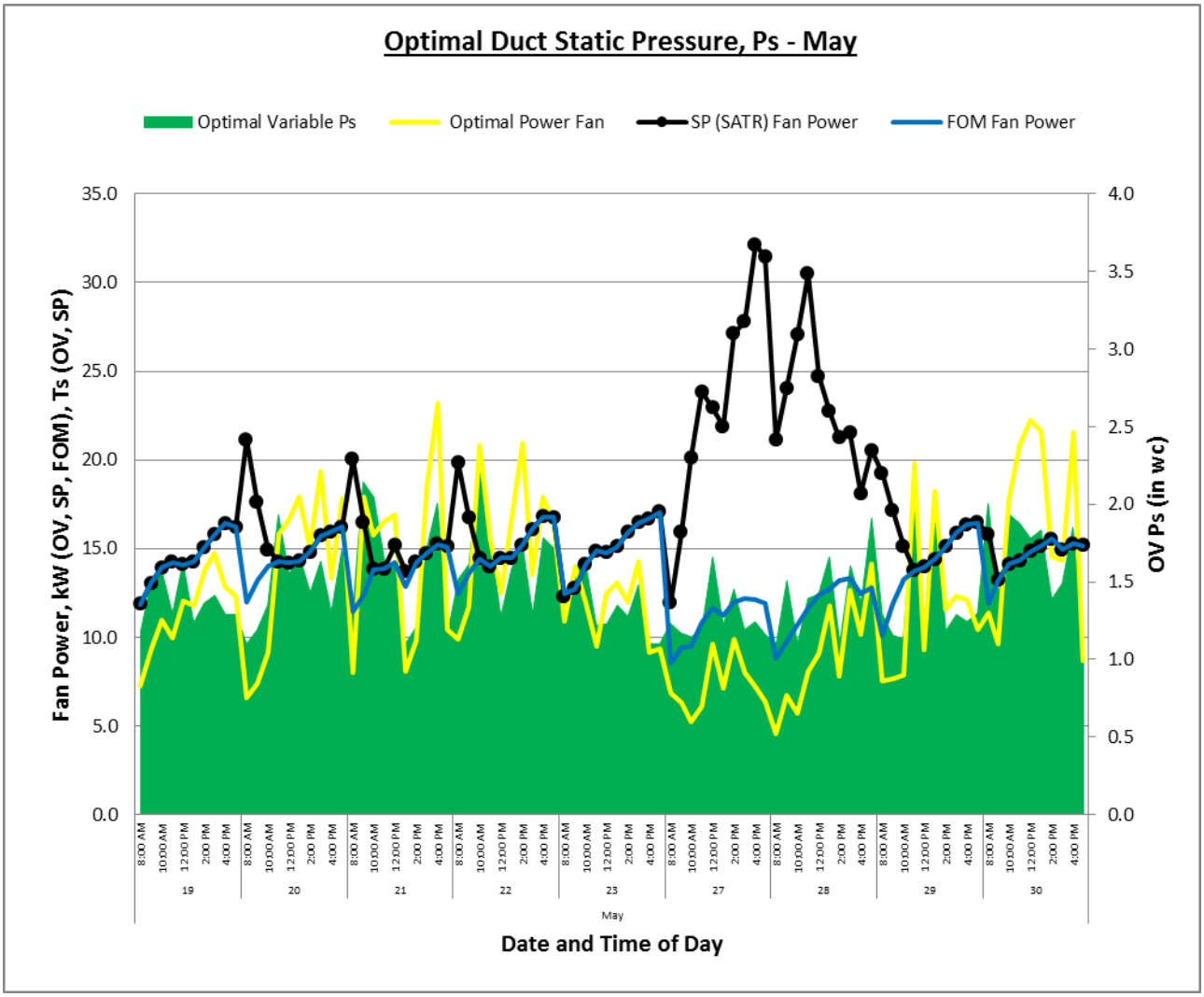

Figure 162. Optimal duct static pressure P_s (May).

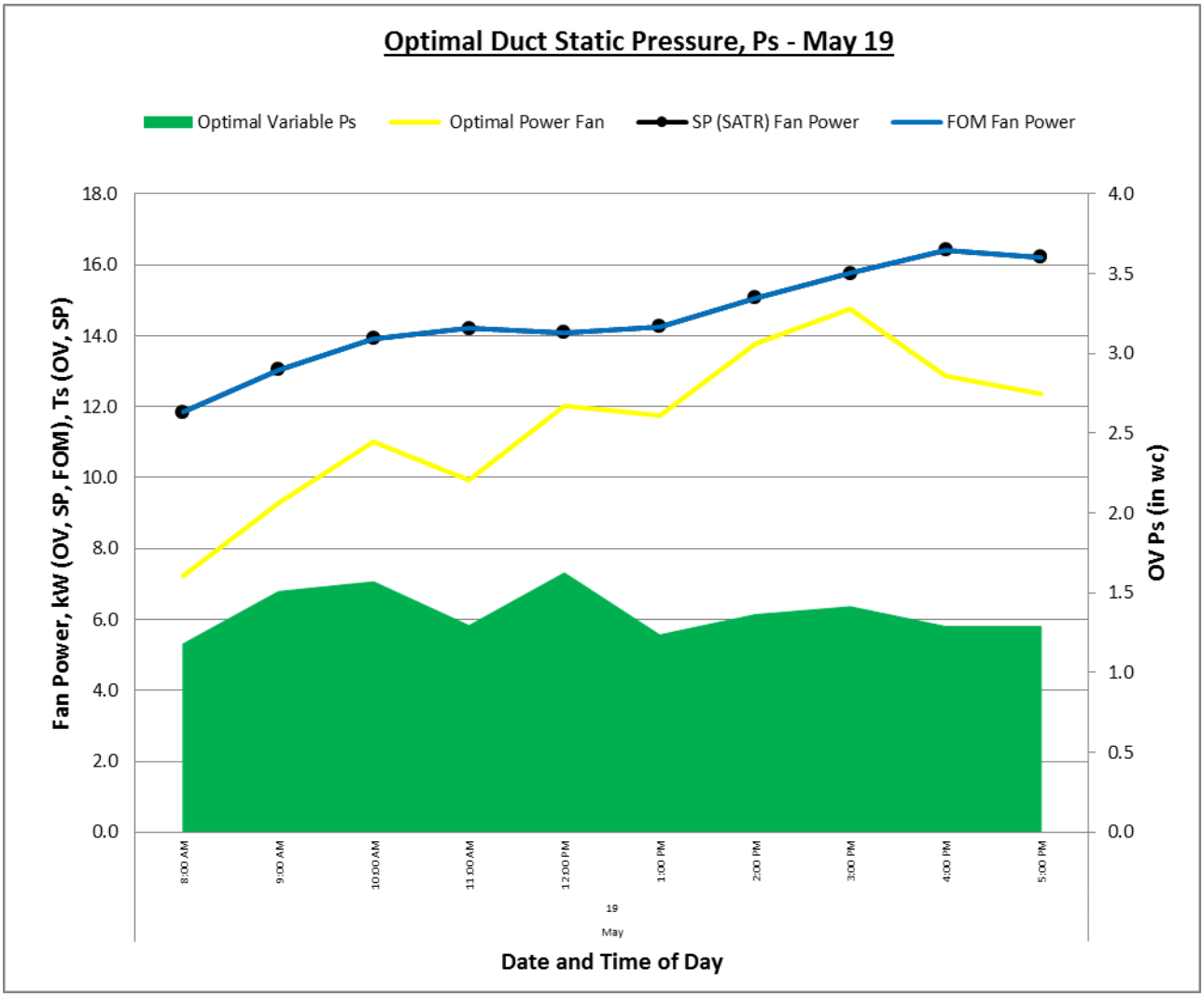

Figure 163. Optimal duct static pressure P_s (May 19).

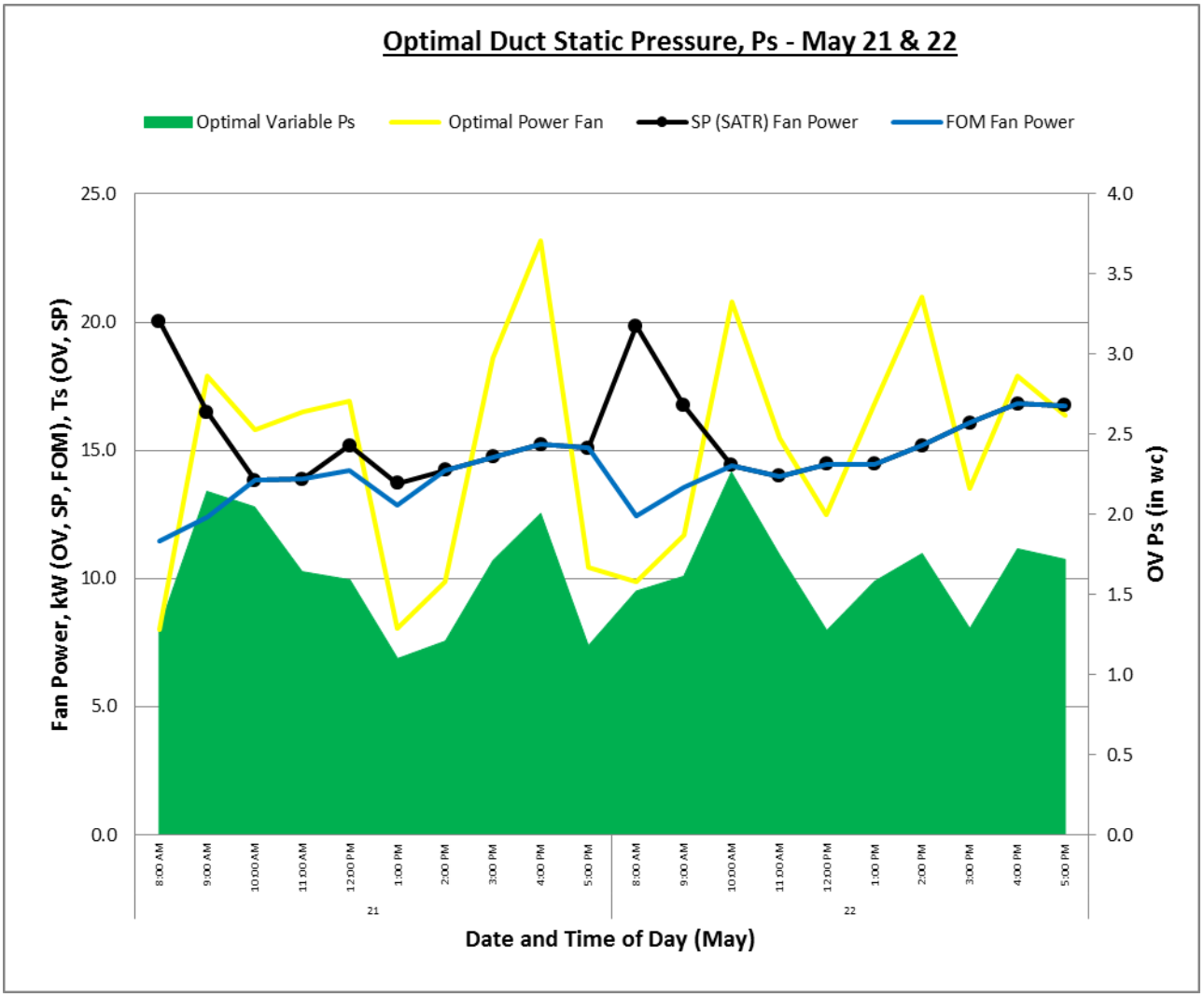

Figure 164. Optimal duct static pressure P_s (May 21 & 22).

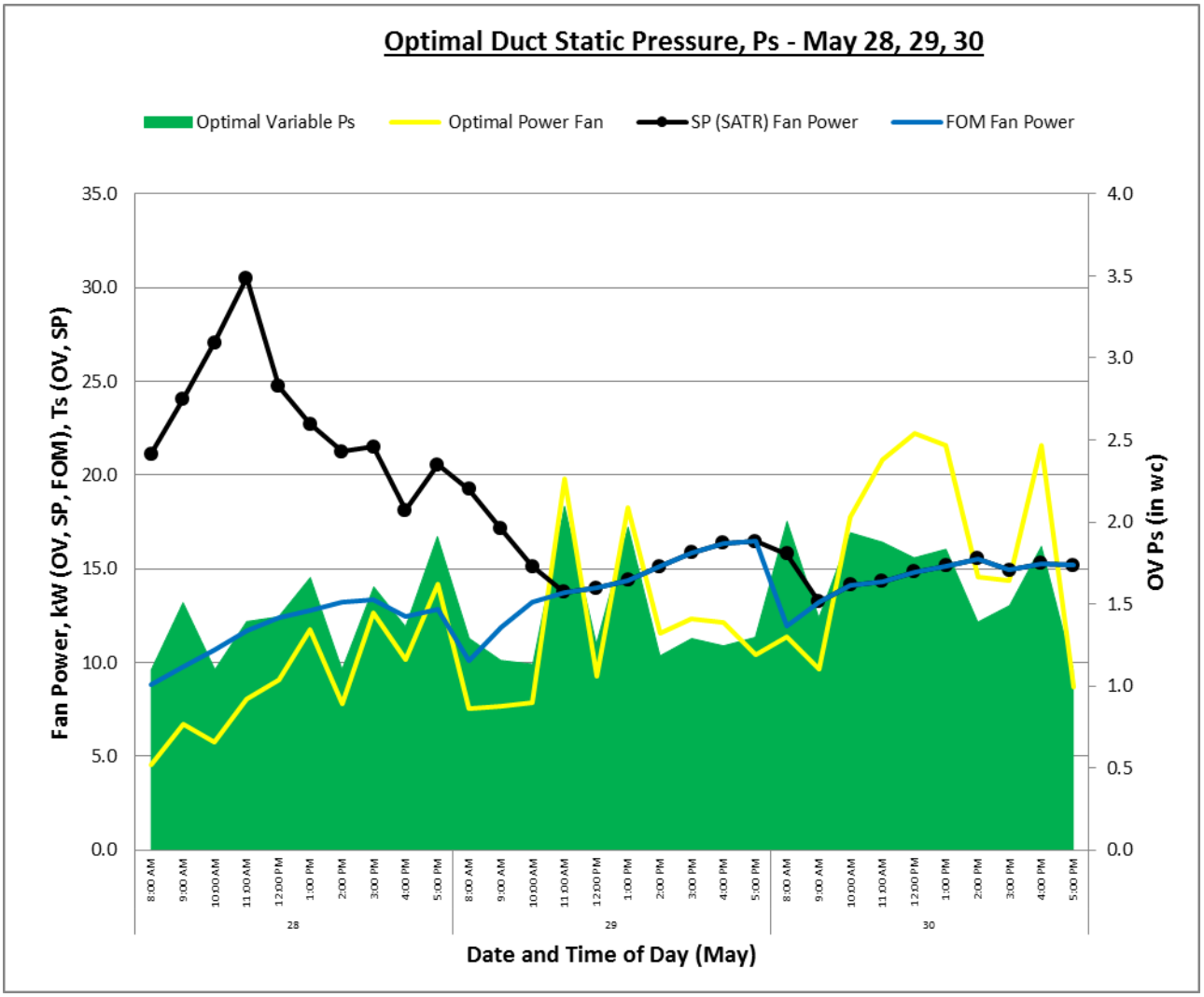

Figure 165. Optimal duct static pressure P_s (May 28, 29, 30).

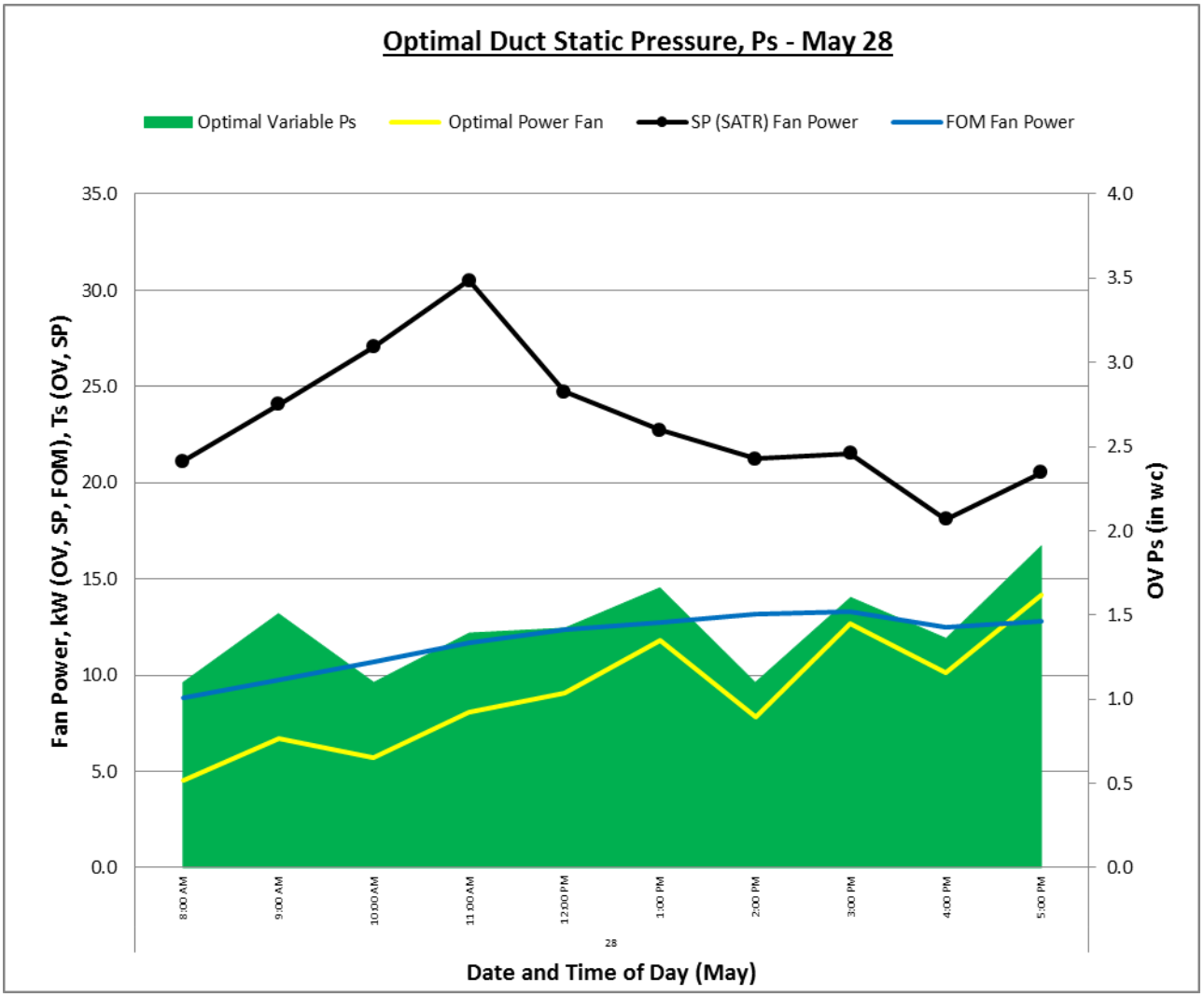

Figure 166. Optimal duct static pressure P_s (May 28).

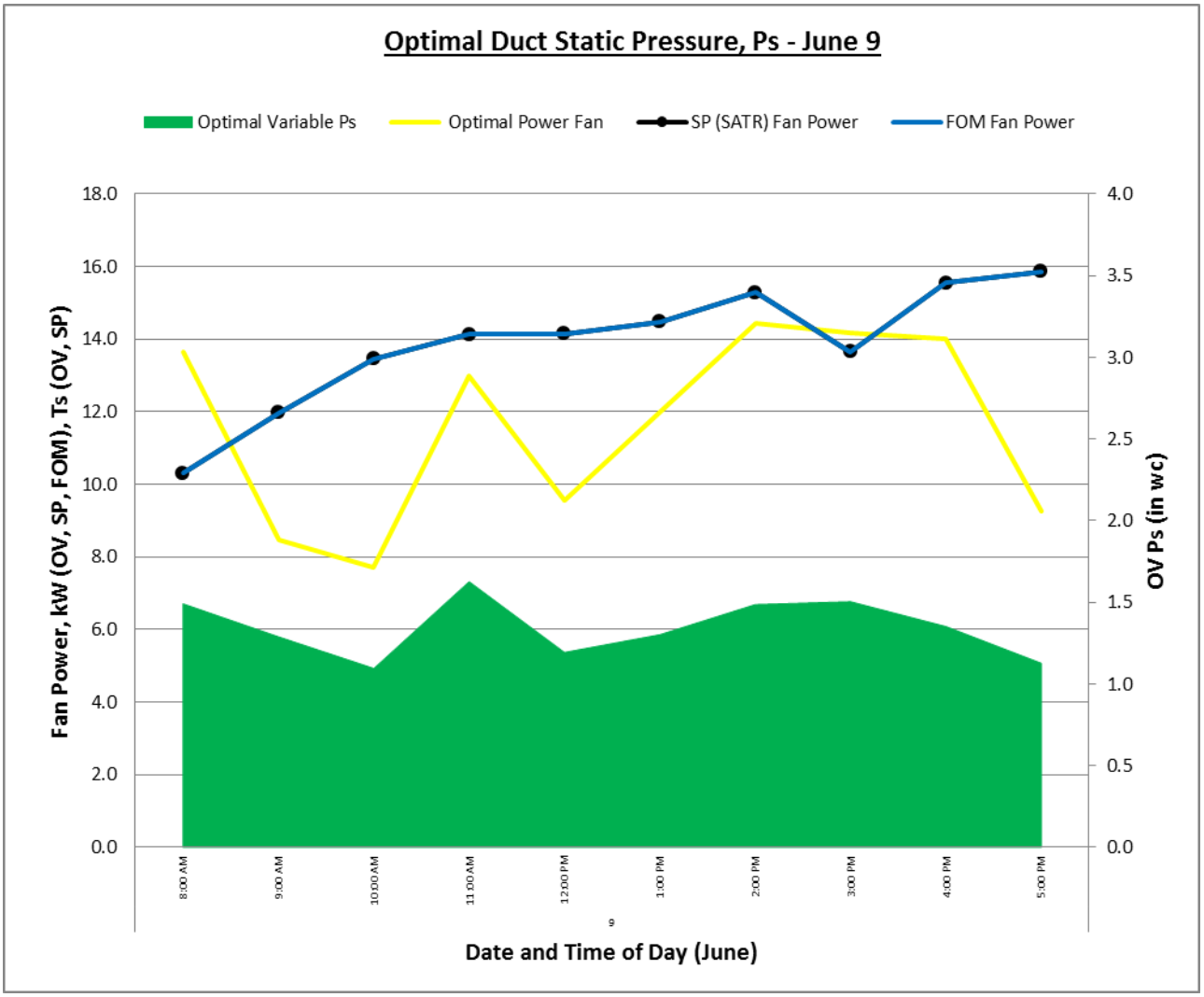

Figure 167. Optimal duct static pressure P_s (June 9).

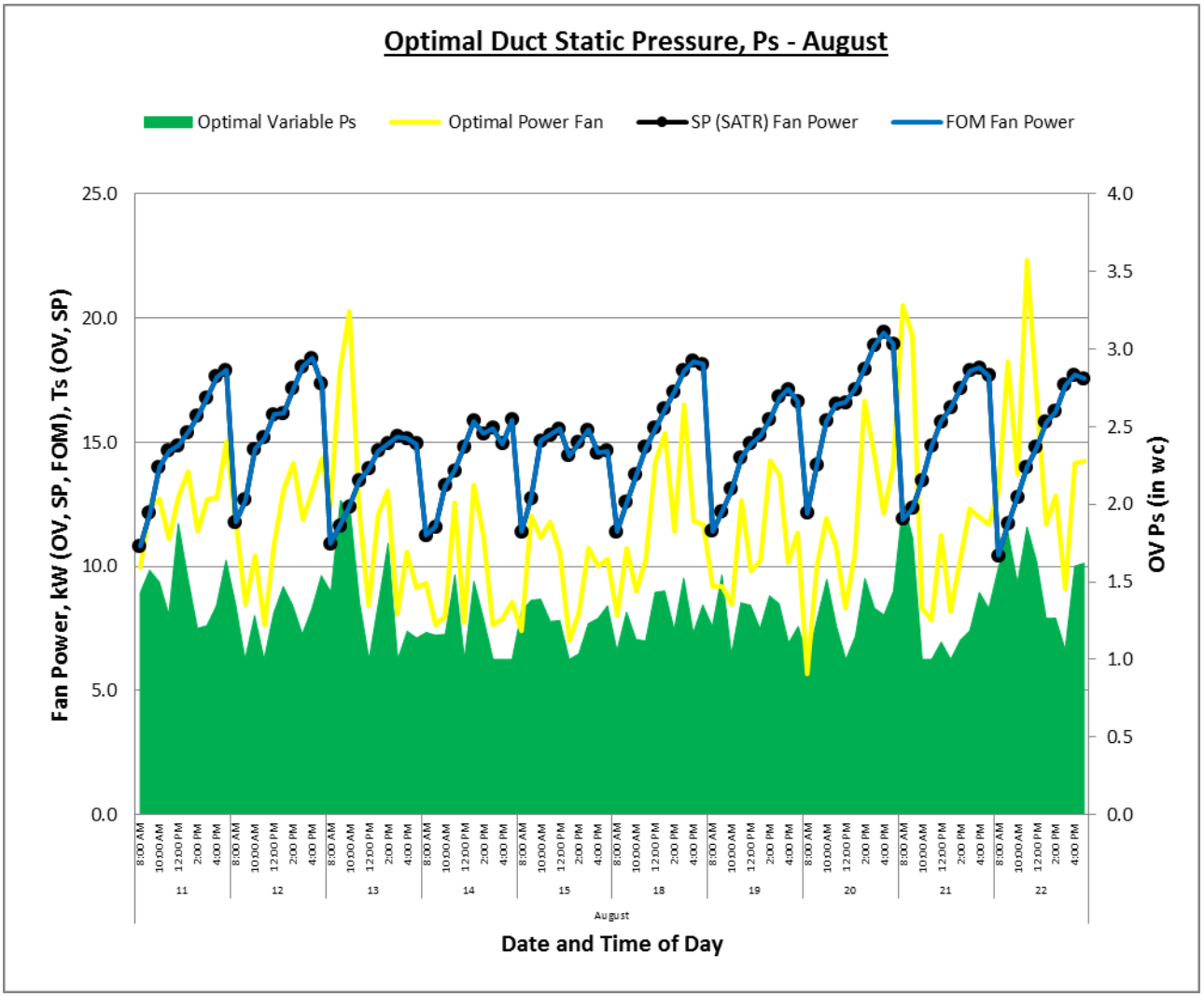

Figure 168. Optimal duct static pressure P_s (August).

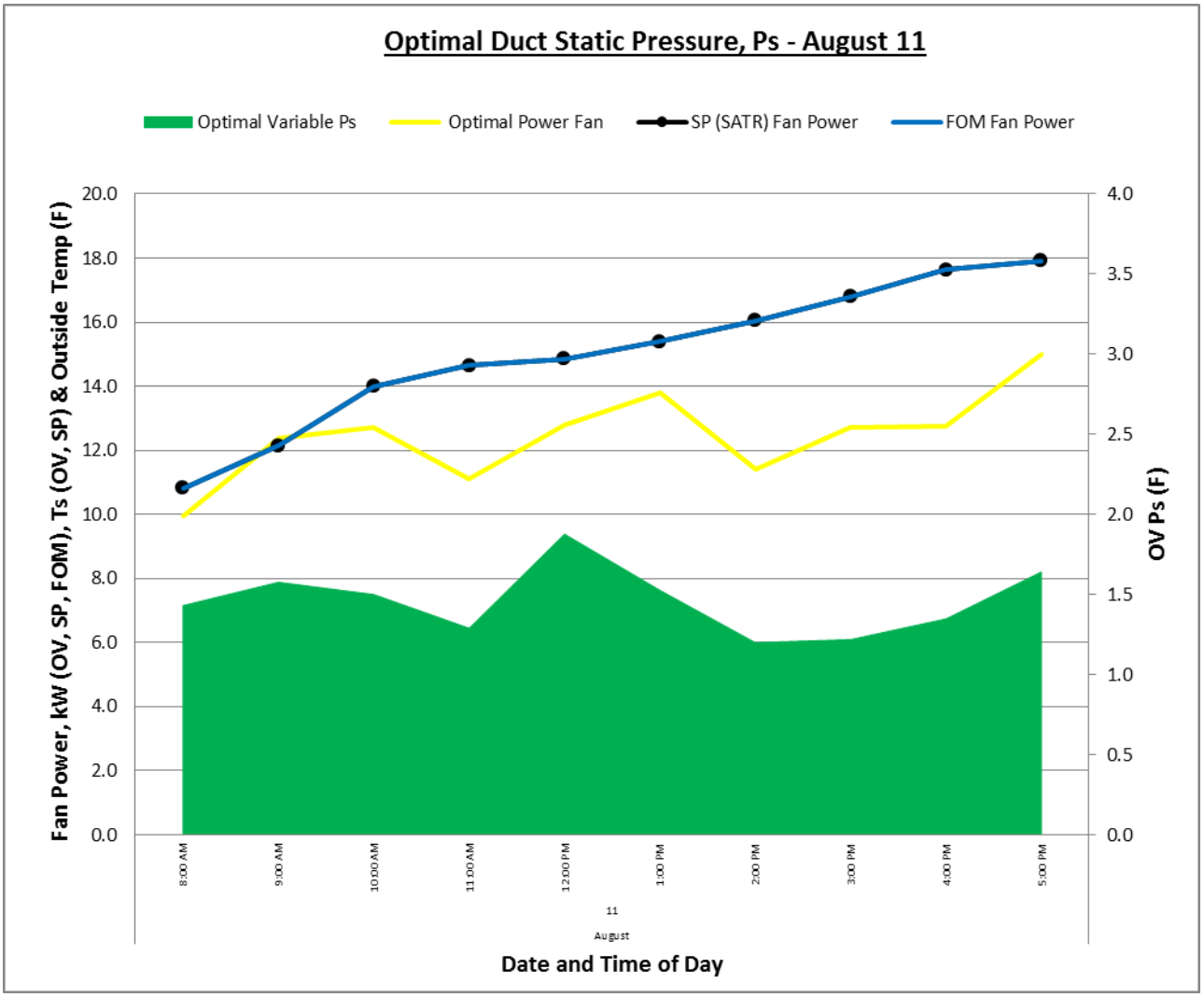

Figure 169. Optimal duct static pressure P_s (August 11).

E.10 OLSTOP Total Power Savings Comparison to SP & FOM Graphs.

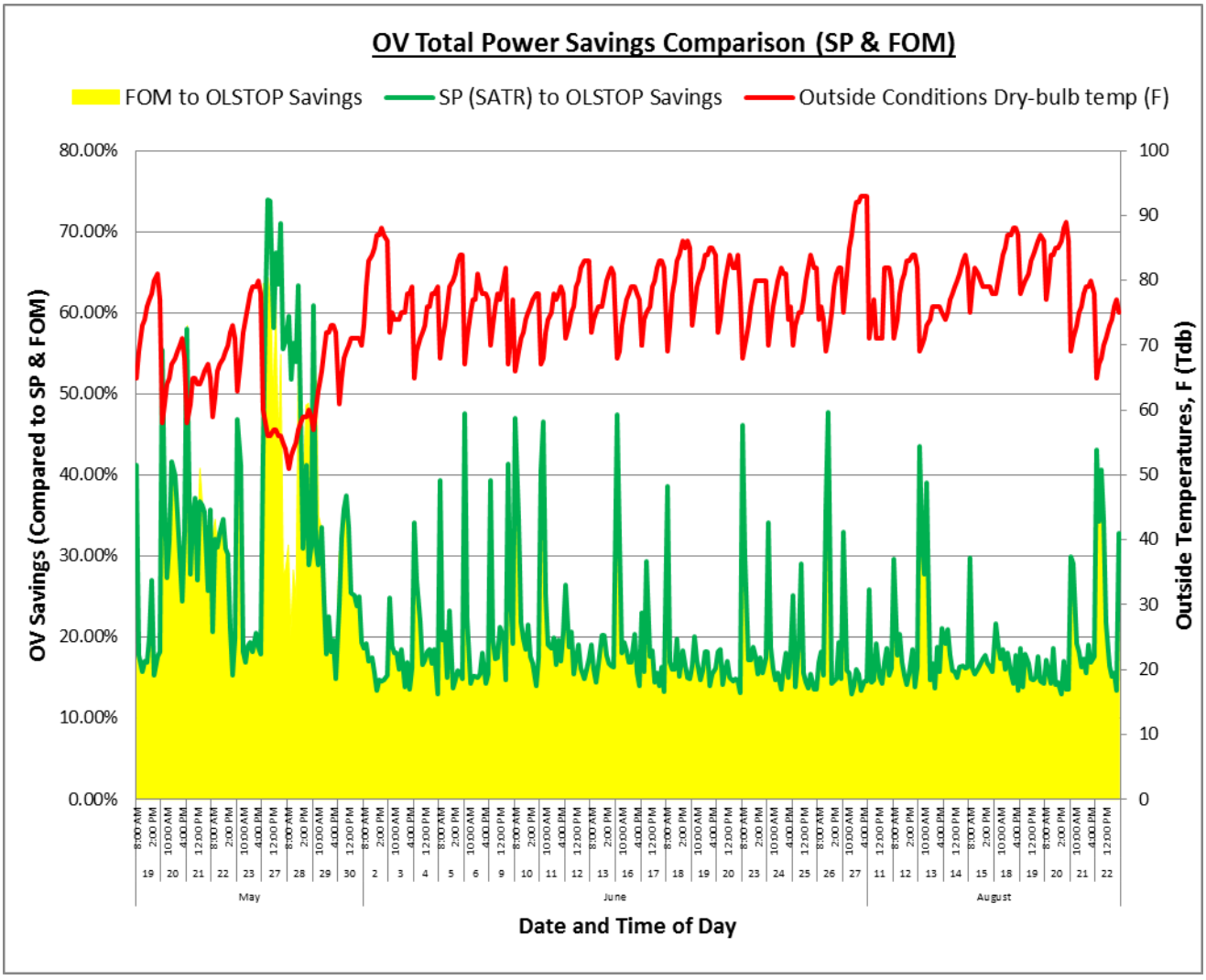

Figure 170. OLSTOP total power savings comparison (May, June, August).

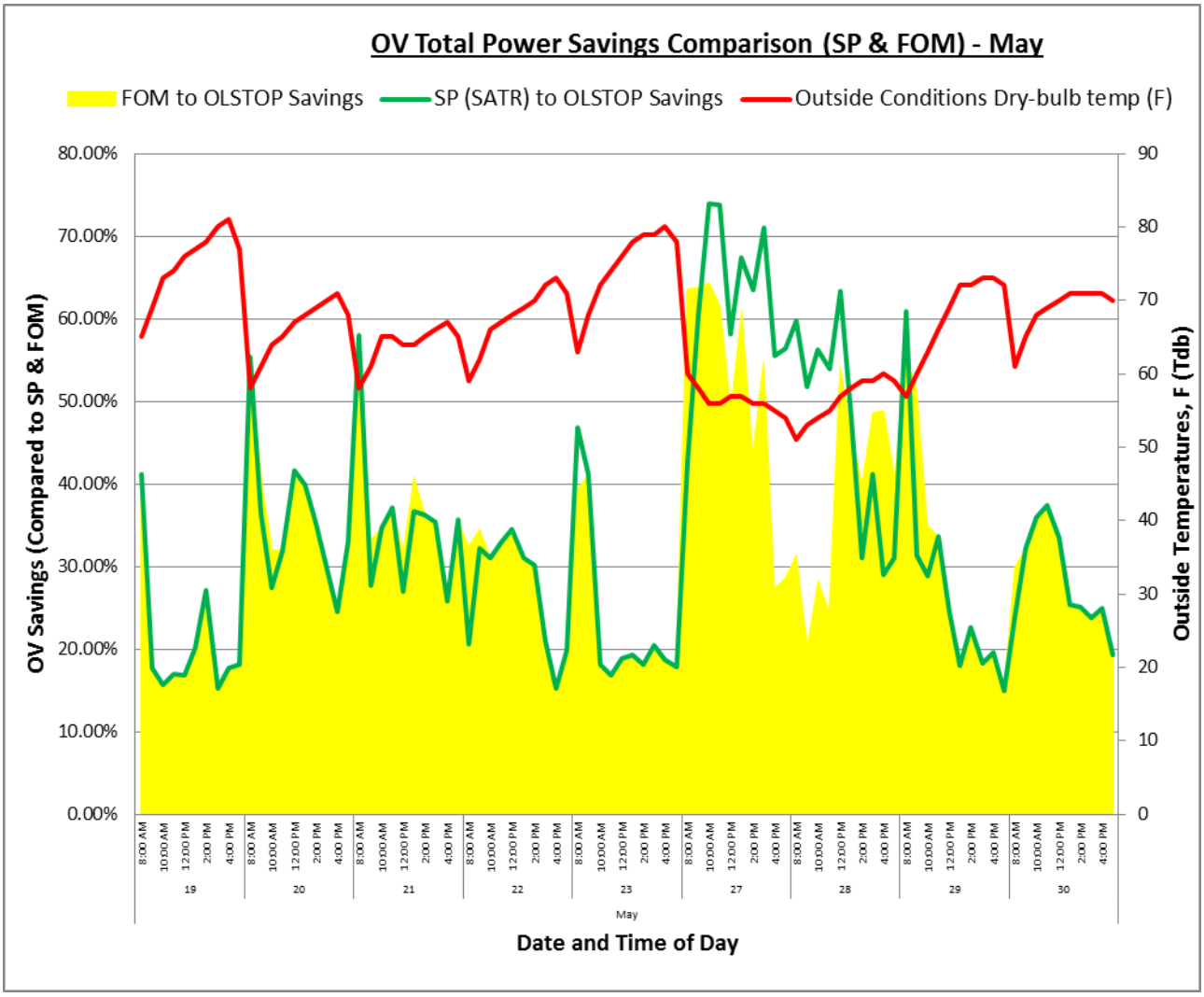

Figure 171. OLSTOP total power savings comparison (May).

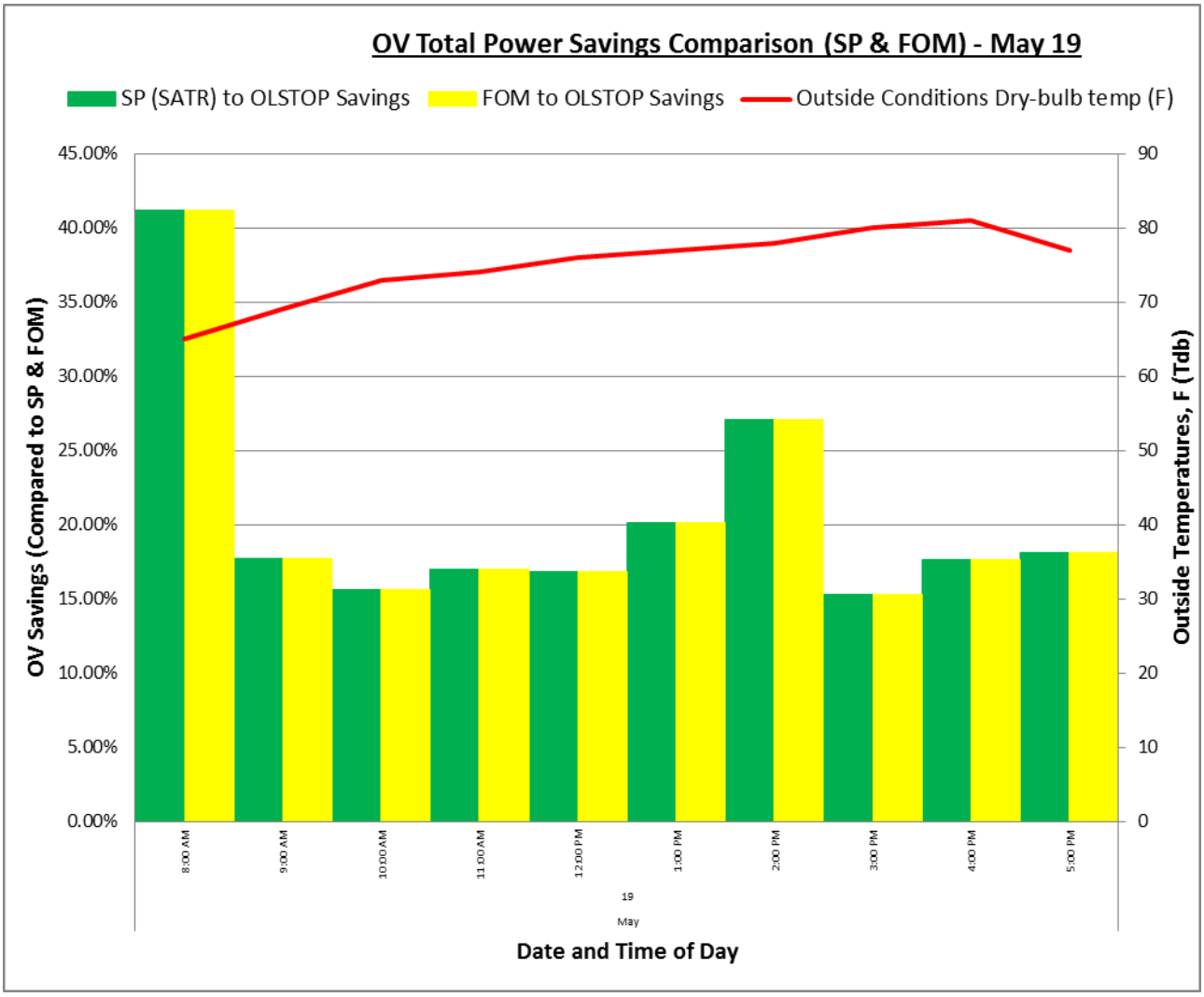

Figure 172. OLSTOP total power savings comparison (May 19).

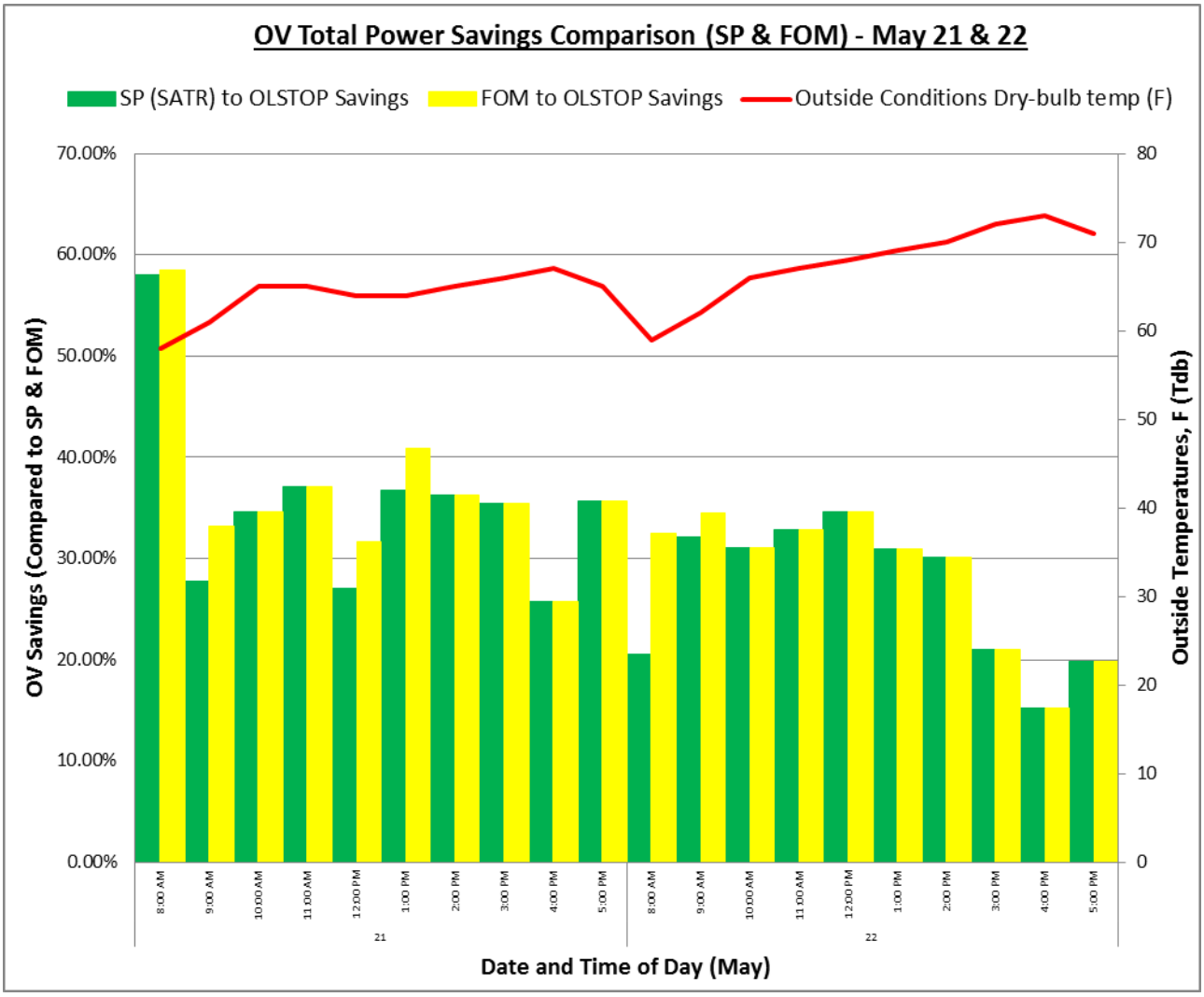

Figure 173. OLSTOP total power savings comparison (May 21 & 22).

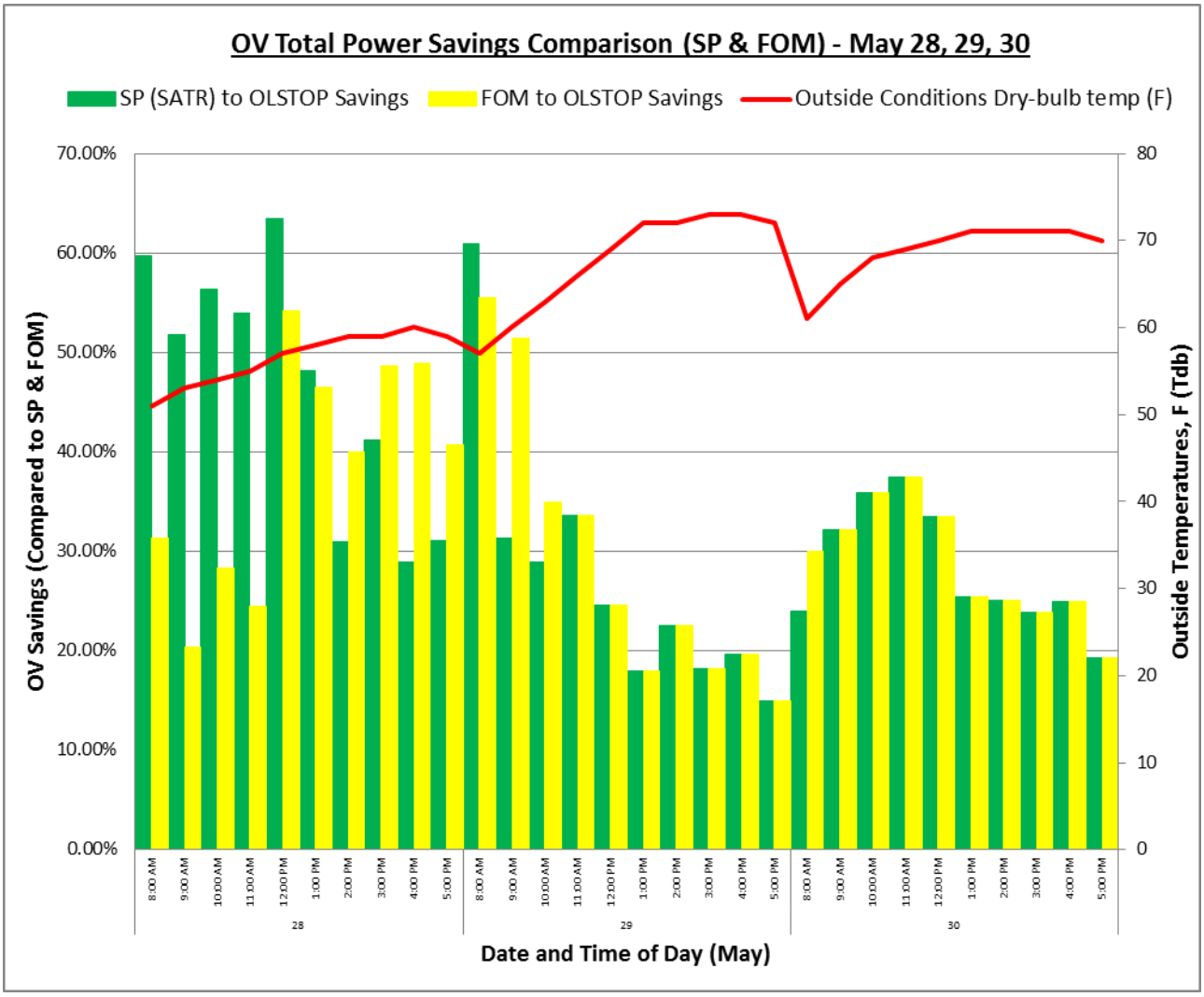

Figure 174. OLSTOP total power savings comparison (May 28, 29, 30).

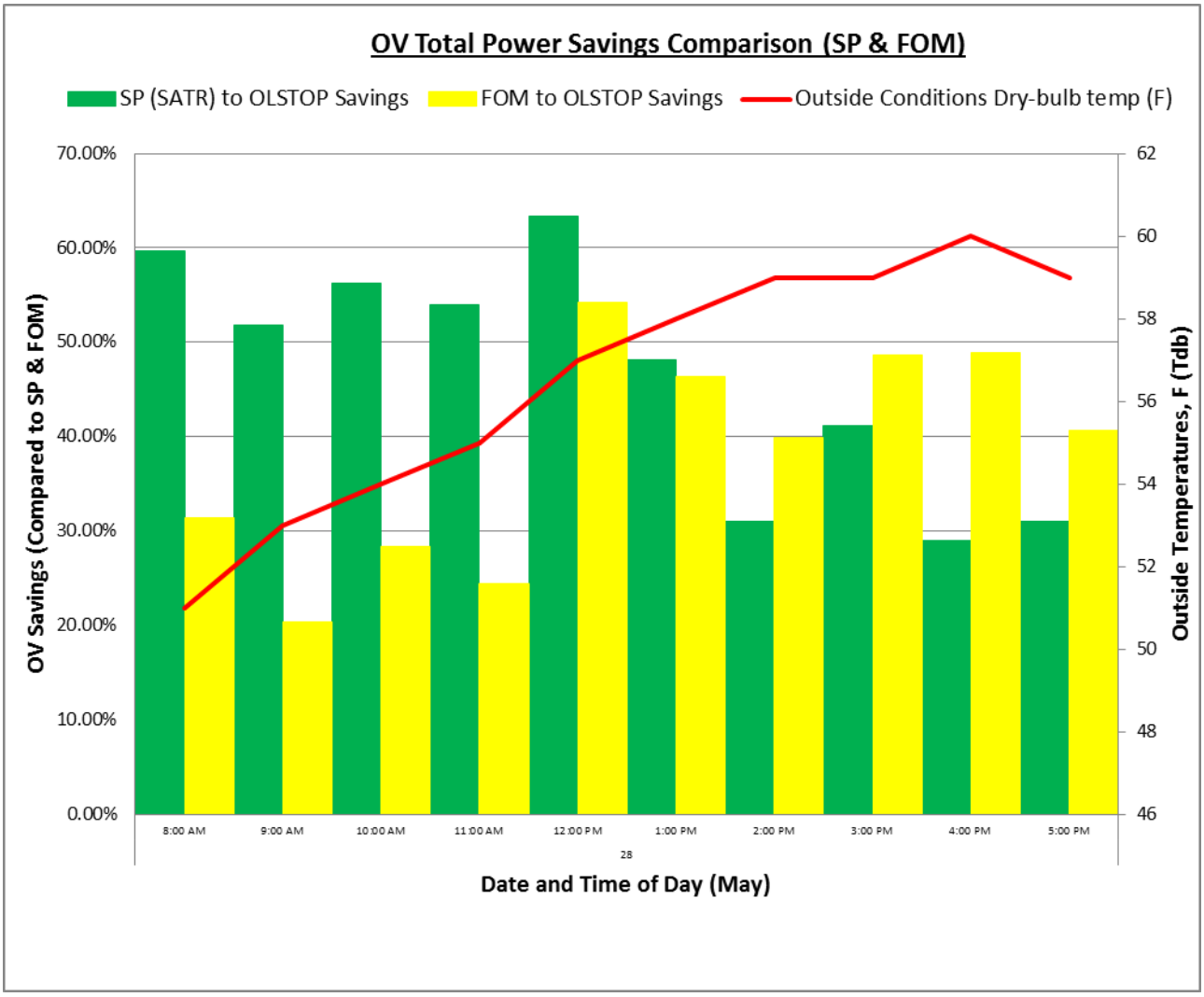

Figure 175. OLSTOP total power savings comparison (May 28).

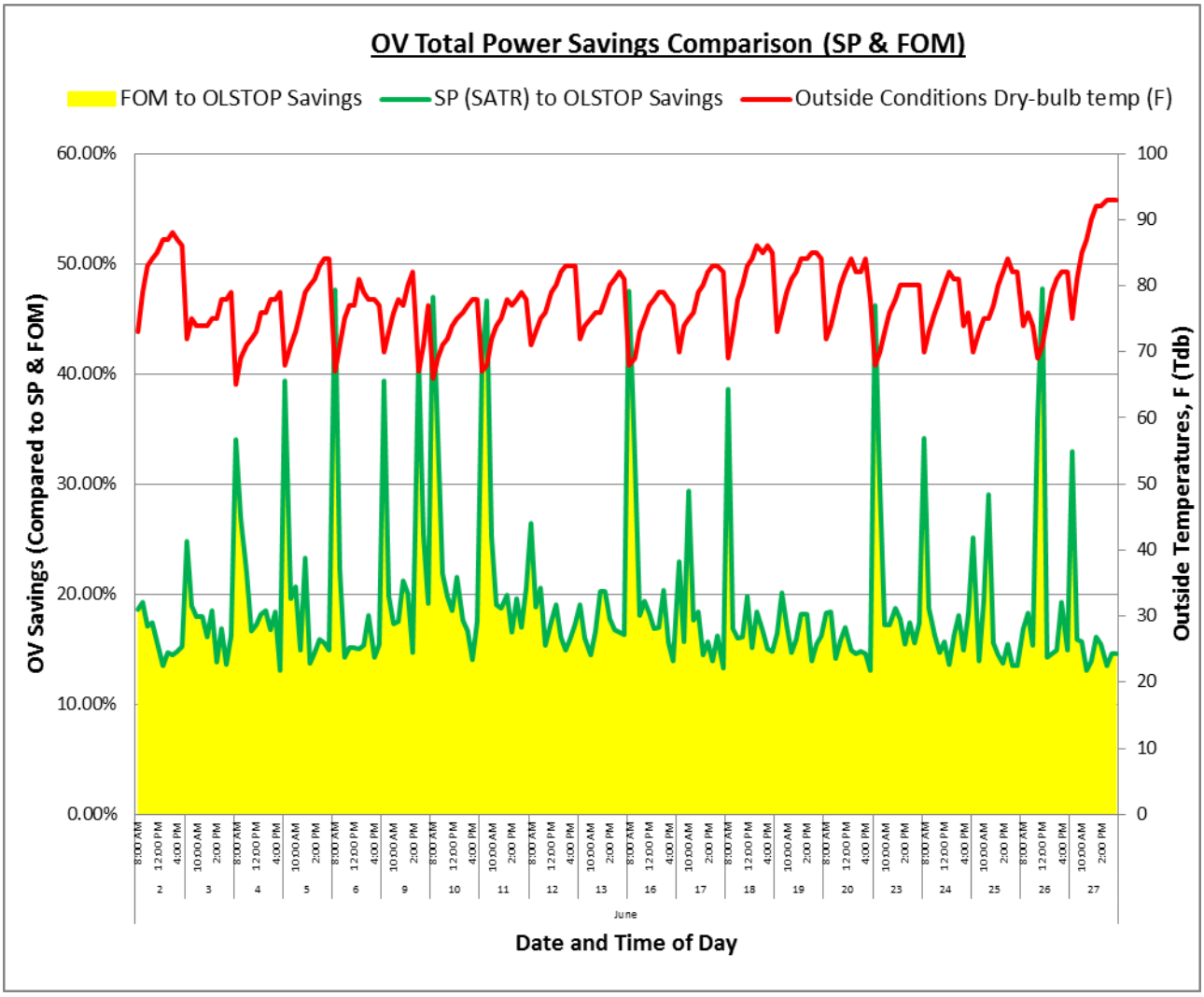

Figure 176. OLSTOP total power savings comparison (June).

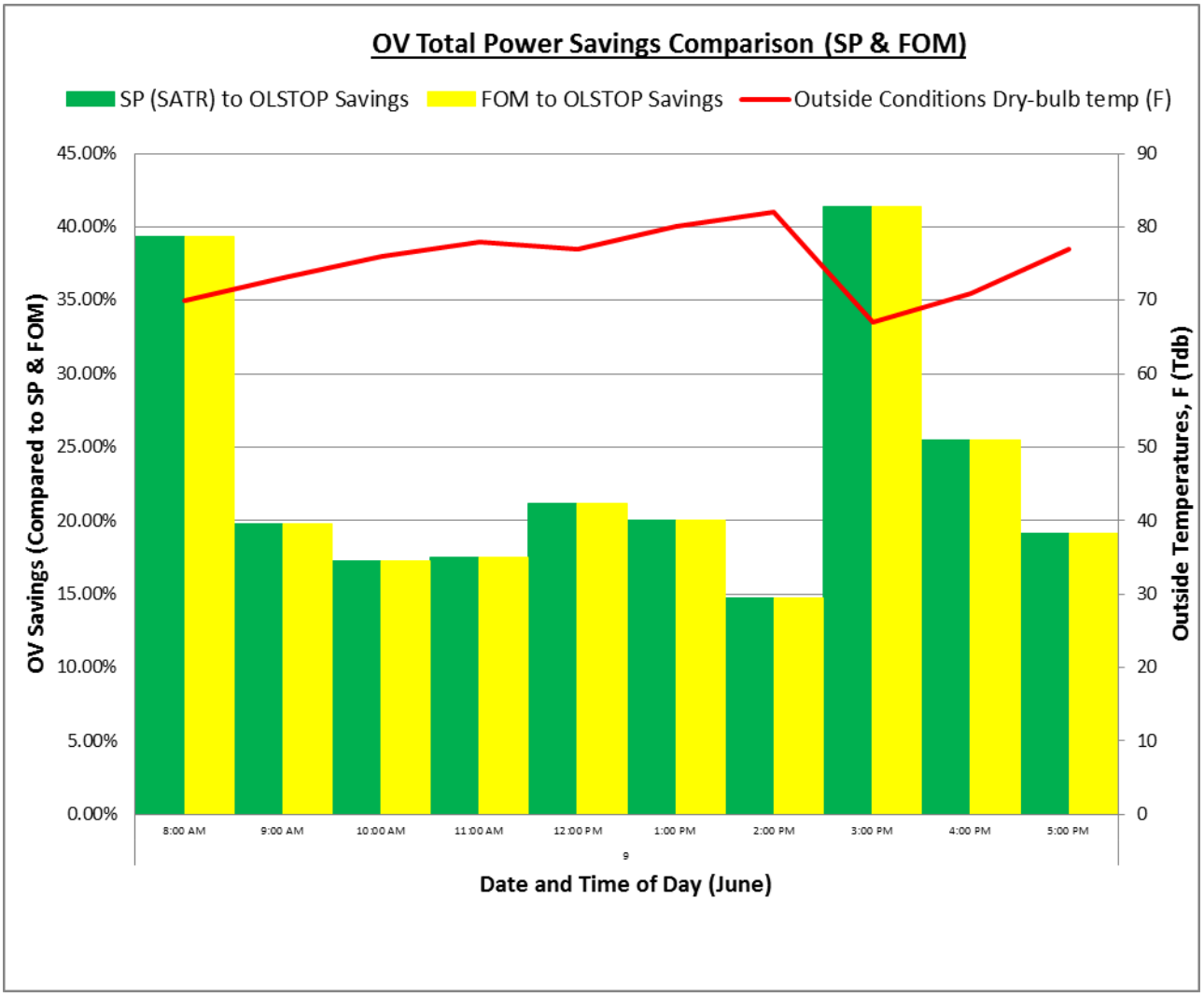

Figure 177. OLSTOP total power savings comparison (June 9).

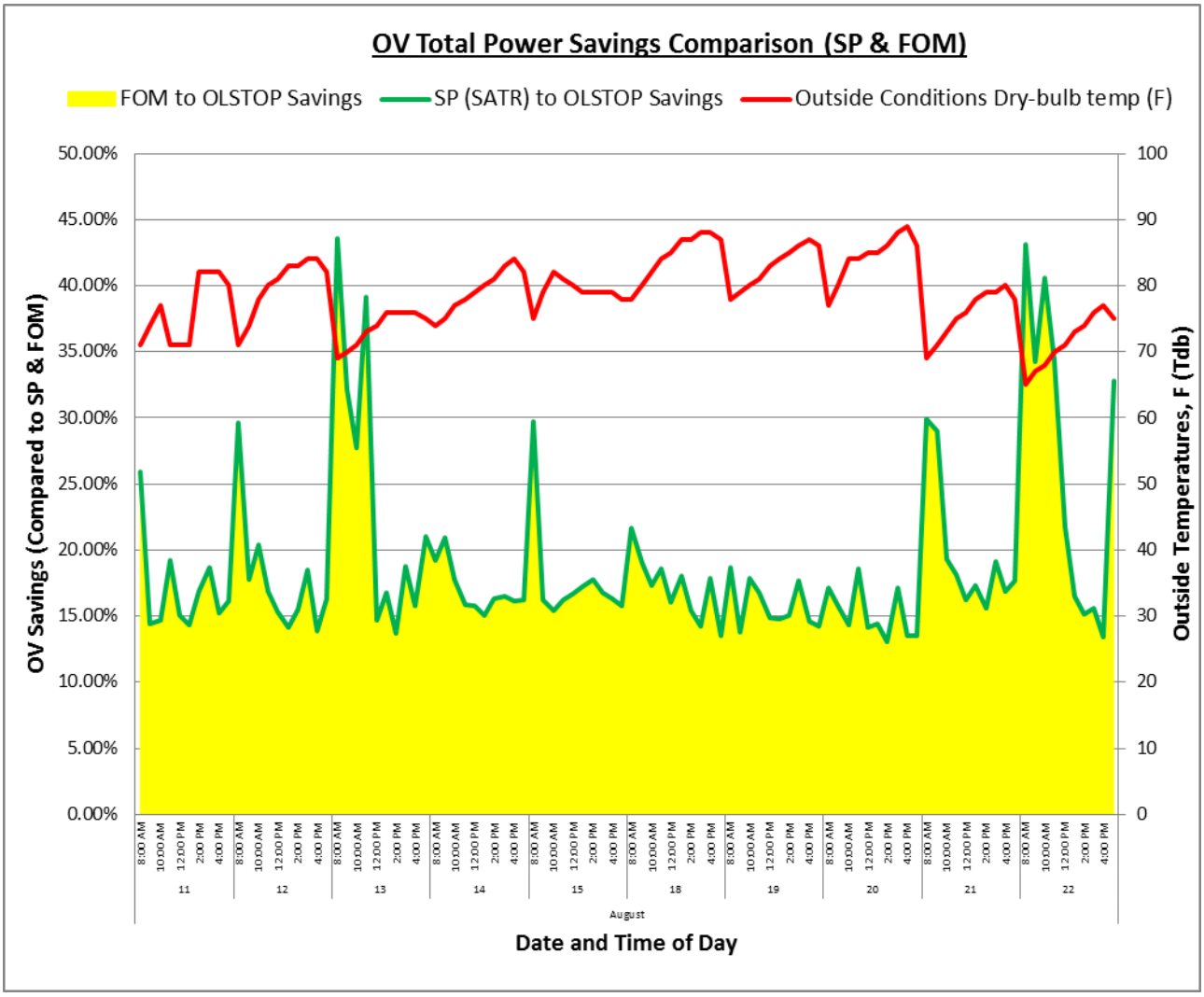

Figure 178. OLSTOP total power savings comparison (August).

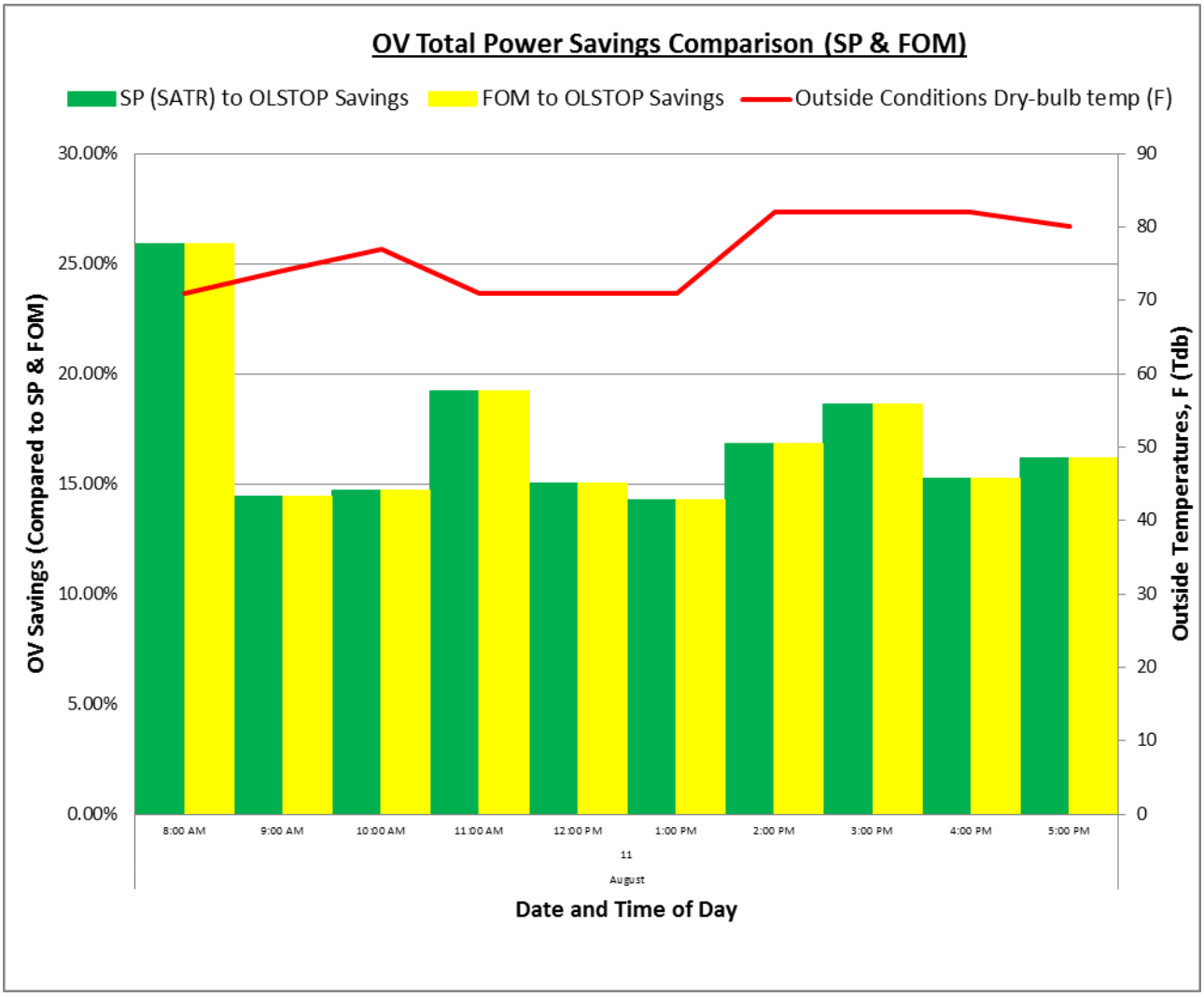

Figure 179. OLSTOP total power savings comparison (August 11).

E.11 OLSTOP Total Power Comparison (OV, SP & FOM) Graphs.

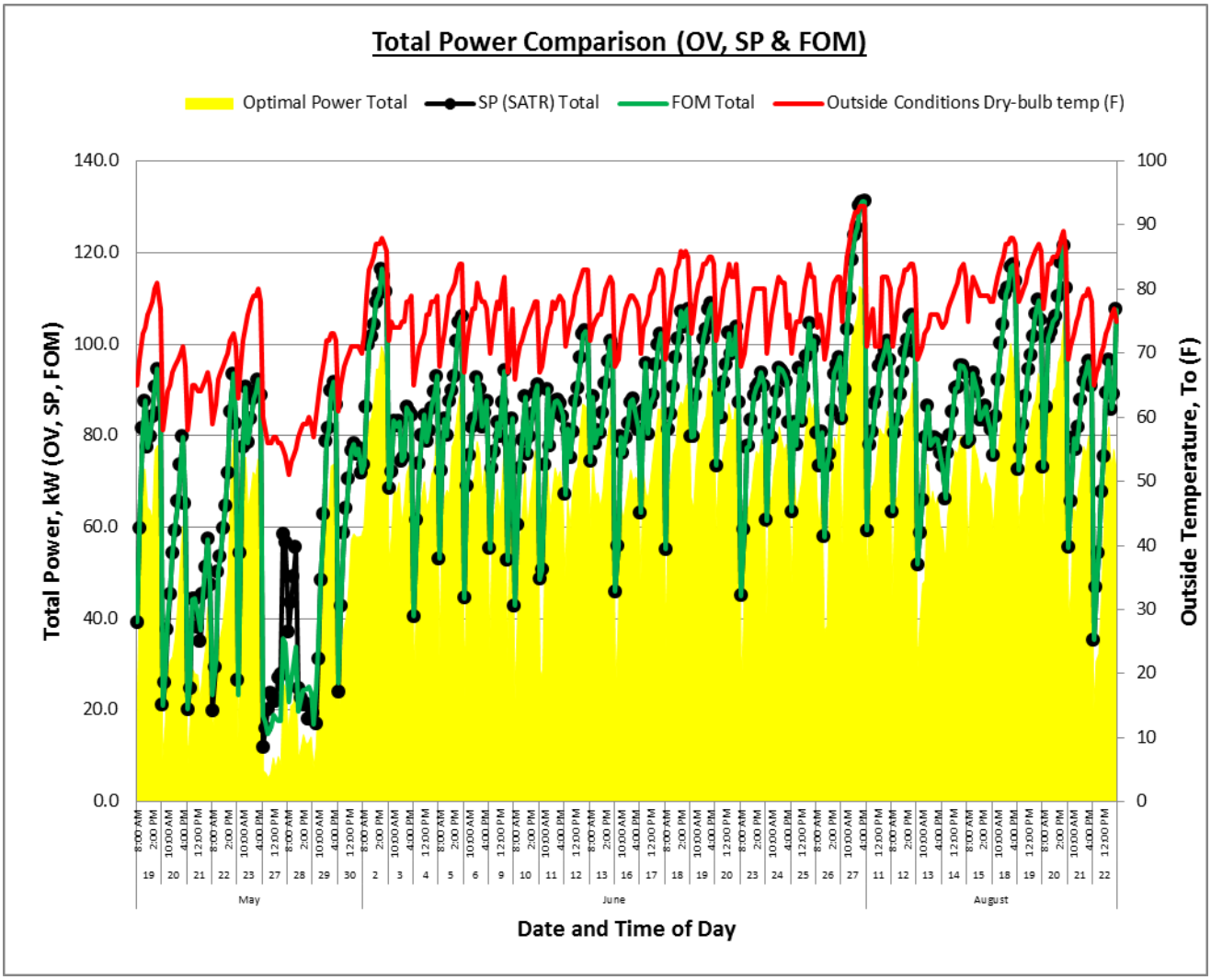

Figure 180. Total power comparison (May, June, August).

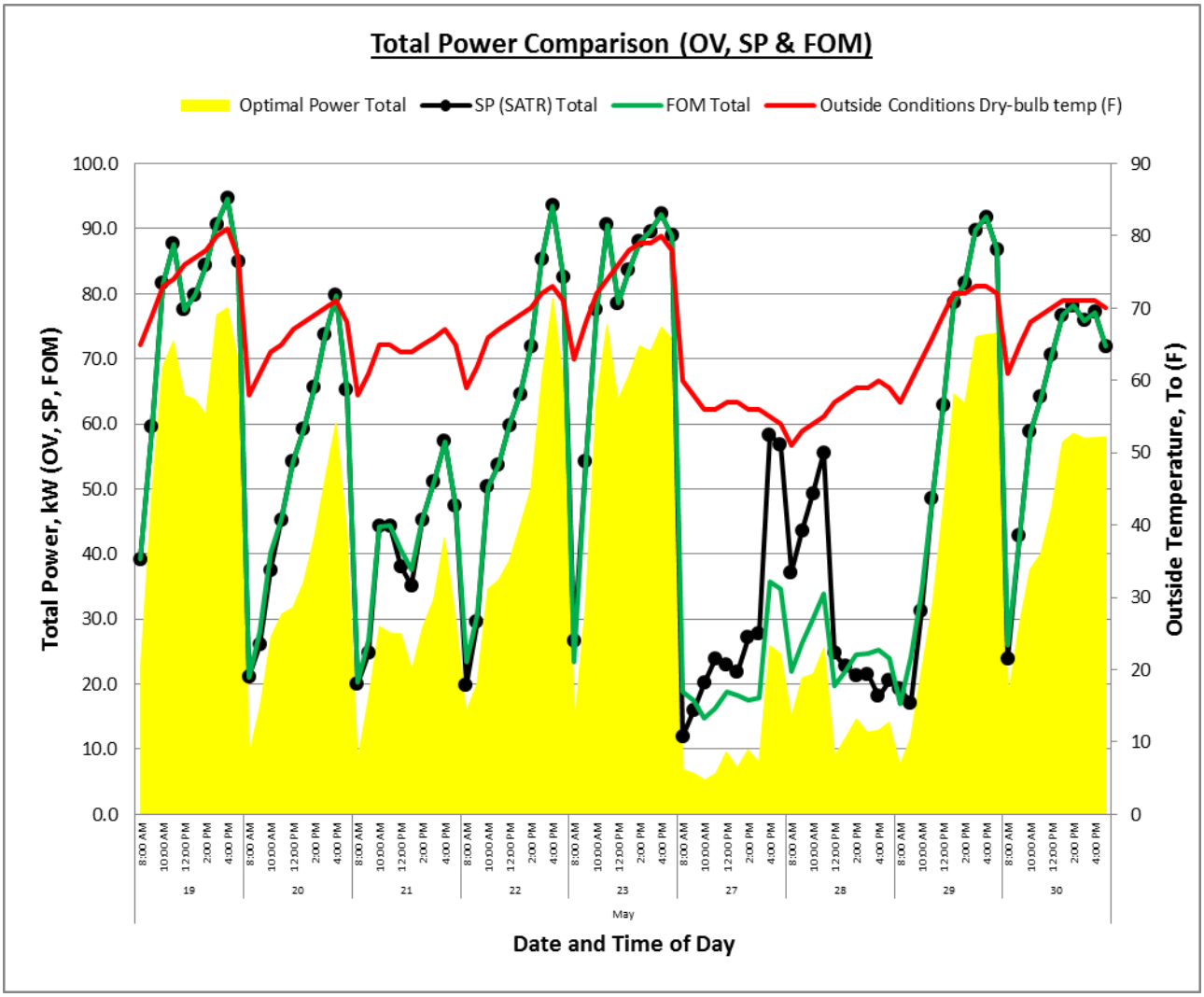

Figure 181. Total power comparison (May).

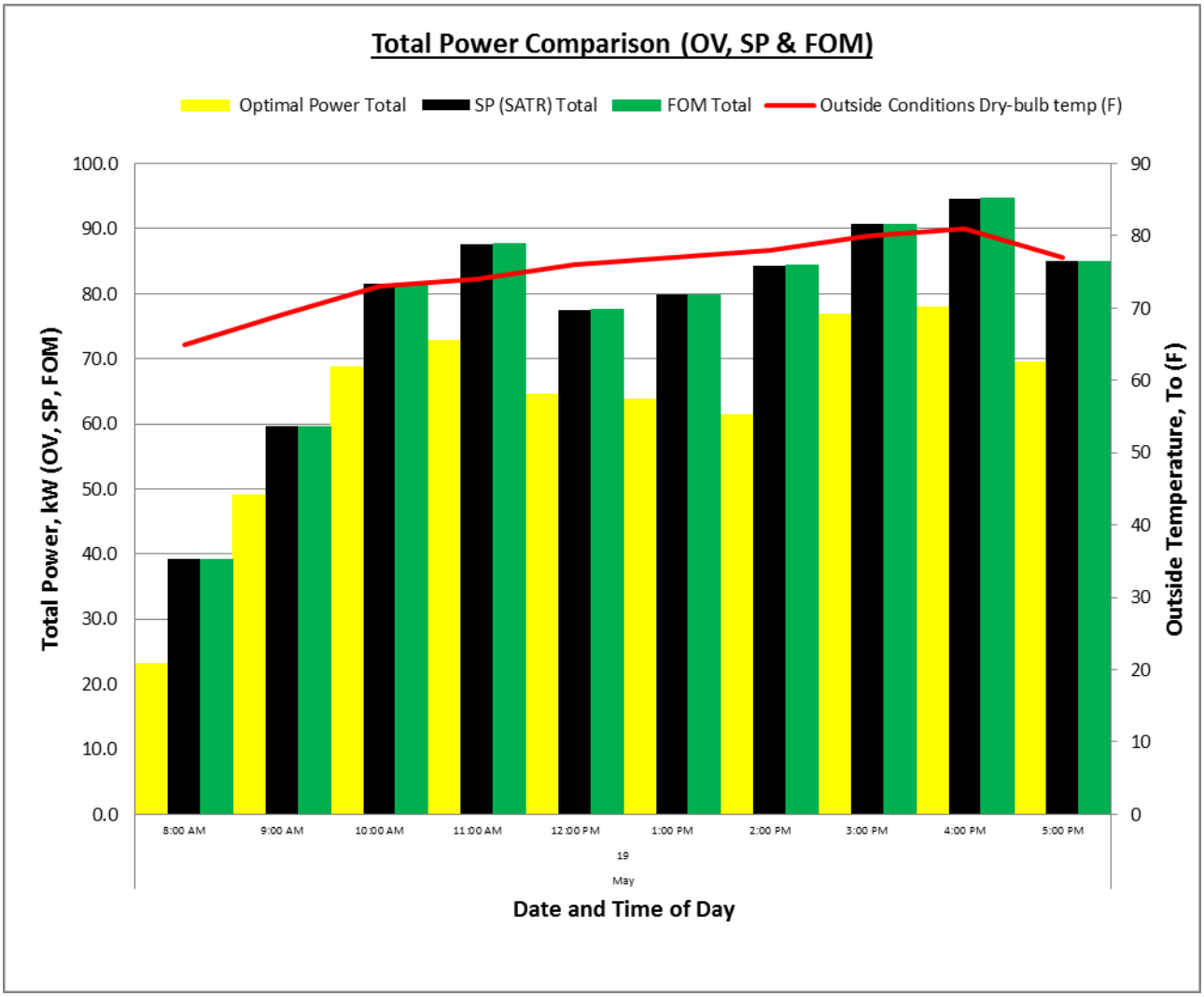

Figure 182. Total power comparison (May 19).

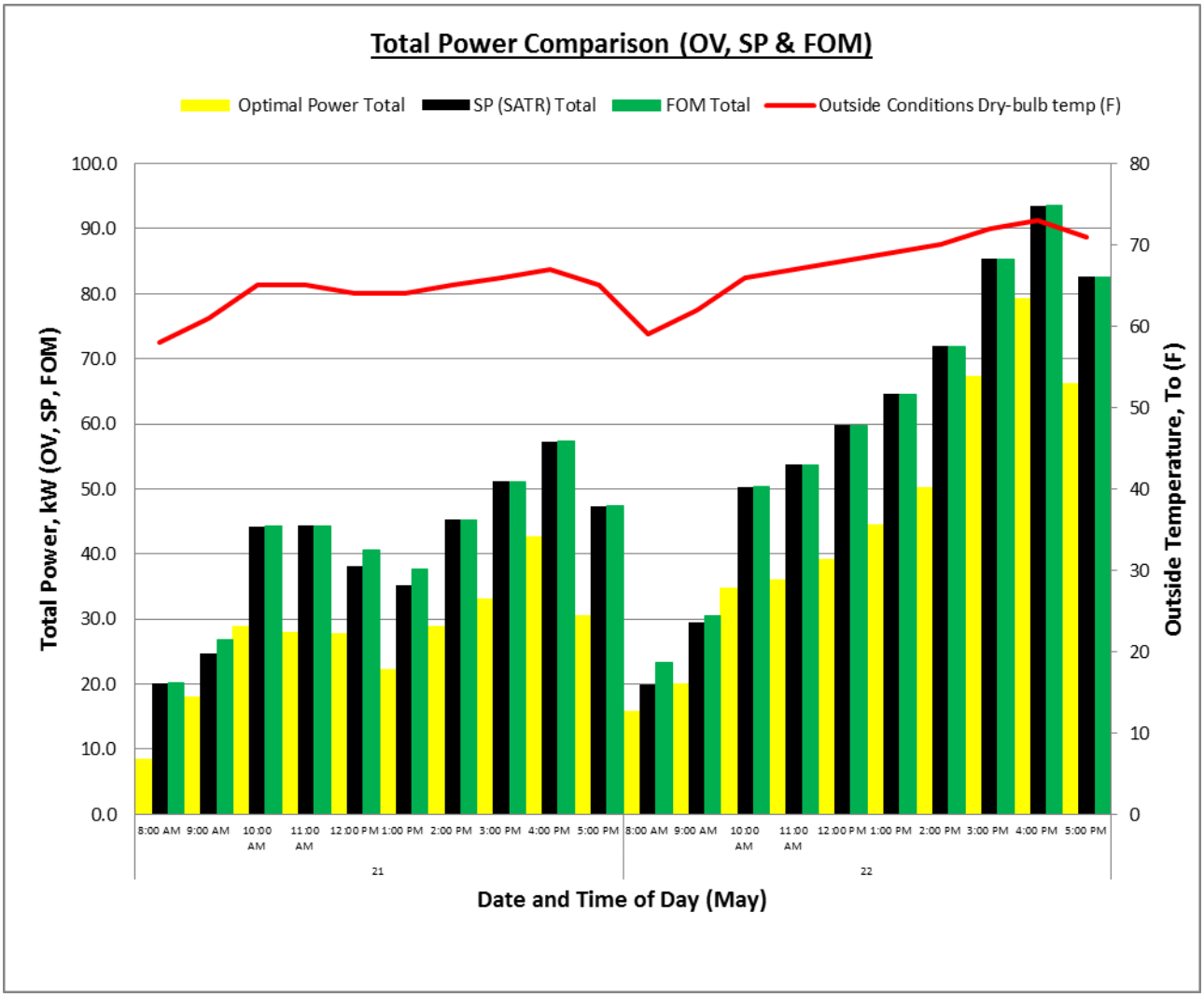

Figure 183. Total power comparison (May 21 & 22).

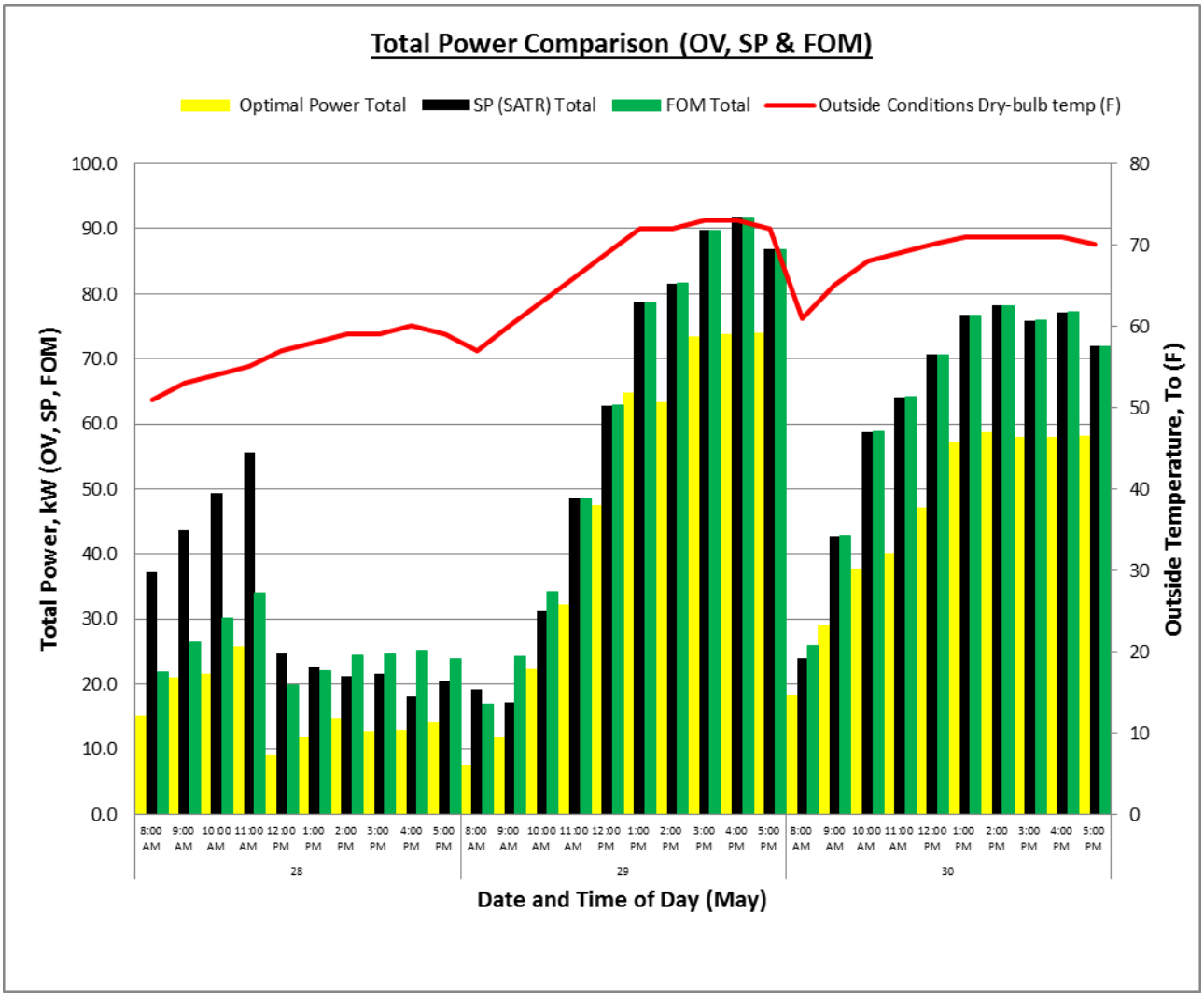

Figure 184. Total power comparison (May 28, 29, 30).

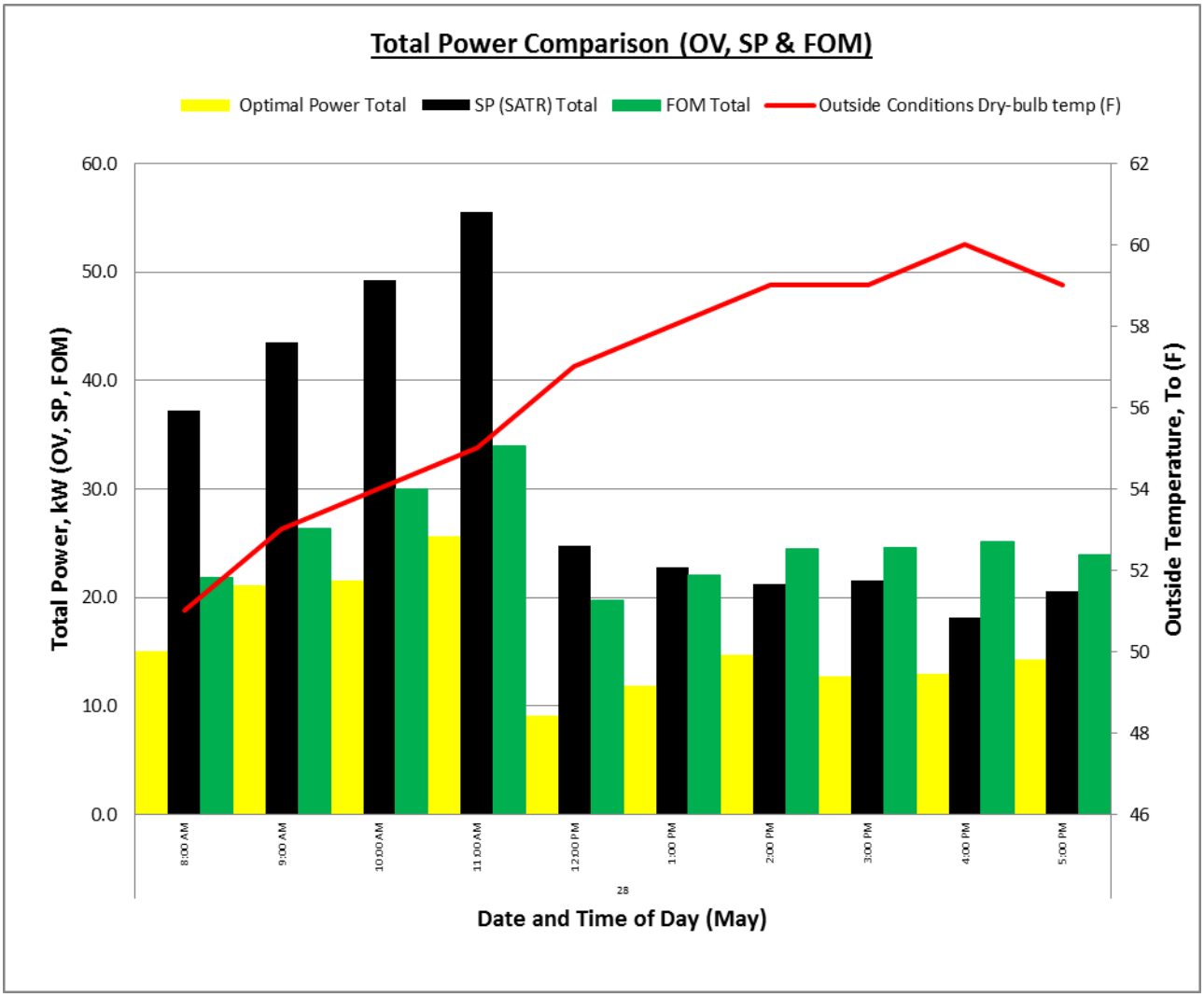

Figure 185. Total power comparison (May 28).

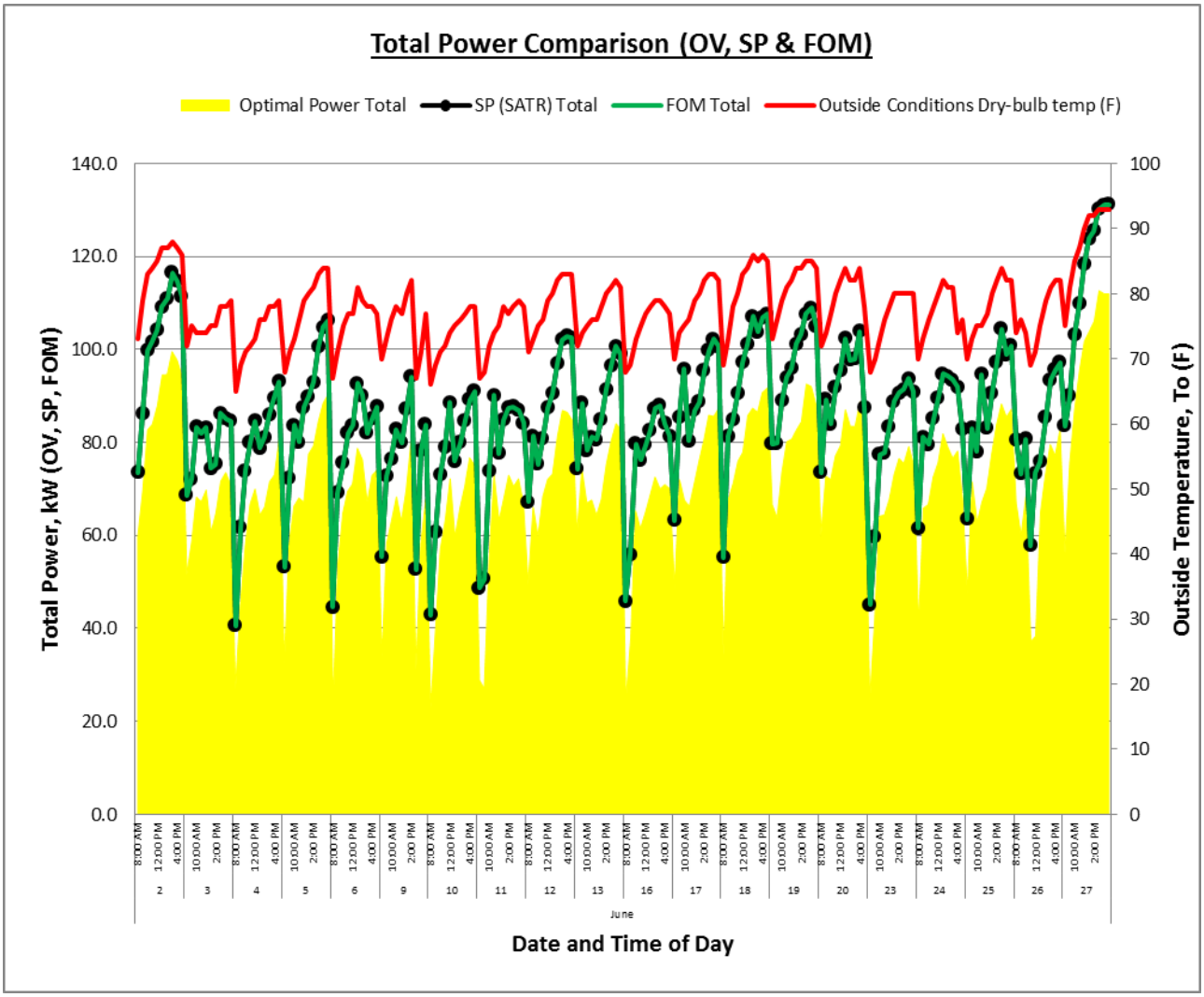

Figure 186. Total power comparison (June).

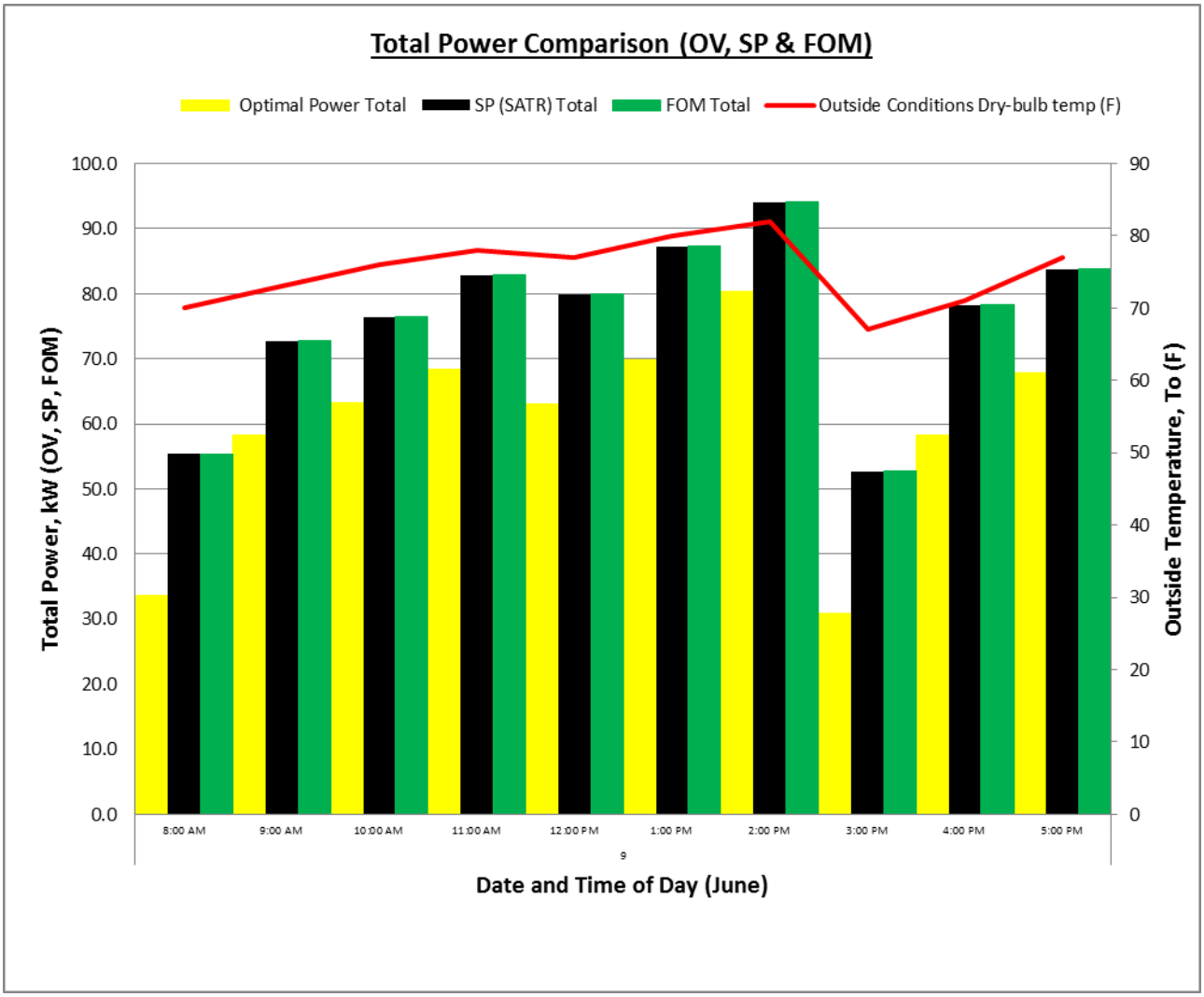

Figure 187. Total power comparison (June 9).

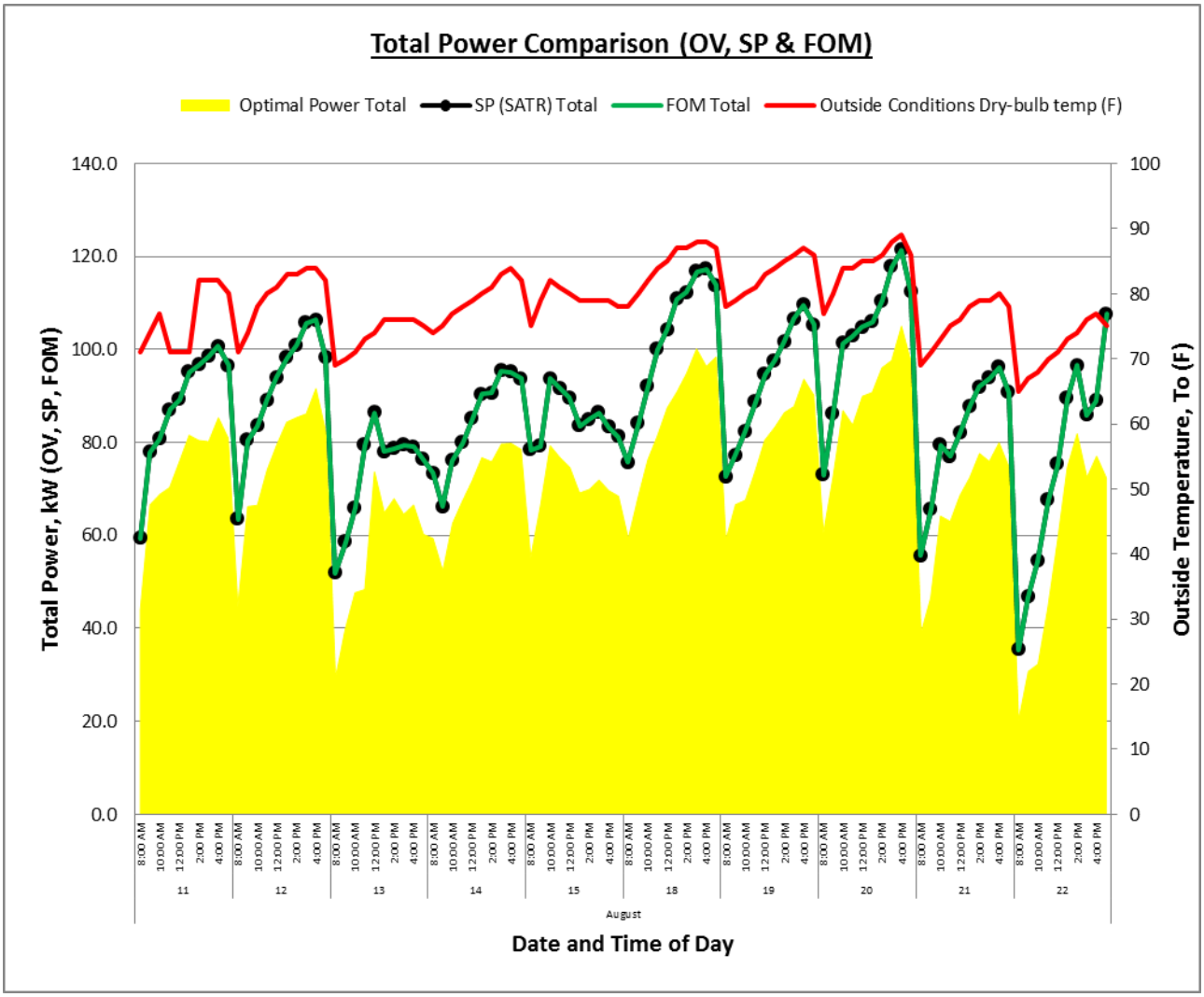

Figure 188. Total power comparison (August).

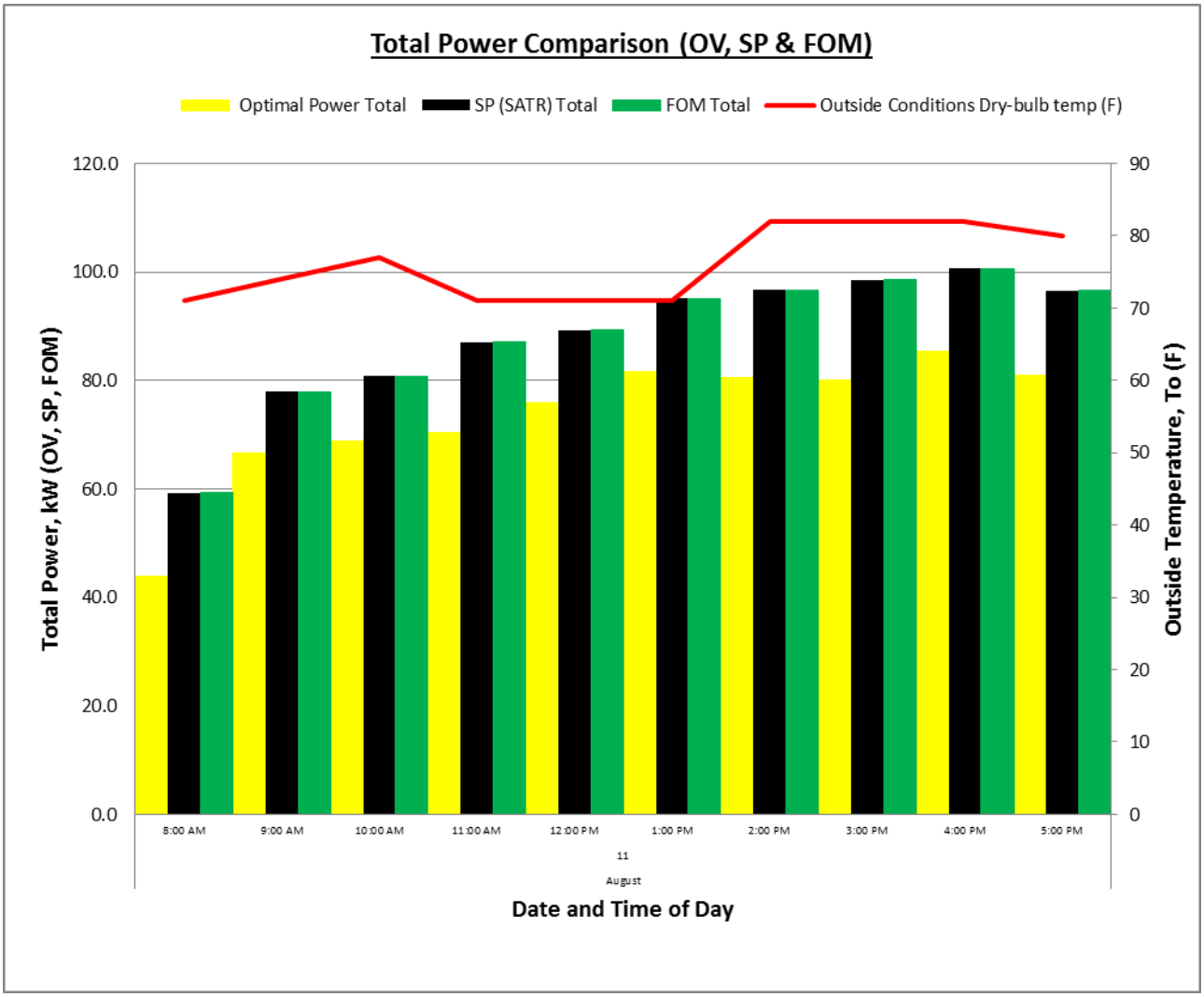

Figure 189. Total power comparison (August 11).

E.12 Q_{sys} and Q_o Comparison (OV & FOM) Graphs.

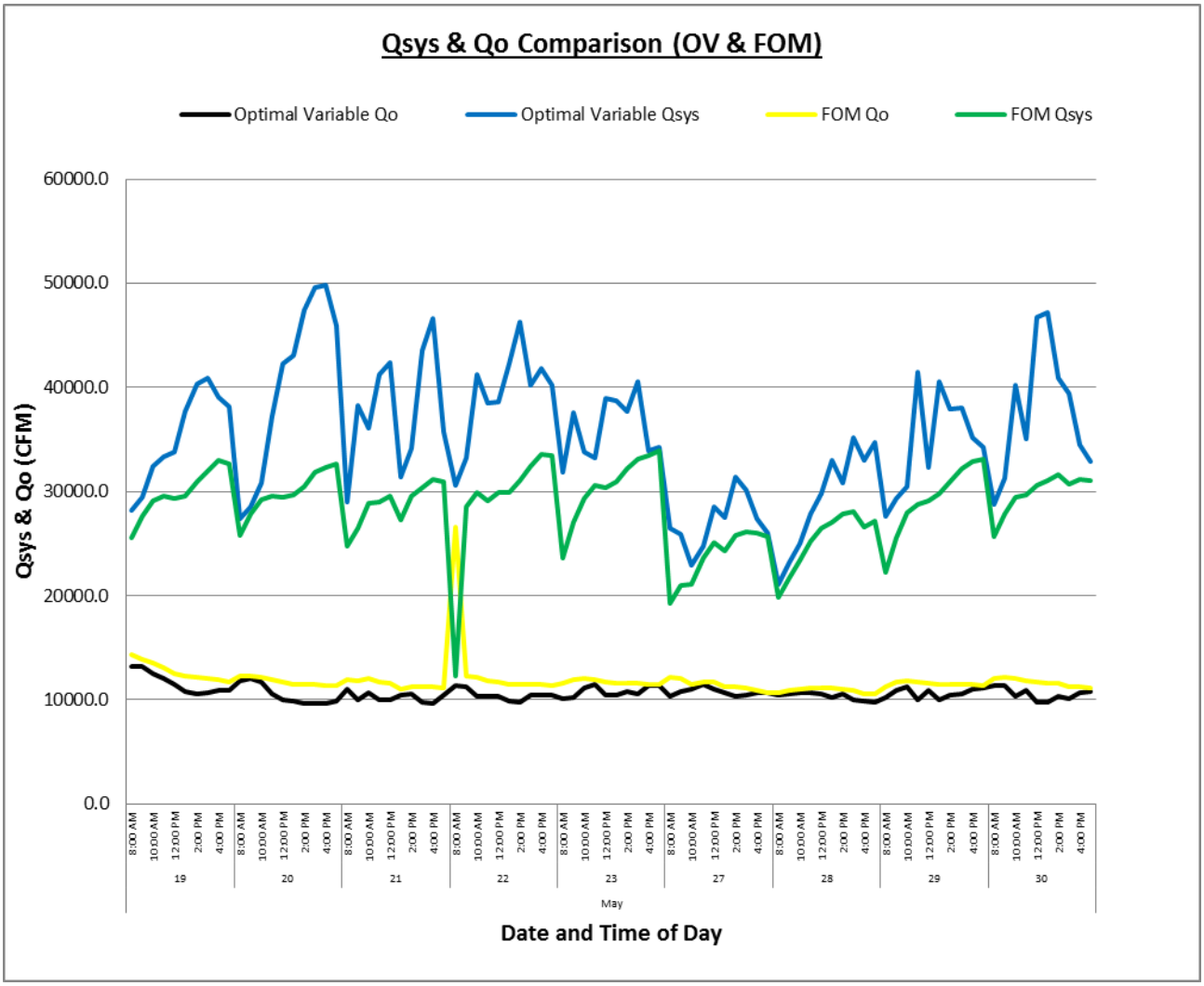

Figure 190. Q_{sys} & Q_o comparison (May).

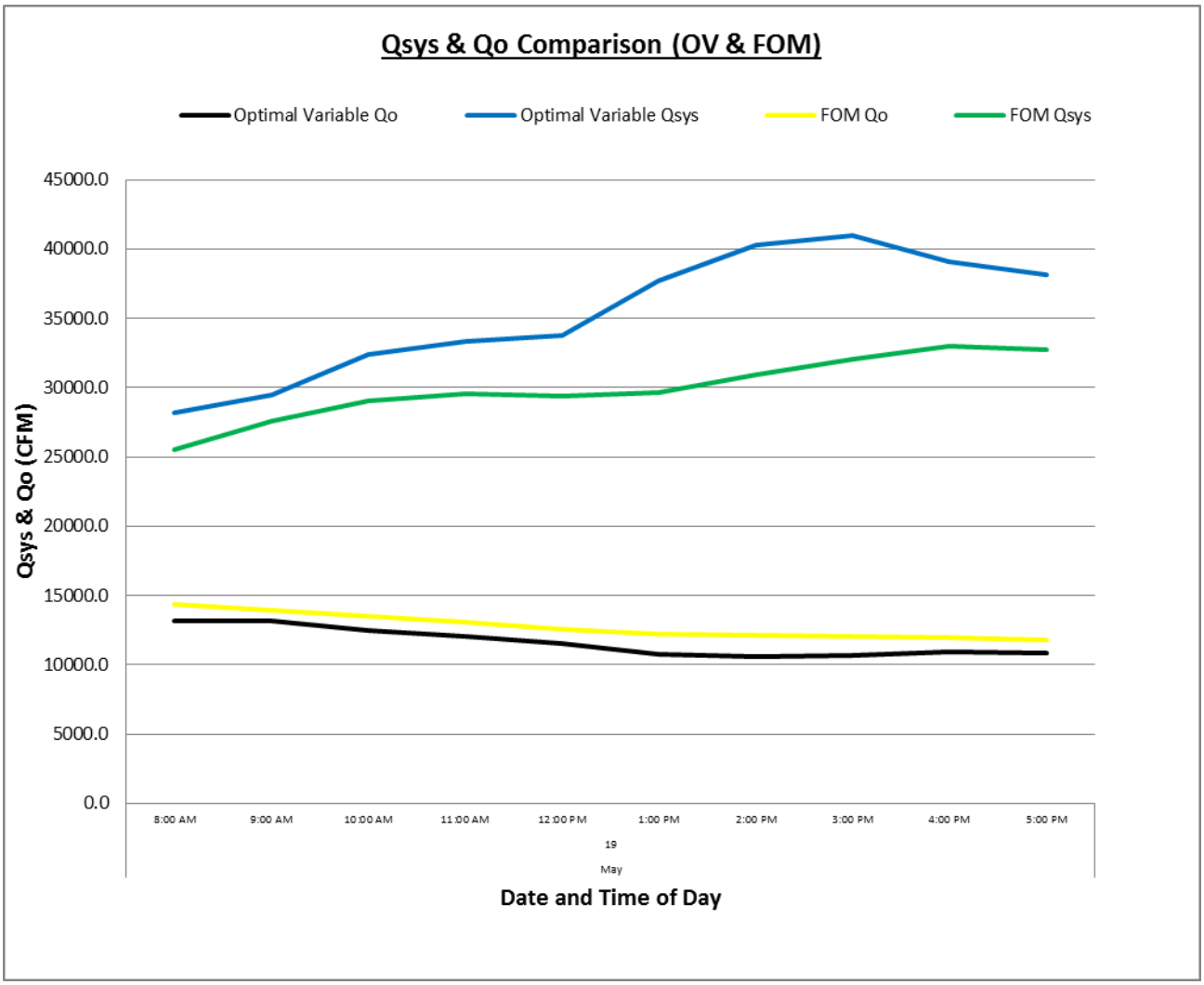

Figure 191. Q_{sys} & Q_o comparison (May 19).

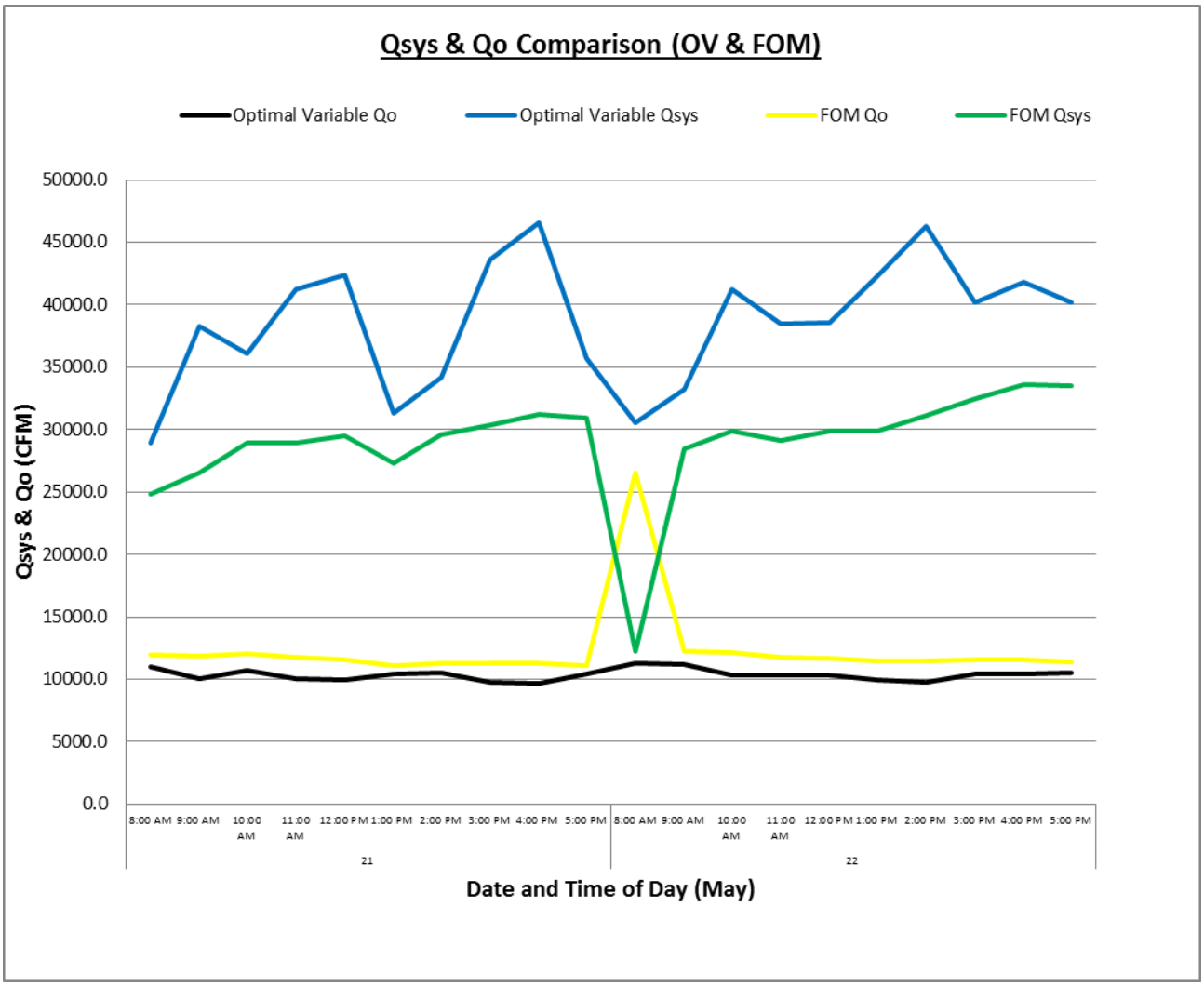

Figure 192. Q_{sys} & Q_o comparison (May 21 & 22).

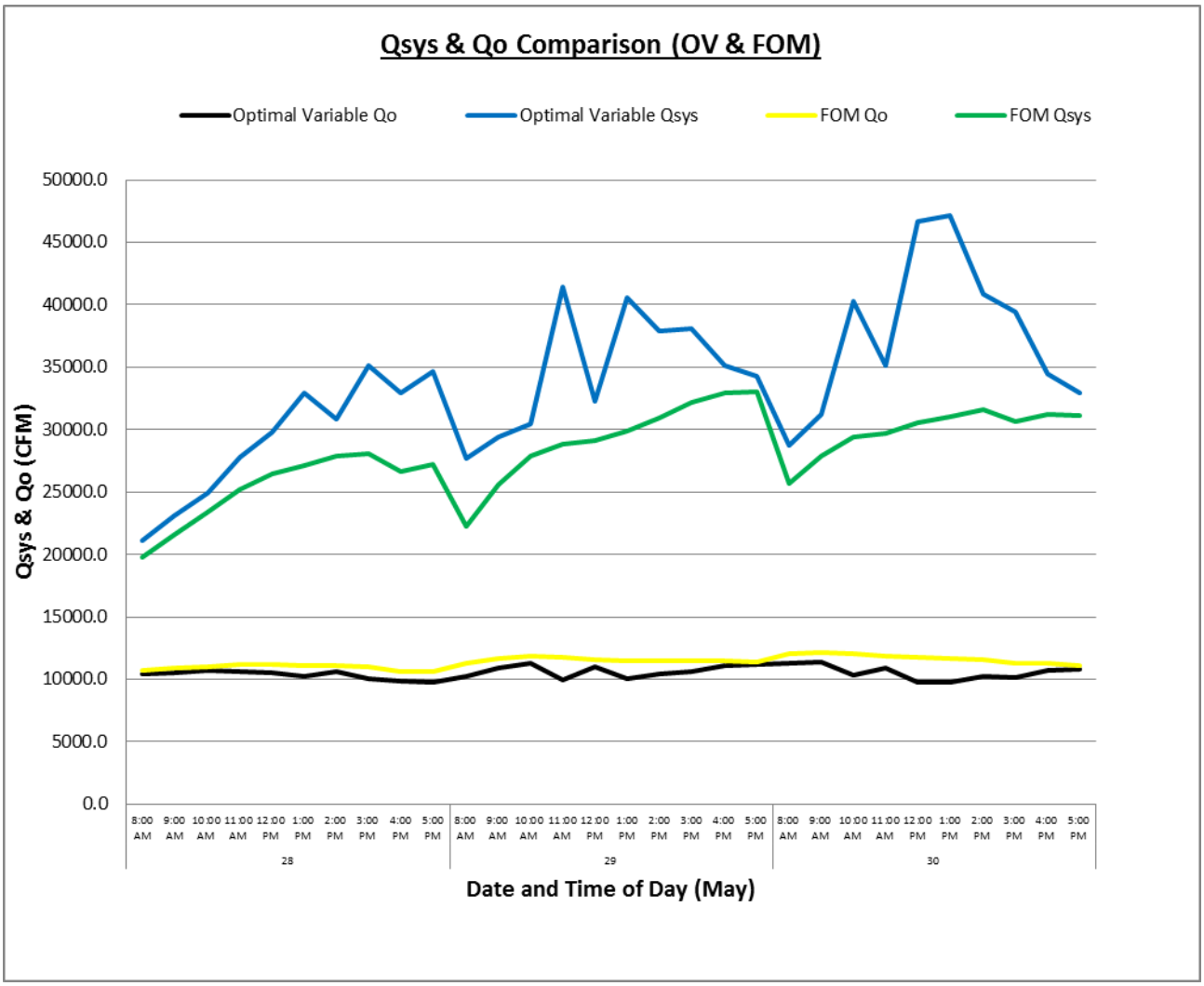

Figure 193. Q_{sys} & Q_o comparison (May 28, 29, 30).

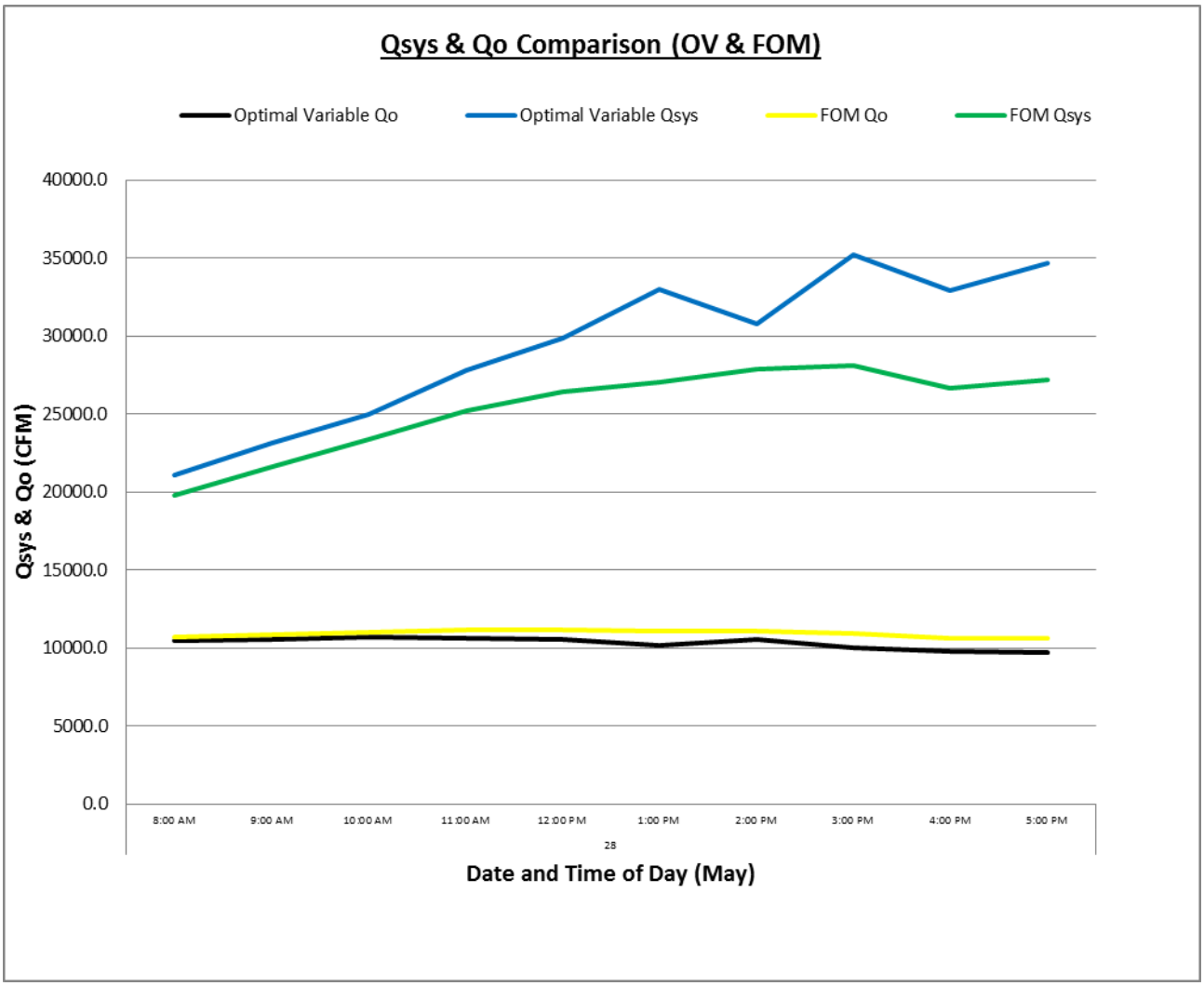

Figure 194. Q_{sys} & Q_o comparison (May 28).

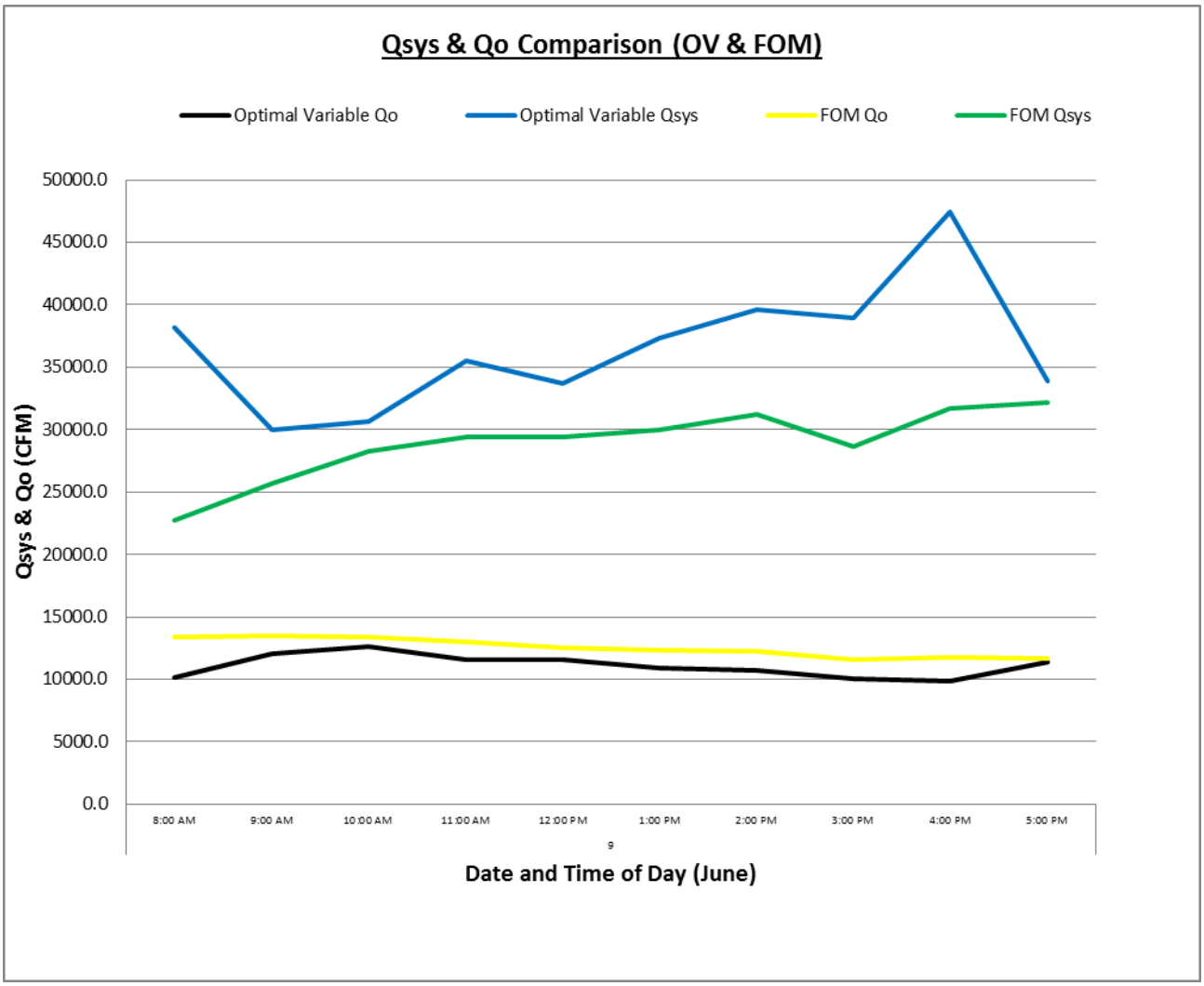

Figure 195. Q_{sys} & Q_o comparison (June 9).

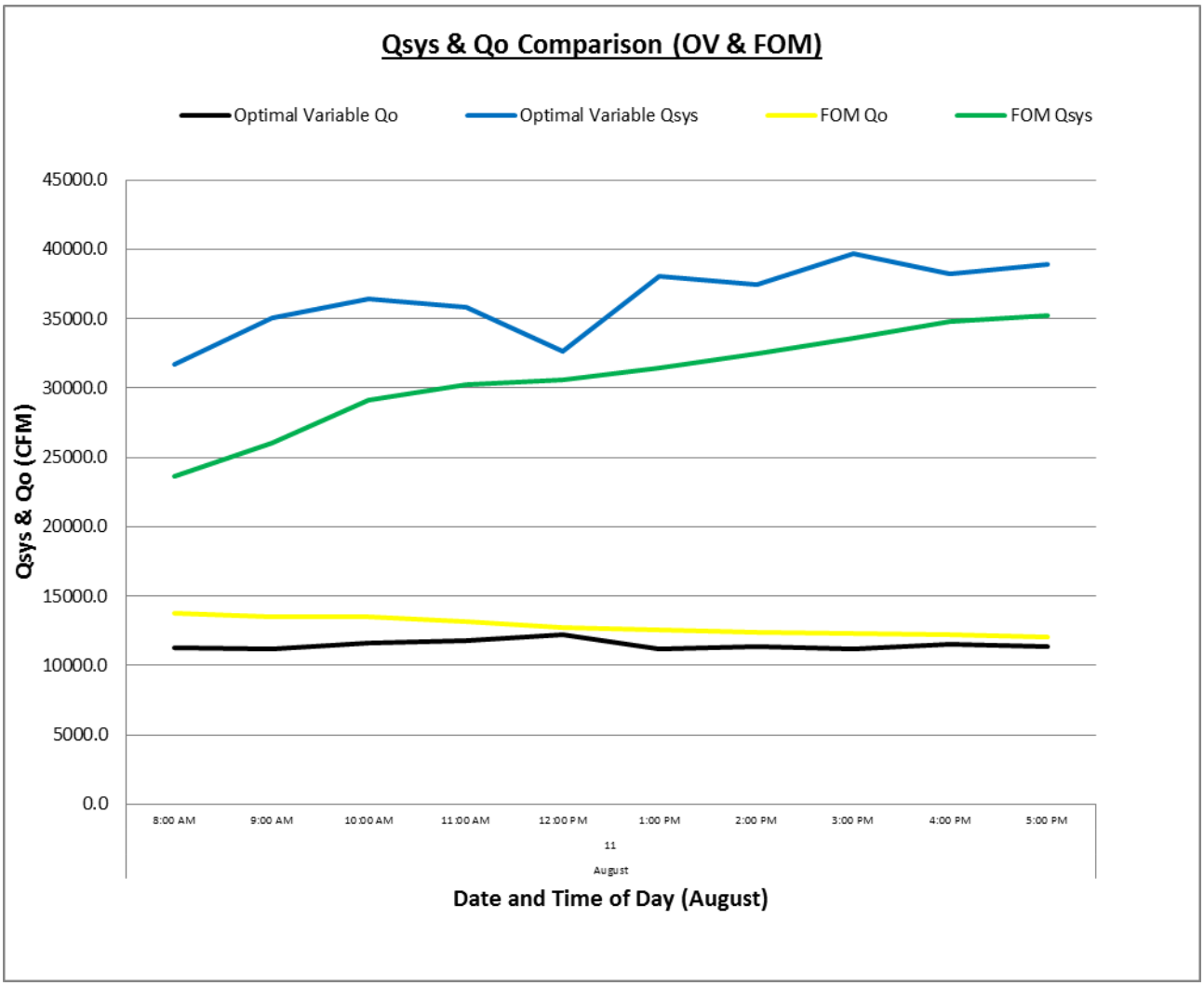

Figure 196. Q_{sys} & Q_o comparison (August 11).

E.13 Optimal Variable Equipment Power (Chiller, Fan & Pump) Graphs.

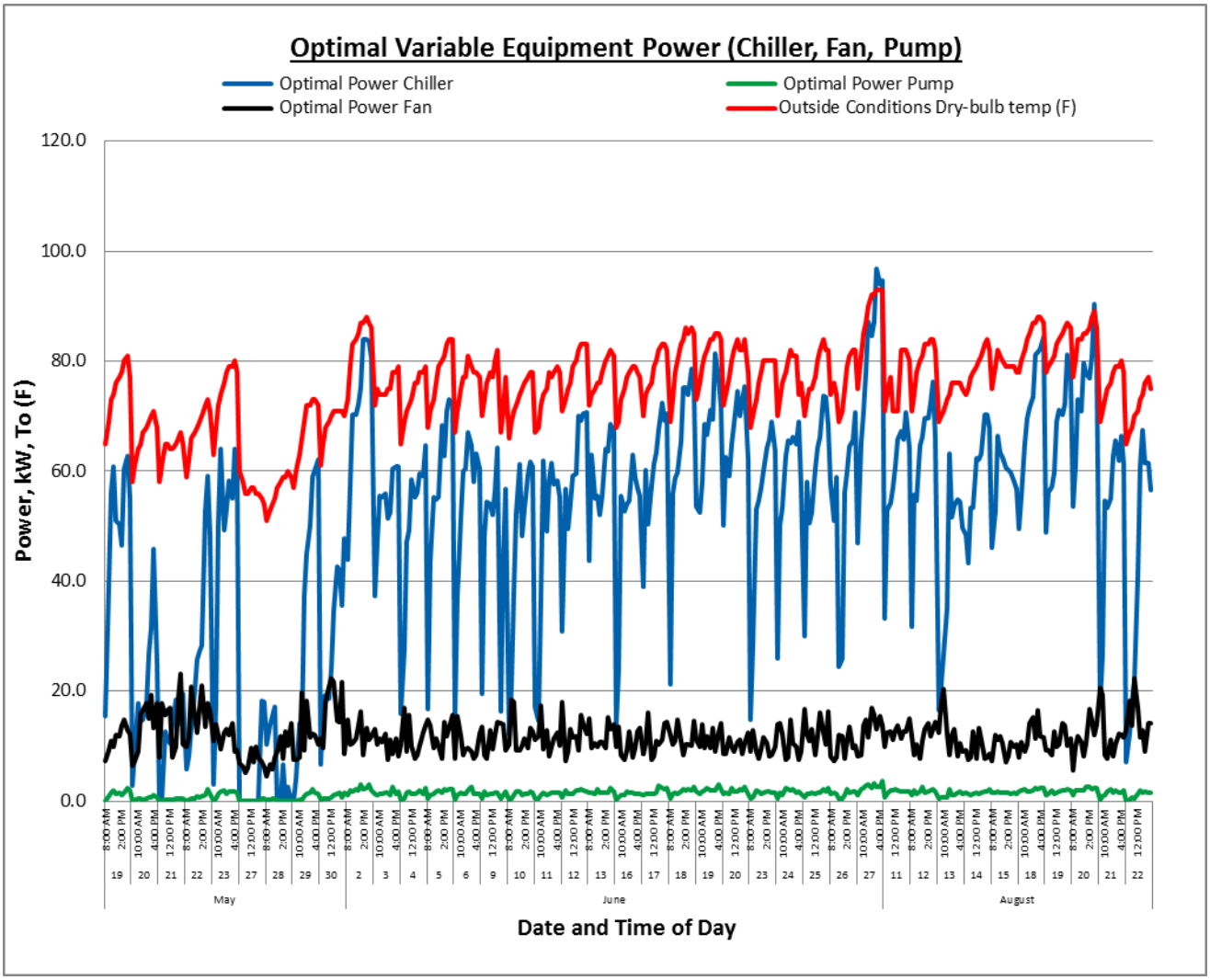

Figure 197. Optimal variable equipment power (May, June, August).

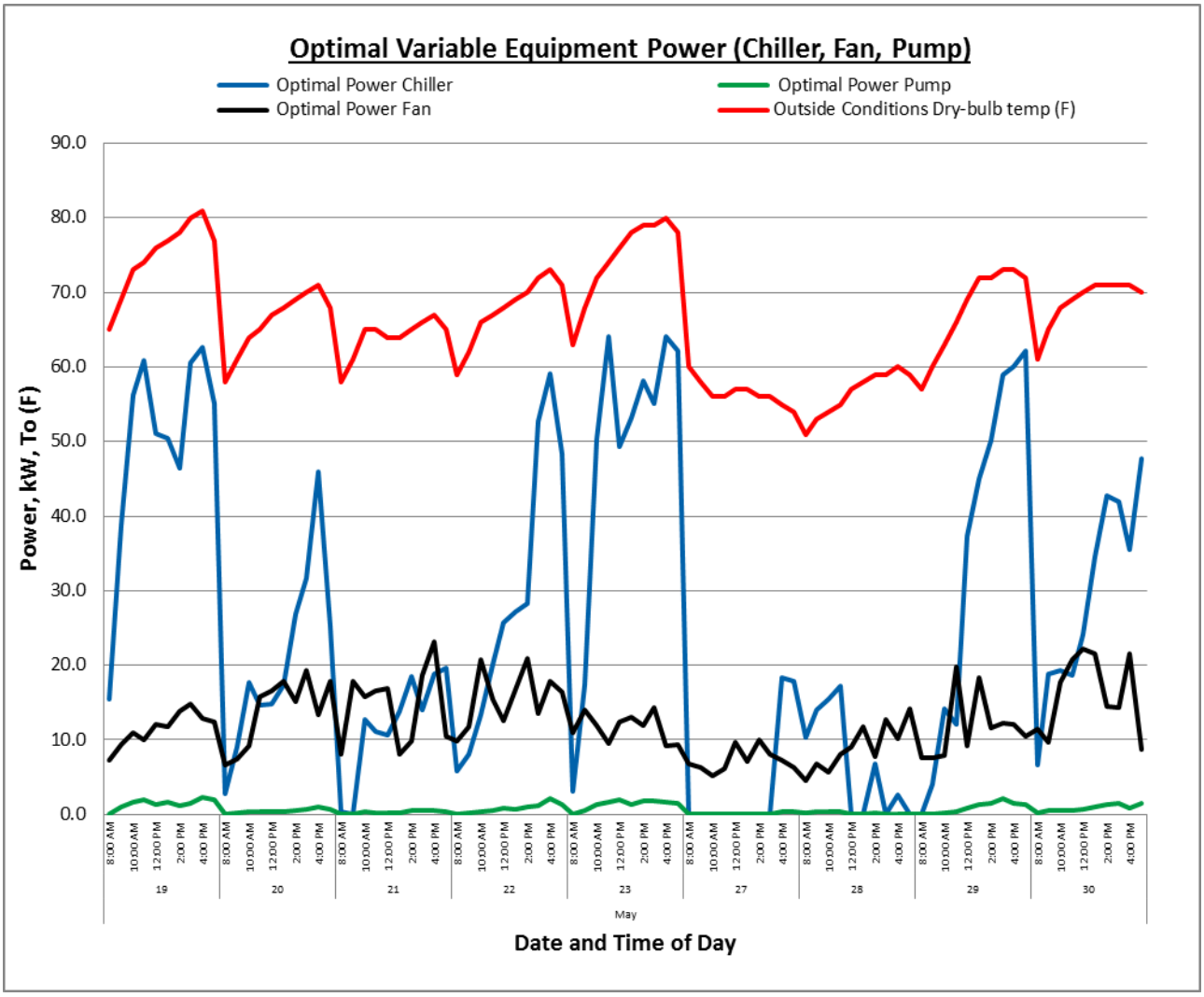

Figure 198. Optimal variable equipment power (May).

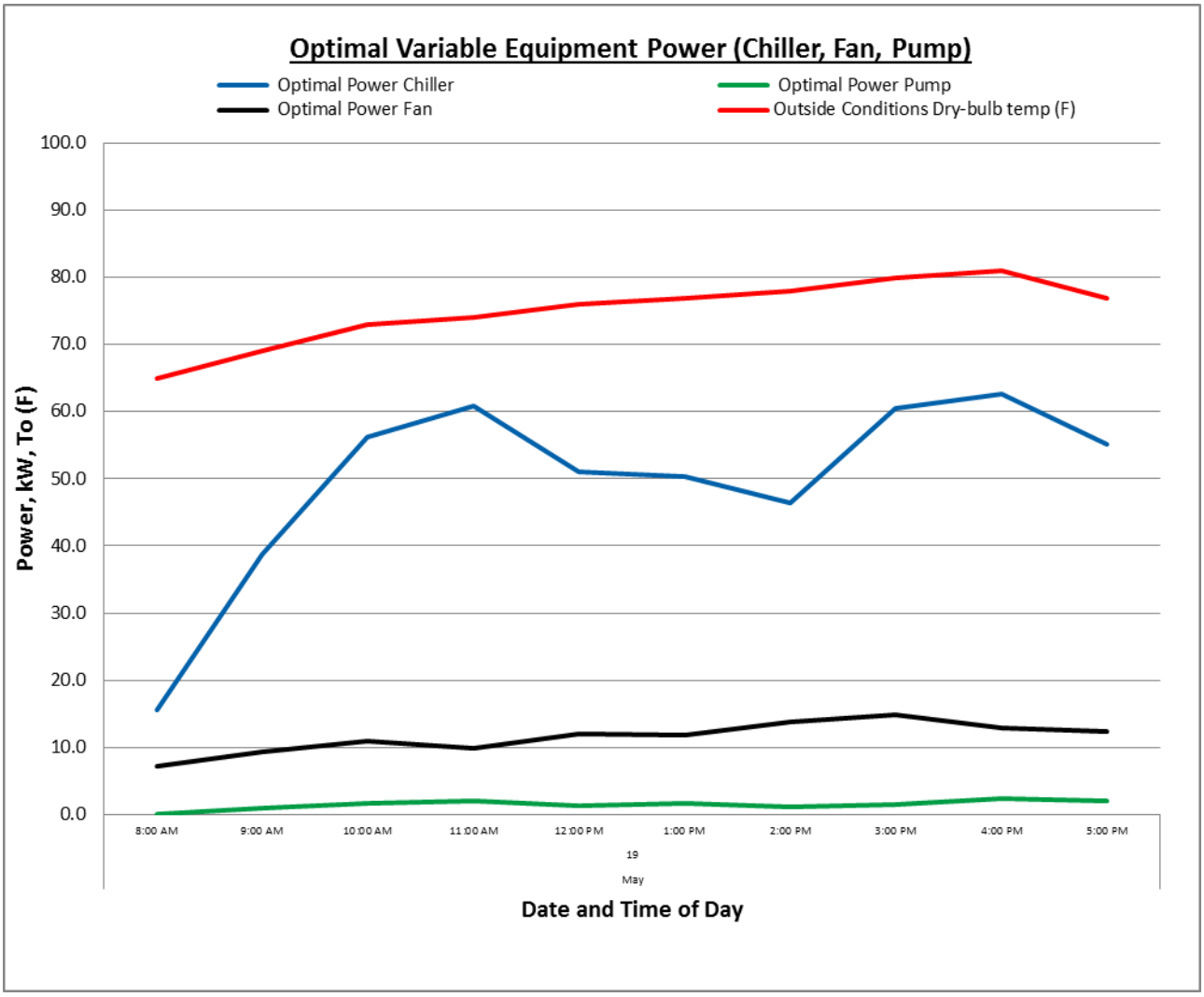

Figure 199. Optimal variable equipment power (May 19).

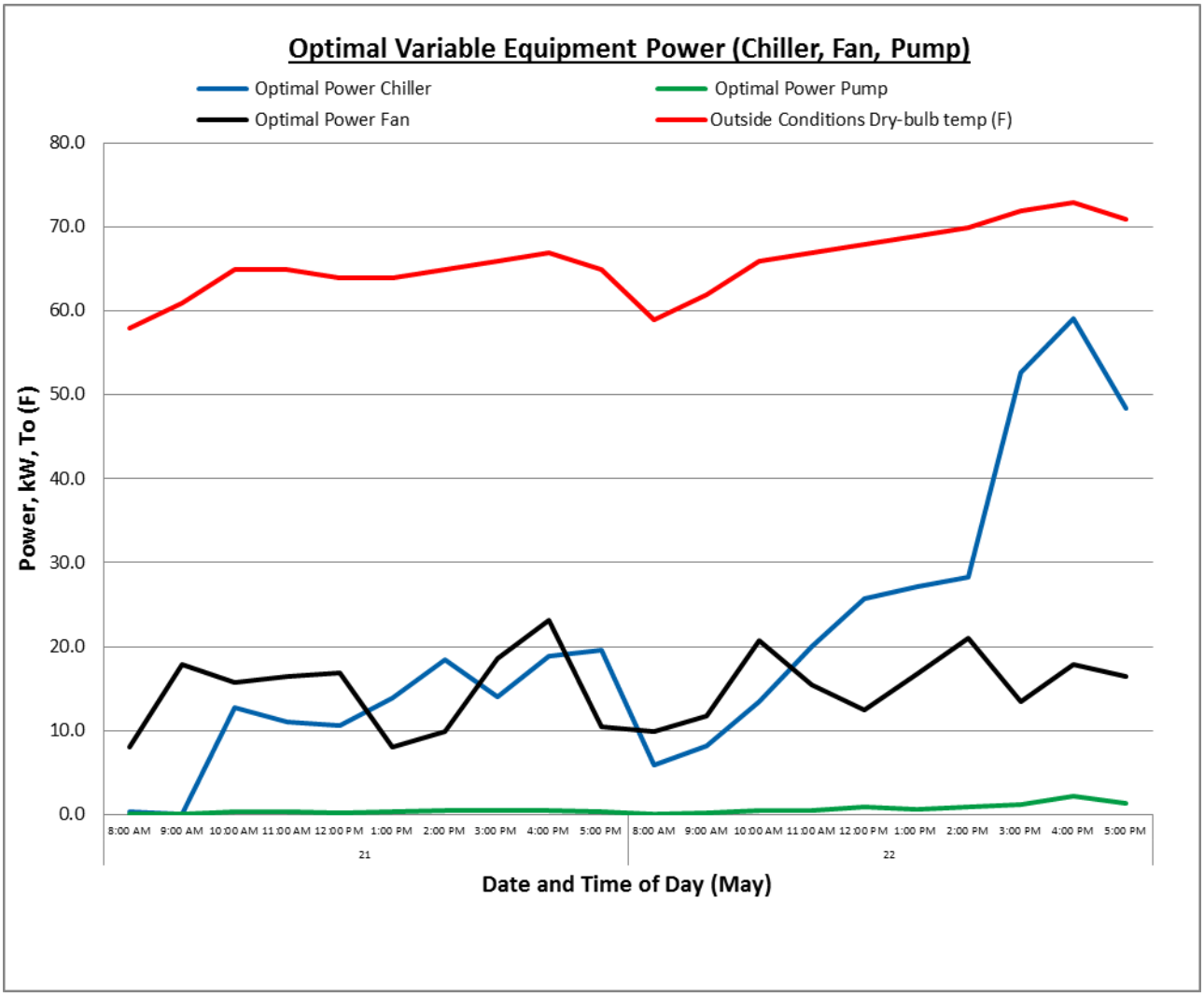

Figure 200. Optimal variable equipment power (May 21 & 22).

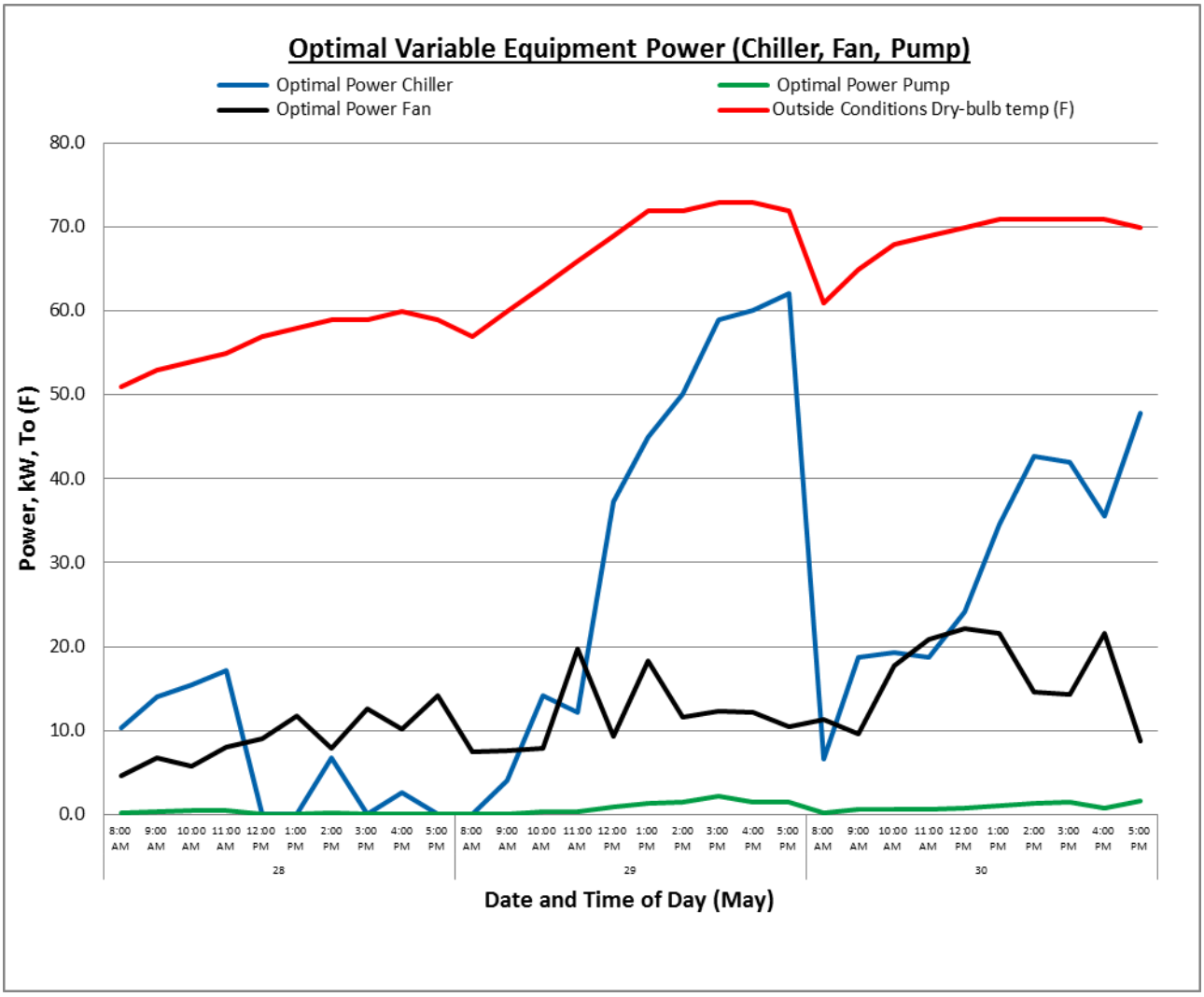

Figure 201. Optimal variable equipment power (May 28, 29, 30).

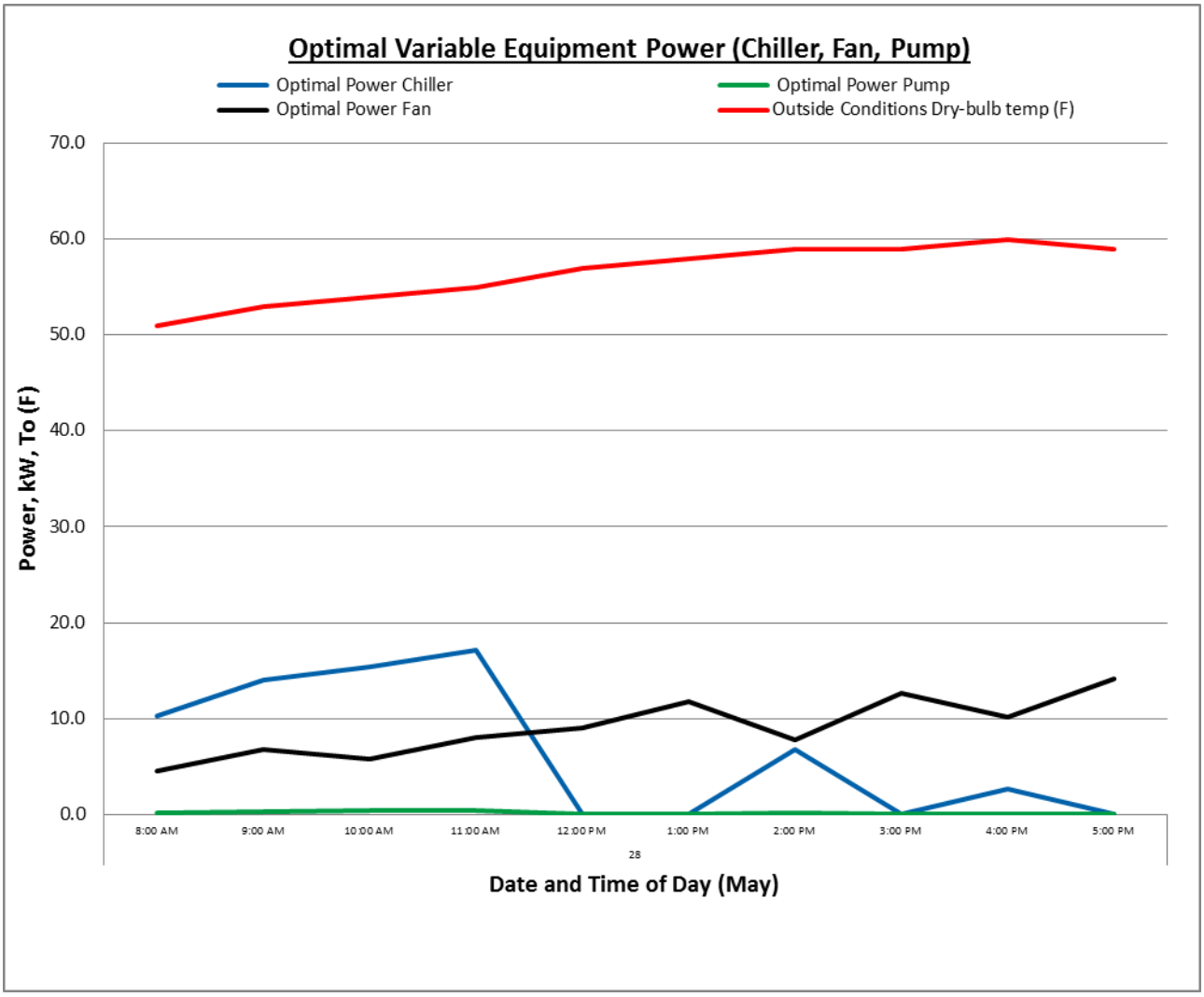

Figure 202. Optimal variable equipment power (May 28).

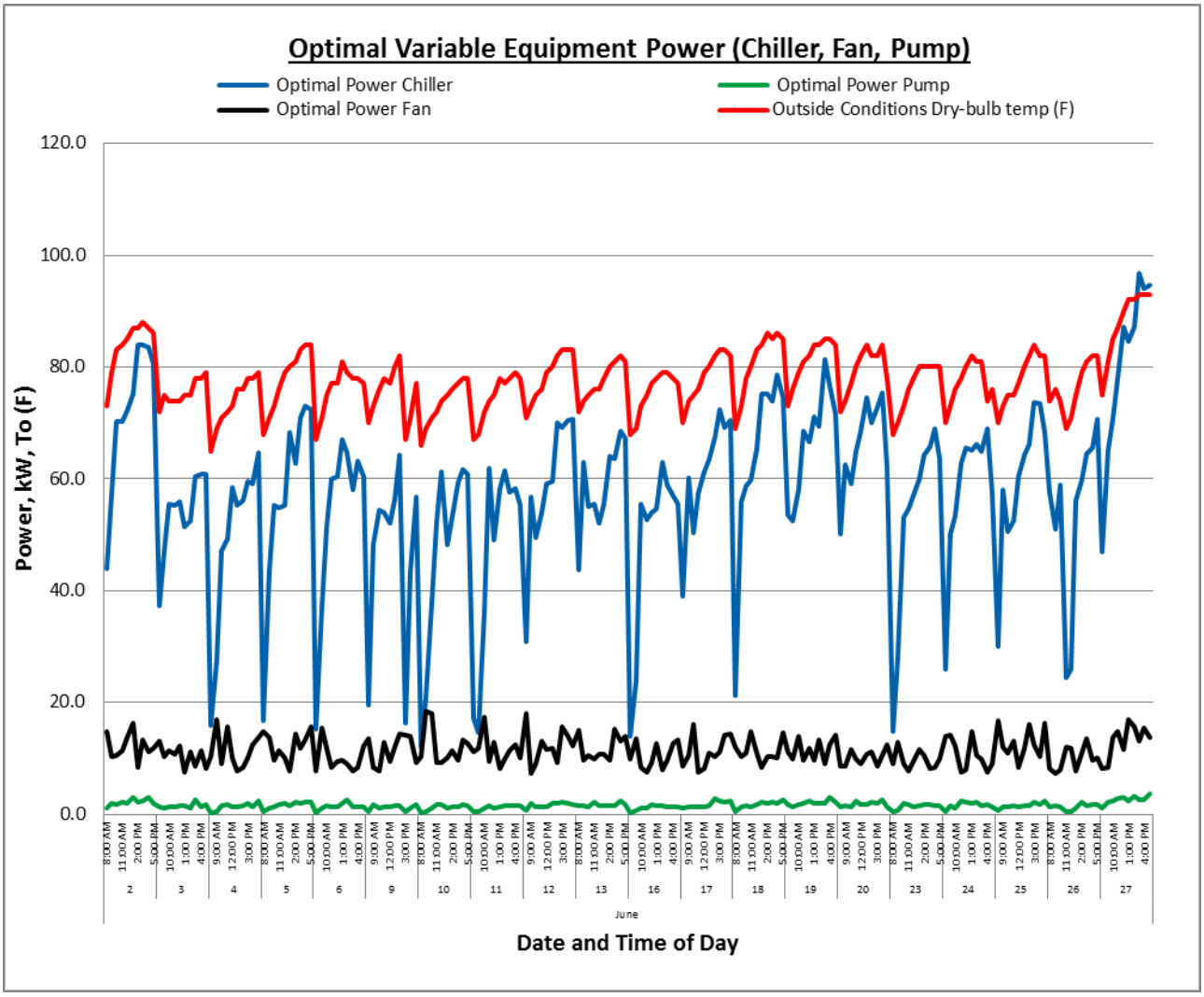

Figure 203. Optimal variable equipment power (June).

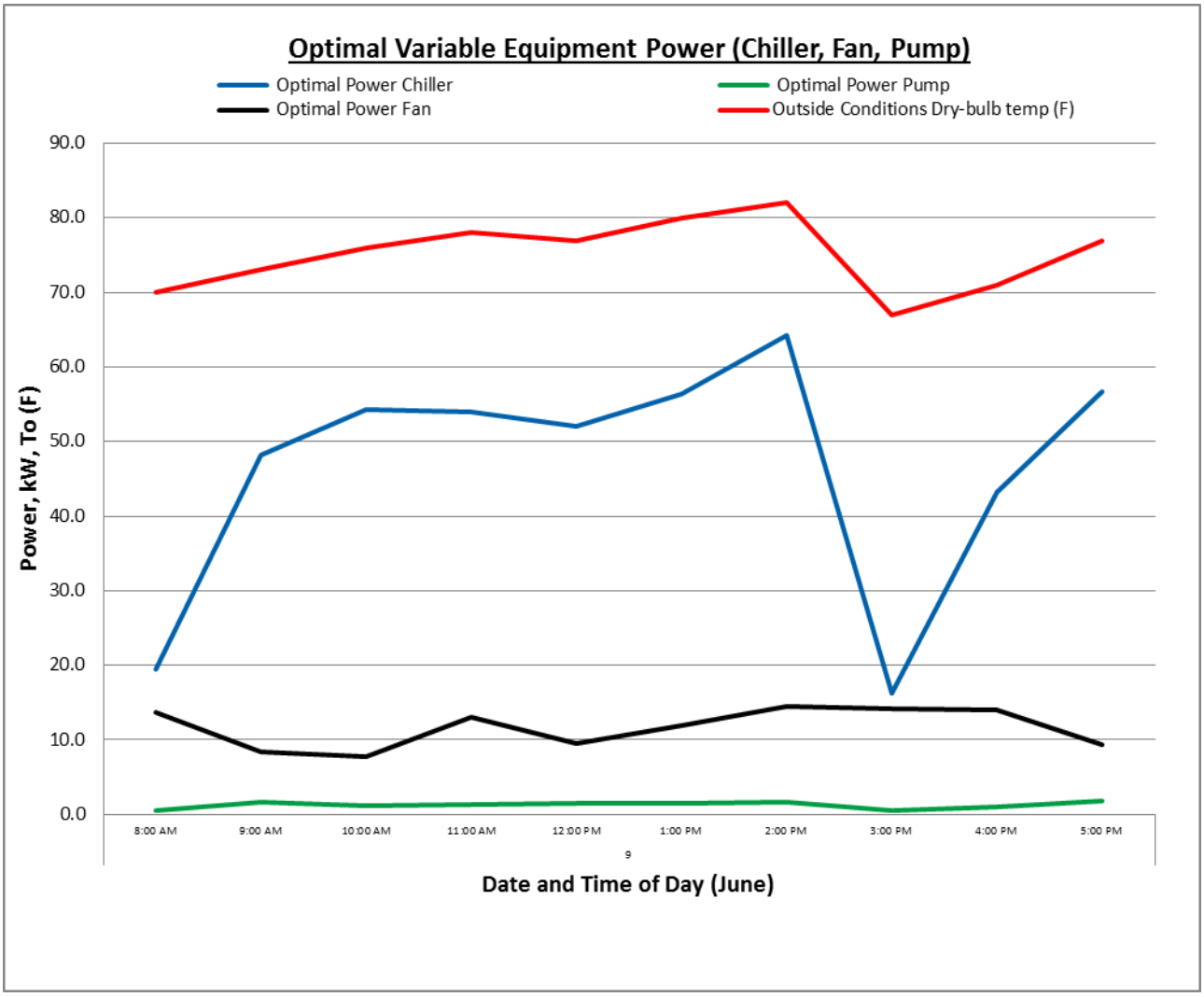

Figure 204. Optimal variable equipment power (June 9).

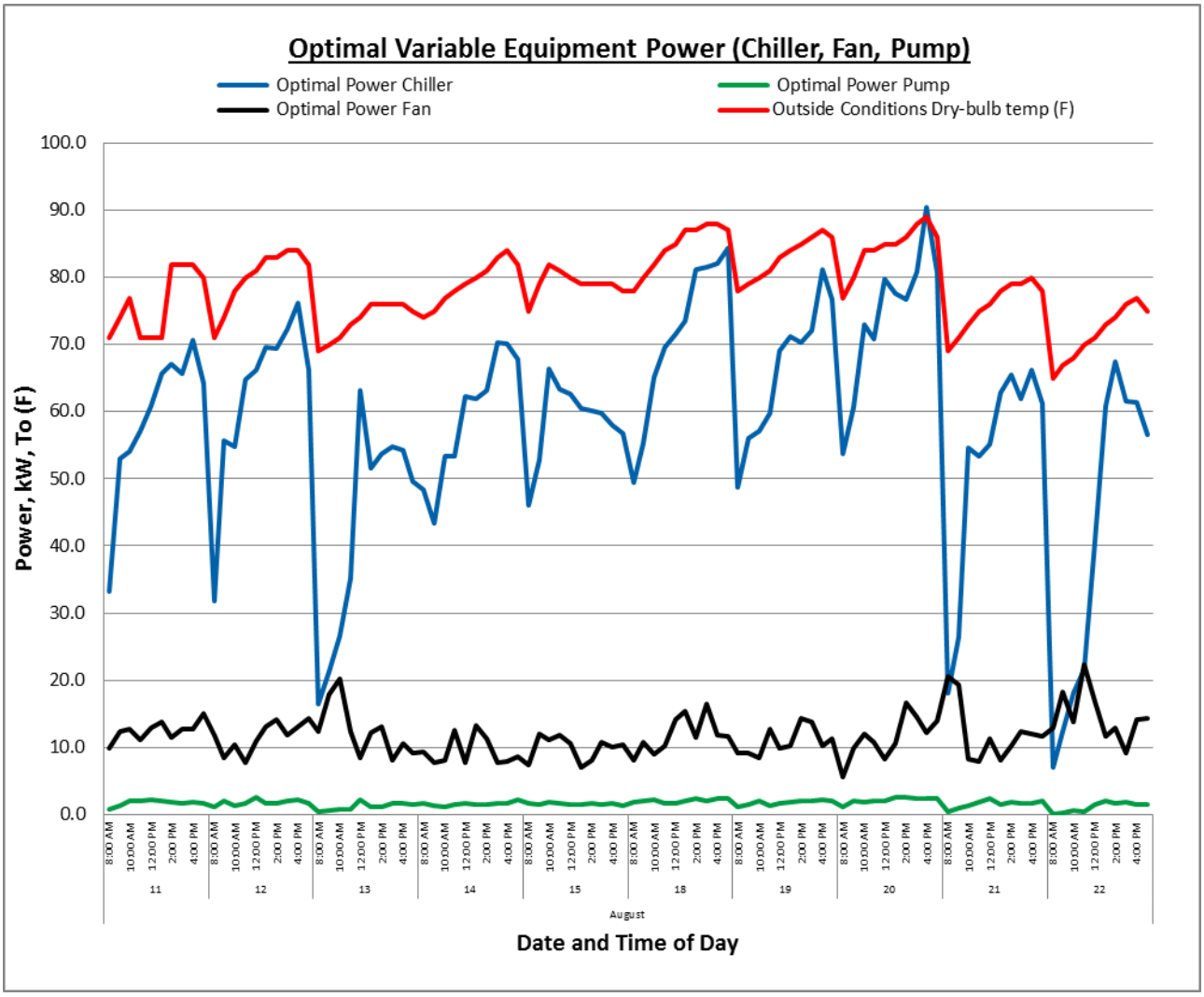

Figure 205. Optimal variable equipment power (August).

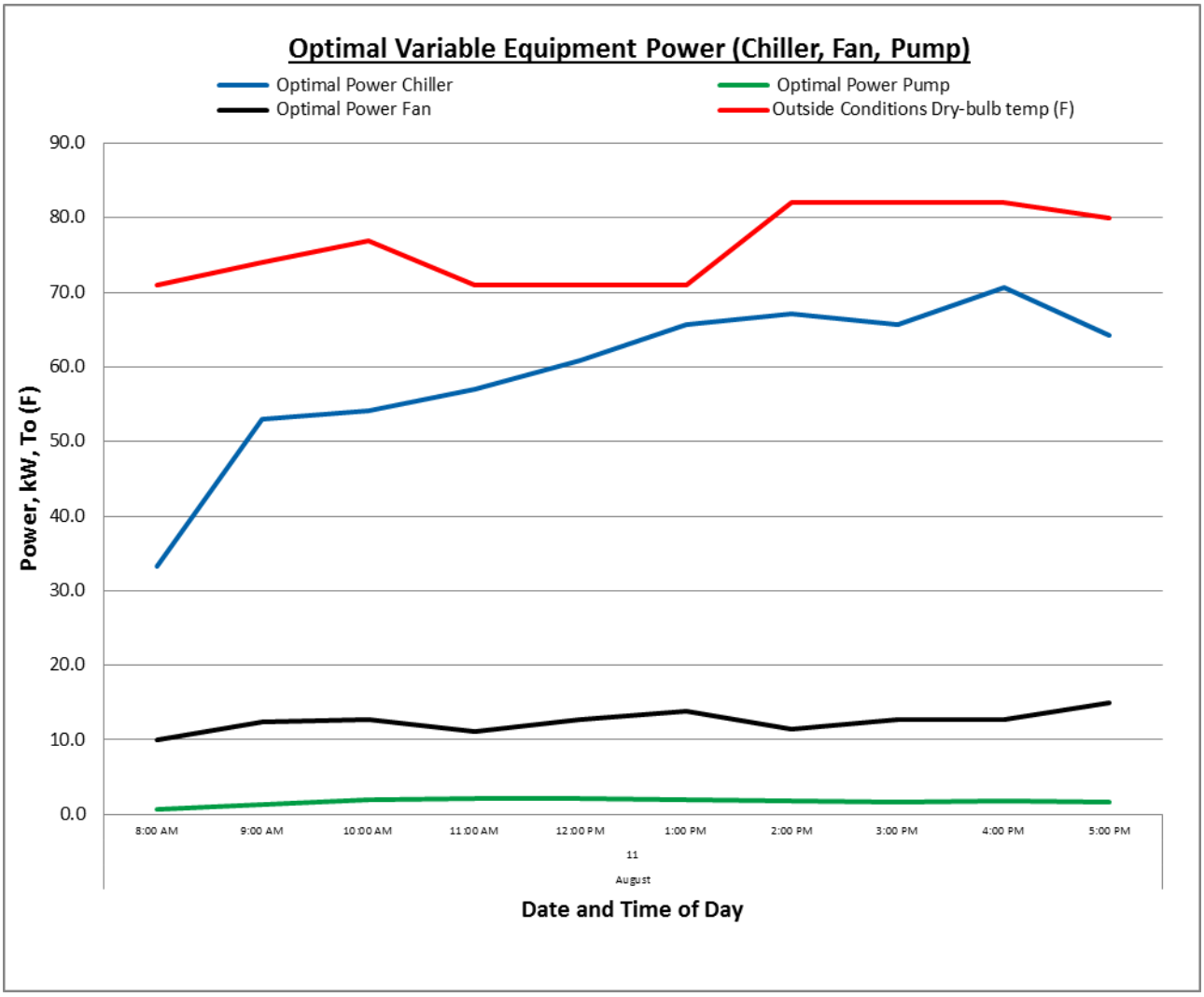

Figure 206. Optimal variable equipment power (August 11).

E.14 Outside Conditions (T_{db} & T_{wb}) Graphs.

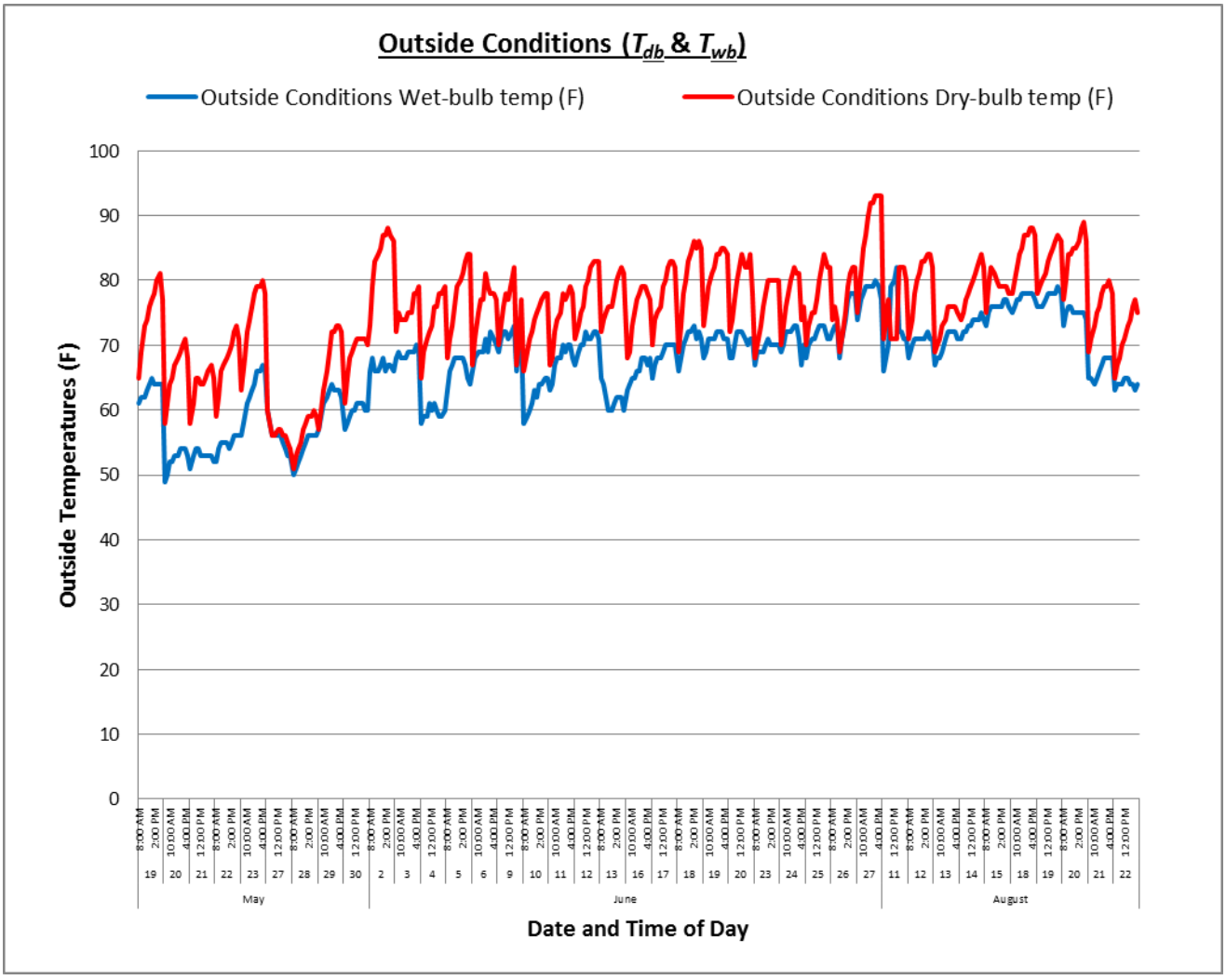

Figure 207. Outside conditions, T_{db} & T_{wb} (May, June, August).

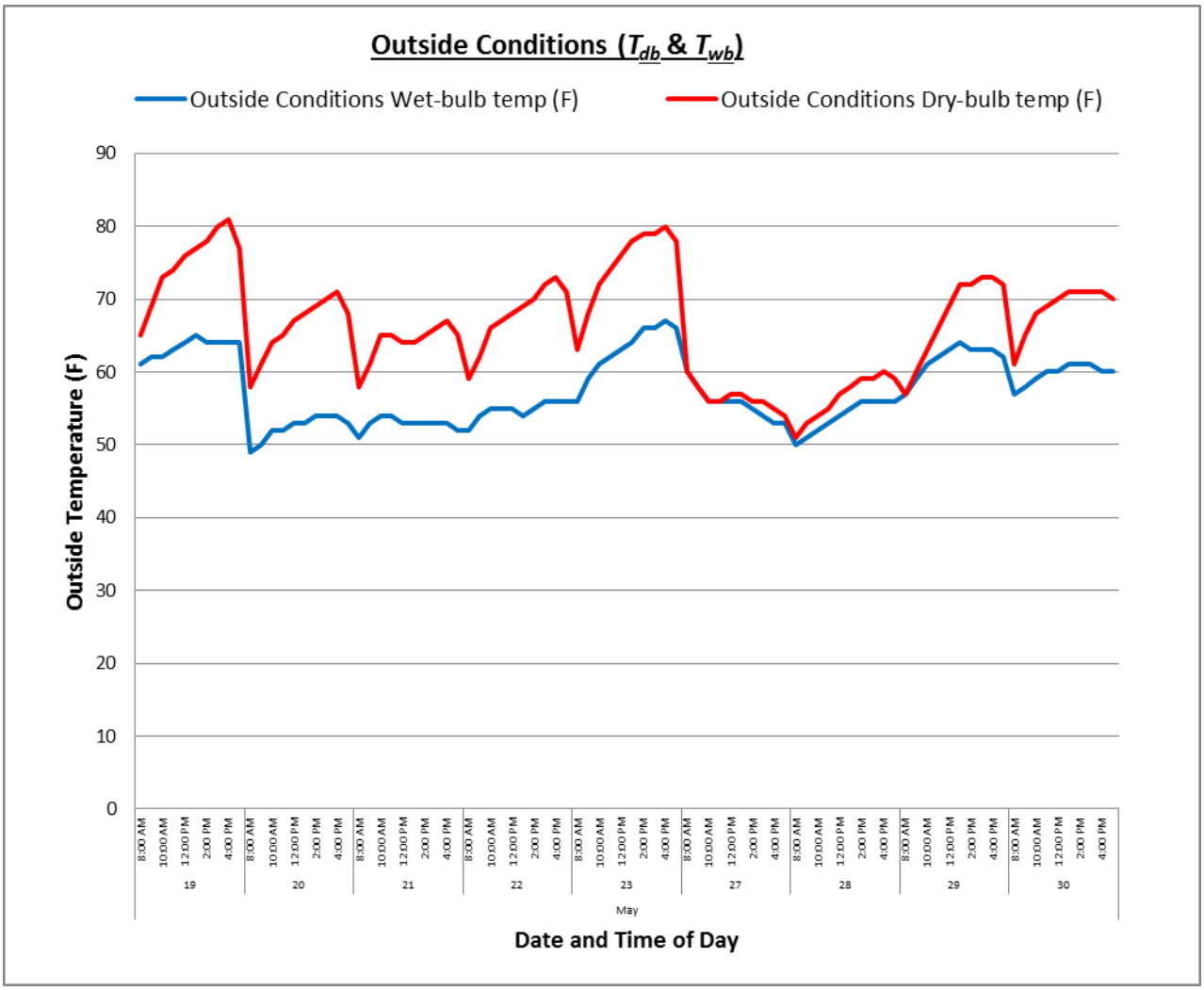

Figure 208. Outside conditions, T_{db} & T_{wb} (May).

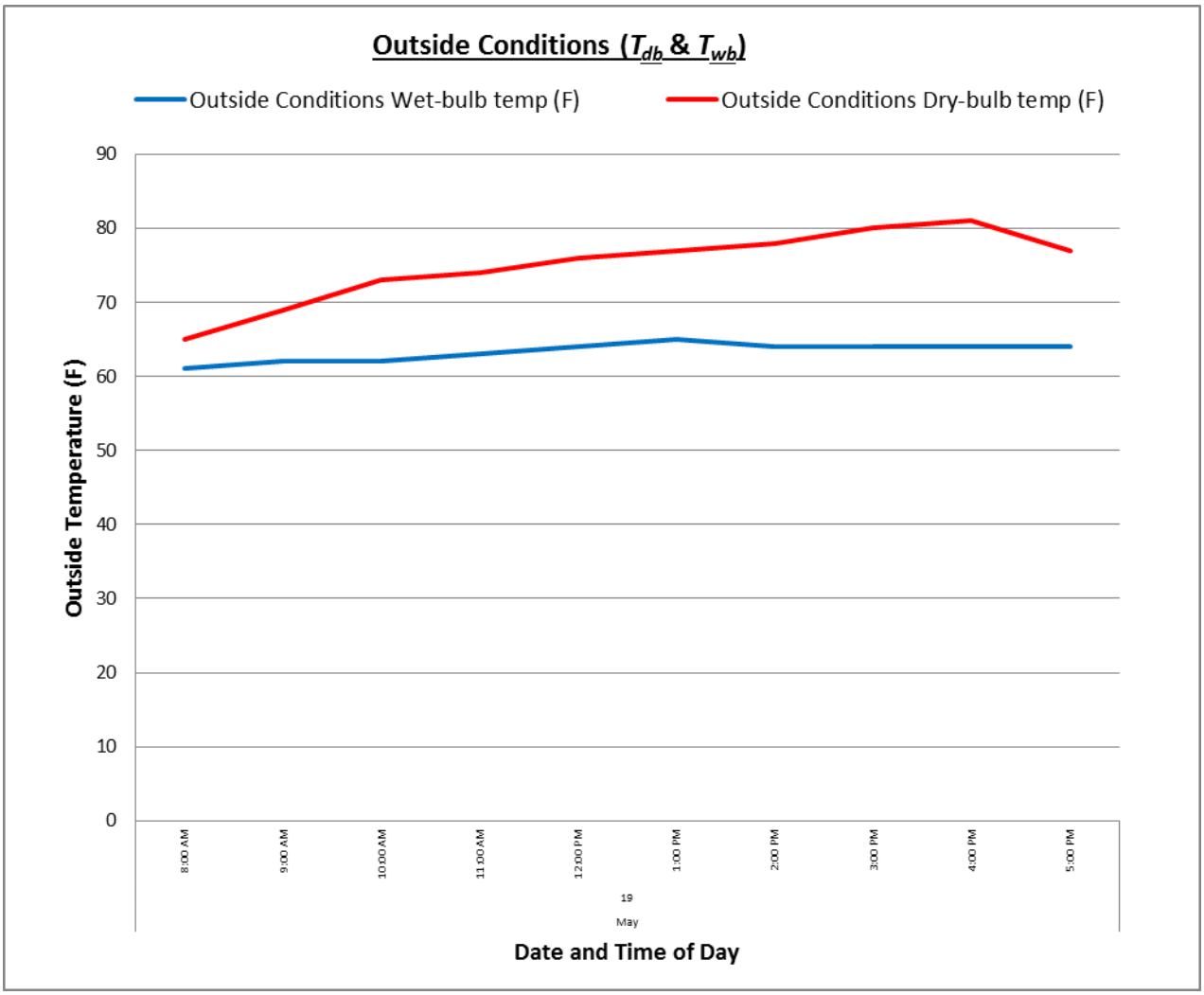

Figure 209. Outside conditions, T_{db} & T_{wb} (May 19).

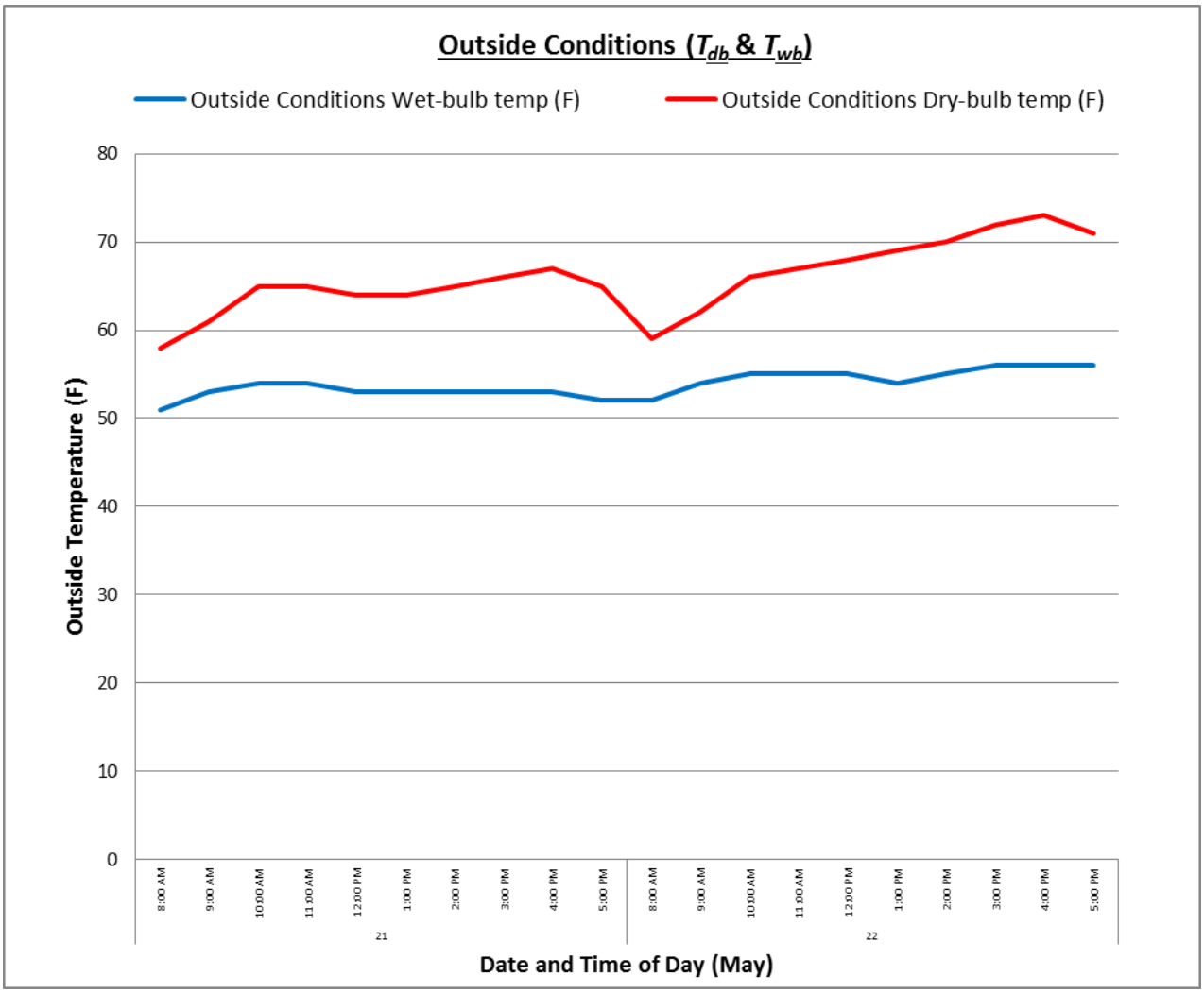

Figure 210. Outside conditions, T_{db} & T_{wb} (May 21 & 22).

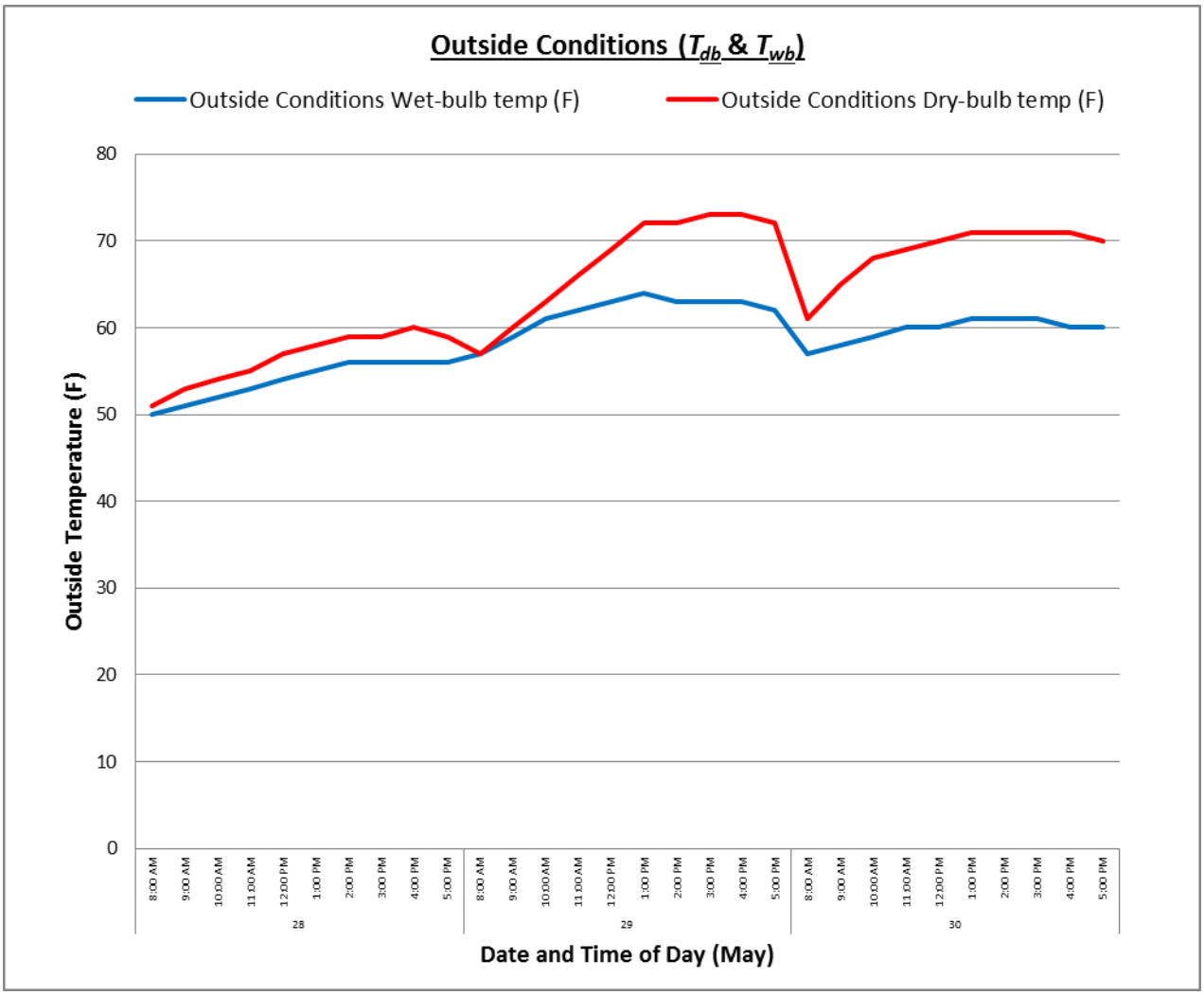

Figure 211. Outside conditions, T_{db} & T_{wb} (May 28, 29, 30).

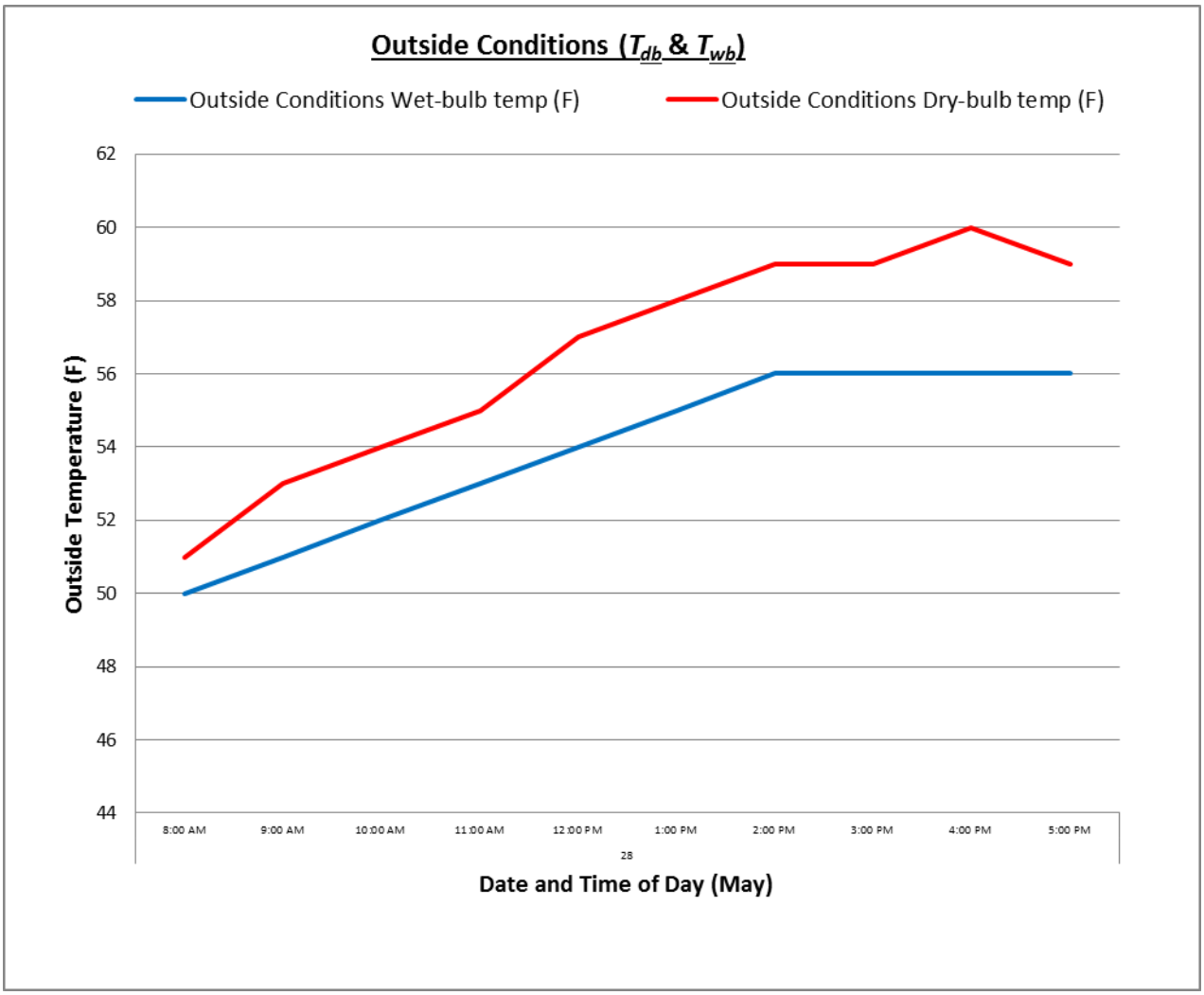

Figure 212. Outside conditions, T_{db} & T_{wb} (May 28).

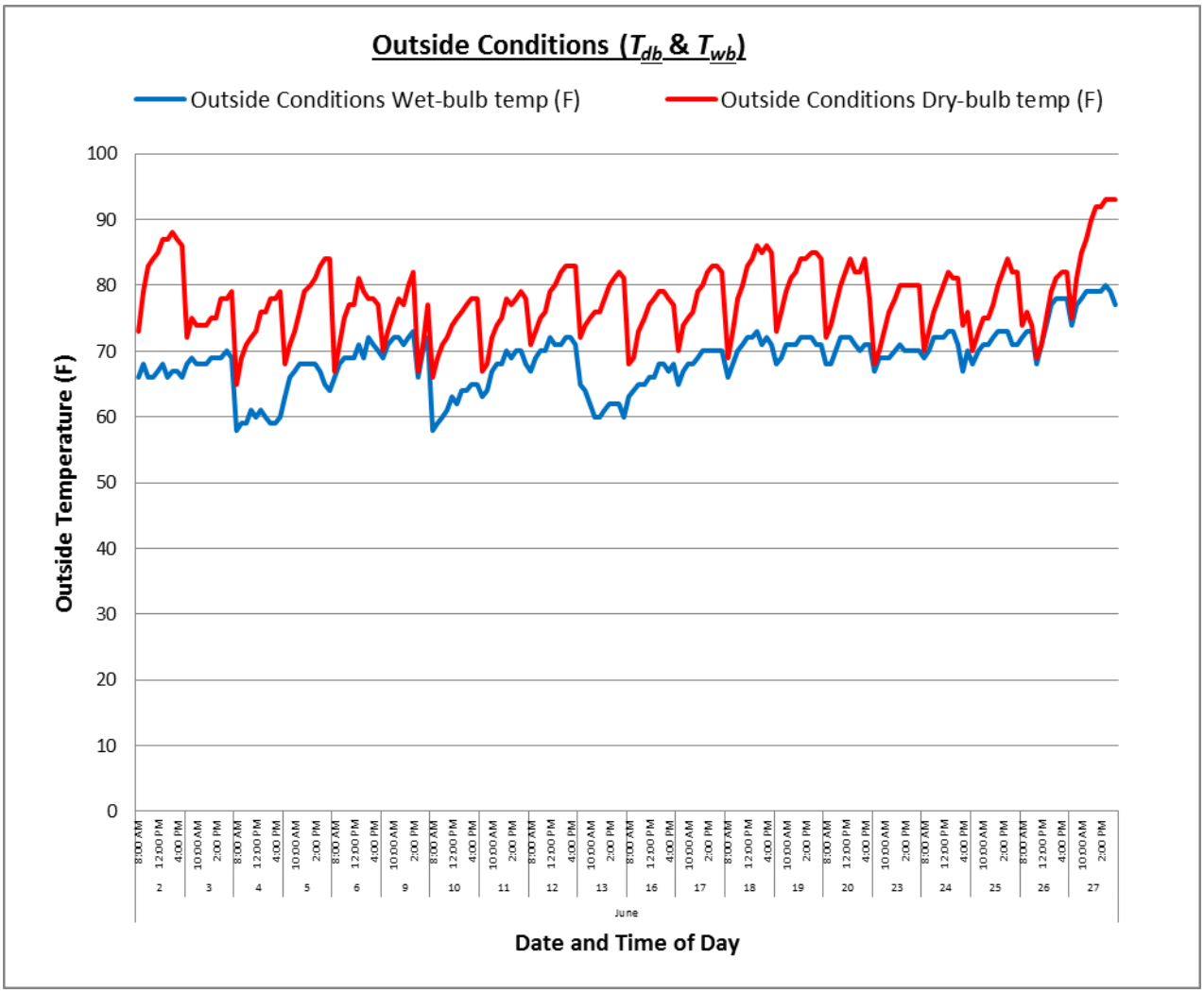

Figure 213. Outside conditions, T_{db} & T_{wb} (June).

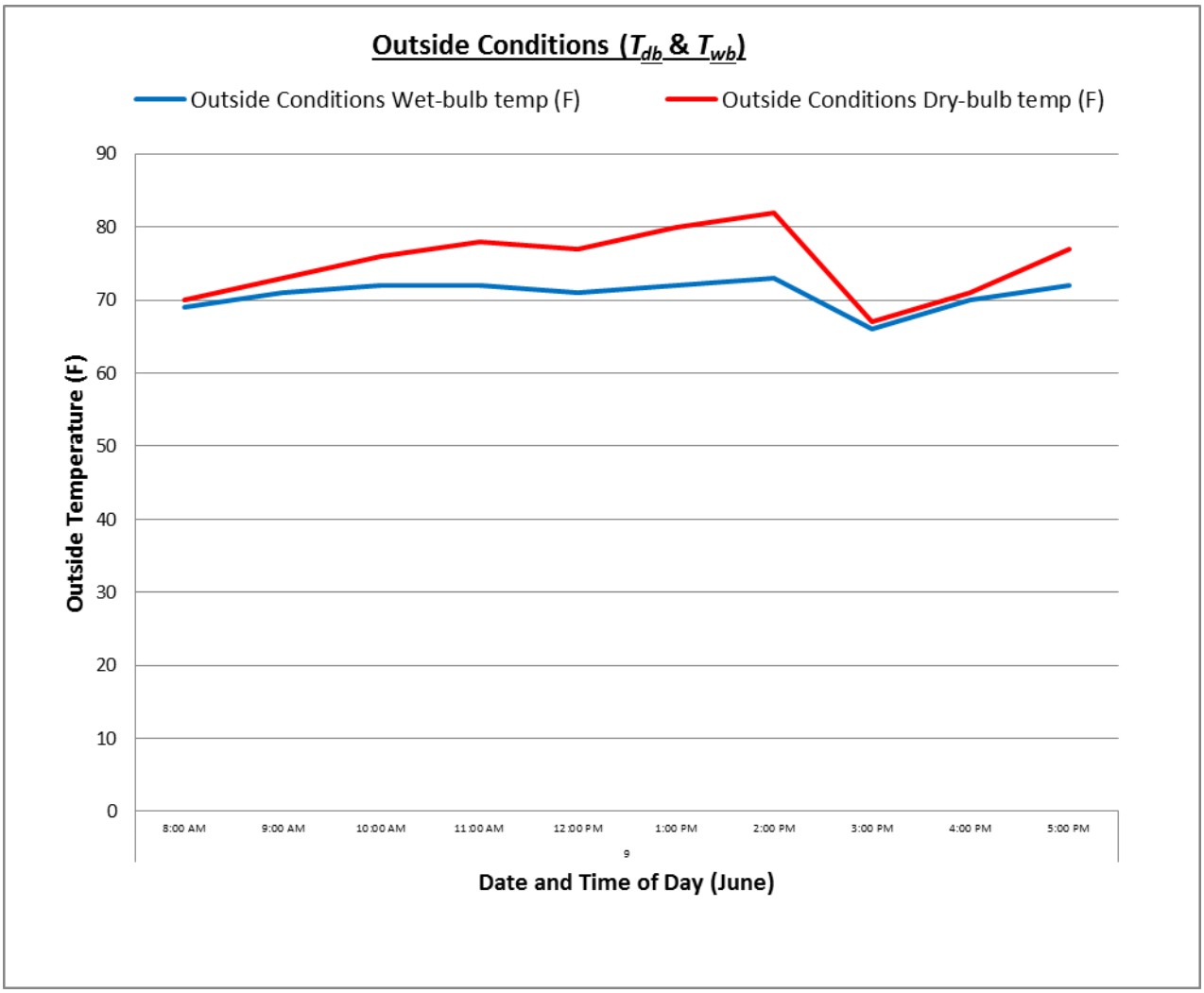

Figure 214. Outside conditions, T_{db} & T_{wb} (June 9).

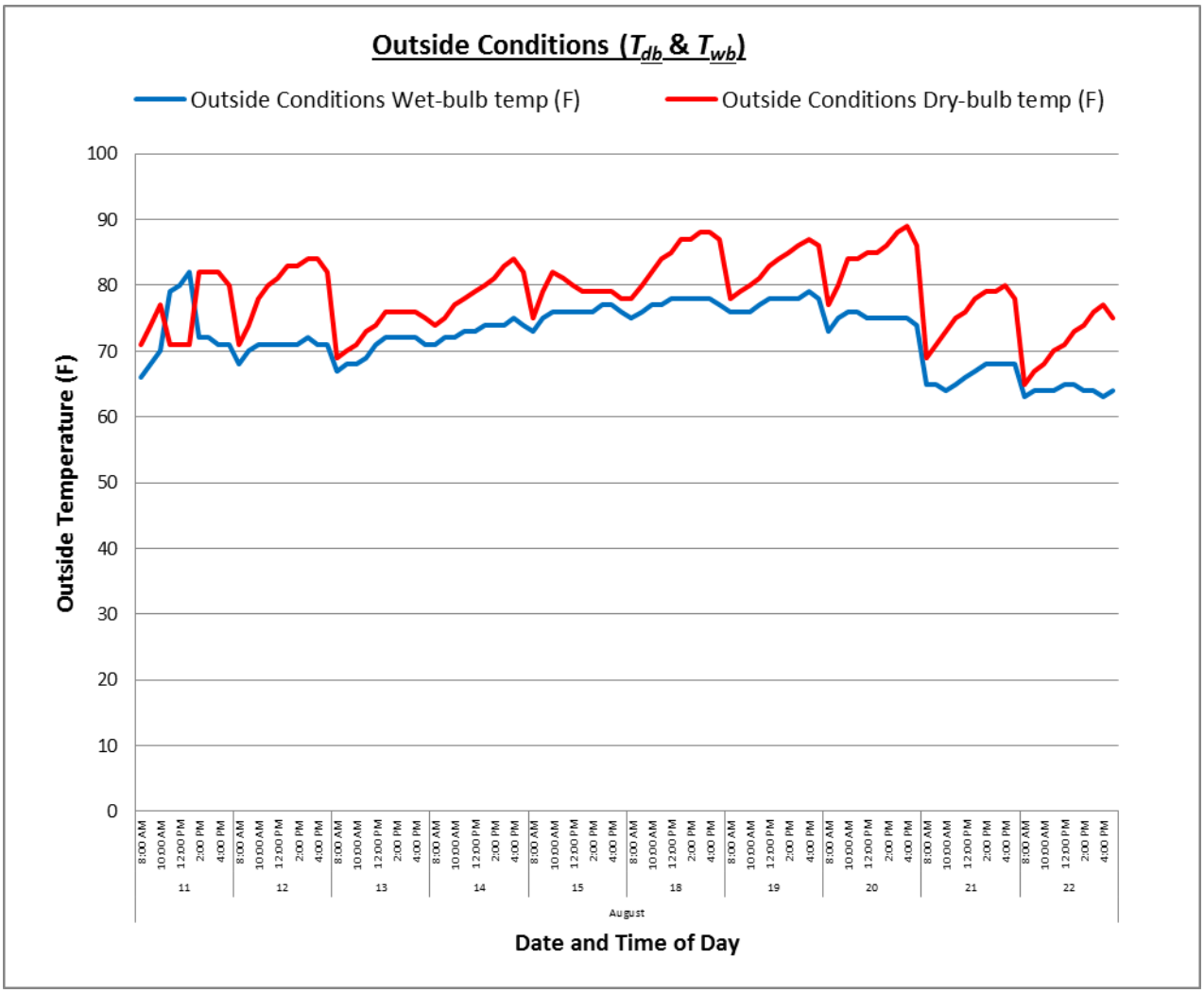

Figure 215. Outside conditions, T_{db} & T_{wb} (August).

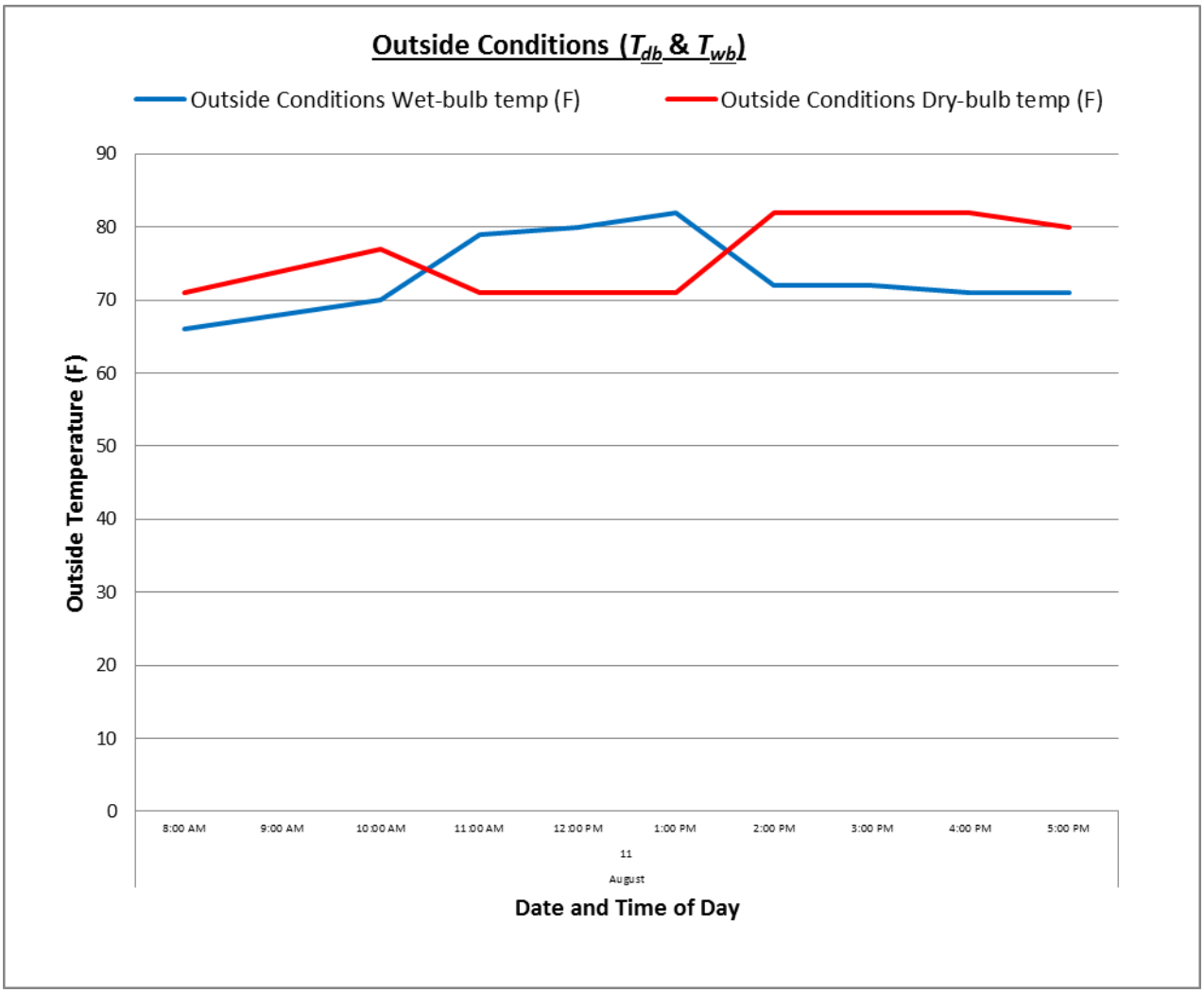

Figure 216. Outside conditions, T_{db} & T_{wb} (August 11).